Effects of overexpression of eIF4E and erbB2 on gene expression profiles and invasive phenotype in human cancer cells

A thesis submitted for the degree of Ph.D.

Dublin City University

By

Isabella Bray B.Sc. (Biotechnology)

This research work described in thesis was performed under the supervision of Prof. Martin Clynes

National Institute for Cellular Biotechnology

Dublin City University

July 2006

I hereby certify that this material, which I now submit for assessment on the programme of study leading to the award of Ph.D. is entirely my own work and has not been taken from the work of others save and to the extent that such work has been cited and acknowledged within the text of my work.

Signed: Isabella Rey (Candidate) ID No.: 95739581

Date: 22.09.06

This thesis is dedicated to my father, Patrick Bray.

Still missed, your memory is ever present, always guiding me.

Acknowledgements

My sincere thanks to Prof Martin Clynes for his patience and kindness, and for giving me so much guidance and support throughout these years. The constant encouragement and reassurance I received from you enabled me to complete this thesis.

I would also like to thank Dr. Padraig Doolan, who co-supervised my work. Thanks Paud, not just for all your help, but also for your friendship (the numerous pep-talks, constant reassurance, up-dates on world politics, shots of brandy, talking me down off the roof etc etc).

Thanks also to Dr. Patrick Gammell. Paddy you went through my Discussion as if it was the Will of some long-lost Gammell who had recently won the lotto! Your help was greatly appreciated.

Thanks to all in the Molecular biology lab, especially Dr. Niall "MacGyver" Barron (the only man who'd try sequencing the human genome with sellotape and a paper clip). Niall thank you so much for your patience over the years in explaining all things molecular, and for never turning me away when I needed help. I don't know what we'd do without you.

Irene and Elaine –I can say with certainty that my thesis would not have gone out without your help. The last couple of weeks were really tough and I can't thank you enough for your support. It's hard to believe that someone as stressed –out and grumpy as me would manage to make friends over the last few years, but I did, and thanks.

Laura, thank you for being so kind and taking care of me when I was preparing for my viva, it's much appreciated.

Madness comes in many forms over the course of a PhD, but it has to be said Finbar was my favourite lunatic in the asylum. Thanks for all your crazy ideas, and for always being able to make me laugh (sometimes with you, sometimes at you…).

Thanks also to Helena, AnneMarie, Jason and Olga for their constant reassurance that I would make it out alive, for all the lunch and coffee breaks, and for their help and support in general.

Eadaoin, and Will (PubMed) - it was reassuring to know that one of you would always be in work, no matter what time of day or night. Thanks for the late-night/early morning chats and the laugh, and for always knowing when things were really bad I could depend on it being worse for one of you!

Carol and Yvonne, thank you both for your kindness and concern, and for always being so patient when I needed help.

Many thanks to Dee and Rasha. I think I would have run screaming during the first couple of years had it not been for them. Thank you all for your help, and your friendship.

John and Yizheng, thanks for the entertainment and company in the sterile room those first few years.

If I don't thank the girls I'll end up with a thesis shaped imprint in the side of my head! Alison, Susan, Ciara, Aoife and Caireann. -thank you all for being so supportive throughout my PhD. Special thanks to Alison (Lovebean), who was always there to cheer me up. You got me through many dark days. Also to Susan, who's always been there with advice and support when I needed it most.

Thanks to all the O'Boyle family, especially Peter – had I not being trying so hard to prove I wasn't as "thick as two short planks" I might never have got this far! I am forever grateful that you cared enough to put me on the right path.

To my sisters Susan and Maria, nephews Patrick and Robert, and nieces Emma and Christine for their love and support. Thanks for always being there, I love you all to bits. Thanks especially to my Mam, Doreen for her incredible patience and invincible good spirits. Mam I can't thank you enough for your unfailing love and support throughout my studies. Love you.

I can't forget family no.2! Thanks to all the Stynes clan, especially Ann and John.

To Derek, thank you for everything. You have had the patience of a saint and the resilience of Stonehenge! I never thought this day would come, but you did, and that constant reassurance got me through the darkest of days. I am forever grateful for your love and caring every step of the way. This thesis is yours as much as it is mine.

ABBREVIATIONS

%P	-	Percentage present
A	-	Absent
ATCC	-	American Tissue Culture Collection
ATP	-	Adenosine Triphosphate
BMP	-	Bone Morphogenic Protein
BSA	-	Bovine Serum Albumin
cAMP	-	Cyclic Adenosine Monophosphate
cDNA	-	Complementary DNA
CFE	-	Colony forming Efficiency
CRE	-	cAMP Responsive Elements
CREB	-	CRE Binding Protein
cRNA	-	Complementary RNA
DEPC	-	Diethyl Pyrocarbonate
DMEM	-	Dublecco's Minimum Essential Medium
DMSO	-	Dimethyl Sulfoxide
DNA	-	Deoxyribonucleic Acid
dNTP	-	Deoxynucleotide Triphosphate (N = A, C, T, G)
EDTA	-	Ethylene Diamine Tetraacetic Acid
EDTA	-	Ethylenediaminetetraacetic Acid
EGF	-	Epidermal Growth Factor
EGFR	-	Epidermal Growth Factor Receptor
EGR1	-	Early growth response 1
eIF	-	Eukaryotic Translation Initiation Factor
EMT	-	Epithelial Mesenchymal Transition
erbB2	-	v-erbB2-Erythroblastic Leukemia Viral Oncogene Homolog 2
FCS	-	Foetal Calf Serum
FGF	-	Fibroblast Growth Factor
GAPDH	-	Glyceraldehyde-6-Phosphate Dehydrogenase
GF(s)	-	Growth Factor (s)
HGF	-	Hepatocyte Growth Factor
HGFR	-	Hepatocyte Growth Factor Receptor

HOXB	-	Homeobox
IGF	-	Insulin Like Growth Factor
IGFR	-	Insulin Like Growth Factor Receptor
IRES	-	Internal Ribosomeal Entry Site
kDA	-	Kilo Daltons
MAPK	-	Mitogen Activated Protein Kinase
Min	-	Minutes
miRNA	-	microRNA
MLR	-	Multiple Linear Regression
MM	-	Mismatch
MMLV-RT	-	Moloney Murine Leukaemia Virus- Reverse Transcriptase
MMPs	-	Matrix Metalloproteases
mRNA	-	Messenger RNA
mTOR	-	Mammalian Target of Rapamycin
MYO	-	Myopalladin
NRG	-	Neuregulin
NSCLC	-	Non-Small Cell Lung Cancer
ODC	-	Ornithine Decarboxylase
%P	-	Percent present
P or M	-	Present or Marginal
PBS	-	Phosphate Buffered Saline
PDGFR	-	Platelet Deriver Growth Factor Receptor
PKA	-	Protein Kinase A
PKC	-	Protein Kinase C
PLIER	-	Probe Logarithmic Intensity ERror Estimation
PM	-	Perfect Match
PTEN	-	phosphatase and tensin homolog
QC	-	Quality Control
qPCR	-	Real-time PCR
R	-	Discrimination Score
RISC	-	RNA-Induced Silencing Complex
RNA	-	Ribonucleic Acid
RNase	-	Ribonuclease
RNasin	-	Ribonuclease Inhibitor

RPM	-	Revolutions Per Minute
RPS6KA3	-	Ribosomal Protein S6 kinase, 90kDa, polypeptide 3
RQ	-	Relative Quantity
RT-PCR	-	Reverse Transcription Polymerase Chain Reaction
SD	-	Standard Deviation
SF	-	Scatter Factor
siRNA	-	Small interfering RNA
TBE	-	Tris-Boric Acid EDTA Buffer
TBS	-	Tris Buffered Saline
TFPI	-	Tissue Factor Pathway Inhibitor
TGFβ1	-	Transforming Growth Factor β1
THBS1	-	Thrombospondin 1
TNFAIP8	-	Tumour necrosis Factor, Alpha-Induced Protein 8
Tris	-	Tris (hydroxymethyl) Aminomethane
TV	-	0.25% Trypsin/ 0.01% EDTA Solution in PBS
UHP	-	Ultra High Pure Water
UTR	-	Untranslated Region
UV	-	Ultraviolet
v/v	-	Volume/Volume
VEGF	-	Vascular Endothelial Growth Factor
VEGFR	-	Vascular Endothelial Growth Factor Receptor
w/v	-	Weight per Volume

Table of Contents

Abstract

Regulation of specific gene expression at the translation level mediated by eukaryotic initiation factor 4E (eIF4E) may play a pivotal role in both tumor formation and metastasis. Non-invasive MCF7 cells, and mildly-invasive DLKP cells were transfected with wild-type eIF4E, eIF4Emut (mutated at serine 209; serine has been replaced with alanine to prevent phosphorylation) and pcDNA (empty plasmid). Up-regulation of eIF4E protein was observed in eIF4E and eIF4E-mutant clones. Increased growth-rate was observed in MCF74E/4Emut and DLKP4E/4Emut compared to the pcDNA clone and parent cell lines. A marked increase in invasion was also observed in DLKP4E and 4Emut clones compared to parent and DLKPpcDNA, but not in the transfected MCF7 clones. MCF74E and MCF74Emut had a greater tendency to grow in suspension, and form colonies in soft agar than parental MCF7. To examine genes related to invasion in a breast cancer cell line, MCF7 cloneH3 (non-invasive) and MCF7H3erbB2 (invasive, erbB2 overexpressing) also were examined.

Whole genome expression microarray experiments and subsequent analysis resulted in gene lists comparing DLKP4E/4Emut to parental DLKP and related to invasion; another specific to MCF7H3erbB2 (compared to non-invasive MCF7, MCF7H3, MCF7pcDNA /4E/4Emut) and related to invasion. A combination of genes with and without previously reported connections to invasion were chosen from each list following application of pathway analysis/literature mining programs to the data. Targets based on analysis of DLKP4E/4Emut had no effect on the rate of invasion of either cell line when individually silenced using siRNA. However, siRNA silencing of EGR1, RPS6KA3, TFPI1 and TNFAIP8, all up-regulated in MCF7erbB2 compared to the parent, caused a decrease in invasion of both invasive DLKP4E and invasive SKBR3 (breast carcinoma) cell lines. THBS1, down-regulated in MCF7H3erbB2 compared to the parent, caused an increase in invasion of mildly-invasive DLKP parent, and non-invasive MCF7 when silenced by siRNA.

This study resulted in the identification of some of the genes involved in development of *in vitro* invasion, and extended the knowledge of known invasion-related genes. It also provided data on what alterations may occur in cancer cells at the mRNA level if eIF4E levels are altered.

Section 1.0

Introduction

1.1 Cancer invasion and metastasis

Cancer is a multistep process and occurs as a result of the loss of control of cell division, leading to the initial tumour formation, which can then be followed by a metastatic spread. A distinguishing feature of malignant cells is their ability to invade surrounding normal tissue, metastasize through the blood and lymphatic systems and re-establish at distant secondary locations. None of the functions of metastasizing cells are unique to cancer cells. An example of physiological invasion is smooth muscle cell migration from the tunica media (which contains smooth muscle fibres, elastic and collagenous tissue) to the intima (endothelial cell layer) of blood vessels. Angiogenesis, nerve growth cone extension and homing, embryogenesis and trophoblast implantation are also examples. During embryonic development, motile cells are tightly regulated in order to ensure proper homing and reversion to a non-motile phenotype after migration into a destined location (Hay, 1995). In contrast, cancer cells have lost the ability to recognise specific targets. Their inappropriate growth signals are accompanied by mechanisms to avoid apoptosis and the potential to elicit angiogenesis for independent nutrient supply. Invasion is not simply due to growth pressure but involves additional genetic deregulation over and above those molecular events that cause uncontrolled proliferation. The difference between the normal process and the pathogenic nature of cancer invasion is therefore one of regulation.

1.1.1 Cancer cell motility: epithelial to mesenchymal transition (EMT)

One of the most critical steps in metastasis is invasion, which involves the active translocation of neoplastic cells across tissue boundaries and through host cellular and extracellular barriers (Liang *et al.*, 2002). In order to translocate across tissue boundaries and through host extracellular matrix barriers, invasive cells must become motile. Tumour cell invasion is most frequently observed in epithelial tumours (carcinomas). The initial phase of tumour cell evasion from well-structured assemblies requires a phenotypic conversion which is referred to as epithelial to mesenchymal transition (EMT) (Gotzmann *et al.* 2004). EMT is an important process during development by which epithelial cells acquire mesenchymal, fibroblast-like properties and show reduced intercellular adhesion and increased motility. EMT is a feature of normal development; gastrulation, neural crest formation, and heart morphogenesis, all of which rely on the transition between epithelium and mesenchyme (Larue

and Bellacosa, 2005). Invasion and metastasis are both critically dependent on the acquisition by the early cancer cell of EMT features (Kang and Massague, 2004; Thiery and Morgan, 2004). This form of movement is characterised by an elongated cell morphology with established cell polarity and is dependent on proteolysis to degrade the extracellular matrix (Sahai, 2005).

Table 1.1 Differences between epithelial and mesenchymal cells

Epithelial cells	Multicellular mesenchymal cells
cohesive interactions among cells, facilitating the formation of continuous cell layers existence of three membrane domains: apical, lateral and basal presence of tight junctions between apical and lateral domains apicobasal polarized distribution of the various organelles and cytoskeleton components	loose or no interactions among cells, so that no continuous cell layer is formed no clear apical and lateral membranes no apicobasal polarized distribution of organelles and cytoskeleton components
lack of mobility of individual epithelial cells with respect to their local environment.	motile cells that may even have invasive properties. During development, certain cells can switch from an epithelial to a mesenchymal status by means of a tightly regulated process defined as the EMT, which is associated with a number of cellular and molecular events. In some cases, EMT is reversible and cells undergo the reciprocal mesenchymal to epithelial transition (MET).

Adapted from (Larue and Bellacosa, 2005)

Several signaling pathways have been found important in EMT, these include tyrosine kinase signaling, the Ras pathway, integrin-linked kinase (ILK) and integrin signaling, Wnt/β-catenin, Notch, Rac1b and reactive oxygen species (ROS), and the phosphatidylinositol 3' kinase (PI3K)/AKT pathway (Figure 1.1) (Larue and Bellacosa, 2005). Activation of the PI3K/AKT signaling cascade is a central feature of EMT. AKT is frequently upregulated and activated in ovarian, breast and pancreatic tumors. AKT is involved in many basic cellular processes, including cell cycle progression, cell proliferation, cell survival, metabolism and EMT (Grille *et al.*, 2003). The EMT

induced by activated AKT involves: loss of cell–cell adhesion, morphological changes, loss of apico-basolateral cell polarization, induction of cell motility, decrease in cell–matrix adhesion, and changes in the production or distribution of specific proteins.

Figure 1.1: Signalling pathways involved in EMT

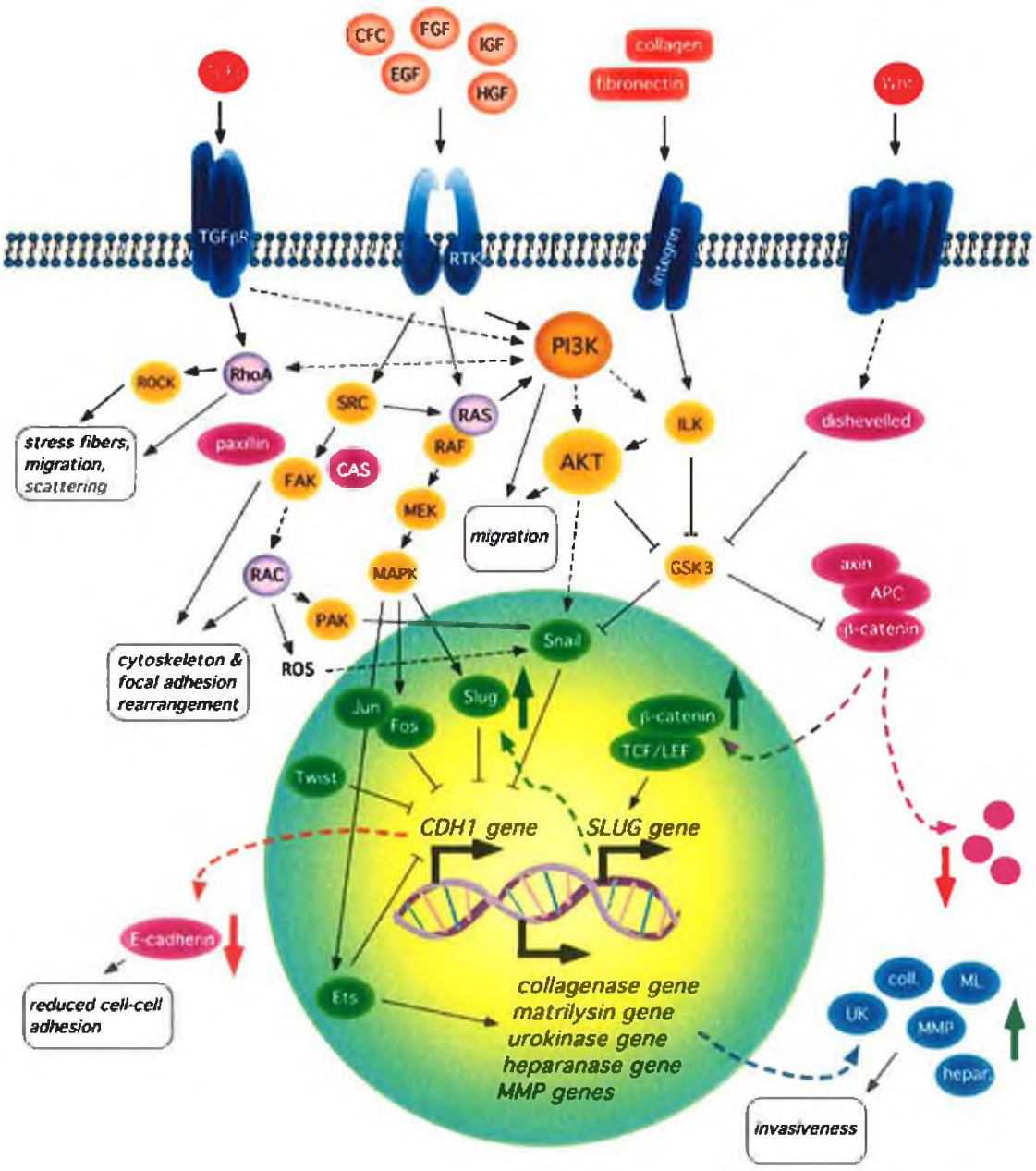

Figure 1.1: Schematic of the signal transduction pathways associated with epithelial–mesenchymal transition. End points of EMT are boxed. RTK: receptor tyrosine kinase; ROS: reactive oxygen species (Larue and Bellacosa, 2005).

1.1.2 Metastasis

The metastatic spread of solid tumours is responsible directly or indirectly for most cancer-related deaths. Metastasis is defined as the escape of tumour cells from their primary site and their re-establishment at distant secondary locations. It occurs as a result of a complex series of interactions between the cancer cell and its surroundings, all of which must be successfully completed to give rise to a metastatic tumour. Following the initial transforming event, neoplastic cells proliferate to form the primary tumour mass, from which cells can detach. There is increasing evidence that in epithelial malignancies, loss or down-regulation of expression of the structures responsible for the maintenance of tissue integrity correlates with an increasing tendency for metastatic spread. Such de-adhesion acts as a prelude to the cells invading the extracellular matrix (Ahmad *et al.*, 1997).

It is important to note that metastasis can occur long after the apparent elimination of the primary tumour. With regard to breast cancer, metastases have been known to occur decades after the primary treatment (Karrison *et al.*, 1999). Investigation of this phenomenon has resulted in a model of discontinuous growth and quiescence (Demicheli, 2001). The current model for metastatic growth indicates that cancer cells can exist in three separate states in a secondary site: solitary cells in quiescence; active pre-angiogenic micrometastases in which proliferation is balanced with apoptosis and no net increase in tumour size occurs; and vascularised metastases, either small and clinically undetectable, or large and detectable by current technology. It is thought that cells in all three states can exist in the same organ at the same time (Chambers *et al.*, 2002).

A recent review by Pantel and Brakenhoff (2004) suggests metastatic spread might follow two models; both complementary but following different specific routes. The first model is dependent on lymph node metastasis. It involves the dissemination of cancer cells during the early stages of tumour growth from the primary tumour to the lymphatic or vascular system. In this model, cancer cells that have been disseminated through the blood either die or remain dormant, whereas solid metastases form in the lymph nodes. Further metastases then occur from the lymph nodes to distant sites, and it is possible that this ability was gained during the selection of these cells in the lymph-node environment. The second model involves the development of solid metastases at distant sites as a result of dissemination through the blood. In this model cells do not passage through the lymphatic system (Pantel and Brakenhoff, 2004).

1.1.3 The metastatic cascade

For successful metastasis, cells must penetrate the vessels (intravasation), travel through the blood stream or lymph system and then exit the vessels at the new site (extravasation), and proliferate. This series of steps are referred to as the metastatic cascade; depicted in Figure 1.2 and outlined in Table 1.1.

Table 1.2 The Metastatic Cascade

Initial transforming event
↓
Growth of neoplastic cells
↓
Neovascularisation/angiogenesis of the tumour
↓
Detachment of neoplastic cells from primary tumour
↓
Local invasion of extracellular matrix by tumour cells
↓
Intravasation of tumour cells into lymphatics or vasculature
↓
Survival of tumour cells in circulation and avoidance of immunological attack
↓
Extravasation of tumour cells from vasculature into secondary organ tissue
↓
Survival and proliferation within organ parenchyma

1.1.3.1 Local invasion

This refers to the penetration of the host tissue surrounding the neoplasm. Invasion is the active process of translocation of neoplastic cells across extracellular matrix barriers. It requires local proteolysis of the extracellular matrix, pseudopodial extension, and cell migration (Liotta, 1986). This usually takes place in the extracellular space, but some carcinomas are thought to be capable of intracellular invasion through the cytoplasm of striated muscle fibres, an example of emperipolesis. The extent of local invasion is thought to be mainly a result of growth, motility and tissue destruction, but differentiation may also play a role.

1.1.3.2 Detachment from primary site

Only rarely can normal cells achieve growth away from their primary site. Apart from pregnancy the only common example is endometriosis (condition in which the mucous membrane (endometrium) that normally lines only the womb is present and functioning in the ovaries or elsewhere in the body). One of the first steps involves the breaking of cell-cell recognition. Breaking of homotypic recognition (same-cell type recognition) and changes in heterotypic recognition (eg. tumour – stroma recognition) are characteristic of invasive and metastatic cancers (Mareel *et al.*, 1992; Elenbaas and Weinberg 2001). A reduction in the expression of proteins such as E-cadherin is often seen in epithelial cancers and results in the ability of cancer cell to break apart. E-cadherin expression is lost early on in breast carcinogenesis. Cell-ECM interactions are also altered in cancer cells. This involves changes in the patterns of integrin expression. Integrins provide a major mechanism whereby cells recognise proteins of the extracellular matrix and basement membrane. Ligands of the integrins include collagen type I, collagen type IV, laminin and fibronectin. In general integrins involved in tissue organisation are decreased while those involved in migration are not. Some examples of changes in integrin expression include the upregulation of $\alpha_v\beta_3$ in melanoma cells, which has abroad range specificity. This means that cells expressing this integrin can migrate over a broad range of matrices. In contrast $\alpha_2\beta_1$ which recognises laminin and collagen is decreased in colon and breast cancers. Integrins $\alpha_3\beta_1$ and $\alpha_6\beta_1$ (laminin receptors) are frequently upregulated in breast and endometrial cancers. An increase in the secretion of proteases also facilitates detachment of cells from the primary through the degradation of the ECM (McGary *et al.*, 2002).

1.1.3.3 Intravasation

As the primary tumour grows it need to develop a blood supply that can support its metabolic needs. This process is known as angiogenesis. Intravasation is the process by which the cells can escape the primary site via the new blood vessels, and enter into the body's circulatory system. Cancer cells attach to the stromal face of the blood vessel basement membrane, digest the membrane with proteases and migrate between the endothelial cells into the bloodstream (Wyckoff *et al.*, 2000).

1.1.3.4 Transport

Cancer cells commonly use three routes of transport. Firstly, body cavities such as the peritoneum facilitate the spread of cancers such as ovary or colon. Cancers invading out from the primary site detach from the surface and then are transported by the peritoneal fluid to other sites. A similar process occurs in the lungs, whereby lung cancers or other cancers invading can colonise the space between the pleural membranes surrounding the lungs. This generates a cancer-containing, growth-supporting fluid, which must be removed to maintain lung function. Secondly, blood vessels such as capillaries which consist of a layer of endothelial cells plus an external basement membrane of glycoproteins. They provide the least difficult barrier to entry and exit of cancer cells. Arteries provide a much more difficult barrier in the form of a smooth muscle layer, and therefore are rarely ever invaded. Thirdly, lymphatic vessels provide even less of a barrier than capillaries as they are not surrounded by a basement membrane. They drain into the subclavian veins and thence into the superior vena cava, hence reaching the blood stream (Evans, 1991).

Once the tumour cells have gained access to the blood system they may be swept away to a distant site which they can colonise. Within the bloodstream the tumour cells may interact with host components such as lymphocytes, monocytes and platelets, through heterotypic adhesion. Transport through blood is very hostile for cancer cells and so for protection against mechanical stress and immune attack they often form aggregates.

1.1.3.5 Lodgement at a distant site

The next step in the metastatic process involves the attachment of the cancer cell to the endothelial lining. Tumour cell attachment to the endothelial cell lining of the circulatory system is of utmost importance in the process of cancer spread. Most tumour cells appear to be arrested in the first capillary bed they encounter, but this does not guarantee growth of a secondary tumour. Tumour cells are seen to lodge in capillaries, arterioles, and occasionally venules, but rarely in arteries (shear may be too high). It is thought that the walls of arterioles may present effective barriers to extravasation, perhaps explaining the low degree of metastasis to tissue such as the skeletal muscle. During the process of lodgement within a blood vessel it is thought that the tumour cell interacts with either the basement membrane or the endothelium. It is thought that there are four possible outcomes from these interactions. Firstly, the cells lodge and go on to form metastasis. This lodgement can occur either by mechanical means, where the cell

literally gets "stuck" as it gets jammed in a vessel whose diameter is less than the cell or clump or cells, by specific adhesion in which the tumour cell "recognises" the wall of the blood vessel, due to the molecular content of the surfaces involved, or lastly by selective adhesion. The second outcome is where cells lodge and become dormant. The cells then exist in a dormant state to become active at a later date. The third outcome is the cells lodge but do not survive and the fourth outcome involves the cells failing to lodge and thus pass through the first organ they meet. Cancer cells deposit based on circulation mechanics and chemokines in target tissue (Hiscox and Jiang, 1997).

1.1.3.6 Extravasation

Extravasation of tumor cells is a prerequisite step during hematogenous metastasis. It is thought to occur due to the retraction of endothelial cells, exposing the glycoproteins of the basement membrane. The tumour cell then attaches to the basement membrane and digests it with proteases and glycosidases, allowing the tumour cell to pass through. Different tumours express different integrins, which recognise different glycoproteins. Thus it follows that the basement membrane composition plays a large role in determining whether tumours are successful at extravasation. Extravasation may occur in a number of ways; the cells may divide and pile up within the lumen of the blood vessel and invade en masse by the destruction of the blood vessel; single cells may migrate between endothelial cells either destructively or non-destructively; single cells may leave by passing through the endothelial cells rather than between them (Heyder *et al.*, 2006).

1.1.3.7 Growth

Proliferation of the cancer cells at their new site is initially confined to within 1mm of the vessel, until the tumour can form new blood vessels (angiogenesis) to supply essential nutrients and oxygen. Tumour growth is dependant on a number of factors including the nature of the environment it finds itself in and the nature of the tumour itself. These factors include resistance to host defence mechanisms of humoral and cellular nature, and response to or requirement for specific growth factors (Evans, 1991).

1.1.3.8 Angiogenesis

Angiogenesis is the growth of blood vessels, and is essential for organ growth and repair. Solid tumours smaller than 1 to 2 cubic millimeters are not vascularised, and in order to spread they need to be supplied by blood vessels that bring oxygen and nutrients and remove metabolic wastes. Beyond the critical volume of 2 cubic millimetres, oxygen and nutrients have difficulty diffusing to the cells in the centre of the tumour, causing a state of cellular hypoxia that marks the onset of tumoral angiogenesis.

Angiogenesis and the development of metastases are intrinsically connected. Growth of metastases are influenced by inhibitors of angiogenesis which keep metastasis in a non-proliferating quiescent (dormant) state. This dormant state is characterized by normal proliferation, increased apoptosis, and insufficient neovascularization. Several endogenous inhibitors of angiogenesis have been identified so far and some of them have already been successfully applied in experimental therapeutic trials (Kirsch *et al.*, 2004).

Figure 1.2 Diagrammatic representation of the metastatic cascade

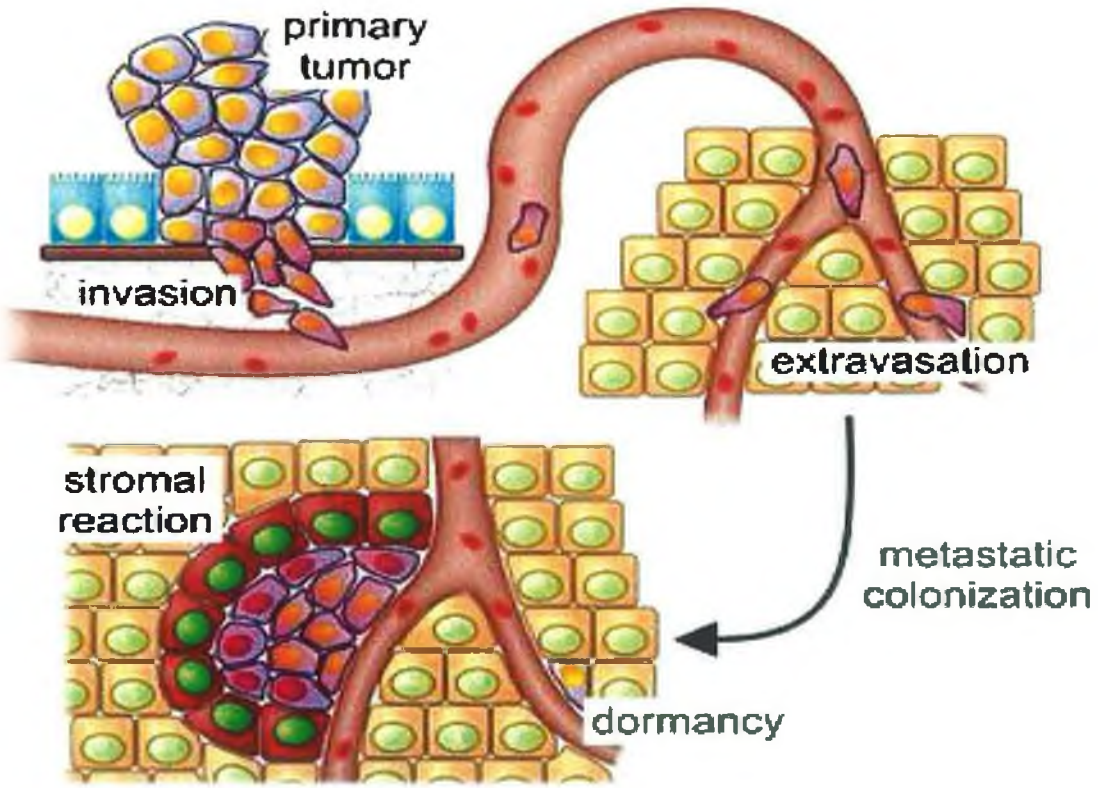

1.1.4 Inefficiency of metastasis

While successful metastasis will facilitate the generation of secondary tumours from primary cancers, few cells have the potential to become motile, and of those that do, less than 0.1% is detected in the bloodstream, the rest having been destroyed by a combination of mechanical stresses, proteolytic degradation and surveillance by the immune system (Weiss, 1990). A combination of in vivo video microscopy and quantitative cell-fate analysis has been used to monitor cell-fate over time. A combination of several such studies has led to the conclusion that the process of shedding of cancer cells into the bloodstream, and subsequent extravasation into a secondary organ is completed efficiently. However, only a small subset of cancer cells initiate growth in a secondary site, and of these only a small portion become vascularised, and an even smaller portion develop to the stage of further metastasis (Chambers *et al.*, 2002).

1.1.5 Molecular regulation of metastatic growth

Gene expression profiles of cancer cells vary greatly with organ microenvironment, and this in turn influences their behaviour and proliferation potential. For example, experimental evidence has shown that the same cancer cells grown in two different sites, expressed very different levels of proteolytic enzymes (Nakajima *et al.*, 1990). This is also seen in the different responses of different organs to chemotherapy (Fidler *et al,* 1994). Growth factor-receptor interactions, which are used extensively for intercellular communications, can initiate signalling pathways that lead to diverse cellular functions. Individual growth factors tend to occur as members of larger families of structurally and evolutionarily related proteins. There are several growth factor families including TGF-beta (transforming growth factor), BMP (bone morphogenic protein), neurotrophins (NGF, BDNF, and NT3) and fibroblast growth factor (FGF).
Different combinations of such interactions lead to different metastasis relevant functions in different organs. These include actin polymerisation, formation of pseudopodia and invasion. The ability of cancer cells to grow in a specific site therefore depends on features that are inherent to the cancer cell, features inherent to the organ, and the active interplay between the two.

1.2 erb-b2 erythroblastic leukemia viral oncogene homolog 2 (erbB2)

1.2.1 Growth factor families and their receptors

Communication between individual cells in multicellular organisms is essential for their regulation and co-ordination of complex cellular processes such as growth, differentiation, migration and apoptosis. The signal transduction pathways mediating these processes are regulated in part by polypeptide growth factors that generate signals by activating cell surface receptors. The primary mediators of such physiological cell responses are receptor tyrosine kinases (RTKs). That is, in most cells, growth factors mediate cellular activity by means of receptors with intrinsic tyrosine kinase activity.

It is widely accepted that cancer cells contain genetic damage that leads to tumourigenesis through deregulation of key signalling pathways. Activation of growth factor receptors and their intrinsic tyrosine kinase activity initiates signalling cascade that involves multiple intracellular signalling pathways, such as the phosphatidylinositol 3-kinase (PI3K) and MAPK pathways, which are responsible for the diverse target actions of these growth factors, which include increased cell division, cell size, protein synthesis, cell migration, and inhibition of apoptosis. While many of the signalling elements that are downstream from tyrosine kinase activation have been characterized, several of the molecular events that occur before or concomitantly with kinase activation and whether these early events can influence the ultimate outcome of growth factor-stimulated signal transduction have not been determined. Malignant cells arise as a result of a stepwise progression of genetic events that include the unregulated expression of growth factors or components of their signalling pathways (Fang and Richardson, 2005; Toker and Yoeli-Lerner, 2006). In this way growth factors and their receptors have been shown to play a major role in cancer development.

RTKs can be divided into 20 subfamilies on the basis of their structural characteristics. All RTKs consist of a single transmembrane domain that separates the intracellular tyrosine kinase domain from the extracellular binding domain. The latter exhibit a variety of conserved elements such as immunoglobulin (Ig)-like or epidermal growth factor (EGF)-like domains, fibronectin type III repeats or cysteine-rich regions that are characteristic for each subfamily. The catalytic domain that displays the highest level of conservation includes the ATP-binding site that catalyses receptor autophosphorylation and tyrosine phosphorylation of RTK substrates. Ligand binding to the extracellular

domain leads to conformational changes that induce and stabilise receptor dimerisation leading to increased kinase activity and autophosphorylation of tyrosine residues (Perona, 2006).

RTK families involved in cancer development include the epidermal growth factor receptor (EGFR/ErbB) family (Section 1.2.2), insulin growth factor receptor (IGFR) family, vascular endothelial growth factor receptor (VEGFR) family, fibroblast growth factor receptor (FGFR) family, hepatocyte growth factor receptor (HGFR) family and platelet-derived growth factor receptor (PDGFR) family.

The IGFR family consists of the insulin receptor (IR) and the insulin-like growth factor (IGF) receptor (IGF-IR). Both receptors consist of two extracellular subunits, which are responsible for ligand binding and two membrane spanning subunits bearing the tyrosine kinase domain and autophosphorylation sites (Ullrich *et al.,* 1986). Ligands for these receptors include insulin, IGF-I and IGF-II. While insulin is mostly a metabolic hormone, IGF-I and IGF-II are crucial for normal development and carcinogenesis. IGF-IR and its ligands have been found to play a major role in breast and prostate cancer (Stephen *et al.*, 2001; Cardillo *et al.*, 2003). In primary breast cancer, IGF-I and IGF-II are primarily expressed by the stromal fibroblasts surrounding the normal and malignant tissue, whereas IGF-IR is overexpressed in breast cancer with enhanced tyrosine kinase activity (Stephen *et al.*, 2001).

VEGF is one of the main inducers of endothelial cell proliferation and permeability of blood vessels. The VEGFR family consists of two receptors VEGFR-1 and VEGFR-2, which are expressed on endothelial cells during embryonic development and are the key regulators of angiogenesis. VEGF is a multifunctional cytokine which potently stimulates angiogenesis in vivo. VEGF expression is elevated in pathological conditions including cancer, proliferative retinopathy, psoriasis and rheumatoid arthritis. Expansion of tumours beyond 1-2mm requires *de novo* formation of vascular network to provide the tumour with oxygen and nutrients. The angiogenesis associated with human tumours is likely a central component in promoting tumour growth and metastatic potential. The regulation of VEGF expression during tumour progression may involve diverse mechanisms including activated oncogenes, mutant or deleted tumour suppressor genes, cytokine activation, hormonal modulators, and a particularly effective activator, hypoxia (Arii *et al.*, 1998).

The human FGF family is composed of 22 members organized into 6 groups based on phylogenetic relationships, and is the largest family of growth factors. Signalling is

mediated through membrane-spanning tyrosine kinase receptors encoded by four independent genes, some of which generate multiple products via alternative splicing or transcription initiation. Unlike other growth factors, FGFs act in concert with heparin or heparin sulphate proteoglycan (HSPG) to activate FGFRs and to induce the pleiotropic responses that lead to the variety of cellular responses induced by this large family of growth factors (Lin *et al.*, 1999). High-affinity interaction between an FGF and its cognate receptor induces receptor dimerization and activation. Two classes of FGFRs have been discovered. The first class comprises the four high affinity FGFRs, whereas the second class is defined by low affinity FGF binding sites. Evidence suggests that the low affinity FGF binding sites represent heparin sulphate proteoglycan molecules (HSPG) located on the cell surface, which may support the fine tuning of cell responses to FGFs. Many FGFs display high-affinity interactions with multiple FGFRs, while some activate unique receptors or receptor isoforms. Deregulated FGFR signalling has been observed in breast, prostate, melanoma, thyroid and salivary gland tumours, bladder cancer and in multiple myeloma (Ezzat and Asa, 2005).

HGFR is encoded by the proto-oncogene met, and plays multiple roles in cancer, by acting as a motility and invasion stimulating factor, promoting metastasis and tumour growth. Furthermore, it acts as a powerful angiogenic factor (Jiang *et al.*, 2005). It is a disulphide-linked heterodimer with glycosylated extracellular chains, which consists of the transmembrane domain and cytoplasmic tyrosine kinase domain. The ligands for HGFR are HGF and scattering factor (SF), which are expressed by mesenchymal-derived cells. Probably the most important biological effect of HGF on cancer cells is its ability to induce motility. Most cancer and normal cells respond to HGF, and stimulation of cancer cells with HGF will result in increased migration over a number of matrices. The motility signals mediated by the HGF receptor, cMET, are multifold and effect downstream key signalling pathways that contribute to the migratory events in cancer cells (Birchmeier *et al.*, 2003).

1.2.2 ErbB Receptor Family of Tyrosine Kinase Receptors

The ErbB receptor family consists of type I growth factor receptors, and is made up of four members, erbB-1 (EGFR), erbB-2 (HER-2/neu), erbB-3 (HER-3) and erbB-4 (HER-4). All ErbBs share an overall structure of two cysteine-rich regions in their extracellular ligand-binding domain, and a single membrane-spanning kinase domain flanked by a cytoplasmic carboxy-terminal tail with tyrosine autophosphorylation sites

(Graus-Porta *et al.*, 1997). With few exceptions (for example, haematopoietic cells), ErbB proteins are expressed in cells of mesodermal and ectodermal origins.

The receptors share 40-50% sequence identity in their extracellular domains, 60-80% identity in their kinase domains and 10-30% identity in their tails. Although the extracellular domain of erbB-3 is homologous to those of the other family members its intracellular domain has diverged significantly (Carraway III and Burden, 1995).

1.2.3 erbB2

erbB-2 has been mapped to chromosome 17q21. No ligand for erbB-2 has been found. Overexpression due to gene amplification has been found in 10-40% of breast cancers, although some carcinomas overexpress erbB-2 in the absence of gene amplification (Suo *et al.*, 1998). Transcription of the erbB-2 gene generates two mRNAs, a 4.6 kb transcript encoding the full length 185 kDa transmembrane protein and a truncated 2.3 kb transcript encoding only the extracellular domain of the erbB-2 protein. The erbB2 gene plays an important role in human malignancies. It is amplified and/or overexpressed in approximately 30% of human breast carcinomas (Slamon *et al.*, 1987, Slamon *et al.*, 1989) and in many other types of human malignancies (Yu and Hung, 2000). Studies of individuals with ErbB2-overexpressing tumours have shown that they have a significantly poor clinical outcome compared to patients whose tumours did not overexpress ErbB2 (Slamon *et al.*, 1987, Slamon *et al.*, 1989). High levels of erbB-2 expression have been shown to correlate strongly with poor prognosis in breast cancer (Carey *et al.*, 2006) and endometrial cancer (Morrison *et al.*, 2006). Another study showed that a subset of pancreatic ductal adenocarcinomas is characterized by erbB2 gene amplification, but in contrast to breast cancer, protein overexpression does not predict this specific gene deregulation mechanism (Tsiambas *et al.*, 2006). Oncogenic activation of erbB-2 can occur by deletion of the extracellular domain or by overexpression as previously mentioned. In rats, but not humans, overexpression can occur through a point mutation in the transmembrane domain (Guy *et al.*, 1992). Two of the major signalling pathways, Ras/Raf/MEK/ERK and PI3K/Akt are triggered by the erbB2/erbB3 heterodimer (Yarden and Sliwkowski, 2001). Such erbB-2 receptor activation leads to activation of early response genes such as c-myc and Elk, both of which have been associated with tumourogenesis. ErbB2 activation also leads to increased intracellular calcium and increased plasma membrane potential, rapidly

inducing c-Fos and c-Jun (both oncogenes (Jariel-Encontre *et al.*, 1997)), leading to a mitogenic response (Suo *et al.*, 1998).

erbB-2 has intrinsic tyrosine kinase activity. As mentioned earlier, no ligands have been found capable of binding directly to erbB-2. However it can be activated by all the ebb ligands through heterodimerisation with other ErbB receptors (Hung and Lau, 1999).

1.2.4 ErbB Receptor Ligands

Under normal physiological conditions, activation of the ErbB receptors is controlled by spatial and temporal expression of their ligands, members of the EGF-related peptide growth factor family (Riese and Stern, 1998). There are a number of ErbB-specific ligands, each of which contains an EGF-like domain that confers binding specificity, allowing them to be divided into three groups. The first group includes EGF, amphiregulin (AR), and transforming growth factor-α (TGF-α), which bind specifically to ErbB1; the second group betacellulin (BTC), heparin-binding EGF (HB-EGF), and epiregulin (EPR), which exhibit dual specificity in that they bind ErbB1 and ErbB4. The third group is composed of the neuregulins (NRG) and forms two subgroups based upon their capacity to bind ErbB3 and ErbB4 (NRG-1 and NRG-2) or only ErbB4 (NRG-3 and NRG-4). Despite the abundance of ligands identified for these three ErbB receptors, no direct ligand for ErbB2 has been discovered (Figure 1.3). Common to all these growth factors is the EGF domain with six conserved cysteine residues characteristically spaced to form three intramolecular disulphide bridges (Prenzel *et al.*, 2001).

After binding to their receptors, EGF-related peptides induce receptor homodimerisation and heterodimerisation leading to activation of the intrinsic kinase domain and subsequent phosphorylation on specific tyrosine residues within the cytoplasmic tail. These phosphorylated residues serve as docking sites for a variety of signalling molecules, whose recruitment leads to the activation of intracellular pathways, including MAPK and PI-3K (Figure 1.4). Different signalling pathways are induced depending on the combination of ligand and homo- hetero-dimer (Yarden and Sliwkowski, 2001).

Figure 1.3 Binding specificities of the epidermal growth factor ligands

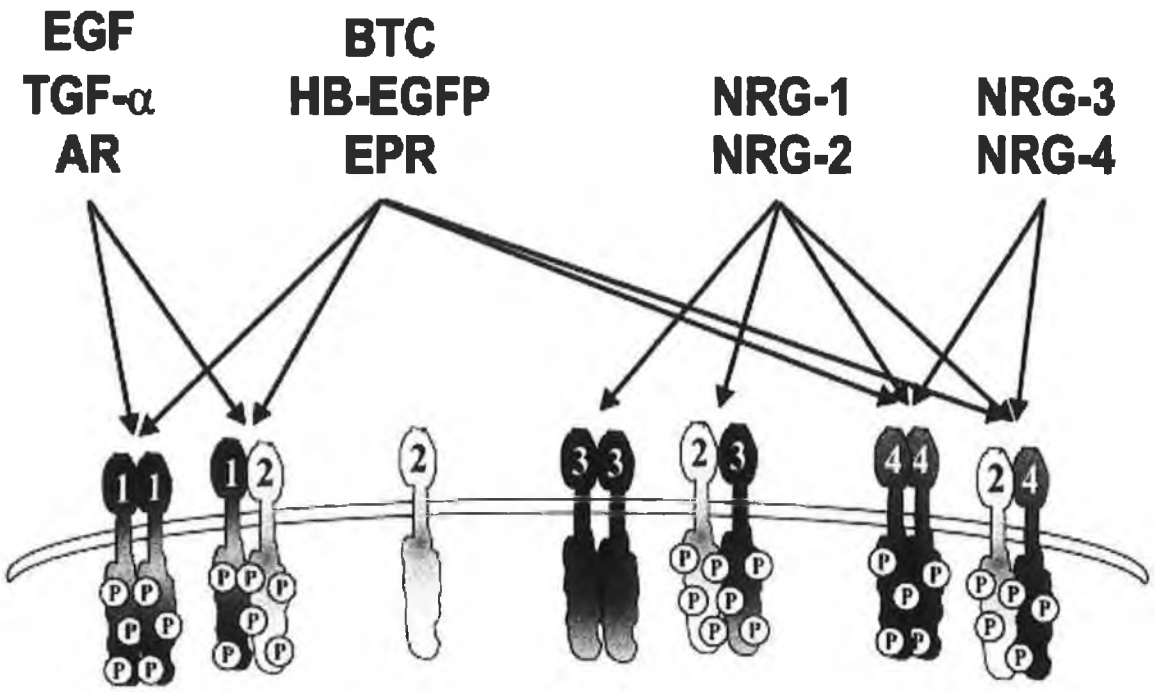

Figure 1.3: The ligands can be divided into categories depending upon binding specificity toward the ErbB receptors. ErbB2 has no direct ligand and needs a heterodimerisation partner to acquire signalling potential (indicated by phosphoresidues). ErbB3 homodimers do not signal, since the receptor has impaired kinase activity. (Holbro *et al.*, 2003)

Although none of these ligands bind directly to erbB-2, they all induce its tyrosine phosphorylation by triggering heterodimerisation and cross-phosphorylation. Earlier work demonstrated ErbB3 was devoid of intrinsic kinase activity, whereas ErbB2 seemed to have no direct ligand (Guy *et al.*, 1994; Klapper *et al.*, 1999). Therefore, in isolation neither ErbB2 nor ErbB3 can support linear signalling. Recent publications describing the structure of the extracellular domains of ErbB1 and ErbB3 suggest that the inability of ErbB2 to bind EGF-related peptides might result from differences in the regions contacting the ligands (Ogiso *et al.*, 2002; Cho *et al.*, 2002).

Figure 1.4 Signalling combinations inducible by the ErbB receptor family members.

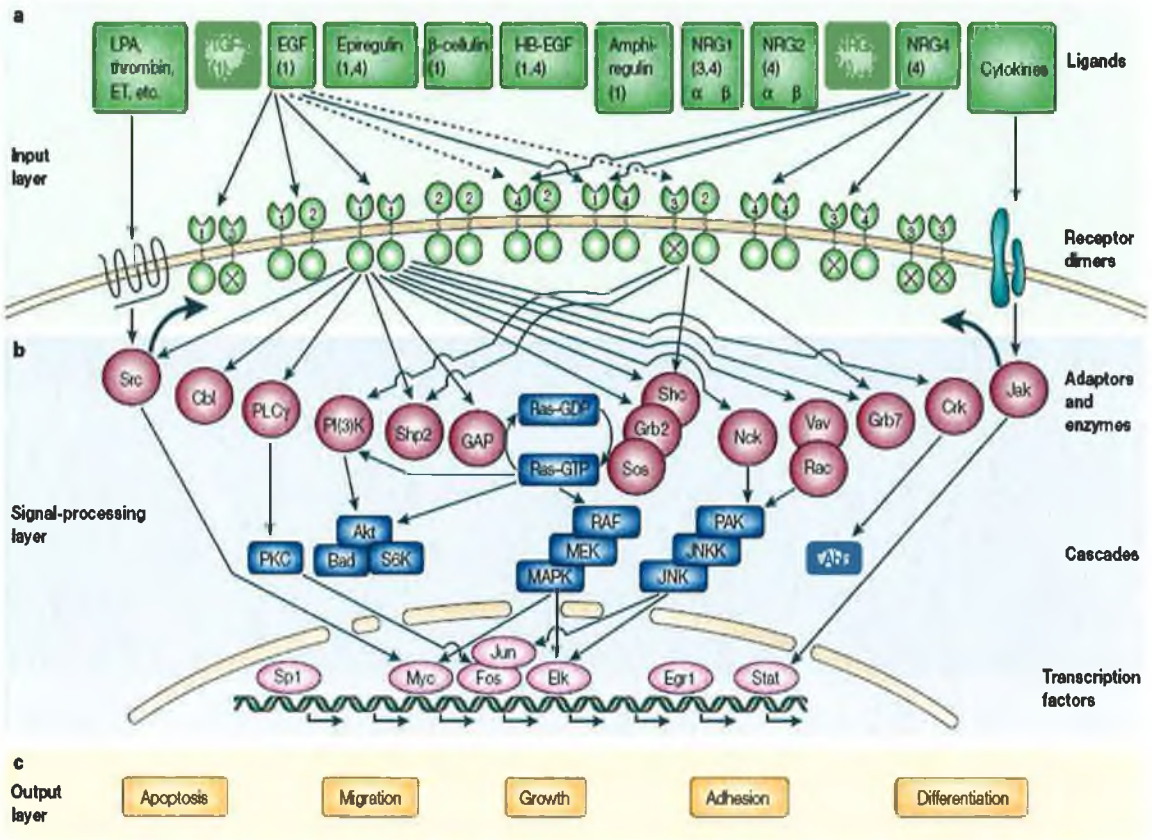

Figure 1.4: ligand binding to a monomeric receptor tyrosine kinase activates the cytoplasmic catalytic function by promoting receptor dimerization and self-phosphorylation on tyrosine residues. The latter serve as docking sites for various ADAPTOR PROTEINS or enzymes, which simultaneously initiate many signalling cascades to produce a physiological outcome (Yarden and Sliwkowski, 2001)

ErbB2, however, has a central role in the family. ErbB receptors have been shown to compete for dimerisation with erbB-2, which is the preferred dimerization partner for the other ErbBs (Graus-Porta *et al.*, 1997). ErbB3 in particular only becomes phosphorylated and functions as a signalling entity when dimerized with another ErbB receptor (Kim *et al.*, 1998). ErbB-2 has been shown to enhance EGF-induced tyrosine phosphorylation of erbB-1 and NRG-induced tyrosine phosphorylation of erbB-3 and erbB-4. This is evident from NRG activation of erbB-3 and erbB-4 heterodimerisation with EGFR, which only occurs when there is no available erbB-2. It also potentiates and prolongs the signal transduction pathways elicited by EGF and NRG. erbB-2 also increases the affinity of both EGF and NRG for their receptors and enhances erbB-3 phosphorylation and association with p85, a subunit of phosphatidylinositol-3-kinase.

These results suggest that erbB-2 acts as a common receptor sub-unit for all the other ErbB receptors (Graus-Porta *et al.*, 1997). Many cancers of epithelial origin have an amplification of the ErbB2 gene, which pushes the equilibrium towards ErbB2 homodimer and heterodimer formation (Yarden and Sliwkowski, 2001).

Figure 1.5 erbB2 receptor dimerisation

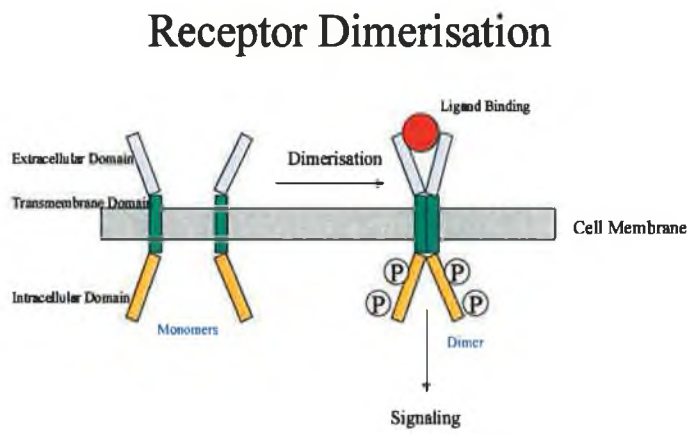

Figure 1.5 diagrammatic representation of the variety of signals activated by the ErbB receptors depending on their dimerisation partners and the ligand occupying their extracellular domains.

After ligand/receptor binding, the next step involves binding of adaptor and enzymes phosphotyrosine proteins to the tail of each ErbB molecule (after dimeric complex formation). Different phosphotyrosine proteins bind depending on the combination of ligand and homo- hetero-dimer (Olayioye *et al.,* 1998). The Ras- and Shc-activated mitogen-activated protein kinase (MAPK) pathway is a target of all ErbB ligands, and p70S6K/p85S6K pathways are downstream of most active ErbB dimmers (Yarden and Sliwkowski, 2001). ErbB ligands also activate the PI3K-activated AKT pathway, with PI3K binding directly with ErbB3 and ErbB4, but indirectly with ErbB1 and ErbB2 (Soltoff and Cantley, 1996). These signalling cascades influence functional effect by regulating of specific transcription factors. These include the proto-oncogenes fos, jun and myc, immediate early response genes including Sp1, Egr1 and Ets family members (Yarden and Sliwkowski, 2001). Therefore erbB2 activation translates in the nucleus into distinct transcriptional programmes.

A number of phenotypic effects result from overexpression of the erbBs. At the nuclear level, the Ras-Raf-MEK-ERK pathway leads to upregulation of the cell cycle protein

cyclin D1, permitting cycle progression from the G1 checkpoint to S-phase and consequently DNA synthesis and mitosis (Shaw and Cantley, 2006). When this pathway is deregulated by up-regulation of the erbBs, it leads to increased proliferation. ErbB overexpression also contributes to cell survival by inhibiting apoptosis. One of the main mechanisms by which tumour cells evade apoptosis is via activation of the PI3K pathway. ErbB family members can lead to activation of PI3-kinase both directly and indirectly through Ras (Yarden and Sliwkowski, 2001), endowing the cell with increased mitosis, cell survival, and influence over the regulation of actin functions and motility.

The ability of cancer cells to invade into surrounding tissue is probably the key property that distinguishes them from normal cells. ErbB receptors can induce many of the phenotypic traits associated with invasion. A recent study looking at squamous cell carcinoma of the head and neck, showed the effects of erbB family overexpression included loss of E-cadherin, acquisition of a motile phenotype and upregulation of a variety of proteolytic enzymes, as demonstrated by Rogers *et al.*, (2005).

1.2.5 The Role of erbB-2 in Human Cancers

Yu and Hung, (2000) examined the expression of erbb2 in 14 different cell lines including, lung, vulvar, ovary and colon. This study found significant correlation of erbB2 expression in tumour cells of epithelial origin. A more advanced study, using a panel of >100 patient-derived nude mouse tumour xenografts of different histological origin, was carried out to investigate the correlation between erbB2 gene amplification, mRNA and protein expression. Based on gene chip expression data, cervical, gastric and adenocarcinomas of the lung emerged as new potential indications for erbB2-directed cancer therapies (Kuesters *et al.,* 2006).

Expression was analyzed in 81 human squamous cell carcinomas of the lung and correlated with clinical parameters of the patients (patient survival, presence of metastases and tumour stage) and with biological characteristics of the tumours (Volm *et al.*, 1992). Pfeiffer *et al.* (1996) examined 186 unselected and systemically untreated patients with non-small cell lung cancer (NSCLC) for erbB-2 and erbB-1 status. ErbB-1 was found to be highly expressed in 55% of tumours while erbB-2 was highly expressed in 26% of tumours. The expression of erbB-1 was higher in squamous cell carcinoma, while erbB-2 was highest in adenocarcinomas. Overexpression of these receptors was found to have no correlation with prognosis. In contrast, Tsai *et al.* (1996) reported that

the intrinsic chemosensitivity of NSCLC cells correlated well with the expression of erbB-2, and transfection of erbB2 cDNA into low erbB2 expressing NSCLC significantly enhanced chemoresistance to adriamycin, cisplatin, mitomycin C and VP-16 (Tsai *et al*, 1996). Kristiansen *et a*l. (2001) also found overexpression of erbB2 was also found to correlate with disease-stage and chromosomal in non-small cell lung cancer.

The majority of normal ovarian tissues express low levels of erbB2. Therefore only tumours that express greater levels of erbB2 can be considered overexpressers. A noted consistency of expression between primary tumours and metastatic sites has been found. No change in expression is seen over time. ErbB2 is overexpressed in approximately 30% of ovarian cancers. Some researchers have shown a positive correlation between overexpression and poor prognosis. On the other hand, other reports have shown no adverse prognostic significance for erbB2 overexpression. No correlation was found between erbB2 overexpression and clinicopathological factors such as age, stage, cell type, histological grade, residual tumour after primary cytoreduction or the likelihood of a negative re-exploration after chemotherapy. However, the uniformly poor prognosis for ovarian cancer may affect these results. Clear cell tumours have been found to have an increase in overexpression, with 68% showing overexpression, as opposed to 9% of other cells (Cirisano and Karlan, 1996). Overexpression of erbB2 has been found in 27% of patients with metastatic disease, as opposed to 4% of patients with disease confined to the uterus. Overexpression correlated with established prognostic variables of grade, stage, depth of invasion, more aggressive disease and disease-related mortality. Heavy staining of cell membrane correlated with 56% 5-year survival, intermediate staining correlated with 83% 5-year survival and negative staining correlated with 95% 5-year survival (Cirisano and Karlan, 1996). A more recent study looking at gene amplification, mutation, and protein expression of erbB2 in ovarian carcinoma showed that both increased copy number and overexpression of EGFR were associated with high tumour grade, greater patient age, large residual tumour size, high proliferation index, aberrant p53, and poor patient outcome. Increased copy number of EGFR was also associated with increased copy number of erbB2 (Lassus *et al.,* 2006). However, another study found that regarding cancer phenotype, there was no statistically significant association between erbB2 copy number changes, histologic and tumour stage of ovarian cancer (Dimova *et al.*, 2006).

Of 396 adenocarcinomas of the stomach, 10.1% overexpressed erbB-2. This overexpression broke down as 15.2% of well differentiated tumours and 3.0% of undifferentiated tumours, showing that erbB-2 overexpression is more prevalent in well differentiated gastric tumours. Gene amplification was detected in all the overexpressing tumours (Ishikawa *et al.*, 1997). Recent studies using microarray analysis to examine gene expression of 12,000 genes in oesophageal adenocarcinoma (EAC) specimens confirmed high levels of the erbB2 gene (Dahlberg *et al.*, 2004).

1.2.6 erbB-2 in Breast Cancer

Early reports showed erbB2 was amplified and/or overexpressed in approximately 30% of human breast carcinomas (Slamon *et al.*, 1987, Slamon *et al.*, 1989). In a study of 166 primary breast cancers, 21.6% showed erbB-2 overexpression, while 27.1% and 85 51.3% showed intermediate and low level expression respectively (Dittadi *et al.* 1996). The majority of studies have found the most useful prognostic factor in breast cancer is the number of positive auxiliary lymph nodes, indeed as the number of metastatic nodes increases, survival rates decrease and relapse rates increase. Breast cancer with 10 or more positive lymph nodes have a poor prognosis with about 30 per cent of patients alive at 5 years after primary surgery alone (Nemoto *et al.,* 1980). A study of 163 tumours from patients with different stages of breast cancer were analysed by Marx *et al.* (1990) in order to evaluate the distribution of erbB2. 33% of cases were found to be erbB2 positive. Only 5% of infiltrating lobular carcinomas (small cell carcinomas) showed positivity. Invasive ductal carcinomas show 33% positivity. Non-invasive and early invasive ductal carcinomas also showed positivity. ErbB2 protein expression was slightly more common in lymph-node positive (37%) than lymph-node negative cancer (30%). 50% of patients with three or more positive lymph-nodes were erbB2 positive. ErbB2 overexpression correlated negatively with steroid receptor status and positively with erbB1 expression.

A study by Quenel *et al.* (1995) of 942 invasive ductal carcinomas found 24% with positive membrane staining for erbB2. They found a significant association between erbB2 and tumour grade. Grading was performed according to Scarff-Bloom-Richardson criteria, with 11.2% of Grade 1, 21.5% of Grade 2 and 35.2% of grade III expressing erbB2. Negative correlation with estrogen and progesterone receptor status was found. No association was found between erbB2 and tumour size, nodal status or

patient age. ErbB2 positivity correlated with the least differentiated tumours, higher mitotic rate and with the most marked polymorphism. Multivariate analysis showed that erbB2 was an independent prognostic factor, associated with earlier relapse or metastasis in node-negative patients. Tsutsui *et al.* (2002) found a high level of concordance in EGFR, erbB2 and p53 expression in primary tumors and matching metastatic auxiliary nodes. These results were not consistent with a study from De la Haba-Rodriguez *et al.* (2004), who found a concordant expression of ER, PgR, p53, and erbB2 in primary tumors and metastatic lymph nodes in only about 40% of cases.

Breast carcinoma *in situ* (CIS) is considered to be the earliest form of breast cancer. Although 90% of patients with CIS are cured by surgery, the hypothesis that CIS lesions are precursors of invasive breast cancer is supported by the reports of a significant rate of local reoccurrence in patients who are not treated with mastectomy. Liu *et al.* (1992) assessed the amplification and overexpression of erbB2 in paraffin-embedded specimens from 27 *in situ* carcinomas of the breast and 122 stage II breast cancers. Gene amplification was detected in 48% of *in situ* carcinomas and in 21% of stage II lesions. ErbB2 protein levels corresponded with amplification levels. These results suggest that the amplification of erbB2 is an early event in human breast cancer.

In a study of 33 patients treated for advanced breast cancer, plasma erbB2 levels were determined (this refers to the extracellular domain shed from the cell surface). 30.3% of the metastatic breast cancer were found to be erbB2 positive. 20 of the patients received standard FEC regimen (5-fluorouracil, epirubicin and cyclophosphamide), 8 received a modified FEC regimen, 2 patients received CMF (5-fluorouracil, methotrexate and cyclophosphamide) and 3 patients received vinorelbine. No statistically significant difference was noted in response to chemotherapy between erbB2+ and erbB2- patients. In the 10 erbB-2+ patients, two increases and eight decreases were seen in plasma concentrations. Remarkably 5 of 23 erbB2- patients had an increase in plasma erbB2 during treatment. One observation made was that plasma erbB2 positivity is associated with advanced breast cancer. Between 34.6-51% of patients with metastatic breast cancer and 33% of patients with locally recurrent breast cancer show plasma erbB2 positivity, while no patients with locoregional non-inflammatory breast cancer showed positivity (Revillion *et al.*, 1996).

1.3 Eukaryotic translation initiation factor 4E (eIF4E)

1.3.1 Eukaryotic translation initiation

The decoding of an mRNA during translation proceeds in the 5'→ 3' direction. The recruitment of the small ribosomal subunit to mRNA must therefore facilitate placement of the ribosome at the 5'end. Two principle pathways are available for attachment of the ribosome in eukaryotes. The first involves recruiting the small ribosomal subunit to a complex secondary structure element within the RNA, known as the internal ribosomal entry site (IRES) (Jackson, 2005).

The second is cap-dependent. All Eukaryotic mRNAs have a cap-structure at their 5'-end, the functions of which include slicing, polyadenylation, nuclear export, stability and recognition of mRNA for translation. The cap-structure consists of a 7-methylguanosine linked to the first nucleoside via a 5'-5' triphosphate bridge added during the synthesis of the primary transcript. One or two methyl groups are usually present at specific locations. The cap structure is added to the 5' end of the pre-mRNA during transcription. The second pathway relies on the cap structure to act as an anchoring point for the cap-binding protein complex. The Cap-site guides the ribosome onto the transcript via the cap-binding protein, eukaryotic translation initiation factor, eIF4E. From here the ribosome scans along the 5' UTR in search of an in-frame AUG start codon (Svitkin *et al.,* 1996).

Once bound to the cap, "scanning" for the AUG initiator codon is regulated by the degree of secondary structure adopted by a particular mRNAs 5' UTR. A strongly competitive mRNA is typically characterised by a short, unstructured 5'UTR. For these mRNAs scanning proceeds easily from the cap through the short leader sequence to reveal the initiation codon. These mRNA represent the majority, and are well translated (e.g., GAPDH). Weaker mRNAs are characterised by long, G+C rich, highly structured 5'UTR's. The stability of the structure formed within the 5'UTR of these mRNAs impedes efficient scanning and cap recognition, rendering these RNAs extremely susceptible to translational regulation (van der Velden and Thomas, 1999). Weak mRNAs usually encode proteins that regulate growth and survival (e.g., ODC, VEGF, c-Myc, cyclin D1).

Initiation of Translation requires 4 specific steps:

1. The ribosome must dissociate into 40S and 60S subunits;
2. The pre-initiation complex is formed when eIF2 binds Met-tRNA with GTP (eIF2.Met-tRNA.GTP), which then binds 40S subunit to form 43S ribosomal subunit. tRNAs (transfer RNAs) carry the Amino Acids to the actively translating ribosome during protein synthesis. The Eukaryotic signal to begin translation is an AUG codon in a particular context, and as such, all proteins begin with a Methionine (encoded by AUG and recognised by t-Met) that is later cleaved (Figure 1.6);
3. The initiation complex binds to the mRNA 5'-UTR at the 7'-Methyl-Gppp Cap, recognised by eIF4E, and the eIF4F trimeric complex is formed (composed of the RNA helicase eIF-4A, the scaffold protein eIF4G, and the cap-binding protein eIF4E);
4. The 60S subunit then associates with the pre-initiation subunit to form the 80S initiation complex.

Figure 1.6: Formation of the pre-initiation complex

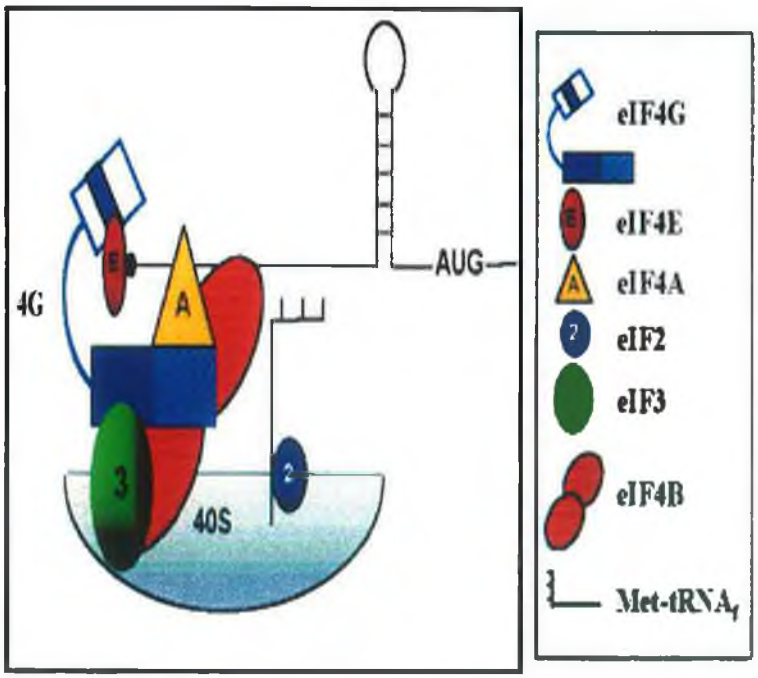

Diagrammatic representation of protein interactions in the 48S pre-initiation-complex. eIF4F component interactions are illustrated. eIF4E is the only factor that specifically recognises the cap structure of mRNA, and so has a crucial role in recruitment of the 40S subunit via its interactions with eIF4G, and indirectly via eIF3, eIF4A and eIF4B (Pain, 1996).

The eIF4F complex consists of three main sub-units, eIF4A, eIF4G and eIF4E. eIF4E, a small, 25 kDa phosphoprotein, is widely accepted as the rate-limiting factor in translation initiation. The synthesis of each protein ultimately depends on the relative abundance of its mRNA, and the capacity of this mRNA to interact with components of the translation initiation machinery. In this way an order of priority is established among mRNA in the initiation process, making translation of mRNAs a highly competitive and tightly regulated step in gene expression. The low abundance of eIF4E creates a competitive environment among 'strongly' and 'weakly' competitive mRNA species. mRNAs regarded as sensitive to available eIF4E levels usually feature long and structured 5' UTRs that interfere with efficient recruitment of the 40S subunits during initiation. Therefore, it is essential in order to allow efficient scanning of the ribosome, that these complex secondary structures be unwound. This function is performed by eIF4A, an RNA helicase which is a subunit of the eIF4F complex. Because one of the roles of the cap-binding complex is to recruit eIF4A to mRNA 5' ends, limitations in availability of eIF4E, and therefore the assembly of the cap complex, might also limit 5'-UTR unwinding. It has recently been reported that the requirement for eIF4A correlates with the stability of secondary structures present in mRNA 5' UTRs (Svitkin *et al.*, 2001).

After binding of eIF4F to the cap and unwinding of the secondary structure, the 43S initiation complex binds to the 5' end of the mRNA via interaction with the eIF4F complex to form the 48S initiation complex. The 48S complex then scans along the 5' UTR in search of an in-context AUG start codon. Recognition involves the Ribosomal mRNA and tRNA and the rate of initiation is influenced by the context of the bases surrounding a particular mRNAs AUG. The 80S ribosomal complex is formed at the initiation codon, ready to commence translation of the coding sequence. This last step requires a prior release of the initiation factors bound to the 40S ribosomal sub-unit, mediated by eIF5. After release the eIF2, GDP is recycled by the guanine-nucleotide exchange factor eIF2B to eIF2.GTP. The event of initiation is cyclic, in that once initiation at the AUG codon occurs the initiation factors dissociate and are recycled for use in another round of initiation (Figure 1.7) (Jackson, 1998).

Figure 1.7: Translation Initiation – a 'recycling' event

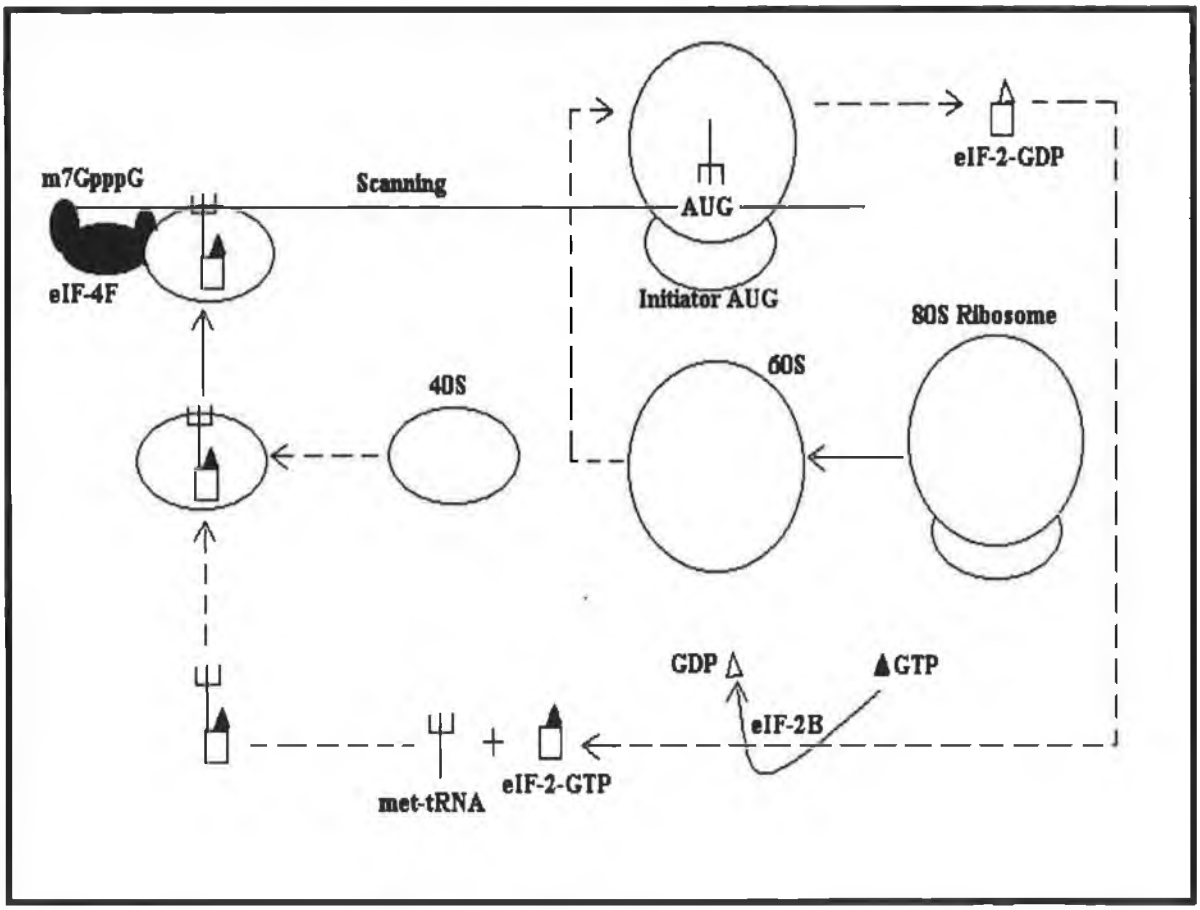

Initiation is the primary target for the control of translation, with the binding of the ribosomal pre-initiation complex to the mRNA and the scanning process being controlled through a number of mechanisms including RNA-binding repressors, modulation of the Initiation Factors involved (usually by phosphorylation), and the effects of secondary structure adopted by a particular mRNAs 5'-UTR.

1.3.2 Structure of eIF4E

The eIF4E molecule is shaped like a cupped hand with dimensions 41 Å (width) × 36 Å (height) × 45 Å (depth) and consists of one domain (Figure 1.8). Secondary structural elements include three long and one short helices and an 8-stranded, antiparallel sheet. The 8 strands are arranged in space making a curved, antiparallel sheet. The three long helices lie almost parallel to the strand direction and top the sheet. The narrow ligand-binding cleft (cap-binding slot) is generated by the concave surface of the sheet, the short helix, and the loop between strands S1 and S2. It is closed at one end by the loop

connecting strands S3 and S4, and open at the other (Marcotrigiano *et al.*, 1997). The 7-methylguanosine cap lies in a hydrophobic pocket on the concave face, sandwiched between two of the eight tryptophan residues that are evolutionarily conserved. Trp102 and Glu103 also hydrogen bond to nitrogen and oxygen of the cap structure (Marcotrigiano *et al.*, 1997; Matsuo *et al.*, 1997).

Figure 1.8 eIF4E bound to a fragment of the cap

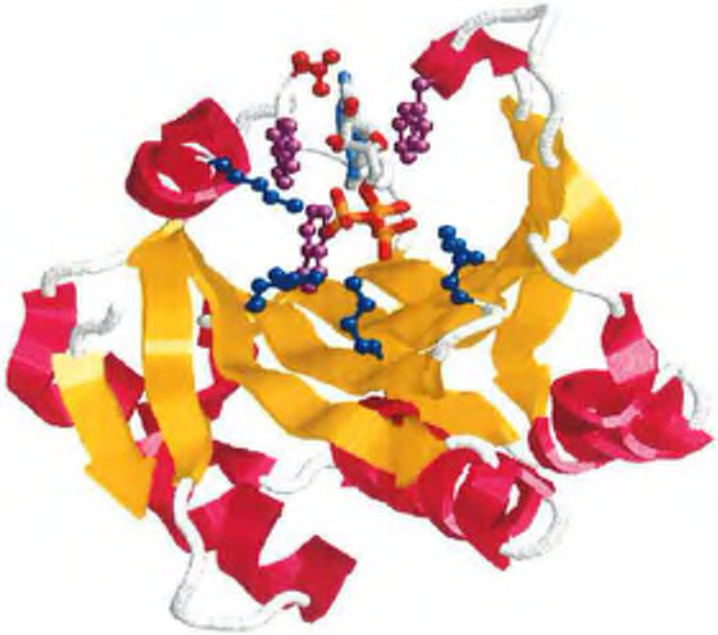

Global fold of eIF4E bound to a fragment of 7 methylguanosine 5'-triphosphate cap. Secondary structure elements are colour coded: yellow - b strands, pink - a helices, white - loops and turns. Amino acid belonging to the cap-binding site are shown as balls and sticks: blue - Lys206, Arg112, Lys162, Arg157 purple – absolutely conserved tryptophans 102, 166, 56, red – glutamic acid 103 (Niedzwiecka et al., 2004).

1.3.3 Phosphorylation of eIF4E

Gene regulation at mRNA translation takes place within minutes and is considered to be due to changes in the activity, or other functions, of components of the translational machinery. Translation is activated in response to hormones, growth factors, and cytokines, as well as nutrients such as amino acids and sugars. Conversely, under stressful conditions such as oxidative or osmotic stress, DNA damage or nutrient withdrawal, the rate of translation is decreased. Regulation is primarily achieved through phosphorylation of the translation components, and seems to be exerted mainly at the stage of translation initiation (Scheper and Proud, 2002).

Phosphorylation of eIF4E takes place on Ser209 in a C-terminal motif that is conserved in eIF4E from all species except *S. cerevisiae* and plants. Murine eIF4E can functionally

replace eIF4E from *S. cerevisiae* (Altmann *et al.*, 1989), and their 3-D structures are very similar (Marcotrigiano *et al.*, 1997; Matsuo *et al.*, 1997; McKendrick *et al.*, 1999). eIF4E phosphorylation is influenced by a variety of extracellular stimuli: treatment of cells in culture with serum, hormones, growth factors, cytokines, mitogens phorbol esters, and in some cell types insulin results in a net increase in eIF4E phosphorylation (Proud, 1992; Flynn and Proud, 1996b). Mitogen-activated protein kinases (MAPK)-interacting kinases 1 and 2 (Mnk1 and Mnk2), are activated by ERK and p38 MAPK in response to mitogens, cytokines or cellular stress, modulate the activity of eIF4E by phosphorylation at Ser209. A recent study has shown that Mnk1 does not interact directly with eIF4E, but uses a docking site in eIF4G, a partner of eIF4E. Consequently, control of eIF4E phosphorylation may not strictly depend on changes in Mnk1 activity. The possibility that integrity of the eIF4E/eIF4G/Mnk1 complex also impinges upon eIF4E phosphorylation is also possible (Pyronnet, 2000).

The phosphorylation state of eIF4E is, in general, correlated with the translation rate and growth status of the cell. An early report showed the pattern of eIF4E phosphorylation varied throughout the cell cycle, with the lowest levels in G0, increasing throughout G1 and S, but was reduced in M phase (Bonneau and Sonnenberg, 1987). eIF4E is also dephosphorylated during apoptosis (Bushell *et al.*, 2000). The correlation between eIF4E phosphorylation and the overall translation rate is, however, not observed in every situation. For example, an increase in eIF4E phosphorylation is observed in response to some types of cellular stress, including exposure to anisomycin, arsenite, tumour necrosis factor and interleukin even though translation rates actually decrease in these situations (Morley *et al.*, 1997). Oxidant stress stimulates phosphorylation of eIF4E without an effect on global protein synthesis in smooth muscle cells (Rao, 2000). However, other types of cellular stress, including heat-shock, or infection with adenovirus or encephalomyocarditis virus are accompanied by a decrease in eIF4E phosphorylation (Raught *et al.*, 1999).The effects of phosphorylation on eIF4E activity are not completely understood. eIF4E phosphorylation has been reported to increase its affinity for mRNA caps. However, a recent study has compared quantitatively the cap affinity for phosphorylated and unphosphorylated eIF4E by a fluorometric time-synchronized titration method and a 1.5- to 4.5-fold reduction of the cap affinity for phosphorylated eIF4E was observed (Zuberek *et al.,* 2003). More recently, it was found that both wild type and mutant (Ser209→Ala) eIF4E interacted equally well with eIF4G, and both were capable of

rescuing a lethal phenotype of eIF4E deletion in *S. cerevisiae*. Slepenkov *et al.*(2000) have recently proposed that phosphorylation of Ser-209, which is located at the entrance to the cap-binding slot, diminishes the rate of association by charge repulsion but has no effect on the rate of dissociation (Slepenkov *et al.*, 2006).

More recent studies have demonstrated that phosphorylation of eIF4E is specific to translation of certain mRNAs. An increase in Ets1 protein expression has been directly correlated with the phosphorylation of MNK1 and eIF4E in natural killer (NK) cells (Grund *et al.*, 2005). This not only suggests Ets1 is an eIF4E sensitive mRNA, but also that its translation is eIF4E phosphorylation dependent. Tumour necrosis factor (TNF)-α mRNA also requires phosphorylation of eIF4E at serine 209 for initiation of translation (Andersson and Sundler, 2006). These studies suggest eIF4E phosphorylation may be important in promoting translation of cancer-promoting proteins, however, another report saw no significant difference between nontransformed cells and carcinoma cell lines with regard to the phosphorylation status of eIF4E (Avdulov *et al.*, 2004).

1.3.4 Regulation of eIF4E

1.3.4.1 Inhibitory proteins of eIF4E

Translation initiation is the rate-limiting step in translation and the common target of translational control. As already mentioned, the mRNA 5' cap is bound by eIF4F, a heterotrimeric protein complex that is the focal point for initiation. eIF4G is the backbone of this complex, and the eIF4E–eIF4G interface is an important target for translational control. Several proteins contain eIF4E-compatable binding motifs, and compete with eIF4E for binding (Mader *et al.*, 1995). In this way the rate of 40S ribosomal subunit association with mRNA, and hence translation initiation, is controlled. Earlier studies suggested that eIF4E was rate-limiting for protein synthesis (Sonenberg, 1994), whereas this factor may, in fact, be relatively abundant in the cell (Rau *et al.*, 1996) and probably present in considerable molar excess over eIF4G (von der Haar and McCarthy, 2002). However, the availability of eIF4E in a functional form can be strongly limited by its association with different eIF4E-binding proteins, the most well characterised being the 4E-BPs (Gingras *et al.*, 1999).

The binding of heat-stable inhibitory proteins called 4EBPs (eIF4E-binding proteins - 4EBP1, 4EBP2 and 4EBP3) to eIF4E is a well documented method of translation regulation. 4EBPs interact with eIF4E at the same site as eIF4G, acting as competitive

inhibitors of eIF4F complex formation (Raught *et al.*, 1999). Phosphorylation of 4EBPs on five residues in the region of interaction with eIF4E causes an "electrostatic repulsion"; 4EBPs fall off and 4E can interact with 4G. By far the best understood of the 4EBPs is 4EBP1. Association of 4EBP1 with eIF4E is regulated by a range of stimuli: for example, insulin, which activates mRNA translation, induces the phosphorylation of 4EBP1 and its release from eIF4E, allowing the protein to bind eIF4G to form initiation factor complexes (Raught *et al.*, 1999).

More recently discovered eIF4E-binding proteins interact with the eIF4E on only specific mRNAs, and do so either because they also interact with certain RNA elements directly, or through affiliations with RNA binding proteins (Richter and Sonenberg, 2005). Modulation of poly (A) tail length is vital for the translation of mRNAs in early development. Cytoplasmic polyadenylation is controlled by CPEB, a protein that interacts with the cytoplasmic polyadenylation element (CPE). CPEB also binds Maskin, a protein that competes with eIF4E. Maskin disrupts eIF4E–eIF4G interactions and the CPEB–Maskin–eIF4E complex inhibits the translation of CPE-containing mRNAs specifically (Stebbins-Boaz *et al.*, 1999).

In humans, two other proteins have been identified as binding partners of eIF4E and appear to act as negative regulators of eIF4E-dependent export of a subset of mRNAs. The promyelocytic leukemia protein (PML) is organized into nuclear bodies which mediate suppression of oncogenic transformation and of growth (Melnick and Licht, 1999). The N-terminal RING motif is required for association of PML with nuclear bodies, and eIF4E is know to directly bind the PML RING. Moreover, this interaction modulates eIF4E activity by significantly reducing its affinity for the cap (Cohen *et al.*, 2001). The proline-rich homeodomain protein, PRH, has also been found to be an inhibitor of eIF4E-dependent cyclin D1 mRNA transport and growth in certain tissues. Interacting with eIF4E through a conserved binding site typically found in translational regulators, PRH inhibits eIF4E-dependent mRNA transport and subsequent transformation (Topisirovic *et al.*, 2003).

1.3.4.2 Transcriptional regulation of eIF4E

The myc family of transcription factors are responsible for the control of genes directly involved in cell growth and proliferation. It is not surprising therefore that the deregulation of myc results in the abnormal growth of tumour tissue (Magrath, 1990). eIF4E is one of few myc-regulated genes which has been characterised. The promoter

region of eIF4E contains two myc binding sites, both of which are required for expression of a heterologous reporter gene (Jones *et al.*, 1996), and as a result, eIF4E expression is up-regulated in c-myc overexpressing genes (Rosenwald *et al.*, 1993b).

Wild-type p53 is a tumour suppressor that can act through several mechanisms, the main one being as a transcriptional factor activating or inactivating the transcription of its target genes (Levine, 1997). In contrast to eIF4E, p53 is important in preventing tumourigenesis, a fact which is highlighted by the occurrences of mutated p53 gene in more than 50% of human cancers. A recent study has shown that the expression of eIF4E is reciprocally regulated by p53 and c-myc, and loss of p53-mediated control over c-myc-dependent transactivation of eIF4E may represent a novel mechanism for eIF4E-mediated neoplastic transformation and cancer progression (Zhu *et al.*, 2005).

Heterogeneous Nuclear Ribonucleoprotein K (hnRNP K) was first identified as a component of hnRNP complexes and is involved in nucleo-cytoplasmic transport of mRNA as well as regulation of mRNA stability (Ostareck-Lederer *et al.*, 2004). As already discussed, eIF4E is a c-myc target gene, and hnRNP is one of the most important transcriptional controls of the c-myc promoter (Michelotti *et al.*, 1996). It has since been identified as a binding protein and positive regulator of eIF4E. Through regulation of eIF4E it has been found to directly contribute to neoplastic transformation (Lynch *et al.*, 2005).

1.3.5 The role of eIF4E in cancer invasion

As already mentioned there are 'strong' and 'weak' mRNAs, and with higher eIF4E levels the translation of weak mRNAs is elevated. Cyclin D1, ODC and FGF-2 are examples of growth factors dependent on eIF4E translation (Rosenwald *et al.*, 1993a; Shantz and Pegg, 1994; Kevil *et al.*, 1995), all of which have a role in cellular growth/proliferation. Because many of these mRNAs code for oncoproteins, regulators of cell cycle, growth factors and their receptors (De Benedetti and Harris, 1999), with increased levels of eIF4E cell growth becomes more rapid, and cells may become neoplastic. Further increase of eIF4E can cause resistance to apoptosis (Polonovsky *et al.*, 1996) and increased mitosis, leading to genetic instability and selection of aggressive survivors (De Benedetti and Harris, 1999). Healthy cells tightly regulate proteins that are necessary in specific cellular environments but which could be potentially oncogenic. With an over-abundance of eIF4E this regulation is lost. To form metastases, individual tumour cells must break from the primary tumour mass, degrade

extracellular matrix, invade the surrounding normal tissue, enter the blood or lymphatic circulation, exit the circulation at a distal tissue and establish satellite colonies within this new tissue environment. This aberrant behaviour of cancer cells requires the cooperative function of numerous proteins – those that facilitate angiogenesis (e.g., VEGF), cell survival (e.g., Bcl-2), invasion (e.g., MMPs), and autocrine growth stimulation (e.g., c-myc, cyclin D1). Although expression of these proteins is regulated at many levels, translation of these key malignancy-related proteins is regulated primarily by the activity of eIF4E. Many of the gene products that drive metastasis are not altered by mutation, but by altered patterns of gene expression. It is the quantity not the quality of key genes that drive the metastatic program (Graff and Zimmer, 2003). Therefore, eIF-4E function contributes to metastatic progression by selectively upregulating the translation of key malignancy-related proteins that together conspire to drive the metastatic process.

After it was observed that overexpression of eIF-4E could result in oncogenic transformation and uncontrolled growth of mammalian cells, a screen of breast carcinomas was carried out. This work showed that eIF-4E was elevated 3- to 10-fold in virtually all the carcinomas analyzed, suggesting eIF-4E to be an essential component in the development of breast cancer (Kerekatte *et al.*, 1995). Since then, several studies have looked at eIF4E levels and effects in cancer. eIF4E gene amplification was associated with malignant progression in infiltrating ductal carcinoma of the breast (IDCA) and in head and neck squamous cell carcinoma (HNSCC) specimens (Sorrells *et al.*, 1999). Recent work carried out to determine the effect of eIF4E overexpression in breast cancer specimens found increasing eIF4E correlated with higher VEGF levels and tumour microvessel density (MVD) counts. Patients whose tumours had high eIF4E overexpression had a worse clinical outcome, independent of nodal status. Thus, eIF4E overexpression in breast cancer appears to predict increased tumour vascularity and perhaps cancer dissemination by hematogenous means (Byrnes *et al.*, 2006).

eIF4E has also been found to play an important role on tumourigenesis, development, invasion and metastases of laryngeal squamous cell carcinoma (Tao *et al.*, 2002), and gastric adenocarcinoma (Chen *et al.,* 2004). In atypical adenomatous hyperplasia and adenocarcinoma of the human peripheral lung, dysregulation of translational control leading to a progressive increase of tumoral and stromal eIF4E is believed to be part of a positive feedback loop for malignant progression (Seki *et al.*, 2002).

1.3.6 Activation of eIF4E through the PI3K/AKT signalling pathway

As a downstream effector of mammalian target of rapamycin (mTOR), eIF4E is regulated by the phosphatidylinositol-3 kinase (PI3K)/AKT signalling cascade, a major cell-survival pathway associated with malignant transformation and apoptotic resistance (Figure 1.9).

Figure 1.9 PI3K/AKT in cell survival and apoptosis resistance

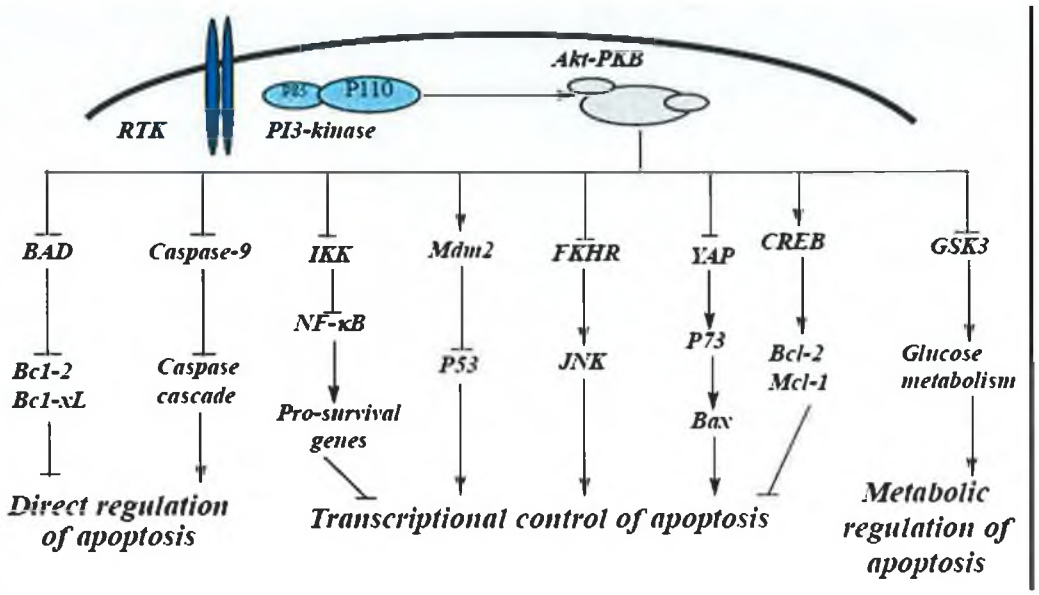

Survival signaling by eIF4E as regulated by this pathway is well documented, and correlates with occurrence of cancer (Wendel *et al.*, 2004a). The PI3K/AKT signaling cascade is activated in response to growth factors or insulin and is thought to contribute to several cellular functions including glucose transport and glycogen synthesis, cell growth, transcriptional regulation and cell survival (Song *et al.*, 2005). This pathway has also been found to be induced by oncogene amplification and mutation (e.g. Ras), mutations in PI3K, and AKT overexpression. It is not surprising therefore that deregulation of AKT is frequently associated with human diseases including cancer and diabetes (Nicholson and Anderson, 2002). AKT is activated by PI3K, which is activated by the tyrosine kinases and G-protein coupled receptors (Wymann *et al.*, 2003). Following recruitment to these receptors, PI3K is activated and phosphorylates PI3K converts phosphatidylinositol-4, 5-bisphosphate (PIP2) to PIP3. PIP3 does not activate AKT directly, but recruits Akt/PKB to the plasma membrane (in its inactive state, AKT is located in the cytosol), alters its conformation and allows subsequent phosphorylation by the phosphoinositide-dependent kinase-1 (PDK1) (Andjelkovic *et al.*, 1997). The

tumour suppressor PTEN, negatively regulates PI3K/AKT but is frequently inactivated in many tumour types, leading to increased activation of AKT (Sansal and Sellers, 2004). The mammalian target of rapamycin (mTOR) lies downstream of the TSC2-TSC1-Rheb complex within the PI3K pathway (Manning, and Cantley, 2003), and also receives nutrient input signals (Jaeschke *et al.*, 2004). The TSC complex, a heterodimer consisting of unphosphorylated TSC2 (tuberin) and TSC1 (hamartin), acts as a GTPase-activating protein (GAP), inhibiting the small G-protein Rheb (*Ras* homolog enriched in brain). By phosphorylating TSC2, AKT disrupts the TSC complex, enabling Rheb to bind to ATP and convert itself from the inactive GDP state to the active GTP state (Zhang *et al.*, 2003). GTP-bound Rheb, in turn, activates mTOR (Inoki *et al.*, 2002). The 4E binding proteins, which regulate interaction between eIF4E and eIF4G, are directly phosphorylated by mTOR. mTOR-mediated signalling causes 4EBP1 to become highly phosphorylated and to dissociate from eIF-4E (Figure 1.10) (Lawrence and Abraham, 1997). eIF-4E then drives the translation of 5′cap mRNAs, including several oncogenic proteins such as FGF, c-Myc, VEGF and cyclin D1, as already mentioned.

Figure 1.10 Regulation of mTOR

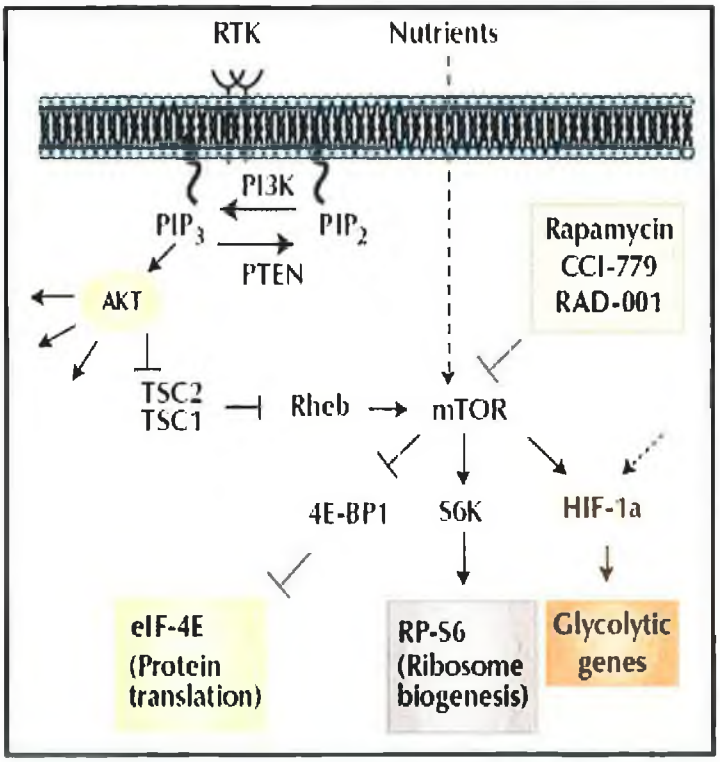

Growth factor receptor tyrosine kinases (RTKs) recruit PI3K to the membrane. PI3K converts phosphatidylinositol-4, 5-bisphosphate (PIP_2) to PIP_3 and activates the serine/threonine kinase AKT. Termination of the PIP_3 signal occurs through the action of PTEN. AKT controls a host of signalling molecules, including tuberin (TSC2). The mammalian target of rapamycin (mTOR) lies downstream of the TSC2-TSC1-Rheb complex within the PI3K pathway, but also receives nutrient input signals. The ribosomal protein S6 kinase (RP-S6) and the eukaryotic initiation factor 4E (EIF-4E) binding protein 1 (4E-BP1) are mTOR effector molecules that function as regulators of ribosome biogenesis and protein translation. mTOR function is inhibited by rapamycin or its derivatives CCI-779 (Wyeth-Ayerst) and RAD001 (Novartis).

1.4 Gene Expression Microarrays

Each cell in the body contains a full set of chromosomes containing identical genes. At any given time only a fraction of these genes are expressed. It is this group of expressed genes that makes each cell type unique. Aberrant gene expression profiles are responsible for many diseases. The completion of the Human Genome project (HGP) in 2003 has led to a huge amount of information becoming available about almost every gene in the genome, and is necessary to understand more about the functions of these gene products. New advances in technology, for example, the development of full genome expression microarrays, have allowed researchers to study the expression of almost every gene simultaneously. It is important to note, however, that we may not yet have identified all genes correctly, from the sequence data, and certainly our knowledge of the range of splice variants is incomplete.

1.4.1 Introduction to microarray technology

Microarrays are artificially constructed grids of DNA such that each element of the grid contains a specific oligodeoxynucleotide probe. This enables researchers to simultaneously measure the expression of thousands of genes in a given sample. Microarray experiments rely on the ability of RNA to bind specifically to a corresponding sequence-complementary probe. DNA microarrays are classified based on the DNA molecule that is immobilised on the slide. There are two basic types: either "oligodeoxynucleotide" or "cDNA" arrays. Oligodeoxynucleotide arrays are typically made up of 25-80 mer oligodeoxynucleotides while cDNA arrays are printed with 500-5000 base pair PCR products.

Microarray technology can be used to detect specific gene changes in, for example, diseased tissue compared to normal healthy tissue, or the changing gene expression profiles of developing tissues at incremental time points. These types of experiments have the potential to explain not only why a disease occurs, but also how best to overcome it by enhancing our understanding of the mechanisms behind diseases, their development and progression. The steps of a microarray experiment are shown in Figure 1.11.

An example of an affymetrix genechip experimental workflow is as follows:

1. Total RNA is isolated from the cells being studied
2. The RNA is enzymatically converted into a double stranded DNA copy known as a complementary DNA (cDNA). This is done through reverse transcription (RT) and second strand synthesis.
3. The cDNA is allowed to go through *in vitro* transcription (IVT) to RNA (now known as cRNA). This RNA is labelled with Biotin by incorporating a biotin-labelled ribonucleotide during the IVT reaction.
4. This labelled cRNA is then fragmented in to pieces anywhere from 30 to 200 base pairs in length by metal-induced hydrolysis.
5. The fragmented, Biotin-labelled cRNA is then hybridized to the array for 16 hours.
6. The array is then washed to remove any unhybridized cRNA and then stained with a fluorescent molecule streptavidin phycoerythrin (SAPE), which binds to Biotin.
7. Lastly, the entire array is scanned with a laser and the information is automatically transferred to a computer for analysis of what genes were expressed and at what approximate level.

Figure 1.11 Steps in a microarray experiment (www.affymetrix.com)

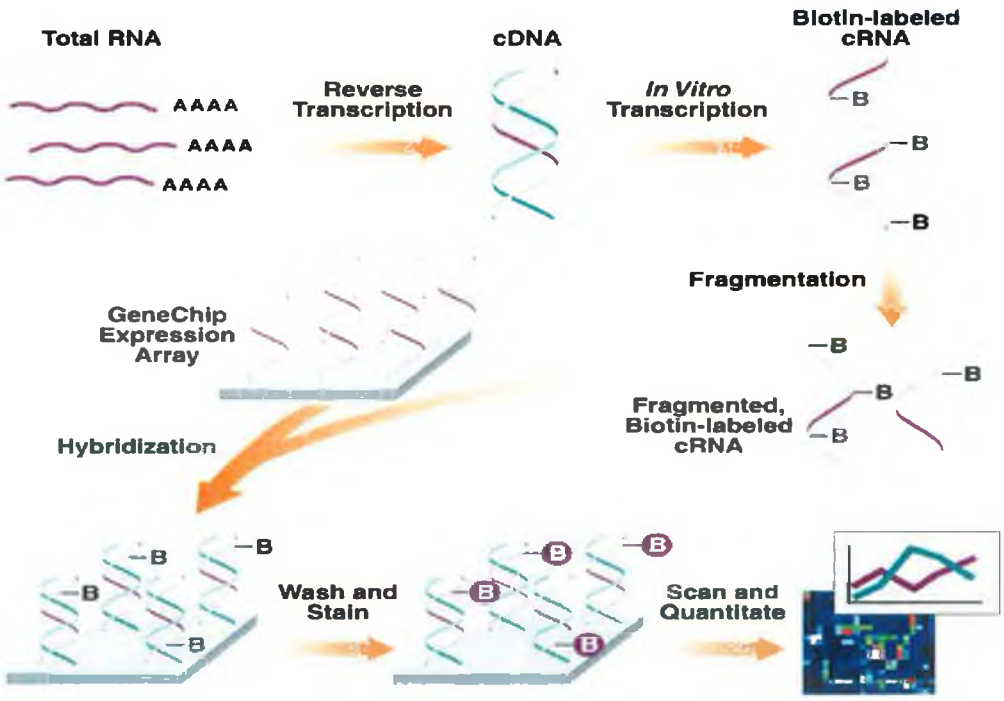

1.4.2 Microarray analysis

Microarray experiments generate vast amounts of data in a short period of time. For the results of a microarray experiment to be acceptable, the raw data from the experiment must be validated. Good experimental design is the first step. It is important that the proper controls and replicates are included in each experiment. Replicates are particularly important since the methods used to identify differentially expressed genes are predominantly statistical. Microarray data is normalised to measure real biological changes by minimising processing variation. This process standardises the data so that the gene expression levels are comparable.

Quality control checks must also be included at all stages of the experiment. These checks would usually include quality checks on the initially isolated RNA and processed sample at regular intervals, e.g. by using an Agilent Bioanalyzer. The Agilent Bioanalyzer analyses sample RNA in order to determine quality. Detailed information about the condition of RNA samples is displayed in the form of highly sensitive electropherograms. Post-experimental quality control checks include the chip controls shown in Table 1.3.

Table 1.3 Array quality control measures

QC measure	Result
Background	Measure of non-specific binding
3'/5' Ratio	Indicates how well IVT reaction has proceeded, or if RNA is degraded
Hybridisation controls	Checks spike controls added to each sample
Percentage present	All samples should have comparable % genes present
Noise	The electrical noise from scanner
Scale factor	Measures the brightness of array- All chips in an experiment should have scale factors within 3-fold of each other

The ideal format for reporting microarray data was reported by Brazma *et al.* (2001), and is called the "minimum information about a microarray experiment" (MIAME). MIAME has two general principles. The first is that there should be sufficient information recorded about each experiment to allow interpretation of the experiment, comparison to similar experiments and replication of the experiment. The second

principle is that the data should be structured to allow automated data analysis and mining.

1.4.3 Affymetrix Gene Chips

The microarray experiments carried out in these studies employed the Affymetrix Genechip system, which is an oligodeoxynucleotide microarray. Affymetrix probes are designed using publicly available information (NCBI database). The probes are manufactured on the chip using photolithography, which is adapted from the computer chip industry. Each genechip contains approximately 1,000,000 features. Each probe is spotted as a pair, one being a perfect match (PM), the other with a mismatch at the centre (MM). Each gene or transcript is represented on the genechip by 11 probe pairs (PM+MM). This can be seen in Figure 1.12. As well as helping estimate and eliminate background, with 22 different probes in total, researchers can be sure that the microarray is detecting the correct piece of RNA. The amount of light emitted at 570nm from stained chip is proportional to the amount of labelled RNA bound to each probe. Therefore, after scanning, the initial computer file generated (.DAT) contains a numerical value for every probe on the array.

Figure 1.12 Perfect match and mismatch probe pairs on Affymetrix Gene Chips (www.affymetrix.com)

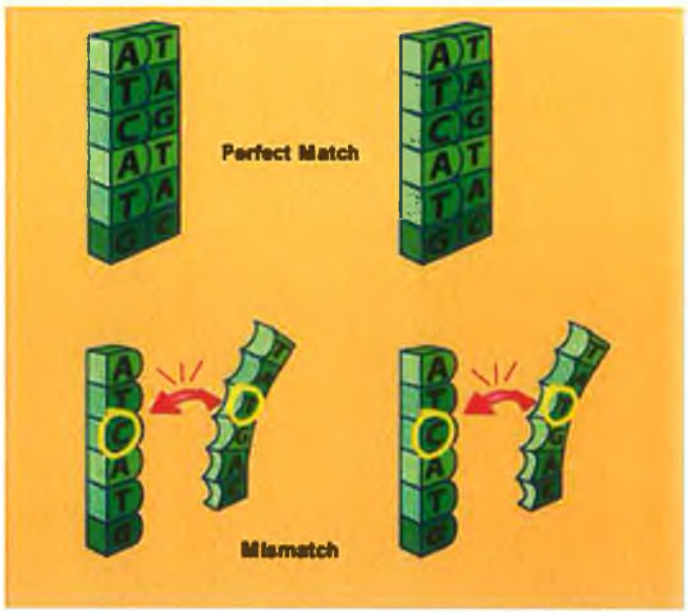

For a valid gene expression measurement, the perfect match 'stick' and the mismatch does not.

1.4.4 Bioinformatics

Bioinformatics is the collection, organization and analysis of large amounts of biological data, using networks of computers and databases. Software packages are available to analyse microarray data e.g. Genespring and Spotfire. The data analysis software used for the analysis of the microarray experiments reported in this thesis was dChip, (Lin *et al.*, 2004). This software is capable of probe-level and high-level analysis of Affymetrix gene expression arrays. High-level analysis in dChip includes comparing samples and hierarchical clustering in order to identify differentially expressed genes. Hierarchical clustering displays the relationships among genes or samples. These are represented by a tree where the length of the branches reflects the degree of similarity between the objects (Eisen *et al.*, 1998). An example of a cluster can be seen in Figure 1.13. There are several other bioinformatics software available which facilitate pathway analysis of genes differentially regulated in the systems studied (Section 2.5.12-19).

Figure 1.13 Hierarchical cluster of microarray samples

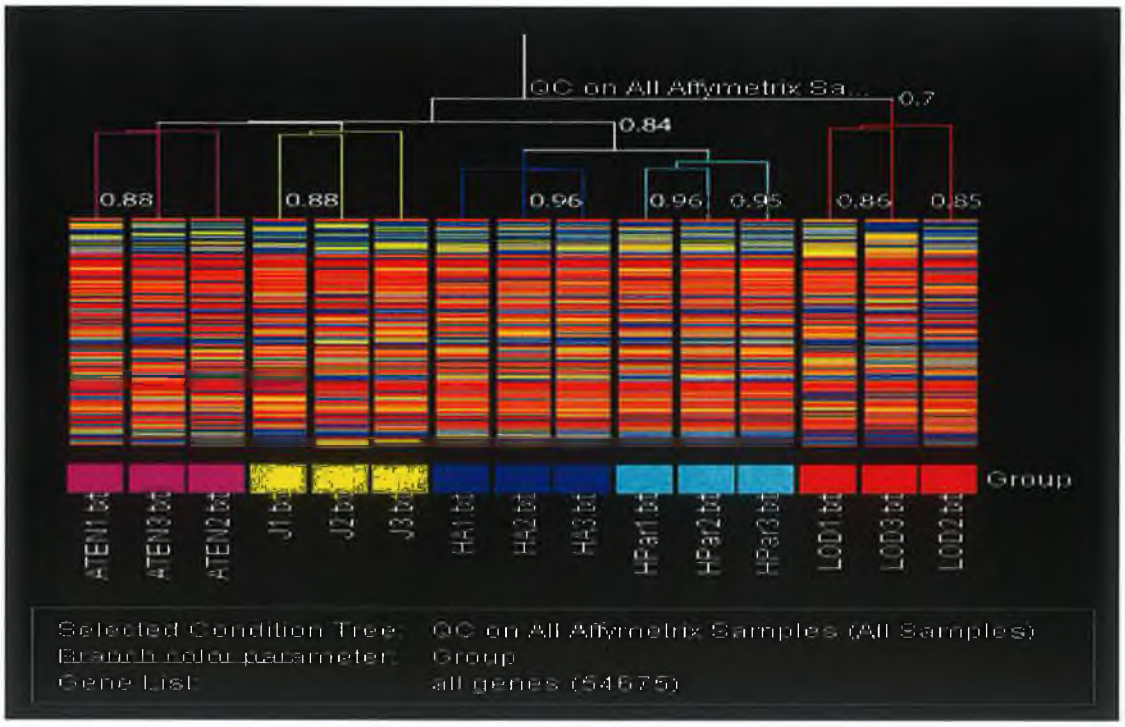

Figure 1.1.3: Hierarchical cluster displaying the relationships among samples. The length of the branches reflects the degree of similarity between samples.

1.4.5 Microarrays and cancer

The initiation and progression of cancers is a complex process, involving an accumulation of genetic aberrations in the cell. Microarrays now provide researchers with the ability to examine whole genomes simultaneously, allowing a complete investigation of the effects of genetic aberrations in many diseases, including cancer. Microarray technology has been used intensively to better understand the development of resistance to chemotherapeutic agents. Whiteside *et al.* (2004) reported a novel method using time-course cDNA microarray analysis designed to evaluate which differentially expressed genes are directly involved in the development of drug resistance. The study used two lung cancer cell lines; one which readily developed resistance to cisplatin and another which after treatment with cisplatin did not display stable resistance. They identified seven genes that are likely to be involved in cisplatin resistance; three of them are newly identified in terms of cisplatin resistance (Whiteside *et al.*, 2004). Another *in vitro* study used human lung cancer cell lines with varying degrees of invasion ability and metastatic potential to determine invasion-related genes (Chen *et al.*, 2001). Hundreds of genes were found significant to the invasive phenotype, several of which had already been associated invasion from previous work. This previous association with invasion validated the analysis and indicated that the more novel genes found may also play a role in invasion/metastasis.

DNA microarrays have also been used to examine RNA profiles of *in vivo* models, and have proven powerful tools in the determination of markers of clinical significance.

Several studies have looked at genes identified as invasion/metastasis markers in *in vivo* and *in vitro* models using microarrays. The significance of chemokine receptor (CR) expression in patients with melanoma and colorectal cancer (CRC) liver metastases was examined using microarray analysis. Tissue samples from patients who underwent hepatic surgery for melanoma or CRC liver metastases were used to obtain RNA for microarray experiments, and CR was found to have prognostic significance for disease outcome (Kim *et al.*, 2006). Conversely, markers significant to cancer have been determined using microarray data alone, and then further examined using *in vitro* and murine models. An example of this was the detection of aberrations of ubiquitin-conjugating enzyme E2C gene (UBE2C) in advanced colon cancer with liver metastases by DNA microarray and two-color FISH (Takahashi *et al.*, 2006). Initially this study identified genes whose expression showed a significant change in primary colon cancers

relative to normal tissue, but could not discover any gene with significant change between the primary tumours and its liver metastases. However, further analysis using FISH revealed that *UBE2C* expression was significantly changed by amplification at 20q13.1, suggesting genomic amplification as one mechanism of increased *UBE2C* expression.

Gene expression profiling has been extensively applied to the study of breast cancer. Recent work has also demonstrated how DNA microarrays can provide prognostic information in patients with newly diagnosed breast cancer, and may be useful in predicting response or resistance to treatment, especially to neoadjuvant chemotherapy (Brennan *et al.*, 2005). Prognostic "signatures" (gene lists) have been established using microarray studies that are purported to be more accurate prognostic factors than well established clinical and pathological features (Nevins *et al.* 2003). In addition, cDNA and oligonucleotide microarrays have also been used to devise predictive "signatures" in the setting of neoadjuvant chemotherapy setting (Hannemann *et al.*, 2005). Although the results are promising, further optimisation and standardisation of the technique and properly designed clinical trials are required before microarrays can reliably be used as tools for clinical decision making (Reis-Filho *et al.*, 2006).

1.5 siRNA

RNA silencing was discovered in plants more than 15 years ago during the course of transgenic experiments that eventually led to silencing of the introduced transgene and, in some cases, of homologous endogenous genes or resident transgenes (Matzke *et al.*, 1989; Linn *et al.*, 1990; Napoli *et al.*, 1990; Smith *et al.*, 1990; van der Krol *et al.*, 1990). The growth of RNAi as a technique has exploded since its discovery to the present day. In the region of 15 RNAi papers were published in 1998 whereas over 1,000 were published in 2005. Many companies have changed their focus from antisense and ribozyme technologies to concentrate on post-transcriptional gene silencing using RNAi, which to date appears far more potent than antisense-based approaches (Wall and Shi 2003).

1.5.1 Mechanism of action

Long double-stranded RNAs (typically >200 nt) can be used to silence the expression of target genes in a variety of organisms, as already mentioned. Upon introduction, the long dsRNAs enter a cellular pathway that is commonly referred to as the RNA interference (RNAi) pathway. During the initiation stage, long dsRNA is cleaved into siRNA and miRNAs (Hamilton *et al.*, 2002), mediated by type III RNase Dicer. RNase III family members are among the few nucleases that show specificity for dsRNAs (Nicholson, 1999) and are evolutionarily conserved in worms, flies, fungi, plants, and mammals (Agrawal *et al.*, 2003). Complete digestion by RNase III enzyme results in dsRNA fragments of 12 to 15 bp, half the size of siRNAs (Yang *et al.*, 2002), however examination of the crystal structure of the RNase III catalytic domain explains the generation of 23- to 28-mer diced siRNA products (Blaszczyk *et al.*, 2001). In this model, Dicer folds on the dsRNA substrate to produce two active catalytic sites having homology with the consensus RNase III catalytic sequence, and two inactive internal sites. The diced products are the limit digests and are double the size of the normal fragments.

During the effector stage, the siRNAs assemble into endoribonuclease-containing complexes known as RNA-induced silencing complexes (RISCs), unwinding in the process (Hammond *et al.*, 2000). Dicers are part of the RISC complex, which includes several different proteins such as the Argonaute gene family members and an ATP-dependant RNA helicase activity that unwinds the two strands of RNA. Argonaute

proteins contain two RNA-binding domains, one that binds the small RNA guide at its 5' end, and one that binds the single stranded 3' end of the small RNA. The siRNA must be 5' phosphorylated to enter the RISC complex. The antisense strand is exposed by the helicase and only one strand of the siRNA guides the RISC to the homologous strand of the target mRNA. Functional RISCs contain only single stranded siRNA or miRNA (Martinez *et al.*, 2002). The siRNA strands subsequently guide the RISC to complementary RNA molecules, where Watson and Crick base pairing takes place between the antisense strand of the siRNA and the sense strand of the target mRNA. This leads to endonuclease cleavage of the target RNA at the phosphodiester bond, 10-11 nucleotides along from the 5' end of the siRNA (Novina and Sharp, 2004). Gene silencing by RISC is accomplished via homology-dependent mRNA degradation (Tuschl *et al.*, 1999; Hamilton & Baulcombe, 1999), translational repression (Grishok *et al.*, 2001) or transcriptional gene silencing (Pal-Bhadra *et al.*, 2002) (Figure 1.14).

Endonucleolytic cleavage is generally favoured by perfect base-pairing between the miRNA /siRNA and the mRNA, although some mismatches can be tolerated and still allow cleavage to occur (Mallory *et al.*, 2004; Guo *et al.* 2005). Translation repression is seen mostly in miRNA, though evidence of siRNA acting like miRNA does exist (Doench *et al.*, 2003). A short RNA with mismatches to a target sequence present in multiple copies in the 3'untranslated region (UTR) of an exogenously expressed gene can silence it by translational repression. A single base mismatch with the target is believed to protect the mRNA from degradation making this type of interference highly specific to the targeted gene (Saxena *et al.*, 2003). Transcriptional gene silencing causes gene expression to be reduced by a blockade at the transcriptional level. Transcriptional silencing by siRNAs probably reflects genome defence mechanisms that target chromatin modifications to endogenous silent loci such as transposons and repeated sequences (Doench *et al.*, 2003; Zilberman *et al.*, 2003).

Figure 1.14 siRNA mechanism of action

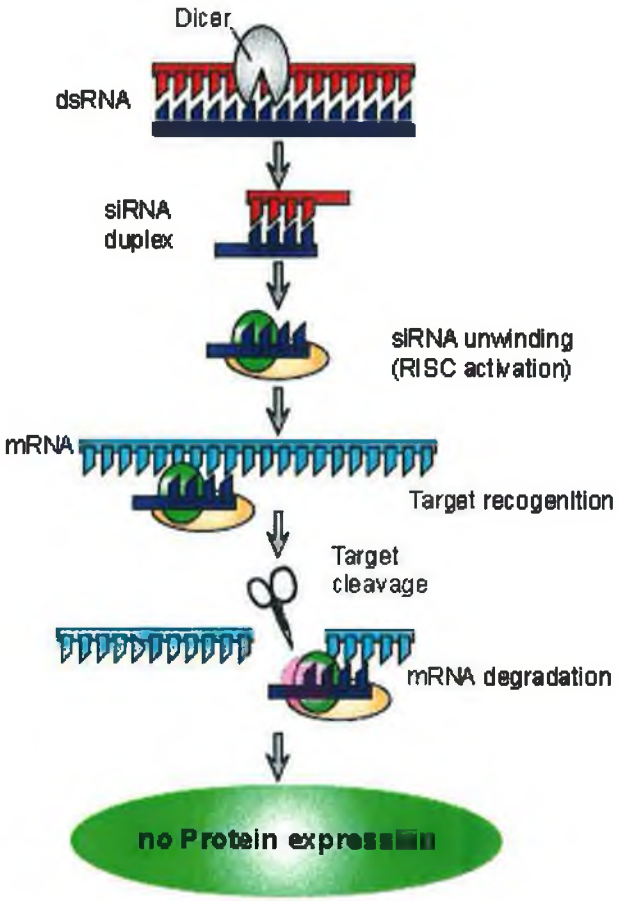

Long dsRNAs are processed by a host RNaseIII called Dicer to form siRNAs (21-23nt long) Dicer-processed siRNAs and synthetic siRNAs undergo ATP dependent unwinding before being incorporated into a high-molecular-weight protein complex called RISC (RNA-induced silencing complex) that contains single stranded siRNAs. The RISC is reconfigured to active RISC which contains the proteins required for cleaving the target mRNA at the point where the antisense siRNA binds. After the cleavage the active RISC is released to cleave additional mRNA molecules whereas the cleaved mRNA is degraded by cellular ribonucleases.

1.5.2 siRNA/miRNA - what's the difference?

RNAi regulation of endogenous genes in mammalian cells occurs via production of short double stranded RNA molecules termed microRNA or miRNA. miRNAs are a class of non-coding RNAs that function as endogenous triggers of the RNAi interference pathway (Hammond, 2006). Mature miRNAs are between 21-23 nucleotides in length and are formed from larger transcripts, 60-80nt. These long precursors are produced by RNA polymerase II, spliced, polyadenylated and resemble mRNAs (though they may or may not have an open reading frame (ORF)). Firstly the larger transcripts fold to produce hairpin structures that are substrates for the RNase III enzymes, Drosha, located in the nucleus. This functional stem-loop structure can be located in an intron or an exon. Following this initial processing pre-miRNAs are escorted through the nuclear pore by exportin-5, a transport receptor (Kim, 2004). As

with siRNA, the pre-miRNA is now processed by Dicer to form mature miRNA duplexes (Lippman and Martienssen, 2004).

siRNA refers to synthetic generation of RNA interference. siRNA are 21-22 nucleotides in a staggered duplex, with two unpaired nucleotides at either end and are perfectly complementary to their target sequence, causing silencing at mRNA level. miRNA on the other hand, possess a strand which is highly, but not perfectly complementary to one or more target mRNAs. The mRNA bound to the miRNA remains untranslated, resulting in reduced expression of the corresponding gene (Lai, 2005).

1.5.3 miRNA in cancer

Recent studies of miRNA expression implicate miRNAs in brain development (Krichevsky *et al.*, 2003), chronic lymphocytic leukemia (Calin *et al.*, 2004), colonic adenocarcinoma (Michael *et al.*, 2003), Burkitt's Lymphoma (Metzler *et al.*, 2004), and viral infection (Pfeffer *et al.*, 2004) suggesting possible links between miRNAs and viral disease, neurodevelopment, and cancer. miRNA has been shown to act as both tumour suppressors and oncogenes. More than 50% of miRNA genes have been found localised in cancer-associated genomic regions or in fragile sites (Calin *et al.*, 2004). Expression profiling methods were developed to analyse 217 mammalian miRNAs from a panel of 200 human cancers. Results showed an overall reduction in expression of miRNAs in cancer compared to normal samples. This indicates that miRNAs act predominately as tumour suppressors (Li *et al.*, 2005). However, a cluster of miRNAs, miR-17 ~ 92, is overexpressed is some lymphoma and solid tumours. Ectopic expression of these miRNAs in a mouse model of Burkitt's lymphoma led to accelerated and disseminated disease (He *et al.*, 2005).

1.5.4 RNAi in cancer research - experimental considerations *in vivo* and *in vitro*

Mammalian tissue culture and animal models have long since been used to study the genetic basis of cancer. The principal methods used, in order to gain knowledge of this complex biological process, are overexpression, deletion or mutation of genes. Cell culture experiments are particularly difficult for obtaining loss-of-function events. A mixed population of cultured cells contains two or more sets of chromosomes, and in most cases inactivation of a single allele will not produce a phenotypic change. A number of methods have been used for this purpose including chemical mutagenesis, antisense and ribozymes (Williams and Flitoff, 1995; Deiss and Kimchi, 1991). These

methods have proved time consuming and unpredictable. In the case of chemical mutagenesis, full-scale genetic screens may be required to detect multiple mutants in order to investigate a single phenotype. Loss-of-function events through expression of an antisense library are inefficient, as it is unlikely that a specific antisense or dominant-negative fragment could be generated for every gene in the genome. Animal models, though currently the best in vivo models of human disorders, are time consuming and expensive. They also rarely reflect the complexity of the disease in humans, with generation of simultaneous mutations beyond the reach of such systems.

With the ability to produce RNA interference for any transcript, RNAi would appear to be the solution to these problems. RNAi is a powerful tool for the generation of tissue culture or animal models with reduced expression of specific genes. However, before embarking on *in vivo* studies using RNAi many important factors need to be taken into consideration. These include site selection, compound design, controls, route of administration and use of a delivery system (Behlke, 2006). It is probable that many adverse effects will be observed *in vivo* using siRNA that may not have occurred in previous experiments using antisense and ribozymes. It is important to be aware of the life span of the chosen RNAi in *in vitro* and *in vivo* experiments. Extracellular degradation of siRNA peaks around 36 to 48hr after their introduction and begins to decrease after 96hr.The levels of silencing vary between species, cells and tissues due to differences in the efficiency with which the siRNAs are taken up by target cells. The duration of gene silencing varies greatly between cells with slow growing cells still showing the effects of siRNA after several weeks, but more rapidly dividing cells not seeing an effect for longer than 1 week (Ryther *et al.*, 2005). Also, the targeting of proteins with a long half-life may not produce the desired phenotypic effect because silencing at the level of transcription will not affect pre-existing proteins. Therefore RNAi has the optimal effect in proteins with a more rapid turnover (Pai *et al.*, 2006).

1.5.5 Targeting individual genes in vitro and in vivo

1.5.5.1 Angiogenesis

Vascular endothelial growth factor (VEGF) has long since been recognized as a key factor in the development and formation of novel blood vessels, and many therapeutic strategies are specifically aimed at VEGF inhibition. It is not surprising therefore that RNAi silencing of VEGF is seen as an attractive opportunity to interfere with

angiogenesis. siRNA was used to silence VEGF in RKO human colon cancer cells, resulting in a decrease in proliferation (Mulkeen *et al.*, 2006). Cationized gelatin delivery of a plasmid DNA expressing VEGF siRNA was used to silence VEGF successfully in vitro and in vivo. In vitro it knocked down expression of three different VEGF isoforms in mouse squamous cell carcinoma NRS-1, and in vivo a mouse model showed a marked reduction in vascularity accompanied by the inhibition of a VEGF siRNA transfected tumour (Matsumoto *et al.*, 2006).

1.5.5.2 Invasion

A characteristic feature of malignant neoplasm is invasion and metastasis. Despite advances in the management of many solid tumours, metastasis continues to be the most significant cause in cancer mortality. Many recent studies have demonstrated that RNAi is a viable approach to inhibit tumour growth and invasion/metastasis. Overexpression of RhoA or RhoC in breast cancer indicates a poor prognosis. This is due to increased tumour cell proliferation, invasion and increased tumour-dependent angiogenesis. A recent study has used siRNA to silence both RhoA and B in MDA-MB-231 breast cancer cells, resulting in a decrease in proliferation and invasion. In a nude mouse model intratumoral injections of these siRNAs almost totally inhibited the growth and angiogenesis of xenografted MDA-MB-231 tumours (Pille *et al.*, 2005). Another study focused on Urokinase plasminogen inhibitor (uPA) and its receptor (uPAR), both of which are essential for tumour cell invasion and metastasis. Silencing of inhibitor and receptor after siRNA transfection resulted in a decrease in invasion and angiogenic potential, and there was also an associated increase in apoptotic cells (Subramanian *et al.*, 2006). S100A4 is a protein which has only recently been associated with the promotion of invasion. A plasmid construct expressing shRNA specific to S100A4 was used to significantly reduce anaplastic thyroid tumours in nude mice. The study also showed tumour cells were sensitized to chemotherapy as a result of S100A4 knock-down (Shi *et al.*, 2006).

1.5.5.3 Apoptosis

The kinase Mirk/Dyrk1B was proven to mediate cell survival in pancreatic ductal adenocarcinoma through siRNA silencing. Transfection of Panc1 pancreatic cells with Mirk/Dyrk1B siRNA was sufficient to cause the induction of apoptosis (Deng *et al.*, 2006). Raf-1, a cytosolic serine-threonine kinase, also plays an important role in

apoptosis, along with tumour cell growth and proliferation. This gene has also been used as a siRNA target both in vitro and in vivo. In this study transfections were performed on a number of cell lines including HUVEC and MDA-MB-435 and results showed a 75% reduction in Raf-1 mRNA compared to control groups. *In vivo* studies showed a 60% decrease in tumour growth after injection with the siRNA (Leng *et al.*, 2005).

The above is a small example of some of the work that has been carried out using RNAi in cancer research. Thyroid carcinoma (Shi *et al.*, 2006), bladder cancer (Nogawa *et al.*, 2005), brain cancer (Boado, 2005), ovarian cancer (Noske *et al.*, 2006) and pancreatic cancer (Bhattacharyya, 2006) have all been the focus of similar studies carried out in the last twelve months.

1.5.6 Clinical use of RNAi

siRNA therapeutics are currently involved in a phase 1 trial of sirna-027 as a therapy for age-related macular degeneration (AMD). Patients have been given intravitreal doses of siRNA and follow up of up to 84 days has shown a dose-dependent improvement of sight. Importantly, the drug is safe and well tolerated (Quinlan, 2005). The same company are also developing an antiviral RNAi against hepatitis C. The treatment has been successful in animal models and is being taken to phase 1 trials this year.

Another company, Alnylam, has developed an intranasal siRNA that is effective against respiratory syncitial virus in mice, and they are also working on siRNA-based treatment for emerging flu strains (Bitko *et al.*, 2005). In March 2006, further research by Alnylam scientist demonstrated in primates, that a systemically delivered RNAi therapeutic can potently silence an endogenous disease-causing gene in a clinically relevant manner. Alnylam and collaborators showed silencing of the gene for apolipoprotein B (apoB), a protein involved in cholesterol metabolism, with clinically significant efficacy as demonstrated by reductions in levels of cholesterol and low-density lipoproteins (LDL) (Zimmermann *et al.*, 2006). In April 2006, Phase I clinical data was presented for ALN-RSV01. The drug was found to be safe and well tolerated when administered intra-nasally in two Phase I clinical studies. ALN-RSV01 is being evaluated for the treatment of respiratory syncytial virus (RSV) infection and is the first RNAi therapeutic in human clinical development for an infectious disease.

1.5.7 Specificity in experimental RNA interference

At present, the most common problem in the use of RNAi is the issue of off-target effects. One study showed that changes occurred in over 1000 genes following the introduction of a siRNA whose target was not expressed in the cell model (Persengiev *et al.*, 2004). This study points out the uncertainty of presuming RNAi elimination of target mRNA based on phenotypic effect alone. It is interesting to note that off-target effects are not observed when complete dsRNAs are introduced instead of synthetic siRNA in primitive organisms. In *C. elegans* expression of dsRNAs of 500 base pairs or more typically results in very efficient gene silencing, irrespective of the sequence of the target mRNA (Fire *et al.*, 1998). One explanation for this could be that endogenously derived siRNA are generated from the cleavage of dsRNA by Dicer and RISC, which may have a proofreading mechanism that protects against the silencing of endogenous genes (Pai *et al.*, 2006).

Local mRNA target structure can also influence siRNA efficacy. Structural accessibility is a critical parameter, with some sequences inaccessible to RNAi therapy due to physical hindrance by RNA-binding proteins or by complex secondary structures. This problem can be overcome by the use of computational analysis to define the structural constraints of the target RNA that are important for the design of effective siRNA species (Overhoff *et al.*, 2005).

Artefacts may be formed by introduced siRNA forming complexes with specific proteins. Although this process has not been confirmed in RNAi, it has previously been observed with antisense oligonucleotides (Chavany *et al.*, 1995). It is also possible that siRNAs can act like miRNAs. miRNAs do not require perfect homology to their target in order to be effective, therefore it is possible that a single siRNA can affect multiple mRNAs, resulting in off target effect at a protein level. Studies have shown that as little as 7 to 11 consecutive homologous bases between the 5' end of either siRNA strand to an mRNA can cause a reproducible reduction in transcript levels (Scacheri *et al.*, 2004; Jackson *et al.*, 2003).

There is also the problem of an immune response. When long stretches of double-stranded RNA are introduced into a cell they trigger an immune response to viral infection. The introduction of shorter 21-23 bp siRNAs seems to overcome this problem (Paddison *et al.*, 2002). However, there have been reports that high concentrations of synthetic or vector-based siRNA can trigger the interferon anti-viral response in sensitive cell lines (Bridge *et al.*, 2003; Sledz *et al.*, 2003). The absence of short over-

hangs, produced by the natural processing of miRNA, as well as the unconventional 5' termini (e.g. triphosphate) might explain the recognition of siRNA (expressed or transfected) as a foreign body (Marques and Williams, 2005). Interferon triggers the degradation of mRNA by inducing 2-5' oligoadenylate synthase, which in turn activates RNase L (Stark *et al.*, 1998). Interferon can also activate dsRNA-dependent protein kinase (PKR), which phosphorylates eIF2. Phosphorylation of the translation initiation factor eIF2 causes its inactivation and global inhibition of mRNA activation.

There is also the theory that high levels of exogenous siRNA can compete with and decrease the efficiency of miRNA, as both are recognized and processed by the same cellular factors (Gartel and Kandel, 2006).

It is clear that there are several artefacts that can arise from siRNA transfection, leading to a misleading result. The most common cause however, is due to siRNA delivery. Whether via transfection or viral transduction, siRNA delivery can result in temporary changes in the cell, and in more extreme cases cells may become resistant to conditions of delivery. Designing siRNAs with resistance to serum RNases without sacrificing biological activity is possible through chemical modification. siRNAs can be encased in cationic liposomes (Matsumoto *et al.*, 2006), lipid complexes (Santel *et al.*, 2006) and collagen complexes (Minakuchi *et al.*, 2004). They can also be coupled with antibodies to cell surface receptor ligands for cell-specific delivery (Schiffelers *et al.*, 2005).

These results emphasize the need for adequate controls in RNAi experiments. One of these is the inclusion of 'scrambled' siRNA, which is designed against a different target, or preferably lacks recognition to any target. However, the non-specific effects on gene expression are dependent upon siRNA concentration in a gene specific manner. Therefore it is possible that the non-specific effects of a given siRNA and a scrambled control differ because of varying transfection efficiencies or have different intercellular stabilities (Persengiev *et al.*, 2004).

The most accurate control for these experiments is to set up repeats targeting the same mRNA using different siRNA sequences. Responses elicited by multiple non-homologous siRNAs can therefore be assumed to be due to target suppression. An even more stringent control would be to examine the effects of multiple non-homologous siRNAs in different cell lines or animal models.

Aims of Thesis:

This thesis aimed to investigate how mRNA profiles changes in cancer cell lines following overexpression of eIF4E, eIF4Emut and erbB2, and to identify genes associated with *in vitro* invasion in lung and breast cell lines. This was to be approached as follows:

1. Generating cell lines over-expressing eIF4E and mutant eIF4E in mildly-invasive DLKP and non-invasive MCF7.

2. Characterising the resulting cell lines to determine: eIF4E expression, growth rate, chemotherapeutic drug resistance, and invasion status (adhesion and colony formation in soft agar was also examined in the case of MCF7 clones).

3. Microarray analysis of invasive eIF4E-overexpressing DLKP4E and DLKP4Emut; non-invasive eIF4E-overexpressing MCF74E, MCF74Emut and invasive MCF7H3erbB2.

4. Analysing the microarray results to determine eIF4E and erbB2 transfectant associated targets, which may contribute to the invasive phenotype.

5. siRNA silencing of chosen invasion targets to determine their functional significance in breast and lung cell lines.

6. Confirmation of siRNA silencing of specific targets at mRNA level using real-time PCR and at protein level using western blot analysis.

7. Performing invasion assays of cell lines post-siRNA transfection to examine the effect on invasive/non-invasive phenotypes.

Section 2.0

Materials and Methods

2.1 Preparation for cell culture

2.1.1 Water

Ultrapure water was used in the preparation of all media and 1x solutions. Pre-treatment, involving activated carbon, pre-filtration and anti-scaling was first carried out. The water was then purified by a reverse osmosis system (Millipore Milli-RO 10 Plus, Elgastat UHP). This system is designed to produce purified water from a suitable municipal water supply. The system utilises a semi-permeable reverse osmosis membrane to remove contaminants from the feed water. This results in water which is low in organic salts, organic matter, colloids and bacteria with a standard of 12-18 MΩ/cm resistance.

2.1.2 Glassware

Solutions pertaining to cell culture and maintenance were prepared and stored in sterile glass bottles. Bottles (and lids) and all other glassware used for any cell-related work were prepared as follows; all glassware and lids were soaked in a 2% (v/v) solution of RBS-25 (AGB Scientific) for at least 1 hour. This is a deproteinising agent which removes proteinaceous material from the bottles. Following scrubbing and several rinses in tap water, the bottles were washed twice by machine (Miele G7783 washer/disinfecter) using Neodisher GK detergent and sterilised by autoclaving. Waste bottles containing spent medium from cells were autoclaved, rinsed in tap water and treated as above. Glassware used for large-scale cell production were treated specially, as outlined in Section 2.2.4.1.

2.1.3 Sterilisation

Water, glassware and all thermostable solutions were sterilised by autoclaving at 121°C for 20 min under 15 p.s.i. pressure. Thermolabile solutions were filtered through a 0.22μm sterile filter (Millipore, millex-gv, SLGV-025BS). Low protein-binding filters were used for all protein-containing solutions. Acrodisc (Pall Gelman Laboratory, C4187) 0.8/0.2μm filters were used for non-serum/protein solutions.

2.1.4 Media Preparation

The basal media used during routine cell culture were prepared according to the formulations shown in Table 2.1.1. 10x media were added to sterile ultrapure water, buffered with HEPES (Sigma, H-9136) and $NaHCO_3$ (BDH, 30151) and adjusted to a pH of 7.45 - 7.55 using sterile 1.5M NaOH and 1.5M HCl. The media were filtered through sterile 0.22 μm bell filters (Gelman, 121-58) and stored in 500ml sterile bottles at 4°C. Sterility checks were carried out on each 500ml bottle of medium as described in Section 2.2.8.

The basal media were stored at 4°C up to their expiry dates as specified on each individual 10x medium container. Prior to use, 100ml aliquots of basal media were supplemented with 2mM L-glutamine (Gibco, 25030-024) and 5% foetal calf serum (PAA laboratories, A15-042) and this was used as routine culture medium. This was stored for up to 2 weeks at 4°C.

Table 2.1.1 Preparation of basal media

	DMEM (Dulbecco's Modified Eagle Medium) (mls) (Sigma, D-5648)	**Hams F12 (mls) (Sigma, N-6760)**
10X Medium	500	Powder
Ultrapure H_2O (UHP)	4300	4700
1M HEPES[1]	100	100
7.5% $NaHCO_3$	45	45

[1] The weight equivalent of 1M N- (2-Hydroxyethyl) piperazine-N'- (2-ethanesulfonic acid) (HEPES) was dissolved in an 80% volume of ultra-pure water and autoclaved. The pH was adjusted to 7.5 with 5M NaOH.

2.2 Routine management of cell lines

2.2.1 Safety Precautions

All routine cell culture work was carried out in a class II down-flow re-circulating laminar flow cabinet (Nuaire Biological Cabinet). Any work which involved toxic compounds was carried out in a cytoguard (Gelman). Strict aseptic techniques were adhered to at all times. Both laminar flow cabinets and cytoguards were swabbed with 70% industrial methylated spirits (IMS) before and after use, as were all items used in the experiment. Each cell line was assigned specific media and waste bottles and only one cell line was worked with at a time in the cabinet which was allowed to clear for 15min between different cell lines. The cabinet itself was cleaned each week with industrial detergents (Virkon, Antec. International; TEGO, T.H.Goldschmidt Ltd.), as were the incubators. A separate Laboratory coat was kept for aseptic work and gloves were worn at all times during cell work.

2.2.2 Cell Lines

The cell lines used during the course of this study, their sources and their basal media requirements are listed in Table 2.2.1. Lines were maintained in 25cm^2 flasks (Costar, 3050), 75cm^2 flasks (Costar, 3075) or 175cm^2 flasks (Nulge Nunc, 156502) at 37°C and fed every two to three days.

Table 2.2.1 Cell Lines used in study

Cell Line	Source	Media	Cell Type
DLKP	NCTCC	ATCC[1]	Poorly differentiated human Lung squamous carcinoma
DLKP4E	NCTCC	ATCC[1]	Clonal subpopulation of eIF4E cDNA transfected DLKP
DLKP4Emut	NCTCC	ATCC[1]	Clonal subpopulation of eIF4E mut cDNA transfected DLKP
DLKPpcDNA	NCTCC	ATCC[1]	Clonal subpopulation of pcDNA transfected DLKP
SKBR3	ATCC[2]	RPMI-1640[3]	Human breast, erbB2 positive
RPMI 2650	ATCC[2]	RPMI-1640[3]	Human nasal septum squamous carcinoma
RPMI Melphalin	NCTCC	RPMI-1640[3]	Melphalin resistant variant of RPMI 2650
MCF7	ATCC[2]	DMEM	Human Breast adenocarcinoma
MCF74E	NCTCC	DMEM	Clonal subpopulation of eIF4E cDNA transfected MCF7
MCF74Emut	NCTCC	DMEM	Clonal subpopulation of eIF4E mut cDNA transfected MCF7
MCF7pcDNA	NCTCC	DMEM	Clonal subpopulation of pcDNA transfected MCF7
MCF7H3	NCTCC	DMEM	Clonal subpopulation of MCF7
MCF7H3erb2	NCTCC	DMEM	Clonal subpopulation of MCF7H3 transfected with erbB2

ATCC[1] = Basal media consists of a 1:1 mixture of DMEM and Hams F12.
ATCC[2] = American Tissue Culture Collection.
NCTCC = National Cell and Tissue Culture Centre.
RPMI-1640[3] = Gibco,52400-025, supplemented with 10% FCS and 2mM L- Glutamine.

2.2.3 Subculture of Adherent Lines

During routine subculturing or harvesting of adherent lines, cells were removed from flasks by enzymatic detachment.

Cell culture flasks were emptied of waste medium and rinsed with a pre-warmed (37°C) trypsin/EDTA (Trypsin Versene - TV) solution (0.25% trypsin (Gibco, 25090-028), 0.01% EDTA (Sigma, E-5134) solution in PBS (Oxoid, BR14a)). The purpose of this was to inhibit any naturally occurring trypsin inhibitor which would be present in residual serum. Fresh TV was then placed on the cells (4ml/25cm^2 flask, 7ml/75cm^2 flask or 10ml/175 cm^2 flask) and the flasks incubated at 37°C until the cells were seen to have detached (5-10 min). The flasks were struck once, roughly, to ensure total cell detachment. The trypsin was deactivated by addition of an equal volume of growth medium (*i.e.* containing 5% serum). The entire solution was transferred to a 20ml sterile universal tube (Greiner, 201151) and centrifuged at 1,200 rpm for 3 min. The resulting cell pellet was resuspended in pre-warmed (37°C) fresh growth medium, counted (Section 2.2.5) and used to re-seed a flask at the required cell density or to set up an assay.

2.2.4 Cell Counting

Cell counting and viability determinations were carried out using a trypan blue (Gibco, 15250-012) dye exclusion technique.

1. An aliquot of trypan blue was added to a sample from a single cell suspension in a ratio of 1:5.
2. After 3 min incubation at room temperature, a sample of this mixture was applied to the chamber of a haemocytometer over which a glass coverslip had been placed.
3. Cells in the 16 squares of the four outer corner grids of the chamber were counted microscopically. An average number per corner was calculated with the dilution factor being taken into account and final cell numbers were multiplied by 10^4 to determine the number of cells per ml. The volume occupied by sample in chamber is 0.1cm x 0.1cm x 0.01cm *i.e.* 0.0001cm^3 (therefore cell number x 10^4 is equivalent to cells per ml). Non-viable cells were those which stained blue while viable cells excluded the trypan blue dye and remained unstained.

2.2.5 Cell Freezing

To allow long term storage of cell stocks, cells were frozen and cryo-preserved in liquid nitrogen at temperatures below –180°C. Once frozen properly, such stocks should last indefinitely.

1. Cells to be frozen were harvested in the log phase of growth (*i.e.* actively growing and approximately 50 - 70% confluent) and counted as described in Sections 2.2.5.
2. Pelleted cells were re-suspended in serum and an equal volume of a DMSO/serum (1:9, v/v) (Sigma, D-5879). This solution was slowly added dropwise to the cell suspension to give a final concentration of at least $5x10^6$ cells/ml. This step was very important, as DMSO is toxic to cells. When added slowly, the cells had a period of time to adapt to the presence of the DMSO, otherwise cells may have lysed.
3. The suspension was aliquoted into cryovials (Greiner, 122 278) which were quickly placed in the vapour phase of liquid nitrogen containers (approximately -80°C). After 2.5 to 3.5 hours, the cryovials were lowered down into the liquid nitrogen where they were stored until required.

2.2.6 Cell Thawing

1. Immediately prior to the removal of a cryovial from the liquid nitrogen stores for thawing, a sterile universal tube containing growth medium was prepared for the rapid transfer and dilution of thawed cells to reduce their exposure time to the DMSO freezing solution which is toxic at room temperature.
2. The cryovial was removed and thawed quickly under hot running water.
3. When almost fully thawed, the DMSO-cell suspension was quickly transferred to the media-containing universal.
4. The suspension was centrifuged at 1,200 rpm. for 3 min, the DMSO-containing supernatant removed, and the pellet re-suspended in fresh growth medium.
5. A viability count was carried out (Section 2.2.5) to determine the efficacy of the freezing/thawing procedures.
6. Thawed cells were then placed into $25cm^2$ tissue culture flasks with 7mls of the appropriate type of medium and allowed to attach overnight.
7. After 24 hours, the cells were re-fed with fresh medium to remove any residual traces of DMSO.

2.2.7 Sterility Checks

Sterility checks were routinely carried out on all media, supplements and trypsin used for cell culture. Samples of basal media were inoculated either into TSB (Oxoid CM129) (incubated at 20-25°C) or thioglycollate broth (Oxoid, CM173) (and incubated at 30-35°C). Both sets were incubated at their specific temperature for up to 2 weeks checking for turbidity and sedimentation. TSB supports the growth of yeasts, moulds and aerobes, while thioglycollate supports the growth of anaerobes and aerobes. Growth media (*i.e.* supplemented with serum and L-glutamine) were sterility checked at least 2 days prior to use by incubating samples at 37°C and checking as before.

2.2.8 *Mycoplasma* Analysis

Mycoplasma examinations were carried out routinely (at least every 3 months) on all cell lines used in this study.

2.2.8.1 Indirect Staining Procedure

In this procedure, *Mycoplasma*-negative NRK cells (a normal rat kidney fibroblast line) were used as indicator cells. These cells were incubated with supernatant from test cell lines and examined for *Mycoplasma* contamination. NRK cells were used for this procedure because cell integrity is well maintained during fixation. A fluorescent Hoechst stain was utilised which binds specifically to DNA and so will stain the nucleus of the cell in addition to any *Mycoplasma* DNA present. A *Mycoplasma* infection would thus be seen as small fluorescent bodies in the cytoplasm of the NRK cells and sometimes outside the cells.

1. NRK cells were seeded onto sterile coverslips in sterile Petri dishes (Greiner, 633185) at a cell density of $2x10^3$ cells per ml and allowed to attach overnight at 37°C in a 5% CO_2 humidified incubator.
2. 1ml of cell-free (cleared by centrifugation at 1,200 rpm for 3 min) supernatant from each test cell line was inoculated onto an NRK Petri dish and incubated as before until the cells reached 20 - 50% confluency (4 - 5 days).
3. After this time, the waste medium was removed from the Petri dishes, the coverslips washed twice with sterile PBS, once with a cold PBS/Carnoys (50/50) solution and fixed with 2ml of Carnoys solution (acetic acid:methanol-1:3) for 10 mins.

4. The fixative was removed and after air drying, the coverslips were washed twice in deionised water and stained with 2 mls of Hoechst 33258 stain (BDH) (50ng/ml) for 10 mins.

From this point on, work proceeded in the dark to limit quenching of the fluorescent stain.

1. The coverslips were rinsed three times in PBS.
2. They were then mounted in 50% (v/v) glycerol in 0.05M citric acid and 0.1M disodium phosphate.
3. Examination was carried out using a fluorescent microscope with a UV filter.

Prior to removing a sample for mycoplasma analysis, cells should be passaged a min. of 3 times after thawing to facilitate the detection of low level infection.

- Cells should be subcultured for 3 passages in antibiotic free medium (as antibiotics may mask the levels of infection).
- Cell lines routinely cultured in the presence of drugs should be sub-cultured at least once in drug free medium before analysis (some drugs such as adriamycin lead to background level of autofluorescence).
- Optimum conditions for harvesting supernatant for analysis occur when the culture is in log-phase near confluency and the medium has not been renewed in 2-3 days.

2.2.8.2 Direct Staining

The direct stain for *Mycoplasma* involved a culture method where test samples were inoculated onto an enriched *Mycoplasma* culture broth (Oxoid, CM403) - supplemented with 20% serum, 10% yeast extract (Oxoid L21, 15% w/v) and 10% stock solution (12.5g D-glucose, 2.5g L-arginine and 250mls sterile-filtered UHP). This medium optimised growth of any contaminants and incubated at 37°C for 48 hours. Sample of this broth were streaked onto plates of *Mycoplasma* agar base (Oxoid, CM401) which had also been supplemented as above and the plates were incubated for 3 weeks at 37°C in a CO_2 environment. The plates were viewed microscopically at least every 7 days and the appearance of small, "fried egg" -shaped colonies would be indicative of a mycoplasma infection.

2.3 Specialised techniques in cell culture

2.3.1 Miniaturised *in vitro* toxicity assays

2.3.1.1 *In vitro* toxicity assay experimental procedure

Due to the nature of the compounds tested in the assays, precautions were taken to limit the risks involved in their handling and disposal. All work involving toxic compounds was carried out in a Gelman "Cytoguard" laminar air flow cabinet (CG Series). All chemotherapeutic drugs used by this researcher were stored and disposed of as described in Table 2.3.1.

Table 2.3.1 Chemotherapeutic drugs used in study

Cytotoxic drug	Supplier	Inactivation	Storage
Vinblastine	David Bull Laboratories Ltd.	Autoclave	Store at 4^0C
Vincristine	David Bull Laboratories Ltd.	Autoclave	Store at 4^0C
Adriamycin	Farmitalia	Hyperchlorite inactivation followed by autoclaving	Store at 4^0C
VP16 (Etoposide)	Bristol-Meyers squib, Pharm. Ltd.	Incineration	Store at RT
Cisplatin	David Bull Laboratories Ltd.	Incineration	Store at RT
Taxol	Bristol-Meyers squib, Pharm. Ltd.	Incineration	Store at 4^0C

1. Cells in the exponential phase of growth were harvested by trypsinisation as described in Section 2.2.3.
2. Cell suspensions containing $1x10^4$ cells/ml were prepared in cell culture medium. Volumes of 100 µl of these cell suspensions were added in to 96 well plates (Costar, 3599) using a multichannel pipette. The plates were divided so that each variable was set up with 8 repeats and 12 variables per plate. A control lane, one to which no drug would be added, was included on all plates. Plates were agitated gently in order

to ensure even dispersion of cells over a given well. Cells were incubated overnight at 37°C in an atmosphere containing 5% CO_2.

3. Cytotoxic drug dilutions were prepared at their final concentration in cell culture medium. The plates were emptied of media and 100 µl volumes of the drug dilutions were added to each well using a multichannel pipette. Plates were mixed gently as above.
4. Cells were incubated for 6 days at 37°C and 5% CO_2. At this point the control wells would have reached approximately 80% confluency.
5. Assessment of cell survival in the presence of drug was determined by acid phosphatase assay (Section 2.3.1.4). The concentration of drug which caused 50% cell kill (IC_{50} of the drug) was determined from a plot of the % survival (relative to the control cells) versus cytotoxic drug concentration.

2.3.1.2 Assessment of cell number - Acid Phosphatase assay

1. Following the incubation period of 6 days, media was removed from the plates.
2 Each well on the plate was washed with 100 µls PBS. This was removed and 100 µls of freshly prepared phosphatase substrate (10mM *p*-nitrophenol phosphate (Sigma 104-0) in 0.1M sodium acetate (Sigma, S8625), 0.1% triton X-100 (BDH, 30632), pH 5.5) was added to each well. The plates were wrapped in tinfoil and incubated in the dark at 37°C for 2 hours.
3 The enzymatic reaction was stopped by the addition of 50 µls of 1M NaOH to each well.
4 The plate was read in a dual beam plate reader at 405 nm with a reference wavelength of 620 nm.

2.4 Analytical Techniques

2.4.1 Western Blot analysis

2.4.1.1 Sample preparation

Cells were grown in flasks until they reached 80-90% confluency. They were then trypsinised and centrifuged at 1,000 rpm. for 5 min. The pellet was washed in PBS and re-pelleted twice. The tube was inverted and drained of supernatant. Further treatment of the cell pellet depended on the type of extract required; lysed or sonicated.

2.4.1.1.1 Lysis of cell pellet

1ml of lysis buffer (PBS, 1% NP-40 (Sigma; N-3516), 1X protease inhibitors and 0.2mg/ml PMSF (Sigma, P7626)) was added to the pellet and left on ice for 20 min. A 100X stock solution of protease inhibitors consisted of 400mM DTT (Sigma, D5545), 1mg/ml aprotonin (Sigma, A1153), 1mg/ml leupeptin (Sigma, L2884), 1mg/ml soybean trypsin inhibitor (Sigma, T9003), 1mg/ml pepstatin A (Sigma, P6425) and 1mg/ml benzamidine (Sigma, B6506). If cell lysis had not occurred after 20 min the cells were subjected to sonication. Whole cell extracts were aliquoted and stored at -80°C.

2.4.1.1.2 Sonication of cell pellet

One protease inhibitor tablet from Complete™ Protease Inhibitor (Boehringer Mannheim, 1 697 498) was added to 2 mls UHP. This was then diluted 1/25 and 200 µls of this diluted solution was added to the pellet. The mix was sonicated in a Labsonic U (Braun) 2-3 times at a repeating duty cycle of 0.5s, while checking under a microscope to make sure all the cells had been lysed. Before loading on to an SDS-PAGE gel, 2 µls of the sonicated sample was removed and diluted to 10 µls with UHP for protein quantification. Sonicated cell extracts were either used immediately in Western analysis or were stored at –80°C.

2.4.1.2 Quantification of Protein

Protein levels were determined using the Bio-Rad protein assay kit (Bio-Rad; 500-0006) with a series of bovine serum albumin (BSA) (Sigma, A9543) solutions as standards. A stock solution of 25 mg/ml BSA was used to make a standard curve. 10 µl samples were

diluted into eppendorfs in a stepwise fashion from 0 – 2 mg/ml BSA. The Biorad reagent was first filtered through 3MM filter paper (Schleicher and Schuell, 311647) and then diluted 1/5 with UHP as it was supplied as a 5-fold concentrate. The diluted dye reagent (490 µls) was added to each standard and sample eppendorf and the mixtures vortexed. The 500 µl samples were diluted out in 100 µl aliquots onto a 96-well plate (Costar, 3599). After a period of 5 min to 1h, the OD_{570} was measured, against a reagent blank. From the plot of the OD_{570} of BSA standards versus their concentrations, the concentration of protein in the test samples was determined. From this, a relative volume for each protein sample was determined for loading onto the gels. Usually 10-20 µg protein per lane was loaded.

2.4.1.3 Gel electrophoresis

Proteins for Western blot analysis were separated by SDS-polyacylamide gel electrophoresis (SDS-PAGE). Resolving and stacking gels were prepared as outlined in Table 2.4.1 and poured into clean 10cm x 8cm gel cassettes which consisted of 1 glass and 1 aluminium plate, separated by 0.75cm plastic spacers. The plates were cleaned by first rinsing in RBS, followed by tap water and finally UHP. After drying, the plates were wiped down in one direction using tissue paper soaked in 70% Industrial Methylated Spirits (IMS). The spacers and comb used were also cleaned in this way. After these had dried, the resolving gel was poured first and allowed to set for 1 hour at room temperature. The stacking gel was then poured and a comb was placed into the stacking gel in order to create wells for sample loading. Once set, the gels could be used immediately or wrapped in aluminium foil and stored at 4°C for 24 hours.

1X running buffer (14.4g Glycine, 3.03g Tris and 1g SDS in 1L) was added to the running apparatus before samples were loaded. The samples were loaded onto the stacking gels, in equal amounts relative to the protein concentration of the sample. The loading buffer (Sigma, S-3401) was added directly at ½ volume to each of the test samples. The samples were loaded including 7µl of molecular weight colour protein markers (New England Biolabs, P7708S). The gels were run at 200V, 45mA for approximately 1.5 hours. When the bromophenol blue dye front was seen to have reached the end of the gels, electrophoresis was stopped.

Table 2.4.1 Preparation of electrophoresis gels

Components	Resolving gel (7.5%)	Resolving gel (12%)	Stacking gel
Acrylamide stock[1]	3.8 mls	5.25 mls	0.8 mls
Ultrapure water	8.0 mls	6.45 mls	3.6 mls
1.875M-Tris/HCl, pH 8.8	3.0 mls	3.0 mls	-
1.25M-Tris/HCl, pH 6.8	-	-	0.5 mls
10% SDS (Sigma, L-4509)	150 µls	150 µls	50 µls
10% Ammonium persulphate (Sigma, A-1433)	60 µls	60 µls	17 µls
TEMED (Sigma, T-8133)	10 µls	10 µls	6 µls

2.4.1.4 Western blotting

Following electrophoresis, the acrylamide gels were equilibrated in transfer buffer (25mM Tris, 192mM glycine (Sigma, G-7126) pH 8.3-8.5 without adjusting) for 10 min. Protein in gels were transferred onto PVDF membranes (Boehringer Mannheim, 1722026) by semi-dry electroblotting. Eight sheets of Whatman 3mm filter paper (Whatman, 1001824) were soaked in transfer buffer and placed on the cathode plate of a semi-dry blotting apparatus (Biorad). Excess air was removed from between the filters by rolling a universal over the filter paper. A piece of PVDF membrane, cut to the same size of the gel, was prepared for transfer (soaked for 30 secs. in methanol, 2 mins. in UHP and finally 5 mins. in transfer buffer) and placed over the filter paper, making sure there were no air bubbles. The acrylamide gel was placed over the PVDF membrane and eight more sheets of presoaked filter paper were placed on top of the gel. Excess air was again removed by rolling the universal over the filter paper. The proteins were

[1] Acrylamide stock solution consists of 29.1g acrylamide (Sigma, A8887) and 0.9g NN'-methylene bis-acrylamide (Sigma, 7256) dissolved in 60ml UHP water and made up to 100ml final volume. The solution was stored in the dark at 4°C for up to 1 month. All components were purchased from Sigma, SDS (L-4509), NH_4-persulphate (A-1433) and TEMED, N,N,N,N'-tetramethylethylenediamine (T-8133).

transferred from the gel to the nitrocellulose at a current of 34mA at 15V for 24-25 mins.

All incubation steps from now on, including the blocking step, were carried out on a revolving apparatus (Stovall, Bellydancer) to ensure even exposure of the blot to all reagents. The PVDF membranes were blocked for 2 hours at room temperature with fresh filtered 5% non-fat dried milk (Cadburys, Marvel skimmed milk) in Tris-buffered saline (TBS) with 0.5% Tween (Sigma, P-1379) pH 7.5. After blocking, the membranes were rinsed once in 1X TBS and incubated with 5 to 10 mls primary antibody. The specific conditions for each antibody are outlined in table 2.4.2 below. Bound antibody was detected using enhanced chemiluminescence (ECL).

Table 2.4.2 List of primary antibodies used for western blot analysis

Antibody	Dilution/ concentration	Supplier	Catalogue no.
eIF 4E (M)[1]	1/500	Transduction laboratories	610270
GAPDH (M)[1]	1/10,000	Abcam	ab 9482
HA tag (M)[1]	1/1000	Roche	1583816
α-tubulin (M)[1]	1/1000	Sigma	T 5168
THBS1 (M)[1]	1/500	Abcam	ab1823-250
TFPI (G)[3]	1/1000	Abcam	ab 9881-100
EGR1 (R)[3]	1/100	Santa Cruz	sc-110
RPS6KA3 (R)[3]	1/150	Abcam	ab18907-100

(M)[1] = Mouse anti-human IgG

(R)[2] = Rabbit anti-human IgG

(G)[3] = goat anti-human IgG

Table 2.4.3 List of secondary antibodies used for western blot analysis

Antibody	Dilution/ concentration	Supplier	Catalogue no.
Mouse	1/1000	Dako Cytomation	P0260
Rabbit	1/1000	Dako Cytomation	P0448
Goat	1/1000	Dako Cytomation	E0466

2.4.1.5 Enhanced chemiluminescence detection

Protein bands were developed using the Enhanced Chemiluminescence Kit (ECL) (Amersham, RPN2109) according to the manufacturer's instructions.

The blot was removed to a darkroom for all subsequent manipulations. A sheet of parafilm was flattened over a smooth surface, *e.g.* a glass plate, making sure all air bubbles were removed. The membrane was placed on the parafilm, and excess fluid removed. 1.5mls of ECL detection reagent 1 and 1.5mls of reagent 2 were mixed and covered over the membrane. Charges on the parafilm ensured the fluid stayed on the membrane. The reagent was removed after one minute and the membrane wrapped in cling film. The membrane was exposed to autoradiographic film (Boehringer Mannheim, 1666916) in an autoradiographic cassette for various times, depending on the signal (30s – 15 mins.). The autoradiographic film was then developed.

The exposed film was developed for 5min in developer (Kodak, LX24, diluted 1:6.5 in water). The film was briefly immersed in water and fixed (Kodak, FX-40, diluted 1:5 in water), for 5min. The film was transferred to water for 5 min and then air-dried.

2.4.1 Immunocytochemistry

2.4.2.1 Fixation of cells

For fixation, medium was removed from 6-wells plates, cells were rinsed 3 times with PBS A and then incubated at -20^{0}C for 7 minutes using ice-cold methanol. The methanol was then removed from the cells, which were allowed to dry at 37^{0}C for a few minutes and then stored at -20^{0}C until required.

2.4.2.2 Immunocytochemical procedure

The avidin-biotin-peroxidase complex (ABC) immunoperoxidase technique combined with the diaminobenzidine (DAB) visualisation procedure was employed to indicate primary antibody binding. The ABC method involves application of a biotin-labelled secondary antibody, followed by the addition of avidin-biotin-peroxidase complex which results in a high staining intensity due to the formation of an avidin-biotin lattice which contains several peroxidase molecules. The peroxidase enzyme reacts with DAB solution to give an insoluble, brown-colour precipitate. Therefore, observation of a brown precipitate following this procedure is indicative of primary antibody reactivity.

Cell preparations (6-well tissue culture plates) which had been previously fixed in methanol and frozen at -20^{0}C were allowed to thaw and equilibrate at room temperature. A grease pen (DAKO, S2002) was used to encircle cells in tissue culture plates to retain the various solutions involved. The cells were equilibrated in Tris-buffered saline (TBS) (0.05M Tris/HCl, 0.15M NaCl, pH 7.6) for 5 minutes. The slides were then incubated for 20 minutes at room temperature (RT) with either normal rabbit (DAKO, X092) or goat (DAKO, X0907) serum diluted 1:5 in TBS to block non-specific binding, depending upon the host source of the primary antibody in question. This was then removed and 25-30µl of optimally diluted primary antibody (Table 2.8.1) was placed on the cells. The slides and tissue-culture plates were placed on a tray containing moistened tissue paper and incubated at 37^{0}C for 2 hours or 4^{0}C overnight. The primary antibodies used in the study are listed in Table 2.8.1. The slides were then rinsed in TBS/ 0.1% Tween (Sigma, P-1379) for 5min x3 times, and then incubated for 30 min with a suitable biotinylated secondary antibody (rabbit anti-mouse immunoglobulins (DAKO, E354); goat anti-rabbit (DAKO, E0432) diluted 1:300 in TBS. The slides were rinsed as before and incubated with strepABComplex/Horse Radish Peroxidase (HRP) (DAKO, K377) for 30 min at RT, after which they were rinsed again in TBS/ 0.1% Tween for 5min x3 times. The cells were then incubated with a DAB solution (DAKO, S3000) for 10-15 min. The plates were then rinsed off with UHP water and counterstained with 2% methyl green solution, and samples mounted using a commercial mounting solution (DAKO, S3023).

2.4.3 RNA Analysis

2.4.3.1 Preparation for RNA Analysis

Due to the labile nature of RNA and the high abundance of RNase enzymes in the environment a number of precautionary steps were followed when analysing RNA throughout the course of these studies.

- All solutions (which could be autoclaved) that came into contact with RNA were all prepared from sterile ultra-pure water and treated with 0.1% diethyl pyrocarbonate (DEPC) (Sigma, D5758) before autoclaving (autoclaving inactivates DEPC), with the exception of Tris-containing solutions (DEPC reacts with amines and so is inactivated by Tris). The Tris-containing solutions were made with DEPC-treated ultra-pure water.
- Disposable gloves were worn at all times to protect both the operator and the experiment (hands are an abundant source of RNase enzymes). This prevented the introduction of RNases and foreign RNA/DNA into the reactions. Gloves were changed frequently.

2.4.3.2 RNA Isolation

Total RNA was extracted from cultured cell lines and plasmid-transfected cell lines. The size of the flasks varied, but the method remained the same.

A standard method of extracting RNA from cells was as follows: cells were seeded into 175cm^2 flasks (Nulge Nunc, 156502) at a density of approximately 2x10^6 per flask and allowed to attach and form colonies for 48-72 hours at 37^{0}C. The cells were trypsinised and the pellet was washed once with PBS. The cells were pelleted and lysed using 1ml of TRI REAGENT™ (Sigma, T-9424). The following procedure is that outlined in the protocol for TRI REAGENT™. The samples were allowed to stand for 5 mins. at room temperature to allow complete dissociation of nucleoprotein complexes. 0.2 mls of chloroform was added per ml of TRI REAGENT™ used and the sample was shaken vigorously for 15 sec and allowed to stand for 15 min at room temperature. The sample was centrifuged at 13000rpm for 15 mins. at 4°C in a microfuge. This step separated the mixture into 3 phases with the RNA contained in the colourless upper aqueous layer. The DNA and protein fractions resulting from the total RNA isolation were retained in

case they were required at some future date. The aqueous layer was transferred to a new Eppendorf and 0.5 mls of 100% isopropanol was added per ml of TRI REAGENT™ originally used. The sample was mixed and allowed to stand at room temperature for 10-15 min before being centrifuged again at 13000rpm for 10 min at 4°C. The RNA formed a precipitate at the bottom of the tube. The supernatant was removed and the pellet was washed with 1ml of 75% ethanol per ml of TRI REAGENT™ used and centrifuged at 4°C for 5 min at 13000rpm. The supernatant was removed and the pellet was allowed to air-dry for 10-15 mins. 20-30 µls of DEPC water was added to the RNA to resuspend the pellet.

2.4.3.3 RNA Quantitation

RNA was quantified spectrophotometrically at 260nm using the following formula:

$$OD_{260nm} \times \text{Dilution factor} \times 40 = \mu g/ml \text{ RNA}$$

An A_{260}/A_{280} ratio of 1.8-2 is indicative of pure RNA, although RNA with ratios from 1.7 – 2.1 were routinely observed and used in subsequent experiments. Partially solubilised RNA has a ratio of <1.6 (Ausubel *et al.*, 1991). The yield of RNA from most lines of cultured cells is 100-200µg/ 90mm plate (Sambrook *et al.*, 1989). In these studies 200 µg RNA per 175cm^2 flask was retrieved. RNA samples were diluted to 500 ng/ µl and stored at –80°C.

2.4.3.4 Micropipette Accuracy Tests

Accuracy and precision tests were carried out routinely on all micropipettes used in all steps of the RT-PCR reactions. The accuracy and precision of the pipettes was determined by standard methods involving repeatedly pipetting specific volumes of water and weighing them on an analytical balance. The specifications for these tests were supplied by Gilson.

2.4.3.5 Reverse-Transcription Polymerase Chain Reaction (RT-PCR) analysis of isolated RNA

2.4.3.5.1 Reverse Transcription of isolated RNA

Reverse transcriptase (RT) reactions were set up on benches using micropipettes, which were specifically allocated to this work.

To form the cDNA, the following reagents were mixed in a 0.5ml eppendorf (Eppendorf, 0030 121 023), heated to 72°C for 5 min and then chilled on ice.

2µl of a 5x buffer (100mM-Tris/HCl, pH 9.0, 50mM-KCl, 1% Triton X-100) (Sigma, P-2317)

1.2µl 25mM-$MgCl_2$ (Sigma, M-8787)

1µl oligo (dT) primers (1µg/µl)

1µl RNasin (40U/µl) (Sigma, R-2520)

0.4µl dNTPs (10mM of each dNTP) (Sigma, DNTP-100)

2µl total RNA (500ng/µl)

7.4µl DEPC water

To this, 4µl water and 1µl Moloney murine leukaemia virus-reverse transcriptase (MMLV-RT) (40,000U/µl) (Sigma, M-1302) were added. The solutions were mixed and the RT reaction was carried out by incubating the Eppendorfs at 37°C for 1 hour. The MMLV-RT enzyme was inactivated by heating to 95°C for 3 mins. The cDNA was stored at -20°C until required for use in PCR reactions as outlined in Section 2.4.3.5.2.

2.4.3.5.2 Polymerase Chain Reaction (PCR) amplification of cDNA

The cDNA formed in the above reaction was used for subsequent analysis by PCR

A standardised polymerase chain reaction (PCR) procedure was followed in this study. Standard Eppendorf tubes were used, as for the RT reactions. All reagents had been aliquoted and were stored at -20°C and all reactions were carried out in a laminar flow cabinet.

A typical PCR reaction contained the following:

9µl UHP

5µl 5x buffer (100mM-Tris/HCl, pH 9.0, 50mM-KCl, 1% Triton X-100)

2µl 25mM-$MgCl_2$

1µl each of first and second strand target primers[2] (250ng/ml)

1µl each of first and second strand endogenous control primer (250ng/ml) (β-actin)

10µl cDNA

Taq/dNTP mixture	1µl dNTPs (10mM each of dATP, dCTP, dGTP and dTTP)
	0.5µl of 5U/µl *Taq* DNA polymerase enzyme (Sigma, D-4545)
	18.5µl UHP

The samples were mixed by pipetting two or three times. A typical reaction would be:

	95°C for 3 min	-	denaturation
Taq/dNTP mixture added here			
30 cycles:	95°C for 30 sec.	-	denaturation
	X[3]°C for 30 sec.	-	annealing
	72°C for 30 sec.	-	extension
And finally,			
	72°C for 7 min.		extension

Following amplification, the PCR products were stored at 4°C for analysis by gel electrophoresis

2.4.3.5.3 Real Time-PCR

RNA was isolated (Section 2.4.3.2) cell and cDNA synthesised as per Section 2.4.3.5.1. The Taqman® Real time PCR analysis was preformed using the Applied BioSystems Assays on Demand PCR Kits, using primer probe pairs as outlined in table 2.4.3. Experiments were preformed in triplicate, following per manufacturer's instructions.

---

[2] All oligonucleotide primers used throughout the course of this thesis were made to order on an "Applied BioSystems 394 DNA/RNA Synthesiser" by Oswel DNA service, Lab 5005, Medical and Biological Services building, University of Southampton, Boldrewood, Bassett Cresent East, Southampton, SO16 7PX.

[3] Temperature dependent on primer type

Table 2.4.4: Applied BioSystems Assays on Demand primer probe pairs

Primer Pair	Supplier	Catalogue No.
TFPI	Applied Biosystems	HS01041344_m1
THBS1	Applied Biosystems	HS00962914_m1
EGR1	Applied Biosystems	HS00152928_m1
RPS6KA3	Applied Biosystems	HS00177936_m1
GAPDH	Applied Biosystems	4326317E-0309005
β-actin	Applied Biosystems	4326315E-0508007
eIF4E	Applied Biosystems	Hs00913390_m1

2.4.3.6 Electrophoresis of PCR products

A 2% agarose gel (Sigma, A-9539) was prepared in 1X TBE (10.8g Tris base, 5.5g Boric acid, 4 mls 0.5M EDTA, 996mls UHP) and melted in a microwave oven. After allowing to cool, 4 µls of a 10mg/ml ethidium bromide solution was added per 100mls of gel which was then poured into an electrophoresis apparatus (BioRad). Combs were placed in the gel to form wells and the gel was allowed to set.

4µl of 6X loading buffer loading buffer (50% glycerol, 1mg/ml bromophenol blue, 1mM EDTA) was added to 20µl PCR of each sample and this was run on the gel at 80-90mV for approximately 2 hours. When the dye front was seen to have migrated the required distance, the gel was removed from the apparatus and examined on a transilluminator and photographed.

2.4.3.7 Densitometric analysis

Densitometric analysis was carried out using the MS Windows 3.1 compatible Molecular Analyst software/PC image analysis software available for use on the 670 Imaging Densitometer (Bio-Rad. CA) Version 1.3. Developed negatives of gels were scanned using transmission light and the image transferred to the computer. The amount of light blocked by the DNA band is in direct proportion to the intensity of the DNA present. A standard area was set and scanned and a value was taken for the Optical Density (O.D.) of each individual pixel on the screen. The average value of this O.D.

(within a set area, usually cm^2) is normalised for background of an identical set area. The normalised reading is taken as the densitometric value used in analysis. As a result, these O.D. readings were unitless.

2.4.4 Plasmid DNA manipulation

pcDNA-eIF4E and its mutant pcDNA-eIF4E-S209 were kind gifts from Dr. Robert Schneider, New York University, USA (Cuestaet al, 2000). The pcDNA-eIF4E vectors code for a fusion protein between eIF4E and hemagglutin (HA epitope tag); this protein appears functionally equivalent to eIF4E (Pyronnet et al, 1999; Cuesta et al, 2000).

2.4.4.1 Transformation of Bacteria

100µl of competent JM109 bacterial cell suspension (Promega, L2001) was mixed with 20ng DNA and placed on ice for 40min after which the mixture was heat-shocked at 42°C for 90sec and then placed on ice for 3min. 1ml of LB broth ((10g Tryptone (Oxoid, L42), 5g Yeast Extract (Oxoid, L21) 5g NaCl (Merck, K1880814))/litre LB, autoclaved before use) was added to the competent cell suspension and incubated at 37°C for 40min. 400µl of this suspension was spread on a selecting agar plate (LB agar containing appropriate antibiotic conc.) and incubated overnight at 37°C. Single colonies, which grew on these selecting plates, were further streaked onto another selecting plate and allowed to grow overnight at 37°C.

2.4.4.2 Large scale plasmid preparation

A single colony was picked from a freshly streaked selective plate and used to inoculate a starter culture of 2-5ml LB medium containing 50µg/ml ampicillin. The culture was incubated at 37°C with vigorous shaking (~300rpm) for ~8hours.A 2ml sample of this suspension was added to 200mls of TB AMP (50µg/ml) and left to grow for 12-16 hours with vigorous shaking. The bacterial cells were harvested by centrifugation at 6000x g for 15 min at 4°C. Plasmid DNA was then extracted using the QIAGEN ® Endofree Plasmid Purification Kit (Qiagen, 12362). DNA concentration was determined by measuring the OD_{260nm}.

2.4.4.3 Restriction enzyme digestion of plasmid DNA

5 µls of each isolated plasmid sample was run out on a 2% agarose gel to check for degradation. Restriction digestion was then carried out to confirm orientation of the insert. All digestions were carried out using the recipe as outlined in Table 2.4.3.

Table 2.4.3 Standard DNA digestion mix

Component	Volume (µls)
DNA sample	10
undiluted enzyme	1
10X Multi-core reaction buffer (Promega, R9991)	1.5
UHP	2.5

All 15 µls were run out on a 1% agarose gel, together with 3 µls loading dye. From the banding patterns observed, the orientation of the insert was correctly discerned. From this information, samples were selected for large-scale plasmid preparation.

2.4.5 Transfection of mammalian cells with exogenous DNA

2.4.5.1 Optimisation of plasmid transfection protocol

Before full transfections involving the various DNA fragments into the different cell lines could proceed, transfection protocols were first optimised for each of the parameters involved. The DNA used was the pCH110 plasmid which codes for beta-galactosidase activity.

The target cell line was trypsinised in the usual fashion (Section 2.2.3) and set up in the container of interest (i.e. 24/6-well plate, 25-75 cm^2 flask) at several different cell concentrations, which were arbitrarily chosen. Following incubation overnight at 37°C, the cells were transfected according to the transfection protocol for the transfectant used. Only the volumes of transfectant and conc. of DNA were altered to ascertain the most efficient combination. Cells were transfected either in the presence of serum overnight or for four hours in the absence of serum, both at 37°C. After transfection, the cells were washed 2X with PBS and fixed by the addition of fix solution (0.4mls 25% glutaraldehyde (Sigma, G-7526), 10mls 0.5M Sodium Phosphate buffer (pH 7.3), 2.5mls 0.1 EGTA (pH 8.0)(Sigma, E-0396), 0.1mls 1.0M $MgCl_2$ (Sigma, M-8266),

37mls UHP) for 10 mins. The cells were then washed for 10 mins. in wash solution (40mls 0.5M Phosphate buffer (pH 7.3), 10mls 1.0M $MgCl_2$ (Sigma, M-8266), 20mg Sodium deoxycholate (Sigma, D-4297), 40µls Nonidet P-40 (Sigma I-3021), 160mls UHP). Staining was carried out on the cells using 2.5mls of stain solution (10mls rinse solution, 0.4mls X-gal (Sigma, B-4252) (25mg/ml in dimethylformamide), 16.5mg potassium ferricyanide (Sigma, P-8131), 16.5mg potassium ferrocyanide (Sigma, P-9387)) overnight at 37°C. After staining, the cells were washed with 10mls rinse solution and examined microscopically. Positive cells were those stained blue - the combination resulting in the most blue colonies was adjudged to be the most efficient association and was thereafter used for that cell line.

2.4.5.2 Transfection of DNA using FuGene® reagents

On the day prior to transfections, the cells to be transfected were plated from a single cell suspension (Section 2.2.3) and seeded into 25cm^2 flasks at 3x10^5 cells per flask. On the day of the transfection, the plasmids to be transfected were prepared along with the FuGene transfection reagents according to the manufacturers protocols (Roche, 11814443001 (1814443).

2.4.5.3 Estimation of transfection effect

For transient transfections 6 flasks were transfected and taken down in sets of two (for RNA and protein samples) at 24, 48 and 72 hours. To establish stable clones, single colonies of stably transfected cells were selected and isolated. Transfected cells were treated with Antibiotic G418 Disulfate salt (geneticin) (Sigma, G5018) 24 hours after transfection. G418 was added in increasing concentrations to transfected and untransfected cells until such a time that all of the untransfected cells died. The plasmids used had a geneticin-resistant gene, therefore, only those cells containing the plasmid will survive treatment with geneticin. In complete media, when the cells grew readily in this concentration of selecting agent, the concentration was increased step-wise to a final concentration of 800µg/ml. At this stage the cells were plated out in 96-well plates (Costar, 3596) at a clonal density of one cell/well. Clonal populations were propagated from these wells, as transfected cells were periodically challenged with geneticin to maintain stability of transfectants and prevent cross-contamination with non-transfected cells.

2.4.5 Invasion assay

2.4.6.1 Preparation of invasion chambers

Invasion assays were carried out using BD BioCoat™ Growth Factor Reduced MATRIGEL™ Invasion Chambers (BD Biosciences, 354483). Inserts were rehydrated as specified by manufacturers protocol. Cell suspensions were prepared in culture media containing 5% FCS at a concentration of 1 X 10^6 cells /ml. 500µl of Media containing the same concentration of FCS was added to the well of the BD Falcon™ TC Companion Plate. 100µl of cell suspension was then added into the insert. The invasion assays were then incubated for 48 hours at 37°C, 5% CO_2 atmosphere. For SKBR3 cell suspensions were prepared in culture media without serum, and 500ul of Media containing 10% FCS was added to the well of the BD Falcon™ TC Companion Plate. The invasion assays were then incubated for 72 hours at 37°C, 5% CO_2 atmosphere.

4.4.6.2 Measurement of cell invasion

2.4.6.2.1 Removal of non-invading cells

After incubation, the non-invading cells were removed from the upper surface of the membrane. The inner side of the insert was wiped with a wet swab (PBS soaked not UHP) while the outer side of the insert was stained with 0.25% crystal violet for 10 minutes and then rinsed in UHP and allowed to dry. Inserts were then viewed under the microscope.

2.4.6.2.2 Counting of invading cells

Cell counting was facilitated by photographing the membrane using an inverted microscope. The cells were observed at 200X magnification. Cells in the central fields of duplicate membranes were counted and an average count calculated from 10 counts per chamber. Data was expressed as the percentage invasion through the GFR Matrigel™ Matrix and membrane relative to the migration through the control membrane.

2.4.6 Extracellular Matrix Adherence Assays

2.4.7.1 Reconstitution of ECM Proteins

Adhesion assays were performed using the method of Torimura *et al.* (1999). Collagen type IV (Sigma C-5533), fibronectin (Sigma F-2006) and laminin (Sigma L-2020) were reconstituted in PBS to a stack concentration of 500 □g/ml. Stocks were aliquoted into sterile eppendorfs. Fibronectin and collagen stocks were stored at -20°C, while laminin stocks were stored at -80°C. Matrigel (Sigma E-1270) was aliquoted and stored at -20°C until use. Matrigel undergoes thermally activated polymerisation when brought to 20-40°C to form a reconstituted basement membrane.

2.4.7.2 Reconstitution of ECM Proteins

Collagen type IV (Sigma C-5533), fibronectin (Sigma F-2006) and laminin (Sigma L-2020) were reconstituted in PBS to a stack concentration of 500µg/ml. Stocks were aliquoted into sterile eppendorfs. Fibronectin and collagen stocks were stored at -20°C, while laminin stocks were stored at -80°C. Matrigel (Sigma E-1270) was aliquoted and stored at -20°C until use. Matrigel undergoes thermally activated polymerisation when brought to 20-40°C to form a reconstituted basement membrane.

2.4.7.3 Coating of Plates

Each of the ECM proteins, collagen, fibronectin and laminin, was diluted to 25µg/ml while matrigel was diluted to 1mg/ml with PBS. 250µl aliquots were placed into wells of a 24-well plate. The plates were gently tapped to ensure that the base of each well was completely covered with solution. The plates were then incubated overnight at 4°C. The ECM solutions were then removed from the wells and the wells rinsed twice with sterile PBS. 0.5ml of a sterile 0.1% BSA/PBS solution was dispensed into each well to reduce non-specific binding. The plates were incubated at 37°C for 20 minutes and then rinsed twice again with PBS.

2.4.7.4 Adhesion Assay

Cells were set up in 75cm^2 flasks and then harvested and resuspended in appropriate serum-free medium. The cells were then plated at a concentration of 2.5×10^4 cells per well in triplicate and incubated at 37°C for 60 minutes. Control wells were those which

had been coated but contained no cells. After 60 minutes, the medium was removed from the wells and rinsed gently with PBS. This was then removed and 200µl of freshly prepared phosphatase substrate (10mM *p*-nitrophenol phosphate (Sigma 104-0) in 0.1M sodium acetate (Sigma, S8625), 0.1% triton X-100 (BDH, 30632), pH 5.5) was added to each well. The plates were then incubated in the dark at 37°C for 2 hours. The enzymatic reaction was stopped by the addition of 100µl of 1N NaOH. 100µl aliquots were transferred to a 96-well plate and read in a dual beam plate reader at 405nm with a reference wavelength of 620nm.

2.4.8 Anoikis assay

Cells were subcultured as described in 2.2.3 and placed in 20ml of appropriate media at a concentration of 3 X 10^4 cells/ml. Cells were incubated in 50ml sterile test-tubes (Greiner bio-one, 210261) for 24 hours at 37°C and shaking. Cells were then counted as described in 2.2.5. The level of anoikis was assessed as the percentage cell death over 24 hours.

2.4.9 Soft agar assay

The agar for these assays was prepared as follows:
1.548g of agar (Bacto Difco, 214040) were dissolved in 100ml of ultra pure water and autoclaved. This agar was then melted in a microwave oven immediately prior to use and incubated at 44°C.

Table 2.4.9.1 : Agar Medium (AgM)

Components	Volume
2X media*	50ml
Pen/Strep	1ml
Foetal calf serum	10ml

*see table 2.2.1

The thermo-labile component Serum was added last to the AgM. 50ml of Agar was then added to the AgM, mixed well and quickly dispensed onto 35mm sterile Petri dishes (Lux Scientific Corp., 5217). The plates were allowed to set at room temperature and

the remaining AgM was returned to the water bath with the temperature reduced to 41°C.

Cells being assayed were harvested and resuspended in medium without serum, ensuring that a single cell suspension was obtained. The cells were diluted to give a concentration of 2 x 10^4 cells per ml in a total of 5ml. 5ml of agar was then added to each suspension, mixed well and 1.5ml was dispensed onto each pre-set agar plate. This was done in triplicate, giving a final concentration of 1.5 x 10^4 cells per plate. The plates were placed on trays containing a small volume of water to prevent the agar from drying out and incubated at 37°C, 5% CO_2 for 10 days.

After this time the colonies were counted using an inverted microscope at 40x. 10 areas were viewed per plate and the total number of colonies present was extrapolated from this. The percentage colony forming efficiency (CFE) was determined by expressing the number of colonies formed as a percentage of the number of cells plated.

2.5 Affymetrix GeneChips®

The microarray gene expression experiments which were performed in this body of work were performed using Affymetrix® GeneChips® Whole genone (Affymetrix, 900467). Affymetrix GeneChip probe microarrays are manufactured using technology that combines photolithography and combinatorial chemistry. Tens to hundreds to thousands of different oligonucleotide probes are synthesised and each of these oligonucleotides is located in a specific area on the microarray slide, called a probe cell. Each probe cell contains millions of copies of a given oligonucleotide and each feature size on the Affymetrix U133 plus 2.0 is 11 microns. The new U133 Plus 2 GeneChips are now comprised of the old Affymetrix U133A and U133B GeneChips on a single slide. The reduction in feature size to 11 microns has resulted in an increase in feature definition, with improved sharpness and signal uniformity.

The most important aspect in efficient probe design is the quality of the sequence information used. Probe selection and array design are two major factors in reliability, sensitivity, specificity and versatility of expression probe arrays. Probes selected for gene expression arrays by Affymetrix are generated from sequence and annotation data obtained from multiple databases such as GenBank, RefSeq and dbEST. Sequences from these databases are collected and clustered into groups of similar sequences. Using clusters provided by UniGene database as a starting point, sequences are further subdivided into subclusters representing distinct transcripts.

This categorisation process involves alignment to the human genome, which reveals splicing and polyadenylation variants. The alignment also extends the annotation information supplied by the databases pinpointing low quality sequences. These areas are usually trimmed for subsequent generation of high quality consensus sequences or alternatively Affymetrix employ quality ranking to select representative sequences, called exemplars, for probe design.

In general, Affymetrix use 11 to 16 probes which are 25 bases in length for each transcript. The probe selection method used by Affymetrix for their U133 GeneChips takes into account probe uniqueness and the hybridisation characteristics of the probes which allow probes to be selected based on probe behaviour. Affymetrix use a multiple linear regression (MLR) model in the probe design that was derived from thermodynamic model of nucleic acid duplex formation. This model predicts probe binding affinity and linearity of signal changes in response to varying target

concentrations. An advantage of this type of model-based probe selection system is that it provides a physical and mathematical foundation for systematic and large-scale probe selection. Also, an essential criterion of probe selection by Affymetrix for quantitative expression analysis is that hybridisation intensities of the selected probes must be linearly related to target concentrations.

A core element of Affymetrix microarray design is the Perfect/Mismatch probe strategy. For each probe that is designed to be perfectly complimentary to a given target sequence, a partner probe is also generated that is identical except for a single base mismatch in its center. These probe pairs, called the Perfect Match probe (PM) and the Mismatch probes (MM), allow the quantitation and subtraction of signals caused by non-specific cross-hybridisation. The differences in hybridisation signals between the partners, as well as their intensity ratios, serve as indicators of specific target abundance.

Table 2.5.1: Equipment required for Microarray experiment

ITEM	Catalogue no.	SUPPLIER
20X SSPE (CAMBREX)	US51214	CAMBREX
Anti-Strep Biotinylated Ab (Goat)	BA-0500	LABKEM
Wheaton 1L Sterile Bottles (Paul Hennessy)	219980	SHAW SCIENTIFIC
Herring Sperm DNA	D1816	MSC
10% Tween 20	28320	MSC
BSA	15561-020	BIOSCIENCES
R-Phycoerythro Streptavidin	S-866	BIOSCIENCES
GeneChip Human Genome U133 Plus 2.0 Array	900470	AFFYMETRIX
Test3 Array	900341	AFFYMETRIX
One-Cycle Target Labelling Kit	900493	AFFYMETRIX
Two-Cycle Target Labelling Kit	900494	AFFYMETRIX
0.5M EDTA	E7889	SIGMA
MES Free Acid Monohydrate	M5287	SIGMA
MES Sodium Salt	M3058	SIGMA
DMSO	D5879	SIGMA
Goat IgG	I5256	SIGMA
Sodium Hypochlorite	42,504-4	SIGMA
20X SSPE (SIGMA)	85637	SIGMA
5M NaCl	9759	AMBION
1.5ml Eppys	12400	AMBION
0.5ml Eppys	12300	AMBION

Rnase Zap	9780	AMBION
RNA ladder	7152	AMBION
0.5M EDTA	9260G	AMBION
Rnase-free UHP	9932	AMBION
5X Megascript T7 kit	1334 (or B1334-5)	AMBION
Rneasy Mini Kit	74106	QIAGEN
QIA Shredder	79656	QIAGEN
Eppendorf Eppy	0030-120-191	UNITECH
RNA 6000 Nano Labchip Kit	5065-4476	Carl Stuart Ltd.

2.5.1 Preparation of total RNA from cells using Rneasy Mini Prep Kit® (QIAGEN, 74104)

2 - 5 X 10^6 cells were harvested by centrifugation and washed with 1 X PBS to remove media. Cells were then lysed in 350µl buffer RLT (as supplied with kit) and homogenised by spinning in Qiashredder for 2 min at room temperature. 350µl of 70% ethanol was added and the cell lysate was applied to the RNeasy column. The column was spun three times at 8000 x g, washed with buffer RW1 and RPE (as supplied with kit). Finally the column was spun for 1 min at maximum speed to dry the pellet. RNA was eluted from the column with a total of 80µl of water. The concentration of RNA was calculated using the Nanodrop (see 2.5.2). Samples were read at OD_{A260}. 1µl of 1:5 dilution of the RNA was then run on Agilent Bioanalyser (see 2.5.4).

2.5.2 Using the Nanodrop to measure nucleic acids

Before applying the RNA sample the pedestal was wiped down using a lint-free tissue dampened with UHP. 1µl of UHP was then loaded onto the lower measurement pedestal. The upper sample arm was then brought down so as to be in contact with the solution. "Nucleic acid" was selected on the Nanodrop software to read the samples.

After the equipment was initialised the "blank" option was chosen, and after a straight line appeared on the screen the "measure" option was selected. All sample readings were automatically saved as tab delimited files which could be viewed using Microsoft excel. The upper and lower pedestals were cleaned with a clean dry wipe between samples. When finished, the pedestal was cleaned with a wipe dampened with UHP followed by drying with a dry wipe.

2.5.3 RNA 6000 Nano Assay.

2.5.3.1 Preparing the Gel

550 µl of RNA 6000 Nano gel matrix was added to a spin filter tube and centrifuged at 1500 g for 10 minutes. The filtered gel was then aliquoted in 65 µl amounts.

2.5.3.2 Sample Preparation

During the 10 minute spin, 2µl aliquots of the RNA samples and an RNA ladder were prepared in 0.5 µl RNAse free tubes, heated to 70 °C for 2 minutes and then cooled on ice.

2.5.3.3 Preparing the Gel Dye Mix

The dye concentrate was allowed to equilibrate to room temperature for 30 minutes before vortexing for 10 seconds. 1 µl of dye was then added to 65 µl of the filtered gel matrix. The solution was well vortexed and then spun in a centrifuge for 10 minutes at 13000 g.

2.5.3.4 Loading the Gel Dye Mix

A new chip was placed on the chip priming station and 9 µl of the gel dye mix was put in to the well marked with a bold **G**. The priming station was then closed and the plunger was pressed down until it was held in place by the clip. Exactly 30 seconds later the plunger was released. 9 µl of gel dye mix was put in to the remaining wells marked G.

2.5.3.5 Loading RNA 6000 Nano Marker

5 µl of RNA 6000 Nano Marker was put in to the well marked with the ladder and into all the 12 sample wells. Any unused wells had 6 µl of Nano Marker added.

2.5.3.6 Loading the sample and ladder

1 µl of sample was put in to each of the sample wells, and 1 µl of ladder was put in the well marked with the ladder. The chip was then placed in the special vortex adapter and vortexed at 2400 rpm for 1 minute. The chip was run on the Agilent Bioanalyzer within 5 minutes.

2.5.4 Running the Agilent 2100 bioanalyser

The Agilent 2100 Bioanalyser is a microfluidics-based platform for the analysis of proteins, DNA and RNA. The miniature chips are made from glass and contain a network of interconnected channels and reservoirs. The RNA 6000 Nano LabChip kit enables analysis of samples containing as little as 5ng of total RNA. The channels are firstly filled with a gel matrix and the sample wells with buffer or sample, there are 12 sample wells per chip. 1µl of each sample is loaded into a sample well along with a fluorescent dye (marker). An RNA ladder is loaded into another sample well for size comparison. When all the samples are loaded, the chip is briefly vortexed and loaded onto the bioanalyser machine (Figure. 2.5.1) for picture of chip). The machine is fully automated and electrophoretically separates the samples by injecting the individual samples contained in the sample wells into a separation chamber (Figure 2.5.2).

Figure 2.5.1 The RNA 6000 Nano chip

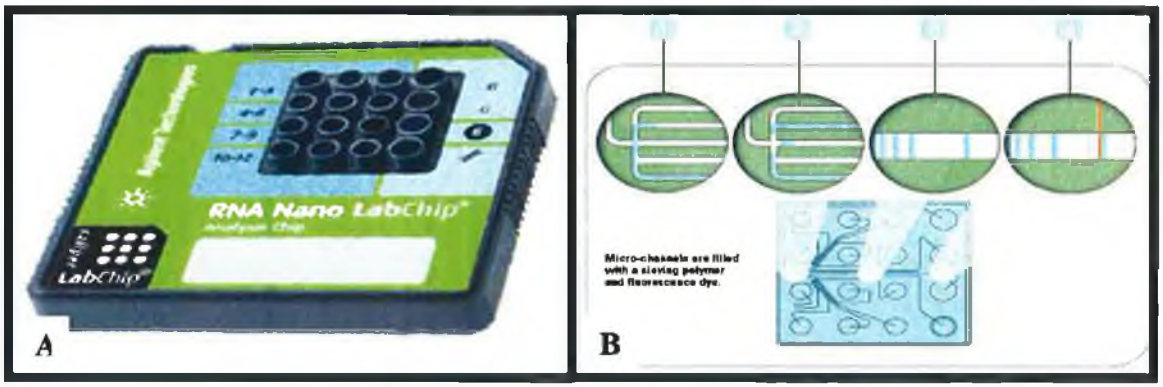

Figure 2.5.1 The RNA 6000 Nano chip, a picture of the front of the RNA Nano chip (A) and a diagram of the microchannels in the chip (B), the sample moves through microchannels (1) and is injected into separation chamber (2) were components are electrophoretically separated (3) and detected by their fluorescence and translated into gel-like images and electropherograms. Both pictures available from http://www.agilent.com/chem/labonachip..

The resulting data is presented as an electropherogram (Figure 2.5.2). The fluorescensce is measured on the Y-axis and the time in seconds is measured on the X-axis. The smaller fragments are detected first and are shown on the left-hand side of the electrophoreogram. Figure 2.5.2 (a) is an example of good quality cell RNA, the 18S

and 28S ribosomal RNA peaks are quite sharp and the 28S is higher than the 18S peak. As RNA degrades, the 28S RNA peak decreases and smaller fragments are visible. An example of slightly degraded cell RNA is shown in Fig. 2.5.2 (b). The 28S peak is smaller than the 18S peak and an extra peak is visible at approximately 25 seconds. This peak represents the fragmented RNA.

Figure 2.5.2 Examples of electrophoreograms generated using the Agilent Bioanalyser.

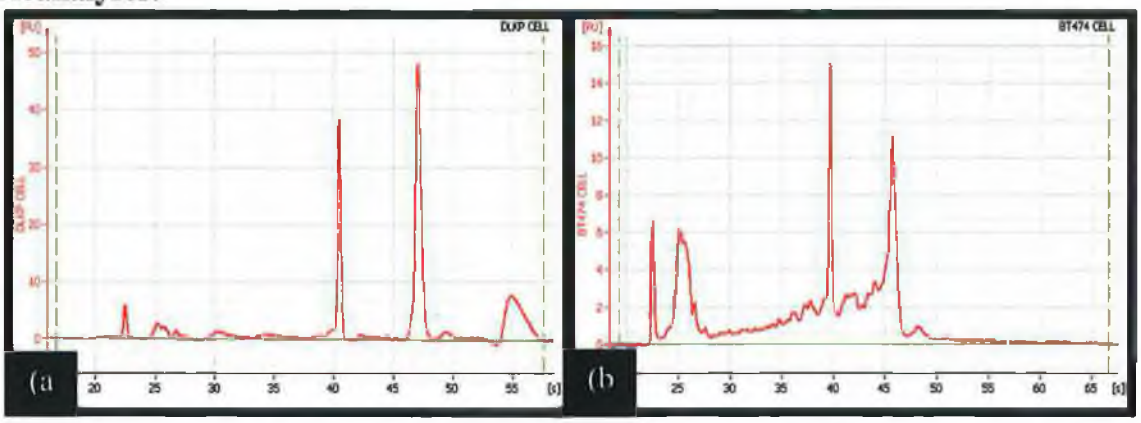

Figure 2.5.2: Examples of electrophoreograms generated using the Agilent Bioanalyser. (a) intact DLKP cell RNA as evident by the sharp 18S and 28S ribosomal bands, (b) slightly degraded BT474 cell RNA as evident by the extra peak at approximately 20secs indicating the presence of smaller fragments of RNA.

2.5.5 cDNA synthesis from Total RNA

After RNA isolation, quantification and purification using the Qiagen Rneasy® isolation method (Section 2.5.1), cDNA was synthesised using the GeneChip® One-Cycle cDNA Synthesis Kit from 10µg total RNA.

Table 2.5.5.1 cDNA reaction for total RNA (10µg)

First strand synthesis:	**volume(µl)**
RNA + Rnase free water	7
Diluted poly-A RNA controls	2
T7/T24 Primer (50pMol/µl)	2
70^{0}C for 10 min.	
Cooled to 42^{0}C.	
5 X 1st strand buffer.	4
0.1M DTT.	2
10mM dNTP's	1
42^{0}C for 2 min.	
Superscript II	2
42^{0}C - 1 hr spin/ice	
Second strand synthesis:	
(< 90 min on ice)	
water	91
5 X 2nd strand buffer	30
10mM dNTP's	3
E.coli DNA Ligase	1
RNaseH	1
E.coli DNA polymerase I	4
130µl of second strand master mix was added to each of the first strand synthesis samples.	
16^{0}C for 2 hr (thermocycler)	
2µl T4 DNA polymerase added	
16^{0}C for 5 min.	
10µl 0.5M EDTA added to stop reaction	
Spin/ice	

2.5.6 Sample cleanup module (SCM) cDNA cleanup

Sample cleanup was carried out using GeneChip Sample Cleanup module (Affymetrix, 900371).600µl of cDNA binding buffer was aliquoted in to a 1.5ml eppendorf. The cDNA was added and mixed thoroughly. 500µl was then transferred to a cDNA cleanup spin column and spun for 1 min at 8000 x g. The flow through was discarded and the remaining 262µl was added and spun for 1 min at 8000 x g. The column was transferred to a new 2ml tube and 750µl of cDNA wash buffer was added. Again, the column was spun for 1 min at 8000 x g and the flow through was discarded. The membrane was dried by spinning for 5 min at the maximum speed. The column was placed in a new 1.5ml eppendorf and 14µl of cDNA elution buffer was added directly to the membrane. This was incubated for 1 min at room temperature and spun for 1 min at maximum speed to elute.

2.5.7 cRNA synthesis from cDNA IVT Amplification

Table 2.5.7.1 cRNA synthesis from cDNA IVT Amplification

Add together in a 1.5ml eppendorf	Volume (µl)
▪ Template cDNA(total RNA 8.1 to 15µg)	6
▪ Water	14
▪ 10X IVT labelling buffer	4
▪ IVT labelling NTP mix	12
▪ IVT labelling enzyme mix	4
▪ 37°C overnight (16 hours)	

2.5.8 cRNA Cleanup

Sample cleanup was carried out using GeneChip Sample Cleanup module (Affymetrix, 900371). For cleanup, all steps were preformed at room temperature. The following were added to cRNA (from 2.5.7):

Water - 60µl (sample was vortexed for 3 seconds)
IVT cRNA Binding Buffer - 350µl (sample was vortexed for 3 seconds)
Ethanol - 250µl (Sample was mixed by pipetting)

The sample was then put into a cRNA cleanup spin column and spun for 15 min at 8000 x g. The flow through was discarded and the column transferred to a new 2ml tube.500µl of cRNA wash buffer was added and the column spun for 15 min at 8000 x g. The flow through was discarded, 500µl of 80% Ethanol was added to column and it was spun for 15 min at 8000 x g. The column was spun for 5 min at maximum speed to dry membrane. The column was transferred to a 1.5ml collection tube,11µl water was added directly to membrane, and it was spun for 1 min at maximum speed. This step was then repeated before the sample was run on the Agilent Bioanalyser and concentration determined using the nanodrop (Read at A260, 1:100 dilution; in duplicate).

2.5.9 Hybridisation of cRNA to chip

Fragmentation reaction (15µg cRNA in 1.5ml eppendorf)	Volume (µl)
▪ cRNA and water	24
▪ 5X Fragmentation buffer	6
Incubate 35 min at 95^0C	

Hybridisation reaction

(Added as a cocktail - 270µl each)

• Herring sperm DNA	3
• Acetylated BSA	3
• 2X Hybridization buffer	150
• Water	114

Prewet chips

- Added 250µl 1X hybridisation buffer
- Rotated 15 min at 45^0C, 60 rpm.
- Removed buffer

Hybridise chips

- Preheated hybridisation solution - 5 min at 95^0C
- 45^0C (for >5min)
- Rotated overnight (16hours) at 45^0C, 60 rpm.

2.5.10 Fluidics on chip

The fluidics station was primed and the hybridisation solution was removed from chips. The chips were then filled with 200µl non-stringent buffer.

Table 2.5.10.1 Preparation of SAPE solution

SAPE solution (stains 1 & 3)	volume (µl)
2X diluent	600
50mg/ml Acetyl BSA	48
1mg/ml SAPE	12
Water	540
Total/chip	1200

Table 2.5.10.2 Preparation of Antibody solution

Ab solution (stain 2)	volume (µl)
2X diluent	300
50mg/ml BSA	24
10mg/ml normal goat IgG	6
0.5mg/ml biotin-α-streptavidin IgG	3.6
Water	266.4

The SAPE and Ab solutions were added to the fluidics station and the fluidics protocol was run on the selected chips (EukGEvs450 for U133 Plus 2.0 chips). The Affymetrix Genechip Operating Software (GCOS) managed the fluidics protocol. All relevant data from the fluidics was stored in the Report file (*.RPT) for each chip.

2.5.11 Chip Scanning

The chips were placed in the scanner and scanned. As for the fluidics, GCOS managed the scanning protocol. The scan generated an initial image file (*.DAT) that contained the values for each gene probe. As there were 11 probes for each gene (one probeset), these values were averaged out into another file that was generated automatically by

GCOS (*.CEL). The user then asked GCOS to generate another file from the .CEL file which contained numerical values for each probeset (*.CHP). Finally, a quality control report file (*.RPT) was generated which was used to check the reliability/QC of each sample.

2.5.12 Microarray Data Normalisation

After the scans from individual chips were generated, the individual pixels were qualified. Following this data for each gene is quantified and whole data is normalised. The purpose of data normalisation is to minimise the effects of experimental and technical variation between microarray experiments so that meaningful biological comparisons can be drawn from the data sets and that real biological changes can be identified among multiple microarray experiments. Several approaches have been demonstrated to be effective and beneficial. However, most biologists use data scaling as the method of choice despite the presence of other alternatives. In order to compare gene expression results from experiments performed using microarrays, it is necessary to normalise the data obtained following scanning the microarray chips. There are two main ways in which this type of normalisation is performed, the first of which is 'Per-chip' normalisation. This type of normalisation helps to reduce minor differences in probe preparation and hybridisation conditions which may potentially result in high intensity of certain probe sets. These adjustments in probe intensity are made to set the average fluorescence intensity to some standard value, so that all the intensities on a given microarray chip go up or down to a similar degree. However, this type of normalisation should only be performed on microarrays using similar cell or tissue types. One drawback from this of normalisation is that some aspects of the microarray data may potentially be obscured, such as whether the RNA samples or the probe preparation steps were equivalent for each sample.

The second way in which most biologist normalise their data sets is by employing 'per gene' normalisation method. The main aim of microarray experiments is to identify genes whose expression changes in different conditions, be that tracking gene changes across a temporal experiment or when comparing gene expression between normal and diseased tissue. Therefore, it is necessary to normalise microarray data sets using 'per gene' normalisation. In 'Per gene' normalisation is necessary to find genes that have similar expression pattern across an experiment. Analysis of raw data from microarray

experiments is useful for identifying genes that are expressed at the same level, for example, genes that are highly abundant in the samples.

The data from each of the chips in this experiment were scaled to 100. This means that the trimmed mean of each chip was scaled to 100 so that direct comparisons between chips could be made.

2.5.13 Detection call

Affymetrix have a system that analyses the raw data and assigns a "presence" or "absence" call to each gene on the array. This analysis generates a Detection *p*-value which is evaluated against user-definable cut-offs to determine the Detection call. This call indicates whether a transcript is reliably detected (Present) or not detected (Absent). Additionally, a Signal value is calculated which assigns a relative measure of abundance to the transcript. Percent Present (%P) values depend on multiple factors including cell/tissue type, biological or environmental stimuli, probe array type, and overall quality of RNA. Replicate samples should have similar %P values.

Each probe pair in a probe set is considered as having a potential vote in determining whether the measured transcript is detected (Present) or not detected (Absent). The vote is described by a value called the Discrimination score [R]. The score is calculated for each probe pair and is compared to a predefined threshold Tau. Probe pairs with scores higher than Tau vote for the *presence* of the transcript. Probe pairs with scores lower than Tau vote for the *absence* of the transcript. The voting result is summarized as a *p*-value. The greater the number of discrimination scores calculated for a given probe set that are above Tau, the smaller the *p*-value and the more likely the given transcript is truly Present in the sample. The *p*-value associated with this test reflects the confidence of the Detection call.

The Discrimination score is a basic property of a probe pair that describes its ability to detect its intended target. It measures the target-specific intensity difference of the probe pair (PM-MM) relative to its overall hybridization intensity (PM+MM):

$$\mathbf{R = (PM - MM) / (PM + MM)}$$

For example, if the PM is much larger than the MM, the Discrimination score for that probe pair will be close to 1.0. If the Discrimination scores are close to 1.0 for the majority of the probe pairs, the calculated Detection *p*-value will be lower (more significant). A lower *p*-value is a reliable indicator that the result is valid and that the probability of error in the calculation is small. Conversely, if the MM is larger than or

equal to the PM, then the Discrimination score for that probe pair will be negative or zero

The next step toward the calculation of a Detection *p*-value is the comparison of each Discrimination score to the user-definable threshold Tau. Tau is a small positive number that can be adjusted to increase or decrease sensitivity and/or specificity of the analysis (default value = 0.015). The One-Sided Wilcoxon's Signed Rank test is the statistical method employed to generate the Detection *p*-value. It assigns each probe pair a rank based on how far the probe pair Discrimination score is from Tau.

The user-modifiable Detection *p*-value cut-offs, Alpha 1 (α1) and Alpha 2 (α 2) provide boundaries for defining Present, Marginal, or Absent calls. At the default settings, determined for probe sets with 16–20 probe pairs (defaults α 1 = 0.04 and α 2 = 0.06), any *p*-value that falls below α 1 is assigned a Present call, and above α 2 is assigned an Absent call. Marginal calls are given to probe sets that have *p*-values between α 1 and α 2. The *p*-value cut-offs can be adjusted to increase or decrease sensitivity and specificity.

2.5.14 dCHIP

DNA-Chip Analyzer (dChip) is a software package implementing model-based expression analysis of oligonucleotide arrays (Li and Wong, 2001) and several high-level analysis procedures. This model-based approach allowed probe-level analysis on multiple arrays. By pooling information across multiple arrays, it was possible to assess standard errors for the expression indexes. In this normalisation procedure an array with median overall intensity was chosen as the baseline array against which other arrays were normalised at probe level intensity. Subsequently a subset of PM probes, with small within-subset rank difference in the two arrays, served as the basis for fitting a normalisation curve. This approach also allowed automatic probe selection in the analysis stage to reduce errors due to cross-hybridizing probes and image contamination. High-level analysis in dChip included comparative analysis and hierarchical clustering. Gene filters employed for this analysis included a raw value difference of at least 100, and a fold change of at least 1.2. After these filters are in place and the relevant genes have been removed, a T-test is carried out to generate p-values for each probe. Only p-values of less than 0.05 were accepted.

This normalisation was downloaded from (http://dchip.org/) along with other data analysis modules.

2.5.15 Microsoft access

This is a database-building package that was used in analysis to compare different gene lists. Access allowed comparison of like genes across multiple lists. It allowed comparison of genes and also relevant information such as probe sets, difference of mean and p-value.

2.5.16 Stanford University on-line gene list comparison tool.

This web page allowed comparison of two list of genes. It was useful because unlike Access it identified not only common genes, but genes present in one list but not in the other. It was located at: http://worm-chip.stanford.edu/~jiml/Compare.html.

2.5.17 GenMAPP

GenMAPP is a free computer application designed to visualize gene expression and other genomic data on maps representing biological pathways and groupings of genes.

A MAPP is a GenMAPP-produced file format that showed biological relationships between genes or gene products. MAPPs could be used to group genes and view data by any organizing principle. Examples of the types of MAPPs represented in GenMAPP are metabolic pathways, signal transduction cascades, subcellular locations, or gene families. GenMAPP automatically linked each gene on a MAPP to data from gene expression experiments which had been imported.

Integrated with GenMAPP were programs to perform a global analysis of gene expression or genomic data in the context of hundreds of pathway MAPPs and thousands of Gene Ontology Terms. MAPPFinder created a global gene-expression profile across all areas of biology by integrating the annotations of the Gene Ontology (GO) Project with GenMAPP. The results were displayed in a searchable browser, allowing rapid identification of GO terms with over-represented numbers of gene-expression changes. Clicking on GO terms generated GenMAPP graphical files where gene relationships could be explored and annotated.

GenMAPP was downloaded from http://www.genmapp.org/introduction.asp

2.5.18 Pathway Assist ®

PathwayAssist is a product aimed at the visualisation and analysis of biological pathways, gene regulation networks and protein interaction maps. It comes with a

comprehensive database that gives a snapshot of all information available in PubMed, with the focus on pathways and cell signalling networks.

This product was useful in assisting in the interpretation of Microarray results. It allowed visualisation of results in the context of pathways, gene regulation networks and protein interaction maps. This was done using curated and automatically created pathways. Graph drawing, layout optimisation, data filtering, pathway expansion and classification and prioritization of proteins were all possible. PathwayAssist worked by identifying relationships among genes, small molecules, cell objects and processes and built pathways based on these relationships (Figure 2.5.3; 2.5.4).

Figure 2.5.3: Pathway Assist® 'nodes'

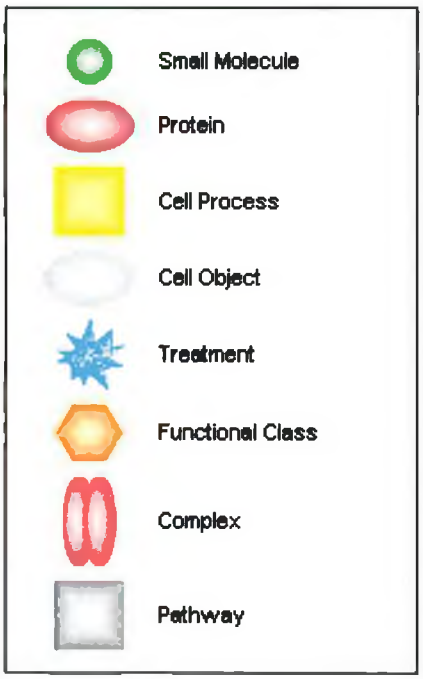

There are 8 different types of 'nodes' and each is represented in a unique graphical form. Each 'node' is clickable to view the annotation information. This includes the molecule name, alias, description, HUGO ID, Swiss Prot ID, MGI ID, OMIM ID, Locuslink ID, RGD ID, Unigene ID, Gene Ontolology terms, and organism name.

Figure 2.5.4: Pathway Assist® 'controls'

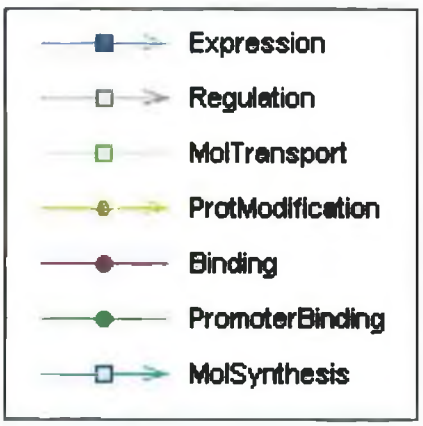

'Controls' are represented as arrows with different colors in the network, each representing a type of control/interaction. The 9 'control' types are shown.The dots on each 'control' arrow is clickable to obtain the description of an interaction and the relevant MedLine articles.

2.5.19 Probe Logarithmic Intensity ERror estimation (PLIER)

The PLIER algorithm (http://www.affymetrix.com) is a new tool introduced by Affymetrix for the use in data analysis of their GeneChips and has replaced the need to normalise microarray data by using the 'per chip' and 'per gene' normalisation methods. This algorithm incorporates model-based expression analysis and non-linear normalisation techniques. PLIER accounts for differences in probes by means of a parameter termed "probe affinity". Probe affinity is a measure of how likely a probe is to bind to a complimentary sequence, as all probes have different thermodynamic properties and binding efficiencies. Probe affinities determine the signal intensities produced at a specific target concentration for a given probe, and are calculated using experimental data across multiple arrays. By accounting for these observed differences, all the probes within a set can be easily compared. An example of how the PIER algorithm works is if one probe is consistently twice as bright as other probes with in a set, PLIER appropriately scales the probe intensities. In the case of a probe set, this enables all set numbers to be compared and combined accurately.

PLIER also employs an error model that assumes error is proportional to the probe intensity rather that of the target concentration. At high concentrations, error is approximately proportional to target concentration, since most of the intensity is due to target hybridisation signal. However, at the low end, error is approximately proportional to background hybridisation intensity, which is the largest component of the observed intensity. Due to this effect, it is inaccurate to treat errors as a proportion of target concentration in all circumstances. The PLIER error model smoothly transitions between the low end, where error is dependent upon background, and the high end, where error is dependent on signal.

The PLIER algorithm supports a multi-array approach that enables replicate sample analysis. PLIER ensures consistent probe behaviour across experiments to improve the quality of results in any one given experiment and helps to discount outliers. Benefits of this algorithm include an improved coefficient of variation of signals from probe sets while retaining accuracy. Also higher differential sensitivity for low expressors maybe achieved using PLIER.

2.5.20 Genomatix Software Suite

One company that is providing software that allows users to explore textual data as well as combine sequence analysis, and genome annotation in order to help researchers to

discover new contexts from biological data; is Genomatix (www.genomatix.de). The analysis offered by Genomatix software is aimed to help researchers gain a better understanding of gene regulation at the molecular level. The Genomatix software suite is comprised of six main tools: ElDorado, Gene2Promoter, BiblioSphere, GEMS Launcher, MatInspector and PromtoerInspector. ElDorado is a gene orientated genome search engine which provides the user with information about functional genomic elements within a specific region of the genome. This piece of software compiles and integrates information from several sources and includes functional information, synonyms and information on gene function and regulatory pathway. In addition, information on mRNAs, their exon/intron structure and coding sequences, single nucleotide polymorphisms (SNPs) and potential promoter regions maybe retrieved using ElDorado.

Since co-regulation of gene transcription often originates from common promoter elements the identification and characterization of these elements provides a more in-depth analysis for expression of microarray clusters. Gene2Promoter allows users to automatically extract groups of promoters for genes that may of interest. This piece of Genomatix software provides access to promoter sequences of all genes annotated in available genomes. Results from Gene2Promoter are presented in a graphical format and common transcription factor binding sites are high lighted along the gene input sequence.

One powerful member of the Genomatix Software Suite, which illustrates the emerging emphasis on the visual presentation of complex data, is BiblioSphere. BiblioSphere is a data-mining tool for extracting and studying gene relationships from literature databases and genome-wide promoter analysis. The data-mining strategy allows to find direct gene-gene co-citations and even yet unknown gene relations via interlinks. BiblioSphere data is displayed as 3D interactive view of gene relationships (Figure 2.5.5). Results can be classified by tissue, Gene Ontology and MeSH. Statistical rating by z-scores indicates over- and under-representation of genes in the referring biological categories.

Figure 2.5.5 Screen shot of BiblioSphere

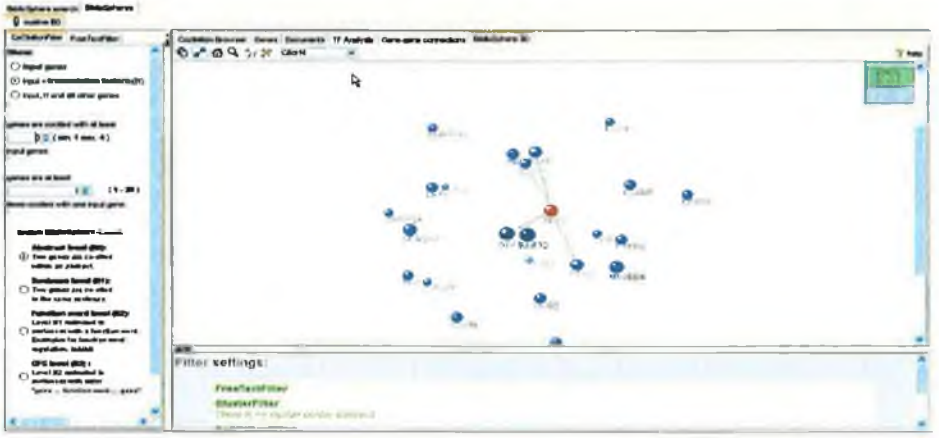

Although transcription is regulated by a variety of DNA sequences, including enhancer and matrix attachment regions, promoters can be seen as the most important part of the sequence because any activator or repressor has to act on the promoter to influence transcriptional initiation of a particular gene. Promoters are DNA regions of several hundred base pairs that contain the transcription start site of genes. The most important functional elements within promoters are binding sites for specific proteins called transcription factors. The control of gene transcription is a common method used in biological systems to regulate protein expression. Transcription regulation in eukaryotes depends on a series of complex signal transduction networks that control gene promoter activity (Figure 2.5.6). Genomatix have develop a software packages, GEMS Launcher with helps researchers to identify transcription factor binding sites in a given gene promoter. GEMS Launcher is divided up into several parts, the first of which is MatInspector.

Figure 2.5.6 Transcription Factor Binding Sites in a Promoter sequence.

Family/matrix	Further Information	Opt.	Position from - to	Str.	Core sim.	Matrix sim.	Sequence
V$AP2F/AP2.01	Activator protein 2	0.89	4 - 16	(+)	0.857	0.931	cgCCCTccggccg
V$EGRF/EGR1.01	Egr-1/Krox-24/NGFI-A immediate-early gene product	0.79	30 - 44	(+)	0.797	0.809	gtgcggtGGGGgaag
V$ZBPF/ZBP89.01	Zinc finger transcription factor ZBP-89	0.93	34 - 46	(-)	1.000	0.930	cccttCCCCcacc
V$CREB/ATF6.02	Activating transcription factor 6, member of b-zip family, induced by ER stress	0.85	43 - 63	(+)	1.000	0.885	aggggtcGACGtggctcagct

MatInspector is a tool that employs a library of matrix descriptions for transcription factor binding sites and locates these binding sites on a given promoter sequence. Graphical display of transcription factor binding sites common to a set of inputted promoters is obtained following MatInspector analysis. FrameWoker software tool that allows users to extract a common *framework* of elements from a set of DNA sequences. These elements are usually transcription factor binding sites since this tool is designed for the comparative analysis of promoter sequences. FrameWorker generates the most complex models that are common to the input sequences. These are all elements that occur in the same order and in a certain distance range in all (or a subset of) the input sequences (Figure 2.5.7).

Figure 2.5.7 Screen shot of FrameWorker Results

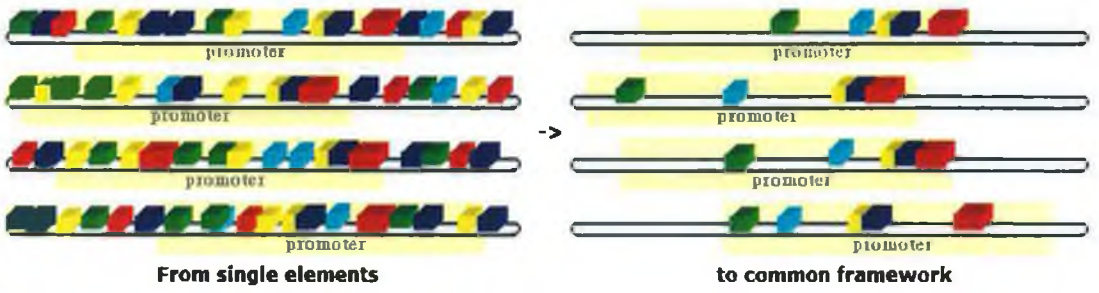

Once a model of transcription factor binding sites is generated using FrameWoker software, it is possible using Genomatix ModelInspector program to scan sequence databases for regulatory units that match the model which have been generated using MatInspector. ModelInspector provides a library of experimentally verified promoter models against which transcription factor models maybe scanned.

It is with software packages provided by companies such as Genomatix, that scientists will have to reply on in order to help them make sense of the vast quantities of data that is being generated by DNA microarray experiments, not only carried out in their own laboratories, but also the great wealth of information that is available in public accesses databases. The type information retrieval, visualisation, standardisation and analysis offered by Genomatix, is and will receive a great deal of attention from countless other companies and bioinformatics will undoubtedly remain an extremely important and ever changing area of scientific research in the future.

2.6 RNA interference (RNAi)

RNAi using small interfering RNAs (siRNAs) was carried out to silence specific genes. The siRNAs used were chemically synthesized and purchased from Ambion Inc. These siRNAs were 21-23 bp in length and were introduced to the cells via reverse transfection with the transfection agent siPORT™ *Neo*FX™ (Ambion Inc., 4511).

2.6.1 Transfection optimisation

2.6.1.1 96-well plate optimisation

In order to determine the optimal conditions for siRNA transfection in 96-well plates, an optimisation with a siRNA for kinesin (Ambion Inc., 16704) was carried out for each cell line. Cell suspensions were prepared at $1x10^4$, $2.5x10^4$ and $5x10^4$ cells per ml. Solutions of negative control and kinesin siRNAs at a final concentration of 30nM were prepared in optiMEM (Gibco™, 31985). NeoFX solutions at a range of concentrations were prepared in optiMEM in duplicate and incubated at room temperature for 10 minutes. After incubation, either negative control or kinesin siRNA solution was added to each NeoFX concentration. These solutions were mixed well and incubated for a further 10 minutes at room temperature. Replicates of 10µl of the siRNA/neoFX solutions were added to a 96-well plate. The cell suspensions were added to each plate at a final cell concentration of $1x10^3$, $2.5x10^3$ and $5x10^3$ cells per well. The plates were mixed gently and incubated at 37°C for 24 hours. After 24 hours, the transfection mixture was removed from the cells and the plates were fed with fresh medium. The plates were assayed for changes in proliferation at 72 hours using the acid phosphatase assay (Section 2.3.1.2). Optimal conditions for transfection were determined as the combination of conditions that gave the greatest reduction in cell number after kinesin siRNA transfection and the least cell kill in the presence of transfection reagent (Table 2.6.1).

Table 2.6.1 Optimised conditions for siRNA transfection in 96-well plates

Cell line	Seeding density per well	Volume NeoFX per well (µl)
MCF7 and variants	7.5×10^3	0.6
DLKP and variants	2×10^3	0.25
SKBR3 and variants	2×10^3	0.25

2.6.1.2 6-well plate optimisation

To determine the optimal conditions for siRNA transfection in 6-well plates, an optimisation with a siRNA for GAPDH (Ambion Inc., 4605) was carried out for each

cell line. Cell suspensions were prepared at $1.5x10^5$, $2.5x10^5$ and $3.5x10^5$ cells per ml. Solutions of negative control and GAPDH siRNAs at a final concentration of 30nM were prepared in optiMEM (Gibco™, 31985). NeoFX and siRNA were prepared as described in section 2.6.1.1.100µl of the siRNA/neoFX solutions were added to each well of a 6-well plate. The cell suspensions were added to each plate at a final cell concentration of $3x10^5$, $5x10^5$ and $7x10^5$ cells per well. The plates were mixed gently and incubated at 37°C for 24 hours. After 24 hours, the transfection mixture was removed from the cells and the plates were fed with fresh medium. After 72 hours cells were removed for protein extraction and western blot analysis carried out (see section 2.4.1). Optimum conditions are shown in Table 2.6.2.

Table 2.6.2 Optimised conditions for siRNA transfection in 6-well plates

Cell line	Seeding density per well	Volume NeoFX per well (µl)
MCF7 and variants	7×10^5	6
DLKP and variants	3×10^5	2
SKBR3 and variants	3×10^5	2

2.6.2 Proliferation effects of siRNA transfection

Using the optimised conditions in Table 2.6.2, each of the siRNAs was tested to see changes in proliferation of the cells after transfection. Two separate siRNAs were used for each target gene (Table 2.6.3). All siRNAs were purchased from Ambion Inc.

Solutions of siRNA at a final concentration of 30nM were prepared in optiMEM (Gibco™, 31985). NeoFX and siRNA solutions were prepared and added to plates as in Section 2.6.1.1. Again, the plates were assayed for changes in proliferation at 72 hours using the acid phosphatase assay (Section 2.3.1.2).

2.6.3 Invasion effects of siRNA transfection

Transfections were carried out in 6-well plates using optimised conditions described in Section 2.6.1.2. After 72 hours cells were used in invasion assays (Section 2.4.6.2).

Table 2.6.3 List of siRNAs used

Target name	Ambion IDs	Target name	Ambion IDs
Scrambled	4613	THBS1	138863, 138862
Kinesin	14851	HOXB4	114927, 114926
RS6KA3	554, 555	HOXB6	114847, 114846
EGR1	146223, 115234	HOXB7	107432, 14758
TFPI	121589, 121587	NRG	45295, 45201
TNFAIP	147518, 147517	MYO	131398, 131397

OVERVIEW OF WORKFLOW

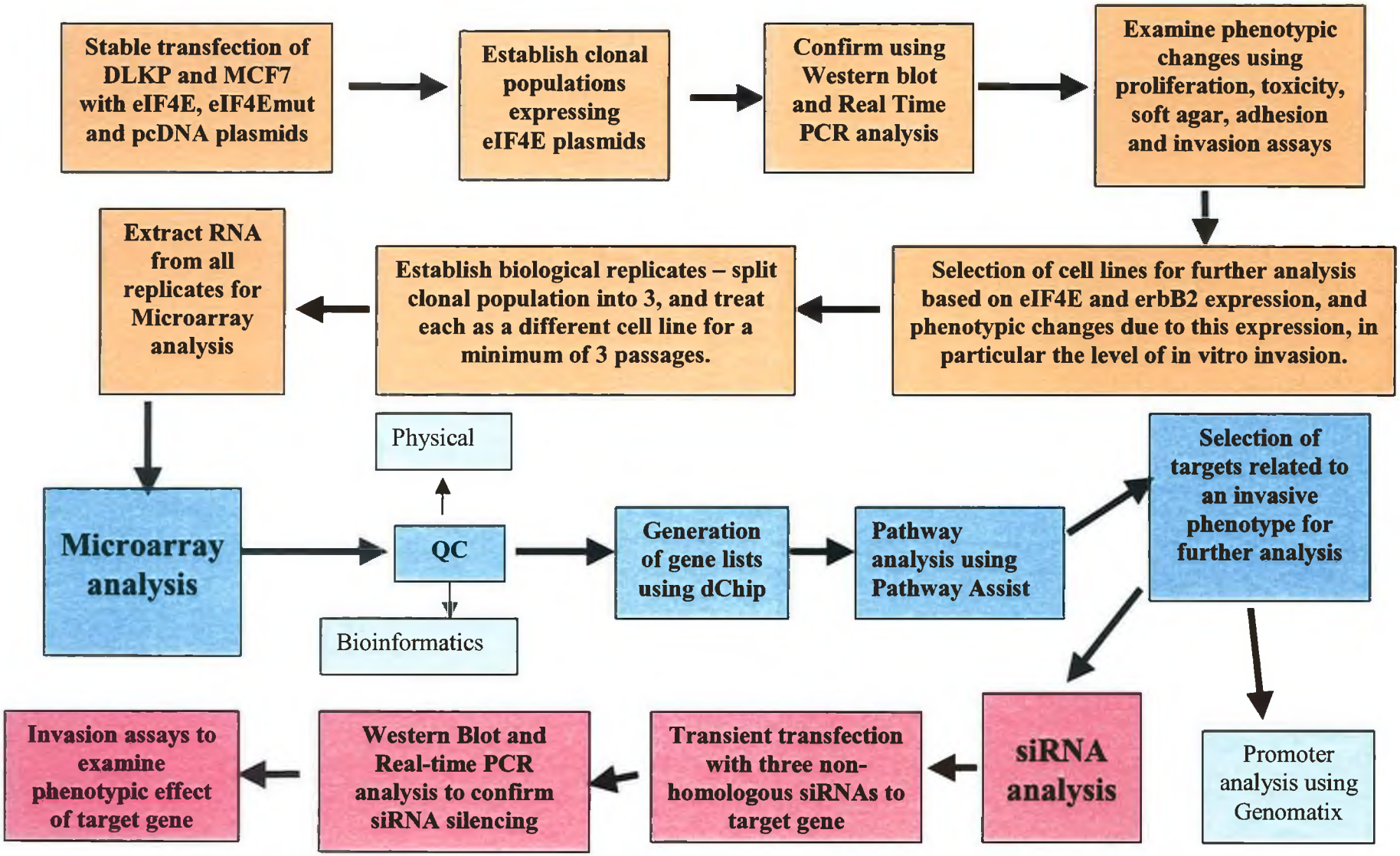

Section 3.0

Results

3.1 Analysis of MCF7 stable transfections with eIF4E, eIF4Emut & pcDNA

The purpose of this set of experiments was to generate an invasive MCF7 cell line through over-expression of eIF4E. Several clones were generated from MCF7 transfections with pcDNA containing HA-tagged eIF4E, HA-tagged eIF4Emut (a phosphorylation-deficient variant of eIF4E) and the empty pcDNA plasmid (see section 2.4.5.3). Western blots for the detection of HAtag were then carried out to determine which clones successfully translated the eIF4E and eIF4Emut plasmids. Cells found expressing HAtag were then examined for expression of eIF4E. Real-time PCR was also used to look at the level of expression of eIF4E at the RNA level. MCF74E6 and MCF74Emut6 were chosen for further analysis based on results from HAtag westerns which showed them to have a similar amount of HAtag expression, and therefore similar expression levels of eIF4E and 4Emut. These clones also showed a high level of overall eIF4E expression at both RNA and protein level. Further analysis showed these clones to have a higher growth rate compared to the parental cell line, and increased ability to grown in an anchorage-independent manner. Toxicity assays carried out showed no significant changes in drug resistance to taxol or 5FU. Finally, invasion assays showed no change in invasion of any of the clones. To further examine the effect of eIF4E overexpression, these clones were forwarded for microarray analysis.

3.1.1 Western blot analysis of HAtag expression in MCF7 transfected cells

MCF7 cells were transfected with HA-tagged pcDNA-eIF4E (eIF4E), its mutant HAtagged pcDNA-eIF4E-S209 (serine 209 has been replaced with alanine to prevent phosphorylation taking place) (eIF4Emut) and the empty pcDNA, as outlined in section 2.4.5.3. The pcDNA-eIF4E vectors code for a fusion protein between eIF4E and hemagglutin (HA epitope tag); this protein appears functionally equivalent to eIF4E (Pyronnet *et al.*, 1999; Cuesta *et al*, 2000).

The success of the transfection was determined using western blot to detect the presence of HAtag protein (see section 2.4.1). As can be seen from Figure 3.1.1, several clones proved HAtag positive. Results showed MCF7 4E 5, 6 and 7 to express the HAtag, as did MCF7 4Emut 3, 4, 5 and 6. In particular, MCF74E6 and MCF74Emut6 appeared to have similar quantities of HAtag protein upon visual inspection of the blot.

Densitometric analysis however showed MCF74E6 to have a much higher level of HAtag expression. This may have been due to the high background present at the 4E clone bands. It was clear from the western blot and from densitometry that MCF74Emut6 and MCF74E6 had the most similar level of HAtag when comparing all of the 4Emut clones to all of the 4E clones (as 4Emut6 was the highest 4Emut-HAtag expressor, and 4E6 was the lowest 4E-HAtag expressor. As there was no perfect match for HAtag expression in any of the 4E and 4Emut clones, these two were picked as the most similar for further analysis. The detection of the HAtag protein in both eIF4E and eIF4Emut clones showed that the transfection was a success.

It was also evident from this western blot that the eIF4Emut clones expressed a lower level of HAtag protein than the eIF4E clones. Technically there is no reason why this would be the case. Most clones would be expected to have a different level of expression of the protein of interest. What was interesting about this result was that there seemed to be a particular pattern of expression which differed between 4Emut clones and 4E clones. It is possible that this was a random occurrence. The alternative explanation would be that phosphorylated eIF4E as opposed to phosphorylation deficient eIF4E played a role in its own translation. The phosphorylation state of eIF4E is, in general, correlated with the translation rate of the cell. It is therefore possible that up-regulation of wild type eIF4E causes a positive feed back loop, resulting in further translation of eIF4E.

Figure 3.1.1 Level of expression of HAtag protein in MCF7 parent, MCF74E & MCF7 eIF4Emut clones

(A)

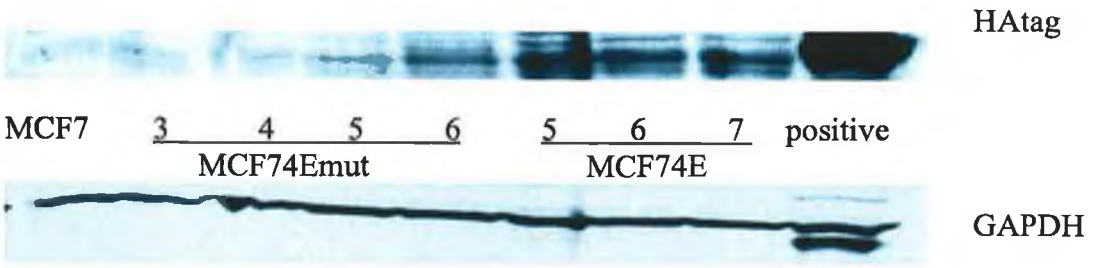

(B)

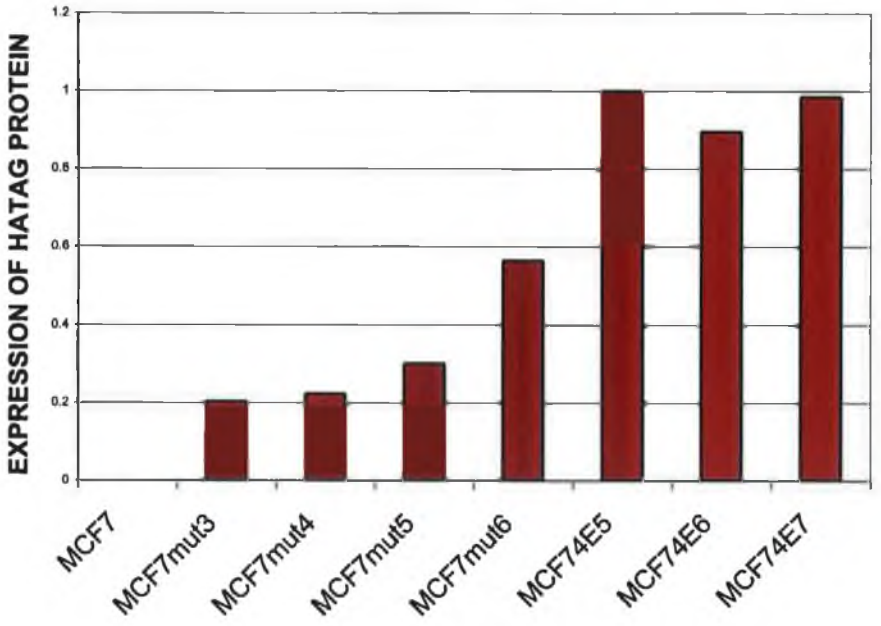

Figure 3.1.1: (A) Western blot showing level of expression of HAtag protein in MCF74E and MCF74Emut clones; (B): Densitometric analysis of western blot results.

3.1.2 Western blot analysis of eIF4E expression in MCF7 clones

The MCF74E and MCF74Emut clones were chosen for further analysis based on the level of HAtag they expressed (Figure 3.1.1). MCF74E 5, 6, and 7, along with MCF74Emut 3, 5 and 6, were used. The pcDNA clones 1 and 2 were also used as controls as neither were expected to have an increased level of eIF4E protein. Western blot analysis was carried out using an eIF4E antibody, as described in see section 2.4.1. Increased expression of eIF4E was seen in all of the MCF74E and MCF74Emut clones, with most significant increases in the eIF4E clones (Figure 3.1.2). Densitometric analysis showed up to a 3.5 fold increase in eIF4E clones. pcDNA 2 showed an increase in expression (1.75 fold), whereas pcDNA 1 showed no significant change when compared with the parent. Up-regulation of eIF4E in the MCF7eIF4E and MCF7eIF4Emut clones correates with HAtag westerns, with higher levels of eIF4E being seen in MCF7eIF4E 5, 6, and 7 as compared to MCF7eIF4Emut 3, 5, and 6. This further confirmed the success of the MCF7 transfections.

3.1.3 Real-time PCR analysis of the level of eIF4E expressed in MCF7, MCF74E and MCF74Emut clones

To verify the levels of eIF4E in the MCF74E and MCF74Emut clones, qPCR was carried out using eIF4E primer-probe pairs (section 2.4.3.5.1, table 2.4.4). Results showed upregulation of eIF4E in all of the MCF74E and MCF74Emut clones compared to the parent (Figure 3.1.3). MCF74E6 and MCF74Emut6 showed a 70% and 30% increase, respectively.

Figure 3.1.2 Level of expression of eIF4E protein in MCF7 parent, eIF4E & eIF4Emut clones

(A):

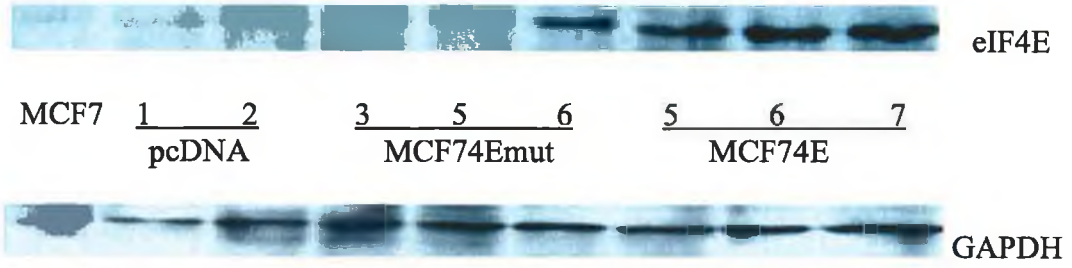

(B):

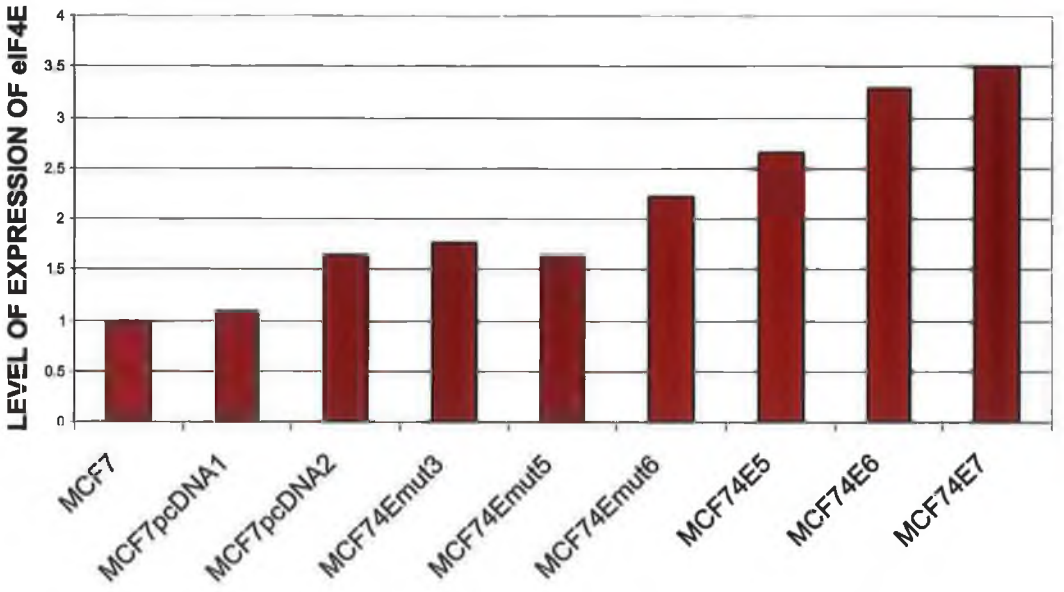

Figure 3.1.2: (A) Western blot showing level of expression of eIF4E in MCF74E and MCF74Emut clones; (B): Densitometric analysis of western blot results.

Figure 3.1.3 Examination of the level of eIF4E expressed in MCF7, MCF74E, and MCF74Emut clones using real-time PCR

(A):

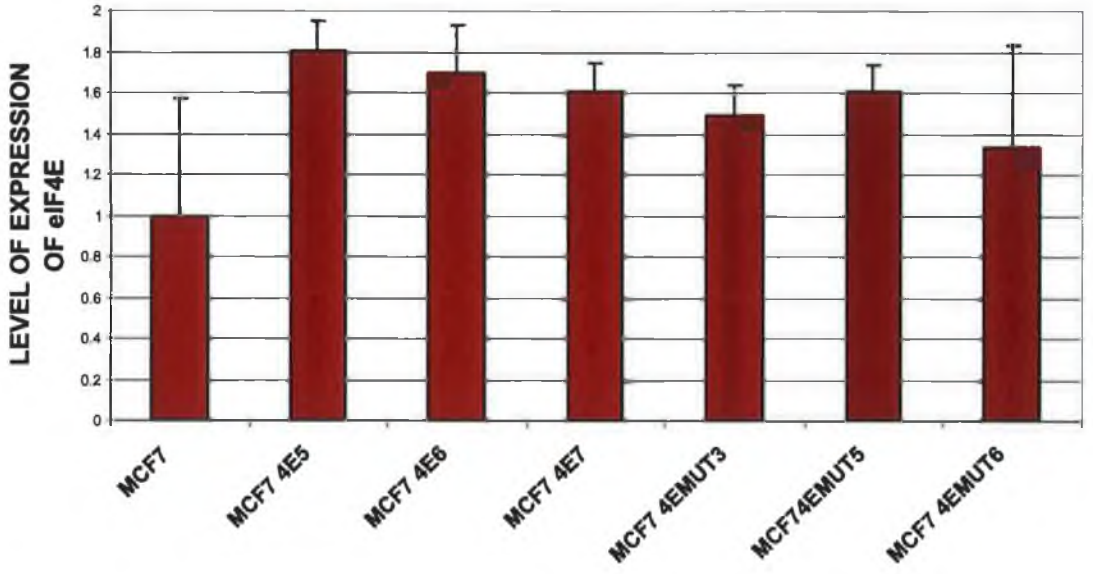

(B):

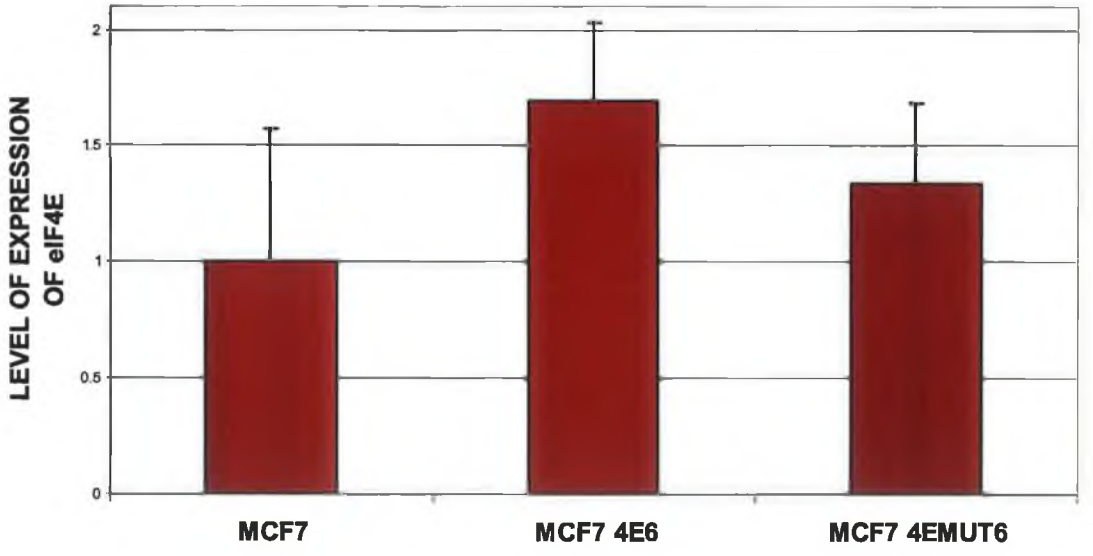

Figure 3.1.3: (A) level of expression of eIF4E in MCF7, MCF7F4E and MCF74Emut clones; (B): level of expression of eIF4E in MCF7 clones used for microarray analysis.

3.1.4 Effect of eIF4E, eIF4Emut and pcDNA on the growth rate of MCF7

Up-regulation of eIF4E has previously been associated with increased growth rate (Flynn and Proud, 1996). Acid-phosphatase proliferation assays (see section 2.3.1.2) along with growth curves (section 2.4.10) were used to determine the growth rate of MCF7 parent, MCF74E6, MCF74Emut6 and MCF7pcDNA1.

3.1.4.1 Proliferation assay

Cells grown in 96 well plates were assayed for changes in proliferation at 72 hours using the acid phosphatase assay (section 2.3.1.2). Both MCF74E6 and MCF74Emut6 grew 3-fold faster than parent MCF7, MCF7pcDNA1 however, grew 10-fold more slowly than the parent (see figure 3.1.4). This result showed that over-expression of both eIF4E and eIF4Emut caused an increase in the rate of growth of MCF7 cells.

3.1.4.2 Growth curve

A growth curve (section 2.4.10) showing the behaviour of cells over a 120hr period also demonstrated an increase in the growth of MCF74E6 and MCF74Emut6 compared to the parent. There was a 2-fold increase in the number of cells after 120hrs in both MCF74E6 and MCF74Emut6 compared to the parent. There was also a decrease in the number of MCF7pcDNA1 cells compared to the parent.

Both assays confirmed that both eIF4E and eIF4Emut had a positive effect on the growth rate of MCF7 cells, they also showed similar trends in growth rate for both 96-well and 6-well plates, with MCF74E6 and MCF74Emut6 cells increasing, and MCF7pcDNA1 decreasing compared to the parental cell line. This result agrees with previous studies which showed correlation between levels of eIF4E and proliferation (Flynn and Proud, 1996). This phenotypic effect of eIF4E transfection further confirms up-regulation of eIF4E in MCF74E6 and MCF74Emut6 cell lines.

Figure 3.1.4: Growth rate of MCF74E, MCF74Emut, and MCF7pcDNA compared to MCF7 parent.

Figure 3.1.4.1:

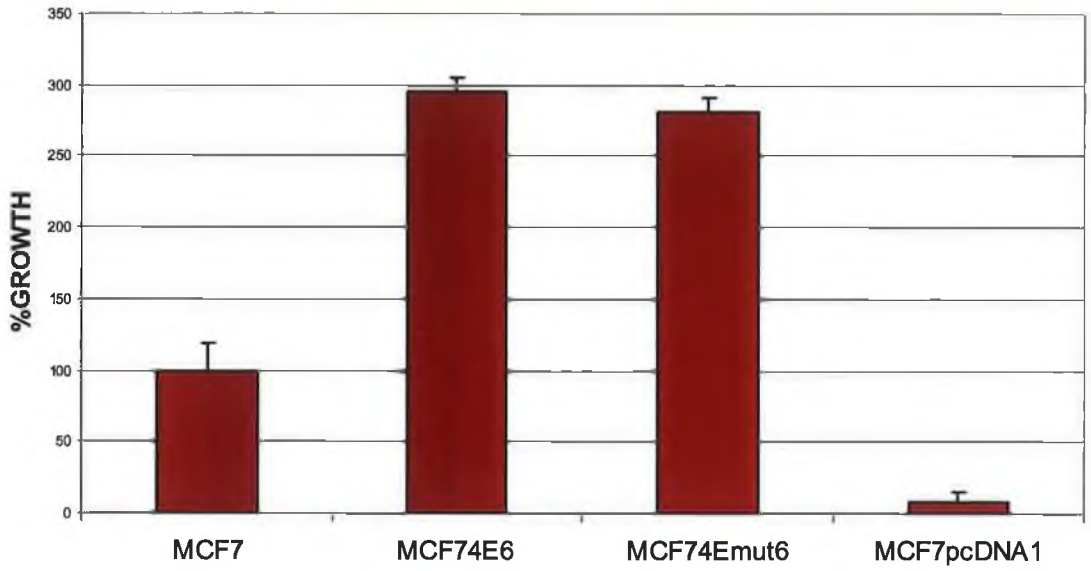

Figure 3.1.4.2:

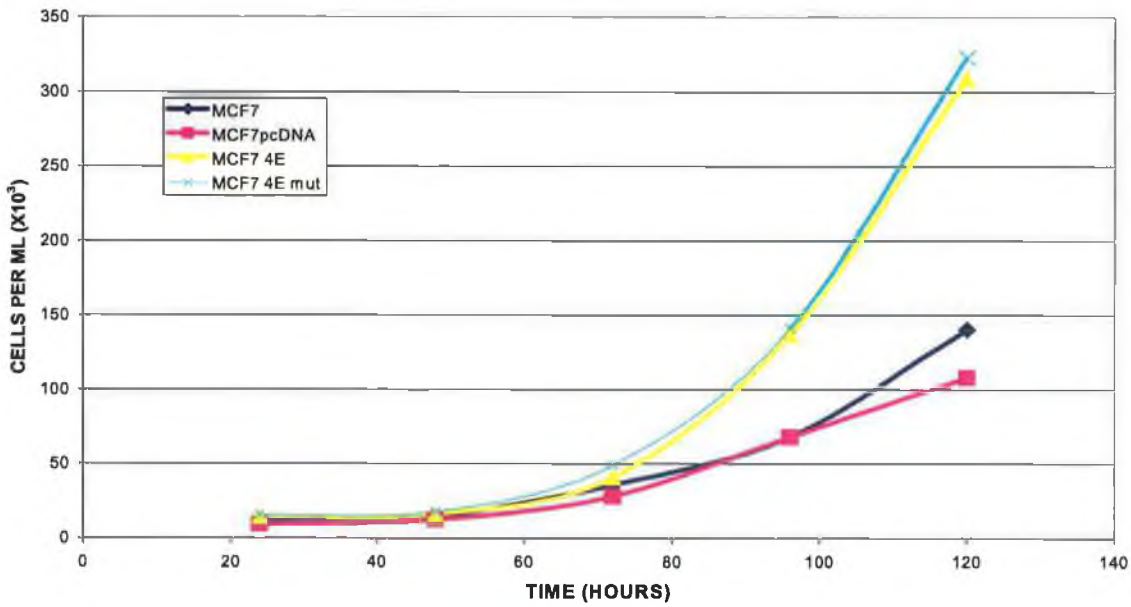

Figure 3.1.4.1: Rate of proliferation of MCF7 clones grown over a 72hr period; Figure 3.1.4.2: Growth curve showing growth rate of MCF7 clones over a 120hr period.

3.1.6 Effect of eIF4E transfection on the adhesion of MCF7 cells

Overexpression of eIF4E has been associated with increased invasion in cancer cell lines (Mamane *et al.*, 2004). To examine whether eIF4E also has an effect on cell adhesion, cell attachment to MATRIGEL was assessed, as was anchorage-dependence using soft agar assays.

3.1.6.1 Adhesion assays

The adhesive properties of the cells were examined by extracellular matrix adherence assays using MATRIGEL® (section 2.4.7). MCF7 parent, MCF74E 5 & 6, MCF74Emut 5 & 6 and MCF7pcDNA 1 & 2 were examined. MCF7 was taken as having 100% attachment, and results showed the MCF7pcDNA and MCF74Emut clones to be between 50 and 60% adherent, whereas the MCF74E clones did not attach after the 60 min incubation (Figure 3.1.6.1). This shows that eIF4E has a greater effect on adhesion than eIF4Emut or the pcDNA control. However, these assays were only performed once, and repeats are necessary.

3.1.6.2 Soft agar assay

The effect of eIF4E and eIF4Emut on the anchorage-dependence of MCF7 was examined using soft agar assays (Section 2.4.9). The percentage colony forming efficiency (CFE) over a 10-day period was determined by expressing the number of colonies formed as a percentage of the number of cells plated. Therefore, CFE was specific for each cell line, and did not refer to comparison with other cell lines. Results for MCF7 parent were then taken as baseline, and the CFE for all other MCF7 clones was compared to this. The highest increase was seen in eIF4E, with a 1.6 fold increase in CFE compared to the parent. (Figure 3.1.6.2). This considerable increase in CFE of MCF7eIF4E suggests eIF4E is involved in cell-adhesion mechanisms in these cells.

Photographic evidence showed an increase in colony size of MCF74E6 and MCF74Emut6 and MCF7pcDNA1 over a 20-day period (Figure 3.1.6.3). Therefore, although the CFE was greater for MCF74E6 and MCF74Emut6 than MCF7pcDNA and MCF7 parent, it would appear that colony size was influenced by transfection of the empty plasmid alone.

Figure 3.1.6.1: Effect of eIF4E transfection on the adhesion of MCF7 cells

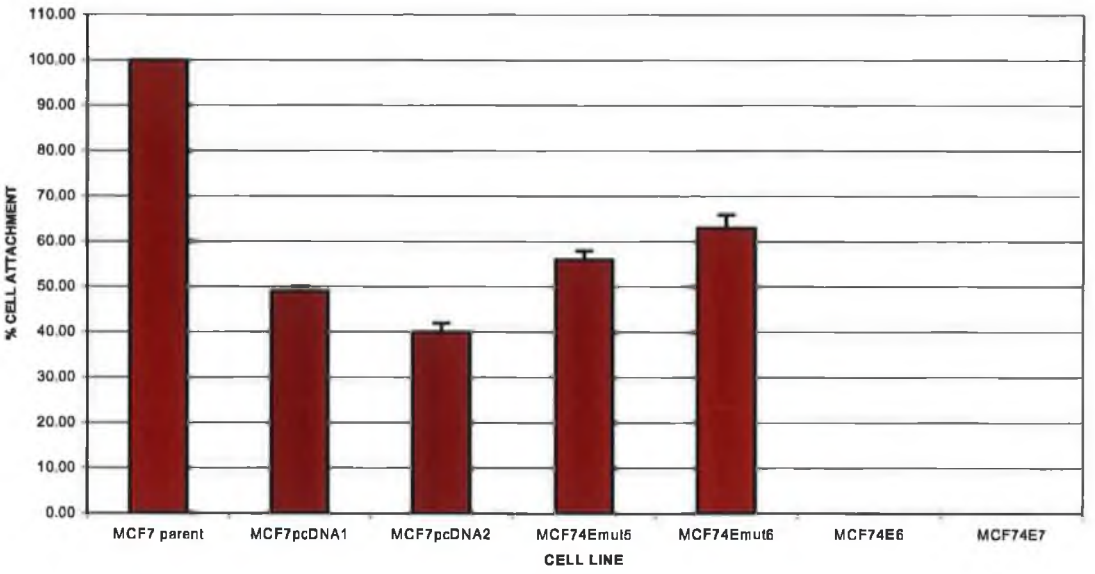

Figure 3.1.6.2: % Colony forming efficiency at 10 days

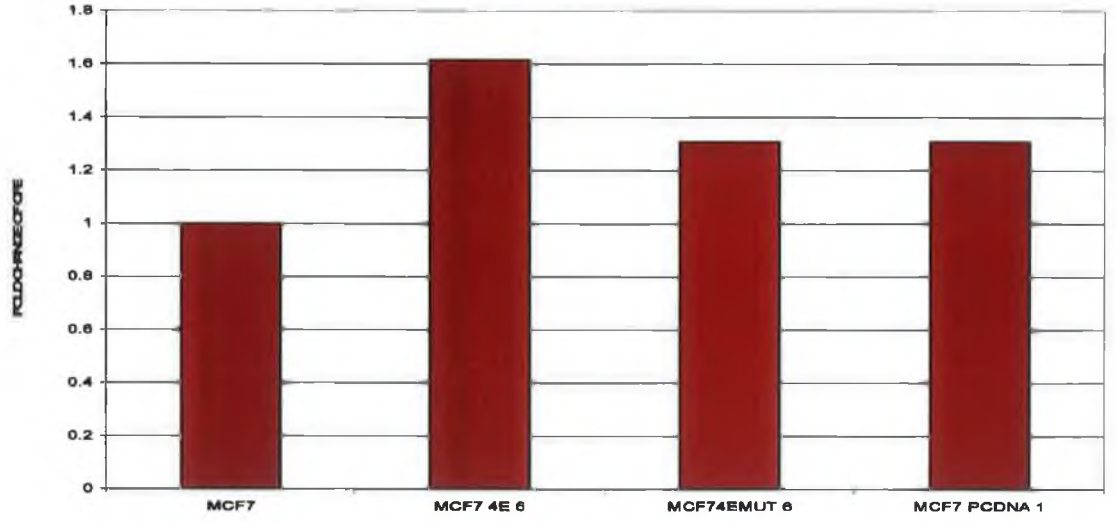

Figure 3.1.6.1: results of adhesion assay showing the % of MCF7, MCF74E, MCF74Emut and MCF7pcDNA that remained attached to MATRIGEL after a 60min incubation; Figure 3.1.6.2: % Colony forming efficiency at 10 days

Figure 3.1.6.3: Photographs of colonies of MCF7, MCF74E, MCF74Emut and MCF7pcDNA in soft agar

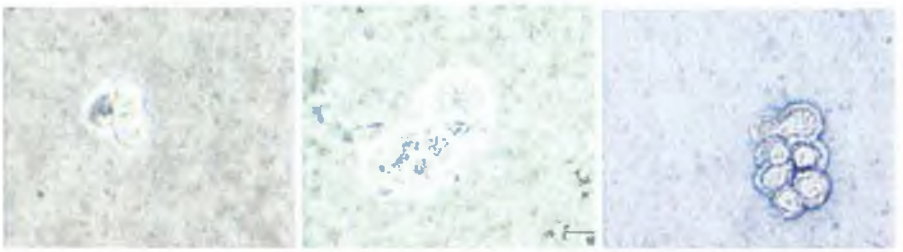

MCF7day 10 MCF7day 15 MCF7day 20

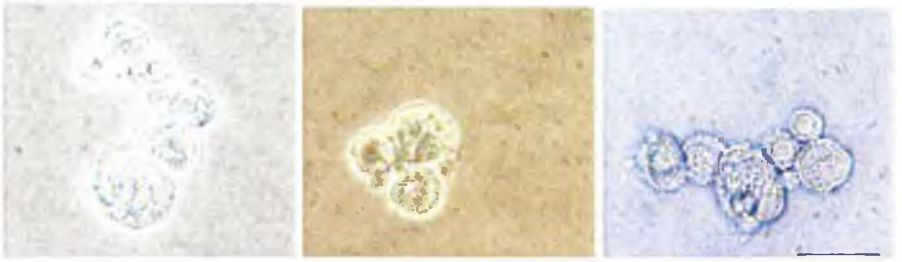

MCF7pcDNA day10 MCF7pcDNA day 15 MCF7pcDNA day 20

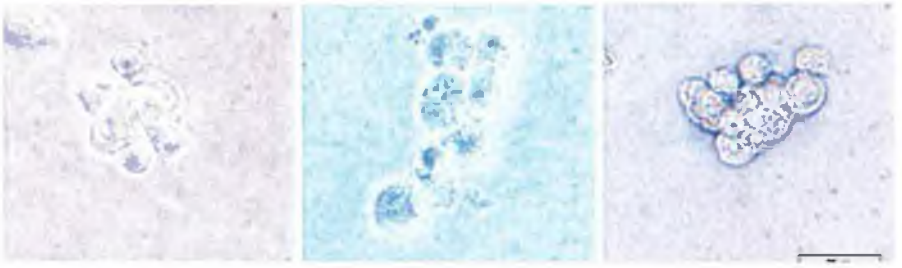

MCF74E day 10 MCF74E day 15 MCF74E day 20

MCF74Emut day 10 MCF74Emut day 15 MCF74Emut day 20

Figure 3.1.6.3: Photographs of colonies grown in soft agar at 40X magnification over a 20 day period.

3.1.7 Effect of eIF4E, eIF4Emut and pcDNA on MCF7 cell invasion

MCF7 is a non-invasive cell line. Invasion assays were carried out to examine changes in invasion following transfection with eIF4E and eIF4Emut (section 2.4.5). MCF7 parent, MCF74E 5, 6 & 7, MCF74Emut 3, 4, 5 & 6 and MCF7pcDNA 1 & 2 were used in this study, and none showed any increase in invasion. Results from MCF7 parent, MCF7eIF4E6, MCF7eIF4Emut6 and MCF7pcDNA1 are shown (Figure 3.1.7). This result showed that eIF4E transfection into MCF7 had no effect on invasion.

3.1.8 Effect of eIF4E, eIF4Emut and pcDNA on drug resistance of MCF7

Over-expression of eIF4E has been associated with increased drug resistance in cancer cell lines. To further investigate the effect of over-expression of eIF4E in MCF7, toxicity assays were carried out (section 2.3.1) on MCF7, MCF7eIF4E and MCF7eIF4Emut cells using 5-Fluorouracil (5FU) and Taxol. 5-FU inhibits protein synthesis by preventing the release of eIF4E from 4EBP1 (binding protein 1), therefore preventing eIF4E participation in translation initiation. Taxol however, is a microtubule antagonist capable of inducing cell-cycle arrest with minimum effect on protein synthesis. These two drugs were chosen so that the effect of eIF4E on drug resistance could be examined using drugs with very different mechanisms of action.

3.1.8.1 Taxol toxicity assays using MCF7, MCF7eIF4E, MCF7eIF4Emut & MCF7pcDNA clones

A selection of clones expressing different levels of eIF4E/eIF4Emut were used for the toxicity assays. Results showed MCF7eIF4Emut clones 2 & 4 and MCF7eIF4E clones 3 & 4 were more resistant to taxol than the parent (Figure 3.1.8.1). However, the pcDNA controls 2 & 3 also displayed greater resistance then the parent. The rest of the clones showed no change or a decrease in resistance compared to the parent. Therefore an increase in levels of eIF4E in MCF7 cells did not effect taxol drug resistance.

3.1.8.2 5FU toxicity assays using MCF7, MCF7eIF4E, MCF7eIF4Emut& MCF7pcDNA clones

Results for 5FU showed both eIF4E and eIF4Emut clones to be more sensitive than the parent, with the exception of MCF74E1, 2 and MCF74Emut4, which showed no change (taking into consideration error bars)) (Figure 3.1.8.2). This result suggests that an increase in eIF4E makes MCF7 more sensitive to 5FU.

Figure 3.1.7: Invasion assays using MCF7, MCF74E, MCF74Emut and MCF7pcDNA clones

---

Figure 3.1.7:

(A) MCF7 parent

(B) MCF7 4E 6

(C) MCF74Emut 6

(D) MCF7pcDNA 1

Figure 3.1.7: Invasion assays showing: (A) MCF7 parent, (B) MCF7eIF4E6, (C) MCF7eIF4Emut 6, (D) MCF7pcDNA 1

Figure 3.1.8.1 Taxol toxicity assays using MCF7, MCF7eIF4E, MCF7eIF4Emut & MCF7pcDNA clones

Figure 3.1.8.1:

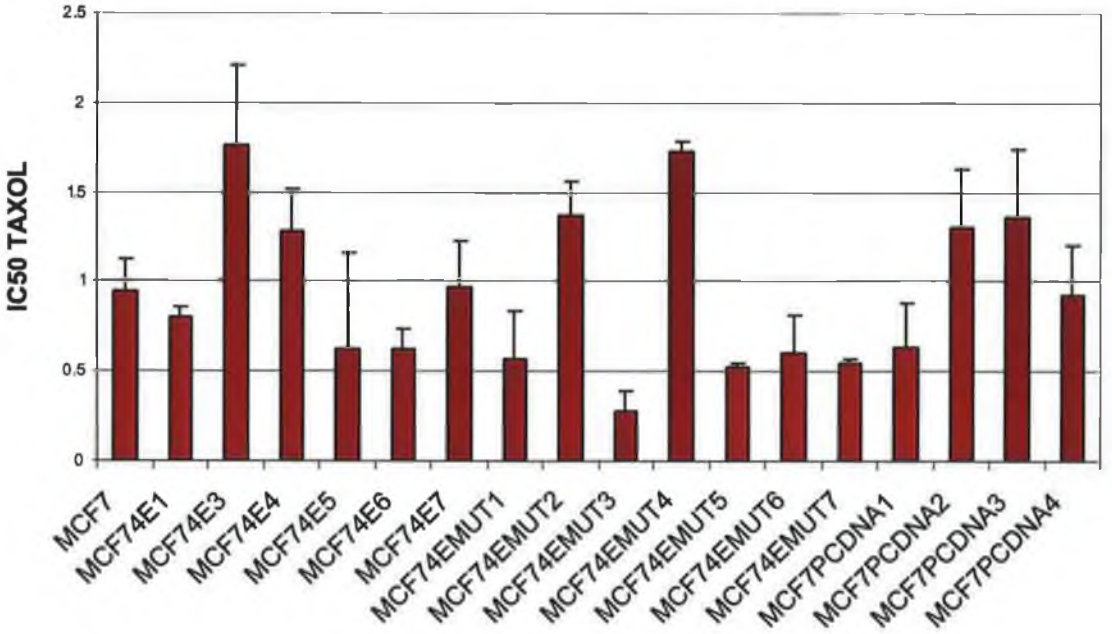

Table 3.1.8.1:

CELL LINE	FOLD CHANGE	CELL LINE	FOLD CHANGE
MCF7	1.0000	MCF7 eIF4Emut3	0.2922
MCF7eIF4E1	0.8499	MCF7 eIF4Emut4	1.8230
MCF7 eIF4E3	1.8640	MCF7 eIF4Emut5	0.5529
MCF7 eIF4E4	1.5946	MCF7 eIF4Emut6	0.6401
MCF7 eIF4E5	0.6603	MCF7 eIF4Emut7	0.5821
MCF7 eIF4E6	0.6609	MCF7PCDNA1	0.6771
MCF7 eIF4E7	1.0256	MCF7PCDNA2	1.3721
MCF7 eIF4Emut1	0.6018	MCF7PCDNA3	1.4345
MCF7 eIF4Emut2	1.4453	MCF7PCDNA4	0.9750

Figure 3.1.8.1: Average IC50 taxol values for MCF7, MCF74E and MCF74Emut clones, where n=3; Table 3.1.8.1: Fold change of IC50 taxol values in clones compared to parent MCF7.

Figure 3.1.8.2 5FU toxicity assays using MCF7, MCF7eIF4E, MCF7eIF4Emut & MCF7pcDNA clones

Figure 3.1.8.2:

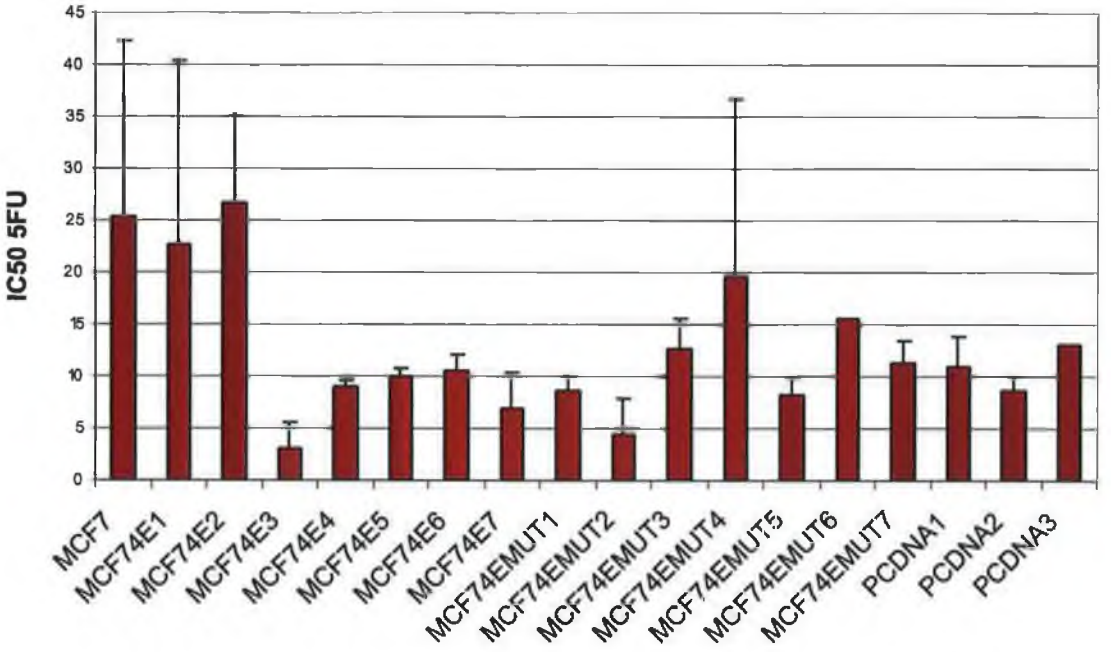

Table 3.1.8.2:

CELL LINE	FOLD CHANGE	CELL LINE	FOLD CHANGE
MCF7	1	MCF7eIF4Emut2	0.1203
MCF7eIF4E1	0.9305	MCF74EeIFmut3	0.0833
MCF7 eIF4E2	1.0277	MCF74EeIFmut4	0.7500
MCF7 eIF4E3	0.0833	MCF74EeIFmut5	0.3333
MCF7 eIF4E4	0.3472	MCF74EeIFmut6	0.1111
MCF7 eIF4E5	0.1527	MCF74EeIFmut7	0.15277
MCF7 eIF4E6	0.1388	MCF7PCDNA1	0.19444
MCF7 eIF4E7	0.1944	MCF7PCDNA2	0.1388
MCF7eIF4Emut1	0.1111	MCF7PCDNA3	0.1111

Figure 3.1.8.2: Average IC50 5FU values for MCF7, MCF74E and MCF74Emut clones, where n=3; Table 3.1.8.2: Fold change of IC50 5FU values in clones compared to parent MCF7.

3.1.9 Invasion assay analysis of MCF7H3erbB2

MCF7H3erbB2 is a clonal subpopulation of MCF7H3 transfected with erbB2. This cell line was previously developed at the NICB by Dr. Sharon Glynn, and was found to be highly invasive. Due to the lack of an invasive MCF74E or 4Emut clone, it was decided to include MCF7H3erbB2 in microarray analysis in order to determine invasion-specific genes in MCF7. Invasion assays (section 2.4.5) were repeated and results confirmed that MCF7H3erbB2 was invasive and MCF7H3 non-invasive (Figure 3.1.9).

Figure 3.1.9 Invasion assays using MCF7H3 and MCF7H3 erbB2

Figure 3.1.9:

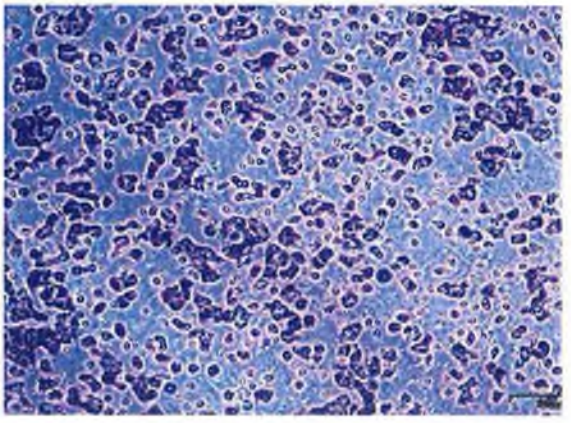

(A)MCF7H3erbB2 (B)MCF7H3

Figure 3.1.9: Invasion assays showing (A) MCF7H3 erb2 and (B) MCF7H3.

3.2 Analysis of DLKP stable transfections with eIF4E, eIF4Emut &pcDNA

The HAtagged-eIF4E and eIF4Emut were transfected into the poorly invasive DLKP parent to examine the effect on invasion. Several clones were generated from transfections with eIF4E, eIF4Emut and pcDNA into DLKP (see section 2.4.5.3). Western blots for the detection of HAtag protein were then carried out to determine which clones were successfully expressing the eIF4E and eIF4Emut plasmids. Cells found expressing HAtag were then examined for overall expression of eIF4E. Real-time PCR was also used to look at the level of expression of eIF4E at RNA level. DLKPeIF4E17 and DLKPeIF4Emut 8 were chosen for further analysis based on results from HAtag westerns which showed them to have a similar amount of HAtag expression, and therefore similar expression levels of eIF4E and eIF4Emut.These clones also showed a high level of overall eIF4E expression at both RNA and protein level. Further analysis showed these clones to have a higher growth rate than the parental cell line. Toxicity assays carried out showed no significant changes in drug resistance to taxol or adriamycin. Invasion assays showed significant increase in eIF4E and eIF4Emut clones compared to pcDNA clones and the parental DLKP. To further examine the effect of eIF4E over-expression these clones were then used in Microarray experiments.

3.2.1 Western blot analysis of HAtag expression

DLKP cells were transfected with pcDNA-eIF4E, mutant pcDNA-eIF4E-S209 and the empty pcDNA, as outlined in section 2.4.5. Because the eIF4E and eIF4Emut are HAtagged, western blot detection of HAtag protein was used to determine whether or not the transfections were successful. Results showed DLKPeIF4E 12, 14 and 17 to express the HAtag, as did DLKPeIF4Emut 2, 3, 6, 7, 8, 9 and 10 (Figure 3.2.1). DLKPeIF4E17 and DLKPeIF4E8 were found to have been successfully transfected and also have a similar level of HAtag. For this reason these cells were chosen for further analysis using microarrays.

Figure 3.2.1a Level of expression of HAtag protein in DLKP parent & DLKP4E clones

(A):

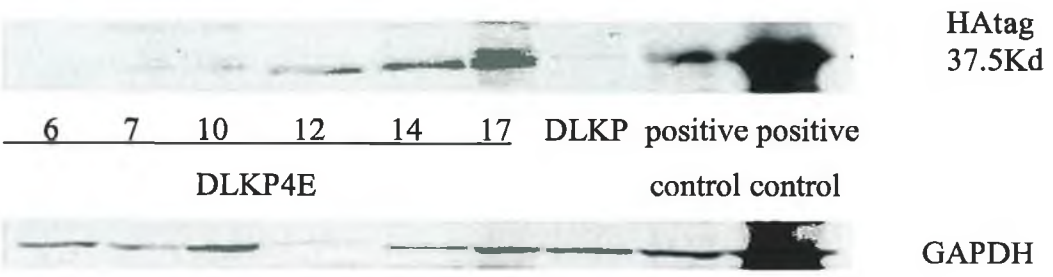

(B):

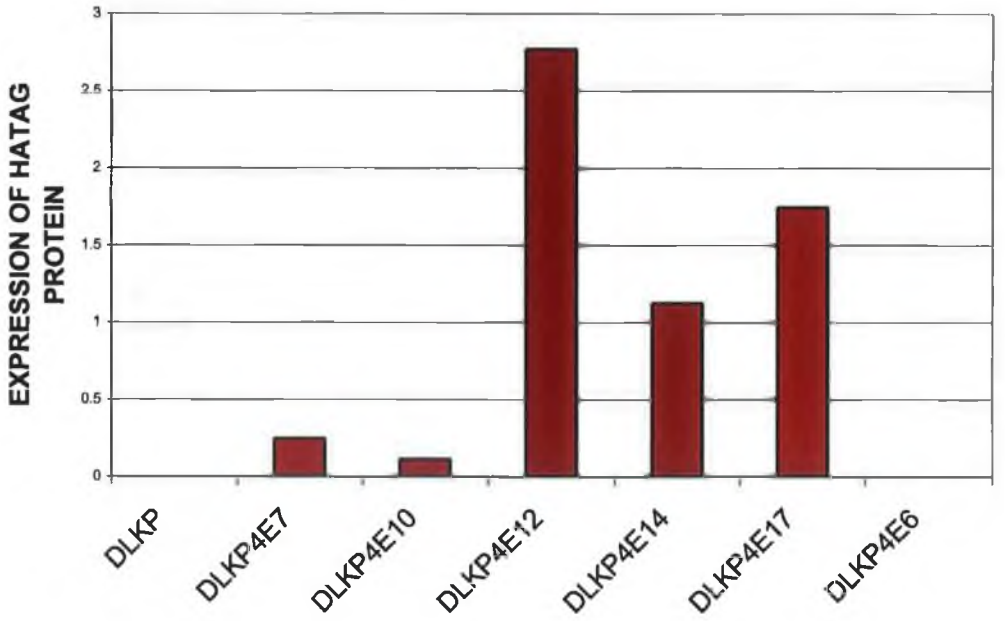

Figure 3.2.1a: (A) Western blot showing level of expression of HAtag protein in DLKPEif4E clones; (B) Densitometric analysis of western blot results

Figure 3.2.1b Level of expression of HAtag protein in DLKP parent & DLKPeIF4Emut clones

(A):

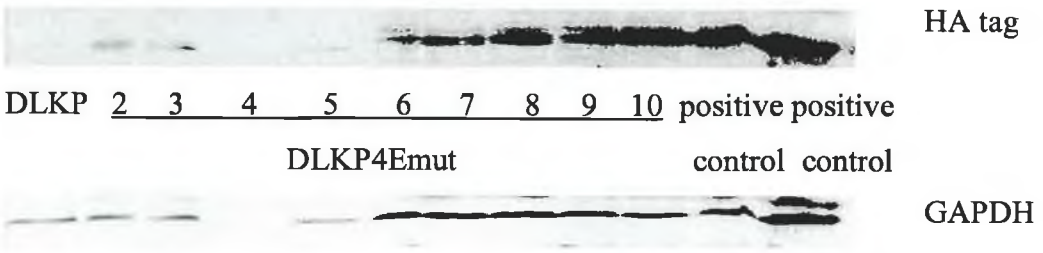

(B):

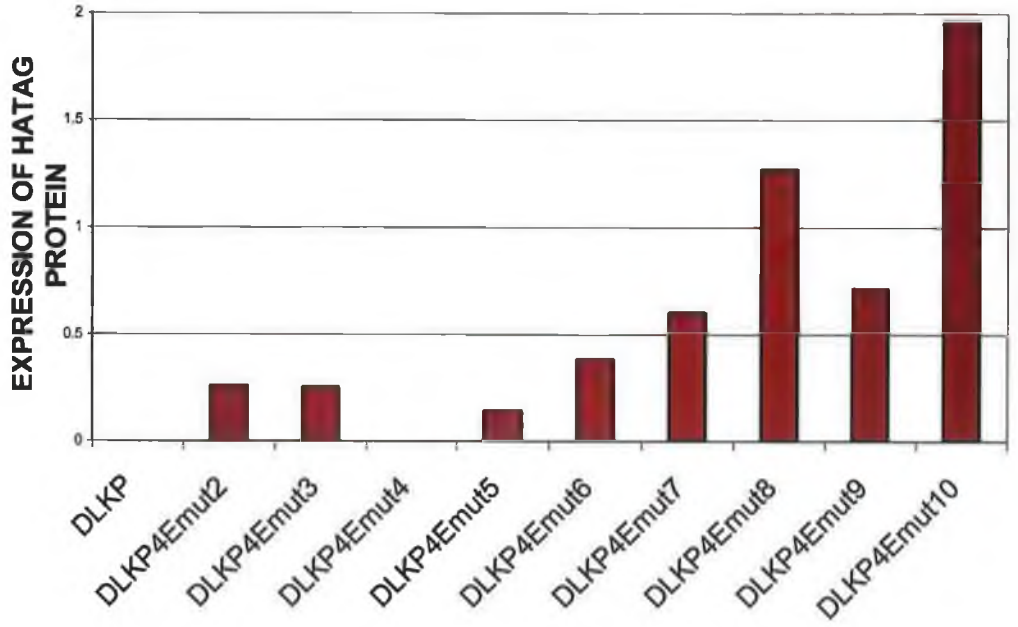

Figure 3.2.1b: (A) Western blot showing level of expression of HAtag protein in DLKP4Emut clones; (B) Densitometric analysis of western blot results.

3.2.2 Western blot analysis of eIF4E expression in DLKP, DLKP4E and DLKP4Emut clones.

Three of the DLKP4E and DLKP4Emut clones were chosen for further analysis based on the level of HAtag they expressed. DLKP4E 12, 14 & 17 along with DLKP4mut 8, 9 & 10 were used to look at the effect of eIF4E and eIF4Emut, on the level of protein expression eIF4E within the cells. When compared to the parent DLKP, no significant upregulation of eIF4E was observed (Figure 3.2.2). It is important to note that antibody used was specific to endogenous eIF4E and not HAtagged-eIF4E.

3.2.3 Real-time PCR analysis of the level of eIF4E expressed in DLKP, DLKPeIF4E17, DLKPeIF4Emut8 and DLKPpcDNA1

Real-time PCR was carried out to look at eIF4E at an RNA level (see section 2.4.3.5). Results showed upregulation of eIF4E in both DLKPeIF4E17 and DLKPeIF4Emut8 compared to the parent (Figure 3.2.3). Therefore up-regulation of eIF4E was observed at an RNA level, but not at a protein level in DLKP transfected with eIF4E/4Emut.

Figure 3.2.2 Level of expression of eIF4E protein in DLKP, DLKP eIF4E & DLKP eIF4Emut clones

(A):

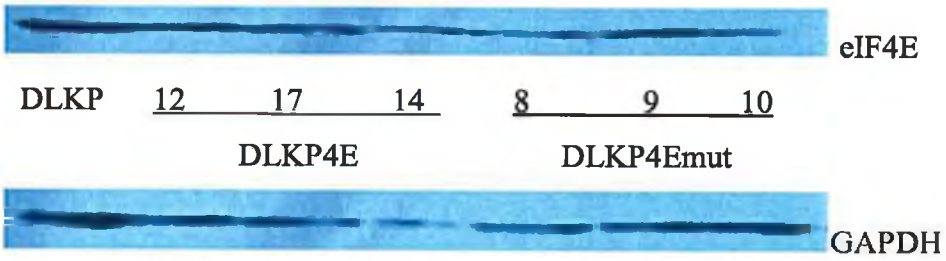

(B):

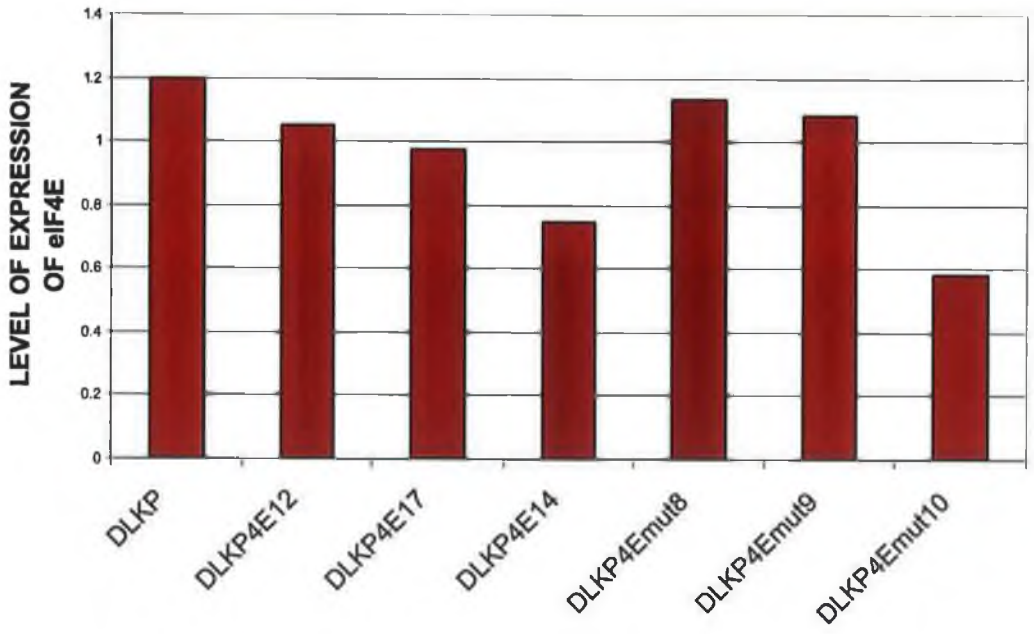

Figure 3.2.2: (A) Western blot showing level of expression of eIF4E inDLKP4E and DLKP4Emut clones; (B) Densitometrie analysis of western blot results.

Figure 3.2.3 Examination of the level of eIF4E expression in DLKP, DLKPeIF4E17, DLKPeIF4Emut8 and DLKPpcDNA1 using real-time PCR

Figure 3.2.3:

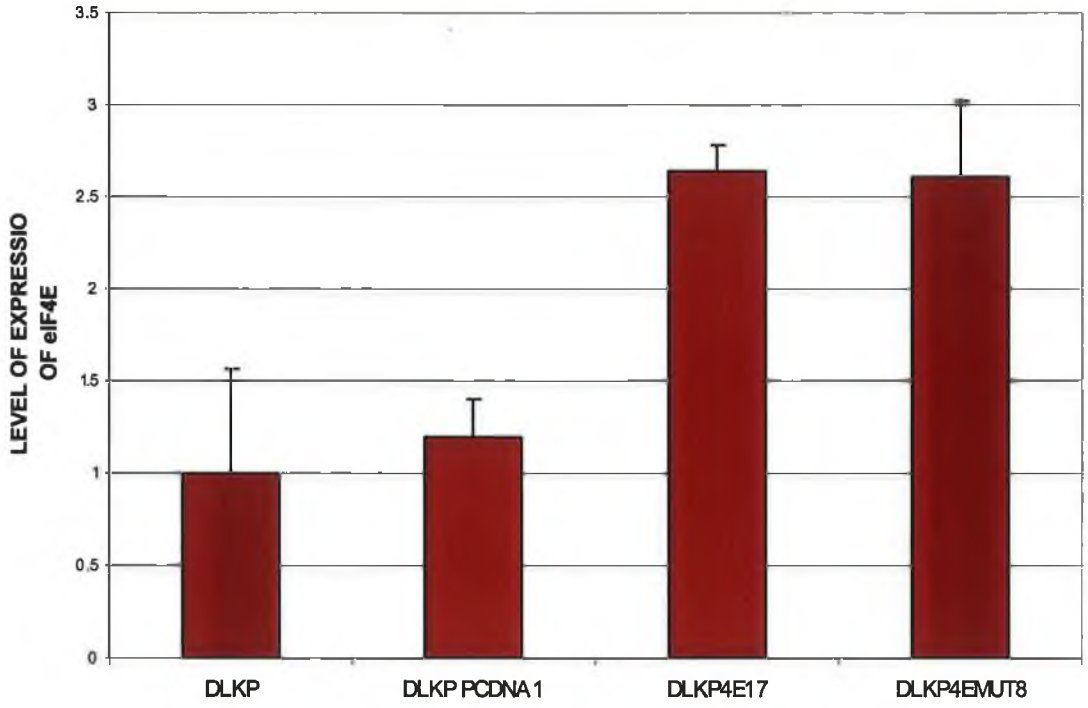

Figure 3.2.3: Level of RNA expression of eIF4E in DLKP, DLKPeIF4E17, DLKPeIF4Emut8 and DLKPpcDNA1 using real-time PCR.

3.2.4 Examination of the growth rate of DLKP parent compared to DLKP4E, DLKP4Emut and DLKPpcDNA.

Increased eIF4E expression has been associated with increased growth rate. Acid-phosphatase proliferation assays (section 2.3.1.2) along with growth curves (section 2.4.10) were carried out on the DLKP parent, DLKP4E, DLKP4Emut and DLKPpcDNA cell lines. The purpose of this experiment was to look at the growth rate of the parent compared to the eIF4E/eIF4Emut clones. DLKP4E17, DLKP4Emut8 and DLKPpcDNA1 were used.

3.2.4.1 Proliferation assay

Both DLKP4E17 and DLKP4Emut8 were observed to grow >2-fold faster than parent DLKP in 96-well plates proliferation assays. DLKPpcDNA grew at an equal rate to the parent (Figure 3.2.4 (A)). This result showed that over-expression of both eIF4E and eIF4Emut caused increased proliferation of DLKP, and that the empty plasmid had no effect.

3.2.4.2 Growth curve

A growth curve showing the behaviour of cells over a 120hr period also showed an increase in the growth of DLKP4E17 and DLKP4Emut8 compared to the parent. There was a 1.3-fold increase in the number of DLKP4Emut8 cells, and a 1.6-fold increase in the number of DLKP4E17 cells compared to DLKP after 120hrs. There was a 0.5-fold decrease in the number of DLKPpcDNA1 cells compared to the parent that was not observed in the 96-well assay. Although a similar trend was not seen for pcDNA in both 96-well and 6-well plates, it is significant that both eIF4E and eIF4Emut had a positive effect on the growth rate of DLKP(Figure 3.2.4 (B)).

Figure 3.2.4: growth rate of DLKP4E, DLKP4Emut and DLKPpcDNA compared to parent DLKP.

(A):

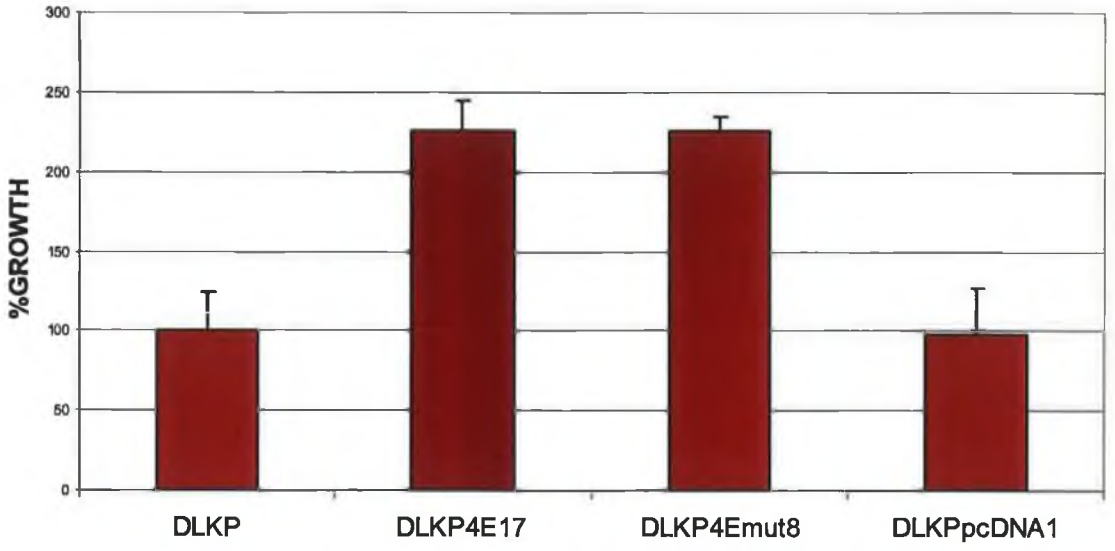

(B):

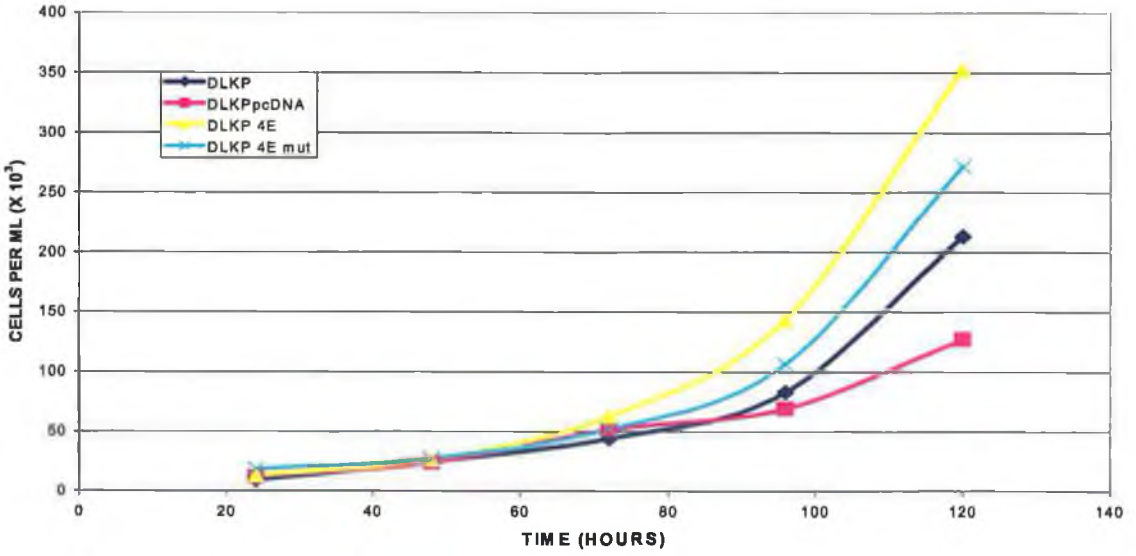

Figure 3.2.4: (A) Rate of proliferation of DLKP clones grown over a 72hr period; (B) Growth curve showing the growth rate of DLKP clones over a 120hr period.

3.2.5 Effect of eIF4E, eIF4Emut and pcDNA on DLKP cell invasion

Invasion assays were carried out to examine if stable transfection of eIF4E into DLKP cells had affected the invasive phenotype of those cells. Invasion assays were carried out on DLKP, DLKP4E, DLKP4Emut and DLKPpcDNA cells using the technique outlined in section 2.4.5. Invasion assay inserts were both photographed and counted at 200X. Overall, there were more DLKP4Emut invasive clones than DLKP4E clones. Both sets of clones were more invasive than parent or DLKPpcDNA. (Figure 3.2.5.1, 3.2.5.2, 3.2.5.3). These results were confirmed with invasion assay cell counts (Figure 3.2.5.4). This result confirms eIF4E and eIF4Emut transfection had a significant effect on invasion in DLKP cells.

Figure 3.2.5.1: Invasion assays using DLKP and DLKPpcDNA

(A) DLKP (B) DLKPpcDNA1

Figure 3.2.5.1: Invasion assay results for (A) DLKP parent and (B) DLKPpcDNA

Figure 3.2.5.2 Invasion assays using DLKP4Emut clones

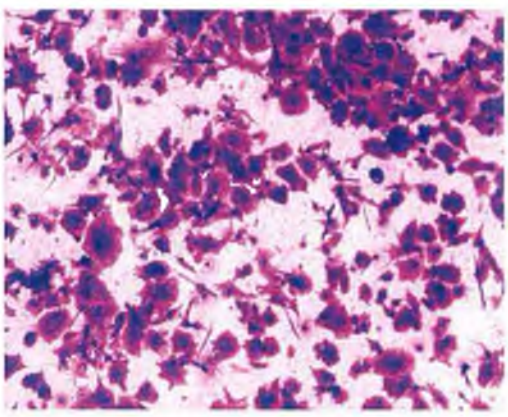

(A) DLKP4Emut2

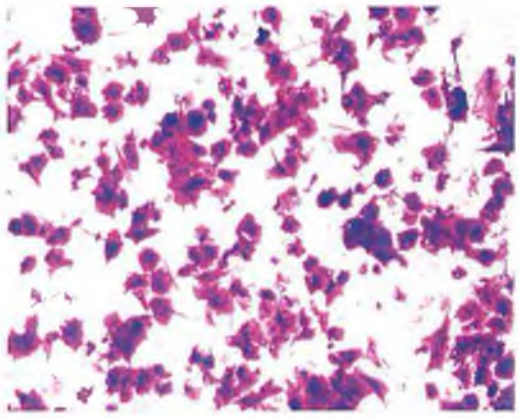

(B) DLKP4Emut3

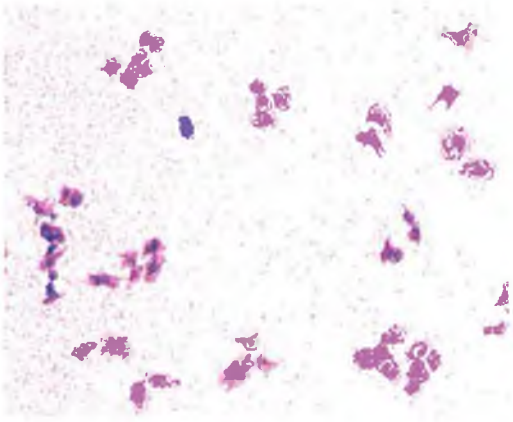

(C) DLKP4Emut6

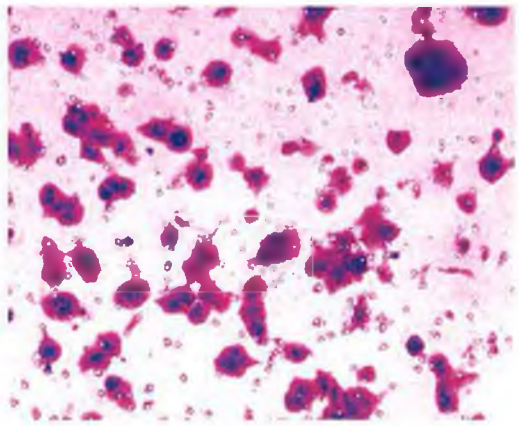

(D) DLKP4Emut7

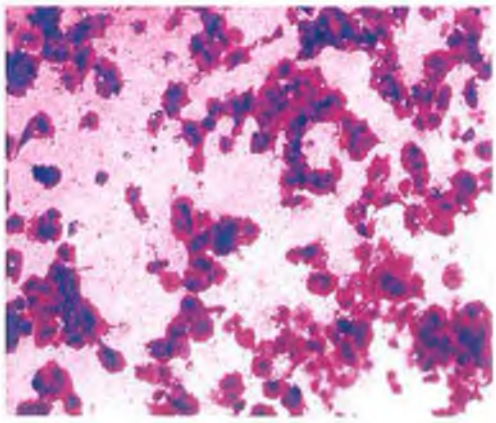

(E) DLKP4Emut8

Figure 3.2.5.2: (A) DLKP4Emut2, (B) DLKP4Emut3 (C) DLKP4Emut6, (D) DLKP4Emut7 and (E) DLKP4Emut8.

Figure 3.2.5.3 Invasion assays using DLKP4E clones

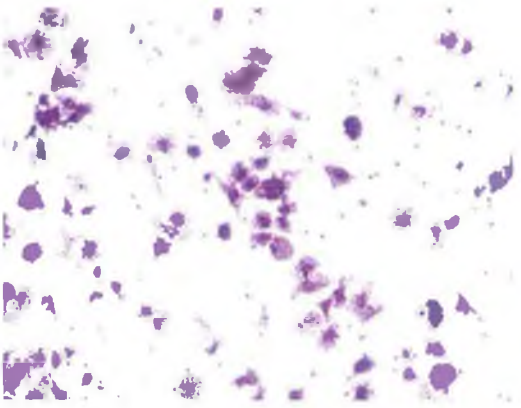

(A) DLKP4E5

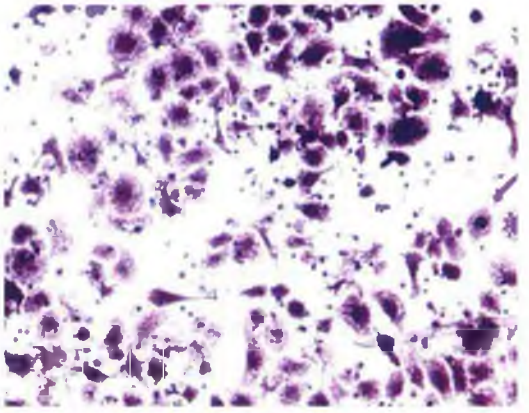

(B) DLKP4E7

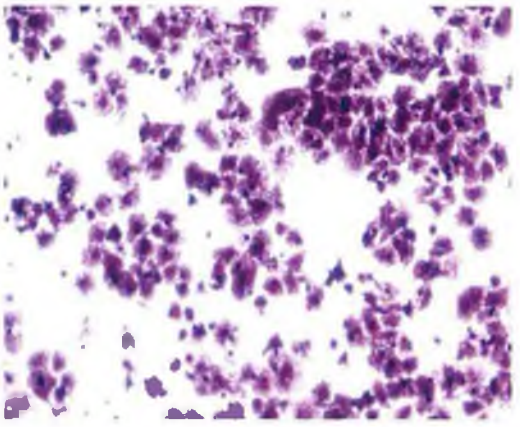

(C) DLKP4E10

(D) DLKP 4E12

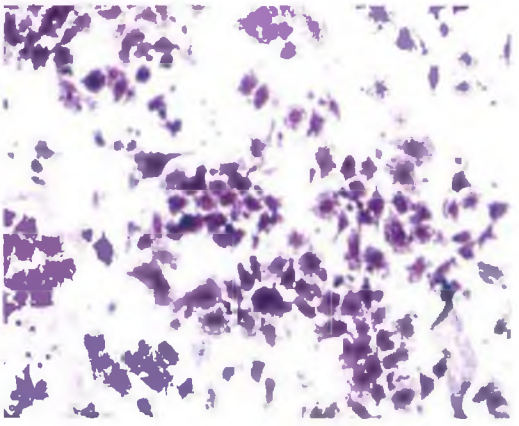

(E) DLKP 4E 17

Figure 3.2.5.3: Invasion assay results for cell lines (A) DLKP4E5, (B) DLKP4E7, (C) DLKP4E 10, (D) DLKP4E12 & (E) DLKP4E17.

Figure 3.2.5.4: Invasion assay cell-counts for parent DLKP, eIF4E/eIF4Emut and pcDNA clones

Figure 3.2.5.4:

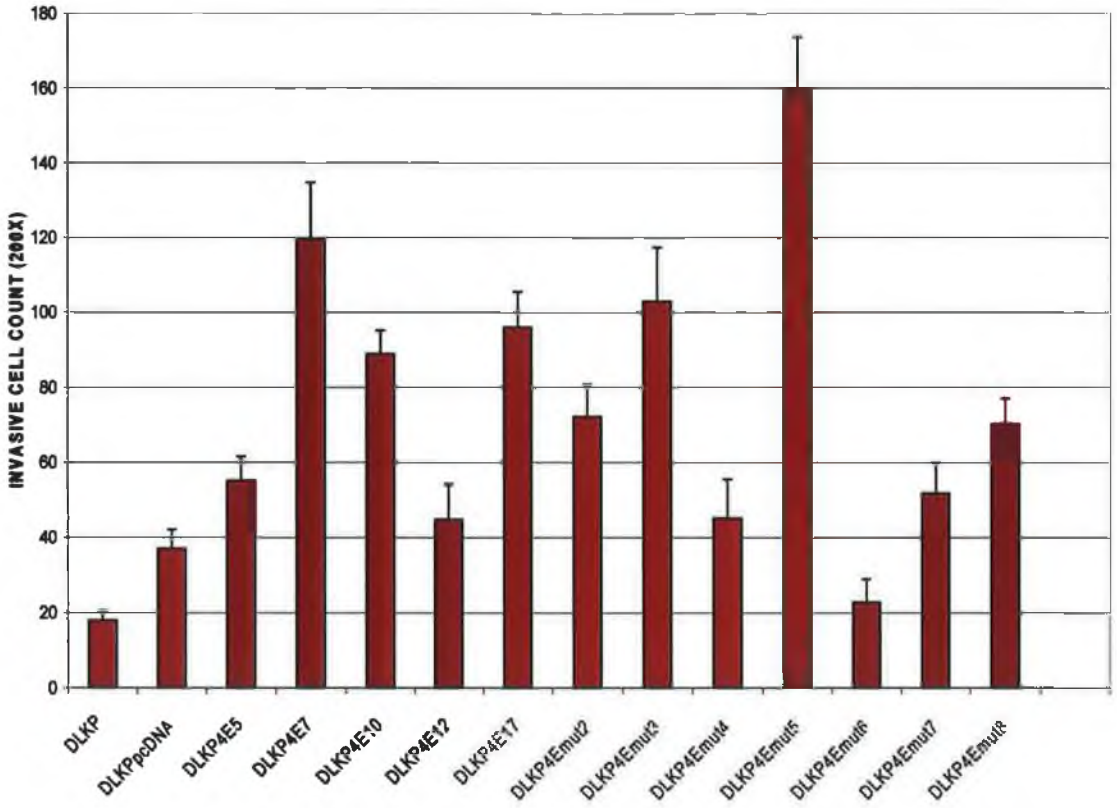

Figure 3.2.5.4: Counts of invasive cells: Cell counting was facilitated by photographing the membrane using an inverted microscope. The cells were observed at 200X magnification.

3.2.6 Effect of eIF4E and eIF4Emut on drug resistance

Toxicity assays were carried out (see section 2.3.1) on DLKP, DLKP4E and DLKP4Emut cells using Adriamycin and Taxol. The purpose of this was to assess the effect, if any, of eIF4E and eIF4Emut on drug resistance. Taxol, as described in section 3.1.9, does not affect protein synthesis. Adriamycin acts by intercalating with double stranded DNA, thus disrupting transcription and translation. This allowed assessment of the role of eIF4E drug resistance across a broader range of drug mechanisms. A selection of clones with different levels of HAtagged-eIF4E and invasion were chosen for this set of experiments (Figure 3.2.6.1 and 3.2.6.2).

3.2.6.1 Taxol toxicity assays using DLKP, DLKP4E & DLKP4Emut clones

Toxicity assays performed using Taxol showed DLKP4Emut 6, DLKP4E 7 and 10 to be more resistant to the drug than the parent (Figure 3.2.6.1), with fold changes from 1.2- to 1.6-fold greater that DLKP. The majority of the clones showed no change or a decrease in resistance to the drug. The results did not correlate with HAtag expression and were therefore inconclusive.

3.2.6.2 Adriamycin toxicity assay using DLKP, DLKP4E & DLKP4Emut clones

DLKP4Emut 7, 8, 9 and 10 showed an increase in resistance, as did DLKPF4E 14 and 17. All of these clones were HAtag positive. However, eIF4Emut 6 also expressed HAtag protein and showed a decrease in resistance (Figure 3.2.6.2). These results showed that most clones that expressed HAtag also displayed an increase in drug resistance, which implies eIF4E plays a role in adriamycin drug resistance in DLKP.

Figure 3.2.6.1 Taxol toxicity assays DLKP, DLKP4E & DLKP4Emut clones

Figure 3.2.6.1:

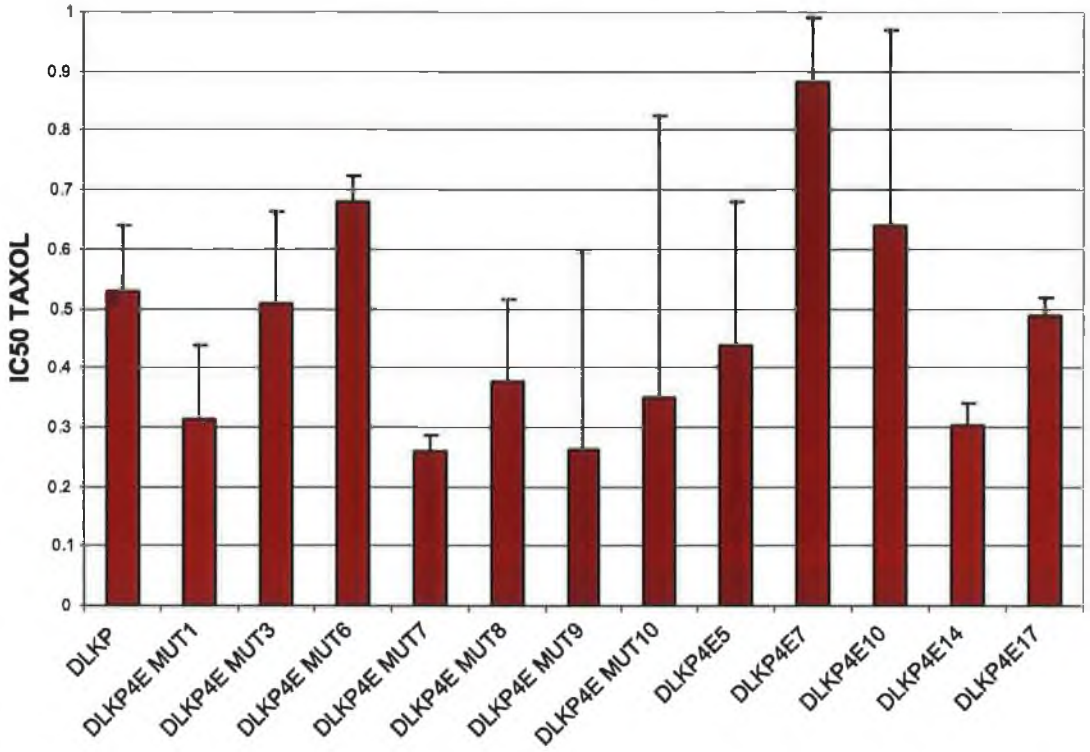

Table 3.2.6.1:

CELL LINE	FOLD CHANGE
DLKP	1
DLKP4E MUT1	0.5876
DLKP4E MUT3	0.95622
DLKP4E MUT6	1.28
DLKP4E MUT7	0.48
DLKP4E MUT8	0.71
DLKP4E MUT9	0.49
DLKP4E MUT10	0.66
DLKP4E5	0.82
DLKP4E7	1.66
DLKP4E10	1.2
DLKP4E14	0.57
DLKP4E17	0.918

Figure 3.2.6.1: Taxol IC50 values for DLKP, DLKP4E and DLKP4Emut clones; Table 3.2.6.1: Fold change of resistance to Taxol.

Figure 3.2.6.2 Adriamycin toxicity assay DLKP, DLKP4E & DLKP4Emut clones

Figure 3.2.6.2:

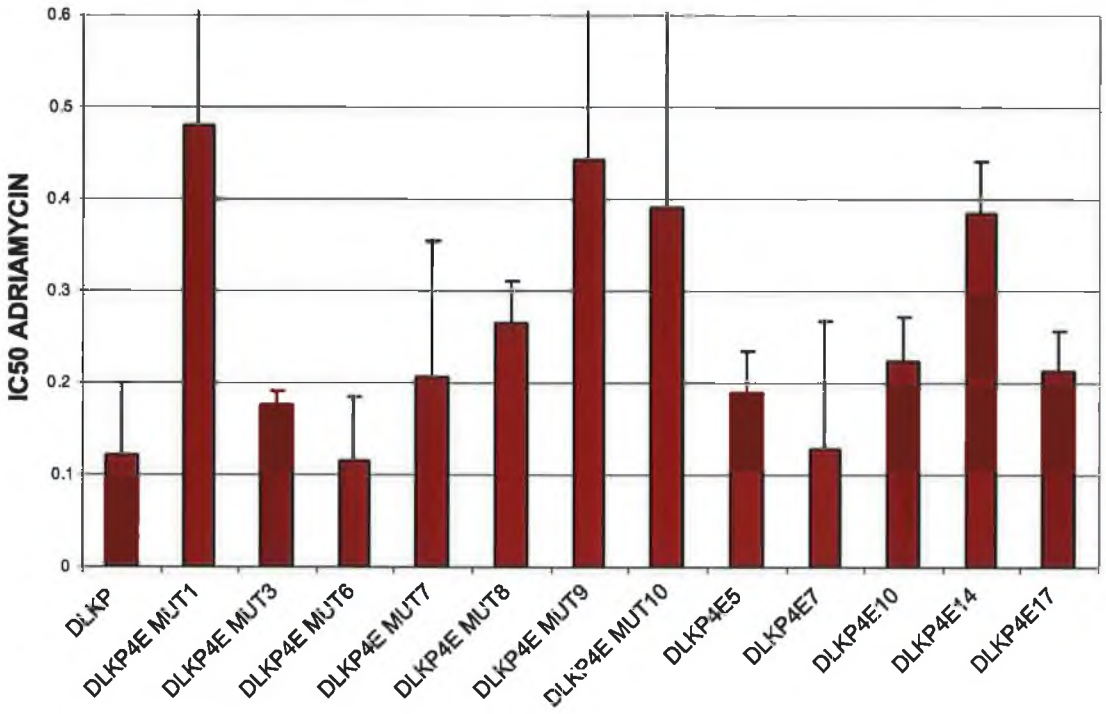

Table 3.2.6.2:

CELL LINE	FOLD CHANGE
DLKP	1
DLKP4E MUT1	3.95
DLKP4E MUT3	0.36
DLKP4E MUT6	0.94
DLKP4E MUT7	1.69
DLKP4E MUT8	2.18
DLKP4E MUT9	6.34
DLKP4E MUT10	3.22
DLKP4E5	1.55
DLKP4E7	1.06
DLKP4E10	1.83
DLKP4E14	3.16
DLKP4E17	1.74

Figure 3.2.6.2: Adriamycin IC50 values for DLKP, DLKP4E and DLKP4Emut clones; Table 3.2.6.2: Fold change of resistance to Adriamycin.

3.3 Microarray analysis

Microarray gene expression experiments were carried out on 10 cell lines (Table 3.3.1). These were DLKP, DLKP4E17, DLKP4Emut8, DLKPpcDNA1, MCF7, MCF74E6, MCF74Emut6, MCF7pcDNA1, MCF7H3erbB2 and MCF7H3. The microarray gene expression experiments which were carried out in this body of work were performed using Affymetrix® GeneChip® Whole genome expression microarray (Section 2.5).

3.3.1 Invasion status of cell lines used for microarray analysis

All cell lines included in microarray analysis were chosen based on their invasion status, obtained from invasion assay results (Section 3.1.7, 3.1.8 & 3.1.9). The purpose of this analysis was to compare invasive and non-invasive cell lines in order to identify genes involved in invasion.

Table 3.3.1 Cell lines used in array analysis

Cell line	Invasion status	Cell type
DLKP	Mildly invasive	Poorly differentiated human Lung squamous carcinoma
DLKP4E	Invasive	Clonal subpopulation of eIF4E cDNA transfected DLKP
DLKP4Emut	Invasive	Clonal subpopulation of eIF4Emut cDNA transfected DLKP
DLKPpcDNA	Mildly invasive	Clonal subpopulation of pcDNA transfected DLKP
MCF7	Non-invasive	Human breast adenocarcinoma
MCF74E	Non-invasive	Clonal subpopulation of eIF4E cDNA transfected MCF7
MCF74Emut	Non-invasive	Clonal subpopulation of eIF4Emut cDNA transfected MCF7
MCF7pcDNA	Non-invasive	Clonal subpopulation of pcDNA transfected MCF7
MCF7H3	Non-invasive	Clonal subpopulation of MCF7
MCF7H3 erbB2	Invasive	Clonal subpopulation of MCF7H3 transfected with erbB2 Clonal subpopulation of MCF7H3 transfected with erbB2

3.3.2 Microarray QC

The U133 Plus 2.0 Affymetrix gene chip contains the probesets for 54,675 gene transcripts. The percentage of genes called present relative to the number of genes present on the array is typically 40-60% for a given experiment, which can be translated to roughly 25-30,000 gene transcript results for each experiment. To reduce the volume of results for further analysis, only probesets found present across all replicates are used. Three microarray chips were run for each cell line used in this experiment, and the resulting data compared based on their degree of similarity. That is, each set of gene transcripts 'present' on each chip were compared to each other set, to find similar genes. The strength of the linear relationship between samples was calculated in terms of a correlation coefficient. The closer this coefficient was to 1, the closer the linear relationship. If any one of the samples did not correlate and a list of genes was chosen from the comparison of all three, this would have increased the number of false negatives, and as a result a lot of important genes would have been overlooked. Removing the rogue sample however, would increase the number of false positives. It was vital that the 'present' call for each sample was accurate in order to ensure an exact comparison between samples. The accuracy with which the percentage of transcripts present was calculated was dependent on stringent physical QC.

3.3.2.1 Physical QC

The array image was monitored using the following control parameters as outlined by Affymetrix®, using Microarray Suite 5.0 (MAS5.0).

3.3.2.1.1 Visual inspection

After scanning the array chips were inspected for the presence of image artefacts. These include spots or regions on the chip with unusually high or low intensity, scratches or overall background. The boundaries of the probe area were easily identified by the hybridization of the B2 oligo, which is spiked into each hybridization cocktail. Hybridization of B2 was highlighted on the image by the following:

1. The 'cross' pattern of intensities on the centre of the chip
2. The checkerboard pattern at each corner

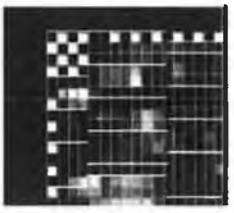

An example of B2 illuminating the corner and edges of the array (affymetrix.com).

B2 Oligo served as a positive hybridization control and was used by the software to place a grid over the image. All of the chips used passed visual inspection.

3.3.2.1.2 Scaling factor

Each array has varying image intensity, and this intensity, or brightness, is measured by the 'scaling factor'. In order to make an accurate comparison of multiple sets of array data the intensities of the arrays were brought to the same level. This process was performed by GCOS® (GeneChip Operating Software) using a mathematical technique known as 'scaling'. Scaling worked by calculating the overall intensity of an array and averaging every probe set on the array (with the exception of the top and bottom 2% of the probe set intensities). The average intensity of the array was then multiplied by the scaling factor to ensure that all of the intensities on the given array went up or down to a similar degree. Scaling allowed normalisation of several experiments to one target intensity. It is recommended that the scaling factor for all of the arrays in a particular experiment should be within 3-fold of each other. All of the scaling factors in this set of arrays were between 0.8 and 1.5 (Table 3.3.2-3.3.4).

3.3.2.1.3 Noise

'Noise' measured the pixel-to-pixel variation of probe cells on the array. It was caused by small variations in the digital signal observed by the scanner as it sampled the array surface. As each scanner has a unique electrical noise associated with its operation, noise values among scanners vary. However, arrays that were scanned on the same scanner would be expected to have similar noise values. Noise values above 3 would normally be deemed excessive and indicate a poor scanning result. All of the noise values for this set of arrays were between 1.3 and 1.7 (Table 3.3.2-3.3.4).

3.3.2.1.4 Background

Affymetrix® have found that typical background values range from 20 to 100 and that arrays being compared should have similar background. Values above 100 would be deemed unacceptable. The background values ranged from 43 to 56 for this set of arrays, which is acceptable (Table 3.3.2-3.3.4).

3.3.2.1.5 %Present

The percentage of genes present determines the number of probe sets called present, relative to the total number of probe sets on the array. Replicate samples should have similar %present calls. Typical % call values for cell lines are 40-60%, lower values usually being attributed to poor quality of sample. Each set of samples used in this study had between 40-47 % present, and each set of replicates were within 3% of each other (Table 3.3.2-3.3.4).

3.3.2.1.6 3'/5' Ratio GAPDH

In addition to the conventional probe sets designed to be within the most 3' 600 bp of a transcript, additional probe sets in the 5' region and middle portion of the transcript have also been selected for certain housekeeping genes, including GAPDH and β-actin. Signal intensity ratio of the 3' probe set over the 5' probe set is often referred to as the 3'/5' ratio. This ratio gives an indication of the integrity of starting RNA, efficiency of first strand cDNA synthesis, and/or indicates whether the in vitro transcription (IVT) of cRNA step proceeded to completion. The signal of each probe set reflects the sequence of the probes and their hybridization properties. A 1:1 molar ratio of the 3' to 5' transcript regions will not necessarily give a signal ratio of 1. A ratio of 1 is considered ideal, and values above 3 indicate incomplete transcripts are being generated, most likely due to poor quality starting RNA. The highest ratio recorded for this set of arrays was 1.3 (Table 3.3.2-3.3.4).

3.3.2.1.7 Bio's Present

BioB, bioC and *bioD* represent genes in the biotin synthesis pathway of *E. coli*. *Cre* is the recombinase gene from P1 bacteriophage. The GeneChip® Eukaryotic Hybridization Control Kit contains 20x Eukaryotic Hybridization Controls that are composed of a mixture

of biotin-labeled cRNA transcripts of *bioB, bioC, bioD*, and *cre,* prepared in staggered concentrations (1.5 pM, 5 pM, 25 pM, and 100 pM final concentrations for *bioB, bioC, bioD*, and *cre*, respectively). The 20x Eukaryotic Hybridization Controls are spiked into the hybridization cocktail, independent of RNA sample preparation, and are thus used to evaluate sample hybridization efficiency on eukaryotic gene expression arrays. *BioB* is at the level of assay sensitivity (1:100,000 complexity ratio) and should be called "Present" at least 50% of the time. *BioC, bioD*, and *cre* should always be called "Present" with increasing signal values, reflecting their relative concentrations. All chips used in this study met this criteria (table 3.3.2-3.3.4).

The 20x Eukaryotic Hybridization Controls can be used to indirectly assess RNA sample quality among replicates. When global scaling is performed, the overall intensity for each array is determined and is compared to a Target Intensity value in order to calculate the appropriate scaling factor. The overall intensity for a degraded RNA sample, or a sample that has not been properly amplified and labeled, will have a lower overall intensity when compared to a normal replicate sample. Thus, when the two arrays are globally scaled to the same Target Intensity, the scaling factor for the "bad" sample will be much higher than the "good" sample. However, since the 20x Eukaryotic Hybridization Controls are added to each replicate sample equally (and are independent of RNA sample quality), the intensities of the *bioB, bioC, bioD*, and *cre* probe sets will be approximately equal. As a result, the signal values (adjusted by scaling factor) for these control probe sets on the "bad" array will be adjusted higher relative to the signal values for the control probe sets on the "good" array.

Table 3.3.2: Physical QC of MCF7, MCF74E, MCF74Emut &MCF7pcDNA

Sample Name	MCF7 1	MCF7 2	MCF7 3	MCF7 4E1	MCF7 4E2	MCF7 4E3	MCF7 4Emut1	MCF7 4Emut2	MCF7 4Emut3	MCF7 PcDNA 1	MCF7 PcDN A2	MCF7 PcDNA3
Visual Inspection	YES	YES	YES	YES	YES	YES	YES	YES	YES	YES	YES	YES
Scaling Factor	1.018	0.865	0.994	0.93	0.931	1.144	1.211	0.847	1.091	1.233	1.531	1.235
Noise	1.67	1.61	1.78	1.47	1.65	1.47	1.49	1.75	1.66	1.54	1.45	1.45
Backround	48.85	47.34	52.86	44.21	48.33	45.28	44.11	51.76	48.65	48.03	43.92	44.94
%Present	43.8	45.6	42.7	46.3	43	43.3	42.9	44	42.9	42.2	41.6	42.8
3'/5' Ratio GAPDH	1.10	1.05	1.05	1.03	1.36	1.31	1.09	1.00	1.00	1.18	1.3	1.28
Bio's Present	YES	YES	YES	YES	YES	YES	YES	YES	YES	YES	YES	YES

Table 3.3.3: Physical QC of MCFH3 & MCF7H3erbB2

Sample Name	MCF7H3 1	MCF7H3 2	MCF7H3 3	MCF7H3 erbB2 1	MCF7H3 erbB2 2	MCF7H3 erbB2 3
Visual Inspection	YES	YES	YES	YES	YES	YES
Scaling Factor	0.868	1.165	0.997	1.134	0.972	1.128
Noise	1.74	1.560	1.8	1.67	1.79	1.5
Backround	52	47.15	54.1	48.15	55.14	44.96
%Present	44.5	41.6	42.5	43.6	44.8	44.8
3'/5' Ratio GAPDH	1.03	1.06	1.06	1.14	1.12	1.10
Bio's Present	YES	YES	YES	YES	YES	YES

Table 3.3.4: Physical QC of DLKP, DLKP4E, DLKP4Emut & DLKPpcDNA

Sample Name	DLKP 1	DLKP 2	DLKP 3	DLKP 4E1	DLKP 4E2	DLKP 4E3	DLKP 4Emut1	DLKP 4Emut2	DLKP 4Emut3	DLKP PcDNA 1	DLKP PcDNA 2	DLKP PcDNA 3
Visual Inspection	YES	YES	YES	YES	YES	YES	YES	YES	YES	YES	YES	YES
Scaling Factor	0.883	0.872	0.966	0.961	0.851	1.204	0.924	1.14	0.99	1.29	0.813	0.972
Noise	1.63	1.73	1.46	1.53	1.63	1.46	1.61	1.58	1.69	1.43	1.72	1.57
Backround	48.58	54.35	44.35	47.88	49.67	45.13	49.03	48.5	51.6	44.29	52.52	47.9
%Present	43.9	44.7	44.5	44.8	43.5	44.1	44.3	42.9	44.3	43	46.5	43.9
3'/5' Ratio GAPDH	1.05	1.06	1.04	1.05	1.06	1.09	1.06	1.09	1.07	1.18	1.16	1.18
Bio's Present	YES	YES	YES	YES	YES	YES	YES	YES	YES	YES	YES	YES

3.3.2.2 Hierarchal clustering

Hierarchical clustering was used to represent the relationship between replicate samples and different sets of replicate samples (section 2.5.14). The tree represents relationships amongst genes in which, branch lengths represent degrees of similarities. This method was useful in its ability to represent varying degrees of similarity and distant relationships among groups of closely related genes. The computed tree was used to organize genes in the original data table, so that genes with similar expression patterns were adjacent. The general procedure for hierarchical clustering followed two steps,

1. The closest points (clusters) were found and merged
2. This process was continued until a single cluster was obtained (all the points).

There were two prerequisites for this procedure:

3. The distance measured between two points
4. The distance measured between clusters.

All of the samples used in the experiment were run in triplicate, and therefore all three replicates of a particular sample were expected to cluster together, and all such clusters were expected to be significantly differently from each of the other clusters. This was not the case for three of the sets of samples (Figure 3.3.1a). DLKP2, DLKP4E2 and MCF74E2 did not behave as expected and did not cluster with their replicates. These samples were removed from further analysis (Figure 3.3.1b).

Figure 3.3.1a Hierarchal clustering of all samples used in microarray gene expression experiments

Figure 3.3.1a:

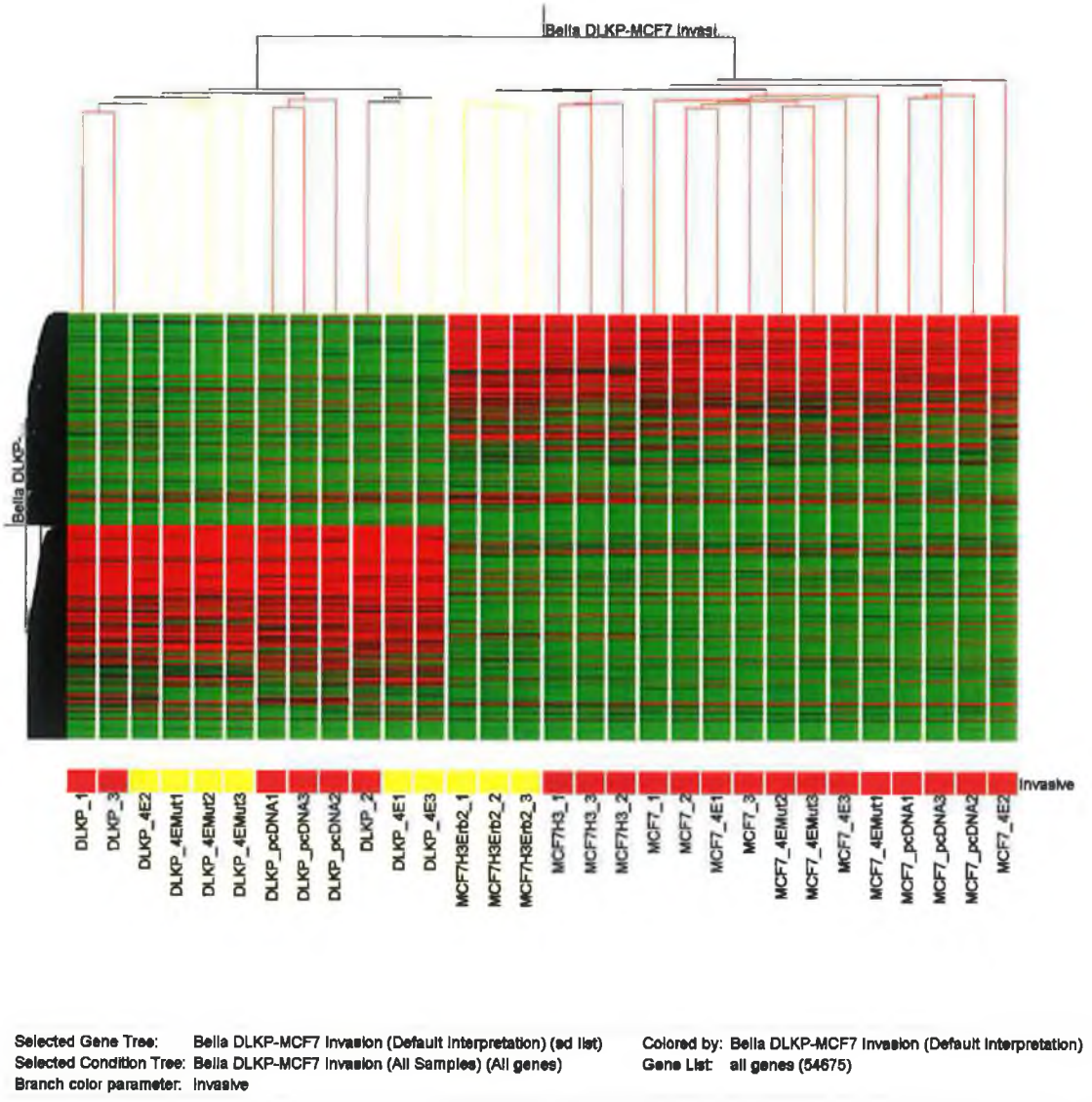

Figure 3.3.1a: Hierarchal clustering of all samples used in microarray gene expression experiments. The tree represents relationships amongst genes in which branch lengths represent degrees of similarities.

Figure 3.3.1b Hierarchal clustering of samples from microarray gene expression experiments used for further analysis

Figure 3.3.1b:

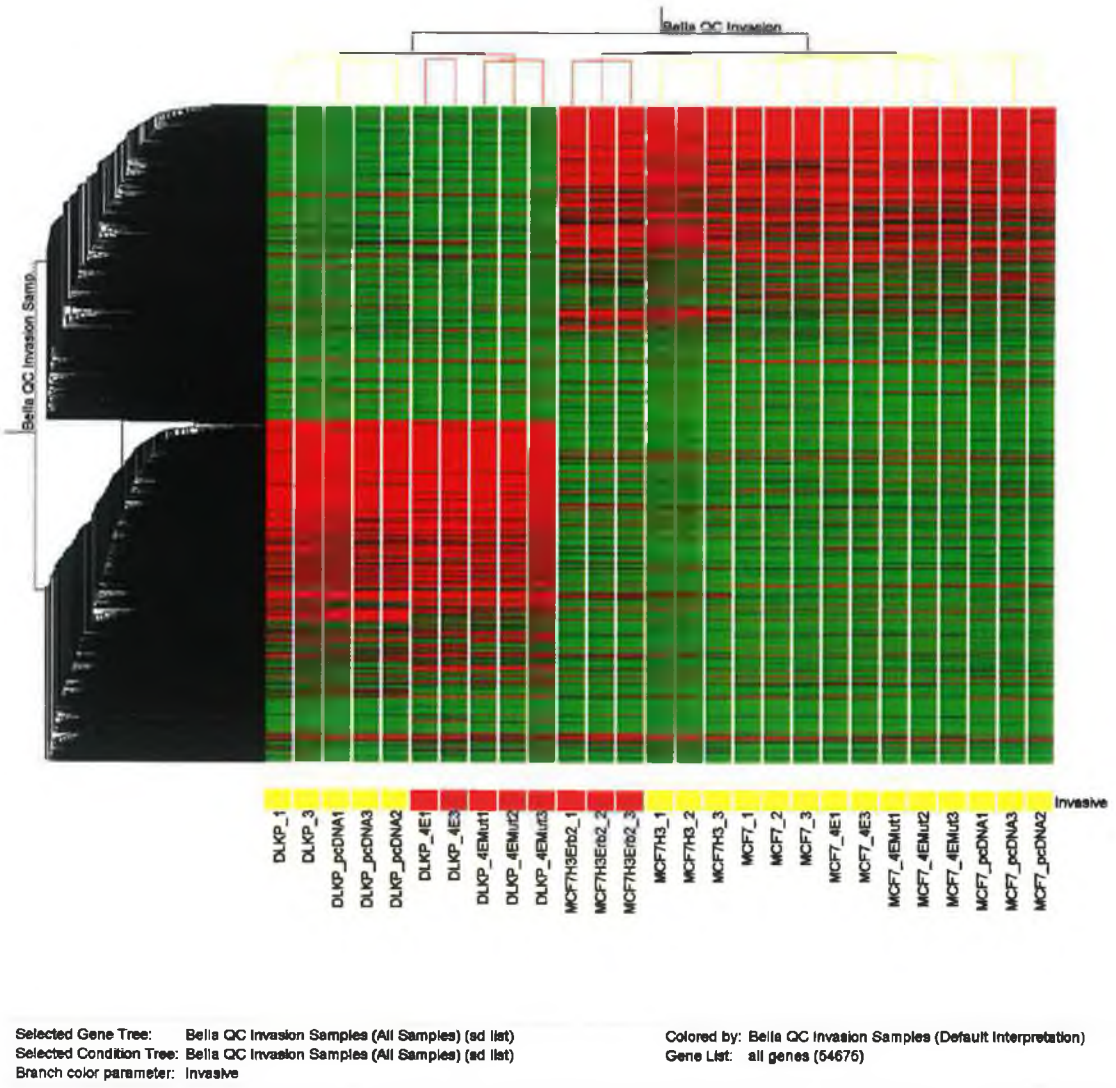

Figure 3.3.1b: Hierarchal clustering after removal of DLKP2, DLKP4E2 and MCF74E2.

3.3.2.2.1 The correlation matrix

In probability theory and statistics, correlation, also called correlation coefficient, indicates the strength and direction of a linear relationship between two random variables. The best known is the Pearson product-moment correlation coefficient, which is obtained by dividing the covariance of the two variables by the product of their standard deviations. In assuming a linear relationship between variables, the correlation coefficient quantifies the strength of the linear relationship between those variables. In microarray experiments, the correlation coefficient measured the amount of variation between groups of genes in replicate samples. The closer the correlation coefficient was to 1 the stronger the relationship. Values closer to 0 implied a poor linear relationship.

Table 3.3.5 (A) shows the correlation coefficients of individual DLKP samples compared with each other. DLKP2 did not perform as it should and only had a correlation value of 0.67 when compared to the other replicates. The correlation matrix for DLKP4E also shows similar results, with DLKP4E2 having a correlation coefficient of 0.53 (Table 3.3.5 (B)). In the case of MCF74E, one of the samples (MCF74Ea) did not cluster initially and the sample was repeated (MCF74Eb). Neither of the two samples had good correlation values (Table 3.3.5 (C)). The maximum correlation coefficient in this group was only 0.63 which is very low, however it is doubtful that repeating the experiment a second time would have improved the correlation between samples. Due to the above results it was decided to continue with three sets of two rather than repeat the arrays for DLKP, DLKP4E and MCF74E. This was done in order to reduce the amount of false negative results, as explained in section 3.3.2.

Table 3.3.5 Summary of correlation matrix results for DLKP, DLKP4E and MCF74E used in microarray analysis

A. DLKP correlation matrix

SAMPLE	DLKP1	DLKP2	DLKP3
DLKP1	1	0.67352	0.828255
DLKP2	0.67352	1	0.672595
DLKP3	0.828255	0.672595	1

B. DLKP4E correlation matrix

SAMPLE	DLKP4E1	DLKP4E2	DLKP4E3
DLKP4E1	1	0.535093	0.801237
DLKP4E2	0.535093	1	0.541529
DLKP4E3	0.801237	0.541529	1

C. MCF74E correlation matrix

SAMPLE	MCF74E1	MCF74E2a	MCF74E2b	MCF74E3
MCF74E1	1	0.477467	0.557717	0.634662
MCF74E2a	0.477467	1	0.604347	0.469049
MCF74E2b	0.557717	0.604347	1	0.599217
MCF74E3	0.634662	0.469049	0.599217	1

Table 3.3.5: A=correlation values for each DLKP sample compared to each other DLKP sample; B= as with A, but using DLKP4E; C=as with A, but using MCF74E.

3.3.3 Generation of gene lists

The aim of the microarray analysis was to generate gene lists that were specific to an invasive phenotype, in order to identify genetic markers for invasion. Before generating these gene lists it was important to examine the relationship between different cell lines as observed by hierarchal clustering (Figure 3.3.1). Firstly, the data can be divided into two distinct groups, one consisting of all the DLKP variants, and one of the MCF7 variants. This result was as expected. As already mentioned, three samples (DLKP2, DLKP4E2 and MCF74E2) did not behave as expected, and this was obvious from the way they clustered compared to their replicate samples. As a result of this analysis, these samples were removed from further study.

3.3.3.1 Initial gene list comparisons

The purpose of initial comparisons was to determine the number of genes changed between the baseline and experiment samples. Gene filters employed for this analysis included a raw value difference (between baseline and experiment) of at least 100, a fold change of at least 1.2. After these filters were in place and the relevant genes were removed, a Welch modified two-sample t-test was carried out to generate p-values for each probe. Only P-values of less than 0.05 were accepted. Gene list comparisons were made using dChip(section 2.5.14) and are summarised in Table 3.3.6.

Table 3.3.6: Initial gene lists comparisons

Cell line comparison	Number of genes changed
DLKP versus DLKP4E	1415
DLKP versus DLKP4Emut	1138
DLKP versus DLKPpcDNA	1950
MCF7 versus MCF74E	864
MCF7 versus MCF74Emut	1828
MCF7 versus MCF7pcDNA	289
MCF7H3 versus MCF7H3 erbB2	3348
MCF7 versus MCF7H3	4106

Table 3.3.6: The above comparisons were made using dChip and Stanford's gene comparison program (see section 2.5.16):

3.3.3.2 Genes specific to invasion in MCF7 variants

Table 3.3.7 generation of genes specific to invasion and MCF7H3erbB2

Cross list comparisons	Number of genes changed
[MCF7H3 versus MCF7H3erbB2] NOT [MCF7 versus MCF7pcDNA] = [A]	1755
[A] NOT [MCF7 versus MCF74E] = [B]	1604
[B] NOT [MCF7 versus MCF74Emut] = [C]	1313
[C] versus [MCF7 versus MCF7H3]= [D]	120

Table 3.3.7: The above comparisons were made using dChip and Stanford's gene comparison program (see section 2.5.14-16):

3.3.3.2.1 Gene changes specific to eIF4E in MCF74E

Comparison of MCF7 (baseline) to MCF74E (experiment) resulted in a list of 864 genes. That is, the expression of 864 genes was up- or down-regulated in MCF7 after exogenous expression of eIF4E.

3.3.3.2.2 Gene changes specific to eIF4Emut in MCF74Emut

When MCF7 was compared to MCF74Emut, again MCF7 was taken as the baseline and MCF74Emut as the experiment. The 1828 resulting gene changes referred to the number of genes expressed in MCF74Emut that were up- or down-regulated compared to those expressed in MCF7. The resulting list of differentially expressed genes are those specific to MCF7 after stable transfection of eIF4Emut.

3.3.3.2.3 Gene changes specific to pcDNA in MCF7pcDNA

Again MCF7 was taken as the baseline and in this case MCF74EpcDNA was the experiment. 2829 genes were found differentially expressed in MCF7pcDNA. This list of genes are those specific to MCF7 after stable transfection of the pcDNA empty

plasmid. There were a surprising number of gene changes due to expression of an empty plasmid.

3.3.3.2.4 Gene changes specific to erbB2 in MCF7H3erbB2

In this comparison, MCF7H3 was taken as the baseline and MCF7H3erbB2 as the experiment. The resulting 3348 gene changes referred to the number of genes expressed in MCF7H3erbB2 that were up- or down-regulated compared to those expressed in MCF7H3. The resulting list of differentially expressed genes are those specific to MCF7H3 after exogenous expression of erbB2.

3.3.3.2.5 Gene changes in MCF7H3 due to clonal variation

As further analysis of the MCF7H3erbB2 invasive phenotype was to involve comparison with non-invasive MCF7, it was necessary to examine the difference between MCF7 and MCF7H3. Taking the parental MCF7 as the baseline, and the clone MCF7H3 as the experiment, 4106 genes were found differentially expressed. This result demonstrates the large number of changes that are possible due to clonal variation alone, and offers an explanation to the high number of gene changes in DLKP and MCF7 after transfection with and empty pcDNA plasmid.

3.3.3.3 Genes related to invasion and specific to MCF7H3erbB2

Analysis found 3348 genes were changed in MCF7H3erbB2 due to up-regulation of erbB2. As up-regulation of erbB2 had caused an increase in invasion in MCF7H3, these genes were also related to an invasive phenotype. Up-regulation of eIF4E, eIF4Emut and pcDNA in mixed-population MCF7 did not result in a change in invasion. Therefore, in order to reduce the number of genes for further analysis, and narrow the search for invasion-related genes, gene changes in non-invasive MCF7 cell lines were removed from those in invasive MCF9H3erbB2. To generate a list of genes related to invasion and specific to MCF7H3erbB2 the following comparisons were made using dChip and Stanford's gene comparison web page (http://wormchip.stanford.edu /~jiml/Compare.html)..

3.3.3.2.1 Genes specific to invasive MCF7H3erbB2 not non-invasive MCF7pcDNA.

In the initial comparison of MCF7H3 to MCF7H3erbB2, 3348 genes changes specific to up-regulation of erbB2 were detected. In order to reduce the number of genes for analysis, gene changes detected in other non-invasive MCF7 cell lines were subtracted from this list. The first of these were gene changes due to MCF7pcDNA (2829 genes). The resulting list of 1755 genes referred to gene changes specific to MCF7H3erbB2 that were not common to gene changes specific to MCF7pcDNA (Figure 3.3.2). This comparison removed gene changes due to pcDNA transfection, but not invasion.

Figure 3.3.2: Genes specific to MCF7H3erbB2 not non-invasive MCF7pcDNA

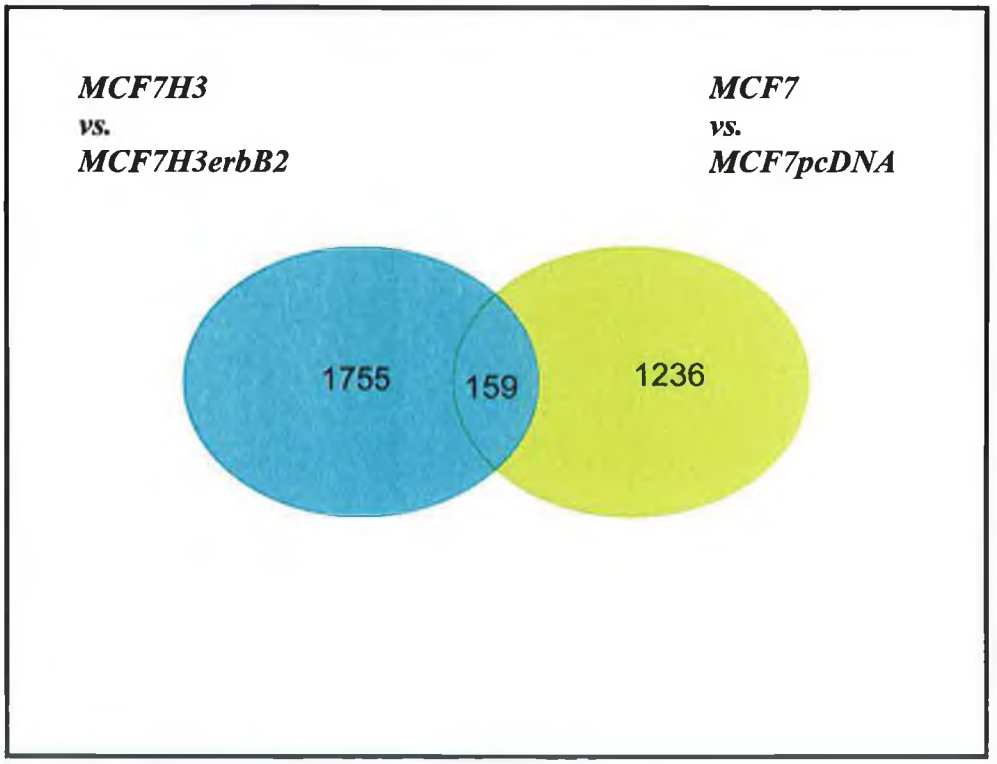

3.3.3.3.2 Genes specific to MCF7H3erbB2, not MCF7pcDNA or MCF74E

dCHip analysis found 306 genes that were specific to MCF74E (Figure 3.3.5), but not invasion. This list was compared to the list of 1755 genes specific to MCF7H3erbB2 from the previous comparison. The result was a list of 1604 genes specific to invasive MCF7H3erbB2 and not non-invasive MCF7pcDNA or MCF74E (Figure 3.3.3).

Figure 3.3.3: Genes specific to MCF7H3erbB2, not MCF7pcDNA or MCF74E

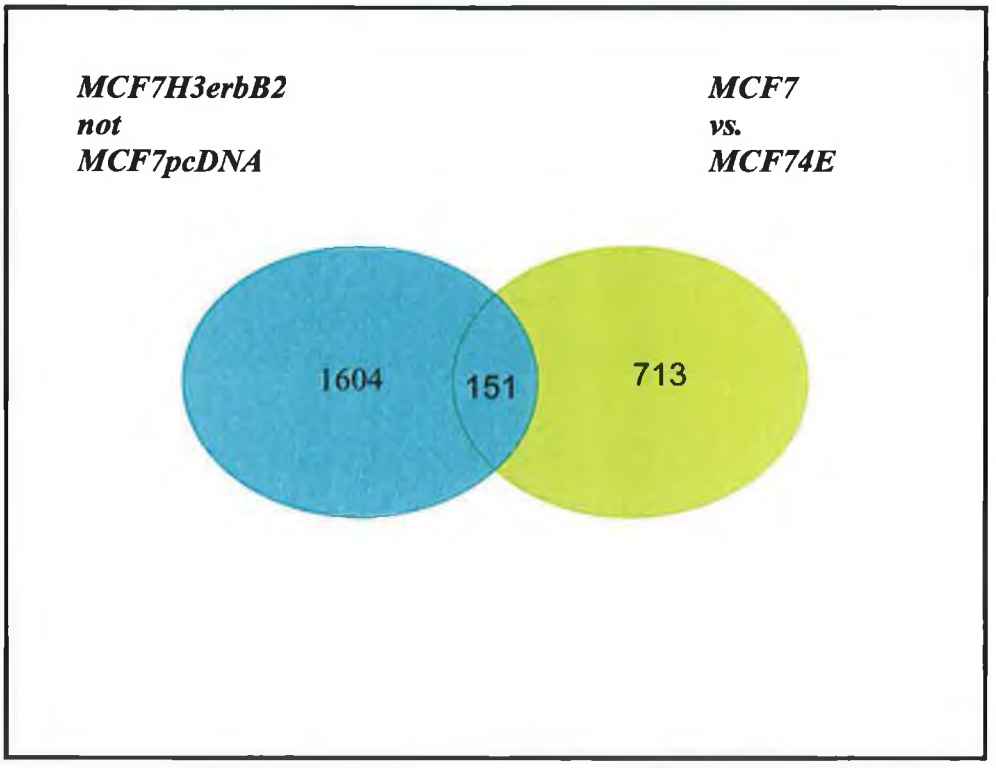

3.3.3.3.3 Genes specific to MCF7H3erbB2, not MCF7pcDNA, MCF74E or MCF74Emut

1828 genes were found differentially expressed in MCF74Emut compared to MCF7. As MCF74Emut was also a non-invasive cell line, these changes were also removed from the MCF7H3erbB2 specific list. When compared to the list of MCF7H3erbB2 specific genes from the previous comparison, 1313 genes were found specific to invasive MCF7H3erbB2 and not non-invasive MCF7pcDNA, MCF74E or MCF74Emut (Figure 3.3.4). Although transfection of MCF7 with eif4E, eif4Emut and pcDNA did not result in invasion, it is possible that genes involved in invasion were changed in these cell lines. However, these changes were not significant enough to cause invasion. That is, the full complement of genes changes required for invasion did not occur. Therefore by making this comparison some genes involved in invasion were removed from the final list, but the genes that made it through were more likely to be significant to invasion.

Figure 3.3.4: Genes specific to MCF7H3erbB2, not MCF7pcDNA, MCF74E or MCF74Emut

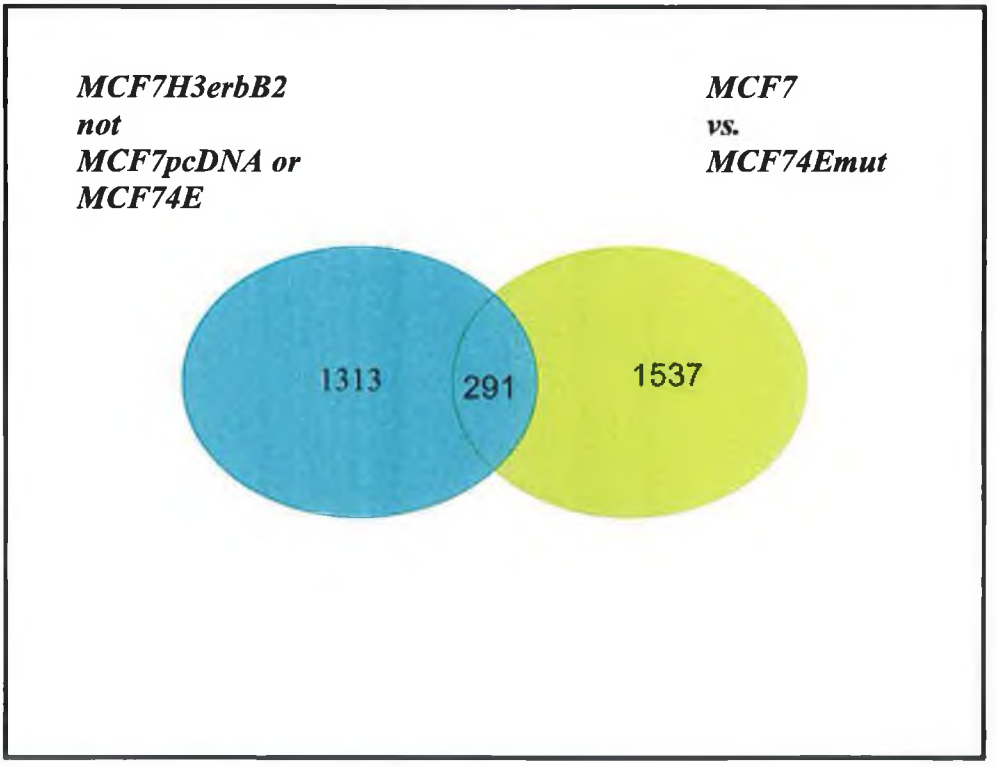

3.3.3.3.4 Gene changes specific to MCF7H3erbB2 and invasion but not due to clonal variation

The purpose of this analysis was to obtain a list of genes specific to invasion and caused by erbB2 up-regulation. This list would then be used to choose targets for siRNA knock-down. For this purpose, the list of genes needed to be further reduced. A comparison was also made between parent MCF7 (mixed population) and MCF7H3 (clone). Although it was not necessary to subtract these changes from the MCF7H3 versus MCF7H3erbB2 comparison, as this was a clone to clone transfection, it is likely that gene changes which occurred due to MCF7 to MCF7H3 clonal variation where not relevant to invasion, and so these genes were also subtracted from the list. This comparison resulted in 120 genes specific to erbB2 up-regulation and related to invasion (Figure 3.3.5).

Figure 3.3.5: Gene changes specific to MCF7H3erbB2 and invasion but not due to clonal variation

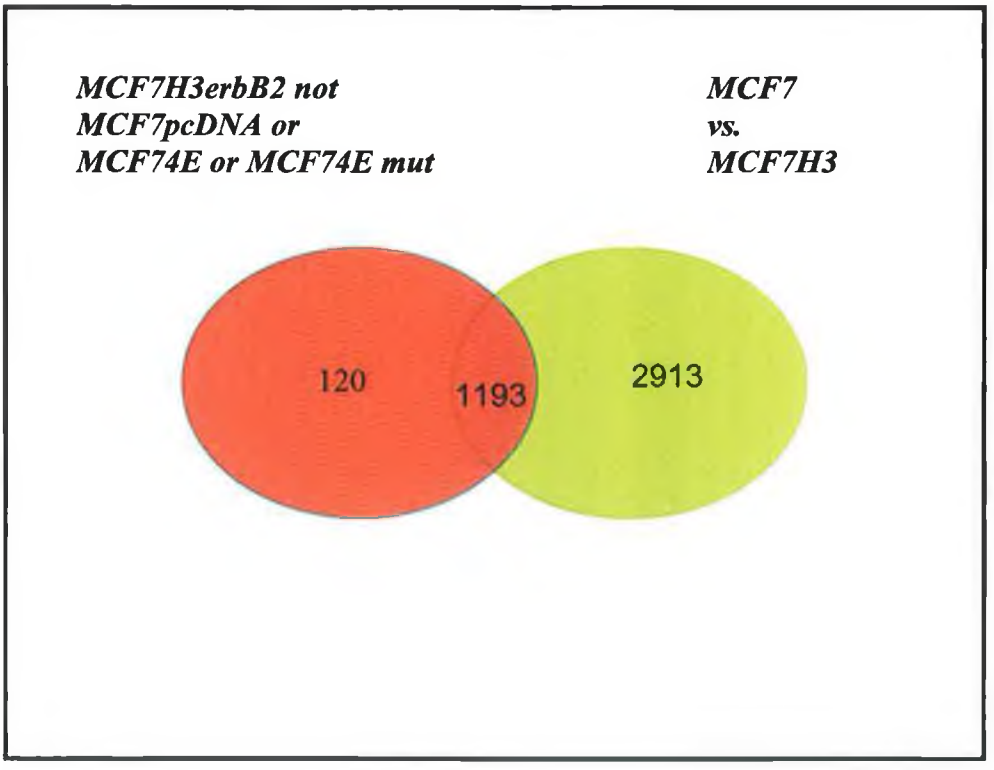

3.3.3.3.5 Final list of 120 genes specific to erbB2 and invasion

This list contained some overlap due to different probe sets targeting various gene transcripts of the same gene. Further examination found there were 108 different genes recognised on this list. Of these, 16 were poorly annotated. Analysis of the literature found 39 of these genes were related to invasion, or processes relevant to invasion. This is 36% of the total list, which demonstrated the accuracy of the microarray analysis, the purpose of which was to identify invasion-specific genes. Gene expression level, which would be an important consideration for further analysis, was also examined. Of the 108 genes, only three had expression levels <100 in either baseline or control experiments. Summary of gene list comparison in Table 3.3.7.

3.3.3.4 Pathway Assist ® analysis of MCF7H3erbB2 invasion-specific genes

PathWay Assist® (section 2.5.18) was used to identify what genes, if any, had direct interaction with each other. 'Direct interaction' identifies only direct biological interactions (controls) between selected biological objects (nodes), in this case the 108 genes (see figure 2.5.18.1 for details of 'nodes' and 'controls'). These interactions are based on information available in the literature to date, and can only take into consideration well-annotated genes. The result of this analysis was a 9-gene pathway (Figure 3.3.6, Table 3.3.5). The relationships between genes are demonstrated using 'controls', which showed MAP3K1 was involved in the regulation of RPS6KA3, ESR1, TNFAIP8 and TANK. It also showed MAP3K1 was capable of binding TANK. RPS6KA3 was shown to be involved in regulation of ESR1, possible through binding. ESR1 was also found to effect RPS6KA3 expression. PTEN was found to regulate TNFAIP8. Pathway assist results show both positive and negative regulation, which implies both are indicated in the literature.EGR1 positively regulated PTEN, and was itself bound by EGR3 and positively regulated by ESR1.

Further examination of the literature found two members of this pathway, PTEN and EGR1, interacted with Thrombospondin 1 (THBS1) (Figure 3.3.7). This gene was not present on the final list but was on the original list of MCF7H3 versus MCF7H3erbB2, with a fold change of – 2.31. What was most interesting about this gene was it linked the 9-gene pathway to tissue factor pathway inhibitor (TFPI) (Figure 3.3.7), the gene with the greatest increase of expression (19.77 fold) on the final list of 108 genes. TFPI

was chosen as a target for siRNA knock-down based on its large fold change, and THBS1 was chosen because of its association with TFPI.

3.3.3.5 MCF7H3erbB2 invasion specific genes chosen for further analysis

Five genes in all were chosen for siRNA knock-down based on specificity to MCF7H3erbB2 and invasion, association with tissue factor pathway inhibitor (as indicated by PathWayAssist®), and relevance to cancer/invasion in the literature. The other targets chosen were tumour necrosis factor alpha-induced protein 8 (TNFAIP8), early growth response 1(EGR1) and ribosomal protein S6 kniase, 90kDa, polypeptide 3 (RPS6KA3). All 3 genes were contained within the 9-gene pathway identified by PathWay Assist (Table 3.3.8).

Figure 3.3.6 Direct interaction between genes specific to MCF7H3erbB2 and invasion.

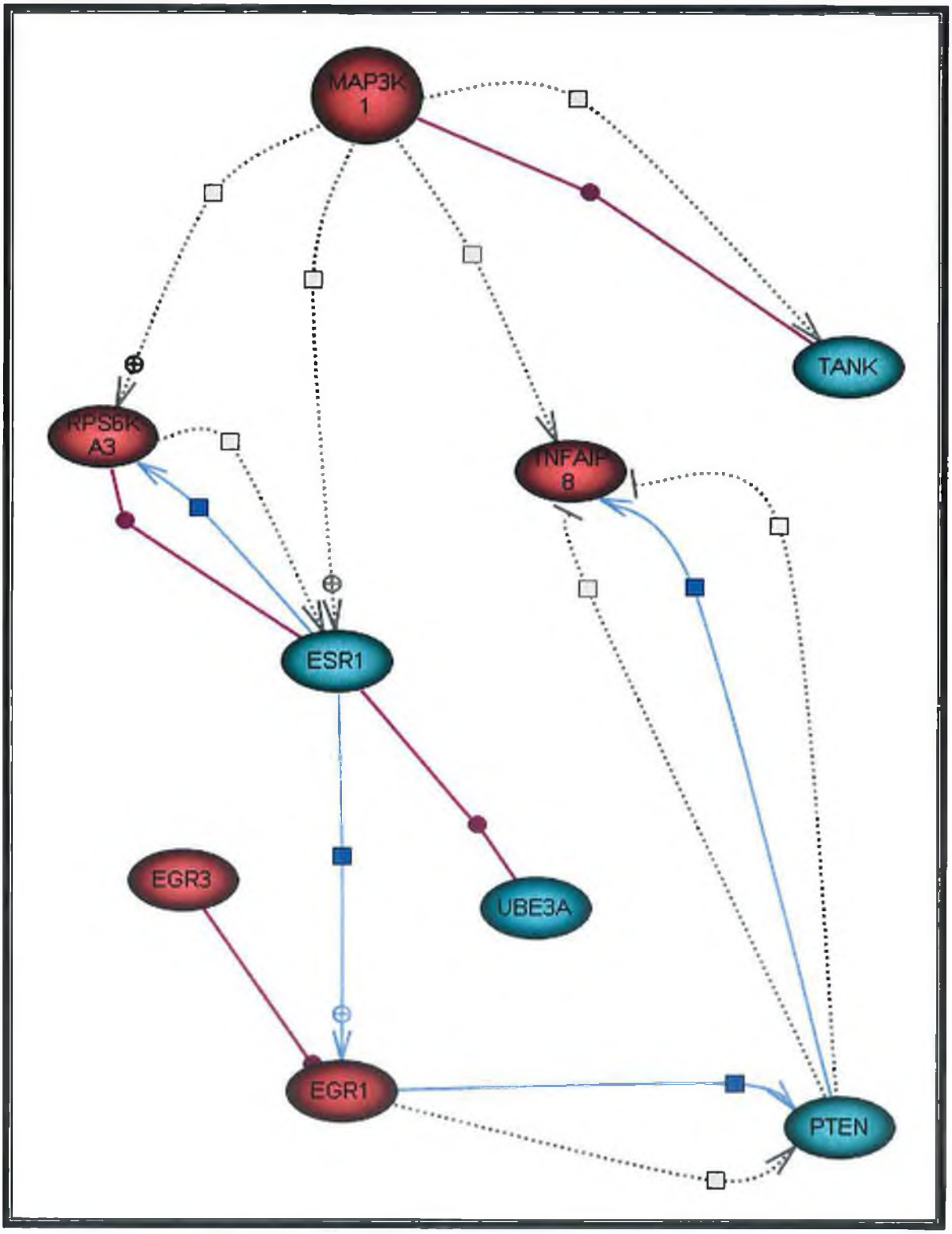

Figure 3.3.6: Pathway 1: direct interaction between genes specific to MCF7H3erbB2 and invasion. Blue = negative fold change; Red = positive fold change (Section 2.5.18)

Table 3.3.8: Genes specific to MCF7H3erbB2 and invasion (Pathway 1)

Name	Description	Fold change
TNFAIP8	tumor necrosis factor, alpha-induced protein 8	2.47
RPS6KA3	ribosomal protein S6 kinase, 90kDa, polypeptide 3	2.36
EGR3	early growth response 3	2.29
EGR1	early growth response 1	2.23
MAP3K1	mitogen activated protein kinase kinase kinase 1	1.45
PTEN	phosphatase and tensin homolog (mutated in multiple advanced cancers 1)	-1.28
ESR1	estrogen receptor 1	-1.32
TANK	TRAF family member-associated Nf-kappa B activator	-1.44
UBE3A	ubiquitin protein ligase E3A (human papilloma virus E6-associated protein, Angelman syndrome)	-1.69

Figure 3.3.7 Direct interaction between Thrombospondin and pathway 1 (genes specific to MCF7H3erbB2 and invasion)

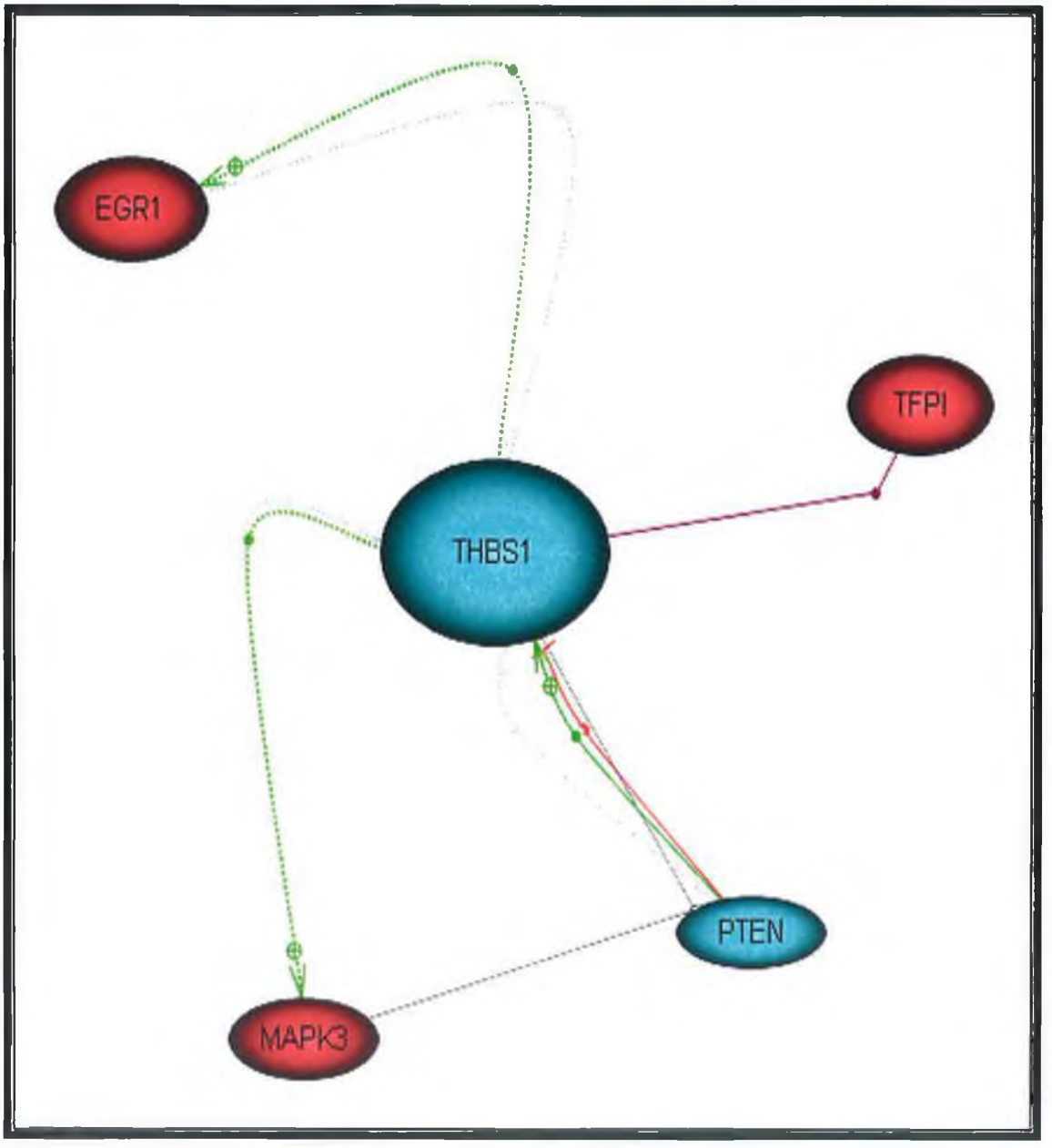

Figure 3.3.7: Pathway 2: Direct interaction between Pathway 1, THBS1 and TFPI.
Blue = negative fold change; Red = positive fold change (Section 2.5.18)

Table 3.3.9: Genes linking TFPI to Pathway 1 (Pathway 2)

Name	Description	Fold change
TFPI	tissue factor pathway inhibitor	20.28
EGR1	early growth response 1	2.99
MAPK3	mitogen activated protein kinase 3	1.31
PTEN	phosphatase and tensin homolog	-1.28
THBS1	thrombospondin 1	-2.31

Table 3.3.10 Genes used for siRNA specific to MCF7H3erbB2/invasion

Gene	Description	Fold Change
TFPI	Tissue factor pathway inhibitor (lipoprotein-associated coagulation inhibitor)	19.77
TNFAIP8	tumor necrosis factor, alpha-induced protein 8	2.47
RPS6KA3	ribosomal protein S6 kinase, 90kDa, polypeptide 3	2.36
EGR1	early growth response 1	2.23
THBS1	thrombospondin 1	-2.31

Table 3.3.9: Fold change of genes in pathway 2; Table 3.3.10: Final list of genes specific to MCF7H3erbB2 and invasion, chosen for further analysis using siRNA knock-down.

3.3.3.6 Genes specific to invasion in DLKP variants

Table 3.3.11 generation of genes specific to invasion, DLKP4E and DLKP4Emut

Cross list comparisons	Number of genes changed
[DLKP versus DLKP4E] AND [DLKP versus DLKP4Emut] = [E]	379
[E] NOT [DLKP versus DLKPpcDNA] = [D]	240

Table 3.3.11: The above comparisons were made using dChip and Stanford's gene comparison program (Section 2.5.14-16).

3.3.3.6.1 Genes changes specific to eIF4E in DLKP4E

In the case of DLKP compared to DLKP4E, DLKP is taken as the baseline and DLKP4E as the experiment. The 1415 genes changed refer to the number of genes expressed in DLKP4E that are up- or down-regulated compared to those expressed in DLKP. The resulting list of differentially expressed genes are those specific to DLKP after stable transfection of eIF4E.

3.3.3.6.2 Gene changes specific to eIF4Emut in DLKP4Emut

When DLKP was compared to DLKP4Emut, again DLKP was taken as the baseline and DLKP4Emut as the experiment. The 1138 genes changed refer to the number of genes expressed in DLKP4Emut that are up- or down-regulated compared to those expressed in DLKP. The resulting list of differentially expressed genes are those specific to DLKP after stable transfection of eIF4Emut.

3.3.3.6.3 Gene changes specific to pcDNA in DLKPpcDNA

Taking DLKP as the baseline and DLKPpcDNA as the experiment, the number of genes differentially expressed in DLKPpcDNA was 1950. This result was surprising as stable expression of an empty plasmid was not expected to greatly affect the parental cell line. It is possible that these changes were due to clonal variation and not pcDNA expression.

3.3.3.6.4 Genes changes common to both DLKP4E and DLKP4Emut

Both DLKP4E and DLKP4Emut were highly invasive, so it was probable that of the genes common to both, some would be involved in invasion. A comparison of genes differentially expressed in DLKP4E and DLKP4Emut compared to parent DLKP, found 378 common genes.

3.3.3.6.5 Genes common to DLKP4E and DLKP4Emut, not DLKPpcDNA

Although there was an increase in invasion in DLKPpcDNA, it was not significant compared to DLKP4E and DLKP4Emut. It is also important to note that the parent DLKP was mildly invasive, and so it was likely that a DLKPpcDNA clone would also be mildly invasive. Therefore, to further reduce the list of genes for analysis, gene changes due to pcDNA were removed. The final list contained 240 (Figure 3.3.7). Gene lists are summarised in table 3.3.11.

3.3.3.6.6 Final list of 240 genes specific to eIF4E/eIF4Emut and invasion

Of the 240 genes on the final list, 31 were poorly annotated. An examination of expression levels showed 20 genes had an expression level below 100, but the expression level of these genes changed sufficiently across cell lines to assume they were either being 'switched on' or 'switched off' by eIF4E or eIF4Emut up-regulation, and so they were considered for further analysis (Figure 3.3.8).

Figure 3.3.8: Final list of 240 genes specific to eIF4E/eIF4Emut and invasion in

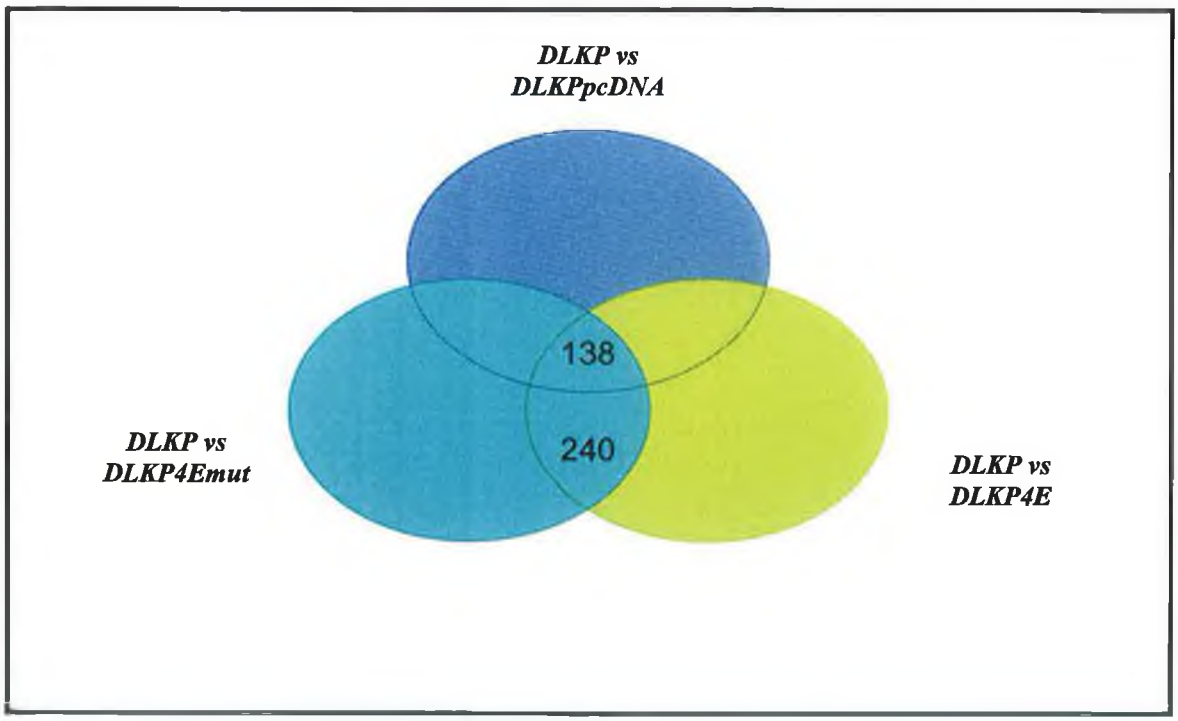

3.3.3.7 Pathway Assist ® analysis of DLKP4E/DLKP4Emut invasion-specific genes

The final list of 240 genes was further studied using Pathway Assist ©. Analysis carried out to identify genes with direct interaction revealed two separate gene pathways (Figure 3.3.9 and 3.3.10). These pathways, as before, were based on information available in the literature.

The first pathway identified several genes which had previously been associated with cancer in the literature (Figure 3.3.9). This fact alone showed the analysis had been successful in identifying invasion-specific genes. From this pathway Neuregulin (NRG) was chosen, based on its significant fold change and direct interaction with 7 genes from the final list. Results from Pathway Assist © showed NRG directly interacted with GRB2, SLC2A3, RPS6KB1 and RPS6KA3, and through these genes may effect CREM and PDGFA. Evidence from the literature suggested some or all of these genes were important for invasion, and so it was thought that knock-down of NRG would have a significant effect.

The last gene chosen was Myopalladin. This did not appear in either pathway and was chosen based on fold change (+9.06), and the fact that although it is known to regulate actin organization, there is no evidence in the literature of its involvement in invasion.

Several HOXB genes showed significant changes in expression on the final list, with fold changes ranging from +6 to +98. Based on this observation, the fact that HOXB genes are transcription factors associated with cancer phenotypes, and the Pathway Assist ® generated pathway (Figure 3.3.10), three of the HOXB genes were chosen for further analysis.

3.3.3.8 DLKP4E/DLKP4Emut invasion specific genes chosen for further analysis

Five genes in all were chosen for siRNA knock-down based on specificity to DLKP4E, DLKP4Emut and invasion, and relevance to cancer/invasion in the literature. These targets were HOXB4, HOXB6, HOXB7, NRG and MYO (table 3.3.14)

Figure 3.3.9 Direct interaction between genes specific to DLKP4E, DLKP4Emut and invasion.

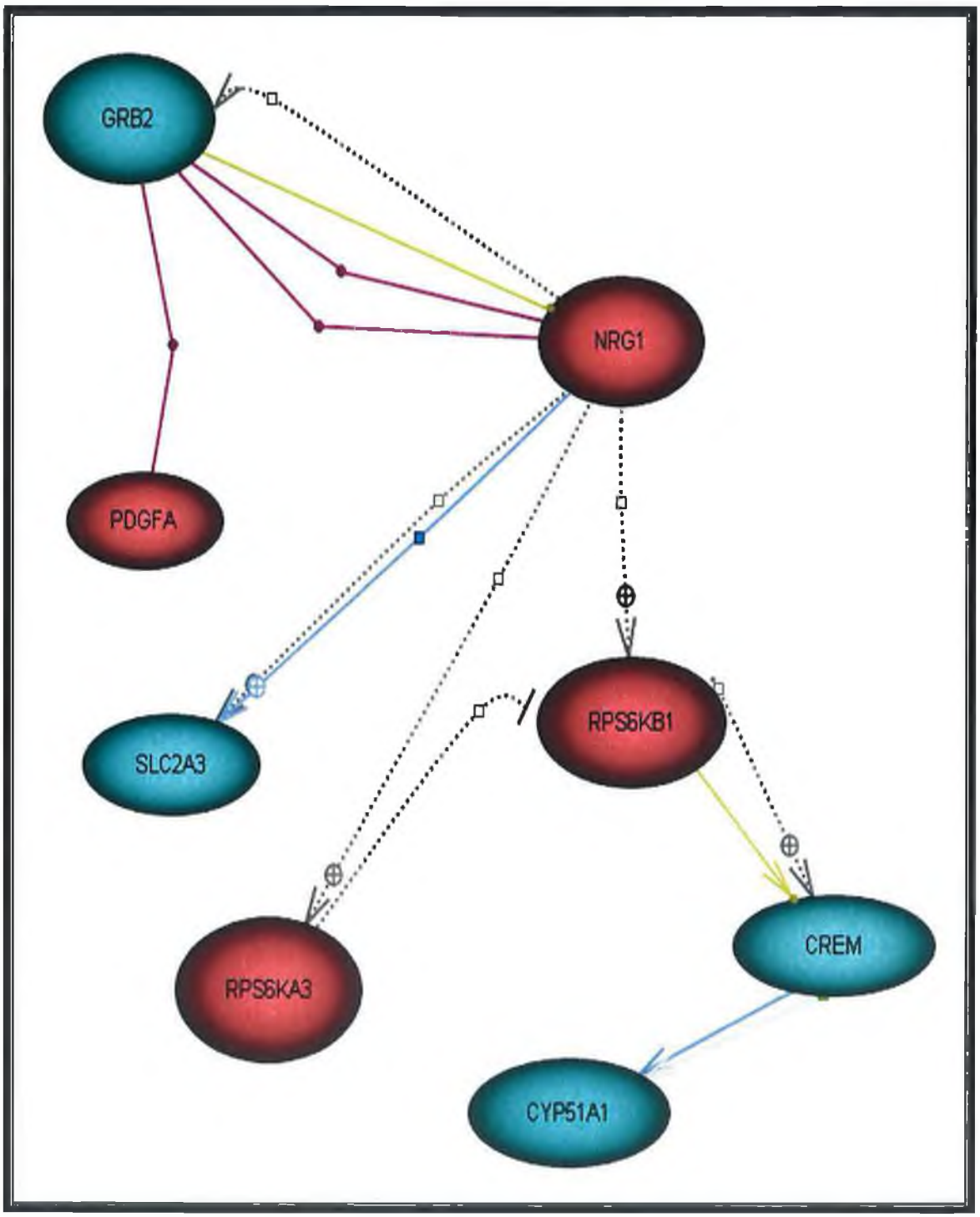

Figure 3.3.9: Pathway 3: direct interaction between genes specific to DLKP4E, 4Emut and invasion. Blue = negative fold change; Red = positive fold change (Section 2.5.18)

Table 3.3.12 Genes specific to DLKP4E, DLKP4Emut and invasion (Pathway 3)

Name	Description	Fold change
NRG1	neuregulin 1	7.36
PDGFA	platelet-derived growth factor alpha polypeptide	4.83
RPS6KA3	ribosomal protein S6 kinase, 90kDa, polypeptide 3	1.67
RPS6KB1	ribosomal protein S6 kinase, 70kDa, polypeptide 1	1.53
GRB2	growth factor receptor bound protein 2	-1.34
CYP51A1	cytochrome P450, family 51, subfamily A, polypeptide 1	-1.36
SLC2A3	solute carrier family 2 (facilitated glucose transporter), member 3	-2.64
CREM	cAMP responsive element modulator	-1.89

Table 3.3.12: fold change of genes in pathway 3.

Figure 3.3.10 Direct interaction between genes specific to DLKP4E, 4Emut and invasion

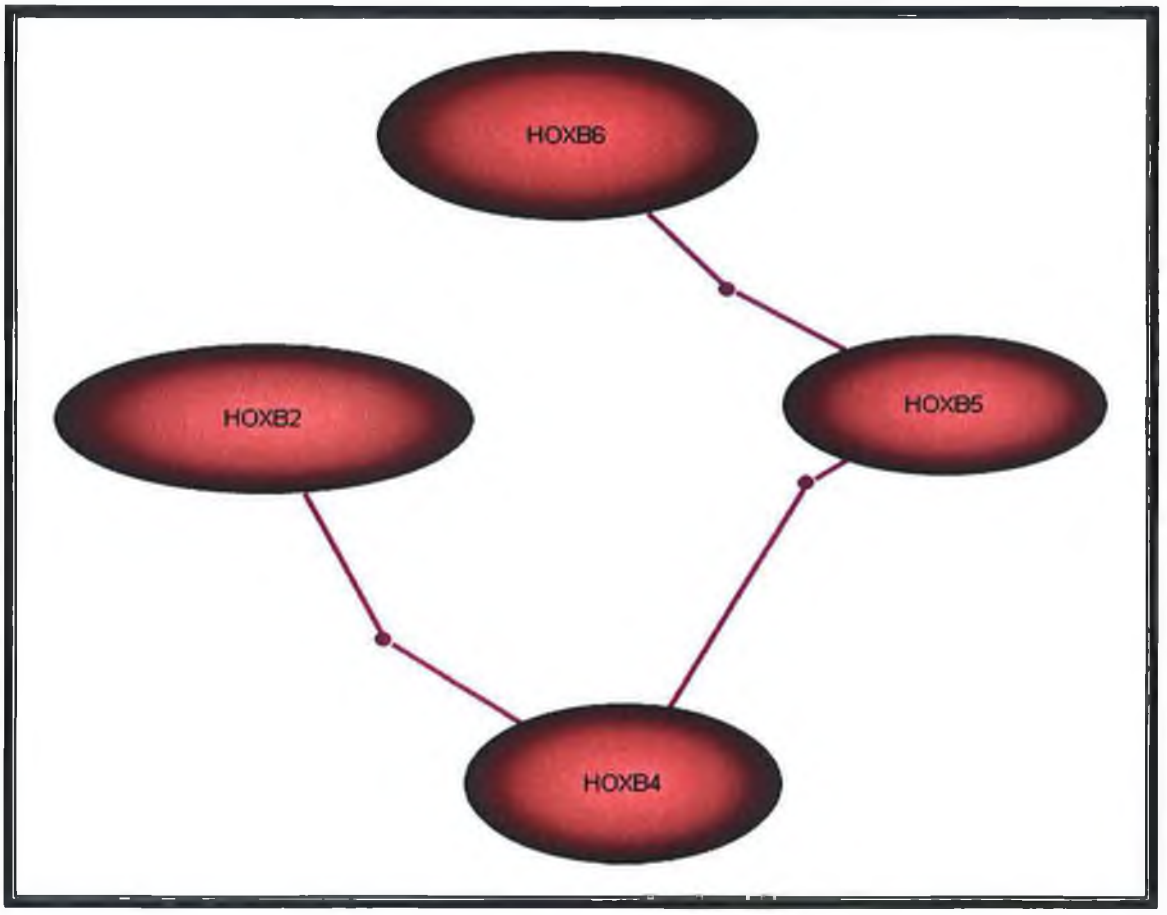

Figure 3.3.10: Pathway 4:direct interaction between genes specific to DLKP4E, 4Emut and invasion. Blue = negative fold change; Red = positive fold change (Section 2.5.18)

Table 3.3.13 genes specific to DLKP4E,4Emut and invasion (Pathway 4)

Name	Description	Fold change
HOXB2	homeo box B2	98.39
HOXB5	homeo box B5	34.38
HOXB6	homeo box B6	33.69
HOXB4	homeo box B4	6.51

Table 3.3.13: Fold change of genes in pathway 4

Table 3.3.14 Genes used for siRNA specific to DLKP4E/DLKP4Emut and invasion

Gene	Description	Fold change
HOXB6	homeo box B6	33.69
HOXB4	homeo box B4	6.51
HOXB7	homeo box B7	7.65
NRG1	neuregulin 1	7.36
MYO	myopalladin	9.06

Table 3.3.14: Final list of genes chosen for further analysis using siRNA knock-down. Specific to DLKP4E/DLKP4Emut.

3.3.4 Genomatix®

Microarray results reflect a multitude of simultaneous cellular processes although only subsets of expression changes are directly caused by the experimental conditions. Therefore, a major task for an in depth analysis is to identify genes whose expression changes due to the experimental setup and distinguish them from effects of biological diversity or general stress response of the cell. Genomatix is based on a combination of statistical, literature and promoter analysis and aims at establishing gene promoter networks on a molecular level.

Array analysis revealed mRNA with significantly changed expression levels but failed to assign these changes to biological events. Projecting microarray data onto information from literature using GenMAPP allowed association of genes with biological processes, but was restricted to current knowledge, and therefore may not have acknowledged genes that are directly pertinent for the experimental conditions. Pathway Assist took this process a step further by identifying direct interaction between genes with significantly changed expression levels, but again this analysis was restricted to previously published data. However, the strong connection between the five genes chosen, combined with statistical relevance (based on p-value) and relation to cancer invasion, implied that they may relate specifically to the experimental conditions. For this reason it was decided that further analysis using Genomatix® (see section 2.5.20) might reveal promoter networks specific to these genes and this experiment. Genomatix combines promoter and pathway analysis allowing for the integration of genes that may have been missed by individual methods.

3.3.4.1 Genomatix analysis of siRNA targets of MCF7H3erbB2

The five genes used in the analysis were: TFPI (Tissue factor pathway inhibitor (lipoprotein-associated coagulation inhibitor)), TNFAIP8 (tumour necrosis factor alpha-induced protein 8), RPS6KA3 (ribosomal protein S6 kinase, 90kDa, polypeptide 3), EGR1 (early growth response 1), THBS1 (thrombospondin 1). As EGR1 is a known transcription factor, it was removed from the analysis. The promoter sequences for all four genes were analysed using the ELDorado^{TM}/ Gene2romoter system (see section 2.5.20). ELDorado is a genome annotation database which is based on a condensation of publicly available data plus Genomatix proprietary annotation, including promoters, transcription factor binding sites, promoter modules, scaffold/matrix attachment regions (S/MARs), and single nucleotide polymorphisms (SNPs) as well as comparative

genomics. Gene2Promoter is a multiple identifier interface to query ELDorado. This allowed retrieval and selection of the promoters for subsequent promoter analysis. Promoter analysis was carried out using FrameWorker (see section 2.5.20), a software tool which allows the extraction of common motifs of transcription factor binding sites from the given set of promoter sequences.

Of the four genes analysed there wasn't a transcription factor model that fit all 4. Two three-element models fit 3/4 genes (TNFAIP8, RPS6KA3, THBS1), with FW scores of 0.60 and 0.43. The FW (FrameWorker) scores showed the ratio of the number of sequences with matches to the number of model matches (overlapping and non-overlapping, respectively). These scores allowed assessment of the quality of the model generated. The higher the scores, the more specific is the extracted model. A very low FW score (<0.5) would indicate a model that is likely to match very often in random DNA sequences. For example, if a model matches 20 times in 10 training sequences, the FW-score is 10/20 = 0.5. A good model would be expected to match not more than once in each sequence (this would yield a FW score of 1.00). Therefore, the first model, with a FW score of 0.6 was more specific (Figure 3.3.11a). In this model, the 3 transcription factors were SP1F, ZF5F and EGRF. It was encouraging that EGRF appeared as EGR1 had previously been chosen through PathWay Assist because of its association with the other four genes (Figure 3.3.6). This provides the first indication that the analytical approach used may have identified a biologically relevant transcription network.

The EGRF transcription factor occurs in 60.0 % of all vertebrate promoters, ZF5F in 25% and SP1F is ubiquitous, so it was clear that individually none were highly specific across the genome. To assess the specificity of the combination of all 3 factors, all human promoters were scanned using ModelInspector, which is connected to Genomatix Promoter Database GPD, containing 50,109 promoters. Only 84 gene promoter regions in the whole genome contained the defined framework suggesting a high degree of specificity of this model.

Figure 3.3.11 3-element Transcription Factor models fitting 3 of 4 selected genes

Figure 3.3.11a: (model 1)

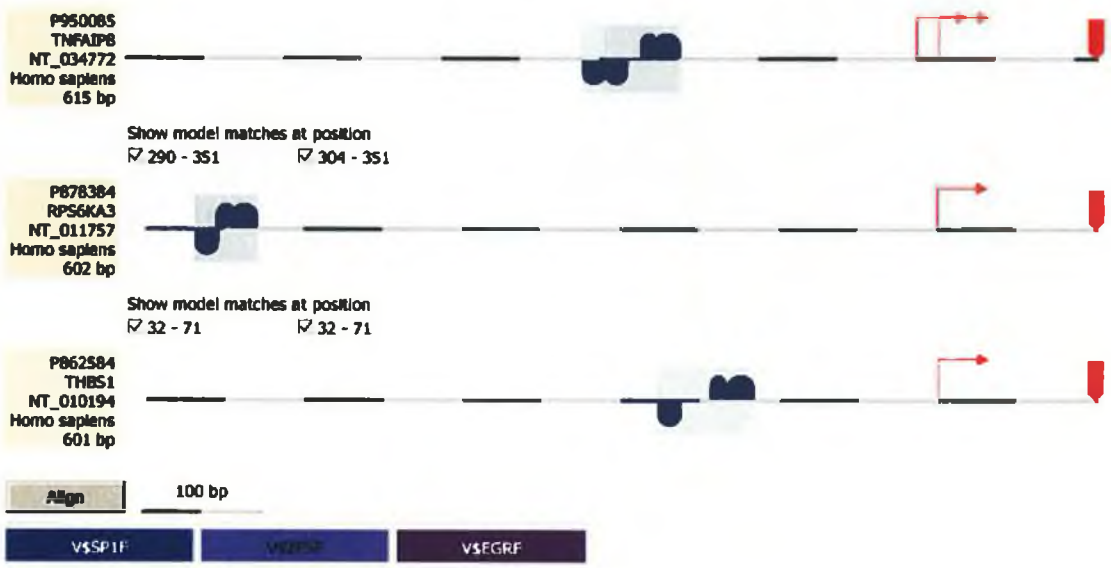

Figure 3.3.11b: (model 2)

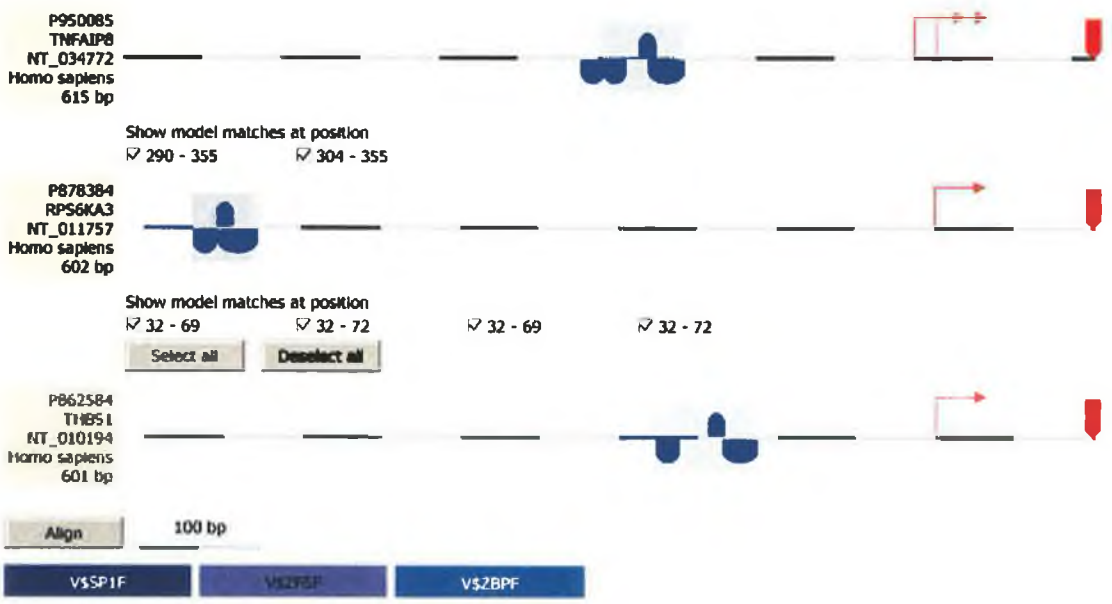

Figure 3.3.11a: FW=0.6, 3-element Transcription Factor model fitting 3 of 4 selected genes (model 1); Figure 3.3.11b: FW= 0.43, 3-element Transcription Factor model fitting 3 of 4 selected genes

3.3.4.2 BiblioSphere analysis

The list of 84 genes was brought into BiblioSphere for further analysis (see section 2.5.20). BiblioSphere is a data-mining solution for extracting and analyzing gene relationships from literature databases and genome-wide promoter analysis. BiblioSphere contains literature data mining strategies using more than 350,000 quality checked gene names and searches over 15 million abstracts. The genes were grouped into the various Gene Ontology (GO) catagories and, ignoring those with only one or two genes, the highest ranking category was Neovascularisation. Only 5.8 genes would be expected in this catagory, but there were 41 found, giving a Z score of 14.69.

The expression level of this group of 84 genes was then checked against the original list of differentially expressed genes from the array experiment (MCF7H3 (non-invasive) compared to MCF7H3erbB2 (invasive)), and it was found that 33 genes were on this list of 3349 genes. This is far more than would be expected randomly (3349 genes = ~6% of 55,000 total but 33 genes = 40% of 84 genes) which provides another line of evidence that this promoter module may be active in this system. The list of 118 genes, from which the original five genes used for the Genomatix analysis were chosen (Section 3.3.3.3.5), was compared to the list of 84 genes with promoter regions specific to this model. The two lists had 3 genes in common. These 3 genes were thrombospondin 1, tumor necrosis factor alpha-induced protein 8 and ribosomal protein S6 kinase, 90kDa, polypeptide 3. These are the 3 genes present in the transcription factor model generated by Genomatix, as would be expected.

The second model generated by FrameWorker had a FW score of 0.43, contained the genes TNFAIP, RPS6KA3, THBS1, and the transcription factors SPI1, ZF5F and ZBPF (Figure 3.3.11b). Again, taken individually none of these transcription factors were highly specific, but combined in this particular Framework they are found in only 118 genes in the entire genome, which indicates a high degree of specificity.

Model 1 and model 2 had 41 genes in common, 9 of which were on the list of MCF7H3erbB2 differentially expressed genes (compared to MCF7H3) (3348 genes Table 3.3.6), and 3 were on the list of 118 genes used to select siRNA targets. Though all of the above genes were found related to cancer, few direct links were found in the literature between erbB2 and this group of genes. Therefore, if these transcription factor motifs are specific to erbB2 up-regulation, they may provide links to novel genes specific to erbB2 up-regulation.

Table 3.3.15 Overview of element distribution in models 1 and 2:

Element 1	V$SP1F
Element 2	V$ZF5F
Element 3	V$EGRF V$ZBPF

Table 3.3.16: Genes common to model 1 and 2 also present in MCF7H3erbB2

Gene	Fold change	P value
ribosomal protein S6 kinase, 90kDa, polypeptide 3	2.72	0.004085
tumor necrosis factor, alpha-induced protein 8	2.52	0.018687
CD99 antigen	2.29	0.000499
transforming, acidic coiled-coil containing protein 1	2.24	0.003028
insulin receptor substrate 2	2.17	0.001826
hypothetical protein FLJ20701	1.74	0.028567
ubiquitin specific protease 32	1.41	0.00361
zinc finger, MYND domain containing 19	-1.29	0.029064
thrombospondin 1	-2.93	0.000328

Neither of the models were found in the literature, but both models were found in rat and mouse. When scanned across the rat and mouse genomes, model 1 was specific for 60 genes in mouse and 14 in rat, and model 2 for 53 genes in mouse and 19 in rat. A final comparison to identify the presence of orthologues in these gene lists would be very useful to further estimate the likely biological relevance of the models – promoter modules that are conserved across species are likely to be functional, otherwise evolutionary mutations would have accumulated.

3.3.5 Analysis of DLKP4E compared to MCF74E

Both DLKP and MCF7 were transfected with HA-tagged eIF4E and eIF4Emut, resulting in an increase in invasion in DLKP but no change in invasion of MCF7. It was clear from these experiments that phosphorylation of eIF4E did not influence the invasive phenotype. It was decided not to include genes differentially expressed as a result of eIF4Emut overexpression in this particular analysis, as it was assumed all gene changes necessary for invasion would be expressed in wild-type eIF4E overexpressing cells.

To examine why overexpression of wild type eIF4E caused DLKP to become more invasive but not MCF7, analysis of MCF74E and DLKP4E microarray results was carried out. Comparison analysis was carried out using dChip and the Stanford gene comparison site: http://worm-chip.Stanford.edu/~jiml/Compare.html (Section 2.5.14-16). DLKP4E specific genes were determined by comparing changes in DLKP to DLKP4E using dChip. This list was reduced by removing genes that had changed due to pcDNA using Stanford 'gene comparison'. MCF74E specific genes were determined in the same way. Two different comparisons were made for this study (Table 3.3.17).

1. Genes present in both DLKP and MCF7 with different patterns of expression, prior to eIF4E transfection
2. Gene changes due to eIF4E overexpression in DLKP4E and not in MCF74E.
3. Genes common to DLKP4E and MCF7H3erbB2 but not MCF74E (with the same pattern of expression).

Table 3.3.17 Gene list: analysis of changes in DLKP4E compared to MCF74E

Cell line comparison	Number of genes changed
DLKP versus DLKP4E	1415
DLKP versus DLKPpcDNA	1950
MCF7 versus MCF74E	864
MCF7 versus MCF7pcDNA	2829
MCF7H3 versus MCF7H3 erbB2	3348
Cross list comparison	**Number of genes changed**
Differentially expressed in DLKP4E not MCF74E	863
DLKP4E & MCF7H3erbB2 common genes, not MCF74E	351
DLKP and MCF7 common genes with different levels of expression i.e. +fold change in DLKP, -fold change in MCF7	239

3.3.5.1 DLKP and MCF7 common genes with different levels of expression

Both cell lines used in this analysis are derived from different tissue types (DLKP=lung, MCF7=breast) and therefore differ greatly; particularly in regards to proliferation and morphology. These differences alone would result in two very different mRNA profiles. With particular relevance to this study, DLKP displayed mildly-invasive characteristics prior to eIF4E transfection. This meant DLKP may have been pre-disposed to an invasive phenotype, already having some of the genes and signalling pathways necessary for invasion 'switched on'. To examine the difference in baseline expression of genes in both cell lines, MCF7 parental cell line was compared to DLKP parental cell line to determine what genes were expressed in both. This comparison resulted in thousands of genes, and so to narrow the search only genes with expression values< 50 in MCF7 and fold change of >10 when compared to DLKP were used for further analysis. This resulted in a list of 239 genes which exhibited very low expression in MCF7 but were expressed at a high level in DLKP.

Pathway Assist® analysis found that several networks of genes existing within this list were relevant to cancer progression. Of note are those involved in the regulation of inflammation, proliferation and survival (Figure 3.3.12-14).

Figure 3.3.12 Genes common to DLKP and MCF7 with different levels of expression - involved in inflammation

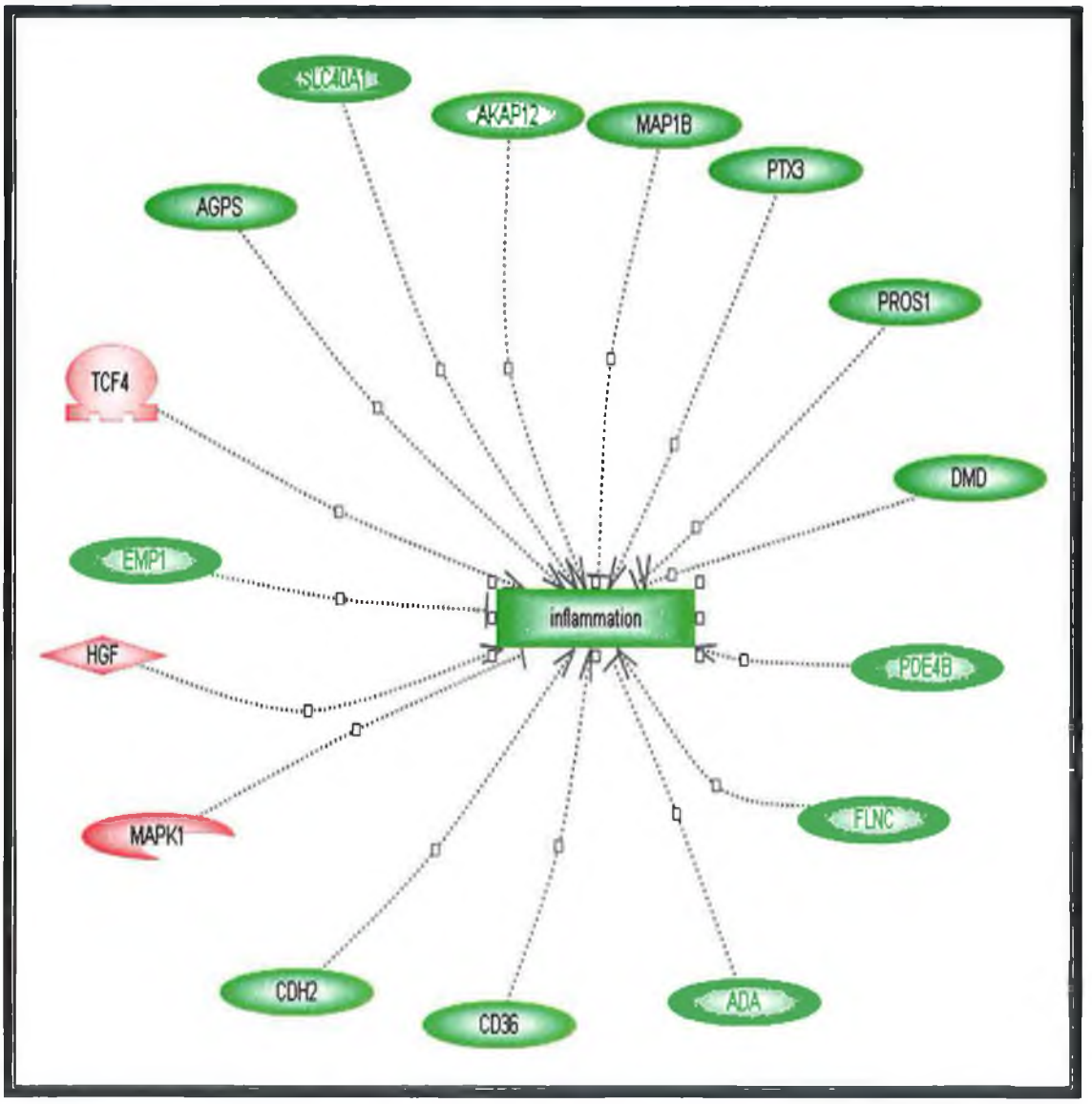

Figure 3.3.12: Representation of genes involved in regulation of inflamation in DLKP not MCF7. Detailed description of nodes and controls in Section 2.5.18.

Table 3.3.18: Genes common to DLKP and MCF7 with different levels of expression - involved in inflammation

Gene	Description	Regulation of Inflamation	Relative fold change: DLKP compared to MCF7
AGPS	alkylglycerone phosphate synthase	unknown	+ 137
AKAP12	A kinase (PRKA) anchor protein (gravin) 12	unknown	+ 747
CD36	CD36 antigen (collagen I receptor, thrombospondin receptor)	unknown	+ 29.03
CDH2	cadherin 2, type 1, N-cadherin (neuronal)	unknown	+ 177
DMD	dystrophin (muscular dystrophy)	unknown	+ 72
EMP1	epithelial membrane protein 1	negative	+ 255
FLNC	filamin C, gamma (actin binding protein 280)	unknown	+ 58.72
HGF	hepatocyte growth factor (hepapoietin A; scatter factor)	unknown	+ 1089
MAP1B	microtubule-associated protein 1B	negative	+ 28
MAPK1	mitogen activated protein kinase 12	negative	+ 16
PDE4B	phosphodiesterase 4B, cAMP-specific (phosphodiesterase E4 dunce homolog, Drosophila)	unknown	+ 168
PTX3	pentaxin-related gene, rapidly induced by IL-1 beta	unknown	+ 98
SLC40A 1	solute carrier family 40 (iron regulated transporter)member1	unknown	+ 79
TCF4	transcription factor 4	unknown	+ 65

Figure 3.3.13 Genes common to DLKP and MCF7 with different levels of expression - involved in proliferation

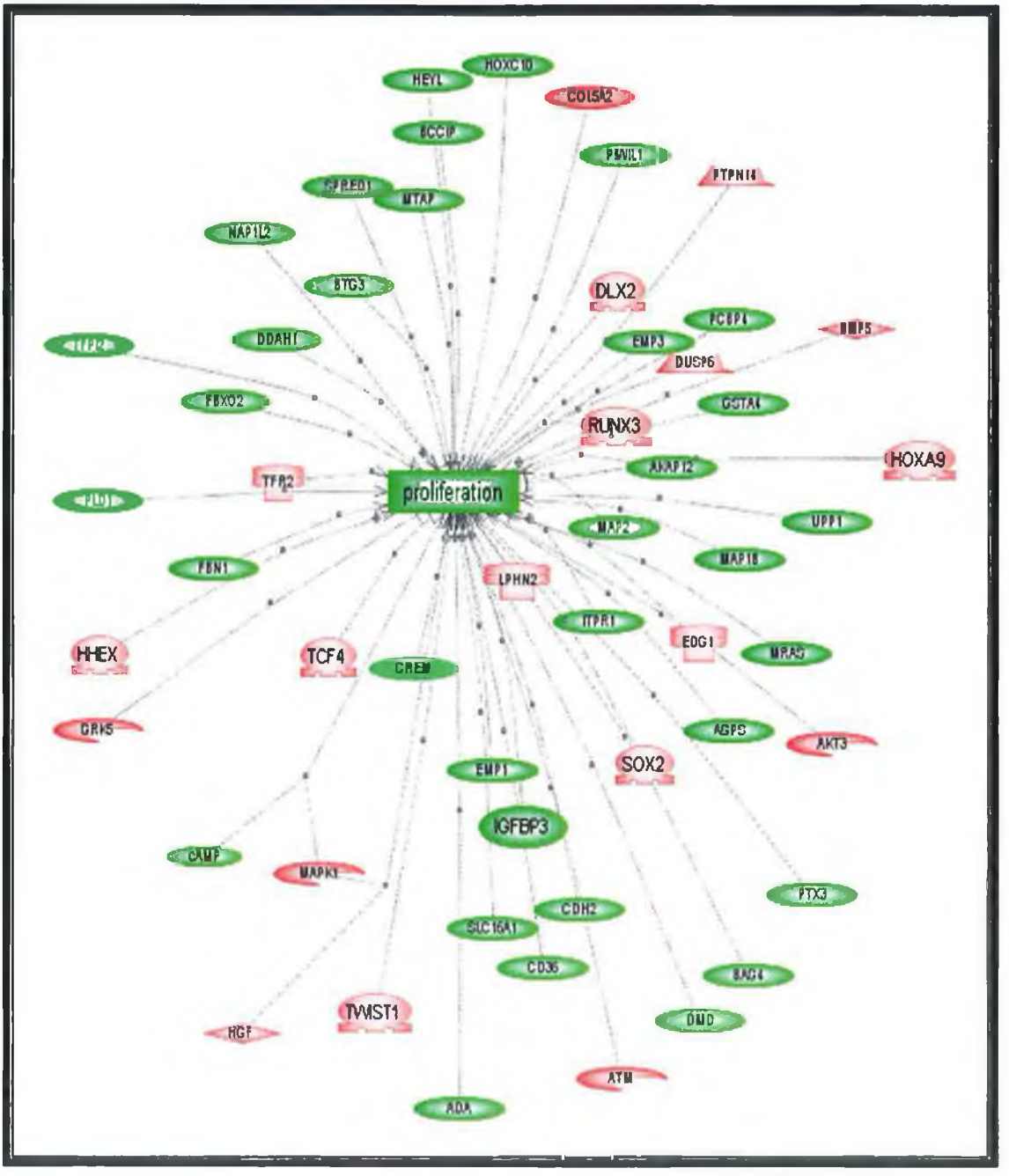

Figure 3.3.13: Representation of genes involved in regulation of proliferation in DLKP not MCF7. Detailed description of nodes and controls in Section 2.5.18.

Table 3.3.19: Genes common to DLKP and MCF7 with different levels of expression - involved in proliferation

Gene	Description	Regulation of proliferation	Fold change
AGPS	alkylglycerone phosphate synthase	unknown	+ 137
AKAP12	A kinase (PRKA) anchor protein (gravin) 12	unknown	+ 747
AKT3	v-akt murine thymoma viral oncogene homolog 3 (protein kinase B, gamma)	unknown	+ 44
BMP5	bone morphogenetic protein 5	positive	+ 25
BTG3	BTG family, member 3	unknown	+ 12
CD36	CD36 antigen (collagen type I receptor, thrombospondin receptor)	unknown	+ 29
CDH2	cadherin 2, type 1, N-cadherin (neuronal)	positive	+ 177
COL5A2	collagen, type V, alpha 2	unknown	+ 96
CREM	cAMP responsive element modulator	unknown	+ 15
DDAH1	dimethylarginine dimethylaminohydrolase 1	positive	+ 22
DLX2	distal-less homeo box 2	unknown	+ 55
DMD	dystrophin (muscular dystrophy, Duchenne and Becker types)	unknown	+ 72
DUSP6	dual specificity phosphatase 6	unknown	+ 146
EDG1	endothelial differentiation, sphingolipid G-protein-coupled receptor, 1	negative	+ 1723
EMP1	epithelial membrane protein 1	positive	+ 255
EMP3	epithelial membrane protein 3	unknown	+76
FBN1	fibrillin 1 (Marfan syndrome)	unknown	+15
FBXO2	F-box protein 2	negative	+19
GRK5	G protein-coupled receptor kinase 5	negative	+ 13
GSTA4	glutathione S-transferase A4	unknown	+24
HGF	hepatocyte growth factor (scatter factor)	positive	+ 1089
HOXA9	homeo box A9	negative	+ 503
HOXC10	homeo box C10	unknown	+ 32
IGFBP3	insulin-like growth factor binding protein 3	negative	+ 36
ITPR1	inositol 1,4,5-triphosphate receptor, type 1	unknown	+ 48
LPHN2	latrophilin 2	negative	+ 27
MAP1B	microtubule-associated protein 1B	unknown	+ 35
MAP2	microtubule-associated protein 2	negative	+ 68
MAPK12	mitogen activated protein kinase 12	unknown	+ 16
MRAS	muscle RAS oncogene homolog	positive	+ 22
MTAP	methylthioadenosine phosphorylase	negative	+ 114
PIWIL1	piwi-like 1 (Drosophila)	unknown	
PLD1	phospholipase D1, phophatidylcholine-specific	unknown	+ 42
PTX3	pentaxin-related gene, rapidly induced by IL-1 beta	unknown	+ 98
RUNX3	runt-related transcription factor 3	unknown	+ 33
SLC16A1	solute carrier family 16 (monocarboxylic acid transporters), member 1	unknown	+ 28
SOX2	SRY (sex determining region Y)-box 2	negative	+ 36
SPRED1	sprouty-related, EVH1 domain containing 1	negative	+ 20
TCF4	transcription factor 4	unknown	+ 88
TFPI2	tissue factor pathway inhibitor 2	unknown	+ 41
TWIST1	twist homolog 1 (acrocephalosyndactyly 3; Saethre-Chotzen syndrome) (Drosophila)	unknown	+ 422
UPP1	uridine phosphorylase 1	negative	+ 168

Figure 3.3.14 Genes common to DLKP and MCF7 with different levels of expression - involved in cell survival

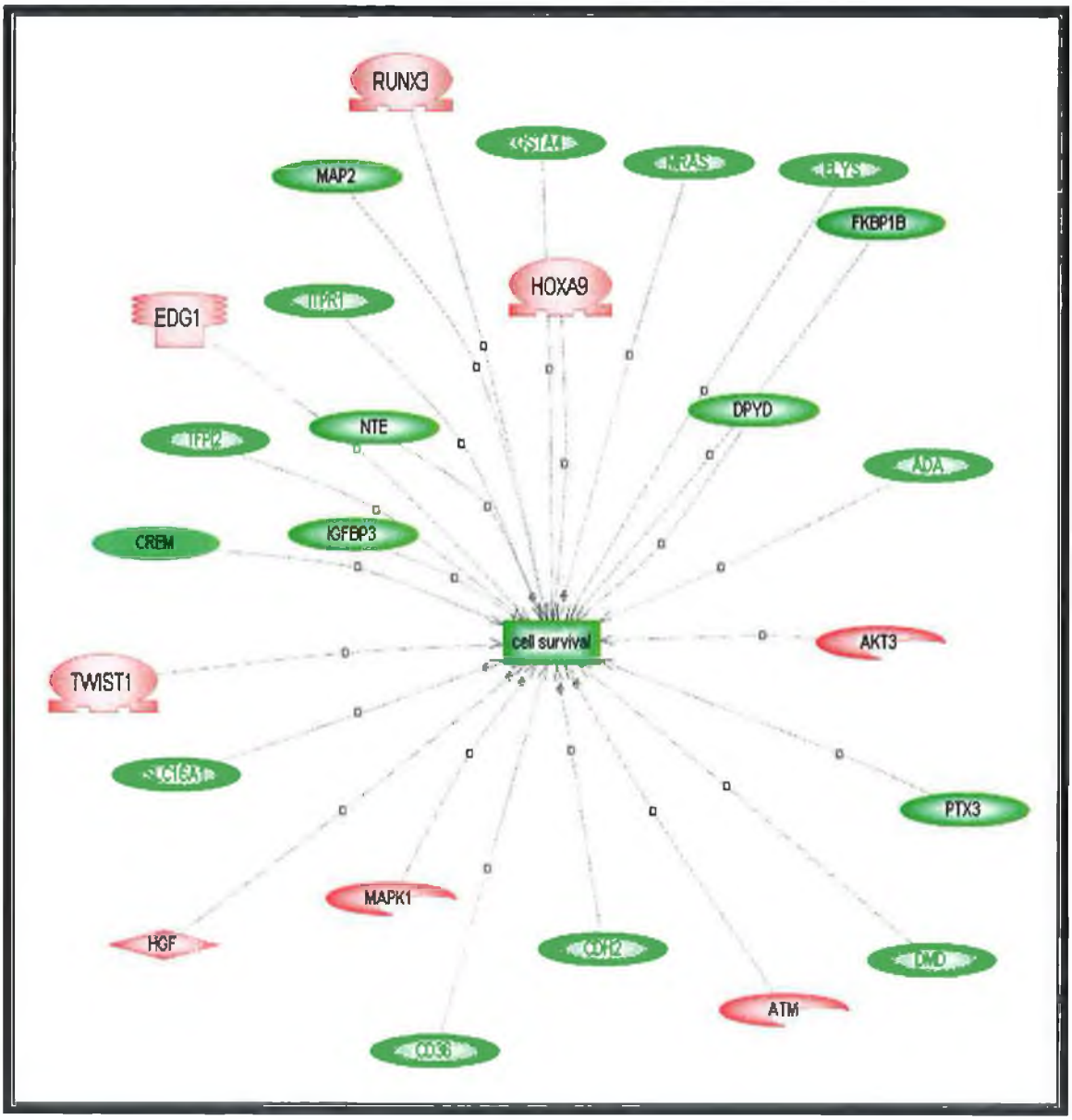

Figure 3.3.14: Representation of genes involved in regulation of cell survival in DLKP not MCF7. Detailed description of nodes and controls in Section 2.5.18.

Table 3.3.20: Genes common to DLKP and MCF7 with different levels of expression - involved in cell survival

Gene	Description	Regulation of cell survival	Fold change
HGF	hepatocyte growth factor (hepapoietin A; scatter factor)	Positive	+ 1089
IGFBP3	insulin-like growth factor binding protein 3	Negative	+ 63
DMD	dystrophin (muscular dystrophy, Duchenne and Becker types)	Unknown	+ 72
SLC16A1	solute carrier family 16 (monocarboxylic acid transporters), member 1	Positive	+ 28
ITPR1	inositol 1,4,5-triphosphate receptor, type 1	Positive	+ 48
MRAS	muscle RAS oncogene homolog	Positive	+ 22
MAP2	microtubule-associated protein 2	Unknown	+ 68
CREM	cAMP responsive element modulator	Unknown	+ 15
CD36	CD36 antigen (collagen type I receptor, thrombospondin receptor)	Unknown	+ 29
AKT3	v-akt murine thymoma viral oncogene homolog 3 (protein kinase B, gamma)	Unknown	+ 41
EDG1	endothelial differentiation, sphingolipid G-protein-coupled receptor, 1	Unknown	+ 1723
FKBP1B	FK506 binding protein 1B, 12.6 kDa	Unknown	+ 18
DPYD	dihydropyrimidine dehydrogenase	Unknown	+ 18
CDH2	cadherin 2, type 1, N-cadherin (neuronal)	Positive	+ 177
PTX3	pentaxin-related gene, rapidly induced by IL-1 beta	Unknown	+ 98
RUNX3	runt-related transcription factor 3	Unknown	+ 33
TFPI2	tissue factor pathway inhibitor 2	Unknown	+ 41
HOXA9	homeo box A9	Unknown	+ 503
GSTA4	glutathione S-transferase A4	Unknown	+ 24
TWIST1	twist homolog 1 (acrocephalosyndactyly 3; Saethre-Chotzen syndrome) (Drosophila)	Unknown	+ 422
ELYS	ELYS transcription factor-like protein TMBS62	Unknown	+ 12

3.3.5.2 Gene changes due to eIF4E in DLKP4E and not in MCF74E

Gene changes in DLKP due to eIF4E and not pcDNA were compared to gene changes in MCF7 due to eIF4E and not pcDNA. A list of 863 genes changed specific to DLKP4E and not MCF74E. As eIF4E caused a change in invasion when transfected into DLKP but not MCF7, these gene changes were associated with an invasive phenotype in DLKP4E, and lack of same in MCF7. The list was further examined using PathwayAssist® (Section 2.5.18).

Pathway analysis found that the genes were predominantly involved in motility and proliferation. Of the 863 genes examined, 67 genes were involved in the regulation of molitity (Figure 3.3.15). 17 of these were known to be negative regulators of motility, and 16 positive regulators. 34 were associated with motility but their exact role unknown (Table 3.3.21). 34% of this set of genes had a fold change greater than 2; a significant change. That is approx. 8% of the group studied. This result provides evidence that the genes selected through PathwayAssist analysis play a significant role in motility, which is important in the invasion process. Therefore no significant change in these genes in the MCF74E cell line may be contributing to the cells lack of invasion.

80 of the 836 genes were involved in proliferation (Figure 3.3.16). Of these 21 were known to be involved in negatively regulating proliferation, and 11 in positive regulation. 47 genes were associated with proliferation in the literature but their exact role was unknown (Table 3.3.22). Dysregulation of proliferation is associated with development of neoplasia, and is also associated with the overexpression of eIF4E. Again, this result indicates that these genes, or lack of in the case of MCF7, may be important in the invasion process.

Figure 3.3.15 Gene changes due to eIF4E in DLKP4E not MCF74E involved in regulation of motility

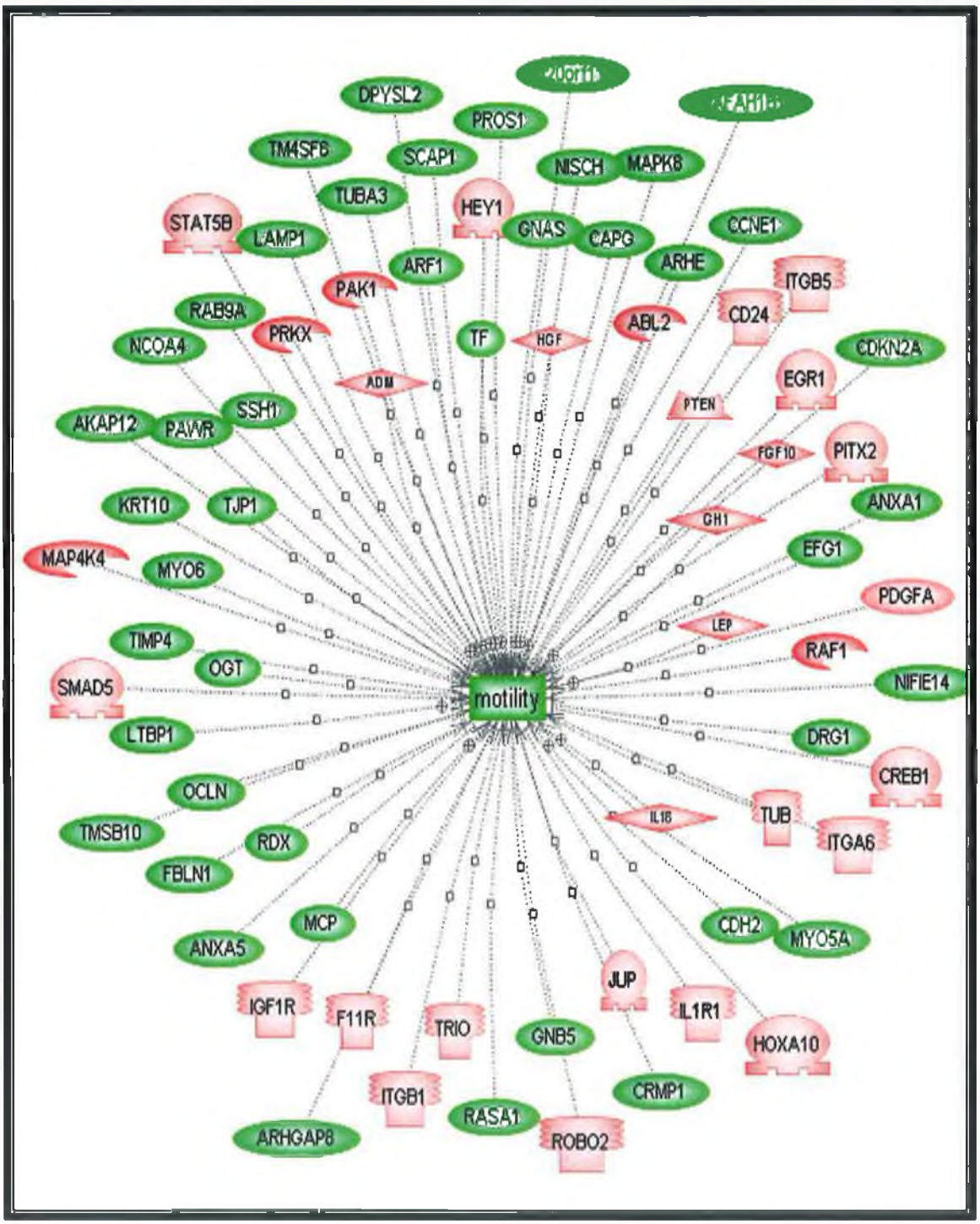

Figure 3.3.15: Representation of genes involved in regulation of motility in DLKP4E specific genes. Detailed description of nodes and controls in Section 2.5.18.

Table 3.3.21 Gene changes due to eIF4E in DLKP4E not MCF74E related to regulation of motility

Gene	Regulation of motility	Fold change	Gene	Regulation of motility	Fold change
ADM	negative	2.27	AKAP12	unknown	3.58
ANXA1	negative	3.31	ARHGAP8	unknown	1.49
ANXA5	negative	2.47	C20orf11	unknown	1.22
CREB1	negative	1.72	CCNE1	unknown	5.54
DRG1	negative	-1.26	CD24	unknown	1.37
FBLN1	negative	1.44	CDKN2A	unknown	3.19
GNB5	negative	1.5	CRMP1	unknown	2.04
HEY1	negative	-1.52	DPYSL2	unknown	-1.43
HOXA10	negative	-3.72	EFG1	unknown	2.4
IL1R1	negative	-1.79	EGR1	unknown	2.64
ITGB5	negative	1.46	F11R	unknown	-1.78
MYO5A	negative	1.66	GH1	unknown	1.22
NISCH	negative	1.37	GNAS	unknown	2.94
PAWR	negative	1.81	ITGA6	unknown	21.63
PTEN	negative	-1.49	JUP	unknown	1.57
TIMP4	negative	-1.32	KRT10	unknown	1.75
TJP1	negative	1.31	MAP4K4	unknown	2.27
TMSB10	negative	1.59	MYO6	unknown	-1.31
ARF1	positive	-1.31	NCOA4	unknown	1.33
ARHE	positive	3.11	NIFIE14	unknown	1.5
CAPG	positive	1.66	OCLN	unknown	1.62
CDH2	positive	2.52	OGT	unknown	1.7
FGF10	positive	4.08	PAFAH1B1	unknown	-2.77
HGF	positive	-1.6	PITX2	unknown	2.25
IL18	positive	5.42	PRKX	unknown	1.73
LAMP1	positive	1.24	PROS1	unknown	1.42
LEP	positive	-1.69	RDX	unknown	-5.65
LTBP1	positive	2.71	ROBO2	unknown	39.23
MCP	positive	-1.48	SCAP1	unknown	1.62
PDGFA	positive	4.14	SMAD5	unknown	2.06
RAB9A	positive	1.69	SSH1	unknown	1.59
STAT5B	positive	1.7	TM4SF6	unknown	1.54
TF	positive	-1.41	TRIO	unknown	1.67
TUBA3	positive	1.43	TUB	unknown	1.56

Table 3.3.21: Role in regulation of motility of DLKP4E specific genes.

Figure 3.3.16 Gene changes due to eIF4E in DLKP4E not MCF74E involved in regulation of proliferation

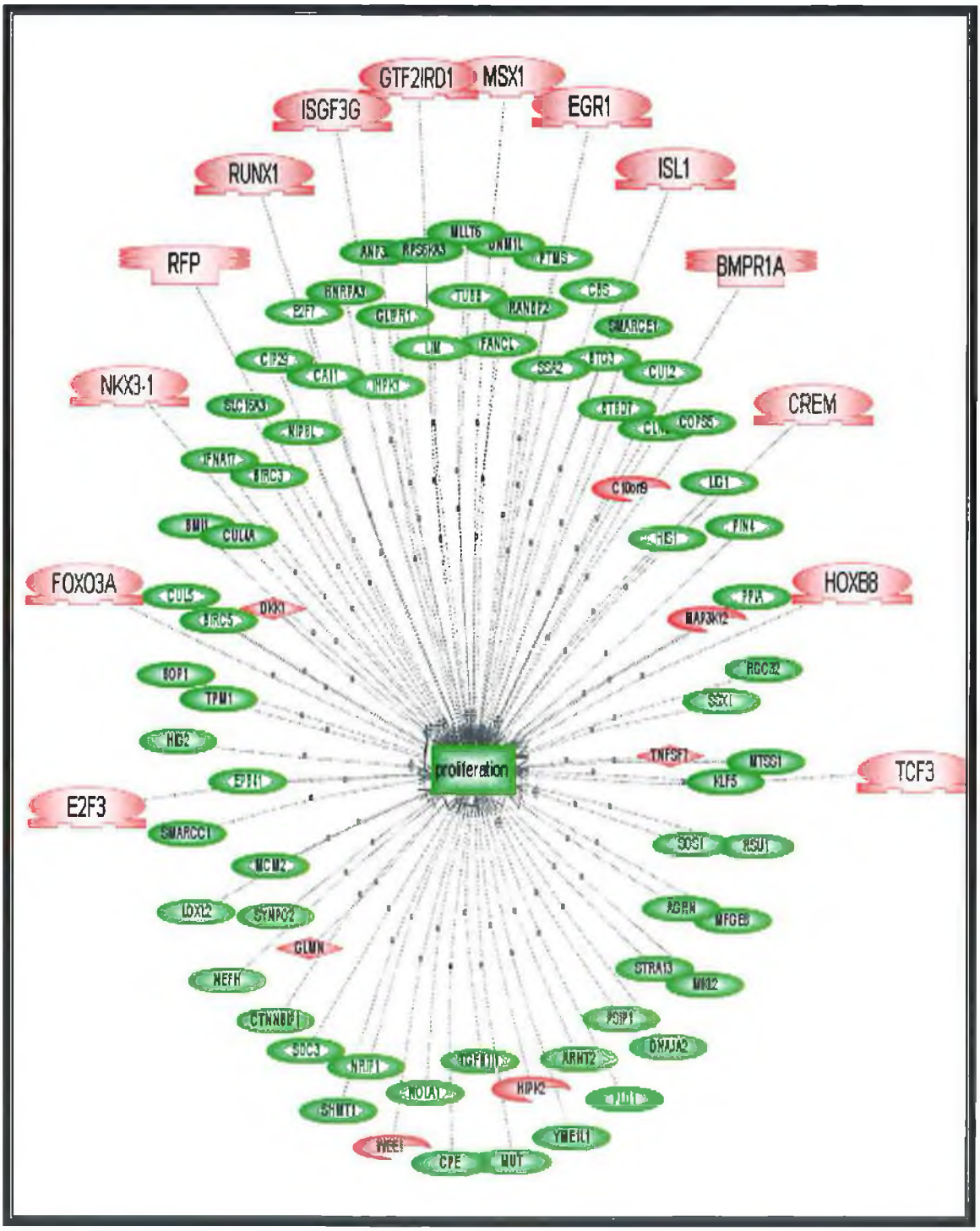

Figure 3.3.16: Representation of genes involved in regulation of proliferation in DLKP4E specific genes. Detailed description of nodes and controls in Section 2.5.18.

Table 3.3.22 Gene changes due to eIF4E in DLKP4E not MCF74E related to regulation of proliferation

Gene	Regulation of motility	Fold change	Gene	Regulation of motility	Fold change
BIRC5	negative	1.26	COPS5	unknown	1.23
BOP1	negative	1.27	CREM	unknown	-1.97
C10orf9	negative	-1.93	CUL2	unknown	-1.43
CPE	negative	-2.04	DNAJA2	unknown	1.21
CTNNBIP1	negative	1.35	DNM1L	unknown	1.3
CUL5	negative	1.31	E2F3	unknown	1.42
E2F7	negative	1.66	EGR1	unknown	2.4
FOXO3A	negative	1.83	EPB41	unknown	2.07
GLMN	negative	1.45	FANCL	unknown	1.29
IHPK1	negative	2.31	HIPK2	unknown	1.87
LOXL2	negative	3.9	HIS1	unknown	1.72
MFGE8	negative	6.39	HNRPA3	unknown	1.28
MKL2	negative	1.65	HOXB8	unknown	20.76
RANBP2	negative	1.34	ISGF3G	unknown	1.51
RSU1	negative	-1.45	ISL1	unknown	4.4
SSA2	negative	1.49	KLF5	unknown	2.47
SYNPO2	negative	1.7	LIG1	unknown	1.68
TGFB1I1	negative	1.6	LIM	unknown	1.47
TPM1	negative	1.57	MCM2	unknown	1.35
TUBB	negative	6.01	MTSS1	unknown	2.31
BIRC3	positive	1.26	MUT	unknown	1.4
BMI1	positive	-1.51	NEFH	unknown	-1.21
BMPR1A	positive	1.5	NIPBL	unknown	1.38
CLN2	positive	1.36	NKX3-1	unknown	-4.27
CUL4A	positive	1.41	NOLA1	unknown	1.3
GTF2IRD1	positive	1.72	NRIP1	unknown	2.19
HIG2	positive	1.89	PIN4	unknown	1.32
MLLT6	positive	1.76	PPIA	unknown	1.27
MSX1	positive	6.26	PTMS	unknown	1.38
PSIP1	positive	1.35	RGC32	unknown	-4.96
RFP	positive	1.46	RPS6KA3	unknown	1.8
AGRN	unknown	1.56	SDC3	unknown	1.65
ANP32A	unknown	1.34	SHMT1	unknown	1.38
ARNT2	unknown	1.61	SLC16A3	unknown	-2.68
BTBD7	unknown	1.71	SMARCC1	unknown	1.83
BTG3	unknown	2.27	SMARCE1	unknown	1.4
CA11	unknown	1.48	SSX1	unknown	-10.19
CBS	unknown	1.36	TCF3	unknown	1.31
CIP29	unknown	1.29	TNFSF7	unknown	3.19
			YME1L1	unknown	-1.47

Table 3.3.22: Role in regulation of proliferation of DLKP4E specific genes.

3.3.5.3 Genes common to DLKP4E and MCF7H3erbB2 but not MCF74E, with the same pattern of expression.

MCF7H3erbB2 is an erbB2-expressing invasive clone of MCF7, and many of the gene changes which occur in this cell line compared to parent MCF7H3 are related to its invasive phenotype. To further investigate gene changes that occur due to eIF4E in DLKP4E and are related to invasion, genes that were common to both MCF7H3erbB2 and DLKP4E but not MCF74E were examined using Pathway Assist ®. This resulted in a list of genes that were differentially expressed with a phenotypical change from non-invasive to invasive in an MCF7 cell line, and also relevant to invasion as a result of eIF4E overexpression. Several pathways were generated which showed common targets for this list of genes. Of the 351 genes on the list 34 were involved in cell survival (Figure 3.3.17), 12 in invasion (Figure 3.3.18), 30 in motility (Figure 3.3.19) and 54 in apoptosis (Figure 3.3.20). Of most likely significance to this study were those involved in invasion and motility. The fact that these genes are significantly changed in two invasive cell lines, and not in non-invasive MCF74E, suggests they may play an important role in invasion in both DLKP and MCF7.

Figure 3.3.17 Gene changes involved in regulation of cell survival common to MCF7H3erbB2 and DLKP4E not MCF74E

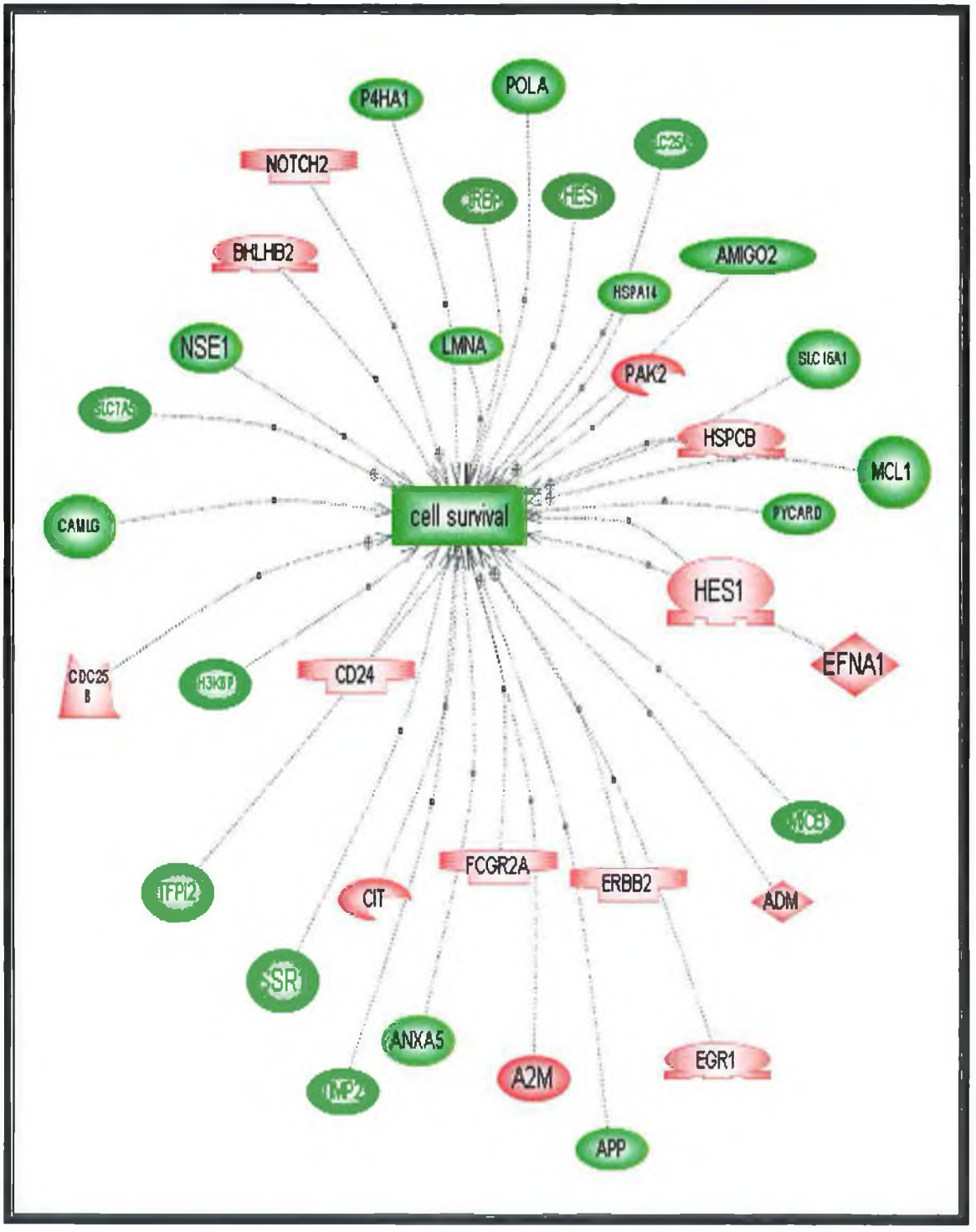

Figure 3.3.17: Representation of genes involved in regulation of cell survival in MCF7H3erbB2 and DLKP4E. Detailed description of nodes and controls in Section 2.5.18.

Table 3.3.23 Regulation of cell survival by DLKP4E MCF7H3erbB2 not MCF74E common genes

Gene	Description	Regulation of cell survival	Fold change DLKP	Fold change MCF7H3erbB2
CIT	citron (rho-interacting, serine/threonine kinase 21)	negative	+ 1.32	+ 1.88
APP	amyloid beta (A4) precursor protein (peptidase nexin-II, Alzheimer disease)	positive	+ 1.22	+ 1.8
CDC25B	cell division cycle 25B	positive	+1.27	+ 1.46
EGR1	Early growth response	positive	+2.4	+3.76
ERBB2	v-erb-b2 erythroblastic leukemia viral oncogene homolog 2, neuro/glioblastoma derived oncogene homolog	positive	+1.34	+1.48
MCL1	myeloid cell leukemia sequence 1 (BCL2-related)	positive	+1.23	+1.27
NOTCH2	Notch homolog 2 (Drosophila)	positive	+1.24	+1.23
SLC16A1	solute carrier family 16, member 1 (monocarboxylic acid transporter 1)	positive	+1.27	+1.8
SLC7A5	solute carrier family 7 (cationic amino acid transporter, y+ system), member 5	positive	+2.13	+1.45
ADM	adrenomedullin	unknown	+2.27	+2.63
ANXA5	annexin A5	unknown	+2.47	+1.6
BHLHB2	basic helix-loop-helix domain containing, class B, 2	unknown	+1.33	+1.98
CAMLG	calcium modulating ligand	unknown	+1.24	+1.47
CD24	CD24 antigen (small cell lung carcinoma cluster 4 antigen)	unknown	+5.81	+1.42
CHES1	checkpoint suppressor 1	unknown	+1.7	+2.67
CIRBP	cold inducible RNA binding protein	unknown	+1.42	+1.34
EFNA1	ephrin-A1	unknown	+2.38	+2.04
FCGR2A	Fc fragment of IgG, low affinity IIa, receptor (CD32)	unknown	-1.44	-1.85
HSPA14	heat shock 70kDa protein 14	unknown	-1.28	-1.46
LMNA	lamin A/C	unknown	+1.6	+1.67
MICB	MHC class I polypeptide-related sequence B	unknown	-1.64	-1.48
P4HA1	procollagen-proline, 2-oxoglutarate 4-dioxygenase (proline 4-hydroxylase), alpha polypeptide I	unknown	-1.38	-1.69
PAK2	p21 (CDKN1A)-activated kinase 2	unknown	-1.2	-1.44
PYCARD	PYD and CARD domain containing	unknown	-90.95	-1.65
SH3KBP1	SH3-domain kinase binding protein 1	unknown	1.72	2.1
SLC25A6	solute carrier family 25 (mitochondrial carrier; adenine nucleotide translocator), member 6	unknown	1.25	1.31
SSR1	signal sequence receptor, alpha (translocon-associated protein alpha)	unknown	-1.21	-1.36
TFPI2	tissue factor pathway inhibitor 2	unknown	-10.96	-1.53

Figure 3.3.18 Gene changes involved in regulation of invasion common to MCF7H3erbB2 and DLKP4E not MCF74E

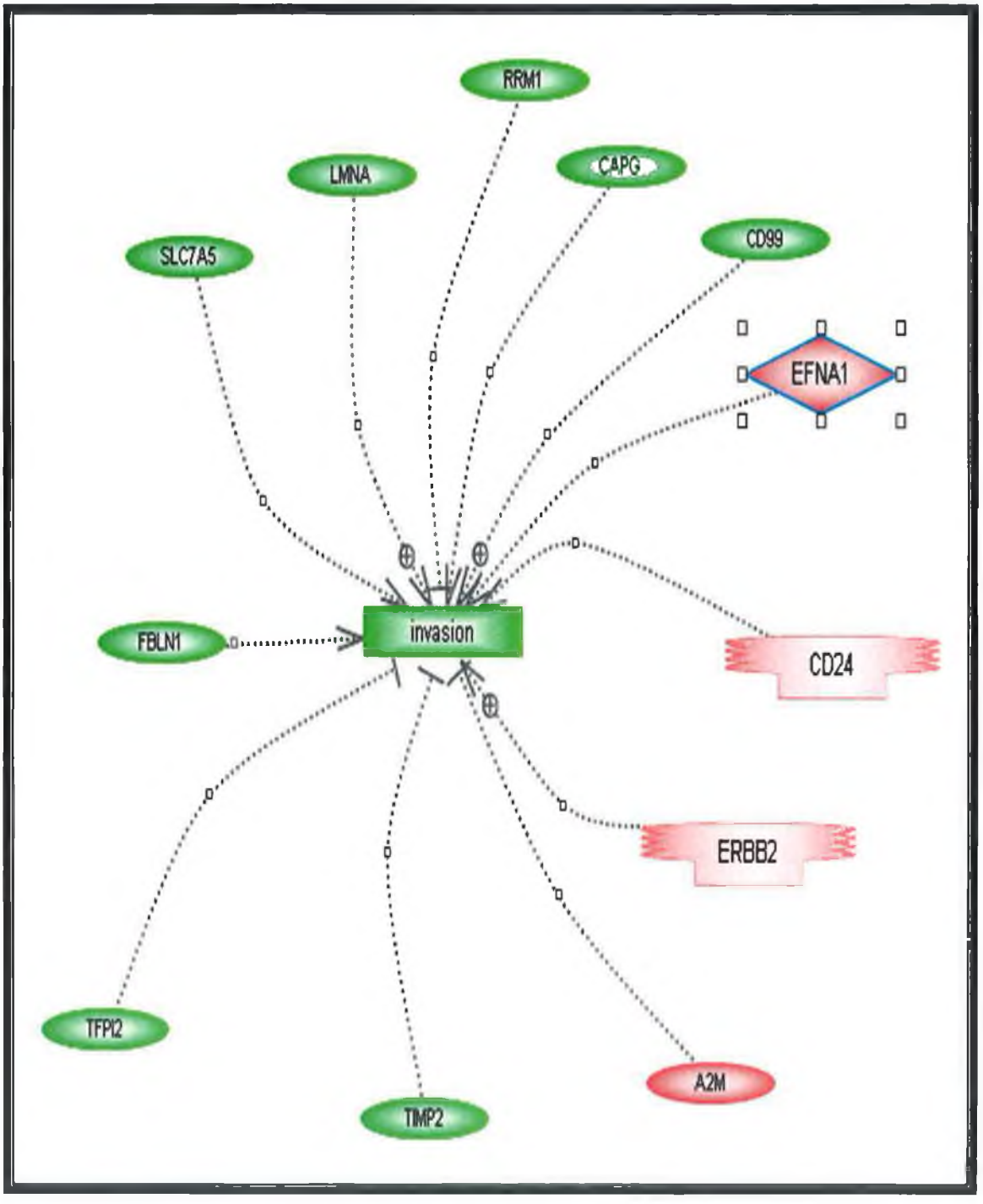

Figure 3.3.18: Representation of genes involved in regulation of invasion in MCF7H3erbB2 and DLKP4E. Detailed description of nodes and controls in Section 2.5.18.

Table 3.3.24 Regulation of invasion by DLKP4E MCF7H3erbB2 not MCF74E common genes

Gene	Description	Regulation of invasion	Fold change DLKP	Fold change MCF7erbB2
RRM1	ribonucleotide reductase M1 polypeptide	negative	1.23	1.42
TFPI2	tissue factor pathway inhibitor 2	negative	-10.96	-1.53
TIMP2	TIMP metallopeptidase inhibitor 2	negative	-1.27	-2.32
LMNA	lamin A/C	positive	1.6	1.67
CD99	CD99 molecule	positive	2.04	2.09
ERBB2	v-erb-b2 erythroblastic leukemia viral oncogene homolog 2, neuro/glioblastoma derived oncogene homolog	positive	1.34	1.48
CAPG	capping protein (actin filament), gelsolin-like	unknown	1.66	1.6
CD24	CD24 molecule	unknown	5.81	1.42
EFNA1	ephrin-A1	unknown	2.38	2.04
FBLN1	fibulin 1	unknown	1.44	2.97
SLC7A5	solute carrier family 7 (cationic amino acid transporter, y+ system), member 5	unknown	2.13	1.45

Figure 3.3.19 Gene changes involved in regulation of motility common to MCF7H3erbB2 and DLKP4E not MCF74E

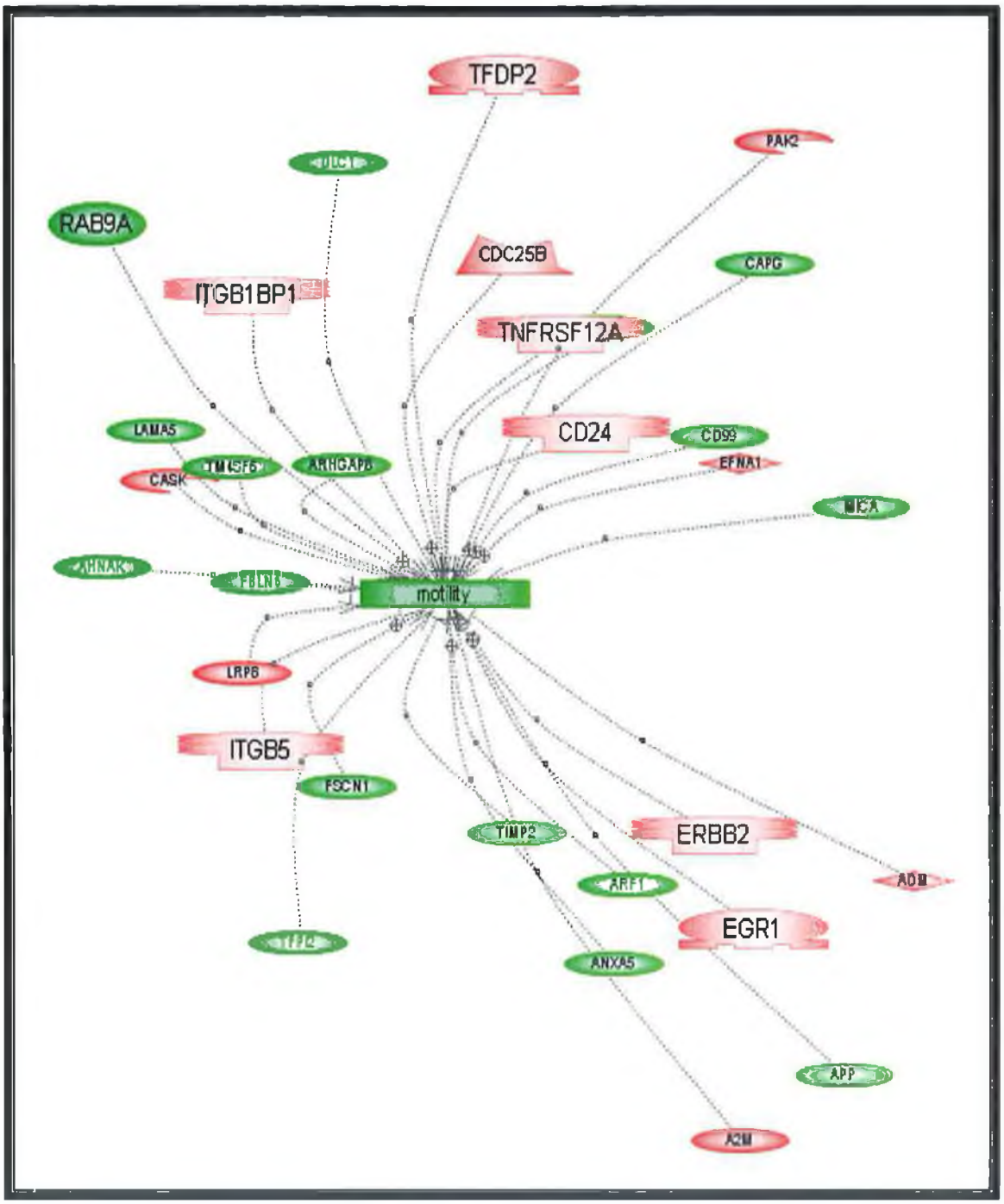

Figure 3.3.19: Representation of genes involved in regulation of motility in MCF7H3erbB2 and DLKP4E. Detailed description of nodes and controls in Section 2.5.18.

Table 3.3.25 Regulation of motility by DLKP4E MCF7H3erbB2 not MCF74E common genes

Gene	Description	D	M	Gene	Description	D	M
MICA	MHC class I polypeptide-related sequence A	-1.69	-1.57	LAMA5	laminin, alpha 5	1.39	1.47
EGR1	early growth response 1	2.4	3.76	CDC25B	cell division cycle 25B	1.27	1.46
ERBB2	v-erb-b2 erythroblastic leukemia viral oncogene homolog 2, neuro/glioblastoma derived oncogene homolog (avian)	1.34	1.48	AHNAK	AHNAK nucleoprotein (desmoyokin)	1.65	1.81
RRM1	ribonucleotide reductase M1 polypeptide	1.23	1.42	ITGB5	integrin, beta 5	1.46	1.44
ADM	adrenomedullin	2.27	2.63	TFPI2	tissue factor pathway inhibitor 2	-10.96	-1.53
CD24	CD24 antigen (small cell lung carcinoma cluster 4 antigen)	5.81	1.42	TNFRSF12A	tumor necrosis factor receptor superfamily, member 12A	-1.37	-1.41
ANXA5	annexin A5	2.47	1.65	CAPG	capping protein (actin filament), gelsolin-like	1.66	1.6
PAK2	p21 (CDKN1A)-activated kinase 2	-1.2	-1.44	FSCN1	fascin homolog 1, actin-bundling protein (Strongylocentrotus purpuratus)	1.81	2.62
TIMP2	tissue inhibitor of metalloproteinase 2	-1.27	-2.32	FBLN1	fibulin 1	1.44	2.97
CASK	calcium/calmodulin-dependent serine protein kinase (MAGUK family)	1.29	1.63	ITGB1BP1	integrin beta 1 binding protein 1	-1.24	-1.45
APP	amyloid beta (A4) precursor protein (protease nexin-II, Alzheimer disease)	1.22	1.8	LRP8	low density lipoprotein receptor-related protein 8, apolipoprotein e receptor	1.26	1.48
DLC1	deleted in liver cancer 1	-1.54	-1.96	TFDP2	transcription factor Dp-2 (E2F dimerization partner 2)	1.92	2.37
ARF1	ADP-ribosylation factor 1	-1.31	-1.32	TM4SF6	transmembrane 4 superfamily member 6	1.59	1.59
RAB9A	RAB9A, member RAS oncogene family	1.69	1.57	ARHGAP8	Rho GTPase activating protein 8	2.58	1.45
EFNA1	ephrin-A1	2.38	2.04	CD99	CD99 antigen	2.04	2.09

D= DLKP4E fold change, M= MCF7H3erbB2 fold change.

Figure 3.3.20 Gene changes involved in regulation of apoptosis common to MCF7H3erbB2 and DLKP4E not MCF74E

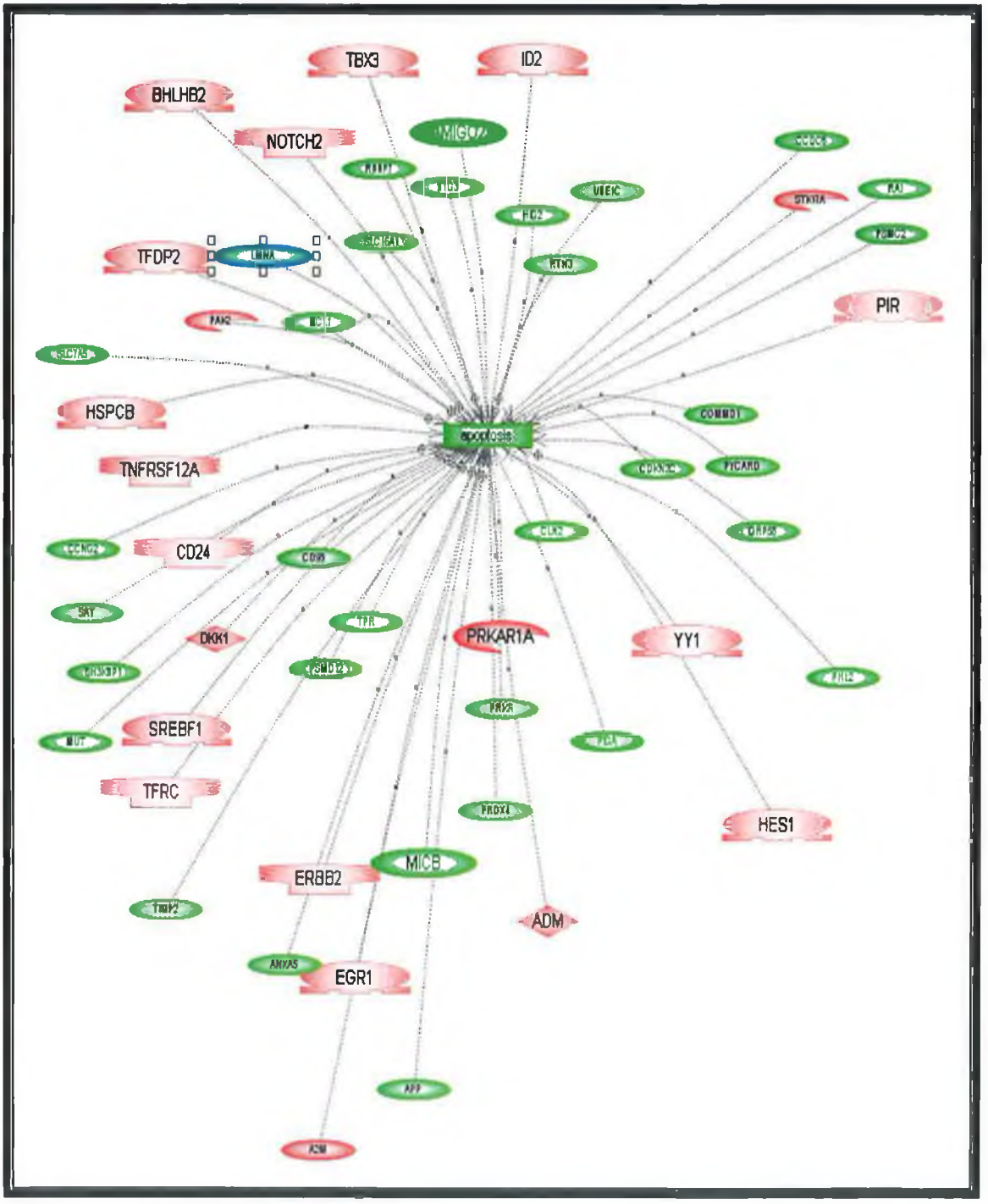

Figure 3.3.20: Representation of genes involved in regulation of apoptosis in MCF7H3erbB2 and DLKP4E. Detailed description of nodes and controls in Section 2.5.18.

Table 3.3.26 Regulation of apoptosis by DLKP4E MCF7H3erbB2 not MCF74E common genes

Gene	Regulation of apoptosis	Gene	Regulation of apoptosis
Nodes	Effect	BTG3	unknown
ADM	negative	CCDC6	unknown
AMIGO2	negative	CCNG2	unknown
BHLHB2	negative	CDKN2C	unknown
COMMD1	negative	CLN2	unknown
ERBB2	negative	EGR1	unknown
HES1	negative	GRP58	unknown
HSPCB	negative	HIG2	unknown
MCL1	negative	ID2	unknown
NOTCH2	negative	PIGA	unknown
RAI	negative	PIR	unknown
ANXA5	positive	PRDX4	unknown
APP	positive	PRKAR1A	unknown
CD24	positive	PRKR	unknown
CD99	positive	PSMC2	unknown
DKK1	positive	PYCARD	unknown
FHL2	positive	SAT	unknown
LMNA	positive	SH3KBP1	unknown
MICB	positive	SLC16A1	unknown
MUT	positive	STK17A	unknown
PAK2	positive	TBX3	unknown
PSMD12	positive	TFRC	unknown
RBBP7	positive	TNFRSF12A	unknown
RTN3	positive	TPR	unknown
SLC7A5	positive	UBE1C	unknown
SREBF1	positive	YY1	unknown
TFDP2	positive	BTG3	unknown

3.4 siRNA analysis of targets specific to invasion in MCF7H3erbB2 and DLKP4E

Two groups of siRNA targets specific to invasion were chosen based on microarray analysis of MCF7H3erbB2 and DLKP4E/DLKP4Emut (Table 3.3.9 and 3.3.14). The levels of silencing vary between species, cells and tissues due to differences in the efficiency with which the siRNAs are taken up by target cells. This problem was overcome by optimising condition for siRNA transfection for each cell line in 96- and 6-well plates using GAPDH and kinesin controls as positive controls, and scrambled siRNA as a siRNA control.

Two to three siRNAs were chosen for each of the 10 targets and transfected into cells (section 2.6). For each set of siRNA transfections carried out, a non-transfected (NT) cell line and a scrambled (SC) siRNA transfected control were used. Scrambled siRNA can be any sequence that does not have homology to any genomic sequence. The scrambled non-targeting siRNA used in this study is commercially produced, and promises limited sequence similarity to known genes. It has also been functionally proven to have minimal effects on cell proliferation and viability. For each set of experiments looking at the effect of siRNA, the cells transfected with target-specific siRNA were compared to cells transfected with scrambled siRNA. This took account of any effects due to the transfection reagents, and also any random effects of the scrambled siRNA.

Transfections were carried out in both 96- and 6-well plates (section 2.6). In order to determine the success of transfection, Kinesin was used as a control in both (Figure 3.4.1 & 3.4.2), and GAPDH siRNA was used as an additional control in 6-well plates (Figure 3.4.3). Kinesin facilitates cellular mitosis, therefore silencing kinesin facilitates cell arrest. In the absence of kinesin dividing cells adopt a rounded morphology in advance of microtubule formation, and this is where the cells arrest. Hence the round morphology of cells transfected with kinesin siRNA. In proliferation assays, non-transfected control cells divide normally while the kinesin siRNA transfected cells do not. The difference in control cell number compared to kinesin siRNA-transfected cells is not a measure of transfection efficiency or related to any cell death. It is a measure of how many times the control cells divided beyond the stage at which Kinesin levels became limiting in the transfected cells and they stopped dividing. GAPDH siRNA used in this study has been validated as a GAPDH-

specific control and has been functionally tested in several common cell lines. GAPDH silencing was seen as a measure of the accuracy of transfection conditions. Proliferation assays (Section 2.6.2) were carried out to assess if transfection of siRNAs had an effect on growth. Real-time PCR (Section 2.4.3.5.3) was used to look at efficiency of mRNA knock-down, and western blots (Section 2.4.1) were used to determine if siRNA had an effect at a protein level. Finally invasion assays (section 2.4.5) were carried out to confirm whether or not these targets played an important role in invasion, as suggested by microarray analysis. 9 out of 10 of the chosen targets were up-regulated in invasive cells, and therefore knock-down of these targets was expected to reduce the level of invasion. THBS1 was the only target down-regulated in invasive cell lines and siRNA silencing was expected to increase invasion.

All ten targets were examined in both DLKP4E and SKBR3. SKBR3, also a human breast, erbB2 positive, invasive cell line, replaced MCF7H3erbB2 for siRNA analysis. This was due to the fact that MCF7H3erbB2 lost its ability to invade. It is important to note that invasion assays were carried out on the MCF7H3erbB2 samples used for microarrays, demonstrating the cells were invasive (section 3.3.1). The THBS1 target, which was predicted to increase invasion when knocked-down using siRNA, was transfected into non-invasive MCF7s and DLKPs.

3.4.1 Proliferation assays using Kinesin siRNA transfection in DLKP, DLKP4E, MCF7 and SKBR3

Proliferation assays were carried out on all cell lines in this study using Kinesin as a positive control. Cellular arrest in the presence of Kinesin siRNA was taken as confirmation of efficient transfection conditions. Reduced growth of Kinesin siRNA-transfected cells compared to scrambled was seen in all cell lines (Figure 3.4.1).

3.4.2 Change in cell morphology after Kinesin siRNA transfection

Kinesin was also used as a control in 6-well plate transfections. Every set of transfections carried out was accompanied by a Kinesin transfection as a positive control. A change in the morphology of the cells indicated that Kinesin had been knocked-down and therefore the Kinesin siRNA transfection was successful. This was taken as an indication of optimum transfection conditions, and successful transfection in this cell line (Figure 3.4.2).

Figure 3.4.1 Proliferation assay results for DLKP, DLKP4E, MCF7 and SKBR3 transfected with kinesin siRNA

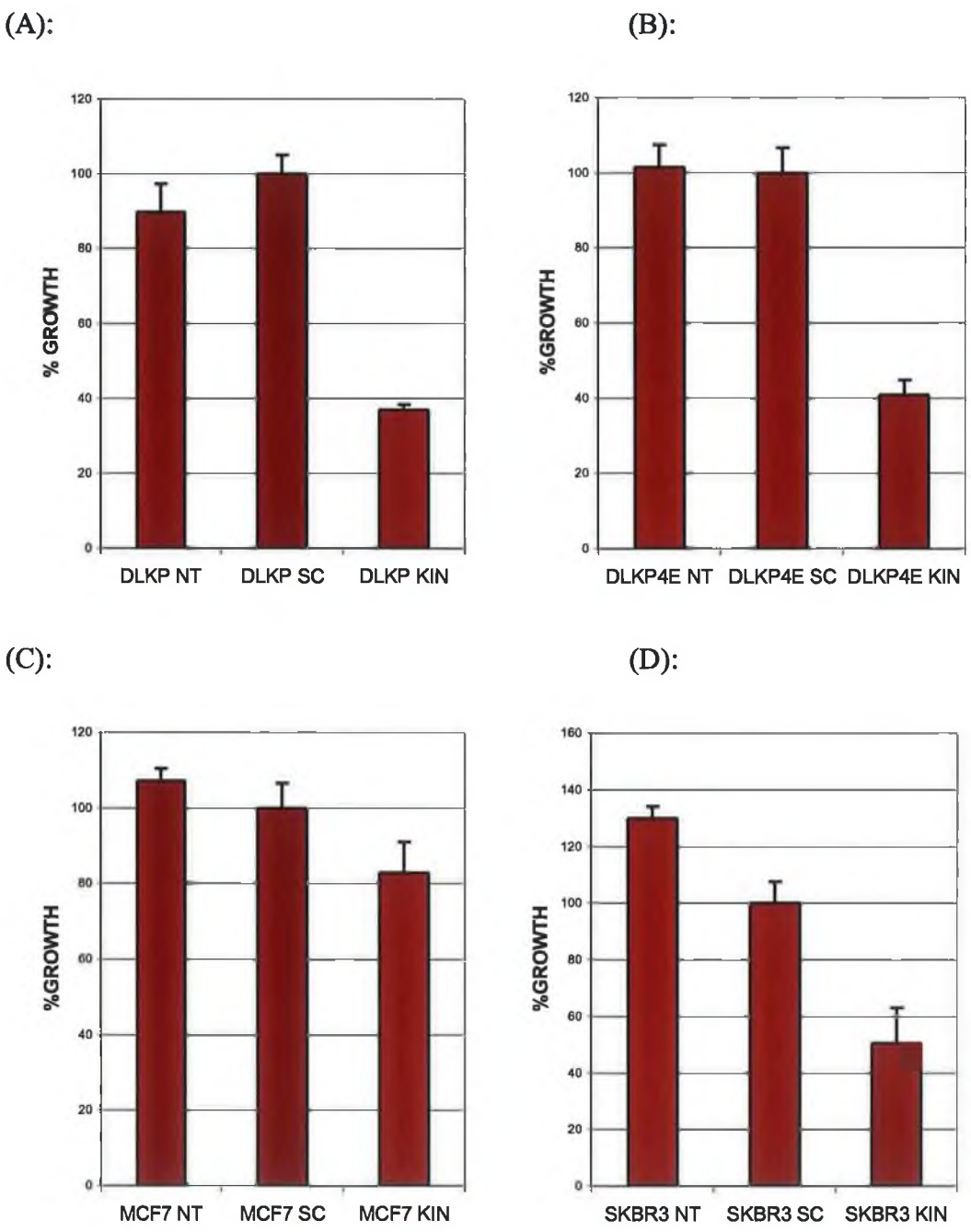

Figure 3.4.1: (A) Growth rate of DLKP after Kinesin siRNA transfection; (B) Growth rate of DLKP4E after Kinesin siRNA transfection; (C) Growth rate of MCF7 after Kinesin siRNA transfection; (D) Growth rate of SKBR3 after Kinesin siRNA transfection.

Figure 3.4.2 Effect of kinesin siRNA on cell morphology

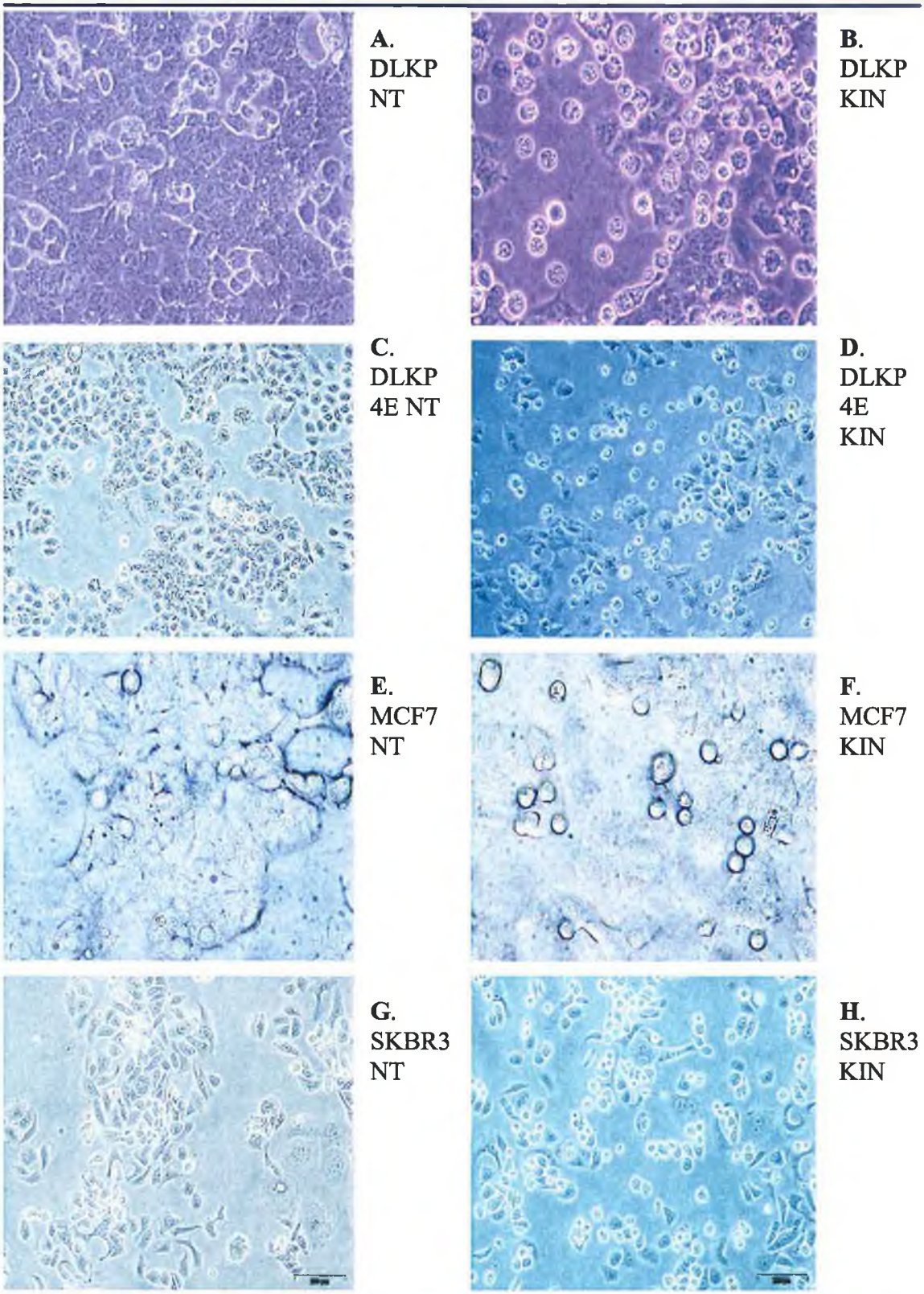

Figure 3.4.2: Photographs of kinesin siRNA transfection cells. Round morphology of cells indicates cell arrest. NT = non-transfected, KIN = Kinesin siRNA transfected. A=DLKPNT, B=DLKPKIN, C= DLKP4ENT, D=DLKP4EKIN, E=MCF7NT, F=MCF7KIN, G=SKBR3NT and H=SKBR3KIN.

3.4.3 siRNA silencing of GAPDH at mRNA level

Every set of 6-well plate transfections was also accompanied by transfection with GAPDH siRNA. This was examined at an mRNA level using real-time PCR. Knock-down of GAPDH in all cell lines confirmed optimum transfection conditions (figure 3.4.3). Results as described in term of relative quantification (RQ). This is the amount of target described in terms of 'fold change' compared to a comparator sample.

Figure 3.4.3 Real-time PCR for GAPDH in DLKP, DLKP4E, MCF7 & SKBR3

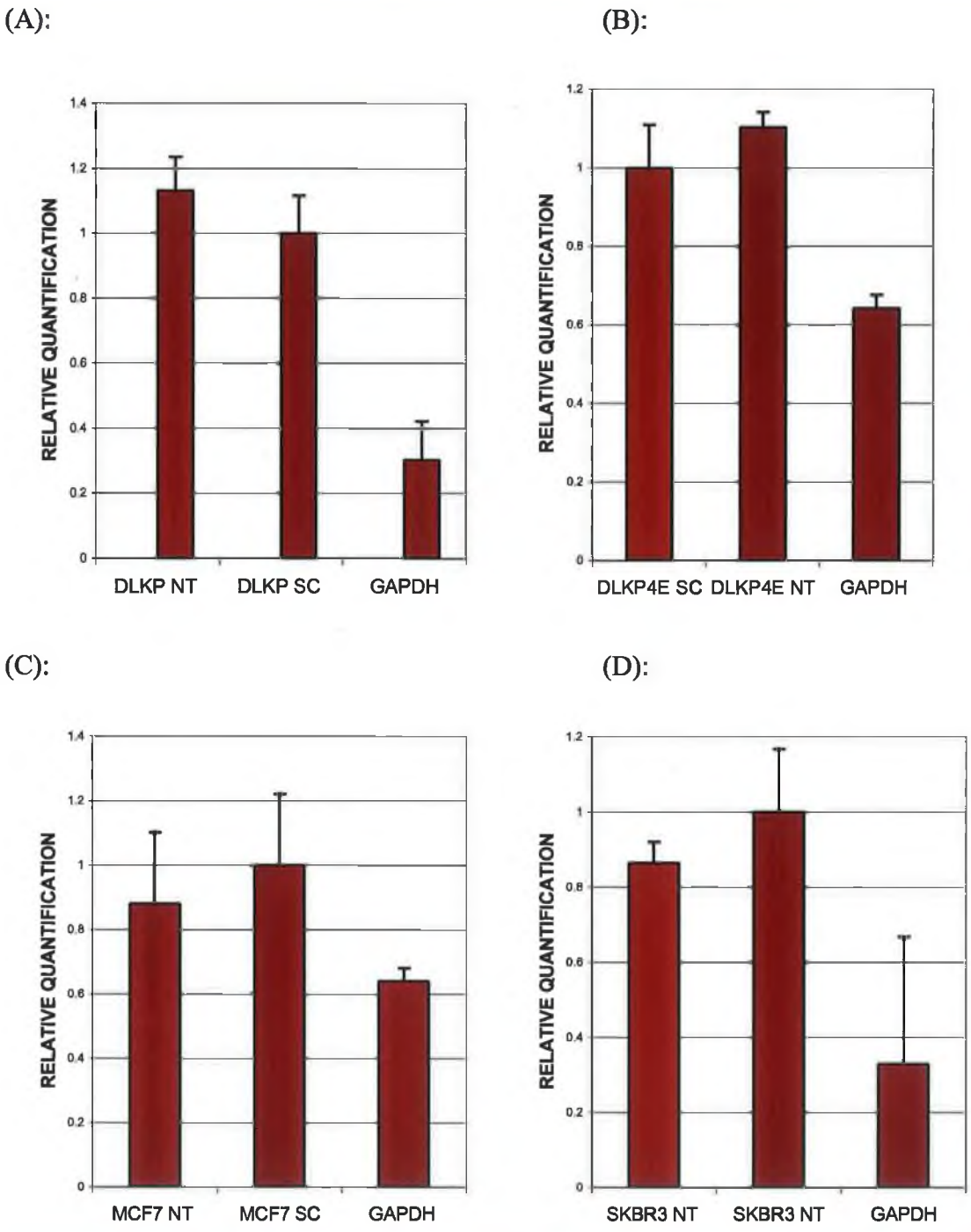

Figure 3.4.3: (A) Relative quantification of GAPDH mRNA 48hrs after GAPDH siRNA transfection into DLKP; (B) Relative quantification of GAPDH mRNA 48hrs after GAPDH siRNA transfection into DLKP4E; (C) Relative quantification of GAPDH mRNA 48hrs after GAPDH siRNA transfection into MCF7; (D) Relative quantification of GAPDH mRNA 48hrs after GAPDH siRNA transfection into SKBR3.

3.5 Tissue factor pathway inhibitor (TFPI)

TFPI was chosen as a target for siRNA based on MCF7H3erbB2 array data analysis that showed a +19.77 fold change in MCF7H3erbB2 (invasive) compared to MCF7H3 (non-invasive). No significant change was seen in DLKP4E, but there was a +10 fold change in DLKP4Emut compared to parent DLKP.

3.5.1 Proliferation assays

Proliferation assays carried out on DLKP4E and SKBR3 transfected with TFPI siRNA A and B showed minor changes in growth rate. Kinesin was used as a control, and the significant decrease in growth rate after knock-down of kinesin demonstrated the accuracy of the transfection conditions (see figure 3.5.1).

3.5.2 Real-time PCR

Real-time PCR carried out on TFPI siRNA A, B and C in both DLKP4E and SKBR3 showed significant knock-down of TFPI mRNA after 24 and 48hrs compared to scrambled siRNA transfections. In DLKP4E, TFPI A decreased TFPI mRNA by 40% at 24hrs, but recovered after 48hrs. TFPI B caused insignificant change at 24hrs but a 60% decrease in mRNA at 48hrs.TFPI C caused a 40% decrease at 24hrs, which increased to 60% after 48hrs (Figure 3.5.2 and 3.5.3). In SKBR3 all 3 siRNAs worked well at 24hrs, with between 70 and 90% decrease in TFPI mRNA. The cells appeared to recover at 48hrs and TFPI mRNA levels increased to only 20 to 30% less than the control (Figure 3.5.4 and 3.5.5).Therefore, transfection of all 3 TFPI siRNAs into DLKP4E and SKBR3 caused silencing of TFPI at mRNA level, with overall much greater effect in SKBR3 cells. In all cases siRNA A and B were treated separately to siRNA C. The reason for this being siRNA C transfections, to obtain RNA, were carried out separately at a later date.

Figure 3.5.1 Proliferation assay for TFPI siRNA A & B in DLKP4E and SKBR3

(A):

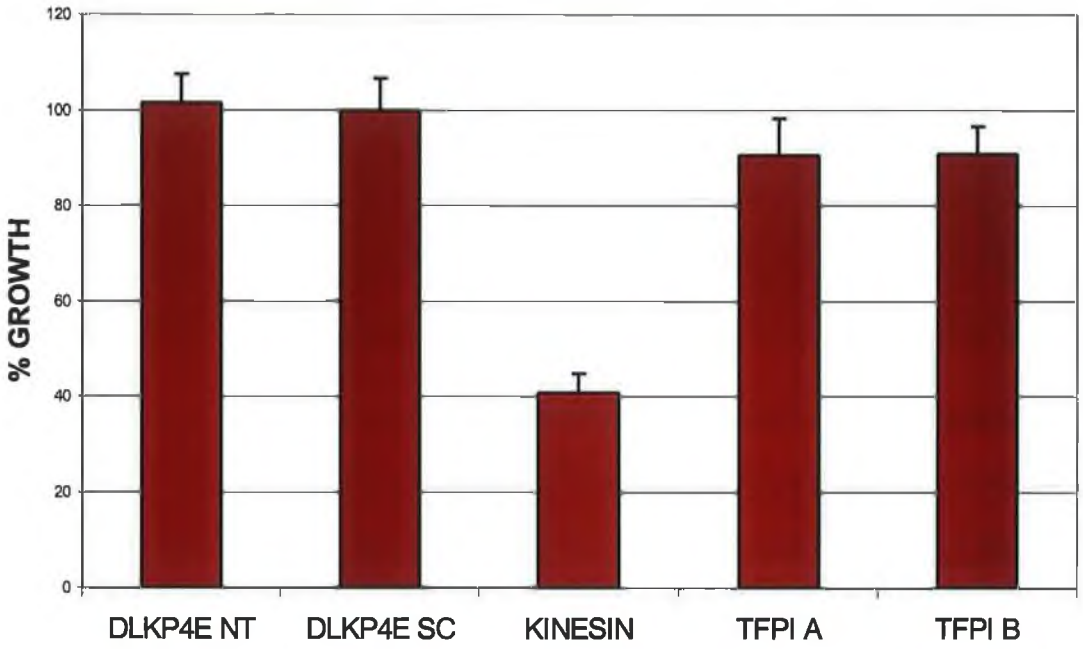

(B):

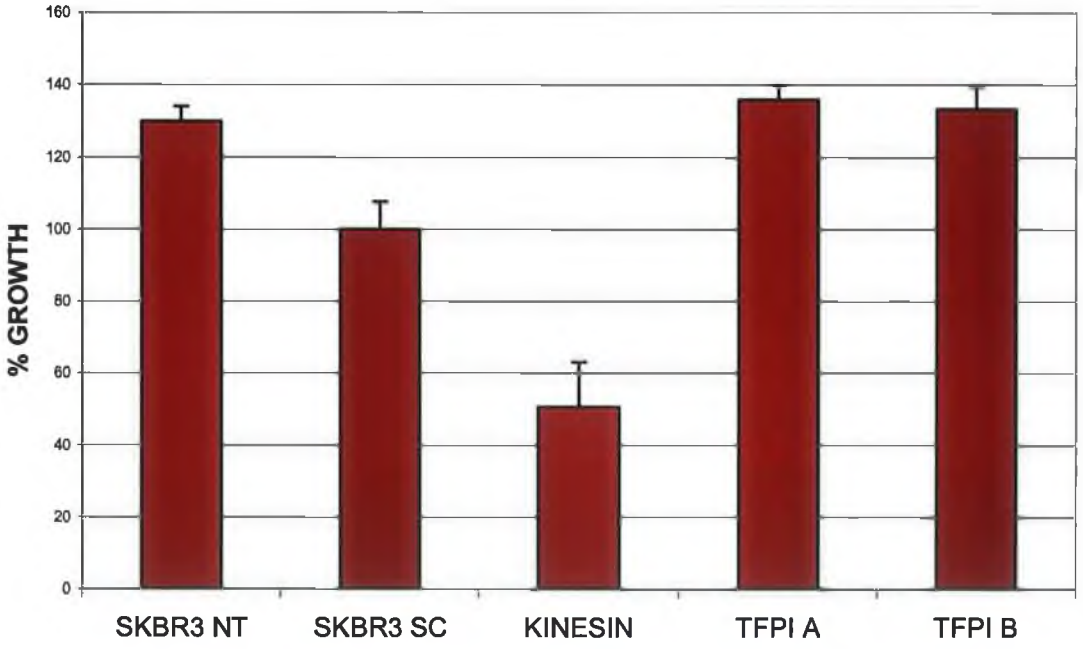

Figure 3.5.1: (A) Growth rate DLKP4E NT, DLKP4E SC and DLKP4E transfected with Kinesin and TFPI A & B siRNA; (B) Growth rate SKBR3 NT, SKBR3 SC and SKBR3 transfected with Kinesin and TFPI A & B siRNA;

Figure 3.5.2 Real-time PCR for TFPI siRNA A, B & C in DLKP4E at 24hrs

(A):

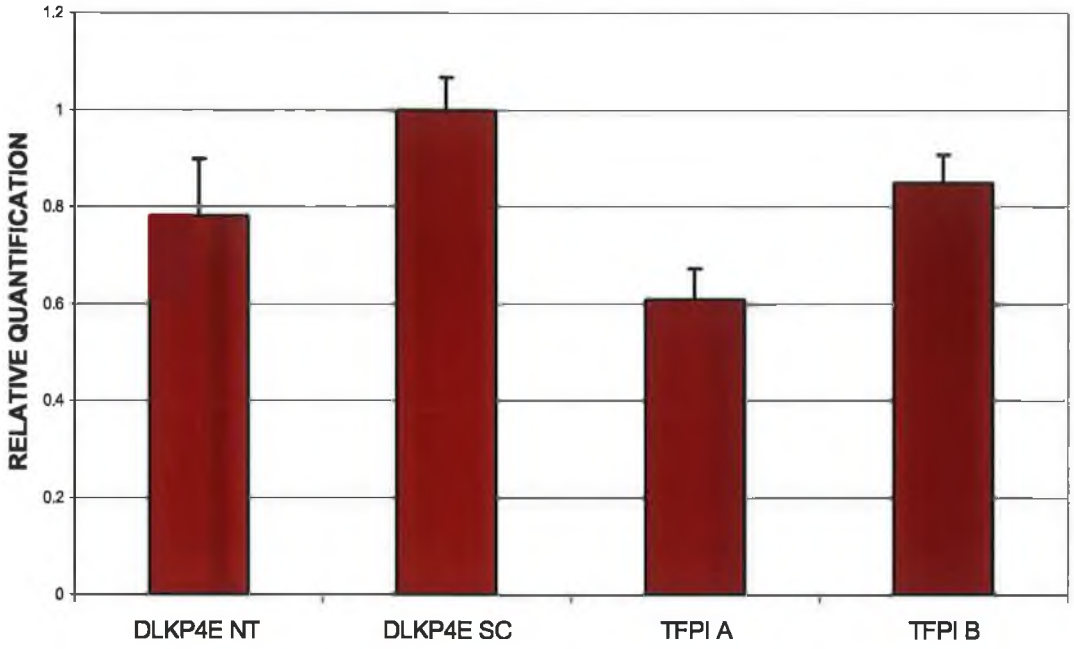

(B):

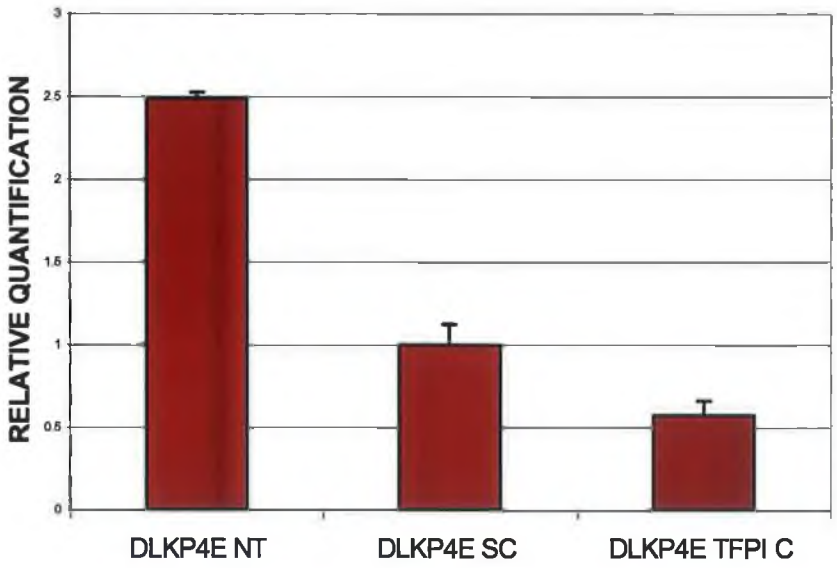

Figure 3.5.2: (A) Relative quantification of TFPI in non-transfected (NT), scrambled (SC), and TFPI siRNA A & B transfected cells after 24hrs; (B) Relative quantification of TFPI in non-transfected (NT), scrambled (SC), and TFPI C transfected cells after 24hrs.

Figure 3.5.3 Real-time PCR for TFPI siRNA A, B & C in DLKP4E at 48hrs

(A):

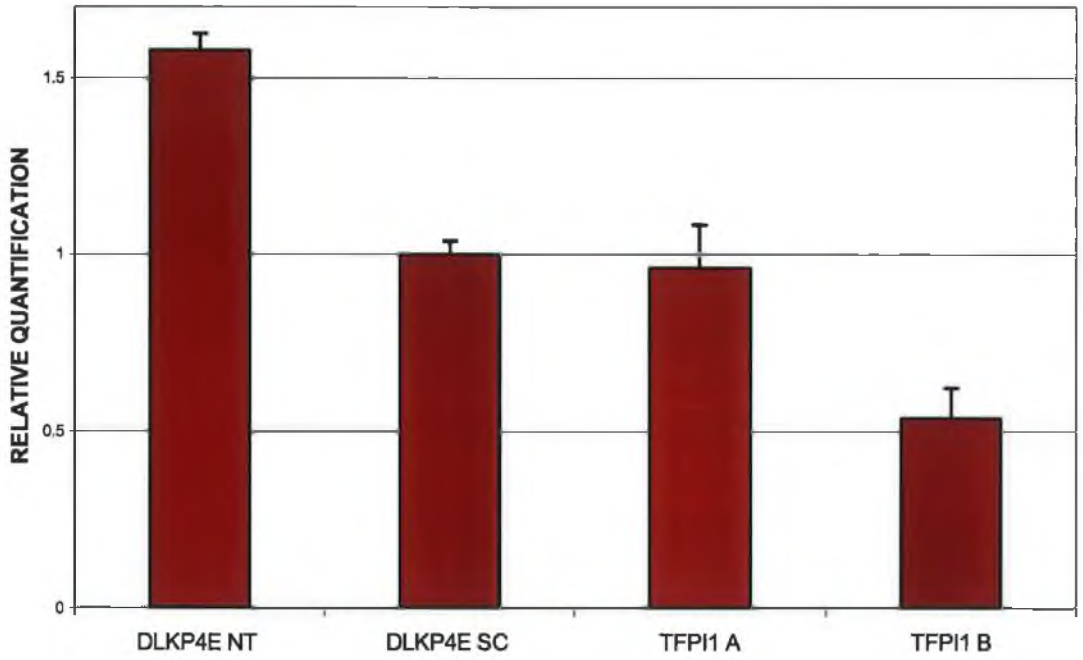

(B):

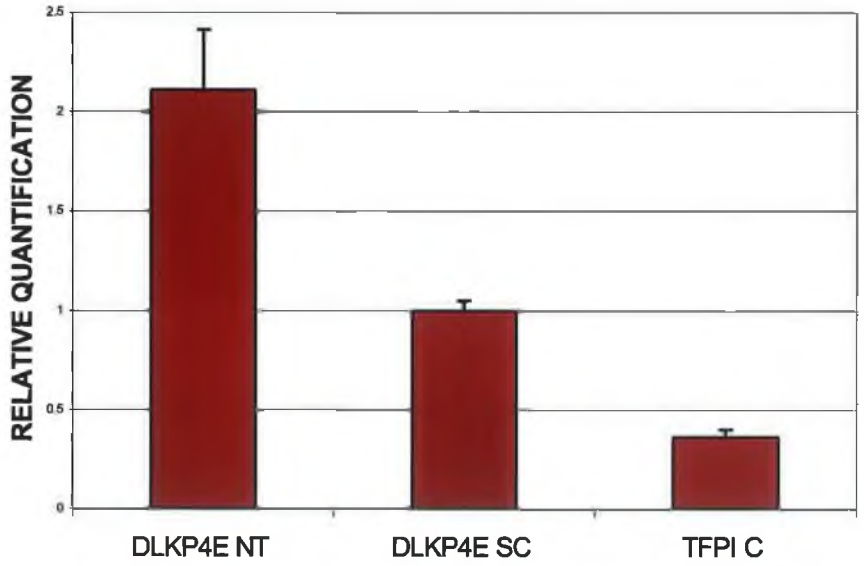

Figure 3.5.3: (A)Relative quantification of TFPI in non-transfected (NT), scrambled (SC), and TFPI siRNA A & B transfected cells after 48hrs; (B) Relative quantification of TFPI in non-transfected (NT), scrambled (SC), and TFPI C transfected cells after 48hrs.

Figure 3.5.4 Real-time PCR for TFPI siRNA A, B & C in SKBR3 at 24hrs

(A):

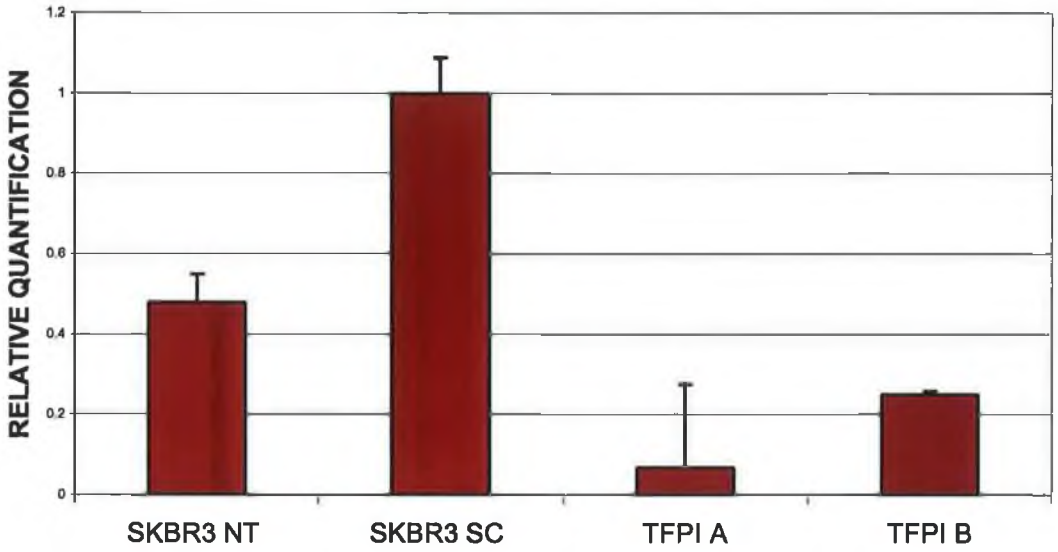

(B):

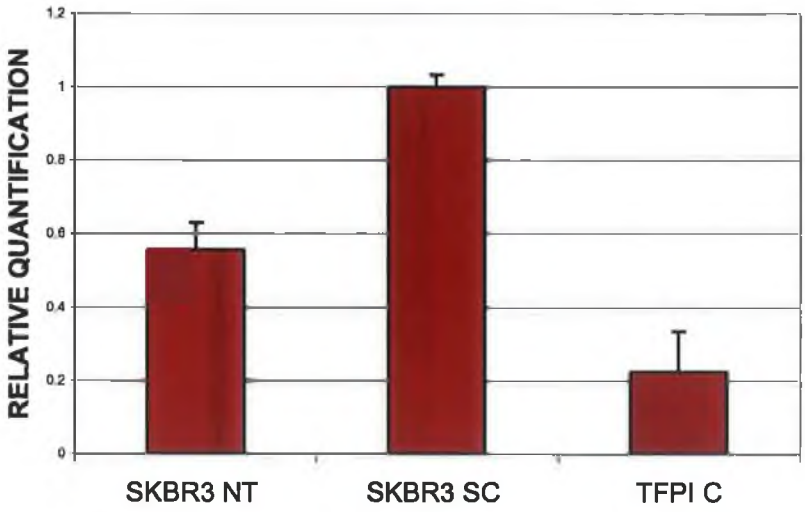

Figure 3.5.4: (A) Relative quantification of TFPI in non-transfected (NT), scrambled (SC), and TFPI siRNA A & B transfected SKBR3 after 24hrs; (B) Relative quantification of TFPI in non-transfected (NT), scrambled (SC), and TFPI C transfected SKBR3 after 24hrs.

Figure 3.5.5 Real-time PCR for TFPI siRNA A, B & C in SKBR3 at 48hrs

(A):

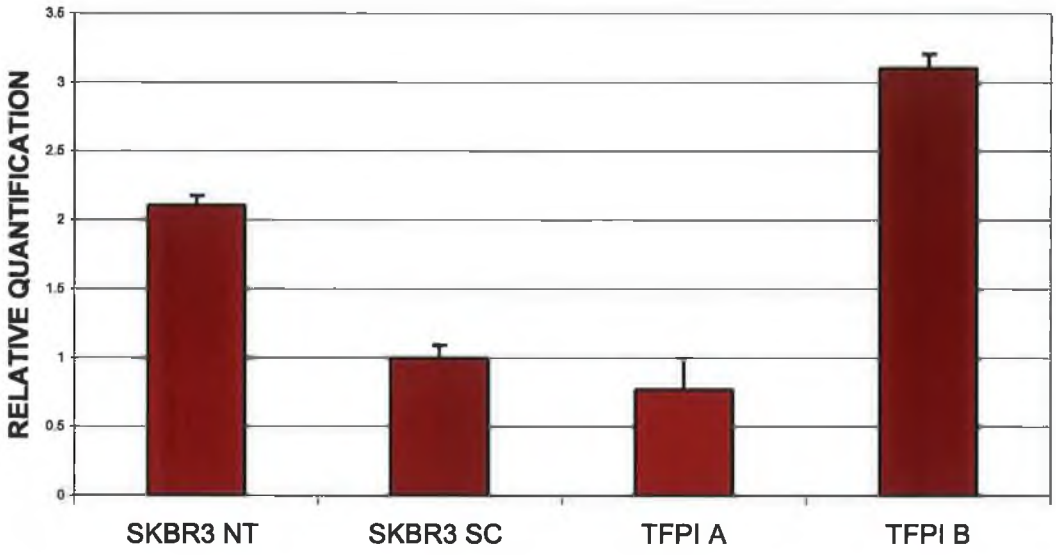

(B):

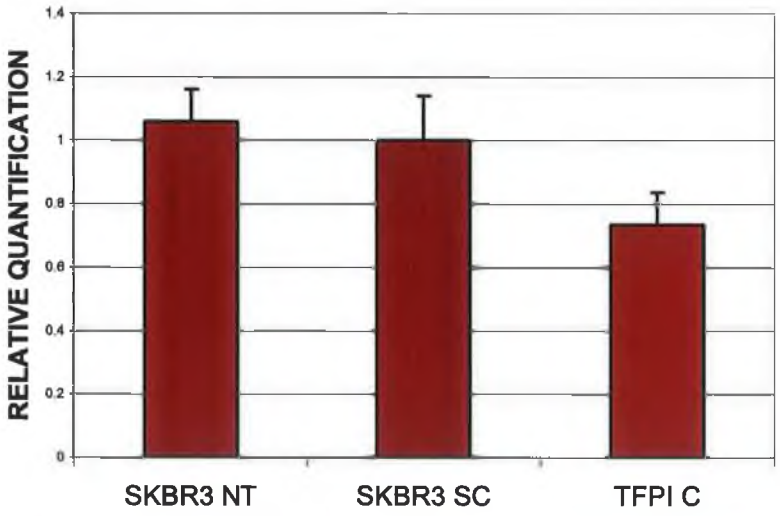

Figure 3.5.5: (A) Relative quantification of TFPI in non-transfected (NT), scrambled (SC), and TFPI siRNA A & B transfected SKBR3 after 48hrs; (B) Relative quantification of TFPI in non-transfected (NT), scrambled (SC), and TFPI C transfected SKBR3 after 48hrs.

3.5.3 Western blot

Western blots were carried out using protein 72hrs after transfection with all 3 TFPI siRNAs in both cell lines. Results showed no significant change in TFPI protein after transfection with any of the TFPI siRNAs in DLKP4E (see figure 3.5.6). TFPI was not detected in SKBR3, this may have been due to low levels of TFPI expression in this cell line.

3.5.4 Invasion assays

72hrs after transfection with TFPI siRNA, cells were assayed for invasion. DLKP4E results showed a reduction in the number of invading cells when transfected with all 3 TFPI siRNAs. This can be seen in both the photographs of the invasion inserts (figure 3.5.7) and in the number of invading cells counted per μm^2 (figure 3.5.8). SKBR3 transfected with the 3 TFPI siRNAs showed dramatic decrease in invasion. Up to an 80% reduction in invading cells was observed after TFPI siRNA A and B transfection into SKBR3. This considerable drop in invasion was obvious from photographs of invasion inserts (see figure 3.5.9) and was confirmed by counting invading cells (see figure 3.5.10). This result combined with those from real-time PCR would strongly suggest that siRNA silencing of TFPI in DLKP4E and SKBR3 decreases invasion.

Figure 3.5.6 Western blot analysis of TFPI protein expression in DLKP4E

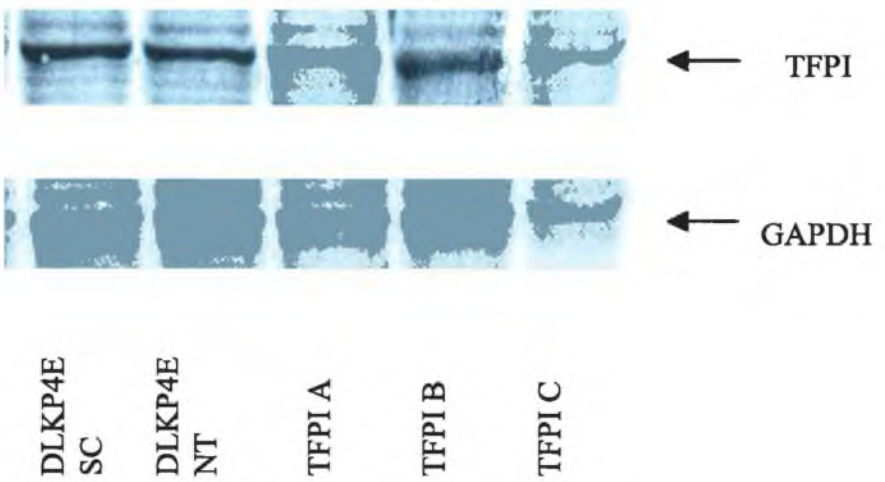

Figure 3.5.6: Western blot showing protein expression of TFPI in DLKP4E NT, DLKP4E SC, and DLKP4E transfected with TFPI siRNA A, B & C.

Figure 3.5.7 Photographs of invasion assays for DLKP4E transfected with TFPI siRNA

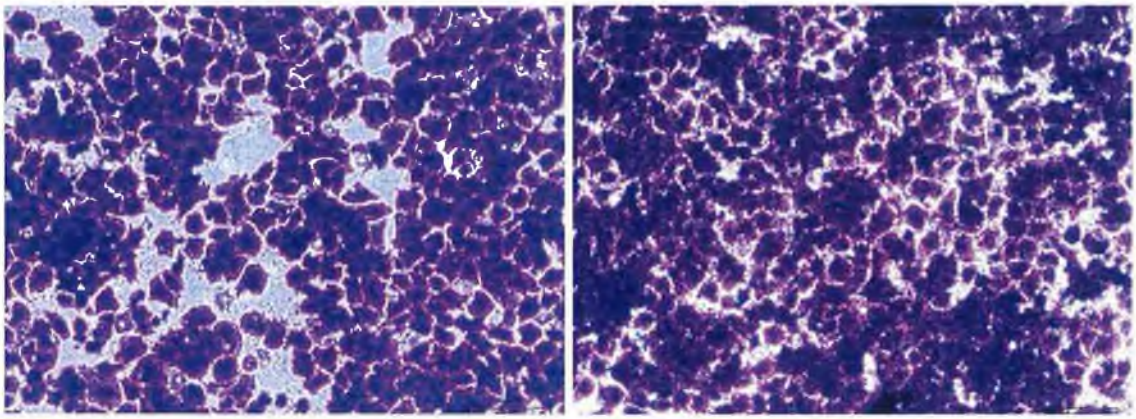

(A) DLKP4E NT

(B) DLKP4E SC

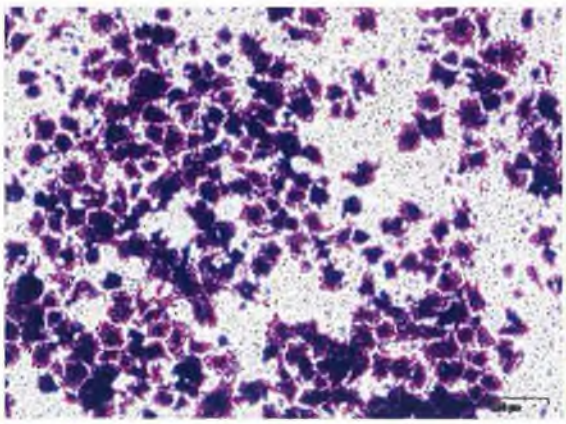

(C) TFPI A

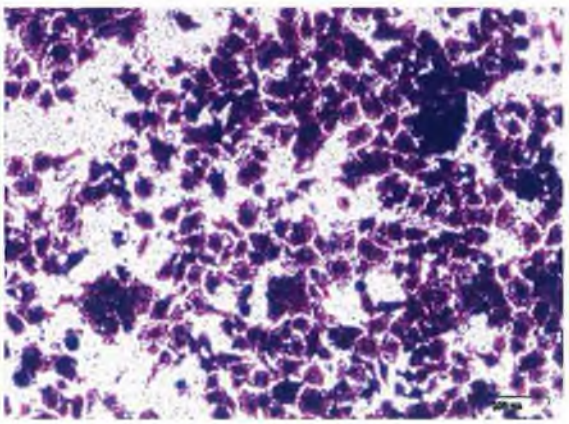

(D) TFPI B

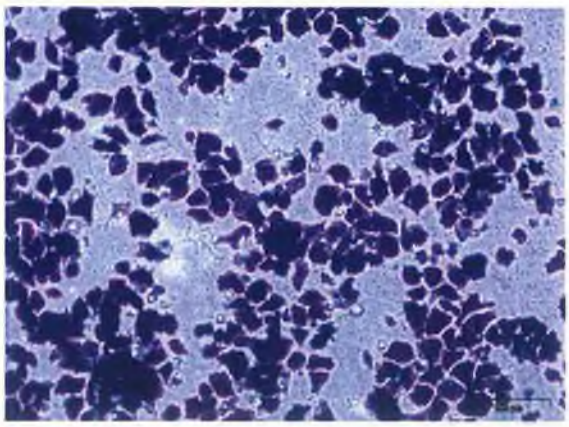

(E) TFPI C

Figure 3.5.7: Photographs of invasion assay inserts at 10X magnification. A=DLKP4E NT, B=DLKP4E SC, C=DLKP4E transfected with TFPI siRNA A, D=DLKP4E transfected with TFPI siRNA B, E= DLKP4E transfected with TFPI siRNA C.

Figure 3.5.8 cell counts of invasion assays for DLKP4E transfected with TFPI siRNA

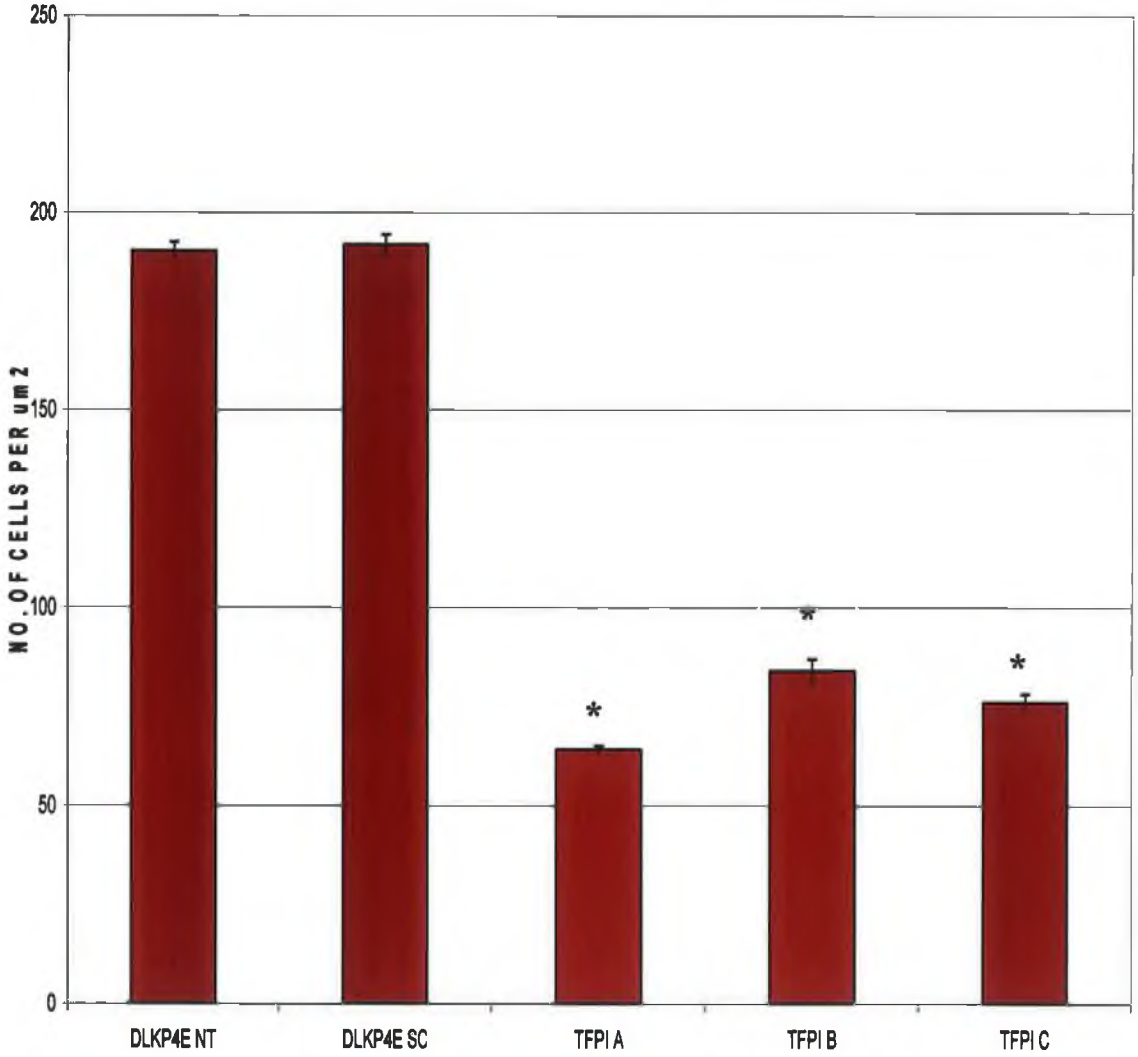

Figure 3.5.8: Number of invading cells detected per μm^2 of invasion assay insert for DLKP4E NT, DLKP4ESC and DLKP4E transfected with TFPI siRNA A, B & C.
n=3, *p-value<0.001

Figure 3.5.9 Photographs of invasion assays for SKBR3 transfected with TFPI siRNA

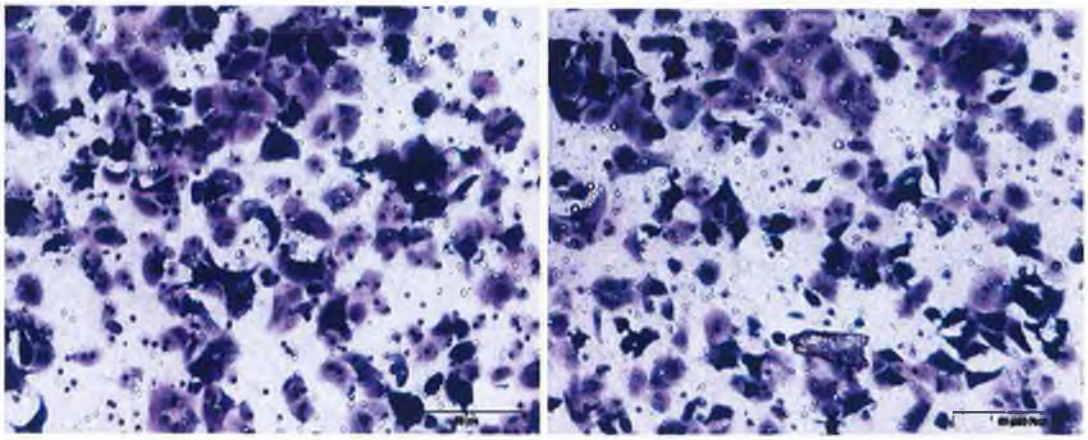

(A) SKBR3 NT (B) SKBR3 SC

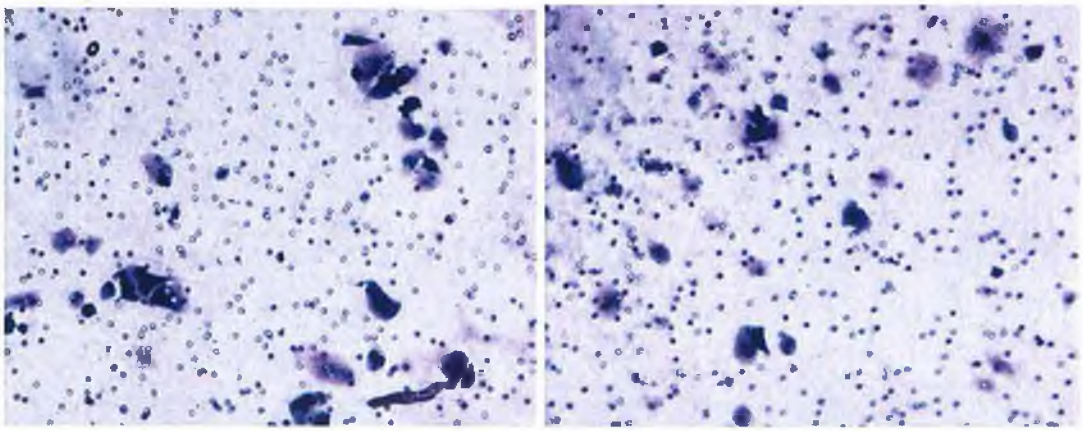

(C) TFPI A (D) TFPI B

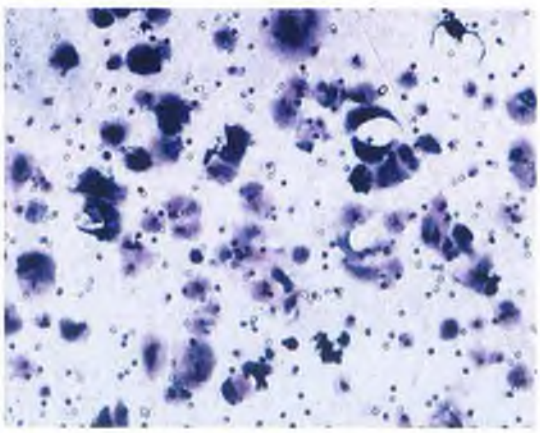

(E) TFPI C

Figure 3.5.9: Photographs of invasion assay inserts at 10X magnification. A= SKBR3 NT, B=SKBR3 SC, C= SKBR3 transfected with TFPI siRNA A, D=SKBR3 transfected with TFPI siRNA B E= SKBR3 transfected with TFPI siRNA C.

Figure 3.5.10 cell counts of invasion assays for SKBR3 transfected with TFPI siRNA

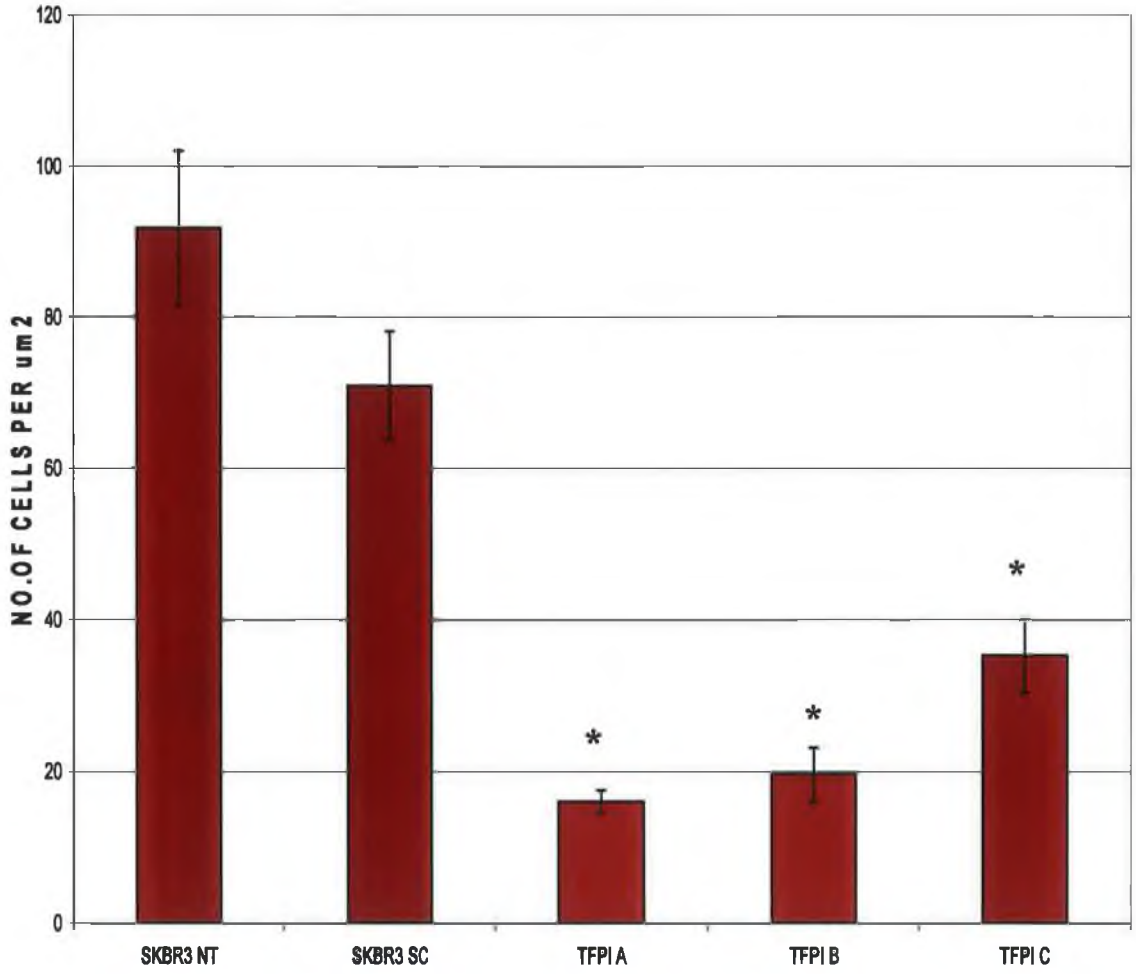

Figure 3.5.10: Number of invading cells detected per μm^2 of invasion assay insert for SKBR3 NT, SKBR3SC and SKBR3 transfected with TFPI siRNA A, B & C.
n=3, *p-value<0.001

3.5.5 Summary of results for TFPI siRNA transfection in DLKP4E and SKBR3

Results from proliferation assays showed that the optimum conditions for transfection were used, as a reduction in growth of cells transfected with kinesin siRNA was observed in both cell lines. This also showed that transfection of TFPI siRNA did not have a major effect on proliferation of DLKP4E or SKBR3 cells. After transfection with three separate TFPI siRNAs in two separate cell lines, a decrease in TFPI mRNA was observed, which indicated the siRNAs were successful in knocking-down TFPI at an mRNA level. Real-time PCR results showing GAPDH silencing under the same conditions also proved transfection conditions were accurate (Table 3.4.3). Although western blots were unable to show TFPI knock-down at a protein level for either cell line, knock-down of TFPI at an mRNA level, accompanied by a significant decrease in invasion of two different cell lines, strongly suggests siRNA knock-down of TFPI led to a reduction in invasion (Table 3.5.1). The implication of these results is that TFPI plays a key role in invasion in both DLKP4E and SKBR3.

Table 3.5.1 Summary of results of TFPI siRNA transfection into DLKP4E and SKBR3

	Real-time PCR – RNA knock-down			Western blot – protein knock-down			Invasion assay – decrease in invasion		
Cell Line	siRNA A	siRNA B	siRNA C	siRNA A	siRNA B	siRNA C	siRNA A	siRNA B	siRNA C
DLKP4E	+	+	+	—	—	—	+	+	+
SKBR3	+	+	+	—	—	—	+	+	+

Table 3.5.1: Summary of results of TFPI siRNA A, B and C transfections into DLKP4E and SKBR3

3.6 Early growth response 1 (EGR1)

EGR1 was chosen as a siRNA target after analysis of MCF7H3erbB2 microarray data showed a +2.99 fold increase in invasive MCF7erbB2 compared to non-invasive MCF7H3. An increase of +1.35 fold was also observed in invasive DLKP4E and, +1.2 fold in invasive DLKP4Emut compared to parent DLKP.

3.6.1 Proliferation assays

Proliferation assays carried out on DLKP4E transfected with EGR1 siRNA A and B showed little change in growth rate, whereas SKBR3 did show an increase in growth of 30-40% compared to the scrambled control. There was no significant change compared to the non-transfected control, and kinesin controls showed the transfection was successful (Figure 3.6.1).

3.6.2 Real-time PCR

Real-time PCR detected no EGR1 mRNA knock-down following EGR1 siRNA A or B transfection at 24 or 48hrs in DLKP4E. However, EGR1 siRNA C caused a 45% decrease in EGR1 at 24hrs and a 35% decrease at 48hrs (Figure 3.6.2 and 3.6.3). EGR1 in SKBR3 was knocked-down by 20%, 70% and 50% by EGR1 siRNA A, B and C, respectively, at 24hrs. At 48hrs, siRNA A and B had began to recovered, with EGR1 mRNA levels increasing. EGR1 siRNA C however, continued to increase silencing of mRNA and at 48hrs, levels were 80% less than the scrambled control (Figure 3.6.4 and 3.6.5). It is interesting to note that EGR1 siRNA C worked similarly in both cell lines, with an increased effect at 48hrs. Overall, EGR1 siRNA C was effective in silencing EGR1 mRNA in both cell lines, but EGR1 siRNA A and B only had an effect in SKBR3. Results for EGR1 siRNA C are shown separately because this RNA sample was from a separate transfection.

Figure 3.6.1 Proliferation assay for EGR1 siRNA A & B in DLKP4E and SKBR3

(A):

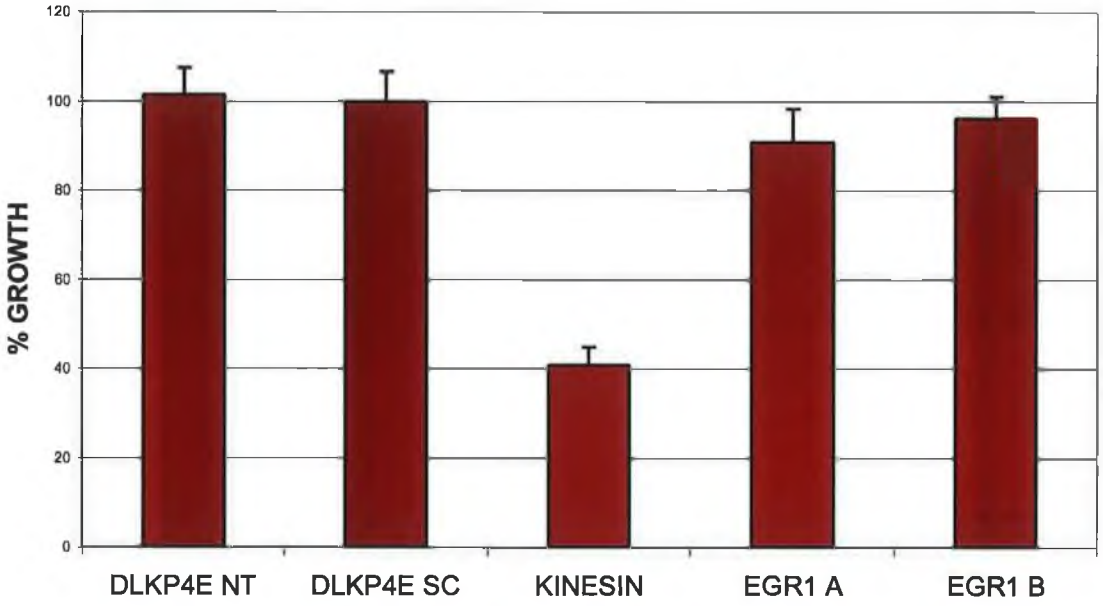

(B):

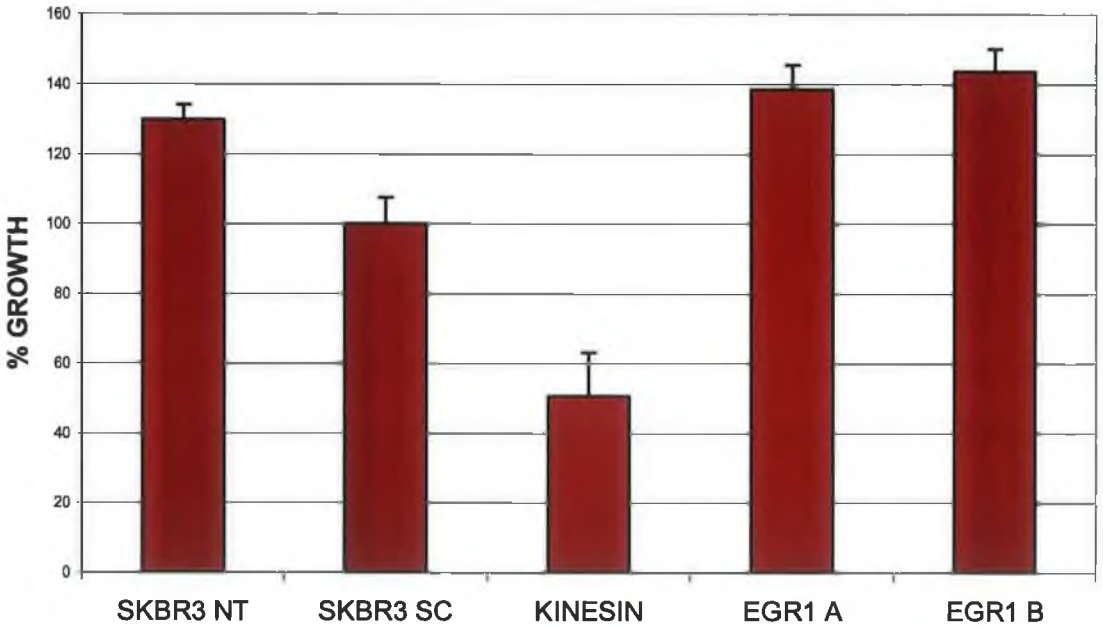

Figure 3.6.1: (A) Growth rate of DLKP4E NT, DLKP4E SC, and DLKP4E transfected with EGR1 siRNA A & B; (B) Growth rate of SKBR3 NT, SKBR3 SC, and SKBR3 transfected with EGR1 siRNA A & B.

Figure 3.6.2 Real-time PCR for EGR1 siRNA A, B & C in DLKP4E at 24hrs

(A):

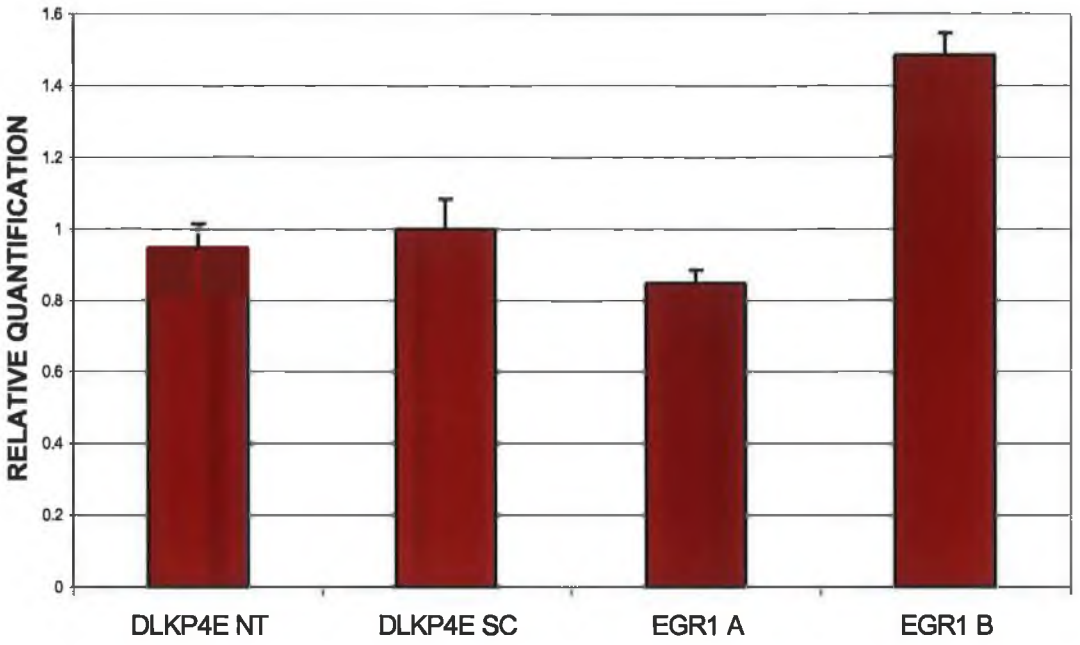

(B):

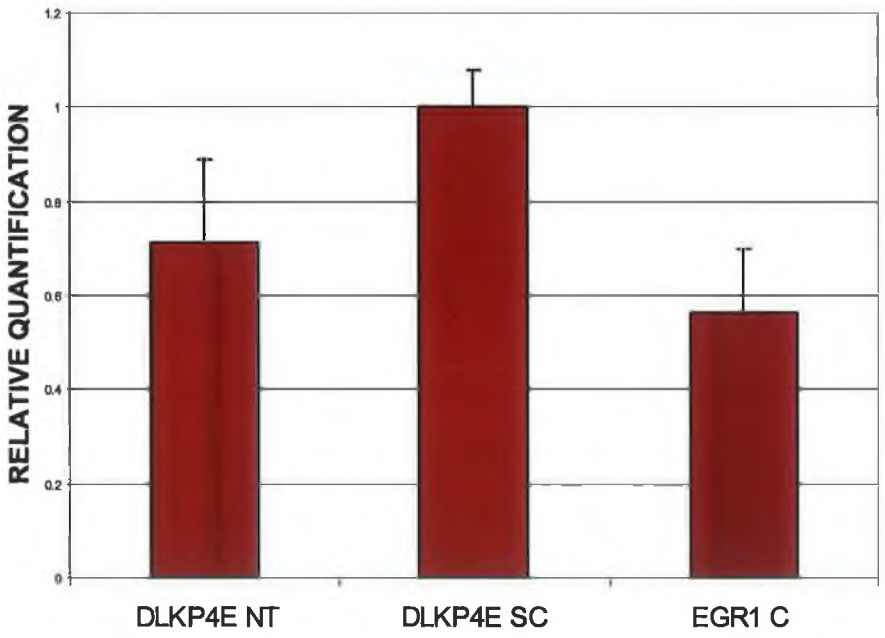

Figure 3.6.2: (A) Relative quantification of EGR1 in non-transfected (NT), scrambled (SC) and EGR1 siRNA A & B transfected DLKP4Es after 24 hrs; (B) Relative quantification of EGR1 in non-transfected (NT), scrambled (SC) and EGR1 siRNA C transfected DLKP4Es after 24 hrs.

Figure 3.6.3 Real-time PCR for EGR1 siRNA A, B & C in DLKP4E at 48hrs

(A):

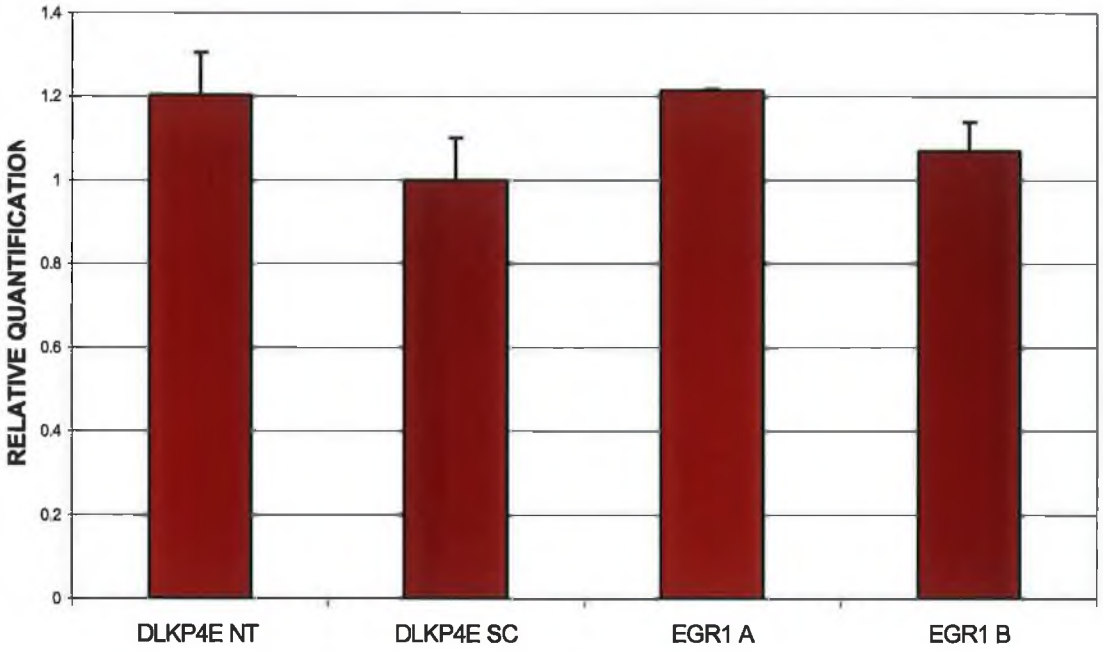

(B):

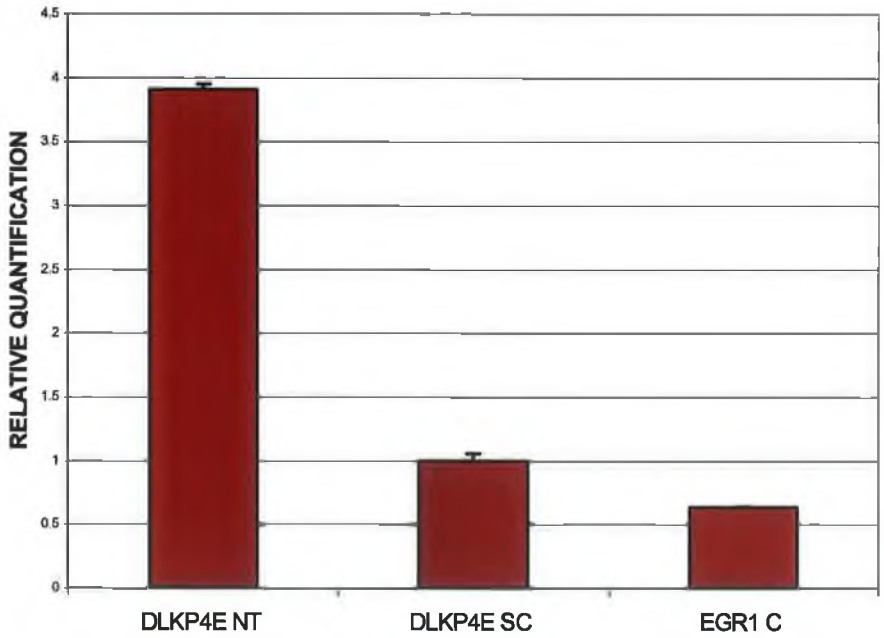

Figure 3.6.3: (A) Relative quantification of EGR1 in non-transfected (NT), scrambled (SC) and EGR1 siRNA A & B transfected DLKP4Es after 24 hrs; (B) Relative quantification of EGR1 in non-transfected (NT), scrambled (SC) and EGR1 siRNA C transfected DLKP4Es after 24 hrs.

Figure 3.6.4 Real-time PCR for EGR1 siRNA A, B & C in SKBR3 at 24hrs

(A):

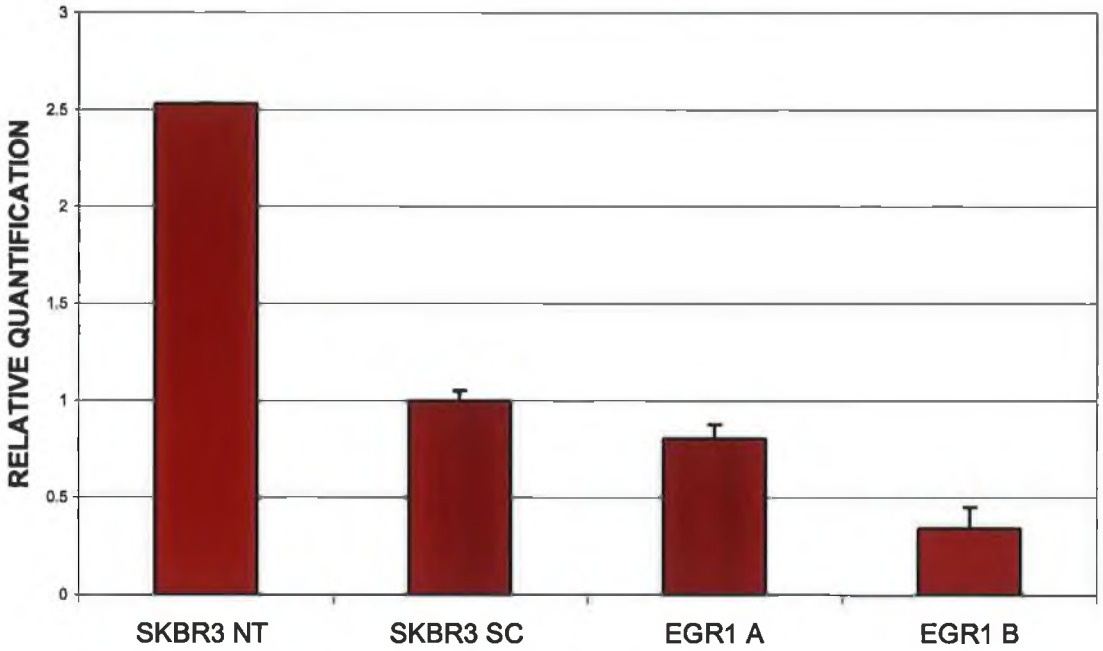

(B):

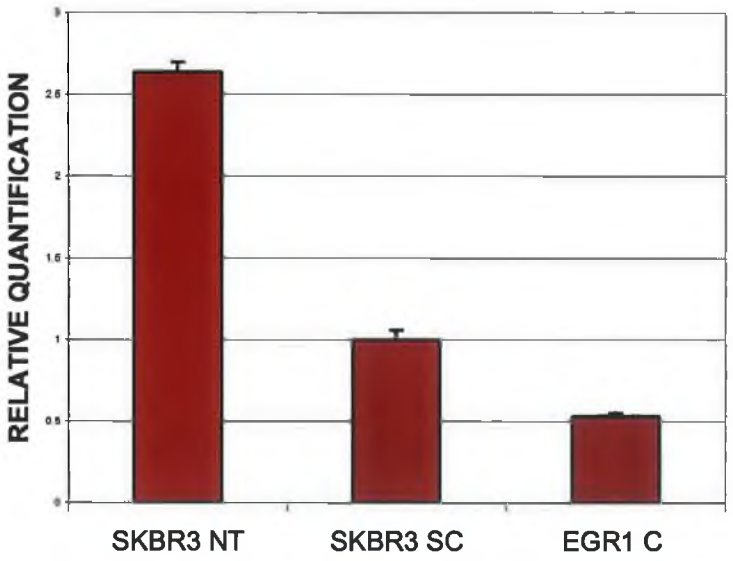

Figure 3.6.4: (A) Relative quantification of EGR1 in non-transfected (NT), scrambled (SC) and EGR1 siRNA A & B transfected SKBR3s after 24 hrs; (B) Relative quantification of EGR1 in non-transfected (NT), scrambled (SC) and EGR1 siRNA C transfected SKBR3s after 24 hrs.

Figure 3.6.5 Real-time PCR for EGR1 siRNA A, B & C in SKBR3 at 48hrs

(A):

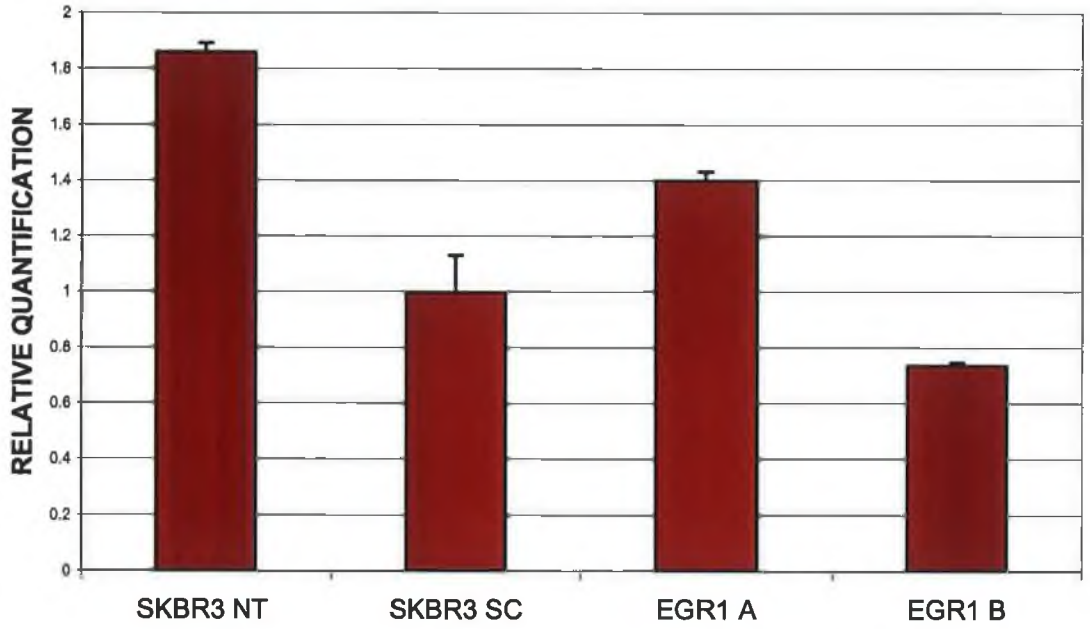

(B):

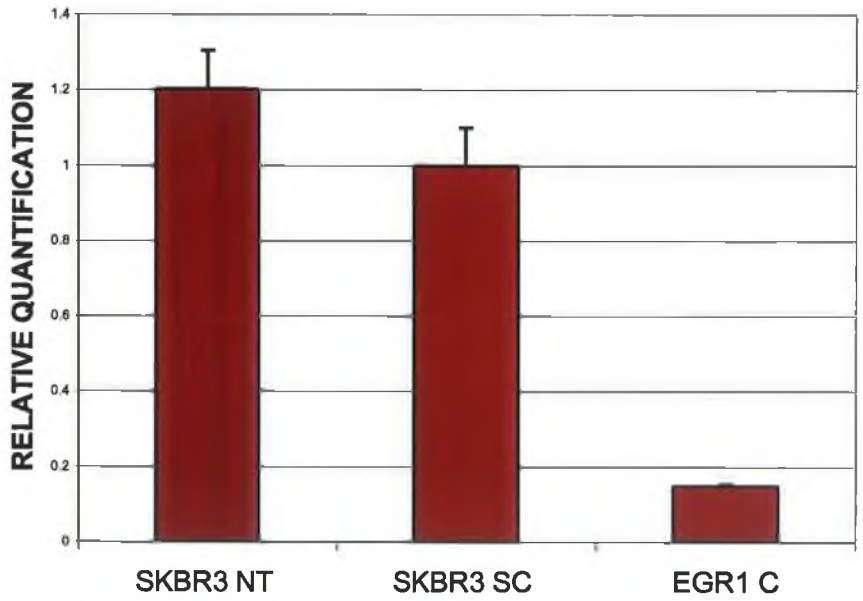

Figure 3.6.5: (A)Relative quantification of EGR1 in non-transfected (NT), scrambled (SC) and EGR1 siRNA A & B transfected SKBR3s after 24 hrs; (B) Relative quantification of EGR1 in non-transfected (NT), scrambled (SC) and EGR1 siRNA C transfected SKBR3s after 24 hrs.

3.6.3 Western blot

Western blots were carried out using an EGR1 specific antibody to detect if EGR1 siRNA transfection had had an effect at protein level (section 2.4.1).Results showed that there was a decrease in EGR1 at a protein level in both cell lines (Figure 3.6.6 and 3.6.7).

DLKP4E transfected with all 3 EGR1 siRNAs showed considerable protein knock-down compared to the non-transfected and scrambled controls. This result implies that despite lack of evidence at an mRNA level, EGR1 siRNA did function in 'knocking-down' EGR1 in DLKP4E (Figure 3.6.6).

In SKBR3 a reduction in EGR1 protein was seen as a result of EGR1 siRNA B and C (Figure 3.6.7). In the case of siRNA C the band is barely detectable, indicating very efficient silencing. Knock-down is not seen in EGR1 siRNA A, although this was observed at mRNA level (Figure 3.6.4 and 3.6.5). With two out of three EGR1 siRNAs showing knock-down of protein in both cell lines, it can be presumed that EGR1 siRNAs worked efficiently.

3.6.4 Invasion assays

Results from invasion assays showed a significant reduction in the number of invading cells after transfection with EGR1 siRNAs. Both photographic evidence and cell counts show that the number of invading cells was halved after EGR1 siRNA transfection in DLKP4E (Figure 3.6.8 and 3.6.9). Similar results are also true of SKBR3 (Figure 3.6.10 and 3.6.11). The most efficient EGR1 siRNA in this case appears to be C, which was also the only siRNA to produce mRNA knock-down in both cell lines.

Figure 3.6.6 Western Blot analysis of EGR1 protein expression in DLKP4E

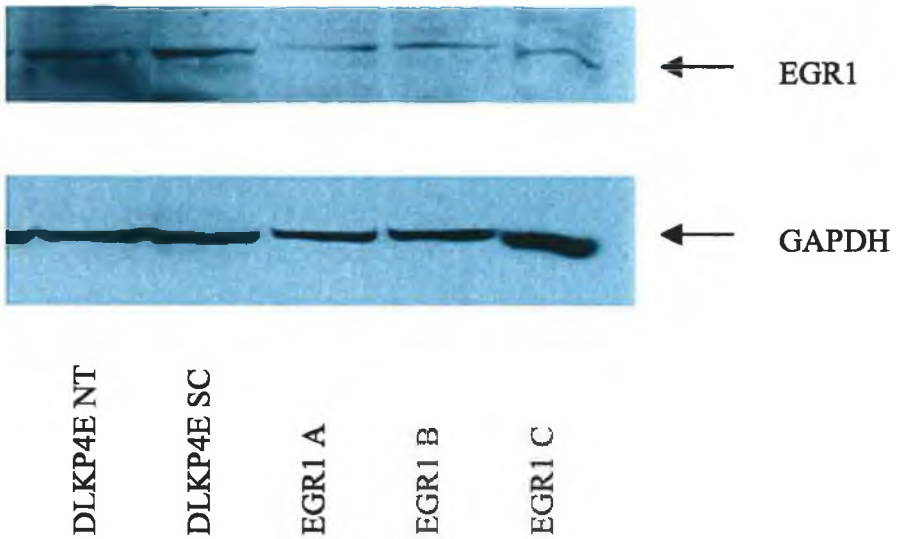

Figure 3.6.6: Western blot showing protein expression of EGR1 in DLDKP4E NT, DLKP4E transfected with scrambled control, and DLKP4E transfected with EGR1 siRNA A, B & C.

Figure 3.6.7 Western Blot analysis of EGR1 protein expression in SKBR3

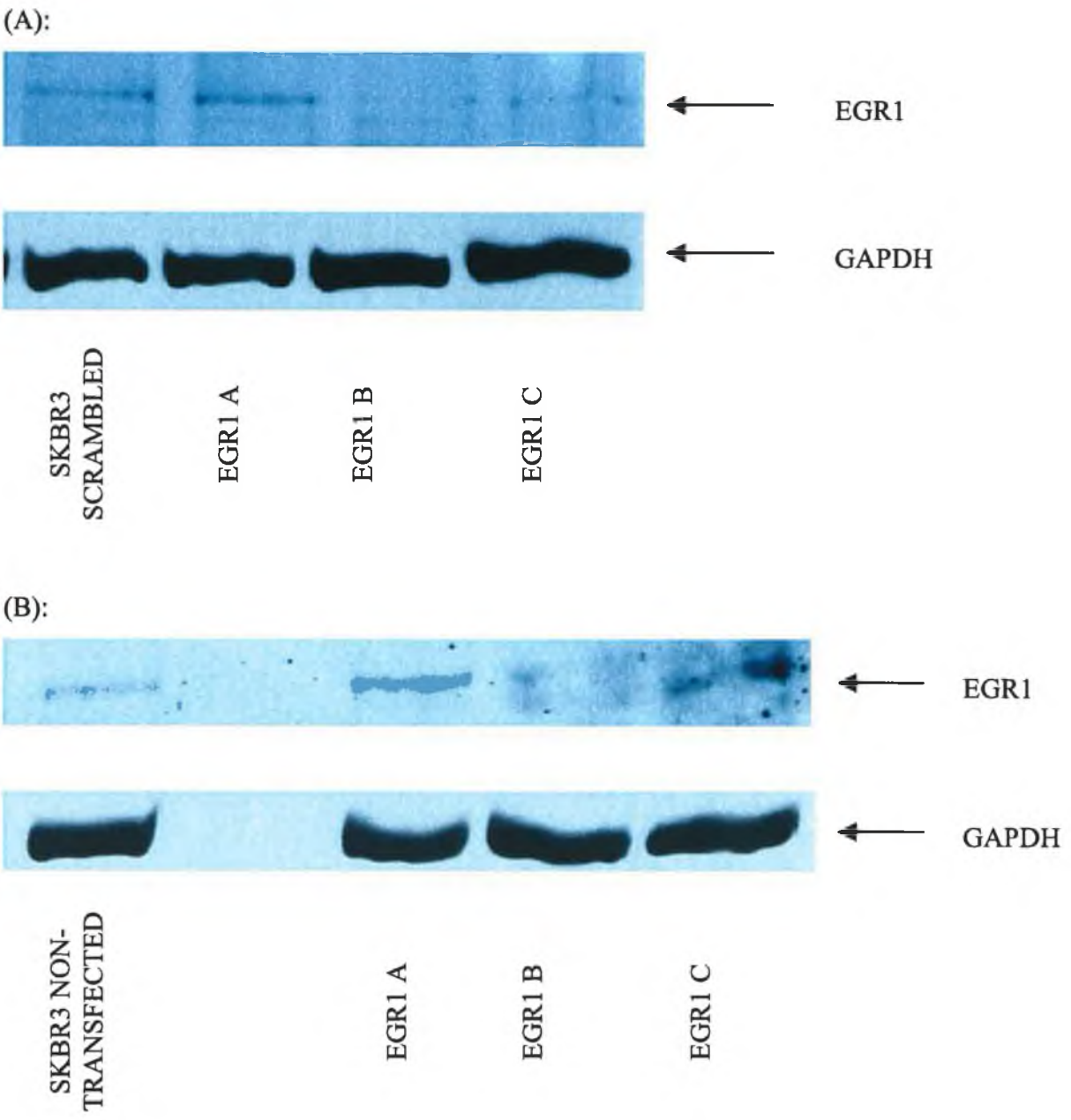

Figure 3.6.7: Western blot showing protein expression of EGR1 in SKBR3 NT, SKBR3 transfected with scrambled control, and SKBR3 transfected with EGR1 siRNA A, B & C.

Figure 3.6.8 Photographs of invasion assays for DLKP4E transfected with EGR1 siRNA

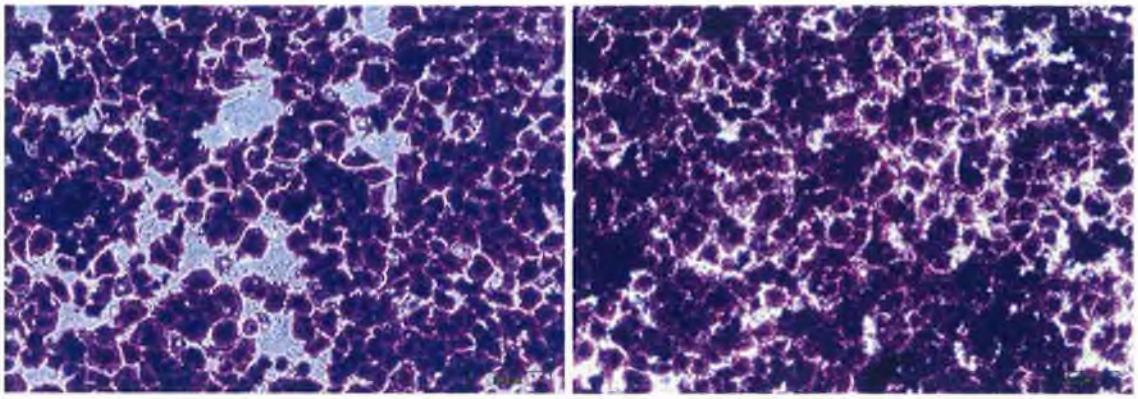

(A) DLKP4E NT

(B) DLKP4E SC

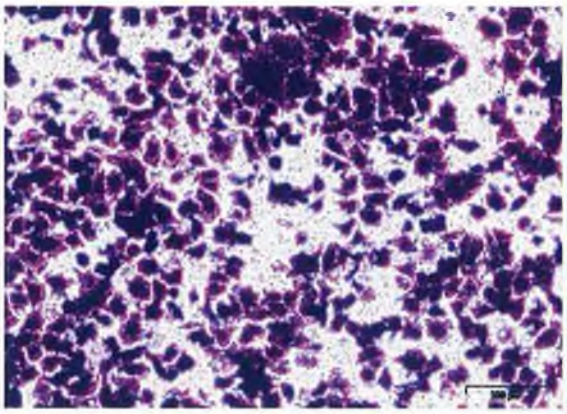

(C) EGR1 A

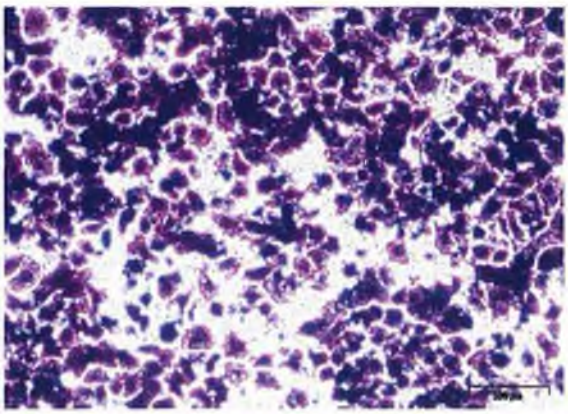

(D) EGR1 B

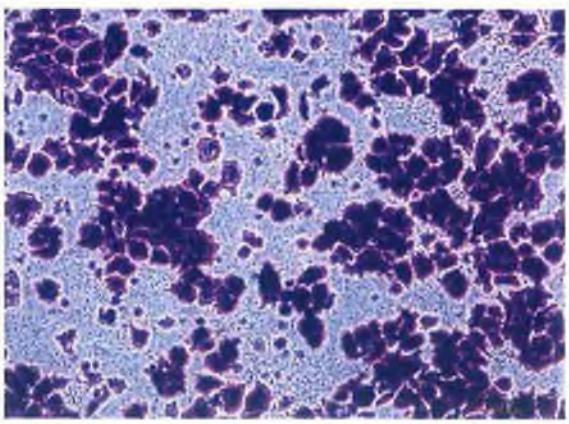

(E) EGR1 C

Figure 3.6.8: Photographs of invasion assay inserts at 10X magnification. A=DLKP4E NT, B=DLKP4E SC, C=DLKP4E transfected with EGR1 siRNA A, D=DLKP4E transfected with EGR1 siRNA B E=DLKP4E transfected with EGR1 siRNA C.

Figure 3.6.9 Cell counts of invasion assays for DLKP4E transfected with EGR1 siRNA

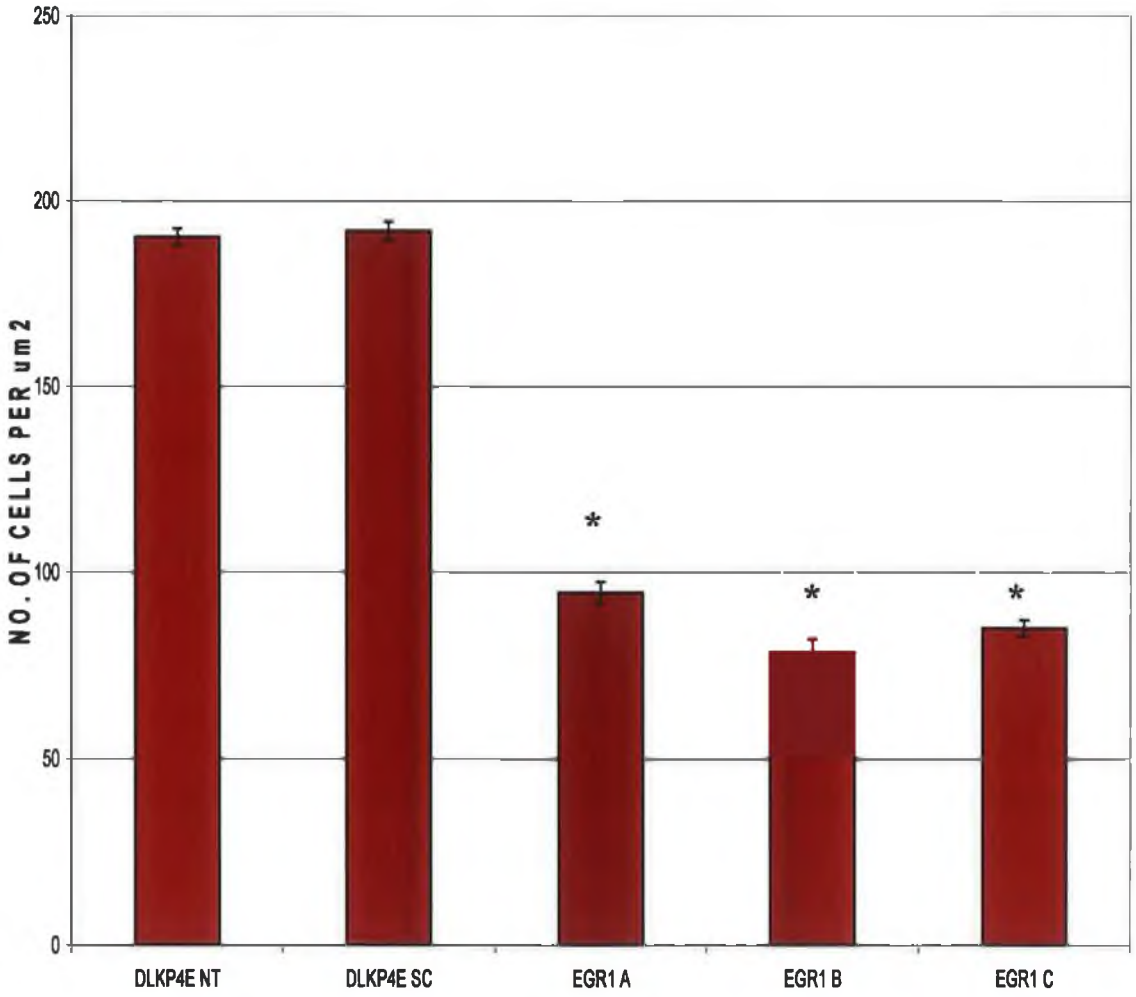

Figure 3.6.9: Number of invading cells detected per μm^2 of invasion assay insert for DLKP4E NT, DLKP4E SC and DLKP4E transfected with EGR1 siRNA A, B & C. n=3, *p-value<0.001.

Figure 3.6.10 Photographs of invasion assays for SKBR3 transfected with EGR1 siRNA

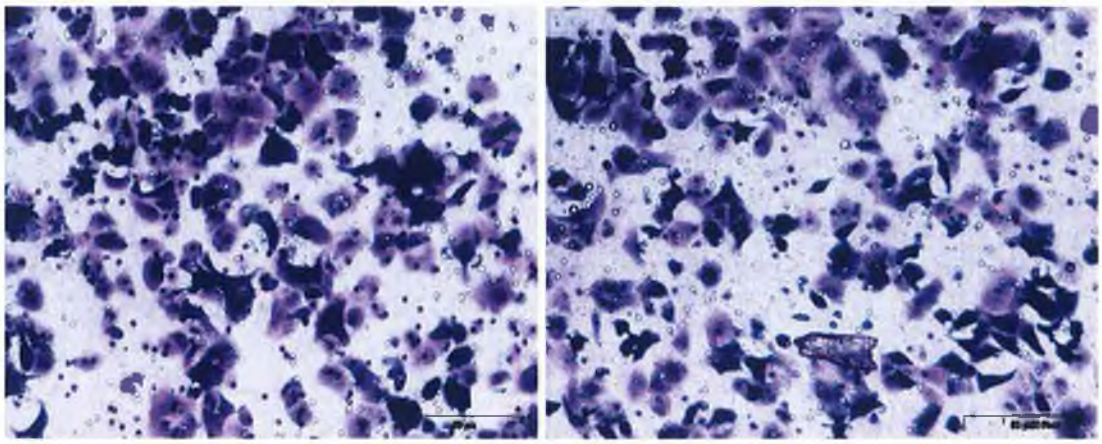

(A) SKBR3 NT (B) SKBR3 SC

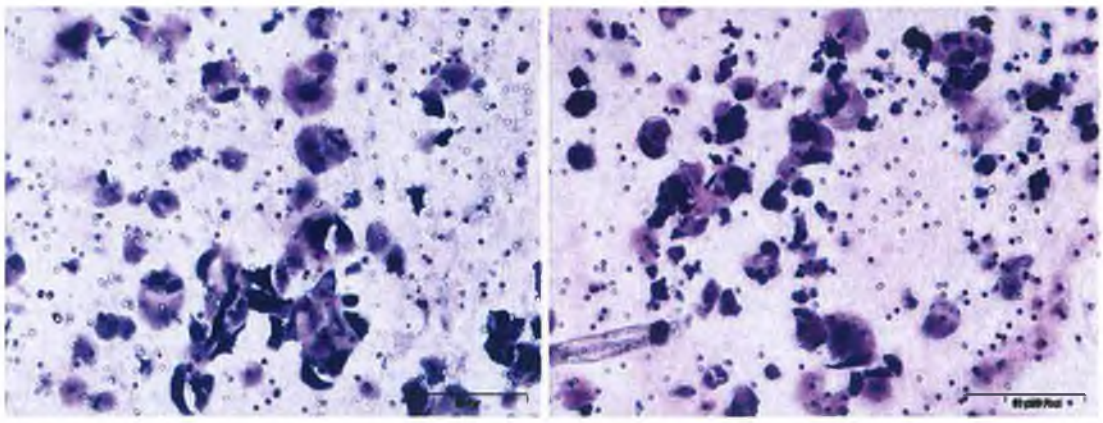

(C) EGR1 A (D) EGR1 B

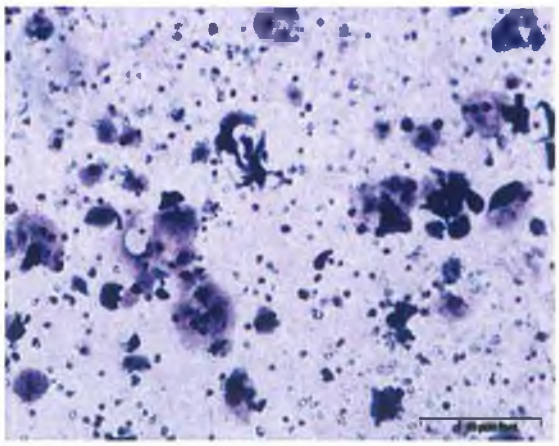

(E) EGR1 C

Figure 3.6.10: Photographs of invasion assay inserts at 10X magnification. A= SKBR3 NT, B=SKBR3 SC, C=SKBR3 transfected with EGR1 siRNA A, D=SKBR3 transfected with EGR1 siRNA B E=SKBR3 transfected with EGR1 siRNA C.

Figure 3.6.11 Cell counts of invasion assays for SKBR3 transfected with EGR1 siRNA

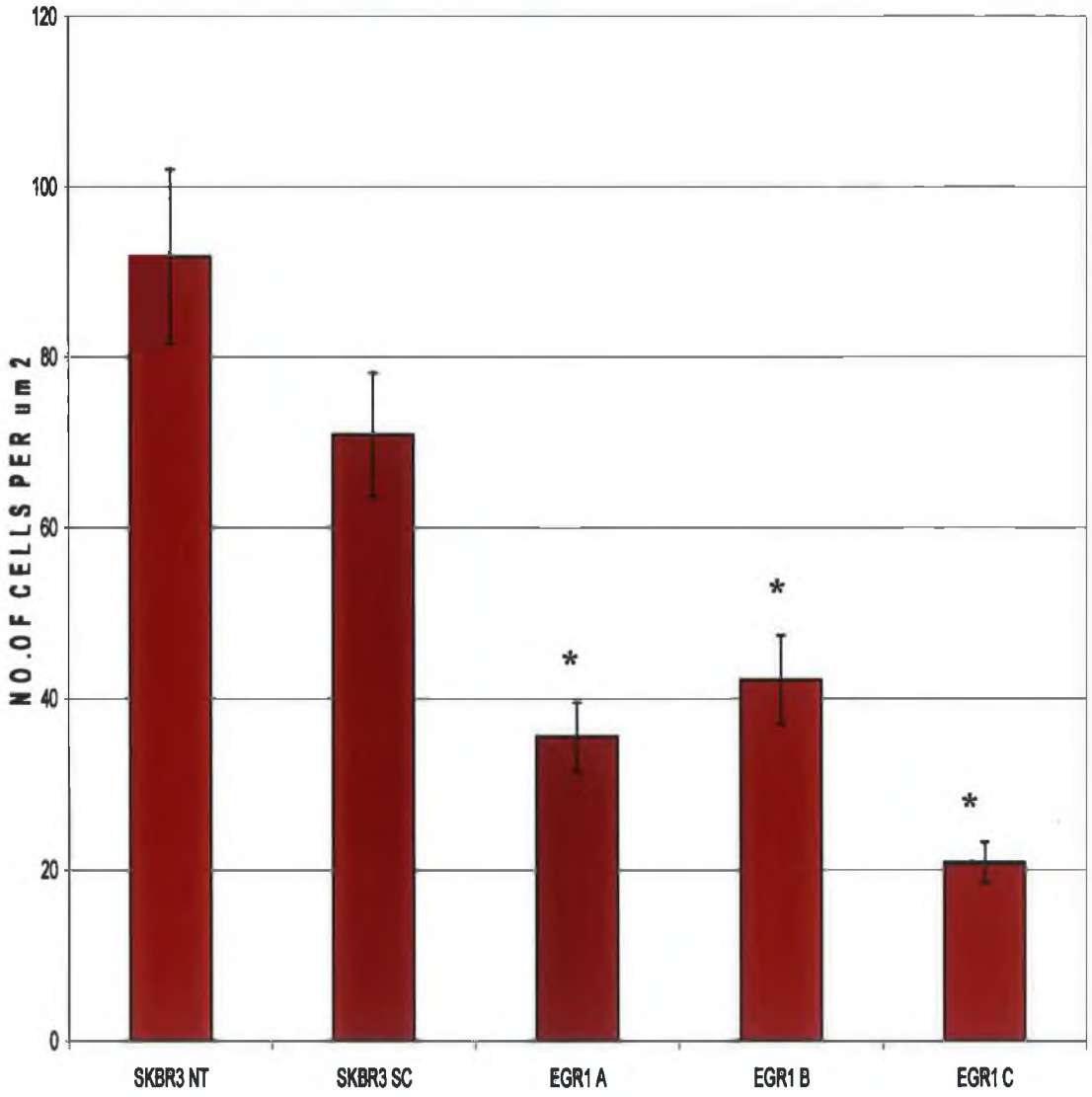

Figure 3.6.11: Number of invading cells detected per μm^2 of invasion assay insert for SKBR3 NT, SKBR3 SC and SKBR3 transfected with EGR1 siRNA A, B & C.
n=3, *p-value<0.001.

3.6.5 Summary of results for EGR1 siRNA transfection into DLKP4E

Proliferation assay results showed a successful transfection with little effect on DLKP4Es, and some increase in proliferation of SKBR3. Both mRNA and protein knock-down was observed for SKBR3, and although mRNA knock-down was not observed in DLKP4E, the decrease in EGR1 protein expression after siRNA transfection shows that the EGR1 siRNA was successful in reducing EGR1 in both cell lines. This is strengthened by the fact that invasion assay results showed a significant decrease in invading cells after EGR1 siRNA transfection in both cell lines. These results show that EGR1 siRNA was successful in silencing EGR1 mRNA and protein, and as a result reduced invasion (Table 3.6.1).

Table 3.6.1 Summary of results of EGR1 siRNA transfection into DLKP4E and SKBR3

	Real-time PCR – RNA knock-down			Western blot – protein knock-down			Invasion assay – decrease in invasion		
Cell Line	siRNA A	siRNA B	siRNA C	siRNA A	siRNA B	siRNA C	siRNA A	siRNA B	siRNA C
DLKP4E	—	—	+	+	+	+	+	+	+
SKBR3	+	+	+	—	+	+	+	+	+

Table 3.6.1: Summary of results of EGR1 siRNA A, B and C transfections into DLKP4E and SKBR3

3.7 Ribosomal protein S6 kinase, 90kDa, polypeptide 3 (RPS6KA3)

Analysis of microarray data found that RPS6KA3 was increased in both of the invasive cell lines, MCF7H3erbB2 and DLKP4E, compared to their non-invasive parent cell lines. A fold change increase of +2.36 was seen in MCF7H3erbB2, and +1.2 in DLKP4E. The array analysis suggested that an increase in RPS6KA3 contributed to an increase in invasion, therefore silencing this gene should reduce invasion. Because of this analysis it was decided to use RPS6KA3 as an siRNA target in the above cell lines to further assess its role in invasion. Only two siRNAs were used for all experiments, as both had been validated by the supplier.

3.7.1 Proliferation assays

Proliferation assays carried out on DLKP4E transfected with RPS6KA3 siRNA A and B appeared to have no effect on growth rate. SKBR3 again showed an increase in the rate of proliferation with siRNA-transfected cells growing up to 45% more than the scrambled control (Figure 3.7.1). A 50- to 60% reduction in proliferation of kinesin transfected cells confirmed a successful transfection (Figure 3.7.1).

3.7.2 Real-time PCR

Results showed no significant RPS6KA3 mRNA knock-down in the presence of RPS6KA3 siRNA A or B at 24 or 48hrs in DLKP4E. A 25% decrease in RPS6KA3 at 24hrs was the largest observed decrease (Figure 3.7.2). Real-time PCR was also used to detect GAPDH knock-down in these cells under the same conditions (figure 3.4.3), and therefore it is unlikely that this result was due to an unsuccessful transfection. The same siRNAs were used to transfect SKBR3 cells, and RPS6KA3 siRNA A also had no effect in this cell line at 24 or 48hrs. RPS6KA3 siRNA B however, did cause a 50% reduction in RPS6KA3 mRNA at 48hrs (Figure 3.7.3).

Figure 3.7.1 Proliferation assay for RPS6KA3 siRNA A & B in DLKP4E and SKBR3

(A):

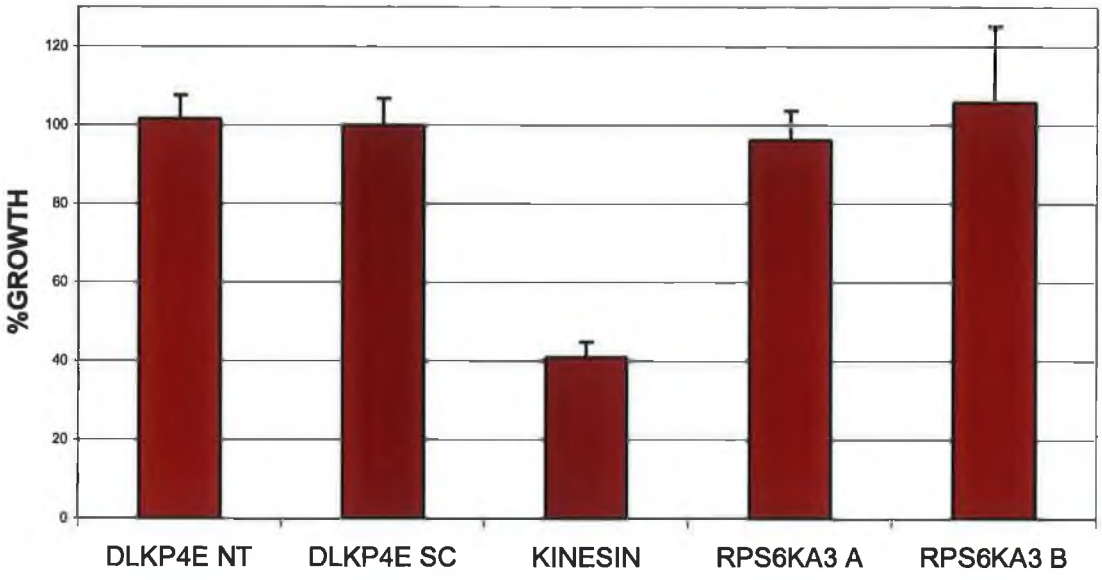

(B):

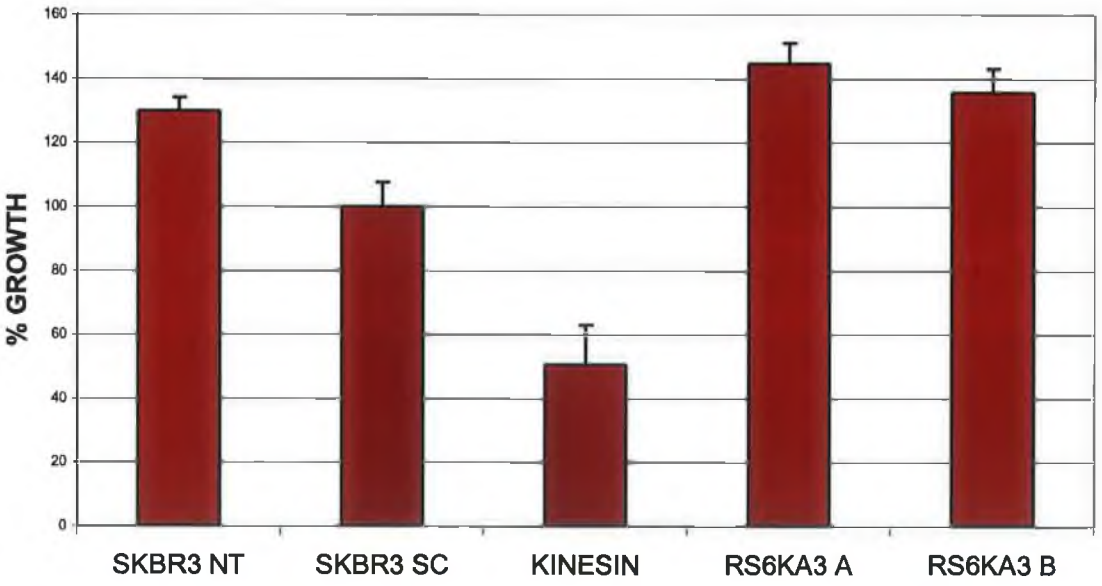

Figure 3.7.1: (A)Growth rate of DLKP4E NT, DLKP4E SC and DLKP4E transfected with RPS6KA3 siRNA A and B. (B) Growth rate of SKBR3 NT, SKBR3 SC and SKBR3 transfected with RPS6KA3 siRNA A and B.

Figure 3.7.2 Real-time PCR for RPS6KA3 siRNA A & B in DLKP4E at 24hrs & 48hrs

(A):

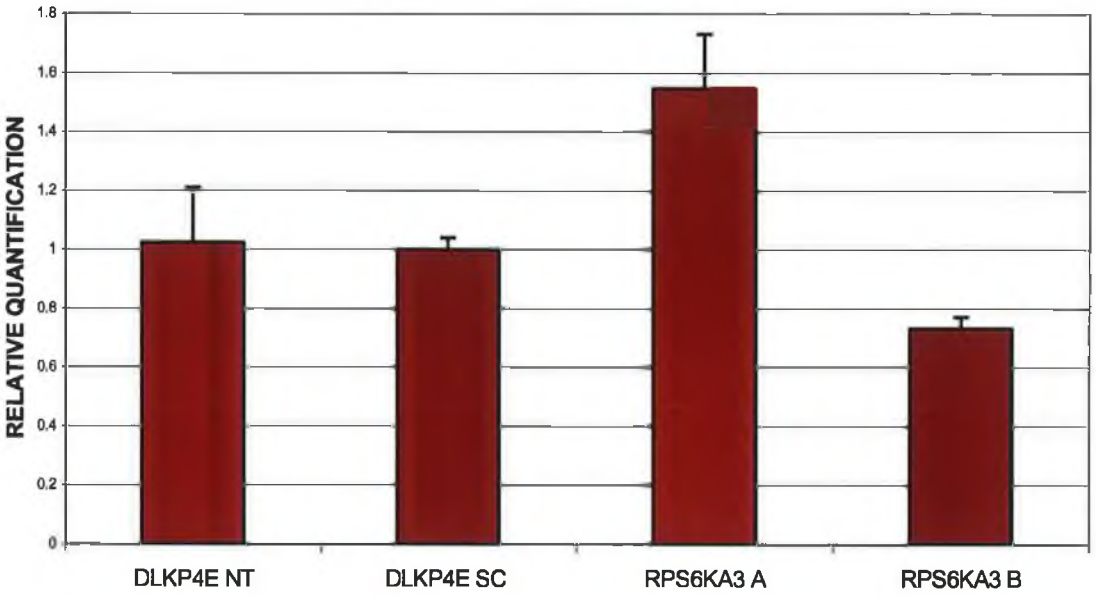

(B):

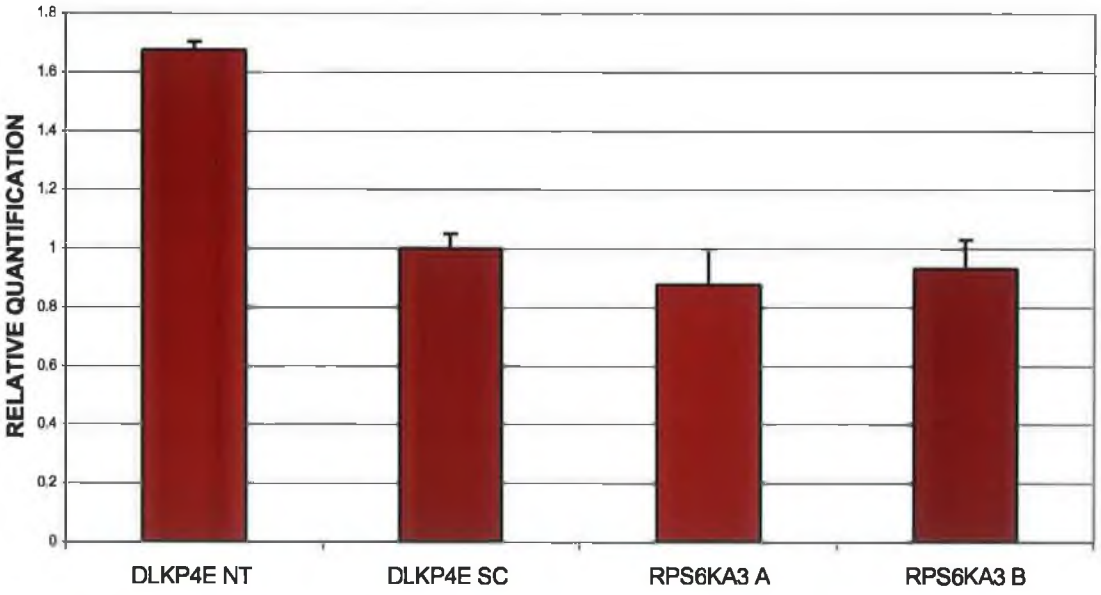

Figure 3.7.2: (A) Relative quantification of RPS6KA3 in non-transfected, scrambled, and RPS6KA3 siRNA A & B transfected DLKP4Es at 24hrs; (B) Relative quantification of RPS6KA3 in non-transfected, scrambled, and RPS6KA3 siRNA A & B transfected DLKP4Es at 48hrs.

Figure 3.7.3 Real-time PCR for RPS6KA3 siRNA A & B in SKBR3 at 24hrs & 48hrs

(A):

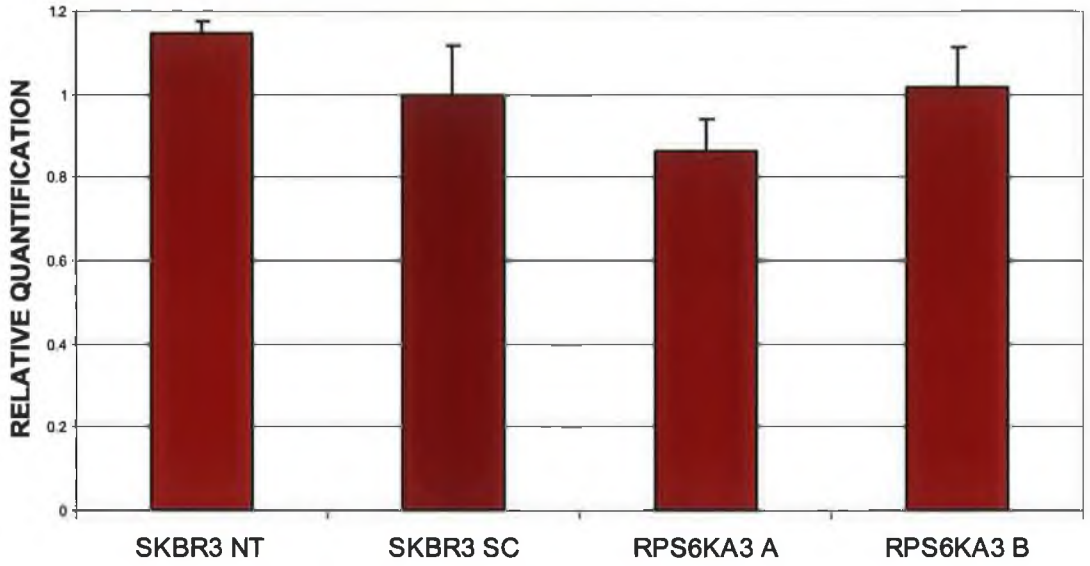

(B):

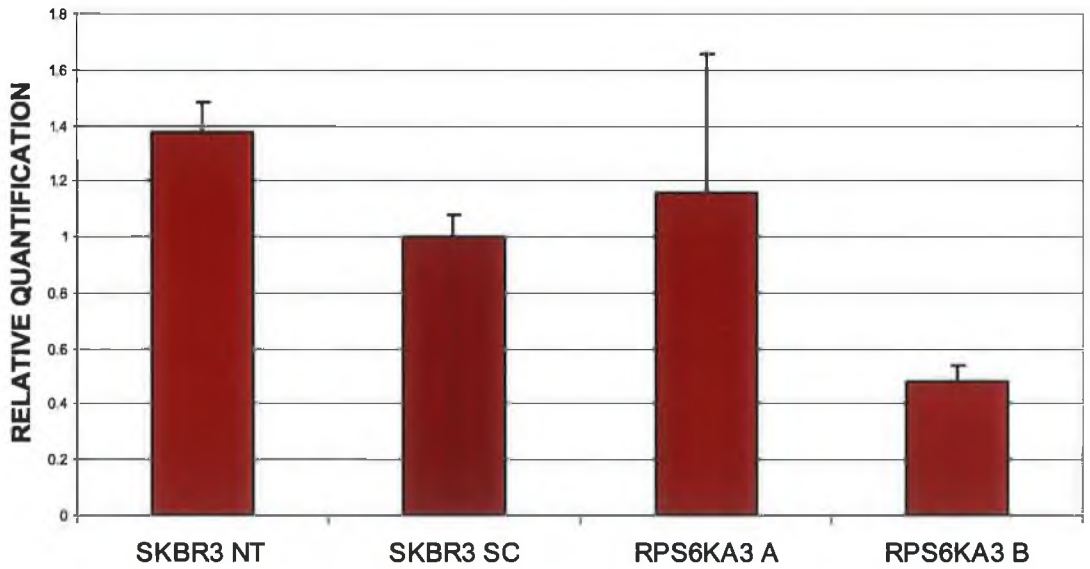

Figure 3.7.3: (A) Relative quantification of RPS6KA3 in non-transfected, scrambled, and RPS6KA3 siRNA A & B transfected SKBR3s at 24hrs; (B) Relative quantification of RPS6KA3 in non-transfected, scrambled, and RPS6KA3 siRNA A & B transfected SKBR3s at 48hrs.

3.7.3 Western blot

Western blots analysis (Section 2.4.1) was carried out using an RPS6KA3 specific antibody to detect if RPS6KA3 siRNA transfection had had an effect on RPS6KA3 protein levels. DLKP4E and SKBR3 transfected with RPS6KA3 siRNA A and B showed protein knock-down compared to the non-transfected and scrambled controls (Figure 3.7.4). Therefore, RPS6KA3 siRNA did succeed in knocking-down RPS6KA3 at a protein level, despite lack of evidence of RPS6KA3 mRNA knock-down.

3.7.4 Invasion assays

Results from invasion assays showed a considerable reduction in the number of invading cells after transfection with both RPS6KA3 siRNAs A and B. Both photographic evidence and cell counts show that the number of invading cells was reduced by at least 50% after RPS6KA3 siRNA transfection (Figure 3.7.5 and 3.7.6). SKBR3 also had a dramatic reduction in invading cells after RPS6KA3 siRNA transfection, again with greater than 50% fewer invading cells (Figure 3.7.8 and 3.7.9). These results show that transfection of RPS6KA3 siRNA caused a decrease in invasion in both cell lines.

Figure 3.7.4 Western blot analysis of RPS6KA3 protein expression in DLKP4E

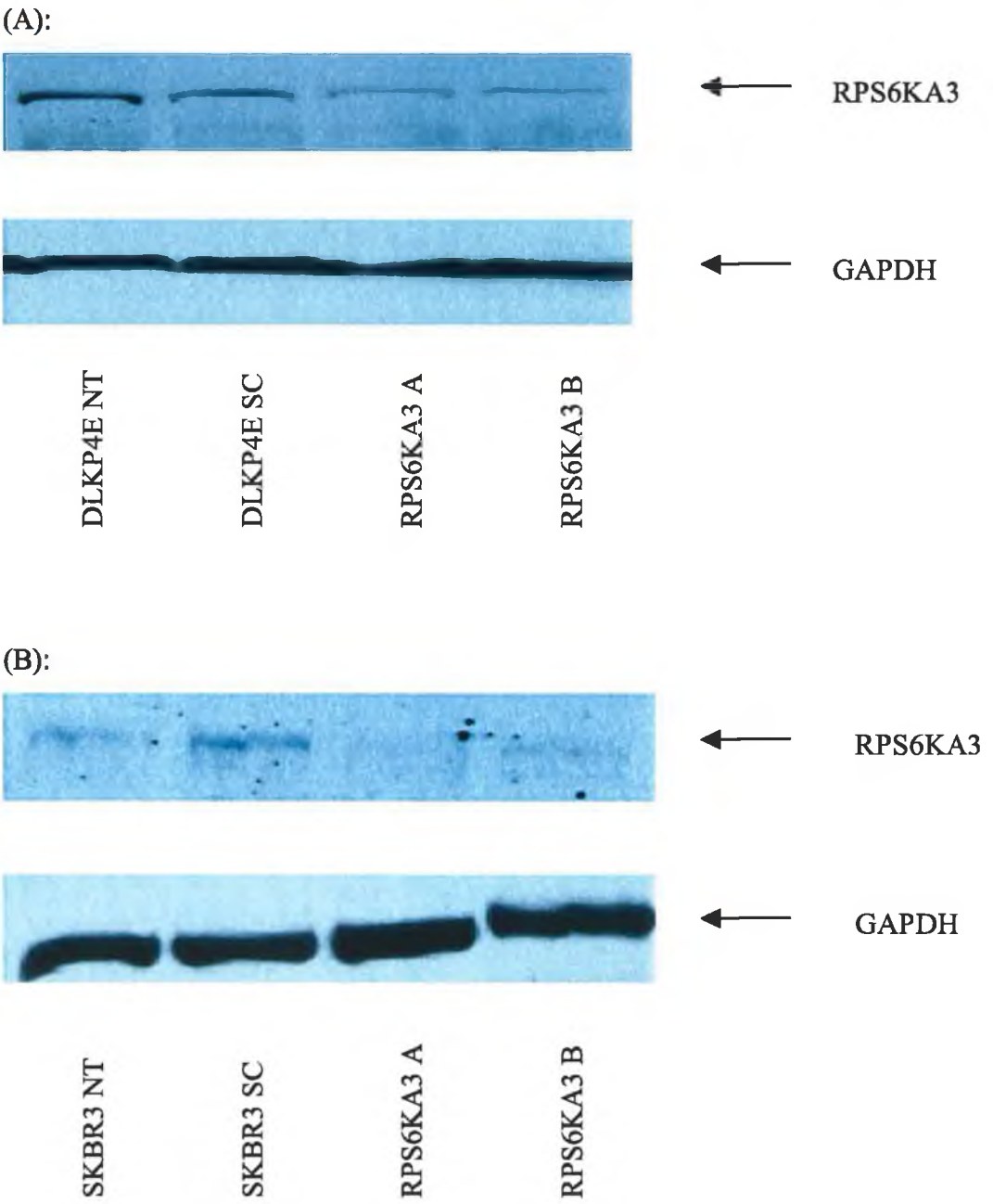

Figure 3.7.4: (A) Western blot showing protein expression of RPS6KA3 in DLKP4E NT, DLKP4E SC, and DLKP4E transfected with RPS6KA3 siRNA A & B; (B) Western blot showing protein expression of RPS6KA3 in SKBR3 NT, SKBR3 SC, and SKBR3 transfected with RPS6KA3 siRNA A & B.

Figure 3.7.5 Photographs of invasion assays for DLKP4E transfected with RPS6KA3 siRNA

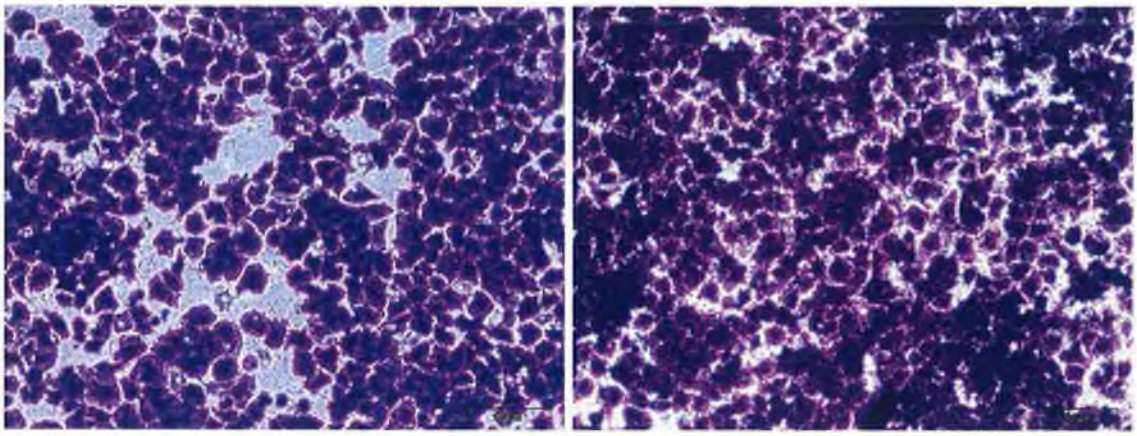

(A) DLKP4E NT (B) DLKP4E SC

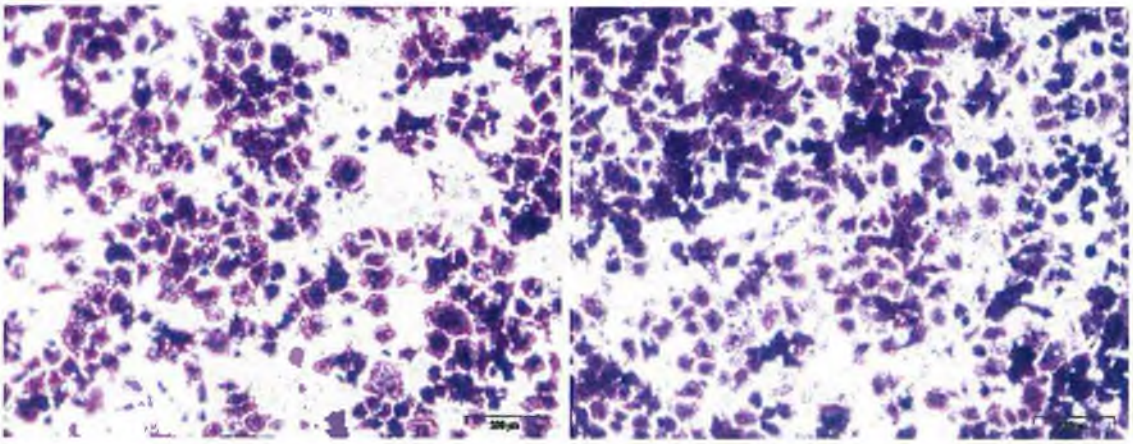

(C) RPS6KA3 A (D) RPS6KA3 B

Figure 3.7.5: Photographs of invasion assay inserts at 10X magnification. A=DLKP4E NT, B=DLKP4E SC, C=DLKP4E transfected with RPS6KA3 siRNA A, D=DLKP4E transfected with RPS6KA3 siRNA B.

Figure 3.7.6 Cell counts of invasion assays for DLKP4E transfected with RPS6KA3 siRNA

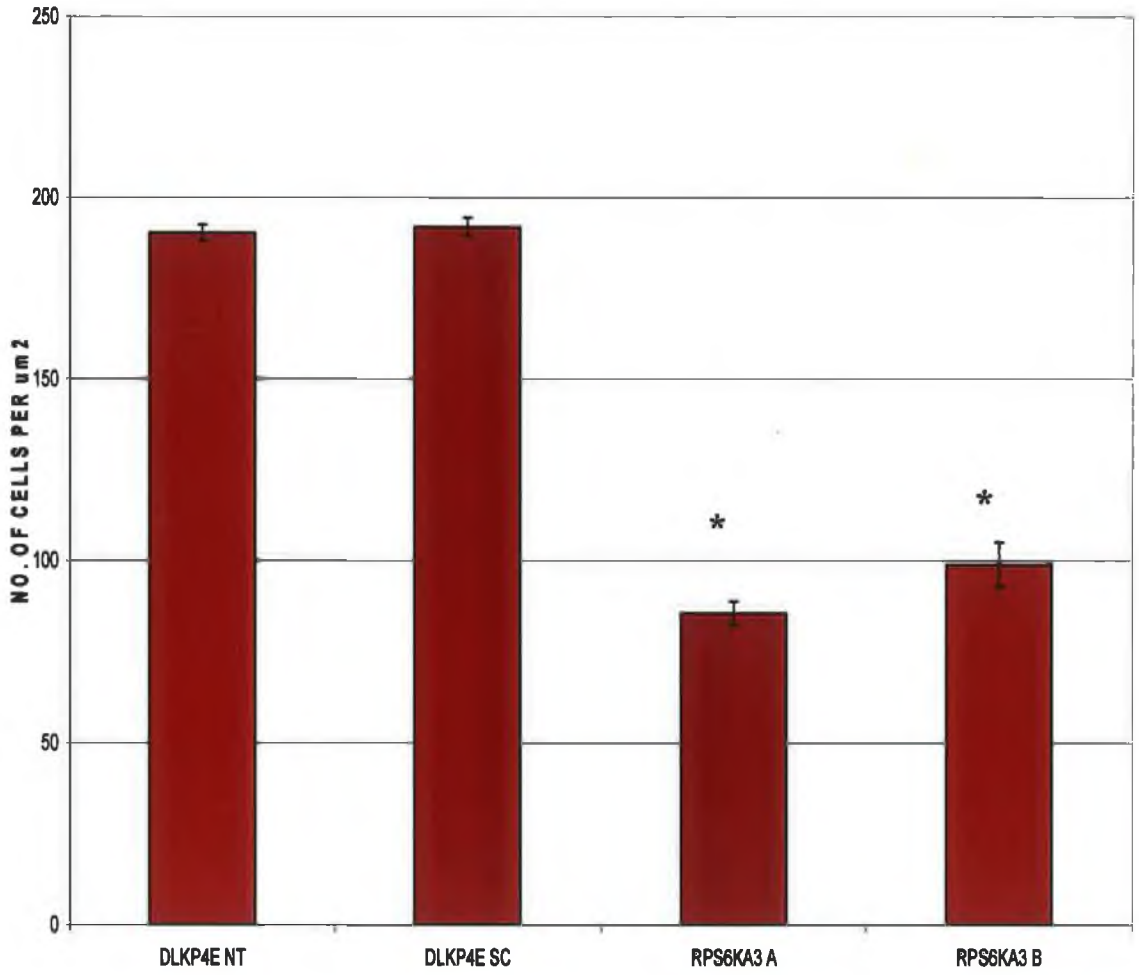

Figure 3.7.6: Number of invading cells detected per μm^2 of invasion assay insert for DLKP4E NT, DLKP4E SC and DLKP4E transfected with RPS6KA3 siRNA A & B. n=3, *p-value<0.001.

Figure 3.7.7 Photographs of invasion assays for SKBR3 transfected with RPS6KA3 siRNA

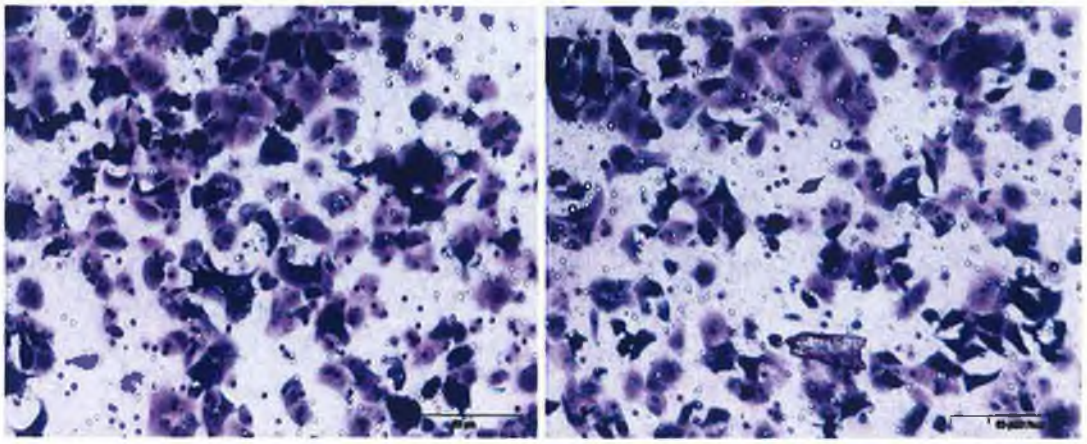

(A) SKBR3 NT

(B) SKBR3 SC

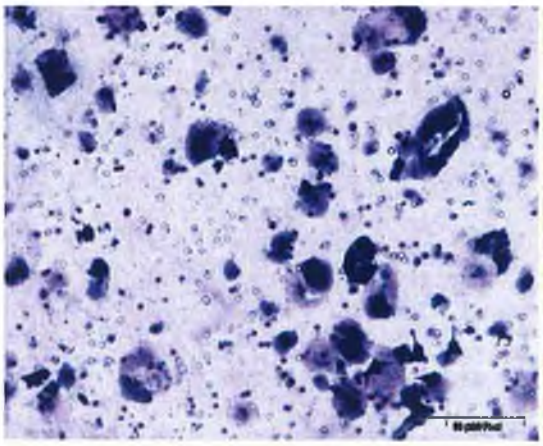

(C) RPS6KA3 A

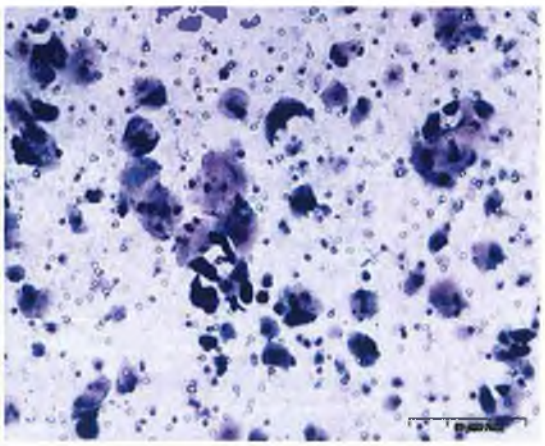

(D) RPS6KA3 B

Figure 3.7.7: Photographs of invasion assay inserts at 10X magnification. A=SKBR3 NT, B=SKBR3 SC, C=SKBR3 transfected with RPS6KA3 siRNA A, D=SKBR3 transfected with RPS6KA3 siRNA B.

Figure 3.7.8 Cell counts of invasion assays for SKBR3 transfected with RPS6KA3 siRNA

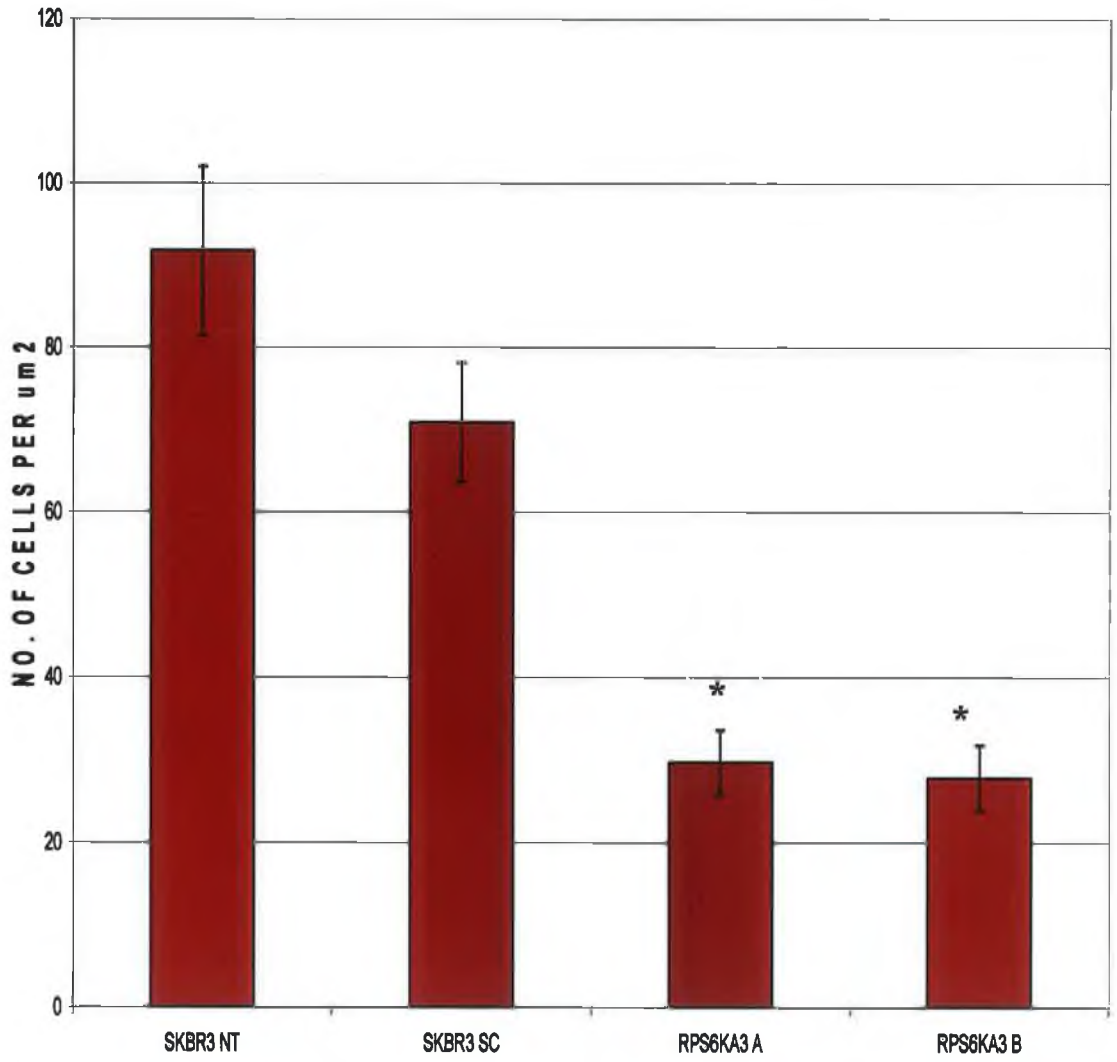

Figure 3.7.8: Number of invading cells detected per μm^2 of invasion assay insert for SKBR3 NT, SKBR3 SC and SKBR3 transfected with RPS6KA3 siRNA A & B.
n=3, *p-value<0.001.

3.7.5 Summary of results for RPS6KA3 siRNA transfection into DLKP4E

Proliferation assay results showed a successful transfection in both cell lines, with insignificant changes in growth of DLKP4E but 30- 40% increased growth in SKBR3. Real-time PCR was used to detect if the siRNA transfection was successful in silencing its target mRNA. mRNA knock-down was not observed at mRNA level for DLKP4E, but western blot showed protein knock-down after siRNA transfection. This confirmed RPS6KA3 siRNA was successful in reducing RPS6KA3 at a protein level within DLKP4E cells. In SKBR3, RPS6KA3 siRNA B reduced levels of RPS6KA3 mRNA after 48hrs, and western blot showed protein knock-down after transfection of both siRNAs. Invasion assay results reinforced this by showing a significant decrease in invading cells after RPS6KA3 siRNA transfection in both cell lines (Table 3.7.1). Proof of knock-down of RPS6KA3 at a protein level, combined with a decrease in invasion after siRNA transfection, validates array analysis which implicated a role for RPS6KA3 in the invasion process.

Table 3.7.1 Summary of results of RPS6KA3 siRNA transfection into DLKP4E and SKBR3

	Real-time PCR – mRNA knock-down		Western blot – protein knock-down		Invasion assay – decrease in invasion	
Cell Line	siRNA A	siRNA B	siRNA A	siRNA B	siRNA A	siRNA B
DLKP4E	—	—	+	+	+	+
SKBR3	—	+	+	+	+	+

Table 3.7.1: Summary of results of RPS6KA3 siRNA A, B and C transfections into DLKP4E and SKBR3

3.8 Tumour necrosis factor, alpha induced protein 8 (TNFAIP8)

TNFAIP8 was one of the siRNA targets chosen after array analysis of invasive MCF7H3erbB2. Comparison of non-invasive parent MCF7H3 to invasive MCF7H3erbB2 found there to be a +2.47 fold increase in TNFAIP8. No change in expression was seen in DLKP4E or DLKP4Emut. Unlike the other siRNA targets, TNFAIP8 was examined only using proliferation and invasion assays, as an antibody was not commercially available due to the novelity of the target. Real-time PCR was attempted but was unsuccessful. The Taqman® Real time PCR analysis was preformed using the Applied Bio Systems Assays on Demand PCR Kits, using primer probe pairs as outlined in Table 2.4.3. The TNFAIP8 primers provided were suitable to detect the same region of TNFAIP8 as detected by Affymetrics probes, and so it is unclear why this procedure did not work.

3.8.1 Proliferation assays

Proliferation assays showed little change in growth rate after TNFAIP8 siRNA transfection into DLKP4E (Figure 3.8.1). TNFAIP8 siRNA transfection into SKBR3 resulted in a 40% increase in growth.

3.8.2 Invasion assays

Both the photographs of the invasion inserts and the cell counts show a considerable decline in the number of invading cells in DLKP4E (Figure 3.8.2 and 3.8.3). DLKP4E cells transfected with TNFAIP8 siRNA A and B were 60%, and C 50% less invasive than DLKP4E transfected with a scrambled control. Results for SKBR3 siRNA A and B were less impressive, with cell counts showing a 20% to 30% reduction in invasive cells. TNFAIP8 C, with a 65% drop in the number of invading cells, was the most considerable change in SKBR3 cells (Figure 3.8.4 and 3.8.5).

Figure 3.8.1 Proliferation assay for TNFAIP8 siRNA A & B in DLKP4E and SKBR3

(A):

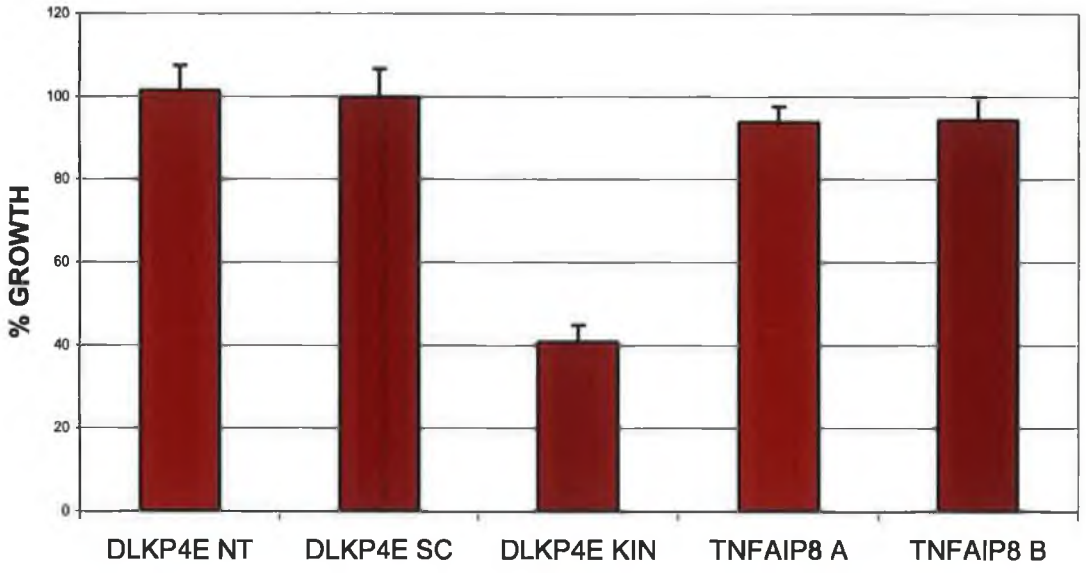

(B):

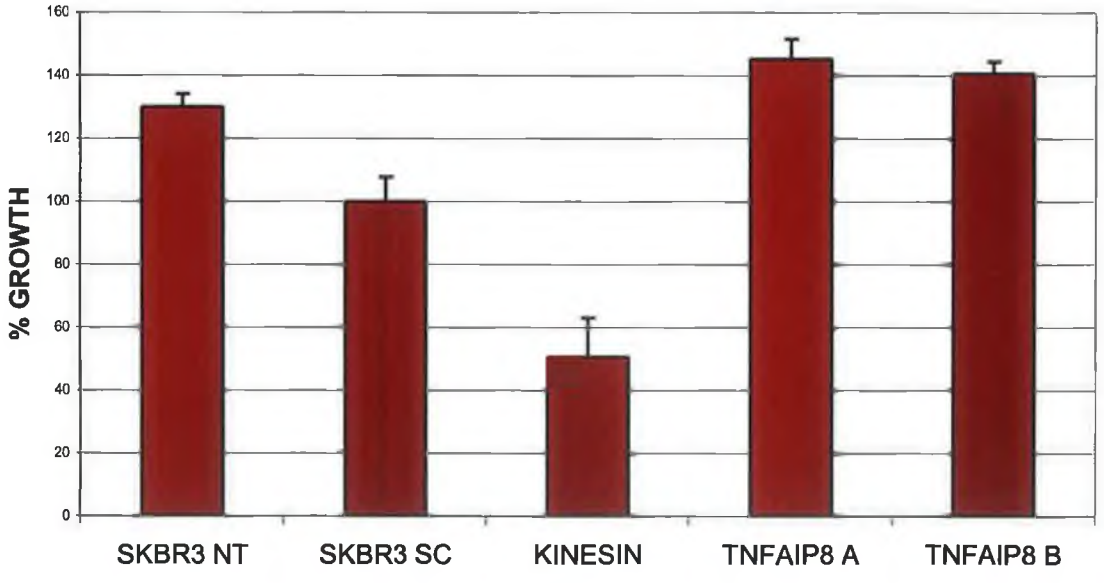

Figure 3.8.1: (A) Growth rate of DLKP4E NT, DLKP4E SC and DLKP4E transfected with TNFAIP8 siRNA A and B. (B) Growth rate of SKBR3 NT, SKBR3 SC and SKBR3 transfected with TNFAIP8 siRNA A and B.

Figure 3.8.2 Photographs of invasion assays for DLKP4E transfected with TNFAIP8 siRNA

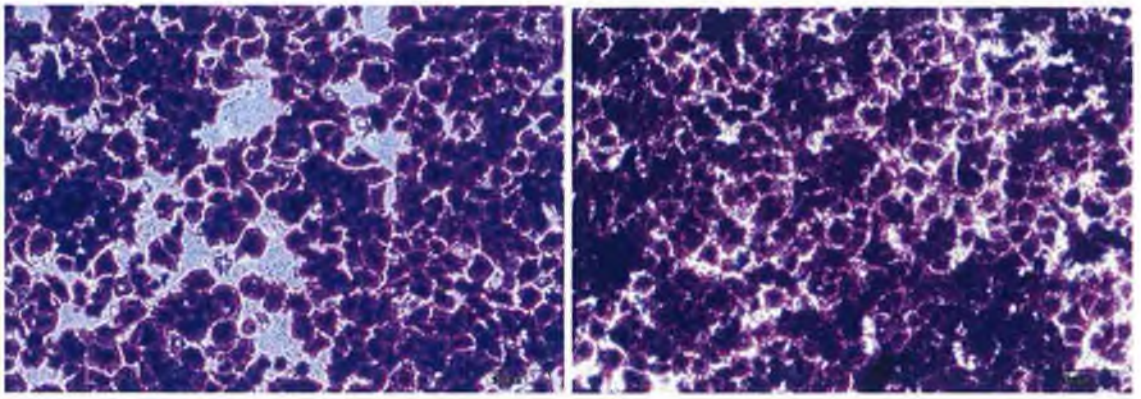

(A) DLKP4E NT

(B) DLKP4E SC

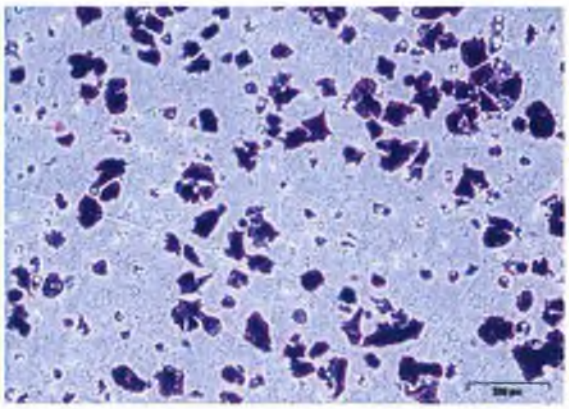

(C) TNFAIP A

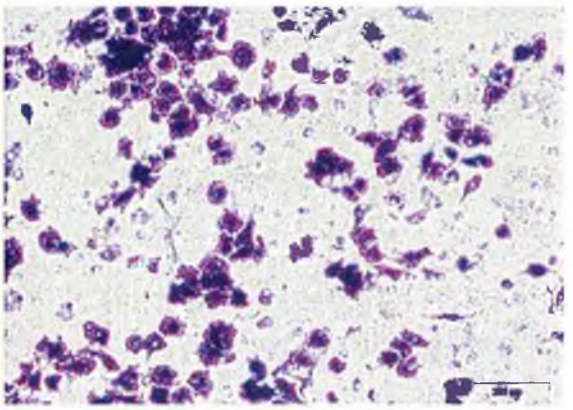

(D) TNFAIP8 B

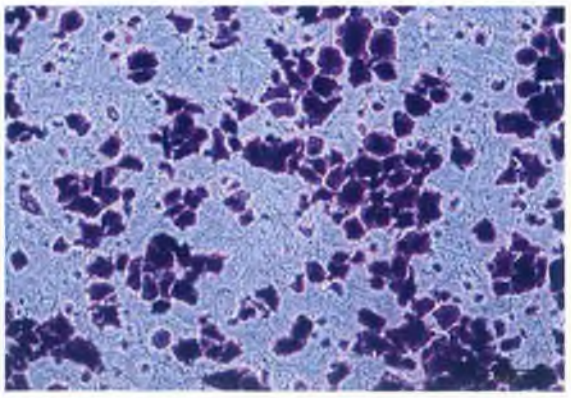

(E) TNFAIP8 C

Figure 3.8.2: Photographs of invasion assay inserts at 10X magnification. A=DLKP4E NT, B=DLKP4E SC, C=DLKP4E transfected with TNFAIP8 siRNA A, D=DLKP4E transfected with TNFAIP8 siRNA B and E=DLKP4E transfected with TNFAIP8 siRNA C.

Figure 3.8.3 Cell counts of invasion assays for DLKP4E transfected with TNFAIP siRNA

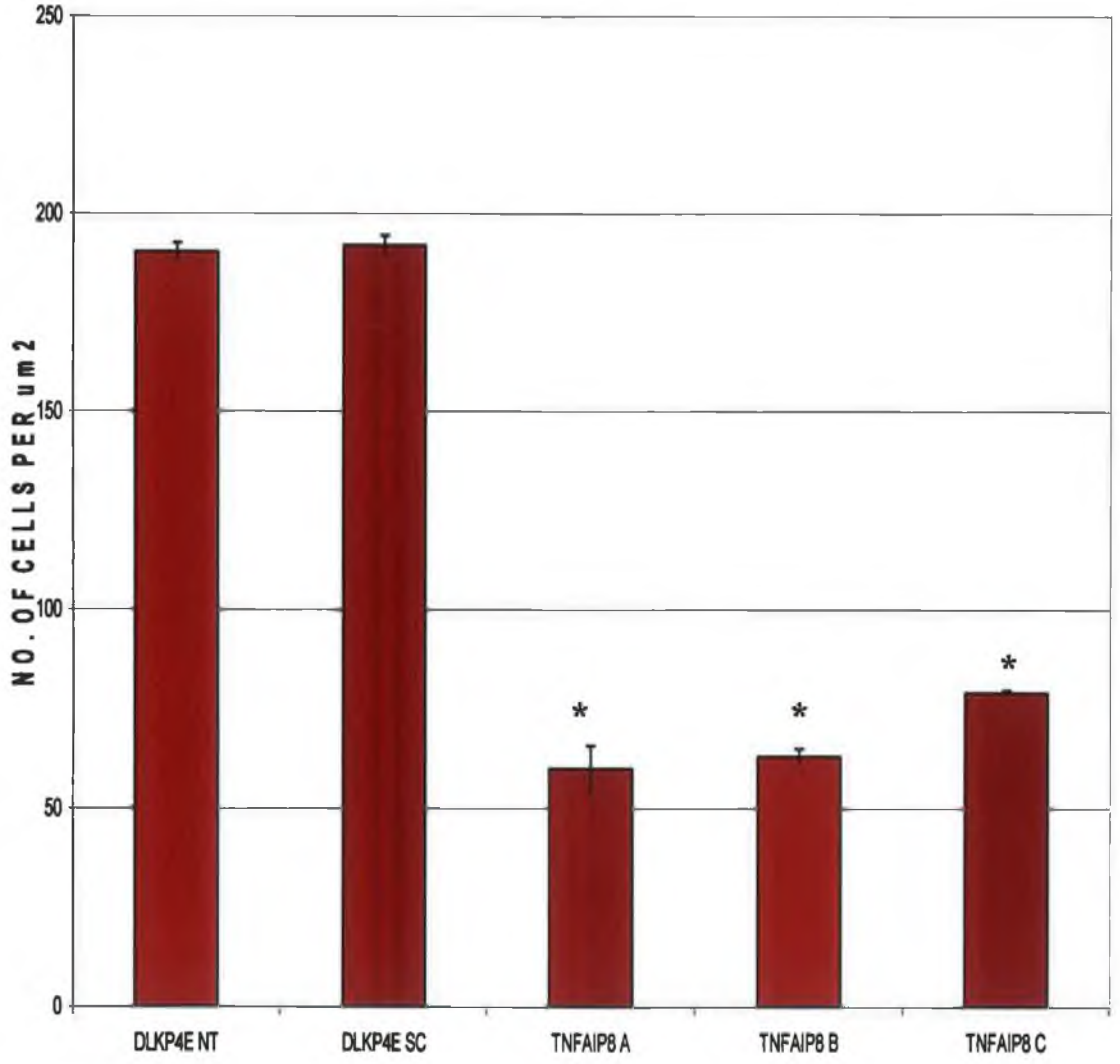

Figure 3.8.3: Number of invading cells detected per μm^2 of invasion assay insert for DLKP4E NT, DLKP4E SC and DLKP4E transfected with TNFAIP siRNA A, B & C. n=3, *p-value<0.001.

Figure 3.8.4 Photographs of invasion assays for SKBR3 transfected with TNFAIP8 siRNA

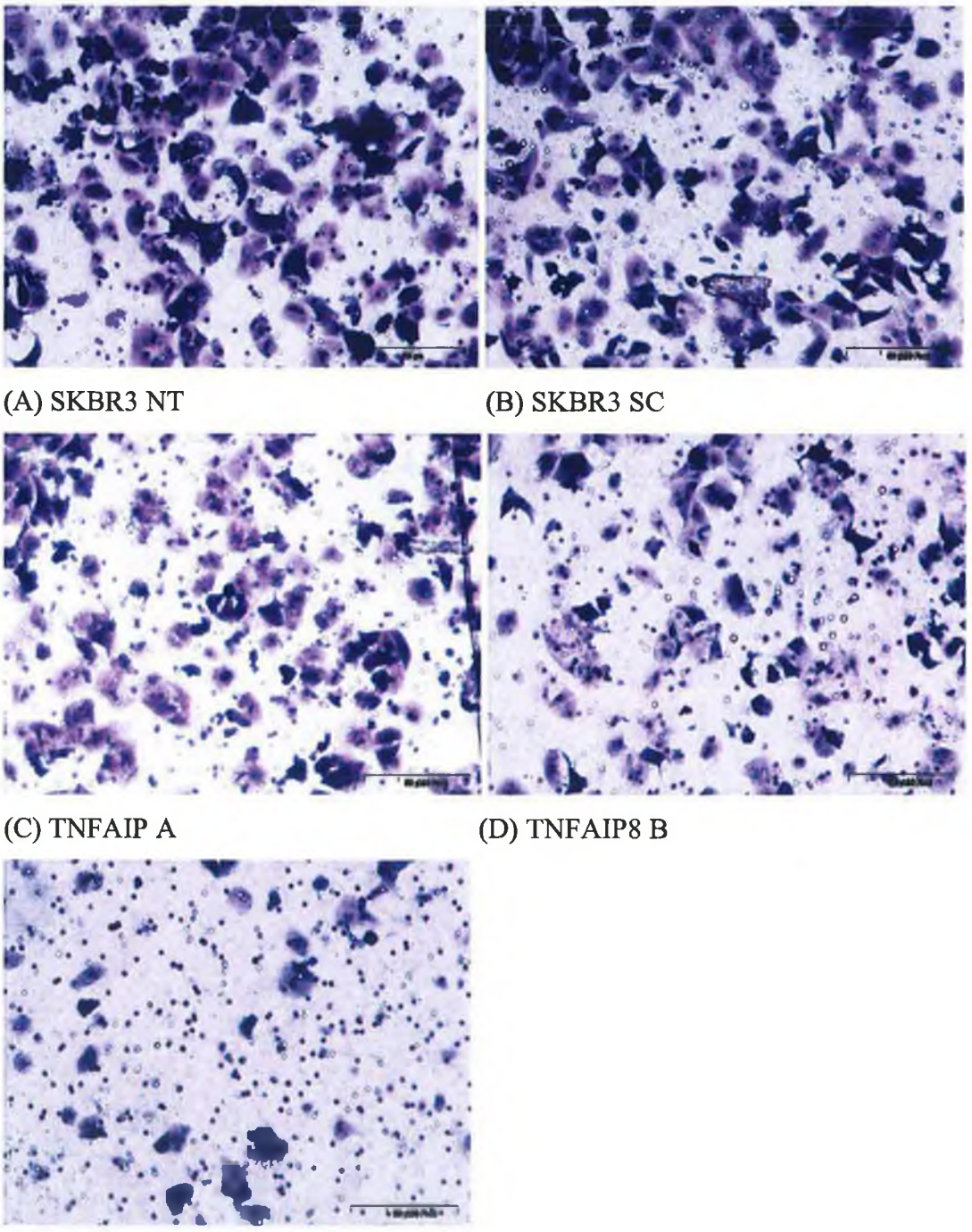

(A) SKBR3 NT (B) SKBR3 SC

(C) TNFAIP A (D) TNFAIP8 B

(E) TNFAIP8 C

Figure 3.8.4: Photographs of invasion assay inserts at 10X magnification. A=SKBR3 NT, B=SKBR3 SC, C=SKBR3 transfected with TNFAIP8 siRNA A, D=SKBR3 transfected with TNFAIP8 siRNA B and E= SKBR3 transfected with TNFAIP8 siRNA C.

Figure 3.8.5 Cell counts of invasion assays for SKBR3 transfected with TNFAIP8 siRNA

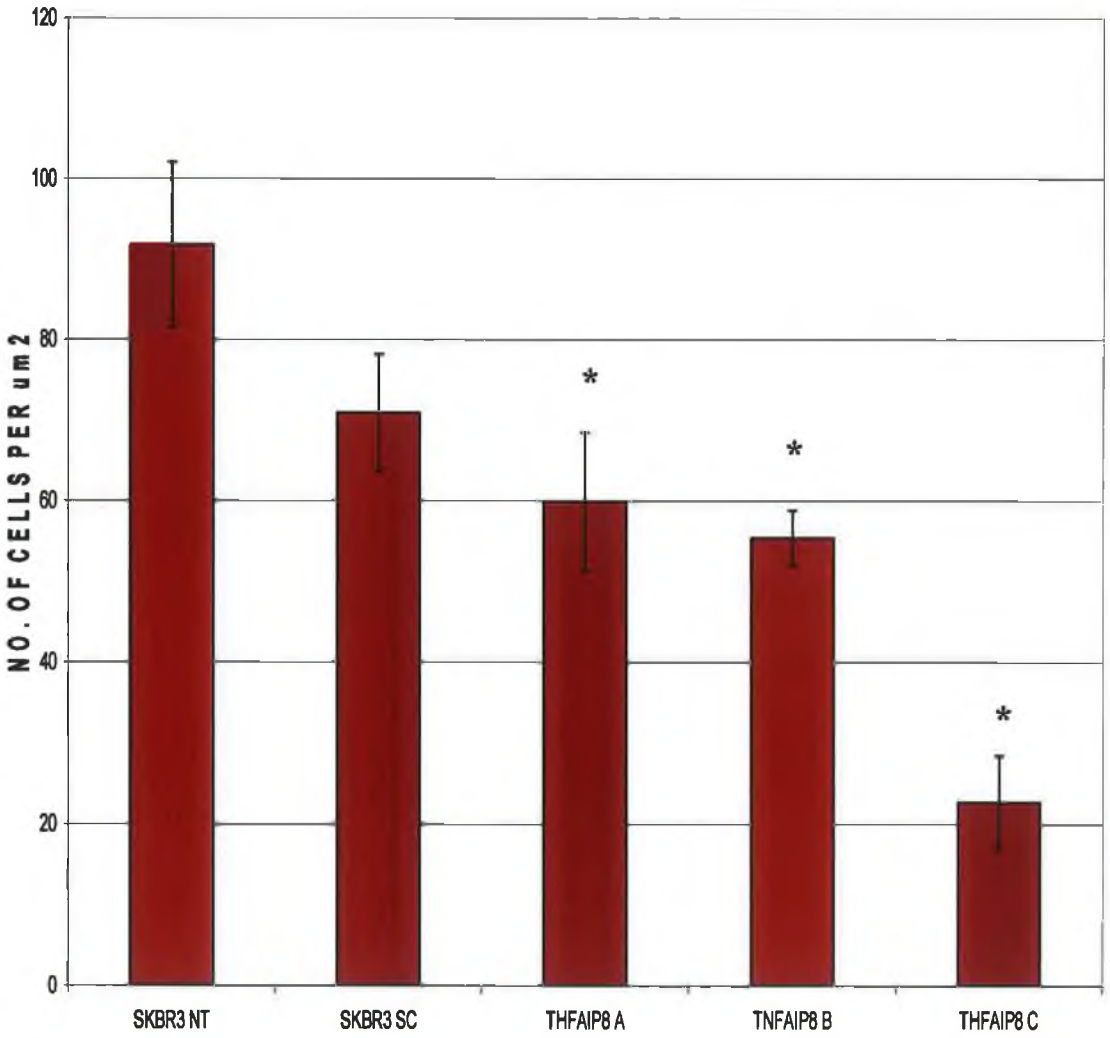

Figure 3.8.5: Number of invading cells detected per μm^2 of invasion assay insert for SKBR3 NT, SKBR3 SC and SKBR3 transfected with TNFAIP8 siRNA A, B & C. N=3, *p-value<0.001.

3.8.3 Summary of results

Array analysis linked up-regulation of TNFAIP8 to invasion, and therefore it proposed that siRNA silencing of this gene would cause a decrease in invasion. Although there was no evidence at either mRNA or protein levels that TNFAIP8 siRNA was working in silencing TNFAIP8, transfection with three different TNFAIP8 siRNAs into DLKP4E resulted in a marked decrease in invasion, and one of the siRNAs also caused a decrease in invasion in SKBR3 (Table 3.8.1). This result demonstrated that transfection of DLKP4E and SKBR3 with TNFAIP8 siRNA reduces invasion, and strongly suggests that the siRNAs are functioning in silencing TNFAIP8.

Table 3.8.1 Summary of results of TNFAIP8 siRNA transfection into DLKP4E and SKBR3

	Real-time PCR – mRNA knock-down			Western blot – protein knock-down			Invasion assay – decrease in invasion		
Cell Line	siRNA A	siRNA B	siRNA C	siRNA A	siRNA B	siRNA C	siRNA A	siRNA B	siRNA C
DLKP4E	—*	—*	—*	—*	—*	—*	+	+	+
SKBR3	—*	—*	—*	—*	—*	—*	—	—	+

Table 3.8.1: Summary of results of TNFAIP8 siRNA A, B and C transfections into DLKP4E and SKBR3

* Real-time PCR primer-probe set did not detect TNFAIP8 and no antibody was available for the TNFAIP8 protein.

3.9 Thrombospondin (THBS1)

THBS1 was chosen as a siRNA target based on microarray analysis of MCF7H3erbB2, an invasive breast cancer cell line. Unlike the other targets chosen from this analysis, THBS1 expression was down-regulated in an invasive cell line (-2.3 fold). Therefore a reduction of THBS1 in a non-invasive cell line would be expected to cause invasion. For this reason MCF7 (non-invasive) and DLKP (mildly invasive) were selected for transfection with THBS1 siRNAs. DLKP4E and SKBR3, which had been used with all other siRNA targets from this analysis, were also included.

3.9.1 Proliferation assays

Results of proliferation assays from MCF7, DLKP and DLKP4E showed very minor changes in growth when transfected with the THBS1 siRNAs. SKBR3 showed a more marked increase in proliferation, with THBS1 siRNA-transfected cells growing up to 35% more than the scrambled control (Figure 3.9.1 and 3.9.2).

Figure 3.9.1 Proliferation assay for THBS1 siRNA A & B in DLKP and MCF7

(A):

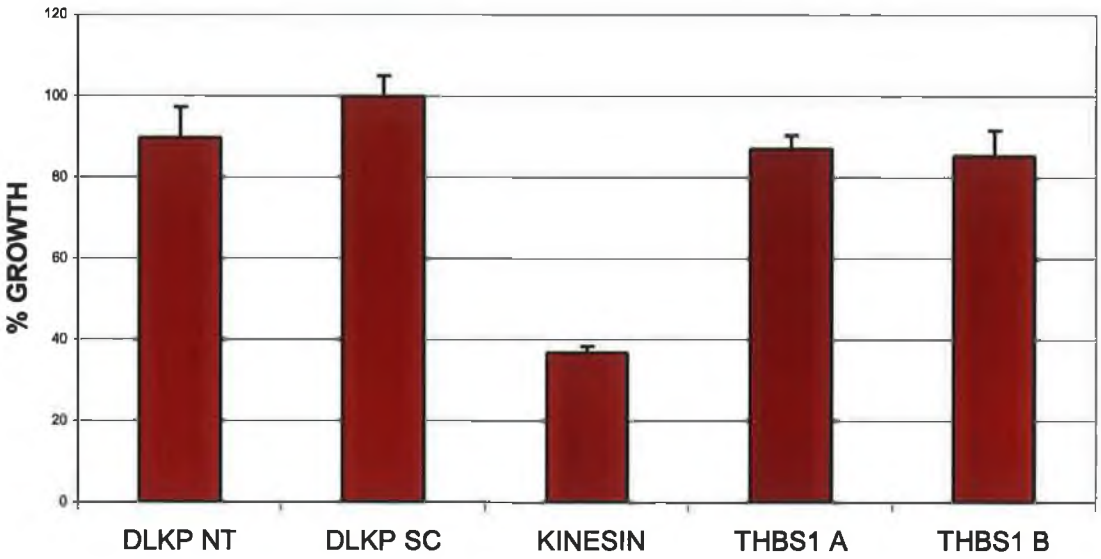

(B):

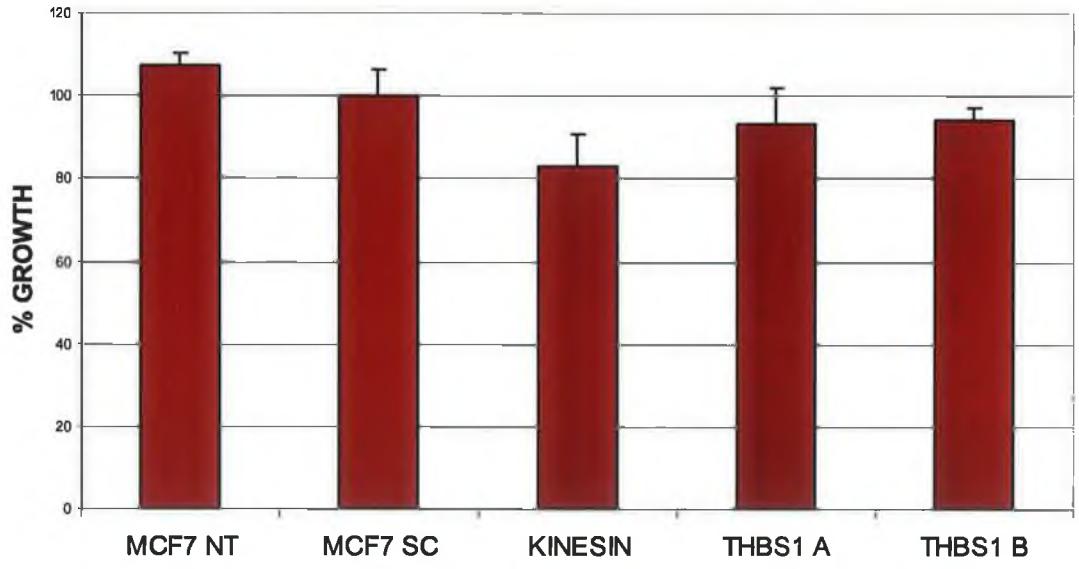

Figure 3.9.1: (A) Growth rate of DLKP NT, DLKP SC and DLKP transfected with THBS1 siRNA A and B. (B) Growth rate of MCF7 NT, MCF7 SC and MCF7 transfected with THBS1 siRNA A and B.

Figure 3.9.2 Proliferation assay for THBS1 siRNA A & B in DLKP4E and SKBR3

(A):

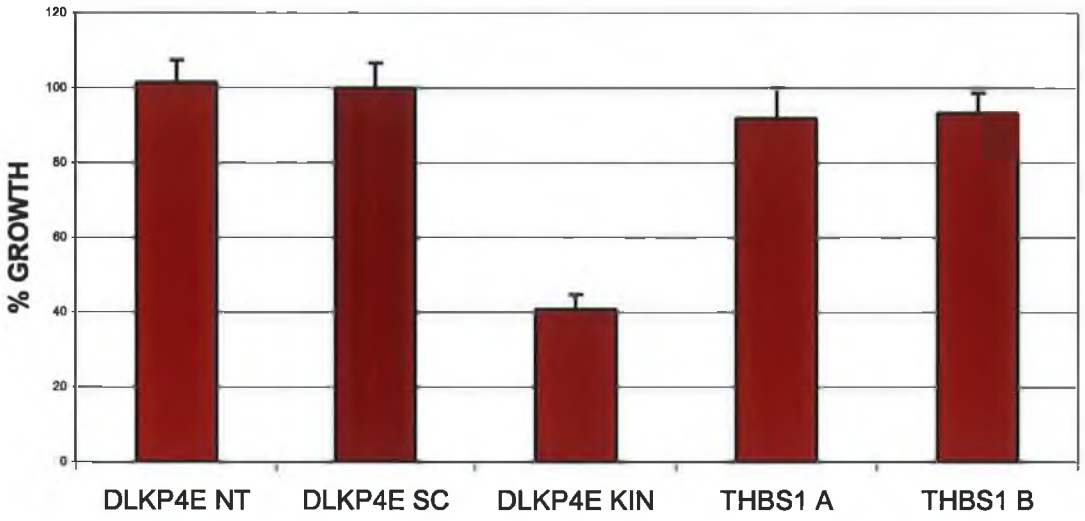

(B):

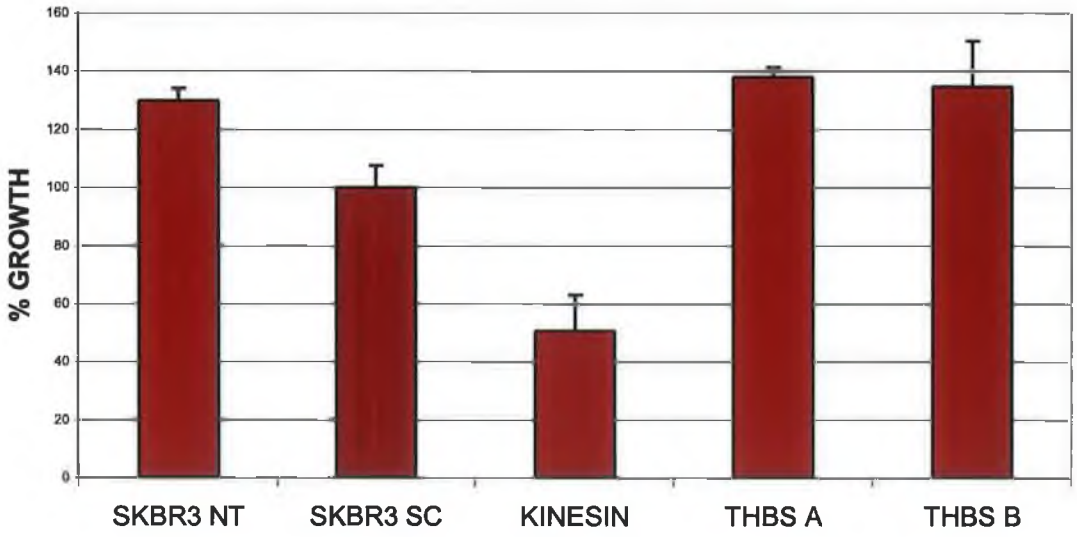

Figure 3.9.2: (A) Growth rate of DLKP4E NT, DLKP4E SC and DLKP4E transfected with THBS1 siRNA A and B. (B) Growth rate of SKBR3 NT, SKBR3 SC and SKBR3 transfected with THBS1 siRNA A and B.

Figure 3.9.3 Real-time PCR for THBS1 siRNA A, B & C in DLKP at 24hrs & 48hrs

(A):

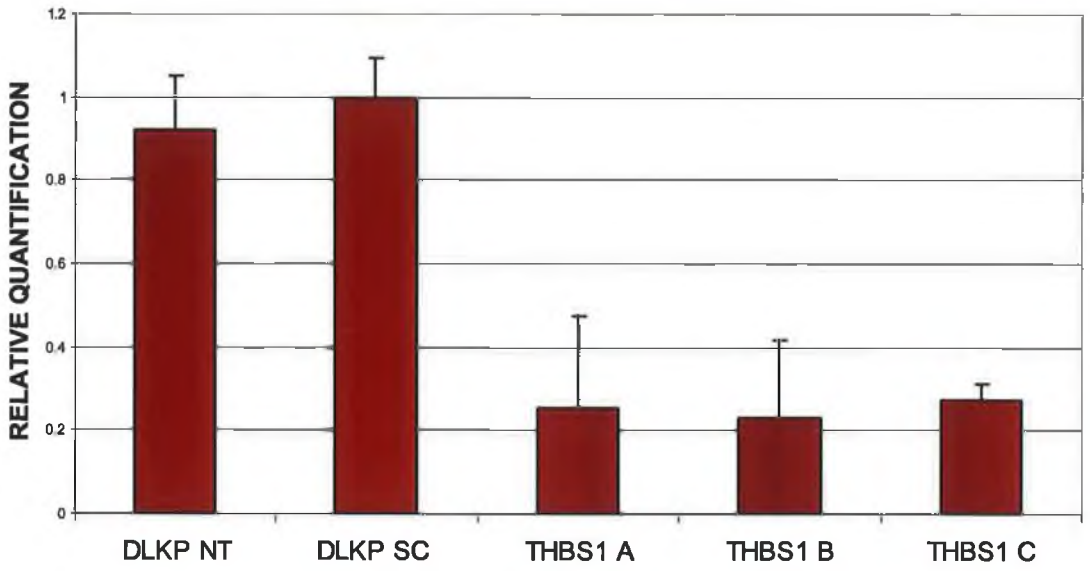

(B):

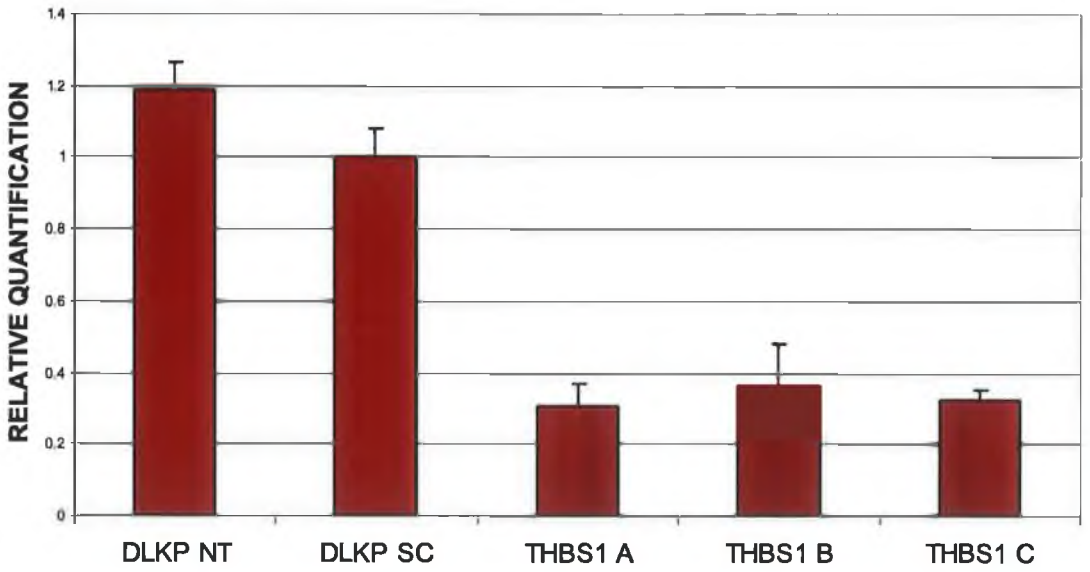

Figure 3.9.3: (A) Relative quantification of THBS1 in non-transfected, scrambled, and THBS1 siRNA A, B & C transfected DLKPs at 24hrs; (B) Relative quantification of THBS1 in non-transfected, scrambled, and THBS1 siRNA A, B & C transfected DLKPs at 48hrs.

3.9.2 Real-time PCR

Real-time PCR was carried out on all four cells lines transfected with all three THBS1 siRNAs to determine if THBS1 mRNA had been successfully silenced. THBS1 mRNA levels were considerably reduced in DLKP after 24 and 48hrs, with all three siRNA transfections showing a drop in THBS1 of between 70% and 80% (Figure 3.9.3). A more moderate response was observed in MCF7 and DLKP4E. In MCF7 THBS1 levels only decreased by 20% to 40% at 24hrs and began to recover after 48hrs (Figure 3.9.4). DLKP4E showed a greater decrease after 48hrs, with siRNA B and C causing a 40% to 50% reduction in THBS1 mRNA (Figure 3.9.5 and 3.9.6).Result for THBS1 siRNA A and B were displayed separately to siRNA C as transfections were carried out on two separate occasions. SKBR3 gave similar results to DLKP, with both THBS1 siRNA A and B causing an 80% to 85% decline in THBS1 mRNA after 24hrs.Unlike DLKP however, THBS1 mRNA levels recovered in SKBR3 48hrs after transfection (Figure 3.9.7 and 3.9.8). Taken as a whole these results showed transfection of 2 out of 3 THBS1 siRNAs caused knock-down of THBS1 at a mRNA level in four different cell lines.

Figure 3.9.4 Real-time PCR for THBS1 siRNA A, B & C in MCF7 at 24hrs & 48hrs

(A):

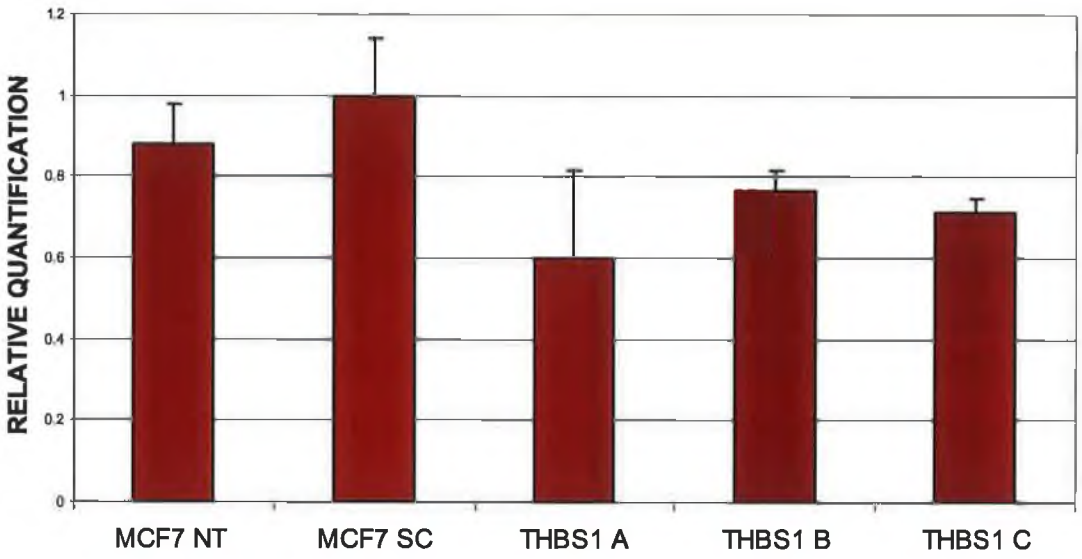

(B):

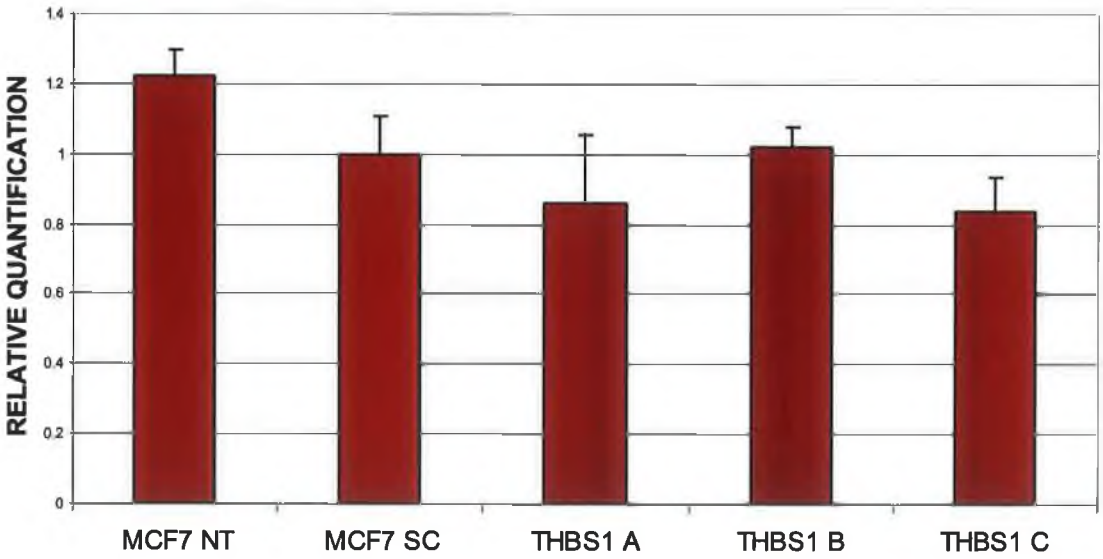

Figure 3.9.4: (A) Relative quantification of THBS1 in non-transfected, scrambled, and THBS1 siRNA A, B & C transfected MCF7s at 24hrs; (B) Relative quantification of THBS1 in non-transfected, scrambled, and THBS1 siRNA A, B & C transfected MCF7s at 48hrs.

Figure 3.9.5 Real-time PCR for THBS1 siRNA A, B & C in DLKP4E at 24hrs

(A):

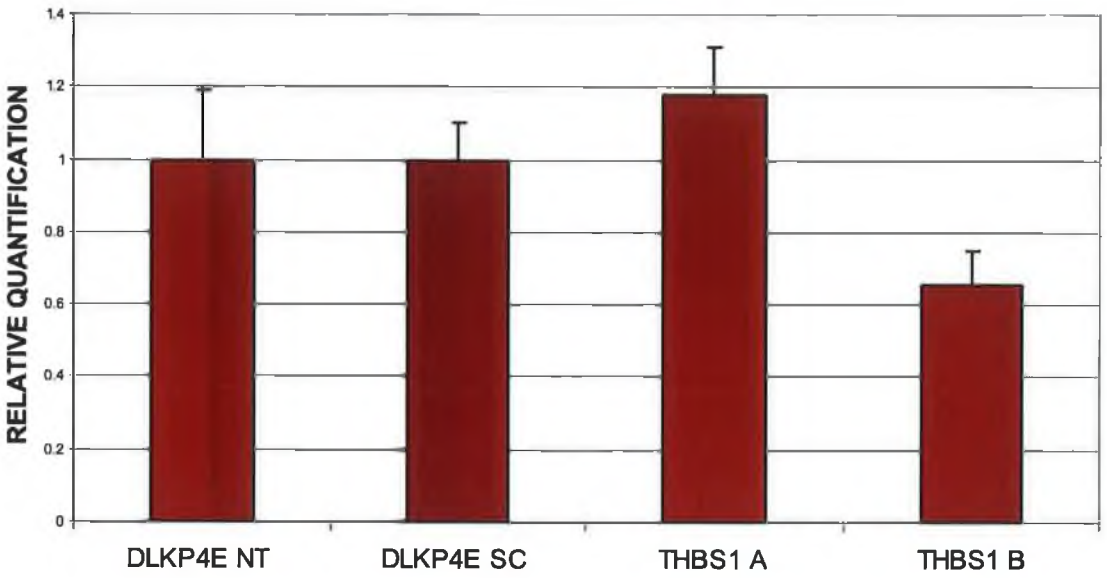

(B):

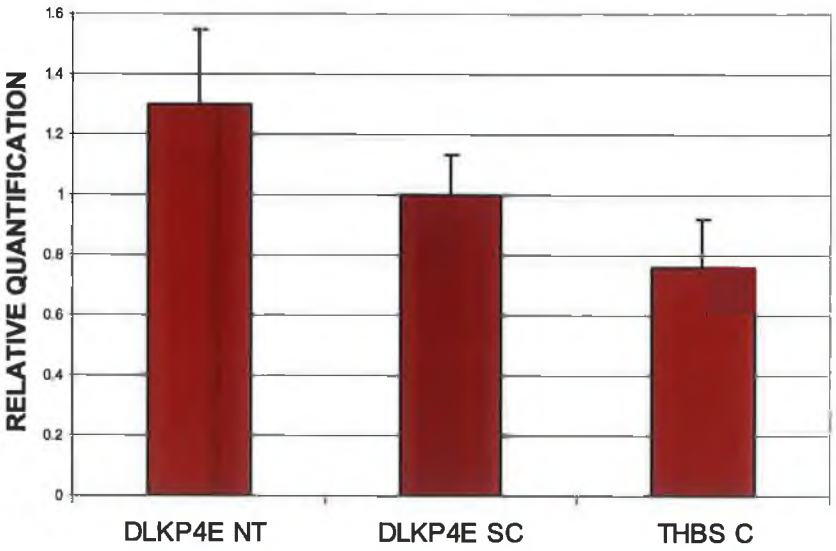

Figure 3.9.5: (A) Relative quantification of THBS1 in non-transfected, scrambled, and THBS1 siRNA A & B transfected DLKP4Es at 24hrs; (B) Relative quantification of THBS1 in non-transfected, scrambled, and THBS1 siRNA C transfected DLKP4Es at 24hrs.

Figure 3.9.6 Real-time PCR for THBS1 siRNA A, B & C in DLKP4E at 48hrs

(A):

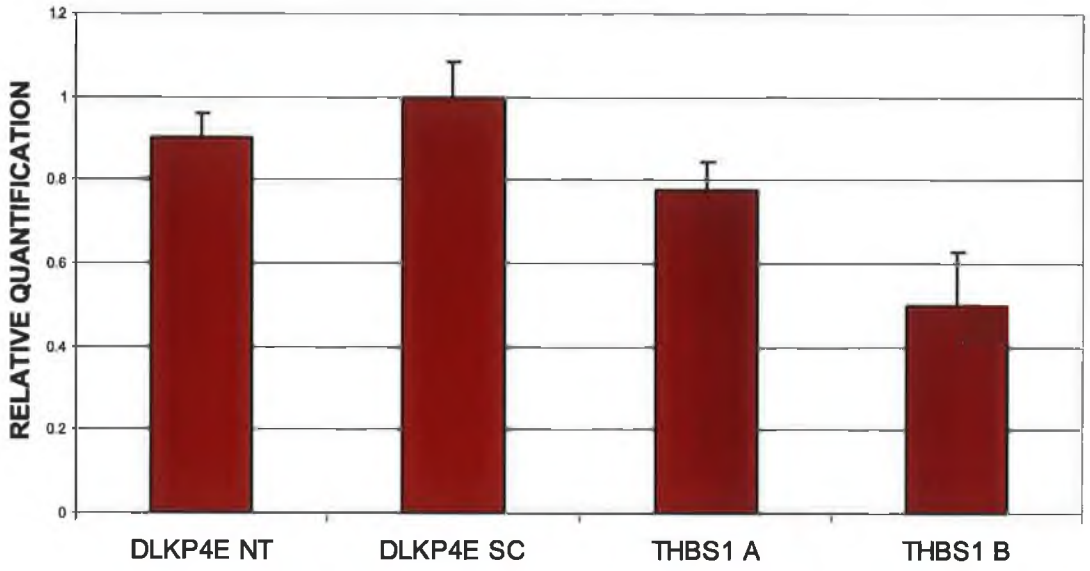

(B):

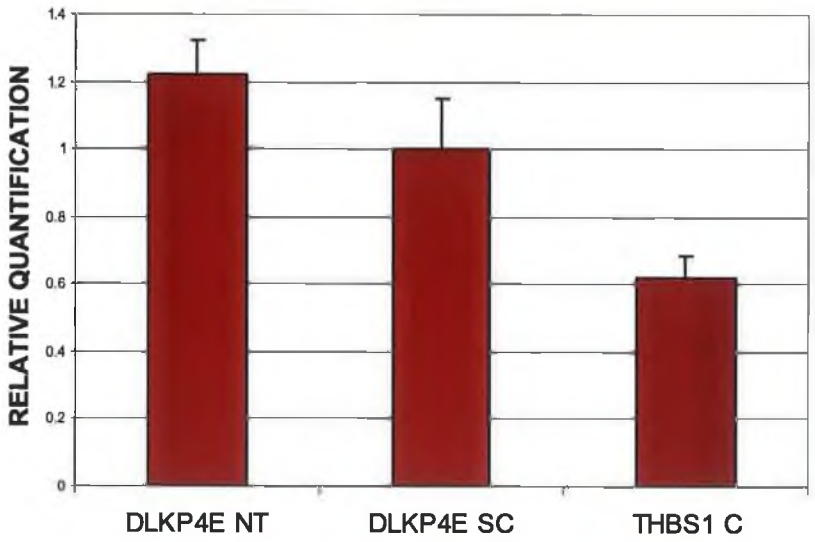

Figure 3.9.6: (A) Relative quantification of THBS1 in non-transfected, scrambled, and THBS1 siRNA A & B transfected DLKP4Es at 48hrs; (B) Relative quantification of THBS1 in non-transfected, scrambled, and THBS1 siRNA C transfected DLKP4Es at 48hrs.

Figure 3.9.7 Real-time PCR for THBS1 siRNA A, B & C in SKBR3 at 24hrs

(A):

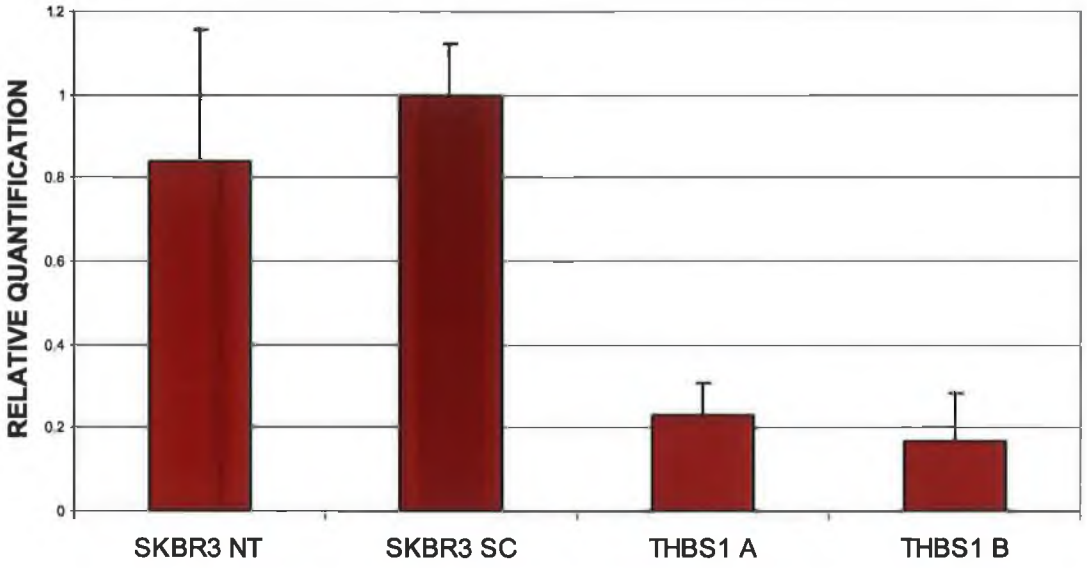

(B):

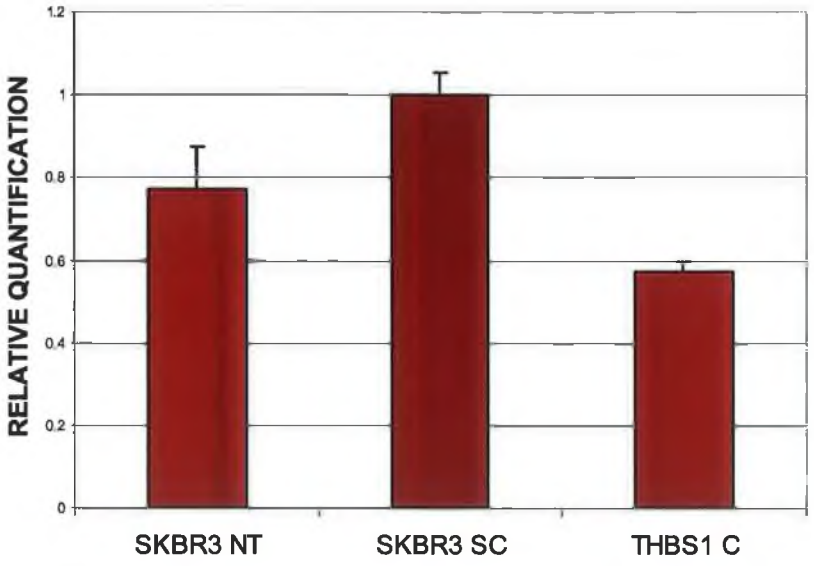

Figure 3.9.7: (A) Relative quantification of THBS1 in non-transfected, scrambled, and THBS1 siRNA A & B transfected SKBR3s at 24hrs; (B) Relative quantification of THBS1 in non-transfected, scrambled, and THBS1 siRNA C transfected SKBR3s at 24hrs.

Figure 3.9.8 Real-time PCR for THBS1 siRNA A, B & C in SKBR3 at 48hrs

(A):

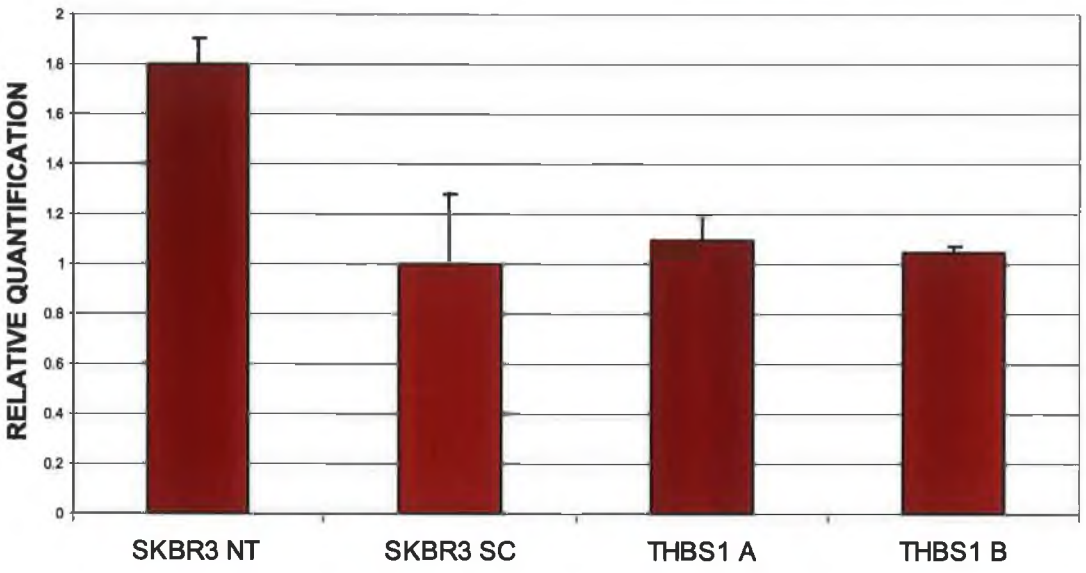

(B):

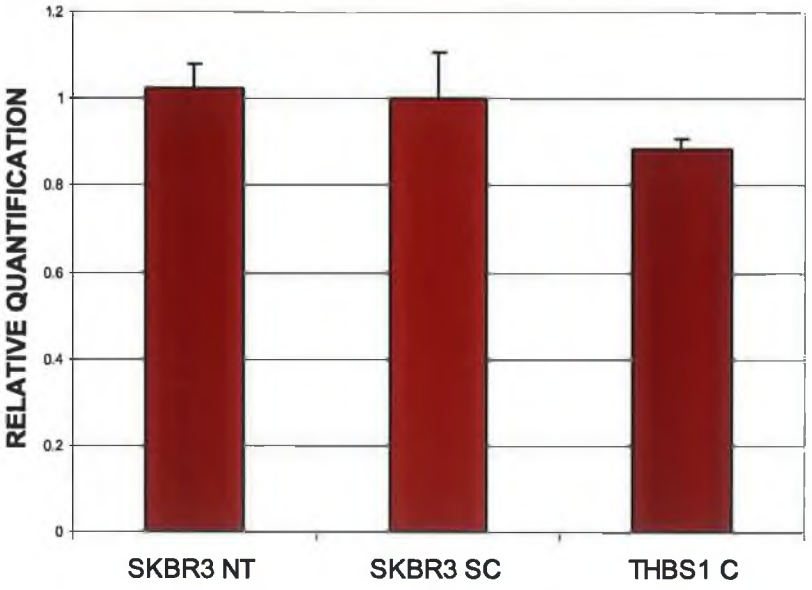

Figure 3.9.8: (A) Relative quantification of THBS1 in non-transfected, scrambled, and THBS1 siRNA A & B transfected SKBR3s at 48hrs; (B) Relative quantification of THBS1 in non-transfected, scrambled, and THBS1 siRNA C transfected SKBR3s at 48hrs.

3.9.3 Western blot

Western blots were carried out on protein isolated from all four cell lines after siRNA transfection. However, MCF7 was the only cell line that had sufficient levels of THBS1 protein for detection by western blot. The results showed that THBS1 protein was reduced after transfection with all three of the THBS1 siRNAs. THBS1 siRNA A and C had the most marked effect, with no detectable band, THBS1 siRNA B, though still visible, is clearly reduced compared to the non-transfected and scrambled controls (Figure 3.9.9). This result proves that the siRNAs used were capable of knock-down of THBS1 at a protein level.

Figure 3.9.9 Western blot analysis of THBS1 protein expression in MCF7

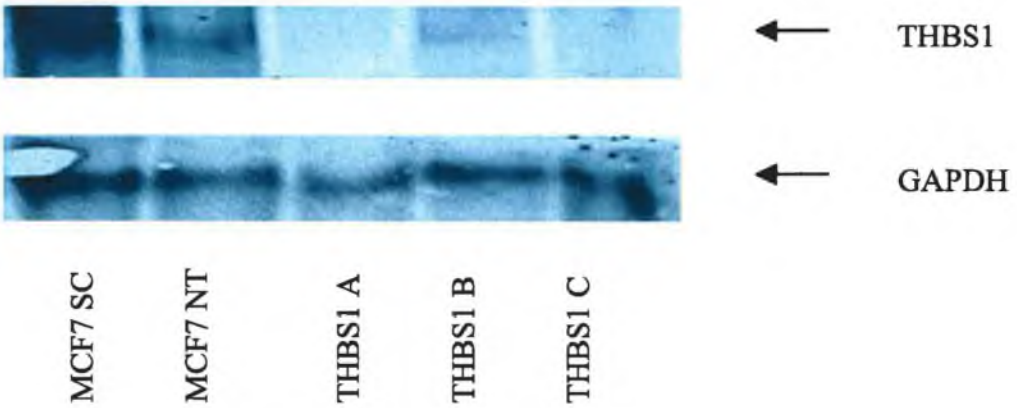

Figure 3.9.9: Western blot showing protein expression of THBS1 in MCF7 NT, MCF7 SC, and MCF7 transfected with THBS1 siRNA A, B & C.

3.9.4 Invasion assays

To establish whether THBS1 silencing seen in mRNA and protein led to a change in the invasion status of the cells, invasion assays were carried out. The most dramatic results were seen in DLKP and MCF7. DLKP, a mildly invasive cell line, showed a 3.5 to 4-fold increase in the number of invading cells when transfected with all three siRNAs (Figure 3.9.10 and 3.9.11). MCF7, a completely non-invasive cell line, became invasive after transfection with THBS1 siRNA (Figure 3.9.12 and 3.9.13). DLKP4E, already a highly invasive cell line, showed a negligible change of 0.1 fold. Combined with the statistical data for these results, this change is insignificant (Figure 3.9.14 and 3.9.15). SKBR3 also showed an increase in invading cells. Though not obvious from photographic evidence of the invasion inserts, cell counts revealed that a 1.3 to 1.7 fold increase was seen in THBS1 siRNA transfected cells (Figure 3.9.16 and 3.9.17). These results show that transfection of THBS1 siRNA produces dramatic increases in invasion across SKBR3 and DLKP, and again, validate results of microarray analysis which suggested reduction of THBS1 should increase invasion.

Figure 3.9.10 Photographs of invasion assays for DLKP transfected with THBS1 siRNA

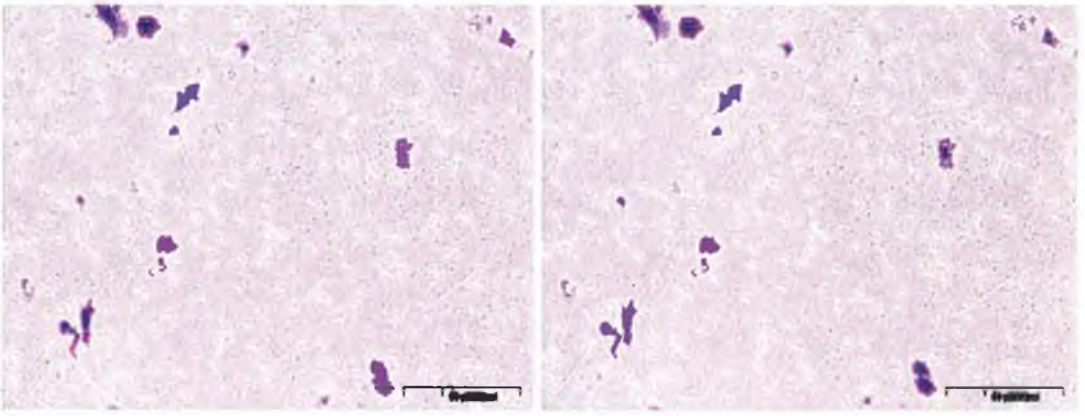

(A) DLKP NT

(B) DLKP SC

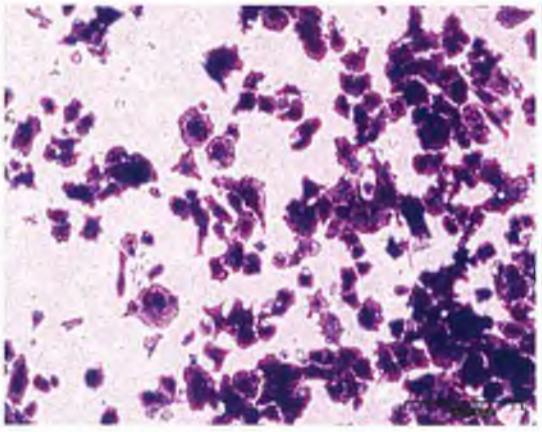

(C) THBS1 A

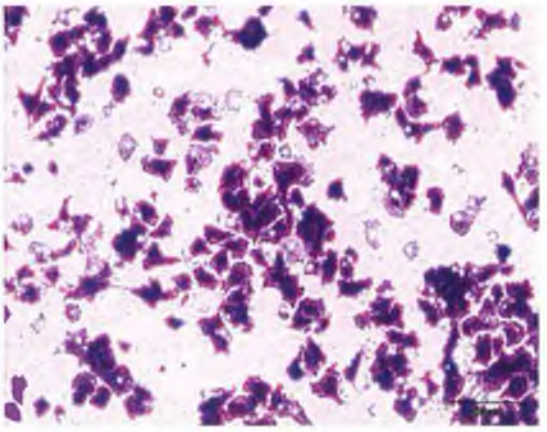

(D) THBS1 B

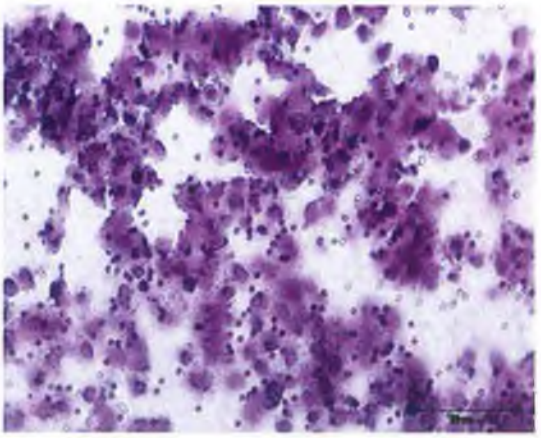

(E) THBS1 C

Figure 3.9.10: Photographs of invasion assay inserts at 10X magnification. A=DLKP NT, B=DLKP SC, C=DLKP transfected with THBS1 siRNA A, D=DLKP transfected with THBS1 siRNA B E=DLKP transfected with THBS1 siRNA C.

Figure 3.9.11 cell counts of invasion assays for DLKP transfected with THBS1 siRNA

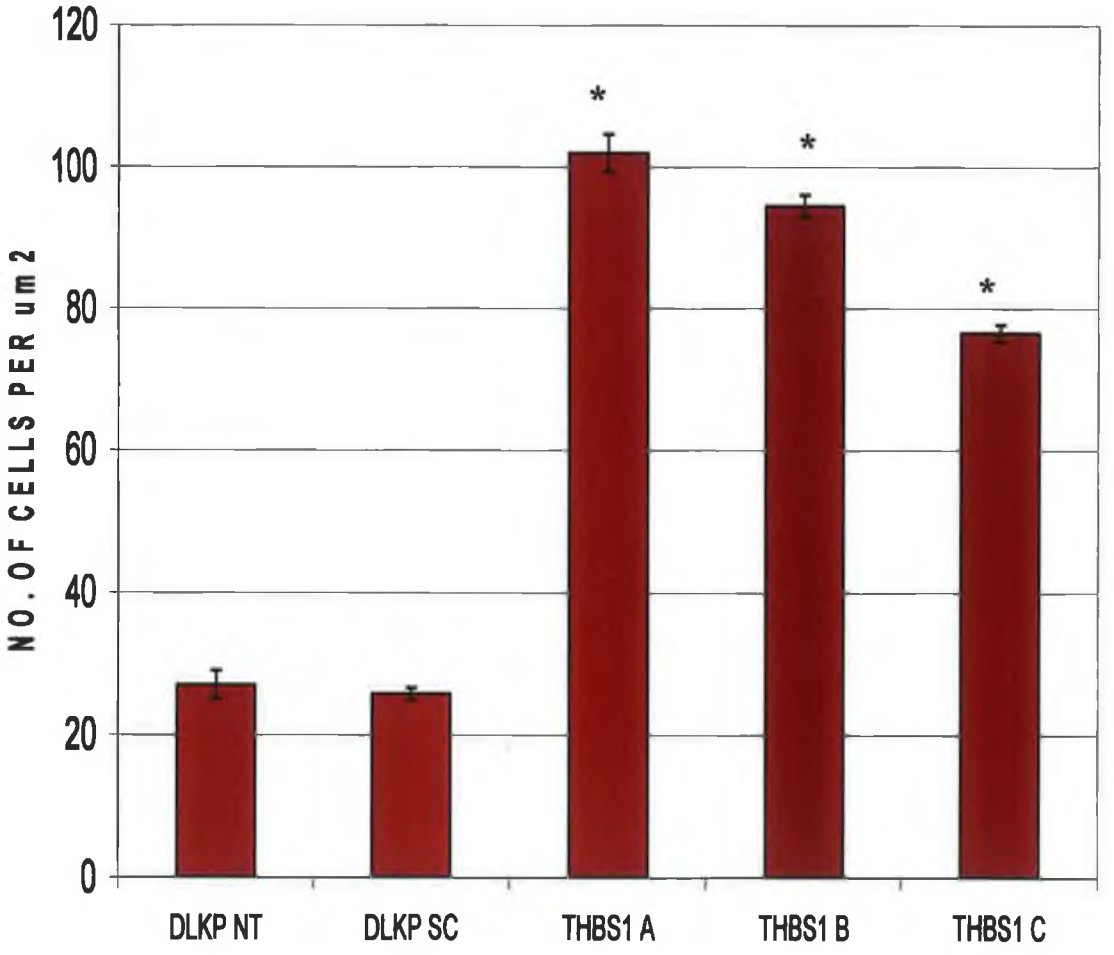

Figure 3.9.11: Number of invading cells detected per μm^2 (at 20X magnification) of invasion assay insert for DLKP NT, DLKP SC and DLKP transfected with THBS1 siRNA A, B & C.

n=3, *p-value<.001.

Figure 3.9.12 Photographs of invasion assays for MCF7 transfected with THBS1 siRNA

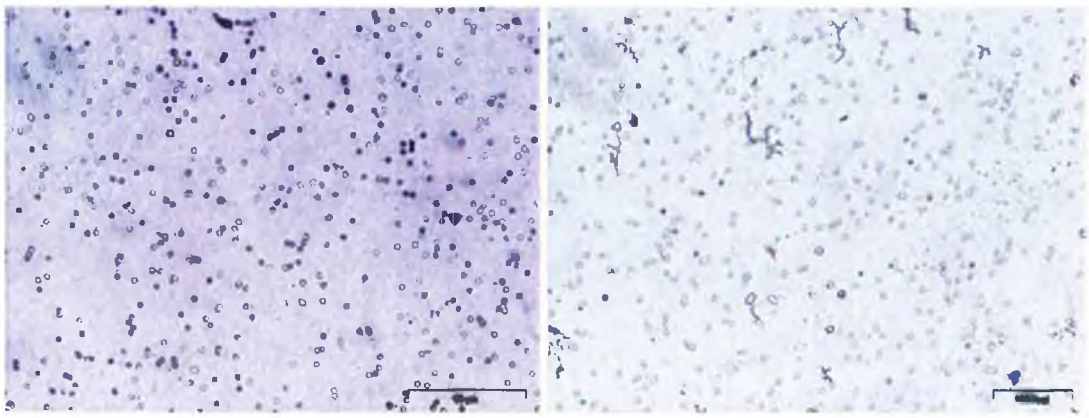

(A) MCF7 NT (B) MCF7 SC

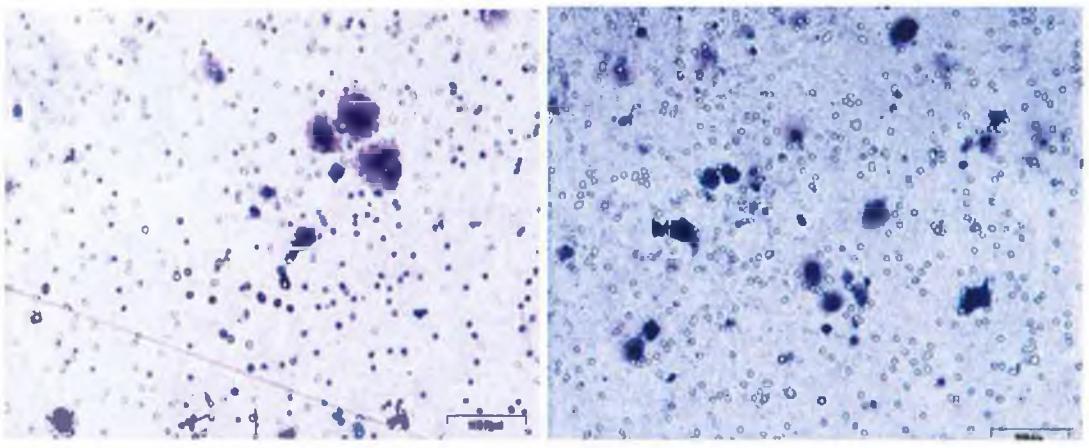

(C) THBS1 A (D) THBS1 B

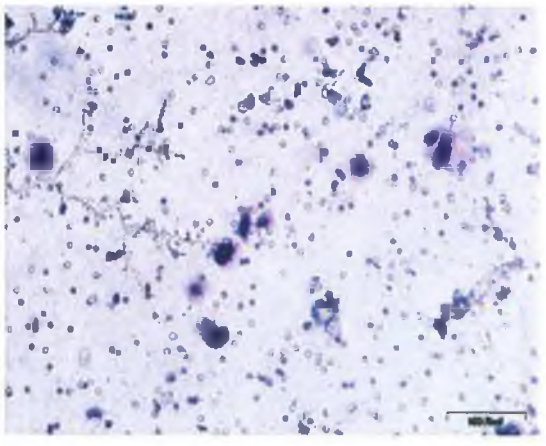

(E) THBS1 C

Figure 3.9.12: Photographs of invasion assay inserts at 10X magnification. A=MCF7 NT, B=MCF7 SC, C=MCF7 transfected with THBS1 siRNA A, D=MCF7 transfected with THBS1 siRNA B E=MCF7 transfected with THBS1 siRNA C.

Figure 3.9.13 cell counts of invasion assays for MCF7 transfected with THBS1 siRNA

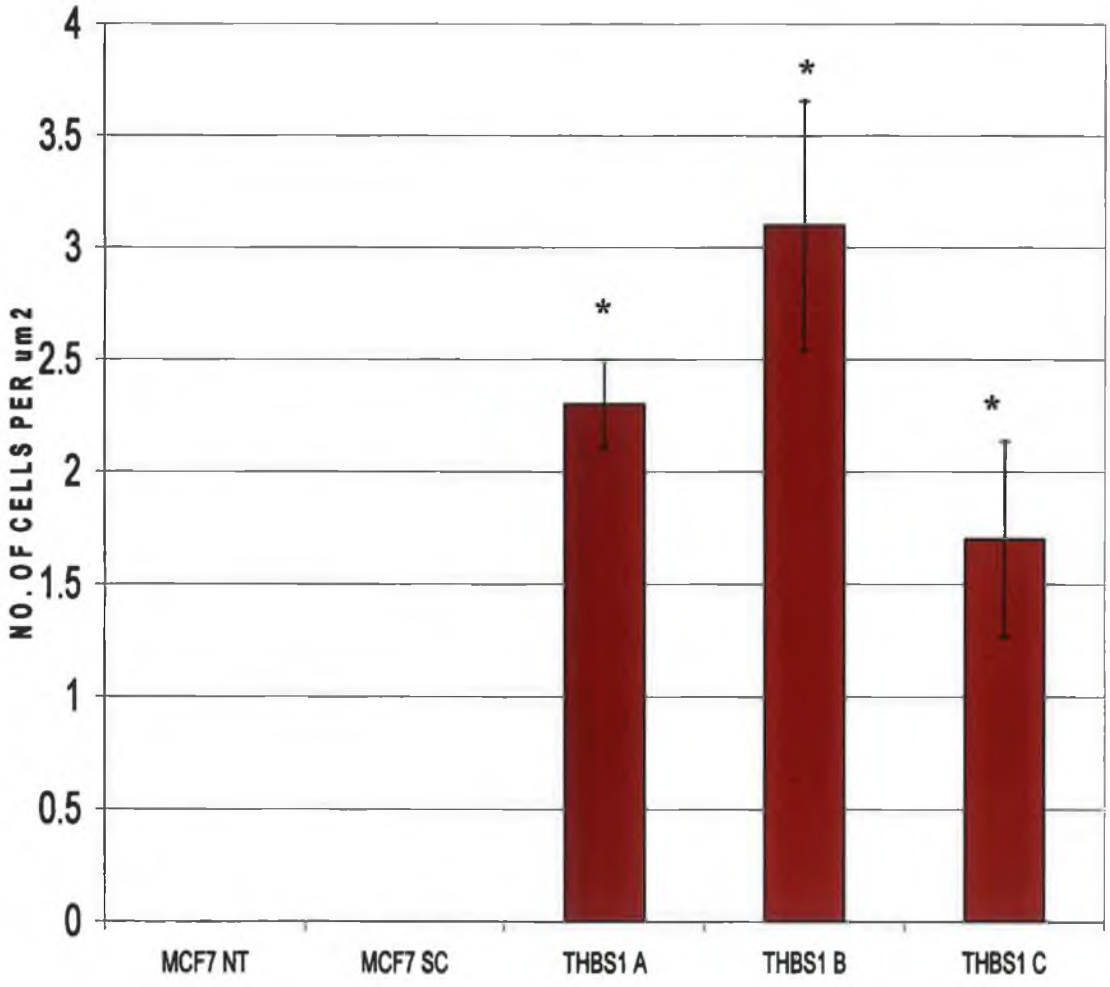

Figure 3.9.13: Number of invading cells detected per μm^2 of invasion assay insert for MCF7 NT, MCF7 SC and MCF7 transfected with THBS1 siRNA A, B & C.
n=3, *p-value<.001.

Figure 3.9.14 Photographs of invasion assays for DLKP4E transfected with THBS1 siRNA

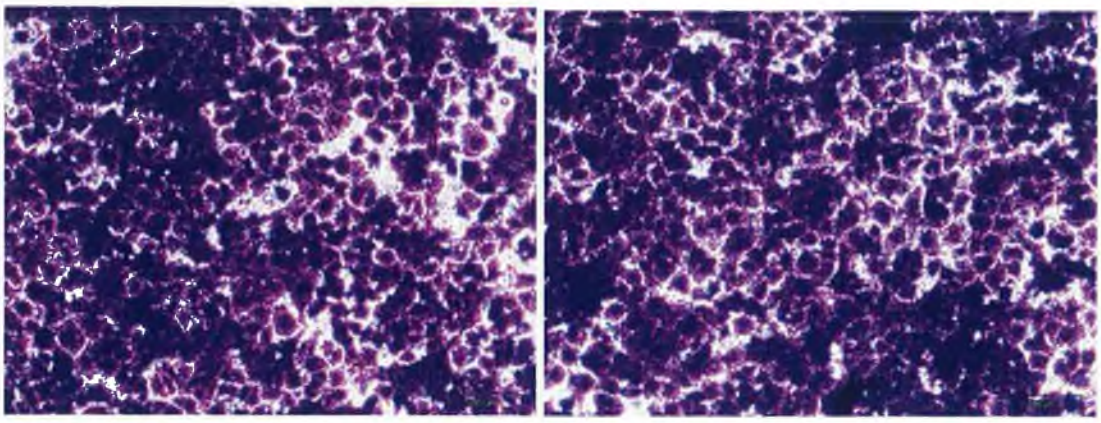

(A) DLKP4E NT

(B) DLKP4E SC

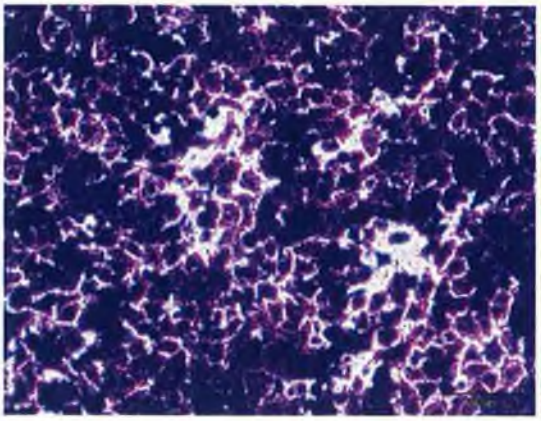

(C) THBS1 A

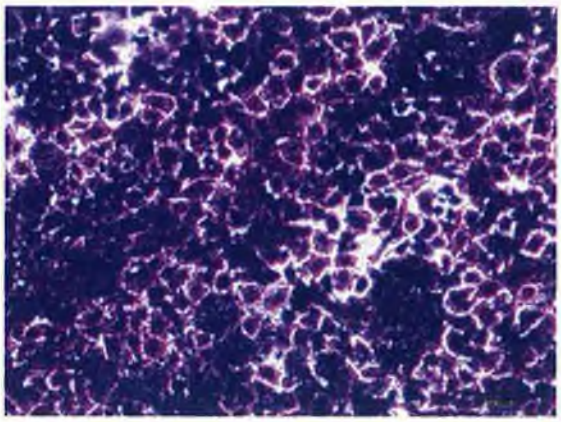

(D) THBS1 B

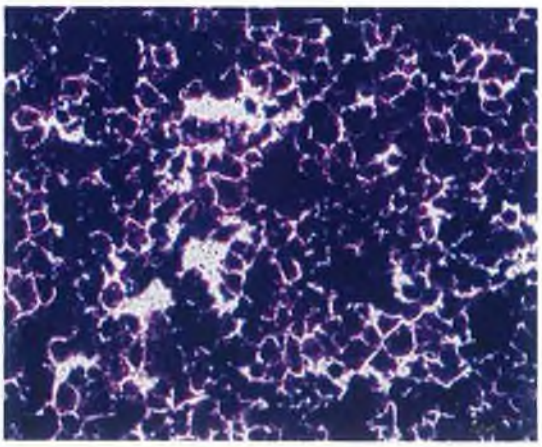

(E) THBS1 C

Figure 3.9.14: Photographs of invasion assay inserts at 10X magnification. A= DLKP4E NT, B=DLKP4E SC, C=DLKP4E transfected with THBS1 siRNA A, D=DLKP4E transfected with THBS1 siRNA B E= DLKP4E transfected with THBS1 siRNA C.

Figure 3.9.15 cell counts of invasion assays for DLKP4E transfected with THBS1 siRNA

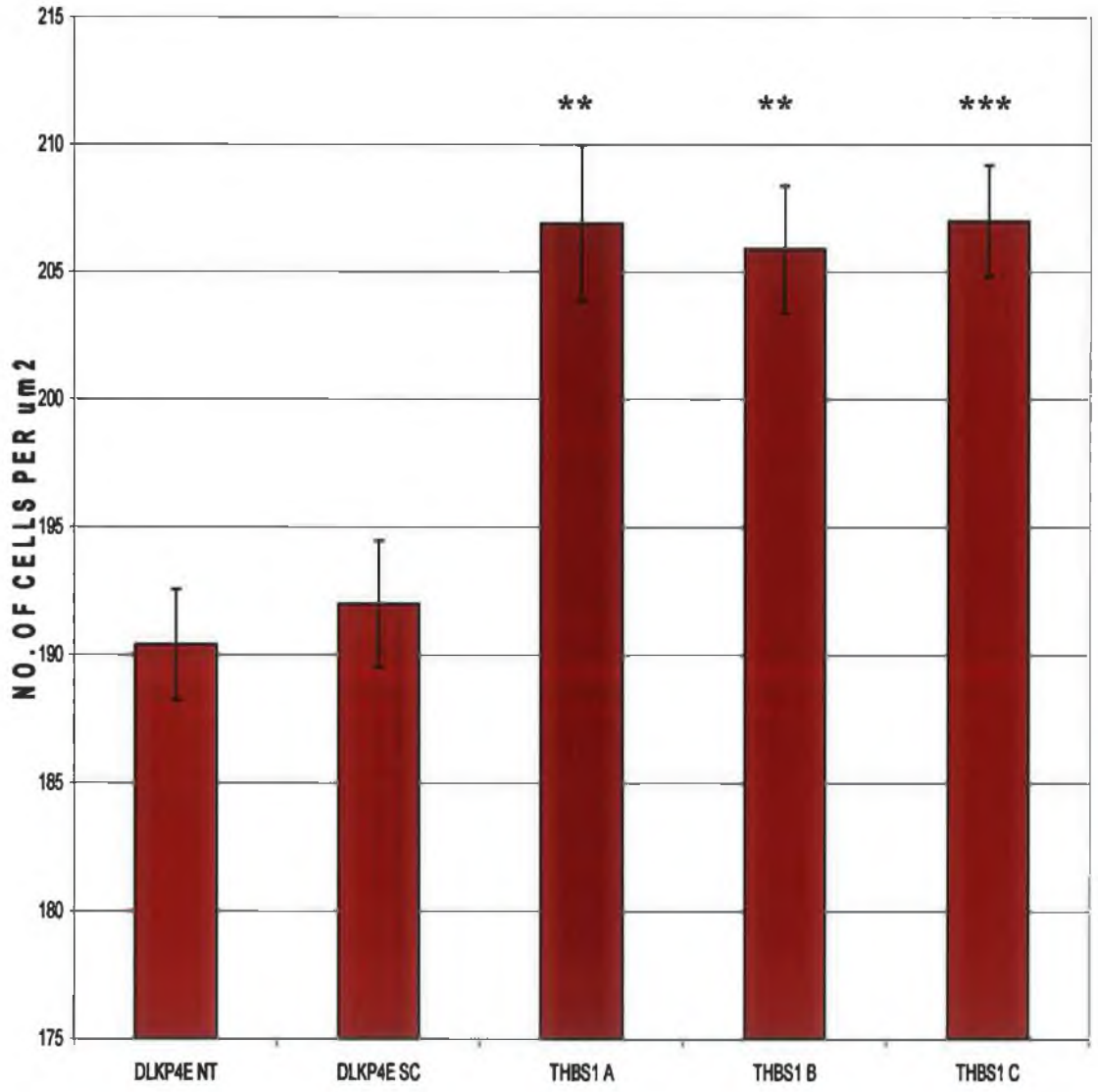

Figure 3.9.15: Number of invading cells detected per μm^2 of invasion assay insert for DLKP4E NT, DLKP4E SC and DLKP4E transfected with THBS1 siRNA A, B & C. n=3, **p-value<0.01***p-value<0.05.

Figure 3.9.16 Photographs of invasion assays for SKBR3 transfected with THBS1 siRNA

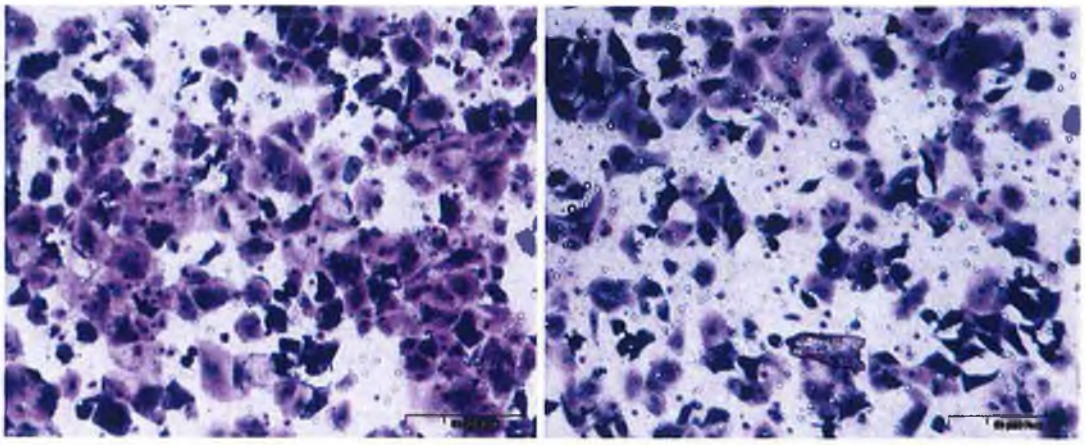

(A) SKBR3 NT

(B) SKBR3 SC

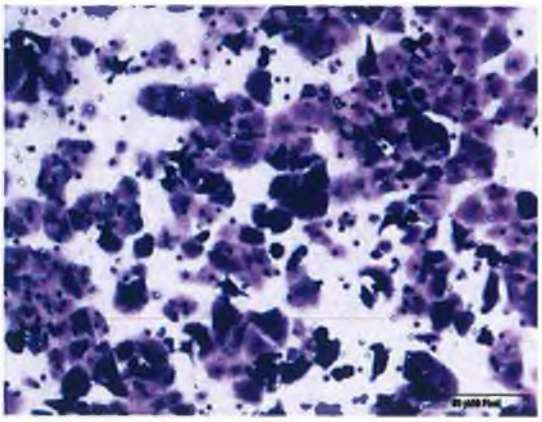

(C) THBS1 A

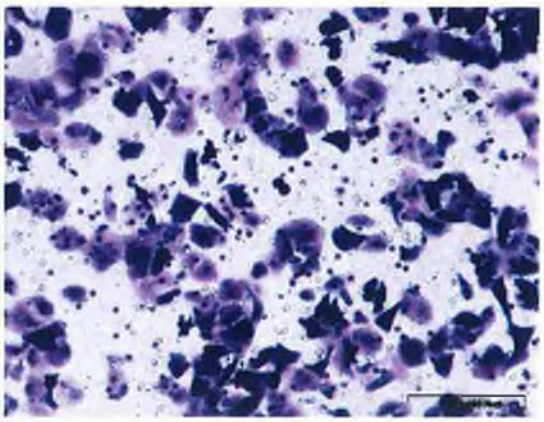

(D) THBS1 B

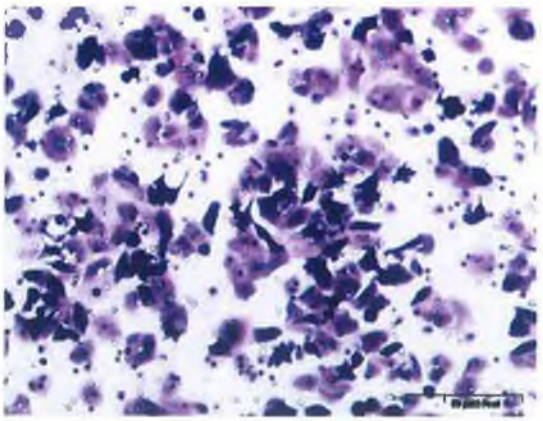

(E) THBS1 C

Figure 3.9.16: Photographs of invasion assay inserts at 10X magnification. A= SKBR3 NT, B=SKBR3 SC, C= SKBR3 transfected with THBS1 siRNA A, D=SKBR3 transfected with THBS1 siRNA B E= SKBR3 transfected with THBS1 siRNA C.

Figure 3.9.17 cell counts of invasion assays for SKBR3 transfected with THBS1 siRNA

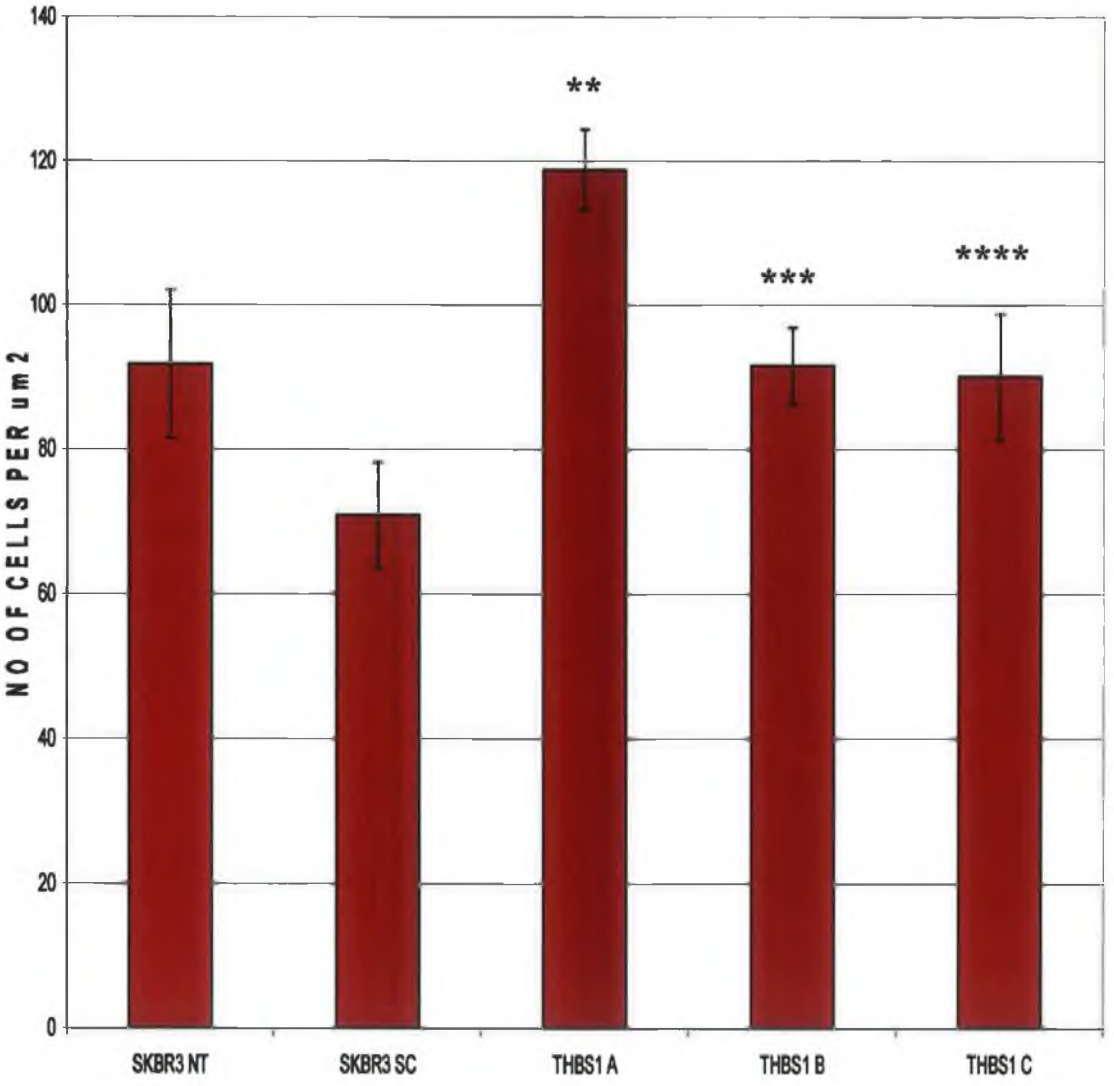

Figure 3.9.17: Number of invading cells detected per μm^2 of invasion assay insert for SKBR3 NT, SKBR3 SC and SKBR3 transfected with THBS1 siRNA A, B & C.
n=3, *p-value<0.001, **p-value<0.01, ***p-value<0.05, ****p-value>0.05

3.9.5 Summary of results for THBS1 in DLKP, DLKP4E, MCF7 and SKBR3

Proliferation assays carried out on all cell lines showed that predominately THBS1 siRNA transfection caused little change in growth rate, with the exception of SKBR3. Real-time PCR revealed efficient knock-down of THBS1 mRNA with all three siRNAs in DLKP and SKBR3, and two of the three siRNAs in DLKP4E and MCF7. Although THBS1 protein expression was too low for detection by western blot in DLKP, DLKP4E and SKBR3, detection and decreased expression was observed in MCF7. Western blot results showed a marked decrease in THBS1 protein in MCF7 cells post-siRNA transfection. THBS1 siRNA A and C both performed best, and this can be seen at both mRNA and protein level, with real-time mirroring western blot results. Invasion assay results were conspicious, with an increase in invasion being inversely proportional to the original level of invasion of the cell lines. Non-invasive MCF7 became invasive, poorly invasive DLKP became highly invasive, and invasive SKBR3 also showed an increase in invading cells. However, DLKP4E, the most highly invasive cell line in the study did not change (Table 3.5.1). Microarray results revealed that expression levels of THBS1 were reduced in an invasive cell line. Results from this study support this idea, with siRNA silencing of THBS1 having a lesser effect on cell lines as they increased in invasion. Microarray analysis would suggest that the higher the level of invasion the lower the level of THBS1. The lower the level of THBS1 the lesser the effect of THBS1 siRNA.

Table 3.9.1 Summary of results of THBS1 siRNA transfection into DLKP, MCF7, DLKP4E and SKBR3

	Real-time PCR – mRNA knock-down			Western blot – protein knock-down			Invasion assay – increase in invasion		
Cell Line	siRNA A	siRNA B	siRNA C	siRNA A	siRNA B	siRNA C	siRNA A	siRNA B	siRNA C
DLKP	+	+	+	—	—	—	+	+	+
MCF7	+	+	+	+	+	+	+	+	+
DLKP4E	+	+	+	—	—	—	+	+	+
SKBR3	+	+	+	—	—	—	+	+	+

Table 3.9.1: Summary of results of THBS1 siRNA A, B and C transfections into DLKP, MCF7, DLKP4E and SKBR3.

3.10 Genes specific to DLKP4E, DLKP4Emut and invasion

Five genes were chosen as siRNA targets based on analysis of DLKP4E and DLKP4Emut microarray data (see section 3.3.4). All five genes displayed increased expression in invasive DLKP4E and DLKP4Emut. siRNA analysis was chosen to silence these genes in order to observe the effect on invasion. As with the genes chosen based on MCF7H3erbB2 data (Section 3.4 to 3.9), all siRNAs were transfected into both SKBR3 and DLKP4E, and two siRNAs were used for each target.

3.10.1 Proliferation assays

Proliferation assays were carried out on both DLKP4E and SKBR3 transfected with all 10 siRNAs to determine the effect on growth rate. Results for DLKP4E showed only minor changes in growth after transfection (Figure 3.10.1.1). The growth rate of SKBR3 increased between 20% and 30% for most transfected cells (Figure 3.10.1.2).

3.10.2 Invasion assays

Invasion assays revealed that none of the siRNA transfections caused any of the expected reduction in invasion of DLKP4E (Figure 3.10.2). Cell counts were not performed because the extent of the invading cells on most inserts made it impossible to get an accurate count. Initially, the photograph of the SKBR3 invasion inserts indicated some decrease in invasion (Figure 3.10.3). However, cell counts revealed no change in the number of invading cells (Figure 3.10.4) and when repeated, results for this cell line were inconsistent. These results showed that transfection of SKBR3 and DLK4E with this set of siRNAs did not result in reduced invasion.

3.10.3 Summary of results

A reduction in Kinesin proliferation and also real-time PCR showing GAPDH knock-down in these cells (Figure 3.4.3) would imply that optimum transfection conditions were used. Therefore invasion assay results suggest that these targets didn't play a significant role in invasion in SKBR3 or DLKP4E. Because of this further analysis was not performed on these targets.

Figure 3.10.1 Proliferation assay for THBS1 siRNA A & B in DLKP and MCF7

(A):

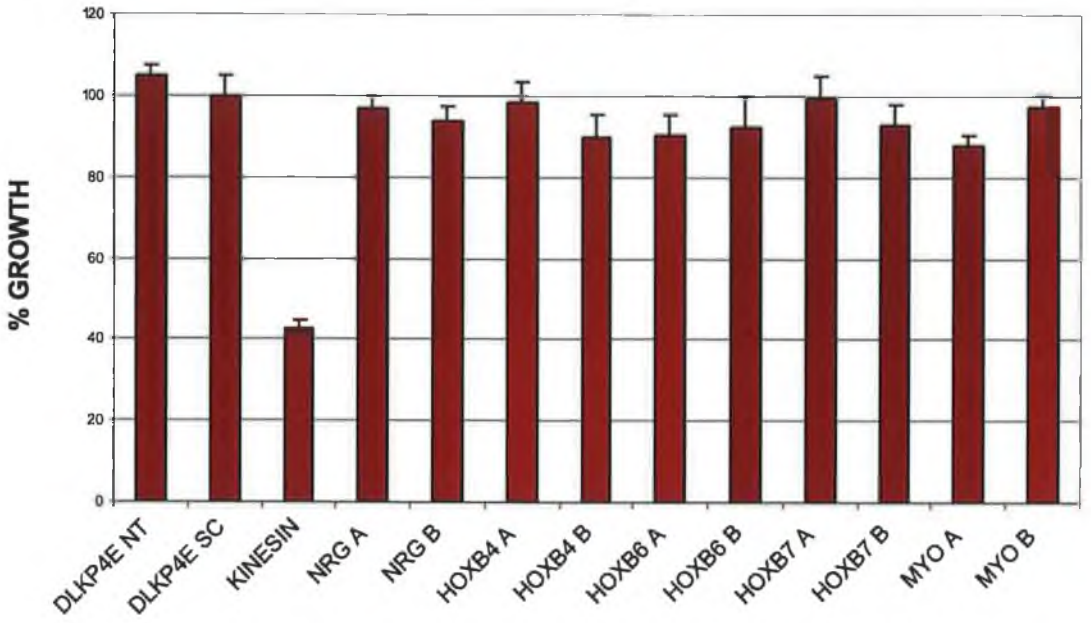

(B):

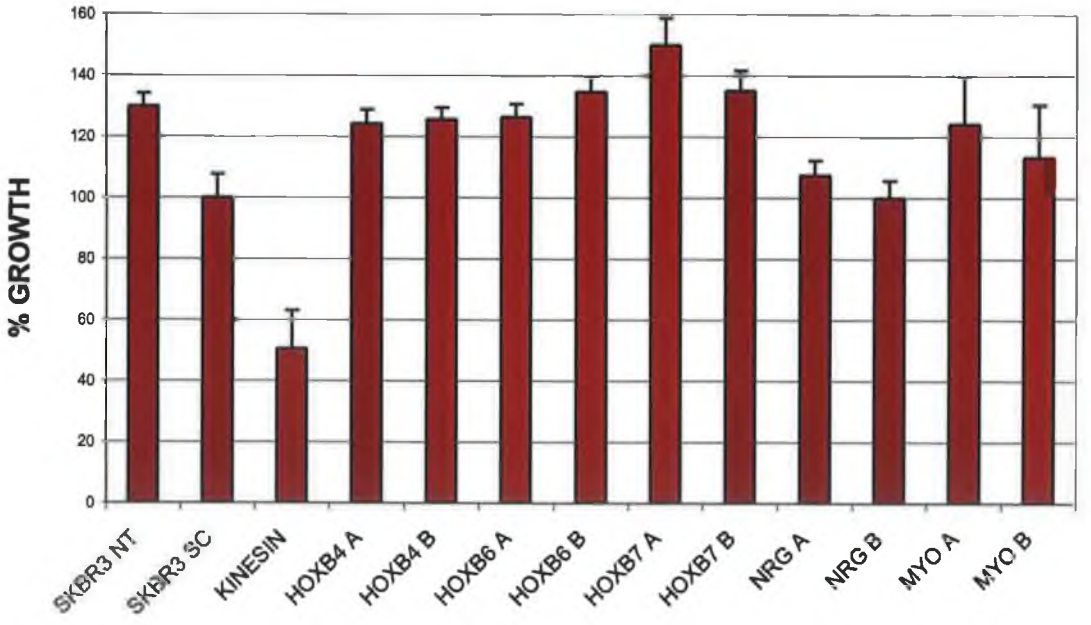

Figure 3.10.1: (A) Growth rate of DLKP4E NT, DLKP4E SC and DLKP4E transfected with DLKP4E/DLKP4E target siRNAs; (B) Growth rate of SKBR3 NT, SKBR3 SC and SKBR3 transfected with DLKP4E/DLKP4E target siRNAs.

Figure 3.10.2 Photographs of invasion assays for DLKP4E transfected with siRNA to target genes specific to DLKP4E, DLKP4Emut and invasion

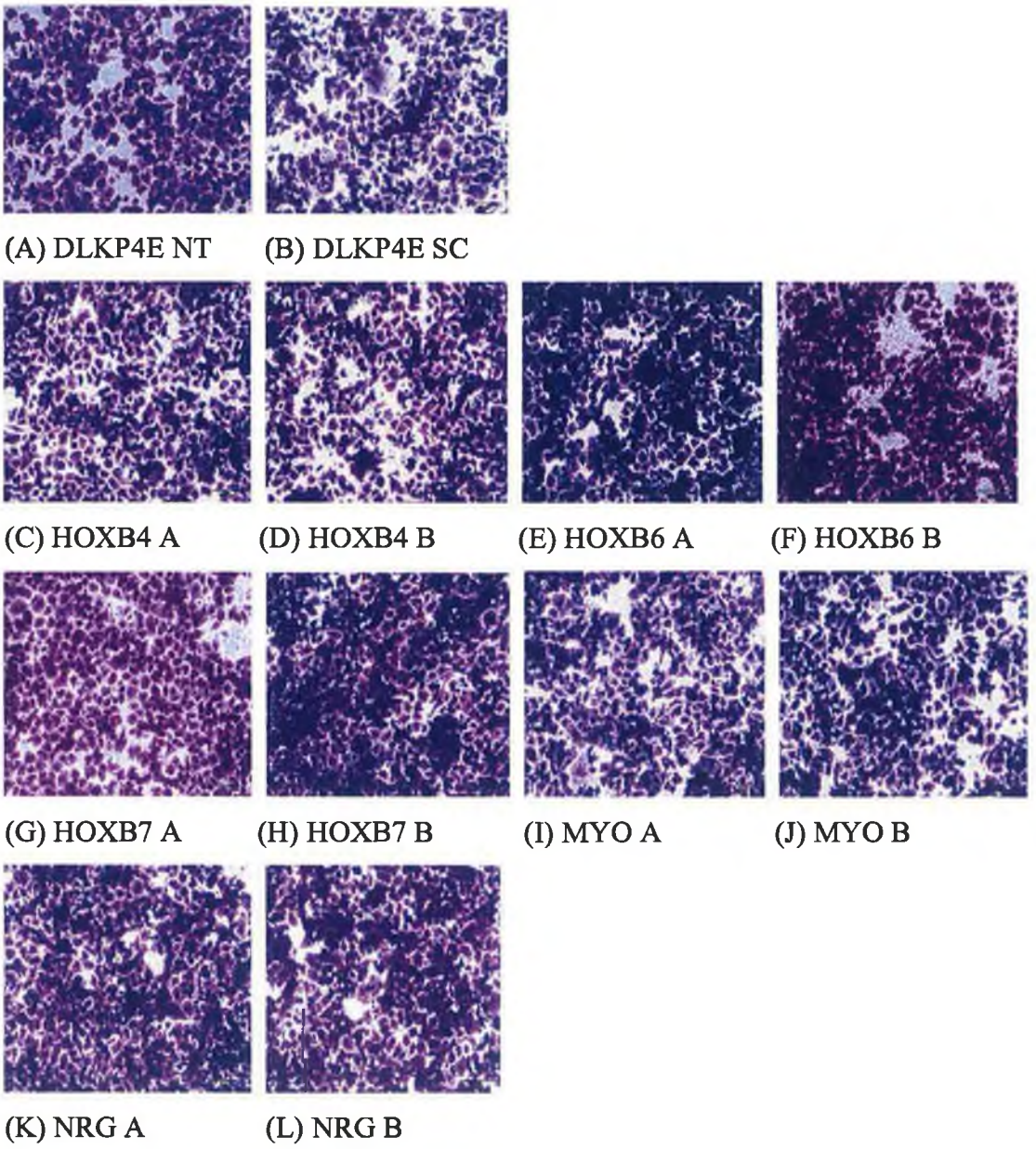

Figure 3.10.2: Photographs of invasion assay inserts at 10X magnification. A=DLKP4E NT, B=DLKP4E SC, DLKP4E transfected with siRNA targeted to (C) HOXB4 A, (D) HOXB4 B, (E) HOXB6 A, (F) HOXB6, (G) HOXB7 A, (H) HOXB7 B, (I) MYO A, (J) MYO B, (K) NRG A, (L) NRG B.

Figure 3.10.3 Photographs of invasion assays for SKBR3 transfected with siRNA to target genes specific to DLKP4E, DLKP4Emut and invasion

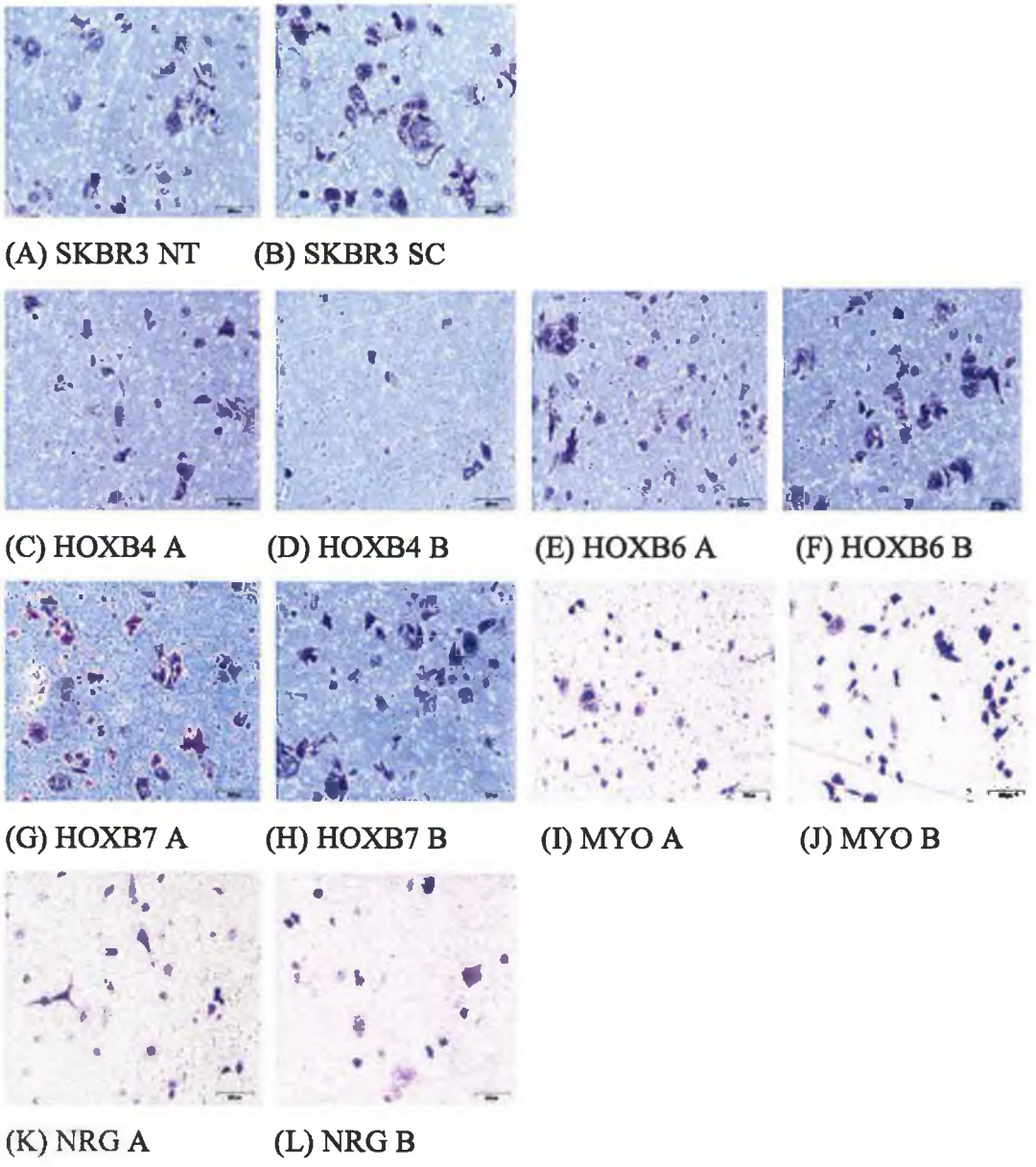

Figure 3.10.3: Photographs of invasion assay inserts at 10X magnification. A=SKBR3 NT, B=SKBR3 SC, SKBR3 transfected with siRNA targeted to (C) HOXB4 A, (D) HOXB4 B, (E) HOXB6 A, (F) HOXB6, (G) HOXB7 A, (H) HOXB7 B, (I) MYO A, (J) MYO B, (K) NRG A, (L) NRG B.

Figure 3.10.4 Cell counts of invasion assays for SKBR3 transfected with siRNA to target genes specific to DLKP4E, DLKP4Emut and invasion

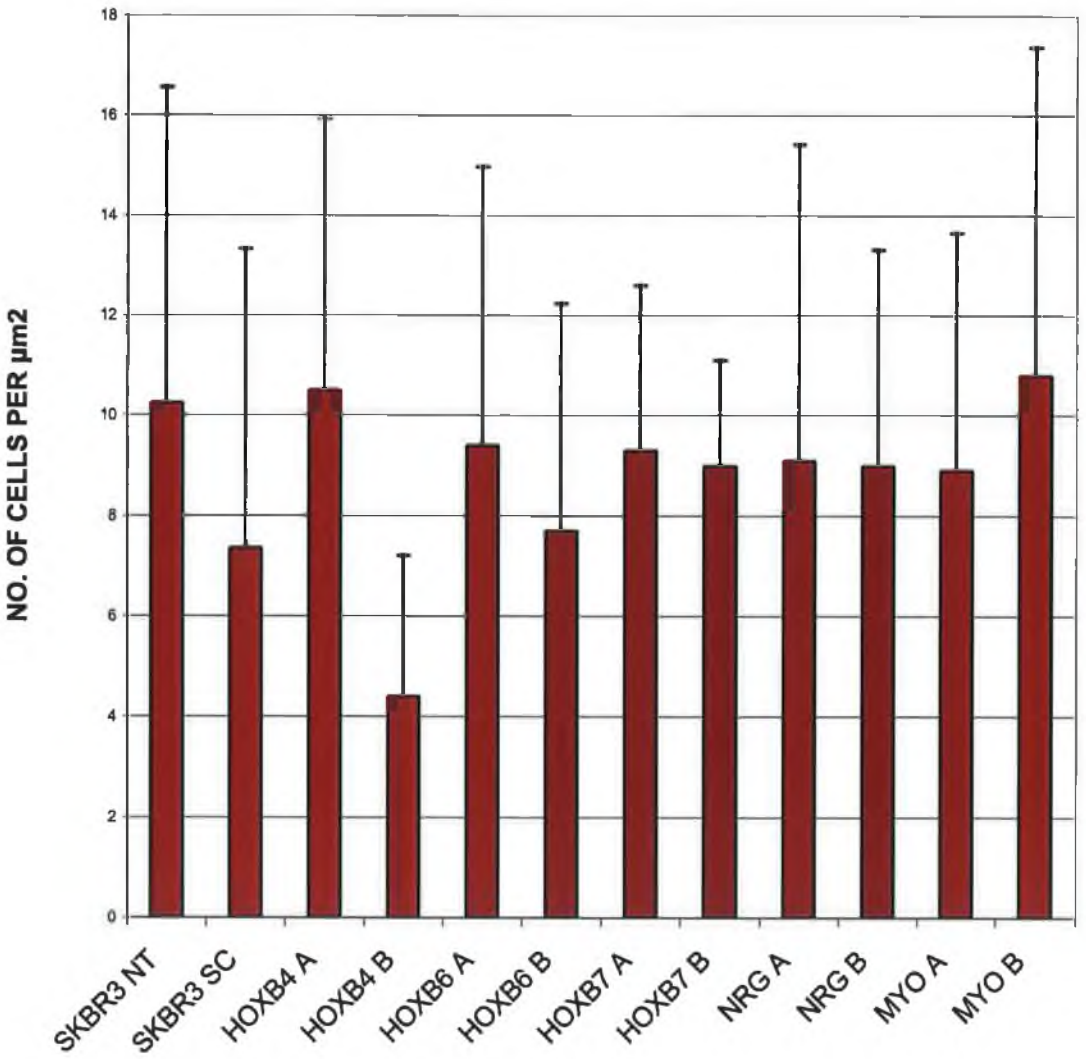

Figure 3.10.4: Number of invading cells detected per μm^2 of invasion assay insert for SKBR3 NT, SKBR3 SC and SKBR3 transfected with siRNA HOXB4 A, HOXB4 B, HOXB6 A, HOXB6, HOXB7 A, HOXB7 B, MYO A, MYO B, NRG A, NRG B.

Section 4.0

Discussion

4.1 Discussion – Overview

The purpose of this thesis was to identify genes which exhibited altered expression as a result of eIF4E or eIF4Emut overexpression in human lung cell lines. More specifically, the effect of eIF4E/eIF4Emut and erbB2 on the invasive phenotype of lung and breast cancer cell lines was investigated using the following approaches:

- Generation and characterisation of DLKP and MCF7 cell lines transfected with wild-type eIF4E and mutant eIF4E.

- Microarray analysis of invasive DLKP4E/4Emut, invasive MCF7H3erbB2 and non-invasive MCF74E/4Emut.

- siRNA expression silencing of genes potentially involved in invasion, chosen based on microarray analysis.

- Investigation of genes up-regulated at transcription level as a result of eIF4E and phosphorylation deficient eIF4Emut.

Several studies have related overexpression of eIF4E to disease progression in the lung (De Benedittis and Graff, 2004). A study of lung adenocarcinomas demonstrated that eIF4E expression was 3.4-7.4-fold higher than in normal lung and that its expression progressively increased in the following order: atypical adenomatous hyperplasia (lowest expression), bronchioloalveolar carcinoma, bronchioloalveolar pattern and minor invasion, and marked invasion (highest expression) (Seki *et al.*, 2002). Many of the known oncogenes and tumor suppressor genes enhance malignant transformation only after they are altered by mutation. However, many of the gene products that drive progression of the primary tumor to metastasis (e.g., MMPs, VEGF) are not altered by mutation but are inappropriately expressed (Sager *et al.*, 1997). Therefore, the formation of metastasis may involve more quantitative than qualitative alterations in the expression of key invasion/metastasis-associated genes, and translation of these proteins is primarily regulated by eIF4E (Graff and Zimmer, 2003).

DLKP is a poorly differentiated, human lung squamous cell carcinoma cell line (Law *et al.*, 1992) which has previously been used as a model to investigate the role of eIF4E in early lung development and carcinogenesis here at the National Institute for Cellular Biotechnology (NICB). Walsh *et al.* (2003) looked at the role of eIF4E in regulating the translation efficiency of differentiation-related mRNAs during early development. They found that increased levels of differentiation correlated with increased phosphorylation of eIF4E. Continuing on from this study, the effects of up-regulation of eIF4E and its phosphorylation-deficient mutant, eIF4Emut, on DLKP cells were examined (Power, PhD thesis, NICB, 2005). This study found through proteomic analysis, that phosphorylation of eIF4E was important for the translation of specific proteins. It also suggests that overexpression of both eIF4E and eIF4Emut increased the level of invasion of DLKP, and that phosphorylation of eIF4E did not influence invasion. The present study was designed to confirm the results in a large range of DLKP transfected clones, and to investigate if eIF4E overexpression would have the same effect in a different cell model. MCF7, a non-invasive, epithelial-like, breast adenocarcinoma cell line was chosen for this purpose. Several studies have demonstrated the overexpression of eIF4E in breast cancer (Li *et al.*, 1998a; McClusky *et al.*, 2005; Byrnes *et al.*, 2006). The most recent of which showed overexpression of eIF4E had poor clinical outcome in stage I to III breast cancer, where outcome endpoints were cancer recurrence and cancer-related death (Byrnes *et al.*, 2006). The same study showed correlation between eIF4E overexpression and increasing levels of vascular endothelial growth factor (VEGF), which plays an important role in angiogenesis and invasion in breast cancer (Skobe *et al.*, 2001).

Several eIF4E/eIF4Emut-overexpressing stable clones were established, and none of them were found to have any increase in invasion (this was determined by level of cell invasion through Matrigel). In order to elucidate why overexpression of eIF4E did not result in a change in invasive phenotype of MCF7, and to enable identification of breast cancer cell specific invasion markers, it was necessary to make a comparison with an invasive MCF7 cell line. MCF7H3erbB2 was chosen for this purpose. This cell line is a clonal subpopulation of MCF7H3 (MCF-7 H3 is a clonal population isolated from MCF7 by Dr. Finbar O'Sullivan (NICB)) transfected with erbB2 and was established at the NICB by Dr. Sharon Glynn. This cell line proved highly invasive after stable expression of erbB2.

The epidermal growth factor (EGF) family of tyrosine kinase receptors (ErbB1, -2, -3 and -4) and their ligands are involved in cell differentiation, proliferation, migration, and carcinogenesis. Overexpression of erbB2 in vitro and in animal studies has been shown to play a role in oncogenic transformation and tumourigenesis (Slamon *et al.*, 1989; Colomer *et al.*, 2001). However, it has proven difficult to link a given erbB receptor to a specific biological process since most cells express multiple erbB members that heterodimerize, leading to receptor cross-activation. In erbB2 homodimerisation results in ubiquitin tagging and rapid digestion by the cell, whereas heterodimerization results in a lower rate of digestion and a higher rate of receptor recirculation. Overexpression of erbB2 on the cell surface appears to lead to constitutive activation of erbB2 homodimers without the need for ligand binding, resulting in unregulated cell growth and oncogenic transformation (Rowinsky, 2003). ErbB2 serves as a critical component that couples erbB receptor tyrosine kinases to the migration/invasion machinery of carcinoma cells. Stimulation of cells with EGF-related peptides resulted in increased invasion of the extracellular matrix, whereas cells devoid of functional ErbB2 receptors showed no change in invasion. ErbB2 facilitates cell invasion through extracellular regulated kinase (ERK) activation and coupling of the adaptor proteins, p130CAS and c-CrkII, which regulate the actin-myosin cytoskeleton of migratory cells (Spencer *et al.*, 2000).

eIF4E translation of complex mRNAs, in particular oncogenes, has previously been associated with cancer progression, and is also involved in the translation of erbB2 protein (Yoon *et al.*, 2006). erbB2 can also control the amount of eIF4E available for translation by activating the Akt/mTOR signalling cascade. In this way, eIF4E and erbB2 are involved in a positive feed-back loop (Figure 4.1). Both eIF4E and erbB2 have individually been associated with invasion and metastasis, and this thesis attempts to look at their relationship with each other, and the influence of this relation on an invasive phenotype *in vitro*. This thesis further strengthens this relationship by showing genes differentially expressed in an invasive erbB2-overexpressing cell line also effect the invasive phenotype of an eIF4E-overexpressing cell line. Many of these genes function as part of the Akt or ERK signalling pathways, both of which can be activated by erbB2.

Figure 4.1 erbB2/eIF4E positive feedback-loop

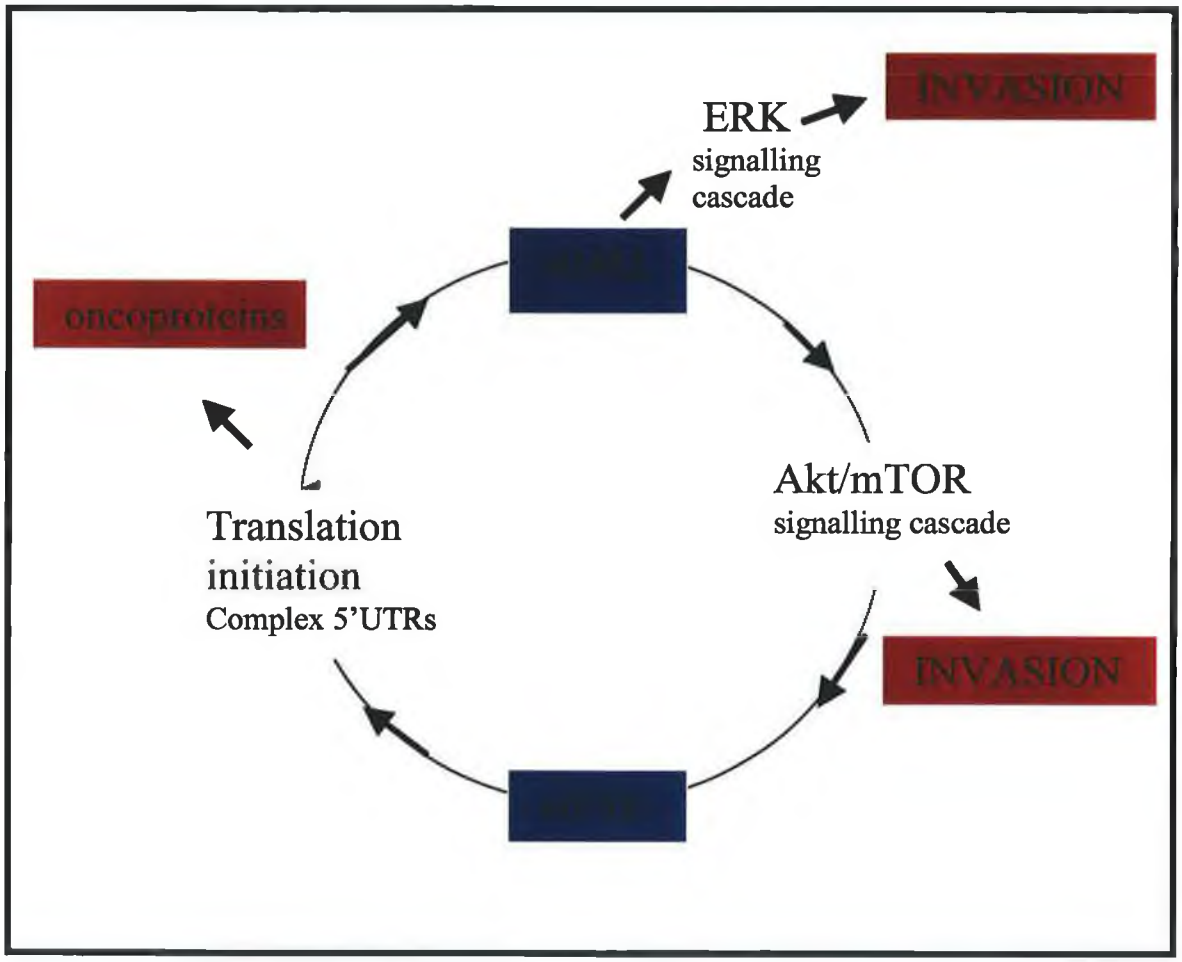

Figure 4.1: Relationship of eIF4E with erbB2. erbB2 regulates eIF4E through the Akt signalling pathway, eIF4E in turn up-regulates erbB2 at a translational level. Both are involved in the ERK and Akt signalling pathways, the deregulation of which has been associated with invasion.

4.2 Phenotypic effects of overexpression of eIF4E

4.2.1 The effect of eIF4E on proliferation of MCF7 and DLKP cells

MCF74E and MCF74Emut cells showed a marked increase (100%) in proliferation compared to the parent and pcDNA-transfected MCF7 (Section 3.1.5). Growth rate of DLKP4E and DLKP4Emut was increased by 66% and 25% respectively (Section 3.2.5). An earlier report showed the pattern of eIF4E phosphorylation varied throughout the cell cycle, with the lowest levels in G0, increasing throughout G1 and S, but was reduced in M phase (Bonneau and Sonnenberg, 1987). eIF4E is believed to play a significant role in proliferation, the disruption of which often leads to oncogenic transformation (Flynn and Proud, 1996a). eIF4E is phosphorylated in many systems in response to extracellular stimuli, but biochemical evidence to date has been equivocal as to the biological significance of this modification. The 4Emut clone used in this work has been transfected with eIF4E where serine 209 has been replaced by alanine to prevent phosphorylation. Therefore, results showed that phosphorylation of eIF4E did not affect the rate of proliferation in MCF7, but did in DLKP cells. Originally it was believed that phosphorylation of eIF4E at Ser-209 occurs as part of the eIF4F complex (Tuazon *et al.*, 1990), greatly enhancing and stabilising its association with the cap structure (Minich *et al.*, 1994; Joshi *et al.*, 1995), and increased levels of eIF4E phosphorylation and its association with eIF4G have been directly correlated with the enhancement of translation which follows mitogenic stimulation of mammalian cells (Morley, 1997; Gingras *et al.*, 1999; Raught *et al.*, 2000). More recent studies demonstrated phosphorylation was not required for protein synthesis in vitro and in vivo (McKendrick *et al.*, 2001). It was found that both wild type and mutant (Ser209→Ala) eIF4E interacted equally well with eIF4G, and both were capable of rescuing a lethal phenotype of eIF4E deletion in *S. cerevisiae*. Slepenkov *et al.* (2006) have recently proposed that phosphorylation of Ser-209, which is located at the entrance to the cap-binding slot, diminishes the rate of association by charge repulsion but has no effect on the rate of dissociation (Slepenkov *et al.*, 2006). Another recent report saw no significant difference between nontransformed cells and carcinoma cell lines with regard to the phosphorylation status of eIF4E (Avdulov *et al.*, 2004). However, a study carried out using *Drosophila melanogaster* provided evidence that eIF4E phosphorylation is biologically significant and is essential for normal growth and

development *in vivo* (Lachance *et al.*, 2002). Results obtained from MCF74E and MCF74Emut suggest that phosphorylation of eIF4E was not essential for growth, whereas DLKP results show an increase in proliferation of DLKP4E compared to DLKP4Emut. Our results are in line with a model, consistent with this recent literature, in which eIF4E phosphorylation is not essential for translation initiation as stimulation of proliferation, but in which phosphorylation does play a role in the efficiency/magnitude of eIF4E targeted effect depending on the precise cellular background. It may be possible that in some situations, eIF4E binding to the cap is 'rate limiting'.

4.2.2 Effect of eIF4E on anchorage-dependence of MCF7 cells

After MCF74E and 4Emut cells were observed growing both in suspension and attached in the same flask, further studies were carried out to examine the level of anchorage-independent growth in these cell lines. The parental MCF7 cells have previously been observed to form numerous large colonies after 2 to 4 weeks of growth in soft agar, indicating that like most transformed cells they do not have an essential requirement for a matrix-derived survival/growth signal (Fiucci *et al.*, 2002; Finlay *et al.*, 1993). The colony forming efficiency (CFE) calculated over a 10-day growth period showed an increase in all lines examined (MCF74E, MCF74Emut and MCF7pcDNA) compared to the parent (Section 3.1.6.2). The largest increase was seen in MCF74E, with a 1.6 fold increase in CFE compared to MCF7. The CFE of MCF74Emut increased by 1.3 fold, but this increase was also achieved by MCF7pcDNA. This may have been a background effect of geneticin selection, which has been known to confer resistance to apoptosis. However, the difference in CFE between MCF7eIF4E and MCF7eIF4Emut clones also suggests that an inability of eIF4E to phosphorylate in these cells had an effect on anchorage-independent growth. Adhesion assays carried out on the same cells also showed eIF4E had a greater effect on adhesion of MCF7 than eIF4Emut or pcDNA. While MCF74Emut and MCF7pcDNA were 50-60% adherent after 60mins, MCF74E showed 0% attachment after the same time period (Section 3.1.6.1). Previous studies have provided evidence that overexpression of eIF4E in human mammary epithelial cells enabled clonal expansion and anchorage-independent growth (Avdulov *et al.*, 2004). Increased CFE of MCF74E showed that sustained increase of eIF4E expression caused an increase in anchorage-independent growth and colony forming efficiency, an *in vitro* event which is frequently associated with malignant transformation.

4.2.3 Effect of eIF4E on drug resistance of MCF7 and DLKP cells

Many chemotherapeutic agents induce apoptosis, and so disruption of apoptosis can promote drug resistance. The complex network of proliferation and survival genes that control apoptosis is frequently disrupted during tumour evolution. eIF4E is described as a potent oncogene *in vivo*, with lymphomas expressing eIF4E highly resistant to drug therapy, producing phenotypes consistent with anti-apoptotic genes (Wendel and Lowe 2004). eIF4E is capable of rescuing cells from Myc-dependent apoptosis by inhibiting the release of mitochondrial cytochrome *c* gene. Experiments achieving gain and loss of function demonstrate that eIF4E-mediated rescue is governed by pre-translational and translational activation of the anti-apoptotic bcl-xl, as well as by additional intermediates acting directly on, or upstream of, the mitochondria (Li *et al.*, 2003). The same group demonstrated in a later study that exogenous expression of eIF4E rescued cells from ER stress-induced apoptosis by mediating the blockade of calcium release from the ER to the cytosol and by preventing activation of caspase-12. This study provided evidence that the integration of critical organelle-mediated checkpoints for apoptosis could be controlled by the cap-dependent translation apparatus, eIF4F (Li *et al.*, 2004). In the present study, DLKP4E and DLKP4Emut were examined using taxol and adriamycin, and MCF74E and MCF74Emut with taxol and 5FU. Due to time constraints, the effects of adriamycin on MCF74E and MCF74Emut were not investigated, nor were 5FU effects examined in DLKP4E or DLKP4Emut.

4.2.3.1 Taxol resistance in DLKP4E/4Emut and MCF74E/4Emut clones.

Taxol is a microtubule antagonist capable of inducing cell-cycle arrest with minimum effect on protein synthesis. It works by binding to microtubules and inhibits their depolymerization into tubulin, therefore blocking the ability to break down the mitotic spindle during mitosis. With the spindle still in place cell division is not possible (Pratt *et al.*, 1984). Taxol has been shown to proceed independently of cell protective effects of PI3K and AKT (Mitsuuchi *et al.*, 2000).

The majority of MCF74E and MCF74Emut clones showed no change or a slight decrease in resistance compared to the parent, as did DLKP4E and DLKP4Emut. Therefore an increase in levels of eIF4E in MCF7 cells did not affect taxol drug resistance. This result is supported by a study by Greenberg and Zimmer, which established that initial chemotherapeutic treatment triggers a stress-related response,

which can lead to an increase in the expression of survival proteins. They found that taxol induced the phosphorylation of 4E-BP1 in the breast cancer cell line, MDA MB 231, which reduced its association with eIF-4E. It could therefore be assumed that taxol increases the functional level of eIF-4E by promoting the phosphorylation and release of 4E-BP1 (Greenberg and Zimmer, 2005). It is unlikely therefore that up-regulation of eIF4E would have any effect on resistance to taxol.

4.2.3.3 5FU resistance in MCF74E and MCF74Emut

eIF4E has been shown to play key roles in cell cycle control and is an important marker for determining chemosensitivity (Wendel and Lowe, 2004; Hartmann *et al.*, 2005). To further investigate the effect of over-expression of eIF4E in MCF7, toxicity assays were carried out on MCF7, MCF7eIF4E and MCF7eIF4Emut cells using 5-Fluorouracil (5FU) and Taxol. Fluorouracil is one of the most commonly used drugs to treat cancer. It is used in the treatment of many types of cancer including, breast, head and neck, colorectal, stomach, colon and some skin cancers. 5FU is part of a group of chemotherapy drugs known as the anti-metabolites, which work by interfering with the production of nucleic acids. It has previously been demonstrated that constitutive AKT levels are the lowest in cell lines that are the most resistant to 5-FU (Saxena *et al.*, 2005). AKT activation regulates mRNA translation via control of phosphorylation of 4E-BP1 and its dissociation from the mRNA cap binding protein elF4E (Cohen *et al.*, 2005). Therefore, 5-FU inhibits protein synthesis by reducing AKT signalling; preventing the phosphorylation of 4EBP1 and the release of eIF4E, therefore preventing eIF4E participation in translation initiation. eIF4E was found sufficient to replace AKT or p53 loss in myc-driven tumours, showing translation regulation can compensate for the AKT survival signal (Wendel and Lowe, 2004).

Based on this information, elevating levels of eIF4E within a cell might have been expected to cause resistance to 5FU. However, results here show the opposite, with MCF74E and 4Emut clones more sensitive to 5FU than the parent cell line (section 3.1.10). Our result suggests that the effect of eIF4E on pathways relevant to 5FU resistance are more complex then previously described in the literature. And so far remain to be fully elucidated.

4.2.3.4 Adriamycin resistance in DLKP4E and DLKP4Emut cells

Adriamycin is an anthracycline antibiotic isolated from *Streptomyces*. It is an intercalating drug that works via nonconvalent DNA-binding, thus disrupting transcription and translation and producing a cytotoxic, mutagenic and carcinogenic effect. However, lymphomas expressing eIF4E were shown to be highly resistant to adriamycin therapy relative to controls (Wendel *et al.*, 2004).

Results presented here show that stable expression of eIF4E and eIF4Emut in DLKP cells cause a fold increase in resistance to adriamycin. Gene expression profiles of adriamycin-resistant cells showed up-regulation of several genes that have been associated with eIF4E (Song *et al.*, 2006). These included p21 (Lazaris-Karatzas and Sonenberg, 1992), tumor necrosis factor superfamily member 7 (TNFSF7) (Wang *et al.*, 2006), programmed cell death 4 (PDCD4) (Kang *et al.*, 2002), proliferating cell nuclear antigen (PCNA) (Jin *et al.*, 2006), MMP-2 and TSP-2 (Van Trappen *et al.*, 2002). eIF4E has also been found to influence adriamycin drug resistance through overexpression of TLK1B, a nuclear serine/threonine kinase that is potentially involved in the regulation of chromatin assembly and is capable of repairing double strand breaks. TLK1B mRNA contains a 5'UTR 1088-nt long with two upstream AUG codons, which was found to be very inhibitory for translation. This inhibition of translation could be relieved by overexpressing eIF4E. TLK1B overexpression protects cells from the genotoxic effects of ionizing radiation (IR) or adriamycin, which is a radiomimetic drug. Therefore it is clear form the literature that there are many ways in which overexpression of eIF4E could influence adriamycin drug resistance. The specific mechanism involved in adriamycin resistance in DLKP4E and DLKP4Emut is unknown, but it is clear from the results that overexpression of eIF4E is involved.

4.2.4 Effect of eIF4E on the invasive status of MCF7 and DLKP cells

To form metastases, individual tumour cells must break from the primary tumour mass, degrade extracellular matrix, invade the surrounding normal tissue, enter the blood or lymphatic circulation, exit the circulation at a distal tissue and establish satellite colonies within this new tissue environment. This aberrant behaviour of cancer cells requires the cooperative function of numerous proteins; those that facilitate angiogenesis (e.g. VEGF), cell survival (e.g. Bcl-2), invasion (e.g. MMPs), and autocrine growth stimulation (e.g. c-myc, cyclin D1). Although expression of these proteins is regulated at many levels, translation of these key malignancy-related proteins

is regulated primarily by the activity of eIF4E (Graff and Zimmer, 2003). This is because the above mRNA contains long, G-C-rich 5'UTRs which are capable of forming stable secondary structures and upstream AUGs, and therefore are dependent on the presence of eIF4E for efficient translation. Many of the gene products that drive metastasis are not altered by mutation, but by altered patterns of gene expression. Therefore it is the quantity not the quality of key genes that drive the metastatic program (Graff and Zimmer, 2003). Not surprisingly, eIF4E is elevated in most solid tumours, contributing to metastatic progression by selectively upregulating the translation of key malignancy-related proteins that together conspire to drive the metastatic process.

It has long since been established that eIF4E plays a critical role in breast cancer (Kerekatte *et al.*, 1995; Byrnes *et al.*, 2006). A marked increased in eIF4E in vascularized malignant ductiles of invasive breast carcinomas has been reported (Nathan *et al.*, 1997), and recent studies have shown direct correlation between invasion and eIF4E in breast cancer cells (Yoon *et al.*, 2006). However, stable expression of the eIF4E and eIF4Emut plasmids alone was not sufficient to cause a change of the invasive phenotype of non-invasive MCF7 (Section 3.1.8). DLKP on the other hand, changed considerably after eIF4E transfection (Section 2.3.6). At a 200X magnification the average number of invading cells was 20/per field in DLKP parent, whereas for DLKP4E and DLKP4Emut clones the average count ranged from 40 to 160 cells per field. This result concurs with previous studies, which have associated eIF4E with increased invasiveness and metastasis of the lung (Graff *et al.*, 1995; Seki *et al.*, 2002).

Why then did eIF4E produce a different effect in MCF7 and DLKP? Microarray analysis of eIF4E and eIF4Emut clones compared to the parent MCF7 and DLKP showed lists of genes differentially expressed when clones were compared to parents. Looking at the eIF4E clones alone, of those changes specific to DLKP4E, almost 900 genes appeared that were not differentially expressed in MCF74E. Likewise, over 200 genes differentially expressed in MCF74E did not change significantly in DLKP4E. Without any further analysis it is clear from this observation alone that eIF4E overexpression has a very different effect on DLKP and MCF7. Combined with the different phenotypic effects of eIF4E in both cell lines, these gene lists point to an invasion mechanism specific to eIF4E in DLKP cells.

4.3 Microarray analysis of DLKP-& MCF7-4E/4Emut stable clones, and MCF7H3 -erbB2

Microarray analysis was used to further examine the impact of eIF4E on transcription in both DLKP and MCF7 cell lines. In particular, one aim of this analysis was to identify genes involved in the invasion process in both DLKP and MCF7. As eIF4E was unable to induce invasion in MCF7, it was important to include an invasive MCF7 cell line. MCF7H3erbB2 was chosen for this purpose. Genes differentially expressed in relation to eIF4E up-regulation were identified by comparing MCF7 parent to MCF74E and MCF74Emut. Genes related to invasion and MCF7 were identified by a MCF7H3 / MCF7H3erbB2 comparison. Further analysis of the MCF7H3erbB2 and MCF7/4E/4Emut gene lists resulted in the identification of invasion-associated gene lists.

Genes differentially expressed in DLKP4E and DLKP4Emut compared to the DLKP parent were related to eIF4E overexpression and invasion, since both DLKP4E and DLKP4Emut are invasive. The end result was two lists of genes, associated with invasion in DLKP and MCF7. In addition, these genes were analysed using software that demonstrated their relationship to each other or a known pathway, based on existing literature.

There are several examples in the literature of microarray analysis as a tool for identifying invasion-associated genes, either by analyzing large numbers of clinical samples or by comparing metastatic and non-metastatic cells in experimental systems. Combination of these studies has resulted in a panel of genes whose expression is linked to the spread of cancer. Some of these studies provided evidence that model cell lines of varying invasiveness and confirmed *in vivo* metastatic properties, evaluated by the cDNA microarray method, constitutes a powerful system to identify invasion- or metastasis-associated genes (Chen *et al.*, 2001; Bai *et al.*, 2006). Resulting data demonstrated the diversity of genes involved in the underlying cellular process of cancer invasion/metastasis, with genes related to cell adhesion, motility, angiogenesis and signal transduction identified as potential participants in the invasion process. Correlation of gene expression patterns in primary tumours with clinical outcome has led to the identification of some genes with cell motility functions whose expression correlates in some way with metastasis (Van't Veer *et al.*, 2002; Ramaswamy and Perou, 2003; Wang *et al.*, 2002). It is encouraging that deregulation of many of the

genes identified in these microarray studies have been demonstrated by traditional, low-throughput immuno-histochemical methods.

4.3.1 Normalisation and Quality control of microarray experiments

Data collected from microarray experiments are random snapshots with errors, noisy and often incomplete. Variability caused by several factors in the fields of experimental design, experimental setup, image analysis and data analysis, disguises actual differences in signal intensities and highlights the necessity for quality control. In order to compare gene expression results from experiments performed using multiple chips, it was necessary to normalise the data obtained following scanning. The purpose of data normalisation was to minimise the effects of experimental and technical variation between microarray experiments so that meaningful biological comparisons could be drawn from the data sets and that real biological changes could be identified. After normalisation all data from microarray chips went through several QC steps, and once satisfactory the data was examined using hierarchical clustering.

Unsupervised hierarchical clustering grouped samples together based on similar expression levels of the genes analysed by the microarrays, and therefore was used to represent the relationship between replicate samples and different sets of replicate samples. Each cell line used in the study was run in triplicate, and it would be expected that biological triplicates should cluster together, and all such clusters be significantly differently from each of the other clusters. First, it is interesting to note that all of the DLKP cell lines, parent and clones, clustered together, as did the MCF7 cell lines. This proved that these particular cell lines retain a similar pattern of expression despite transfection and clonal variation, which would have been expected. Most importantly, this QC step proved crucial in the analysis as it identified three cell lines with biological replicates that did not cluster. DLKP2, DLKP4E2 and MCF74E2 did not behave as expected and did not cluster with their replicates. The percentage of genes present relative to the number of genes present on the array is typically 40-60%, which relates to approximately 25-30,000 gene transcripts. Three microarray chips were run for each cell line used in this experiment, and the resulting data compared based on their degree of similarity. That is, each set of gene transcripts 'present' on each chip were compared to each other set, to find similar genes. A correlation coefficient, generated by dChip for each sample, measured the amount of variation between groups of genes in replicate samples. The closer this coefficient was to 1, the stronger the linear relationship. If any

one of the samples did not correlate and a list of genes was chosen from the comparison of all three, this would have increased the number of false negatives, and as a result a lot of important genes may be overlooked. On the other hand, removing the rogue sample would increase the number of false positives. It was vital that the 'present' call for each sample was accurate in order to ensure an exact comparison between samples. The accuracy with which the percentage of transcripts present was calculated was dependent on stringent physical QC. Because results showed a poor linear relationship for these samples within their biological triplicate, it was decided to continue with three sets of two rather than repeat the arrays for DLKP, DLKP4E and MCF74E.

This was a surprising result as great lengths had been taken to ensure that all biological replicates were treated in the same way prior to RNA extraction and microarray processing. Due to the sensitivity of microarray analysis all cell culture conditions including media, incubation and cell number were the kept the same for all samples. Despite this, it is clear that some event occurred that brought about 'drift' in gene expression within certain cells, significant enough to produce a different microarray profile. DLKP is a mixed population of cells, and over a number of passages a different sub-population could have inadvertently been selected. The reason as to why MCF74E and DLKP4E did not cluster is more difficult to explain, as both were clonal populations.

4.3.2 Selection of differentially expressed MCF7H3erbB2 genes for further analysis

The first step in analysis of microarray data was to identify differentially expressed genes. These are genes whose expression levels were significantly different between two cell lines. In all initial gene list comparisons, samples were assigned to two groups, e.g. DLKP1, 2 &3 =group A and DLKP4E1, 2 & 3=group B. P-value and fold change are the most common parameters utilised to generate gene lists from microarray experiments. The most important factor for consideration is the p-value. Before considering the significance of this value, one must first consider that all statistical hypothesis tests are based on the concept of comparing a test statistic to a pre-hypothesised value, or null-hypothesis. The null hypothesis is an assumption made about the data before the comparison. In the present study, the null-hypothesis was the assumption that the average level of expression in of a particular gene in group A was the same as the average level of expression in group B. Expression level in relation to microarray results is the level of intensity of a particular probe. This in turn is related to

the amount of that probe which bound to the target gene, and therefore the level of expression of that gene. This intensity is given a numerical value, calculated by a dChip algorithm and represents the level of expression of the gene. In order to establish if the mean expression level in A was significantly different to B, the observed t-statistic for each gene was calculated (using dChip). The t-statistic measured the distance between samples in units of standard deviation. The p-value measured the probability of observing a value of the test statistic (t-statistic) at least as extreme as that observed *if* the null-hypothesis was true. Therefore the lower the p-value, the greater the likelihood that the null-hypothesis is NOT true, and that the samples are significantly different. The limitation of p-value is if expression levels for a gene are very high or very low, the amount of background noise is increased, and this affects the accuracy of statistical analysis.

Fold change was also considered when filtering genes. The shortcoming of this parameter is that there is a bias towards genes that are expressed at very low levels in the parent samples, and "turned on" in the experimental samples. For example, when looking at genes with differential expression across DLKP4E and DLKP4Emut compared to DLKP, the genes hypothetical protein FLJ14503 and RPS6KA3 have similar fold-change of 1.67 and 1.69, respectively. However, for hypothetical protein FLJ14503 the average intensity difference is 181.17, but for RPS6KA3 it is 534.91. The result for hypothetical protein FLJ14503 is still significant, but less so than RPS6KA3. For this reason, it was important to consider difference of mean (of normalised expression levels) when filtering genes. Genes that were differentially expressed were uncovered using parameters of p-value of ≤ 0.05, fold change of 1.2, and normalised expression level > 100.

The end result of the gene list comparison was two gene lists, one comprised of 240 genes differentially expressed in both DLKP4E and DLKP4Emut compared to DLKP parent. The other was MCF7H3erbB2 specific genes, differentially expressed compared to parent MCF7H3, and not expressed in non-invasive MCF7 cell lines (MCF7pcDNA, MCF74E and MCF74Emut). This list consisted of 120 genes. It is important to note that in order to filter down possible targets for further analysis to a controllable quantity, many other potentially interesting genes were discarded.

4.3.3 Genes related to invasion and specific to MCF7H3erbB2

The final list of 120 genes specific to MCF7H3erbB2 and invasion contained some overlap due to different probe sets targeting various gene transcripts. Further examination found there were 108 different genes on this list. Literature searches found 39 of these genes were related to invasion, or processes relevant to invasion. This was 36% of the total list, which supported the relevance to invasion of our microarray and follow-up bioinformatics analysis, the purpose of which was to identify invasion-specific genes. It was also a strong indication that many other genes on the list may be related to the invasion process, although this is not currently reflected in the literature. It seemed plausible that a pathway that existed within a group of genes already chosen based on their association with an invasive phenotype, was most likely an invasion-relevant pathway. This information could, in turn, lead to the discovery of novel genes and/or pathways associated with invasion/metastasis. Pathway Assist® was then used to identify what genes, if any, had direct biological interaction with each other, or previously annotated pathways. Pathway Assist® generated this list based on relationships between genes previously demonstrated in the literature. Pathway Assist® is equipped with a comprehensive database that gives a snapshot of all information available in PubMed, with the focus on pathways and cell signalling networks. Of the 108 genes specific to MCF7H3erbB2 and related to invasion, 9 were found to have direct biological interaction with each other (Table 3.3.12). Further literature searches related this pathway to thrombospondin (THBS1). Although THBS1 was not present on the final gene list, it provided a link between the MCF7H3erbB2 9-gene pathway and tissue factor pathway inhibitor (TFPI). TFPI was significant because of its considerable fold change (+19.77). Pathway Assist © showed that THBS1 was not only associated with TFPI, but also with early growth response 1 (EGR1) and phosphatase and tensin homolog (PTEN), both of which were on MCF7H3erbB2 the 9-gene pathway.

The relationships between genes as determined by Pathway Assist©, was demonstrated using 'controls'. These showed MAP3K1 was involved in the regulation of RPS6KA3 (Shelton *et al.*, 2003), ESR1 (Lee and Bai, 2002) TNFAIP8 (Aggarwal *et al.,* 2006) and TANK (de Martin *et al.*, 2000). It also showed MAP3K1 was capable of binding TANK (Pisegna *et al.*, 2004). RPS6KA3 was shown to be involved in regulation of ESR1, and ESR1 in turn was found to effect RPS6KA3 expression (Clarke *et al.*, 2001). PTEN was found to regulate TNFAIP8 (Panner *et al.*, 2005). Results indicated both positive and negative regulation, probably a reflection of the opposing functions of the TNF family

(Idriss and Naismith, 2000). EGR1 positively regulated PTEN (Baron et al., 2006), and was itself bound by EGR3 (O'Donovan *et al.*, 1999) and positively regulated by ESR1 (Pratt *et al.*, 1998). Further examination of the literature found two members of this pathway, PTEN and EGR1, interacted with thrombospondin 1 (THBS1) (Wen et al., 2001; Shingu and Bornstein, 1994). This gene was not present on the final list of 108 genes, but was on the original list of MCF7H3 versus MCF7H3erbB2, with a fold change of – 2.31. What was most interesting about this gene was it linked the MCF7H3erbB2 9-gene TFPI, the gene with the greatest increase of expression (19.77 fold) on the final list of genes. TFPI was chosen as a target for siRNA silencing based on its large fold change, and THBS1 was chosen because of its association with TFPI. THBS1 was the only target chose which was down-regulated in association with an invasive phenotype.

4.3.4 Limitations of Pathway Assist® analysis

Pathway Assist® was useful in assisting in the interpretation of Microarray analysis as it allowed visualisation of results in the context of pathways and networks, gene regulation networks and protein interaction maps. However, many of the 'direct interaction' as indicated by Pathway Assist® were based on two of the chosen genes appearing in the same publication, which did not always mean they were capable of biological interaction. 'Direct interactions' did not always refer to the two genes from the pathway, but with a gene or family of genes which was associated with the chosen gene. Therefore it was important that all literature referenced by Pathway Assist® was checked before proceeding with a target based on this characterisation. Despite this, this software did give an indication of the interaction between genes, which in most cases could be associated as indicated, if not directly, then through signalling-pathways associated with 'directly interacting' genes.

4.3.5 MCF7H3erbB2 invasion specific genes chosen for further analysis

Five genes in all were chosen for siRNA silencing based on specificity to MCF7H3erbB2 and invasion, association with tissue factor pathway inhibitor (as indicated by PathWayAssist®), and relevance to cancer/invasion in the literature (Table 4.1). Fold change represents the fold difference between expression in the parent MCF7H3, and MCF7H3erbB2.

Table 4.1 Genes specific to MCF7H3erbB2 and related to invasion chosen for further analysis

Gene	Description	Fold Change	Mean Expression Difference
TFPI	Tissue factor pathway inhibitor (lipoprotein-associated coagulation inhibitor)	+19.77	406
TNFAIP8	tumor necrosis factor, alpha-induced protein 8	+2.47	299
RPS6KA3	ribosomal protein S6 kinase, 90kDa, polypeptide 3	+2.36	299
EGR1	early growth response 1	+2.23	950
THBS1	thrombospondin 1	-2.31	-322

4.3.5.1 Tissue factor pathway inhibitor (TFPI)

Tissue factor pathway inhibitor (TFPI) is an endogenous anticoagulant protein of the serine protease family TFPI comprises of three Kunitz type domains flanked by peptide segments; an N-terminal acidic region followed by the first Kunitz domain (K1), a linker region, a second Kunitz domain (K2), a second linker region, the third Kunitz domain (K3), and the C-terminal basic region. The K1 domain inhibits factor VIIa complexed to tissue factor (TF) while the K2 domain inhibits factor Xa. TFPI binds and inactivates Factor Xa (FXa) in an inhibitory complex (FXa–TFPI), which then binds and inactivates tissue factor (TF) and Factor VIIa (FVIIa) (Rapaport and Rao, 1995). No direct protease inhibiting functions have been demonstrated for the K3 domain. Importantly, the Xa-TFPI complex is a much more potent inhibitor of the VIIa-TF than TFPI by itself (Bajaj *et al*, 2001). The third Kunitz domain and the C-terminal basic region of the molecule have heparin-binding sites (Kato, 2002). TFPI is the only protease inhibitor known to down regulate TF procoagulent activity at physiologically significant rates. Once bound to TFPI, the TF/VIIa complex is much less likely to dissociate back to TF and VIIa. Within the cell the TFPI-TF-VIIa complex dissociates after 12hours. TF and TFPI are recycled but 75% of the VIIa is degraded. Once bound to TFPI, the TF-VIa complex is much less likely to dissociate back to TF and VIIa (Broze, 1995).

TFPI is mainly produced by microvascular endothelial cells and pooled in the endothelium (50-80%), plasma (10-15%) and platelets (<2.5%) (Werling *et al.,* 1993; Novotony *et al.,* 1989; Sandset, 1996). The free TFPI fraction in plasma, although constituting only 10–20% of total plasma TFPI, carries most of the TFPI anticoagulant

activity (Lindahl *et al.*, 1991). Cancer cells may express TF and FX activator, which produce FXa, an activator of coagulation; this may explain why most cancer patients exhibit signs of hypercoagulation (Iversen and Abildgaard, 1998). TF is thought to initiate the extrinsic pathway of coagulation, with collagen playing the same role in the intrinsic pathway (Price *et al.*, 2004). Therefore TFPI inhibition of TF shifts coagulation from the extrinsic to the intrinsic pathway. The precise mechanism responsible for the elevation of TFPI is unknown, however down-regulation of extravascular TF initiated coagulation by TFPI is thought to involve the release of TFPI from activated platelets, or the transfer of endothelial associated TFPI to the extravascular space (Mast *et al.*, 2000). Present in plasma, TFPI exists both as a full-length molecule and as a variably carboxy-terminal truncated forms, and is also circulated in complex with plasma lipoproteins (Lwaleed and Bass, 2006). Optimal inhibition of extrinsic coagulation is obtained by the full-length molecule, while the truncated form can bind other surface receptors such as very low-density lipoprotein (VLDL) receptor (Hamik *et al.*, 1999). Independent of its fVIIa/TF inhibitory activity, TFPI also displays antiproliferative activity which results from association with the very low-density lipoprotein (VLDL) receptor (Todd *et al*, 2001).

High plasma levels of TFPI have been reported in cancer patients with solid tumours, whereas those with leukaemia and related blood malignancies have normal levels of TFPI (Lindahl *et al.*, 1989, 1992; Iversen *et al.*, 1998). However, the theory that high TFPI levels in cancer were a consequence of activated coagulation was disproved by Inversen (1998) who demonstrated there was no correlation between the two. It was concluded that TFPI was related to the biology of the disease rather than the degree of coagulation (Inversen *et al.*, 1998). Microarray results showed a 19.77 fold increase of TFPI in invasive MCF7H3erbB2 compared to non-invasive parent MCF7H3. With mean expression values increasing from 21 to 428, this implies that after erbB2 overexpression, TFPI was essentially 'switched on'. This agrees with previous work that shows elevated levels of TFPI have been found in breast cancer, (Erman *et al.*, 2004). It has also been found that TFPI levels correlate with cancer progression (Lindahl and Sandset, 1992; Lindahl *et al.*, 1993). This evidence combined with results from the microarray analysis of MCF7H3erbB2 strongly link TFPI to the invasion process. Despite this no function effect of TFPI has been published in relation to invasion.

4.3.5.2 Early growth response 1 (EGR1)

Early growth response 1 (EGR1), is an 80- to 82-kd protein consisting of 533 amino acids. EGR1 is inducibly expressed in many different cell types; among the vascular cells known to express EGR1 are endothelial cells, smooth muscle cells, fibroblasts, and leukocytes (Silverman and Collins, 1999). It acts as a transcriptional regulator that activates genes involved in differentiation and mitogenesis. The EGR1 gene is a transcription factor that acts as both a tumour suppressor and a tumor promoter. Analysis of certain human tumour cells and tissues has indicated that EGR1 exhibits prominent tumour suppressor function. Many human tumor cell lines have been shown to express little or no EGR1 in contrast to their normal counterparts, and furthermore, EGR1 is decreased or undetectable in small cell lung tumors, and human gliomas (Krones-Herzig *et al.*, 2005). Re-expression of EGR1 in these human tumor cells inhibited transformation. Paradoxically, EGR1 is oncogenic in prostate cancer (Eid *et al.*, 1998), where up-regulation of EGR1 is associated with down-regulation of PTEN and p53. It has been suggested that these defects in the suppressor network allow for the unopposed induction of transforming growth factor β1 (TGFβ1) and fibronectin, which favor transformation and survival of prostate tumor epithelial cells, explaining the role of EGR1 in prostate cancer (Baron *et al.*, 2006).

Because of its role in proliferation, up-regulation of other oncogenes may induce transcription of EGR1, and thereby elevate the expression of genes involved in growth, proliferation, apoptosis and angiogenesis. Mutant p53 has been found to induce EGR1, enhancing transformation and resistance to apoptosis (Weisz *et al.*, 2004). Several groups have demonstrated how mutant p53 can facilitate the transcription of transformation-related genes, and various p53mutants have been found overexpressed in human tumours (Hussain and Harris, 1998). Weisz *et al.*, (2004) showed mutant p53, through EGR1, could facilitate the up-regulation of VEGF expression. Bcl2 (Huang *et al.*, 1997), fibronectin (Liu *et al.*, 2000) and nuclear factor kB (NFkB) (Cogswell *et al.*, 1997), all of which are associated with differentiation and cell survival, and VEGF and tissue factor, both of which are involved in angiogenesis, are regulated by EGR1. In head and neck squamous call carcinoma hepatocyte growth factor/scatter factor (HGF), which has been found to play a significant role in invasion/metastasis (Vande Woude *et al.*, 1997), induces expression of EGR1 through the MEK and AKT signaling pathways. This up-regulation of EGR1 in turn results in transcriptional activation of platelet-derived growth factor (PDGF) and vascular endothelial growth factor (VEGF). This

may explain how HGF contributes to the mediation of angiogenesis (Worden *et al.*, 2005).

EGR1 has been found differentially expressed in breast cancer in some reports (Bertucci *et al.*, 2002; Bièche *et al.*, 2004), and undetected in breast tumours in others (Krones-Herzig *et al.*, 2005). However, there is evidence that EGR1 levels are influenced by the estrogen receptor (ER) status of a cell, and a recent report has shown EGR1 is deleted in an ER negative human breast carcinoma (Ronski *et al.*, 2005). Other studies have shown that in ER positive cells induce expression of EGR1 through activation of Raf-1 kinase (Pratt *et al.*, 1998). Microarray results for MCF7H3erbB2 showed a down regulation of ER and up-regulation of EGR1, which suggested ER did not play a part in EGR1 up-regulation in this system. However, further examination of microarray results showed expression levels of ER were still high, even in MCF7H3erbB2, with average expression values being 1370, as opposed to MCF7H3 values of 1850. These results support the idea that EGR1 is induced by ER expression, and support work done by Ronski *et al.*, (2005).

Array results showed expression of EGR1 in MCF7H3 to be 700, increasing to 1700 in MCF7H3erbB2. This increase in expression could have been due in part to erbB2-overexpression. There is evidence that activation of the ras/MAP kinase pathway is important in erbB2 signal transduction, and an increases in MAP kinase activity of erbB2-overexpressing human breast cancer cells is associated with enhanced transcription of the EGR1 (Reese and Slamon, 1997). The complex mechanism controlling regulation of EGR1 between non-transformed and chronically transformed cells is not yet understood, and EGR1 seems to be equally involved in regulation of tumour-suppressors (Huang *et al.*, 1997; Baron *et al.*, 2006) and mechanisms involved in tumour progression (Fudge *et al.*, 1994; Toretsky and Helman, 1996). EGR1 was found differentially expressed in MCF7H3erbB2, and the level of expression increased 2.23 fold compared to MCF7H3. EGR1 was also identified by pathway assist as having direct interaction (based on information available in the literature) with eight other genes differentially expressed in MCF7H3erbB2. Combined with evidence in the literature that suggest a role for EGR1 in invasion, these results provide a strong argument in favour of EGR1 as a pro-invasion gene in MCF7H3erbB2.

4.3.5.3 p90 Ribosomal S6 Kinase, polypeptide 3 (RPS6KA3)

p90 ribosomal S6 kinase polypeptide 3 (RSK2)(RPS6KA3)($p90^{rsk}$) is one of the four $p90^{rsk}$ family genes (RSK1 to RSK4), it maps to Xp22 and encodes a 90 kDa ribosomal S6 serine/threonine kinase (Guimiot *et al.*, 2004). The RSK genes are a subfamily of mitogen-activated protein kinase-activated protein kinases (MAPKAPKs) (are downstream effectors of mitogen-activated protein kinase (MAPK) (Zhao *et al.*, 1996) that contain two distinct kinase catalytic domains in a single polypeptide chain. The four mammalian isozymes of ribosomal S6 kinase, which are encoded by separate genes are phosphorylated and activated *in vivo* by extracellular signal-regulated kinase (ERK) (Smith *et al.*, 1999) and 3-phosphoinositide-dependent protein kinase 1 (PDK1) (Jensen *et al.*, 1999). Recent work looking at adult human tissue using northern blots showed RPS6KA3 was expressed in several tissues, with strongest expression in skeletal muscle, cerebellum, the occipital lobe and the frontal lobe (Zeniou *et al.*, 2002).Of the four RSK isoforms identified, evidence suggests that RPS6KA3 may play the most important role in gene regulation. Previous studies have shown that RPS6KA3 can regulate gene expression by effecting chromatin remodelling through phosphorylation of histone H3 (Sassone-Corsi *et al.*, 1999). Although the mechanism of RPS6KA3 activation has been the subject of many studies, little progress has been made in understanding its biological function.

Protein phosphorylation, catalysed by protein kinases, is a ubiquitous, intracellular post-translational modification found in eukaryotes and prokaryotes. The state of protein phosphorylation is controlled by the relative activity of two families of enzymes with opposing actions. These are the protein kinases and the protein phosphatases. Reversible protein phosphorylation is involved in the regulation of diverse biological processes such as proliferation, apoptosis, differentiation and metabolism (Cohen, 2002). Eukaryotic protein kinases can be categorised into two categories based on their target amino acids: protein tyrosine kinases and protein serine/threonine kinases. Modification of serine and threoinine residues is much more prevalent compared with tyrosine phosphorylation (Hanks and Hunter, 1995).

RPS6KA3 was found to be up-regulated (2.36 fold) not only in the final list for MCF7H3erbB2-invasion specific genes but also in the final list for DLKP4E-invasion specific genes (1.67 fold change), and therefore stood out as a potential marker for invasion. Though RSK family mechanism of action has been the subject of many studies, few have examined their biological function. Using a specific inhibitor for the

RSK family, it was discovered that they played an important role in proliferation, and gene-silencing of RPS6KA3 (RSK2) using RNAi resulted in a 57% decrease in proliferation of MCF7 cells (Smith *et al.*, 2005). A similar study carried out using a prostate cancer cell line confirmed these results (Clarke *et al.*, 2005). Both reports also observed a 50% increase in RSK family members in breast and prostate cancer tissue compared to normal tissue, which would suggest dysregulation in cancer cells. Although no direct association is documented between RPS6KA3 and invasion, many of its substrates have been identified as key players in tumour progression, these include; Estrogen receptor α, cyclic AMP response element-binding protein (CREB), c-Fos and nuclear factor-κB (Smith *et al.*, 2005). Therefore the role of RPS6KA3 in phosphorylation and subsequent activation of many factors involved in the invasion process would suggest an important role in tumour progression and invasion. Combined with the results obtained from the present study, this makes RPS6KA3 a good candidate for further analysis.

4.3.5.4 Tumour necrosis factor, alpha-induced protein 8 (TNFAIP8)

TNFAIP8 was up-regulated by 2.47 fold in invasive MCF7H3erbB2 compared to non-invasive MCF7H3. TNFAIP8 was originally discovered by a comparison looking at differentially displayed transcripts in human primary and matched metastatic head and neck squamous cell carcinoma cell lines. In this work TNFAIP8 was identified as having association with an invasive phenotype (Patel *et al.*, 1997). The examination of clinical samples showed higher expression levels of TNFAIP8 protein in certain human tumour tissues as compared to the matched normal adjacent tissues (Kumar *et al.*, 2004).Both studies concur with results of the present work, which found TNFAIP8 differentially expressed in an invasive MCF7H3erbB2 compared to the non-invasive parent MCF7H3.

The isolation and characterization of TNFAIP8 has only occurred recently (Kumar *et al.*, 2000). This study found TNFAIP8 was detectable in most human normal tissues, with relatively higher levels in spleen, lymph node, thymus, thyroid, bone marrow, and placenta and lower levels in spinal cord, ovary, lung, adrenal glands, heart, brain, testis, and skeletal muscle. TNFAIP8 mRNA was expressed in all cancer cell lines tested, with relatively higher levels in chronic myelogenous leukemia cells, lymphoblastic leukemia cells, A549 lung carcinoma cells and lower levels in SW480 colorectal adenocarcinoma cells. Other studies to date have shown up-regulation of TNFAIP8 in MDA-MB 435

cancer cells caused an increased growth rate and an increase in cell migration in collagen I, and in athymic mice, TNFAIP8 transfectants showed significantly enhanced tumor growth as compared to control transfectants (Zhang *et al.*, 2006).

A more recent study has demonstrated that expression of TNFAIP8 cDNA in MDA-MB 435 human breast cancer cells was associated with enhanced invasion *in vitro* and increased frequency of pulmonary colonization of tumor cells in athymic mice (Zhang *et al.*, 2006). These results show TNFAIP8 as a novel invasion marker, and confirm the accuracy of the microarray analysis used in the present work to identify invasion-associated genes in MCF7H3erbB2. This study combined with results from the present work was sufficient evidence to choose TNFAIP8 for further analysis with regards to its role in invasion.

4.3.5.5 Thrombospondin (THBS1)

THBS1 was different to all of the other genes chosen for further analysis as it was found down-regulated (-2.31 fold) in the invasive MCF7H3erbB2 compared to the non-invasive MCF7H3, which suggested it played a role in the inhibition of invasion. Although it was not present in the 9-gene pathway constructed by pathway assist analysis, further literature searches found it to be transcriptionally regulated by EGR1 and also play a role in the binding of TFPI to tissue factor (TF). It was decided to further investigate these possible anti-invasion properties by using THBS1 as a target for siRNA. Overexpression of THBS1 has been associated with migration in many cancer tissues. Experimental evidence has indicated that THBS1 can be both adhesive and anti-adhesive, can foster and retard metastasis, stimulate and inhibit angiogenesis and increase and reduce proteolytic activity and fibrinolysis.

THBS1 is an adhesive, extracellular matrix glycoprotein that mediates cell-to-cell and cell-to-matrix interactions through binding of fibronectin, fibrinogen, laminin, type V collagen and integrins α_V/β_1. Transforming growth factor β (TGFβ) and platelet-derived growth factor (PDGF) have also been found to bind to THBS-1. Evidence to date would suggest THBS-1 functions in directing formation of multi-protein complexes that modulate cellular phenotype (Esemuede *et al.*, 2004) There are five family members, each representing a separate gene product, which have been found to exist in most vertebrates. Specific patterns of expression have been found for each of the five proteins in embryonic and adult tissues, with most tissues expressing at least one family member. Expression of most THBS gene products were observed in heart, cartilage and

brain tissue (Lawler, 2000). The THBSs appear to function at the cell surface to bring together membrane proteins and cytokines that regulate extracellular matrix structure and cellular phenotype. The membrane proteins found to participate in these complexes include integrins, the integrin-associated protein (also known as CD47 or IAP), CD36 and proteoglycans (Lawler, 2000).

Thrombospondin-1 (THBS1) is a large (450 kDa) glycoprotein that is released into the extracellular matrix by several cell types (cultured endothelial cells, fibroblasts and monocytes have all been found to synthesize and secrete THBS1). THBS1 expression is increased in response to growth factors, heat shock and hypoxia, and is downregulated in response to IL-1β and TNFα. Due to the presence of a SRE in the THBS1 promoter, it is synthesised by most cells in culture (Adams, 1997). It is released by platelets at the end of the coagulation process during the formation of a hemostatic plug, hence the name 'thrombospondin' was proposed, to indicate that the protein was released in response to thrombin (Lawler *et al.*, 1977). During thrombus formation, fibrinogen at the wound site binds to platelet membrane glycoproteins (GPIIb and GPIIIa). THBS1 creates crosslinks between multiple fibrinogen- GPIIb/GPIIIa complexes leading to stabilization and formation of platelet macroaggregates (Bonnefoy *et al.*, 2001). THBS1's role in this process is important during the initial stages of hemostasis, and is relevant to the formation of an irreversible platelet plug.

Because each cell expresses a different repertoire of receptors, the composition of the complexes and the cellular responses vary among different cell types. The stimulation or inhibition of migration of vascular smooth muscle cells or endothelial cells, respectively, is an example of THBS-1 diversity (Lawler, 2000). Experimental evidence has indicated that THBS1 can be both adhesive and anti-adhesive, can foster and retard metastasis, stimulate and inhibit angiogenesis and increase and reduce proteolytic activity and fibrinolysis (Bornstein, 1995). Interaction of THBS1 with structural proteins such as collagens, proteoglycans, fibronectin and lamins, could cause THBS1 to present to the cell surface, and modulate interaction of those proteins with their own receptors. These actions would have a diverse effect on proliferation, adhesion and migration depending on cellular and extracellular matrix content, explaining how differential expression of different cell surface receptors can dictate the response of a particular cell type to THBS1.

THBS1 displays distinct biological activities in different cell types, which is attributed to its multiple functional domains that engage corresponding receptors on the surface of targeted cells (Figure 4.2).

Figure 4.2: THBS1 Structure

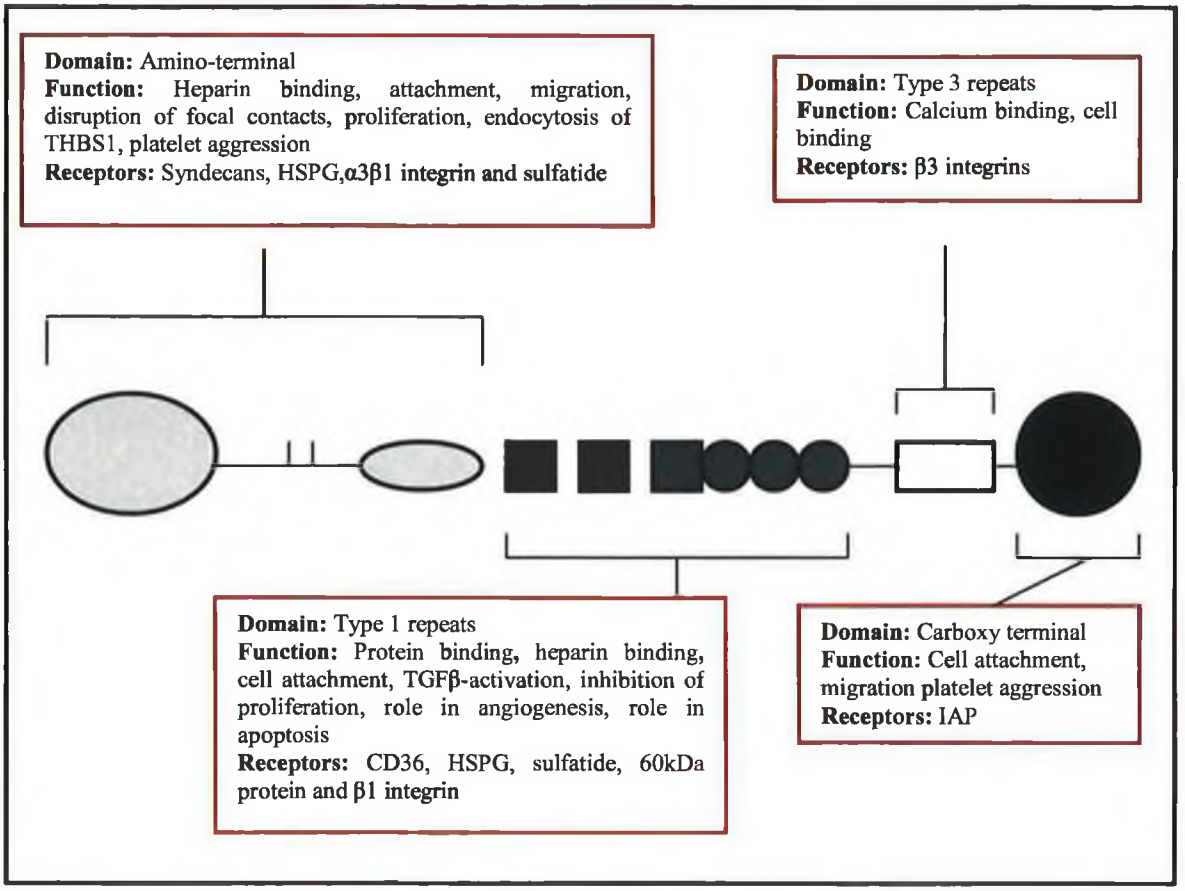

Figure 4.2: Schematic representation of the structure and function of Thrombospondin-1. THBS1 contains an amino-terminal domain, type 2 and type 3 repeat sequence and a carboxy-terminal domain

The specificity of THBS1 activity is dictated by the receptors expressed by the cells surrounding the protein, rather than its inherent activity. Because of this fact THBS1 has been found to have many different contradictory functions in relation to tumour progression. THBS1 has been located at the border between tumour and stroma in primary tumours, and from here can contribute to tumour progression or deterioration depending on the THBS1 receptor repertoire of the tumour (Bastian *et al.*, 2005). The events that take place during tumor progression enable the tumor to interact with its stromal environment in ways that enhance its ability to proliferate in the primary site and, in highly malignant tumors, to metastasize to distant sites in the body (Brown *et*

al., 1999). However, contrary to microarray results, many previous studies have identified THBS1 as a promoter of invasion (Qian, 2001; Boire *et al.*, 2005). Because each cell expresses a different repertoire of receptors, the composition of the complexes and the cellular responses vary among different cell types. Experimental evidence has indicated that THBS1 can be both adhesive and anti-adhesive, can foster and retard metastasis, stimulate and inhibit angiogenesis and increase and reduce proteolytic activity and fibrinolysis (Bornstein, 1995). Conformation of calcium (Ca^{+}) binding repeats in THBS1, and therefore affinity for binding integrins and proteases, can be influenced by calcium concentration (Sun *et al.*, 1992). Therefore it is possible that the ionic state of the cell could regulate THBS1 function. Interaction of THBS1 with structural proteins such as collagens, proteoglycans, fibronectin and lamins, may cause THBS1 to present to the cell surface, and modulate interaction of those proteins with their own receptors. These actions would have a diverse effect on proliferation, adhesion and migration, depending on cellular and extracellular matrix content, explaining how differential expression of different cell surface receptors can dictate the response of a particular cell type to THBS1.

4.3.6 Selection of differentially expressed DLKP4E and DLKP4Emut genes for further analysis

Both DLKP4E and DLKP4Emut were highly invasive, so it was probable that of the genes common to both, some would be involved in invasion. 379 genes changes were common to 4E, 4Emut. Although there was an increase in invasion in DLKPpcDNA, it was minor compared to invasion in DLKP4E and DLKP4Emut, and could have been a non-specific effect of selection with geneticin. It is also important to note that the parent DLKP was mildly invasive, and so it was likely that a DLKPpcDNA clone would also be mildly invasive. To further reduce the list of genes for analysis, gene changes due to DLKPpcDNA were removed. The final list contained 240 genes.

4.3.6.1 Genes related to invasion and specific to DLKP4E and DLKP4Emut

The final list of 240 genes was further studied using Pathway Assist ®. Analysis carried out to identify genes with direct interaction revealed two separate gene pathways. These pathways, as before, were based on information available in PubMed. The first pathway identified several genes which had previously been associated with cancer invasion and metastasis (Table 3.3.13), for example Neuregulin (NRG) (Stove and Bracke, 2004), platelet-derived growth factor alpha polypeptide (PDGFA) (Jechlinger *et al.*, 2002), ribosomal protein S6 kinase, 70kDa, polypeptide 1 (RPS6KB1) (Harrington *et al.*, 2005), growth factor receptor bound protein 2 (GRB2)(Sugiyama *et al.*, 2001), solute carrier family 2 (facilitated glucose transporter), member 3 (SLC2A3) (Higginset *et al.*, 2003) and cAMP responsive element modulator (CREM) (Taki *et al.*, 2002). This fact alone showed the analysis had been successful in identifying invasion-specific genes. RPS6KA3 also appeared on the list of MCF7H3erbB2-specific genes, which strengthens the association of this gene with an invasive phenotype. From this pathway Neuregulin (NRG) was chosen, based on its significant fold change and direct interaction with 5 other genes from the final list. Results from Pathway Assist® showed NRG directly interacted with GRB2 (Lim *et al.*, 2000), SLC2A3 (Ghosh *et al.*, 2005), RPS6KB1 (Canto *et al.*, 2004) and RPS6KA3 (Rahmatullah *et al.*, 1998), and through these genes may effect CREM (de Groot *et al.*, 1994) and PDGFA (Matuoka *et al.*, 1993). As previous work had associated some or all of these genes with cancer and invasion, it was thought that knock-down of NRG would have a significant effect.

A second pathway identified interaction between four of the homeo box genes (HOXB2, 5, 6, & 4). Several HOXB genes showed significant changes in expression on the final list, with fold changes ranging from +6 to +98. Based on this observation, the fact that HOXB genes are transcription factors associated with cancer phenotypes (Flagiello *et al.*, 1996; Lopez *et al.*, 2006), and the Pathway Assist® results, three of the HOXB genes (homeo box B6 (HOXB6), homeo box B4 (HOXB4) homeo box B7 (HOXB7)) were chosen for further analysis.

The last gene chosen was Myopalladin. This did not appear in either pathway and was chosen based on fold change (+9.06), and the fact that although it is known to regulate actin organization (Bang *et al.*, 2001), there is no evidence in the literature of its involvement in invasion.

4.3.6.2 DLKP4E and DLKP4Emut invasion-related genes chosen for further analysis

Five genes in all were chosen for siRNA knock-down based on specificity to DLKP4E, DLKP4Emut and invasion, and relevance to cancer/invasion in the literature. These targets were HOXB4, HOXB6, HOXB7, NRG and MYO.

Table 4.2 Genes specific to DLKP4E/DLKP4Emut and related to invasion chosen for further analysis

Gene	Description	Fold Change	Mean Expression Difference
HOXB6	homeo box B6	+33.69	756
HOXB4	homeo box B4	+6.51	199
HOXB7	homeo box B7	+7.65	412
NRG1	neuregulin 1	+7.36	596
MYO	myopalladin	+9.06	599

4.3.6.2.1 HOX gene family in cancer

Alterations in the expression of transcription factors is believed to constitute another step in carcinogenesis. HOX genes are a family of transcription factors that contain a highly conserved sequence of 183bp that encodes a 61 amino acid homeodomain, which binds to specific DNA sequences in target genes, regulating their expression (Gehring *et al.*, 1994). The Homeobox-containing gene family primarily play a crucial role during development. Several indications suggest their involvement in the control of cell growth

and, when dysregulated, in oncogenesis. For example, deregulation of homeobox gene expression has been invoked as the molecular basis of a number of leukemias (Cillo *et al.*, 1999). Several HOX genes are differentially expressed in many neoplasias, such as primary and metastatic colorectal cancer, and neoplastic human kidney, and several reports show a relationship between HOX gene expression and specific human tumors (Cillo *et al.*, 1999). So when so many HOXB genes appeared on the final list of genes for analysis, they seemed an obvious choice for further examination. It was thought because this family of genes were so closely related, down or up-regulation of one may have a knock-on effect on the others.

4.3.6.2.2 HOXB4

HOXB4 was also found differentially expressed in array analysis, with a fold change of 6.5 in DLKP4E compared to the parent DLKP. An examination of the expression levels for HOXB4 showed that the gene had been 'switched on' after DLKP transfection with eIF4E, and that the gene was exclusive to DLKP4E and DLKP4Emut. Expression levels rose from 13 in the parent to 235 in DLKP4E. HOXB4 gene expression has previously been found in cervical tumor tissues, suggesting a role in cervical cancer (Lopez *et al.*, 2006). The expression pattern of HOXB4 gene products were examined immunocytochemically in 11 human breast carcinoma tissues. In all observed breast cancer cases, HOXB4 was present in over 90% of the neoplastically transformed cells (Bodey *et al.*, 2000a). HOXB4 has also been implied in the development of leukemia, and when expressed at high levels, HOXB4 concomitantly perturbs differentiation and thus likely predisposes the manipulated cells for leukemogenesis (Will *et al.*, 2006). Up-regulation of HOXB4 has also been observed in lung (Bodey *et al.*, 2000b) and osteocarcinoma (Bodey *et al.*, 2000c).Though HOXB4 expression has been observed in a variety of tumour types, it has not been directly related to invasion, and therefore was chosen as a potential novel marker for further analysis.

4.3.6.2.3 HOXB6

Animal studies indicate that the HOXB genes play an essential role in lung development. Microarray analysis of HOX genes in human lung tissue found HOX genes were expressed in normal human adult lung and among them HOXA5 was the most abundant, followed by HOXB2 and HOXB6 (Golpon *et al.*, 2001). Microarray results from the present study showed that in DLKP4E, which is a lung cancer cell line,

HOXB2, 5 and 6 were the most highly differentially expressed of all HOXB genes (with fold changes of +98, +34 and +33 respectively).The expression of these genes in a lung cell line would not be unexpected, however, what was unusual was they appeared to be 'switched on' in the eIF4E over-expressing cell line compared to the parent. HOXB6 for example had an expression value of 20 in DLKP and 780 in DLKP4E. This would suggest that the upregulation of eIF4E, which also led to a considerable increase in invasion, caused up regulation of the HOXB6 gene. Of these three genes, HOXB6 was chosen. Overexpression of HOXB6 has previously been associated with colon cancer (Vider *et al.*, 1997), and leukemia cell lines (Ohnishi *et al.*, 1998).Dispite the association of HOXB6 with cancer in the literature, it had not been directly assocated with invasion, and so was chosen as a possible novel marker of invasion in DLKP4E cells.

4.3.6.2.4 HOXB7

Microarray analysis showed HOXB7 to be differentially expressed in DLKP4E, and have a fold change of +7.65 compared to DLKP parent. This gene was also 'switched on' after eIF4E overexpression, with expression levels of 60 in the parent increasing to 470 in the DLKP4E clone. Previous work had identified HOXB7 as a possible oncogene. In vivo and in vitro transformation assays have been used to demonstrate that the overexpression of homeobox genes is the basis of transformation and tumourgenesis (Maulbecker and Gruss,1993). This study identified HOXB7 as part of a new family of nuclear protooncogenes. Misexpression of HOXB7 in primary colon cancer as well as in metastatic liver lesions originated from colorectal tumors, also implicates a role for HOXB7 in the evolution and invasion of colon cancer (Cillo *et al.*, 1999). HOXB7 has also been directly linked to the invasive phenotype of cells. A recent study showed a reduction of invasion following HOXB7 antisense introduction into ovarian cancer cells (Yamashita *et al.*, 2006). Another study found that the expression level of HOXB7 was lower in lymph node metastasis-positive breast cancer tissues than metastasis-negative cancer tissues (Makiyama *et al.*, 2005). These findings concured with microarray results that showed HOXB7 expression to be of significance to the DLKP4E/DLKP4Emut invasive phenotype. This added strength HOXB7 as a target for further analysis.

4.3.6.2.5 NRG

NRG was found to have an expression level +8.6 fold greater in DLKP4E than in DLKP. The NRG1 proteins play essential roles in the nervous system, heart, and breast. There is also evidence for involvement of NRG signalling in the development and function of several other organ systems, and in human disease, including the pathogenesis of schizophrenia and breast cancer (Falls, 2003). Human epidermal growth factor (EGF) receptor (HER) family of receptor tyrosine kinases has long since been implicated in cancer. Overexpression or mutation of these receptors is most often the trigger for tumour progression, but the aberrant autocrine or paracrine activation of HERs by EGF-like ligands is also thought to play an important role in the process. Neuregulins are a family of EGF-like ligands that bind to HER3 or HER4, preferably forming heterodimers with the orphan receptor HER2 (erbB2). Mesenchymal neuregulin typically serves as a pro-survival and pro-differentiation signal for adjacent epithelia. Disruption of the balance between proliferation and differentiation, because of autocrine production by the epithelial cells, increased sensitivity to paracrine signals or disruption of the spatial organization, may lead to constitutive receptor activation, in the absence of receptor overexpression (Stove and Bracke, 2004). The association of NRG with the human epidermal growth factor receptor (HER) family is well documented, as is the association of the HER family with invasion/metastasis. It was encouraging to see a gene so obviously linked with an invasive phenotype appear on the final list of genes. This gene was chosen not only based on its significance in the array analysis, but also because it was already so closely related to the HER family and invasion it was expected to have some effect if downregulated. Pathway analysis of the final list of DLKP4E and DLKP4Emut specific genes produced a pathway of directly related genes which included NRG. It was hoped that disrupting expression of NRG would have a knock-on effect on the other genes in the pathway, and therefore amplify the anti-invasive effect.

4.3.6.2.6 MYO

MYO expression levels increased +9.06 fold in DLKP4E compared to the parent DLKP. MYO is a member of a recently discovered family of proteins that function as scaffolds regulating actin organization (Bang *et al.*, 2001). The dynamic remodeling of the actin cytoskeleton plays a critical role in cellular morphogenesis and cell motility, and it is not surprising therefore that these cytoskeletal filaments are the targets of a

growing number of anti-cancer drugs. Actin-associated scaffolds are key to this process, as they recruit cohorts of actin-binding proteins and associated signaling complexes to subcellular sites where remodeling is required (Otey *et al.*, 2005). Microtubules and actin filaments play important roles in mitosis, cell signaling, and motility. Despite the obvious potential for MYO in the invasion process, no evidence is available in the literature to connect the two. Therefore MYO was chosen for further analysis based on its significant fold change in an invasive cell line and the fact that it could prove a novel marker for invasion.

4.4 RNA Interference – further analysis of genes chosen from microarray analysis

In order to further examine the genes chosen from microarray analysis, it was decided to use RNA interference to silence these genes and look at the resulting effect on invasion. RNA interference has been used in several other studies to examine the effect of individual genes on the invasion process (Subramanian *et al.*, 2006; Rodrigues *et al.*, 2005) Two groups of siRNA targets specific to invasion were chosen based on microarray analysis of MCF7H3erbB2 and DLKP4E/DLKP4Emut, as discussed in the previous section. In total, 10 targets were chosen, 5 specific to invasion in MCF7H3erbB2 (TFPI, TNFAIP8, THBS1, RPS6KA3 and EGR1), and 5 specific to invasion in DLKP4E (HOXB4, HOXB6, HOXB7, MYO and NRG). Of the ten targets chosen, 9 were found to be up-regulated in invasive cells. It was therefore logical to presume that a reduction in expression of these genes would result in a reduction in invasion. To this end, all 9 targets were examined in the invasive cell lines DLKP4E and SKBR3. SKBR3, also a human breast, erbB2 positive, invasive cell line, replaced MCF7H3erbB2 for siRNA analysis, due to the fact that MCF7H3erbB2 lost its ability to invade. It is important to note that invasion assays were carried out using MCF7H3erbB2 prior to microarrays, showing the cells were invasive (Section 3.3.1). The THBS1 target, which was predicted to increase invasion when silenced using siRNA, was transfected into non-invasive MCF7s and DLKPs.

4.4.1 Kinesin and GAPDH siRNA transfection in DLKP, DLKP4E, MCF7 and SKBR3

Proliferation and all 6-well optimisation assays were carried out using kinesin as a positive control (Figure 3.4.1; 3.4.2). Kinesin facilitates cellular mitosis, therefore silencing kinesin causes cellular arrest. Kapitein *et al.* (2005) concluded that members of the kinesin-5 family were likely to function in mitosis, pushing apart interpolar microtubules as well as recruiting microtubules into bundles that are subsequently polarized by relative sliding. Dividing cells adopt a rounded morphology in advance of microtubule formation, and in the absence of kinesin 11 the cells arrest, leading to a round morphology. Examination of cell morphology after transfection in both 96- and 6-well plates indicated as to whether the transfection had been a success. A change in the morphology of the cells indicated that kinesin had been silenced and therefore the

kinesin siRNA transfection was successful. This was taken as an indication of optimum transfection conditions, and successful transfection in this cell line. In the proliferation assays, the control cells divided normally while the kinesin siRNA transfected cells did not. The difference in control cell number versus kinesin siRNA transfected cells was not a measure of transfection efficiency or related to any cell death, but rather a measure of how many times the control cells divided beyond the stage at which the kinesin levels became limiting in the transfected cells. Cellular arrest in the presence of Kinesin siRNA was taken as confirmation of efficient transfection conditions. Reduced growth of kinesin siRNA transfected cells compared to scrambled was seen in all cell lines.

GAPDH, often used as an endogenous control, has been found to be an 'easy target' for siRNA, with efficient silencing observed in many different systems (www.Ambion.com). Every set of 6-well plate transfections was also accompanied by transfection with GAPDH siRNA. This was examined at an mRNA level using real-time PCR. Knock-down of GAPDH in all cell lines confirmed optimal transfection conditions.

4.4.2 Genes related to invasion and specific to MCF7H3erbB2

4.4.2.1 Effect of TFPI1 siRNA on DLKP4E and SKBR3

TFPI was chosen as a target for siRNA based on MCF7H3erbB2 array data analysis that showed a +19.77 fold change in MCF7H3erbB2 (invasive) compared to MCF7H3 (non-invasive). No significant change was seen in DLKP4E, but there was a +10 fold change in DLKP4Emut compared to parent DLKP. Sefter *et al.* (2002) carried out microarray experiments to identify invasion markers by comparing non-invasive to invasive human uveal melanoma cells. Their results also found TFPI up-regulated in an invasive cell line, though no further analysis was carried out (Sefter *et al.*, 2002).

4.4.2.1.1 Effect of TFPI siRNA on proliferation

Proliferation assays carried out on DLKP4E and SKBR3 transfected with TFPI siRNA A and B showed minor changes in growth rate, demonstrating transfection did not have a major effect on proliferation of DLKP4E or SKBR3 cells (Section 3.5.1). Previous work by Sato *et al.* (1997) showed that TFPI inhibited smooth muscle cell (SMC) migration that is induced by the factor VIIa-TF complex (Sato *et al.*, 1997), and Kamikubo *et al.* (1997) demonstrated that the growth of cultured human neonatal aortic

SMCs was inhibited by TFPI (Kamikubo *et al.*, 1997). TFPI has also been found to inhibited proliferation and induced apoptosis of cultured human umbilical vein endothelial cells (HUVECs) (Hamuro *et al.*, 1998). A more recent study also demonstrated TFPI deficiency enhances neointimal proliferation and formation in a murine model of vascular remodelling (Singh *et al.*, 2003). It has previously shown that TFPI is also a potent inhibitor of endothelial proliferation in vitro and of primary and metastatic tumor growth in vivo (Hembrough *et al.*, 2001). The Tissue factor dependent extrinisic pathway of blood coagulation is known to support tumour progression through promotion of cellular proliferation (Rak *et al.*, 2006), and the anti-proliferative effect of TFPI was thought to be associated with its TF inhibitory role. However, antiproliferative activity in TFPI has been localized to a short, very low density lipoprotein (VLDL) receptor-binding sequence found in its carboxyl terminus. This activity is independent of the hemostatic activity of TFPI and represents a previously unrecognized nonhemostatic mechanism whereby TFPI can regulate tumor growth and angiogenesis (Hembrough *et al.*, 2004). This previous work suggests a model where a reduction of TFPI results in an increase in proliferation. This did not happen in DLKP4E or SKBR3 cells. However, it is evident from results that siRNA silencing did not reflect a decrease in TFPI protein. This was most likely due to the rapid turnover of TFPI (Valentin *et al.*, 1991), and may explain why TFPI siRNA transfection did not have a marked effect on proliferation. TFPI exists in plasma both as a full-length molecule and as a variably carboxy-terminal truncated forms. Both forms take can influence cellular proliferation. Optimal inhibition of extrinsic coagulation is obtained by the full-length molecule, while the truncated form can bind other surface receptors such as very low-density lipoprotein (VLDL) receptor, and still cause an anti-proliferative effect (Hamik *et al.*, 1999). As TFPI was already expressed at relatively low levels (evident from western blot and qPCR), it is possible that silencing of TFPI mRNA was sufficient to effect proliferation.

4.4.2.1.2 Effect of TFPI siRNA on mRNA and protein levels

As mentioned above, TFPI silencing was seen at mRNA level using real-time PCR in both cell lines, using three different TFPI siRNAs (Section 3.5.2). However, fluctuations were observed between the non-transfected and scrambled-siRNA transfected controls. This was not expected, as the scrambled control should have minimal affect on TFPI mRNA. It is possible that because TFPI was expressed at a low

level in both cell lines (this is evident from microarray results for DLKP4E and real-time PCR results for SKBR3 showed the cycle threshold for TFPI to be 25 to 29, indicating it was lowly expressed) background noise had a greater effect. In qPCR, the detection threshold is the level of detection or the point at which a reaction reaches a fluorescent intensity above background noise. The cycle at which the sample reaches this level is called the Cycle Threshold, Ct. If the intensity of the signal is low to begin with due to a poorly expressed gene, background noise will have a greater effect on data analysis. It is also possible that differences in expression between the non-transfected and scrambled controls was due to residual effects of the transfection reagent, in this case NeoFX (Section 2.6.1.2).

Western blot analysis of cells transfected with TFPI siRNA showed no change in TFPI at a protein level in DLKP4E, and was not sensitive enough to detect TFPI in SKBR3 (likely due to low level of expression already discussed) (Section 3.5.3). Previous studies have demonstrated that the targeting of proteins with a long half-life may not produce the desired phenotypic effect because silencing at the level of transcription will not affect pre-existing proteins (Pai *et al.*, 2006). For this reason, it was important to be aware of the life span of the chosen RNAi in *in vitro* experiments. Extracellular degradation of siRNA peaks around 36 to 48hrs after their introduction and begins to decrease after 96hrs. However, TFPI has a short half-life (60-120mins) (Valentin *et al.*, 1991), and RNAi has the optimal effect in proteins with a more rapid turnover (Pai *et al.*, 2006). It is possible that the siRNA effect at an mRNA level was not reflected at a protein level because turnover of TFPI was so rapid new protein masked the effect of siRNA. It is also possible that the newly synthesized protein may not yet have undergone some essential post-translation modification, and therefore may not yet be functional. Alternative mRNA splicing of TFPI generates two forms, TFPIα and TFPIβ. A portion of expressed TFPI remains associated with the cell surface through both direct (TFPIβ) and indirect (TFPIα) glycosylphosphatidyl-inositol (GPT)-mediated anchorage (Chang *et al.*, 1999). Based on protein mass, TFPIβ (28 kDa) is considerably smaller than TFPIα (36 kDa), but both migrate with the same apparent molecular mass (46 kDa) on sodium dodecylsulfate-polyacrylamide gel electrophoresis (SDS-PAGE). Recent studies have demonstrated this is due to a difference in post-translational modifications, with both TFPIα and β containing differing levels of glycosylation (Piro and Broze, 2005). TFPI β uses an alternative exon in the 3' coding region compared to TFPI α, resulting in a protein (isoform β precursor) with a shorter and distinct C-

terminus compared to isoform α precursor. TFPIA, B and C siRNAs used in the present study target Exons 6, 7, and 8 respectively, and therefore would be effective for both splice variants. It is therefore uncertain which variants were silenced. The antibody used in western blot analysis could not distinguish between either, nor could the real-time PCR primers. This fact might explain why mRNA silencing is observed but not protein silencing. To date the role of TFPIα and β in invasion have not been studied. Information available tells us cell stimulation with a variety of pro-inflammatory agents does not affect surface-TFPI content or TFPIα and β mRNA levels; TFPIα is the most abundant form of surface TFPI; although TFPIβ represents only ~20% of total surface-TFPI, it accounts for most of the anti-TF-FVIIa activity, suggesting a potential alternative role for cell-surface TFPIα (Piro and Broze, 2005).

4.4.2.1.3 Effect of TFPI siRNA on invasion

Although no change in protein was observed, a phenotypical change was seen after siRNA transfection. Invasion assays carried out 72hrs after siRNA transfection showed a marked decrease in the number of invading cells (Section 3.5.4). The duration of gene silencing varies greatly between cells with slow growing cells still showing the effects of siRNA after several weeks, but more rapidly dividing cells not seeing an effect for longer than 1 week (Ryther *et al.*, 2005). This was important to consider when choosing time points for RNA, protein, and also invasion analysis. All assays were carried out within 6 days of the initial transfection to ensure the siRNA was still having effect.

Besides mRNA and protein analysis to detect a change in TFPI post-siRNA transfection, several other steps were taken to ensure that the results obtained were due to siRNA silencing of TFPI and not because of off target effects. siRNA delivery through transfection can result in temporary changes in the cell, and in some cases cells may become resistant to conditions of delivery. siPORT™ *NeoFX*™, a lipid-based agent was used to minimize serum RNase digestion of siRNA and to maximize delivery of siRNA to the cells.

Because of the several artifacts that can arise from siRNA transfection, leading to a misleading result, it was vital to include proper controls. As already mentioned, GAPDH and kinesin controls were included for all transfections. A 'scrambled' siRNA, which was designed so as to lack recognition to any target, was also included in every experiment. Previous studies have pointed out the uncertainty of presuming RNAi elimination of target mRNA based on phenotypic effect alone, and emphasises the

necessity for a 'scrambled' control, as well as examining siRNA effecs at both an RNA and protein level (Persengiev *et al.*, 2004). In the present study real-time PCR and western blot analysis were used to confirm RNA/protein silencing, and 'scrambled' siRNA controls were used in all experiments. Invasion assay results showed that the scrambled control had little effect on DLKP4E and SKBR3 compared to TFPI siRNA, and this validated that reduced invasion was as a result of TFPI silencing.

The most accurate control for any set of siRNA experiments is to set up repeats targeting the same mRNA using different siRNA sequences. Responses elicited by multiple non-homologous siRNAs are more likely to be due to specific target suppression. Three non-homologous TFPI siRNAs were used in this set of experiments, each targeted to a different TFPI exon (Figure 4.3).

Figure 4.3: Exon targets of TFPI siRNA A, B & C.

TFPIA

TFPIB

TFPIC

www.Ambion.com

An even more stringent control would be to examine the effects of multiple non-homologous siRNAs in different cell lines or animal models. Here a lung (DLKP4E) and breast (SKBR3) cancer cell line were transfected using the same TFPI siRNA and both produced similar results; TFPI siRNA silencing reduced the level of invasion. Therefore, it is most likely that the reduction in invasion observed in both SKBR3 and DLKP4E was due to siRNA silencing of TFPI. This result not only validates the

microarray analysis but provides the first evidence of a functional effect of TFPI in relation to invasion.

4.4.2.1.4 Role of TFPI in invasion

TFPI production by endothelial cells may be stimulated by cytokines secreted by the cancer cells, possibly as a means of inhibiting coagulation by the host. Increased concentration of free and total TFPI in cancer may also contribute to increased (factor Xa) FXa–TFPI complex. Coagulation factor Xa is crucial for the conversion of prothrombin to thrombin, in both the extrinsic and intrinsic pathways of coagulation. FXa–TFPI complex has been described as slowing activation of coagulation (Iversen *et al.*, 2002), and thus slowing tumour progression. In contrast, other studies have demonstrated up-regulation of TF during angiogenesis results in a more pro-coagulant vascular surface, and although expression of TFPI triggers anti-coagulant mechanisms, the result is a balance in the coagulation process, maintaining an exclusive vascular bed within the tumour and allowing sustained growth (Gruel *et al.*, 2005).

Microarray results showed a +19.77 fold increase of TFPI in invasive MCF7H3erbB2 compared to non-invasive parent MCF7H3. This was in concurrence with previous work, which showed elevated levels of TFPI have been found in breast cancer, and patients whose tumours were completely removed showed significant decline in the level of total, free and lipid-bound TFPI (Erman *et al.*, 2004). It has also been found that TFPI levels correlate with cancer progression (Lindahl and Sandset, 1992; Lindahl *et al.*, 1993). Despite this, little work has been done to further investigate the precise role of TFPI in cancer invasion. Fisher *et al.* (1999) suggested a specifc role for TFPI in invasion in primary bladder carcinoma cells, observing that TFPI could serve as an adhesive ligand for cancer cells to extracellular matrices (ECM). This study showed that heparin enhanced cancer cell adherence to TFPI present in the ECM, a process which was dependent upon TF/VIIa/TFPI interactions. More importantly, it found that the TF-VIIa complex localizes to the invasive edge, in proximity to tumor-infiltrating vessels that stain intensely TFPI, demonstrating TFPI played a functional role in promoting cell migration. In culture, binding of VIIa to TF-expressing tumor cells was sufficient to allow cell adhesion, migration, and intracellular signaling on immobilized TFPI-1. This study provided evidence for a novel mechanism of protease-supported migration via protease-dependent bridging of TF's extracellular domain to TFPI (Fischer *et al.*, 1999).

TFPI may also influence invasion by dictating whether coagulation proceeds through the intrinsic or extrinsic pathway. The end product of the extrinsic pathway of coagulation, as triggered by TF, is thrombin. Two components of invasion (i) proteolysis of extracellular matrix and (ii) cellular movement through it are promoted by thrombin (the serine proteinase derived from the ubiquitous plasma protein prothrombin) Thrombin has been observed to promote the invasion of MDA-MB231 breast tumour cells (a highly aggressive/invasive cell line) but not MDA-MB436 and MCF-7 cells, less aggressive/invasive cell lines (Henrikson *et al.*, 1999). As TFPI inhibits Xa and therefore thrombin production, it is difficult to explain how up-regulation of TFPI can in fact increase invasion. It is important to note in the context of the present study, that although the TFPI-TF-VIIa-Xa complex inhibits thrombin formation through the extrinsic pathway, factor X, which is necessary for the activation of prothrombin to thrombin, can be activated independently through the intrinsic pathway (Lwaleed and Bass, 2006). Therefore TFPI switches the coagulation cascade from the extrinsic to the intrinsic, which may reduce, but does not prevent thrombin production. The serine protease thrombin, independently of its participation in hemostasis and thrombosis, has been involved in tissue repair and remodeling, embryogenesis, angiogenesis, and development and progression of atherosclerosis. Many of these functions appear to be mediated by specific thrombin receptors, particularly the protease-activated receptor-1 (PAR1) (Archiniegas *et al.*, 2004). Recent studies have highlighted the role played by PAR1 in both negative and positive invasion pathways. In *in vitro* studies carried out using the collagen type I substratum, PAR-1 and the pertussis toxin (PTx)-sensitive Gαo/i subunits were shown to exert a dominant invasion suppressor role toward several proinvasive pathways controlled by oncogenes and tumor-secreted growth factors (Faivre *et al.*, 2001). Conversely, neutralization of Gαo/i signaling by pertussis toxin (PTx)-sensitive Gαo/i subunits led to the pro-invasive activity of thrombin and PAR-1 through the Gα12/13/RhoA cascade, myosin light chain (MLC) phosphorylation, and activation of the actomyosin system (Kureishi *et al.*, 1997; Nguyen *et al.*, 2005). The pro-invasive potential of PAR-1 in collagen type I was also revealed by inhibition of RhoA GTPase by RhoD (Nguyen *et al.*, 2005). In this case, PAR-1 is connected with the Gαq/phospholipase Cβ–Ca^{2+}/calmodulin-MLC kinase (CaM-MLCK) cascades that bypass RhoA blockade (Nguyen *et al.*, 2005). This study defined a new function for the small GTPases RhoA and RhoD acting as a molecular switchs controlling the negative and positive invasive pathways triggered by PAR-1 in

the presence of a collagen type 1 substratum (the intrinsic pathway is stimulated by the exposure of collagen to a vessel surface. PAR-1 had previously been found to induce invasion of Matrigel by breast cancer cells through requirement of $\alpha v\beta 5$ integrins (Even-Ram *et al.*, 2001), suggesting that the PAR-1 invasive potential is controlled by the matricellular context (Nguyen *et al.*, 2005). The $\alpha v\beta 5$ integrins have been shown to play an important role in cell-collagen attachment (Hoffman *et al.*, 2005). Evidence suggests that the activated of PAR-1 by thrombin, and subsequent involvement in positive invasion pathways, is influenced by the level of collagen. This in turn implicates the intrinsic coagulation pathway in the producion of thrombin certain cancer cells.

It is also of note that activation the intrinsic pathway has been associated with patients with advanced disease or receiving chemotherapy. Patients with advanced colon and pancreatic cancer have increased levels of plasma TFPI with progression of the malignancy, while the concentration of the other coagulation inhibitors (antithrombin and activated protein C) decrease (Lindahl *et al.*, 1992). High concentration of TFPI has also been associated with apoptotic or antiproliferative effects on smooth muscle and endothelial cells (Mikhailenko *et al* 1995; Hamuro *et al*, 1998). This may be due to the fact that although the extrinsic pathway is the quickest route to thrombin, it requires a consistent level of TF, whereas the intrinsic pathway can be triggered by relatively small quantities of thrombin, and is sustainable due to a positive feedback loop (Louvain-Quintard *et al.*, 2005). This might explain why in the case of MCF7H3erbB2, SKBR3 and DLKP4E, up-regulation of TFPI is being observed, supporting the idea that the intrinsic over the extrinsic is being chosen in support of an invasive phenotype.

Functional effects of TFPI knock-down in relation to invasion have not yet been examined. Here TFPI was identified as a possible invasion-related gene based on microarray analysis, and further investigation confirmed through siRNA silencing that TFPI did in fact play an important role in invasion in both DLKP4E and SKBR3.

Figure 4.4: The Role of TFPI in invasion

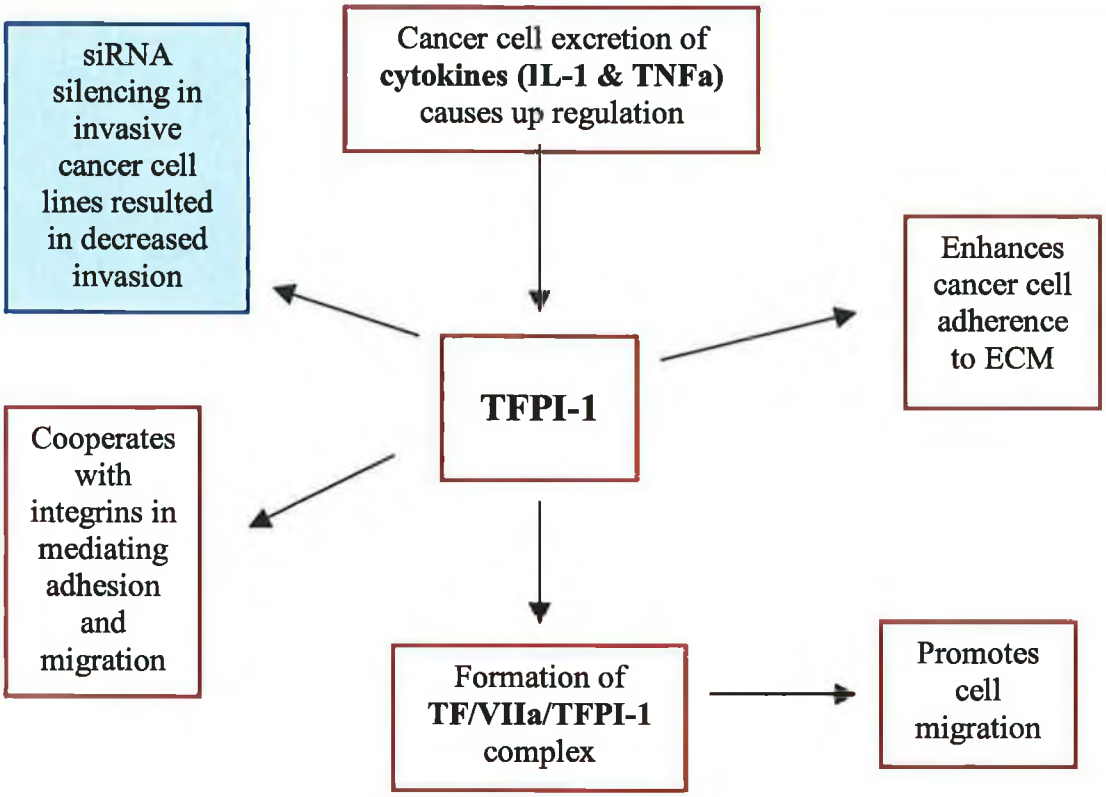

Figure 4.4: Overview of the many roles of TFPI related to invasion

4.4.2.2 Effect of EGR1 siRNA on DLKP4E and SKBR3

EGR1 was chosen as a siRNA target after analysis of MCF7H3erbB2 microarray data showed a +2.99 fold increase in invasive MCF7erbB2 compared to non-invasive MCF7H3. An increase of +1.35 fold was also observed in invasive DLKP4E and, +1.2 fold in invasive DLKP4Emut compared to parent DLKP. This contradicts previous work in lung, brain and breast tissue where EGR1 was associated with tumour suppression (Calogera *et al.*, 2001; Huang *et al.*, 1997). However, EGR1 has been found to promote survival of prostate cancer cells (Abdulkadir *et al.*, 2001), and is associated with proangiogenic activity in head and neck squamous carcinoma (Worden *et al.*, 2005).

4.4.2.2.1 Effect of EGR1 siRNA on proliferation

EGR1 plays a significant role in cell growth and proliferation, which can be seen from the correlation between mitogen activation and EGR1 biosynthesis (Goetze *et al.*, 1999). It would therefore be expected that over-expression of EGR1 may lead to cancer progression. Despite its obvious role in proliferation, EGR1 is predominately described as having a negative effect on tumour cell growth. Up-regulation of EGR1 is reported to result in apparently contradictory activities. These include differentiation (Nguyen *et al.*, 1995), mitogenesis (Kaufmann and Thiel, 2001), tumour suppression (Huang *et al.*, 1995), apoptosis (Virolle *et al.*, 2001), and protection from apoptosis (Virolle *et al.*, 2003). Likewise, EGR1 has been found to be equally involved in regulation of tumour-suppressors (Huang *et al.*, 1998; Baron *et al.*, 2006) and mechanisms involved in tumour progression (Fudge *et al.*, 1994; Toretsky and Helman, 1996). As a result, EGR1 expression in many different cancer cell lines is varied, and seems to be dependent on tissue type.

Proliferation assays carried out on DLKP4E transfected with EGR1 siRNA A and B showed little change in growth rate. As EGR1 was up-regulated in invasive DLKP4E, its down-regulation would be expected to have a negative effect on proliferation. This was not the case, with only 5-10% reduction in proliferation observed compared to scrambled siRNA transfected controls. EGR1 influences proliferation through regulation of several genes. Mitogen-activated protein kinase (MAPK) cascades are involved in the transduction of signals from mitogens and cellular stresses into appropriate cellular responses and are required for many functions including cell

proliferation (Chang and Karin, 2001). Mitogen-activated transcription of a number of immediate-early genes, such as EGR1, is dependent on the activation of MAPK cascades. However, the MAPKs activate several factors that are important for proliferation, and silencing of EGR1 alone may not be adequate to influence the rate of proliferation in DLKP4E.

SKBR3 showed an increase in growth of 30-40% compared to the scrambled control (Section 3.6.1). There was no considerable change compared to the non-transfected control, and kinesin controls showed the transfection was successful. These results implied that either EGR1 siRNA transfection had a positive effect on proliferation of SKBR3 cells, or scrambled siRNA control had a negative effect on SKBR3. EGR1 has been associated with both enhanced (Virolle *et al.*, 2003), and reduced (Ferraro *et al.*, 2005) rates of proliferation, depending on the cell line, and therefore it is possible that EGR1 siRNA would have a different effect in SKBR3 than in DLKP4E. It is also possible that the scrambled siRNA control had a negative effect on proliferation in SKBR3, as the cells transfected with target siRNA had a similar rate of proliferation as the non-transfected SKBR3 control. As this effect was also observed in SKBR3 using other target siRNAs, it is most likely the case.

4.4.2.2.2 Effect of EGR1 siRNA on mRNA and protein levels

Real-time PCR results showed that all three EGR1 siRNAs were effective in silencing EGR1 mRNA in SKBR3 at 24hrs (~50% reduction), and EGR1 siRNA C was effective in DLKP4E (Section 3.6.2). Other studies looking at EGR1 silencing by siRNA, used an appropriate EGR1-specific sequence inserted into the pSUPER plasmid (direct synthesis of siRNA in mammalian cells). The results of this study showed a single EGR1 siRNA was effective in reducing mRNA levels by 40-50% after 48hrs (Weisz *et al.*, 2004), which support the results presented in this work. Real-time PCR results for DLKP4E and SKBR3 showed fluctuations in EGR1 expression were observed between the non-transfected and scrambled-siRNA transfected controls at mRNA level. This was not expected, as the scrambled control was a nontargeting siRNAs designed to have limited sequence similarity to known genes, and therefore minimal affect on EGR1 mRNA. It is unlikely that this is due to qPCR background noise, as although expression levels for SKBR3 had not been determined by microarray results showed the cycle threshold value to be 20, which implies a sufficient level of expression for accurate qPCR analysis. This result may be due to non-specific effects of siRNA on gene expression.

These effects are dependent upon siRNA concentration in a gene specific manner. Therefore it is possible that the non-specific effects of a given siRNA and a scrambled control differ because of varying transfection efficiencies or have different intercellular stabilities. One study showed that changes occurred in over 1000 genes following the introduction of a siRNA whose target was not expressed in the cell model (Persengiev *et al.*, 2004). Although care was taken to avoid this type of effect by using < 50nm siRNA, it is possible that non-specific effects of scrambled control caused fluctuation in mRNA results for EGR1.

Western blots showed a decrease in EGR1 at protein level in both cell lines (Section 3.6.3). DLKP4E transfected with all 3 non-homologous siRNAs showed marked reduction in protein levels compared to the non-transfected and scrambled controls. This result implies that despite the apparent lack of silencing at an mRNA level, EGR1 siRNA A and B did function in silencing EGR1 in DLKP4E. In SKBR3 a reduction in EGR1 protein was seen as a result of EGR1 siRNA B and C, with the barely detectable siRNA C band indicating very efficient silencing. The fact that EGR1 siRNA A and B did not have an effect on DLKP4E at mRNA level, but did at protein level might suggest these siRNAs were functioning like miRNA. siRNA are 21-22 nucleotides in a staggered duplex, with two unpaired nucleotides at either end and are perfectly complementary to their target sequence. On the other hand, miRNA possess a strand which is highly, but not perfectly complementary to one or more target mRNAs. This causes the assembly of an mRNA-protein complex on the target mRNA, preventing translation.

4.4.2.2.3 Effect of EGR1 siRNA on invasion

The invasion assay results following EGR1 silencing were impressive, with all three siRNAs causing a considerable drop in the number of invading cells. EGR1 siRNA C produced the greatest effect, and was the only siRNA that showed knock-down at mRNA and protein level for both cell lines, proving it the most efficient of the three (Section 3.6.4).

It has been suggested that EGR1 is plays a role in tumour supression:

1. Through inducing synthesis of p53, a known tumour suppressor, by directly activating the p53 promoter (Weisz *et al.*, 2004).

2. By binding to the transcription factor c-Jun and augmenting its pro-apoptotic activity (Whitmarsh *et al.*, 1995).
3. Through transactivation of PTEN, also a tumour suppressor (Ferraro *et al.*, 2005).

Equally, EGR1 has also been implicated in cancer progression:

1. Mutant P53 can induce induction of EGR1 leading to enhanced transformed properties and resistance to apoptosis (Weisz *et al.*, 2004).
2. It is activated through signaling in a number of pathways which have been associated with cancer progression e.g. JNK, ERK, AKT. As a result it regulates the expression of many genes involved in survival (BCL2, Fibronectin, NFkB) and angiogenesis (VEGF and TF) (Worden *et al.*, 2005).
3. It is suggested in the present study that up-regulation of EGR1 does not necessarily mean up-regulation of PTEN, and therefore EGR1 doesn't always play a role in tumour supression.

Recent studies indicate that EGR1 is a direct regulator of multiple tumour supressors including TGFβ1 (Adamson *et al.*, 2003), PTEN (Ferraro *et al.*, 2005) and p53 (Weisz *et al.*, 2004). The downstream pathways of these factors display multiple nodes of interaction with each other, suggesting the existence of a functional network of suppressor factors. This mechanism, once activated, would support maintenance of normal growth and resistance to transformed variants. It is interesting to note that although EGR1 has been identified as a transactivator of PTEN, results from the present microarray study show a decrease in PTEN, while EGR1 is up-regulated. This suggests EGR1 does not enhance the tumour suppressor activities through PTEN in MCF7H3erbB2. PTEN functions as a tumour suppressor by antagonizing the P13K/AKT signaling cascade. The P13K/AKT pathway plays a vital role in cell growth and survival. This pathway is targeted by genomic aberrations including mutation, amplification and rearrangement, all of which, including down-regulation of PTEN, which is observed in the present study (-1.28 fold change) can lead to uncontrolled growth and survival. This in turn leads to competitive growth advantage, metastatic competence and drug resistance (Hennessy *et al.*, 2005). This model has also been observed in prostate cancer where EGR1 is oncogenic. In this case up-regulation of EGR1 is associated with down-regulation of PTEN and p53 in prostate cancer tissue (Eid *et al.*, 1998). EGR1 deficiency was also found to significantly delayed the

progression from prostatic intra-epithelial neoplasia to invasive carcinoma in EGR1 $^{-/-}$ mice (Abdulkadir *et al.*, 2001). It has been suggested that these defects in the suppressor network allow for the unopposed induction of transforming growth factor β1 (TGFβ1) and fibronectin, which favor transformation and survival of prostate tumor epithelial cells, explaining the role of EGR1 in prostate cancer (Baron *et al.*, 2005). Interestingly, fibronectin is also found up-regulated in MCF7H3erbB2 compared to parent, which suggests a common mechanism of invasion in prostate and breast cancer cells.

The P13K/AKT signalling cascade also regulates IkB kinase, causing degradation of IkB, an inhibitor of NFkB (Kane *et al.*, 1999). Nuclear translocation and activation of NFkB leads to the transcription of NFkB-dependent genes including Bcl-xl, caspase inhibitors and c-Myb, all of which have an antiapoptotic effect on the cell (Barkett and Gilmaore, 1999). EGR1 is known to regulate NFkB, and upregulation of EGR1 in MCF7H3erbB2 as a result of unregulated activation of the P13K/AKT pathway may result in up-regulation of NFkB, preventing apoptosis and facilitate the invasive phenotype of the cells.

The fact that EGR1 itself is upregulated by several growth factors and oncogenes supports the idea that it functions as a growth-promoting protein in cancer cells. It is also clear that EGR1 is involved in many key signaling pathways in the invasion process (JNK, ERK, AKT). The present study has demonstrated how siRNA knock-down of EGR1 alone in breast and lung cancer cell lines was sufficient to reduce invasion. Evidence from the literature would suggest that up-regulation of EGR1 is a downstream effect of defective MAPK pathway signaling. Although its exact role in the invasion process is unclear, it is still a probable marker of invasion in certain types of cancer. The present study suggests EGR1 may be a promising target for future anti-invasion interventions.

Several contradictory reports have been published on the role of EGR1 in invasion. A recent study showed invasion inhibition by COX inhibitors is mediated by EGR1. Overexpression of EGR1 was found to weakened the cellular invasion of A549 lung cancer cells, and suppression of EGR1 expression by siRNA enhanced the invasion of A549 cells compared with control RNA-transfected cells. These results indicated that the inhibition of tumor cell invasion by COX inhibitors was mediated by the increased expression of EGR1 (Moon *et al.*, 2005). However, in agreement with the present study, Weisz *et al.* (2004) showed that siRNA knock-down of EGR1 resulted in a decrease in

colony forming efficiency of H1299 (also a human lung cancer cell line) a phenotypic effect often associated with invasion (Weisz *et al.*, 2004).

All possible precautions to ensure efficient and accurate EGR1 silencing were carried out (as outlined for TFPI), including use of appropriate controls, multiple non-homologous EGR1 siRNAs, carrying out siRNA transfection in two different cell lines, and detection of EGR1 silencing at RNA and protein level. Therefore, we can say with confidence that a reduction in invasion of DLKP4E and SKBR3 was due to silencing of EGR1, and accordingly that EGR1 plays a significant role in the invasion process of both cell lines, confirming the accuracy of genes chosen by microarray analysis.

4.4.2.3 Effect of RPS6KA3 siRNA on DLKP4E and SKBR3

Analysis of microarray data found that RPS6KA3 was increased in both of the invasive cell lines, MCF7H3erbB2 and DLKP4E, compared to their non-invasive parent cell lines. A fold change of +2.36 was seen in MCF7H3erbB2, and +1.2 in DLKP4E. As this analysis suggested an increase in RPS6KA3 contributed to an increase in invasion. Because of this analysis it was decided to use RPS6KA3 as a siRNA target to further assess its role in invasion in the above cell lines. Unlike the other targets, only two siRNAs were used for all experiments, as both had been validated by the supplier (that is, they were functionally tested and guaranteed to work).

4.4.2.3.1 Effect of RPS6KA3 siRNA on proliferation

The involvement of RPS6KA3 levels in breast was recently examined and it was found that mean levels of RPS6KA3 were statistically higher than normal tissue, being overexpressed in ~50% of human breast cancer tissue samples (Smith *et al.*, 2005). The same study showed an inhibitor of RPS6KA3 caused inhibition of proliferation in MCF7 cells, producing a cell-cycle block in G1 phase. RNA interference of RPS6KA3 showed same. Work carried out with prostate cancer tissues produced similar results, with ~50% of samples overexpressing RPS6KA3, and inhibition of proliferation after inhibition of RPS6KA3 (Clarke *et al.*, 2005). Identification of RPS6KA3 as a gene up-regulated in invasive DLKP4E and MCF7H3erbB2 would support a proliferation-enhancing role for RPS6KA3, and concur with the above studies. However, proliferation assays carried out on DLKP4E transfected with RPS6KA3 siRNA A and B had no substantial effect on growth rate. It is clear from previous studies that inhibition of RPS6KA3 alone is sufficient to have a negative effect on proliferation, and it is therefore unclear why no such effect was seen here.

SKBR3 again showed an increase in the rate of proliferation with siRNA transfected cells growing up to 45% more than the scrambled control (Section 3.7.1). As RPS6KA3 has been found up-regulated in DLKP4E and MCF7H3erbB2, both invasive cell lines, its down-regulation would not be expected to have a positive effect on proliferation. Although expression levels for SKBR3 had not been determined by microarray, real-time PCR results suggest the level of expression was sufficiently high as to not be greatly effected by background noise. This was also observed with EGR1, and it seems likely that the scrambled siRNA control had a negative effect on proliferation of

SKBR3 cells, as the cells transfected with target siRNA had a similar rate of proliferation as the non-transfected control. Therefore it is likely that this is a SKBR3-specific effect.

4.4.2.3.2 Effect of RPS6KA3 siRNA on mRNA and protein levels

Results showed no considerable RPS6KA3 mRNA reduction in the presence of RPS6KA3 siRNA A or B at 24 or 48hrs in DLKP4E. A 25% decrease in RPS6KA3 at 24hrs was the largest observed decrease (Section 3.7.2). The same siRNAs were used to transfect SKBR3 cells, and RPS6KA3 siRNA A also had no effect in this cell line at 24 or 48hrs. RPS6KA3 siRNA B however, did cause a 50% reduction in RPS6KA3 mRNA at 48hrs. Real-time PCR detected GAPDH knock-down in these cells under the same conditions (Figure 3.4.3), and therefore it is unlikely that this result was due to an unsuccessful transfection. Western blot showed a considerable decrease in protein in DLKP4E and SKBR3. Cells transfected with both siRNAs showed protein silencing compared to the non-transfected and scrambled controls. This result implies that despite lack of silencing at an mRNA level, RPS6KA3 siRNA did function in 'knocking-down' RPS6KA3 in both cell lines. The fact that EGR1 siRNA A and B did not have an effect on at mRNA level, but did at protein level may suggest these siRNAs were functioning like miRNA. This would not affect the level of mRNA transcription but prevent translation of RPS6KA3 protein. It is also possible that the mRNA was being regulated so rapidly silencing was not detected 24hrs after transfection. There is also the possibility that the RPS6KA3 primer used was not specific, and picked up another transcript. This would cause a decrease in the observed mRNA silencing at mRNA level. Other studies looking at the effects of RPS6KA3 have shown protein silencing, but did not address silencing at mRNA level (Woo *et al.*, 2004; Aggarwal *et al.*, 2006).

4.4.2.3.3 Effect of RPS6KA3 siRNA on invasion

Results of invasion assays showed transfection of RPS6KA3 siRNA caused a decrease in invasion in both cell lines. A considerable reduction in the number of invading cells was observed after transfection with both RPS6KA3 siRNAs A and B in both cell lines. Both photographic evidence and cell counts showed that the number of invading cells was reduced by at least 50% (Section 3.7.4). Proof of knock-down of RPS6KA3 at a protein level, combined with a decrease in invasion after siRNA transfection, validated

array analysis and confirmed RPS6KA3 is important in the invasive mechanism of SKBR3 and DLKP4E.

Particularly relevant to the present study is the connection between RPS6KA3 and phosphoinositide dependent protein-kinase-1 (PDK1). RPS6KA3 is phosphorylated and activated *in vivo* by ERK and 3-phosphoinositide-dependent protein kinase 1 (PDK1) (Jensen *et al.*, 1999). The isolated N-terminal kinase of RSK2 is phosphorylated at Ser^{227} by PDK1, a constitutively active kinase, leading to 100-fold stimulation of kinase activity. Previous studies have demonstrated that active PDK1 may account for basal RPS6KA3 activity in cells, whereas stimulation of RPS6KA3 by growth factors requires the collaborative regulation by ERK and PDK1 (Jensen *et al.*, 1999).PDK1 was first identified as a protein-Ser/Thr kinase that linked PI3K to Akt activation in response to growth factor receptor stimulation. Recent reports have demonstrated that PDK1 confers a marked growth advantage, promotes invasion and can activate matrix metalloproteinases (Xie *et al.*, 2006). Ser386 in the hydrophobic motif of RPS6KA3 is a recognised docking site for PDK1 (Frodin *et al.*, 2000). At the same time, the N-terminal of RPS6KA3 is phosphorylated at Ser227 by PDK1. Therefore a mechanism exists whereby both PDK1 and RPS6KA3 activate each other. Interestingly, microarray results for MCF7H3erbB2 showed a -1.72 fold change in PDK1, but a +2.36 change in RPS6KA3. This may indicate that ERK plays a more significant role in RPS6KA3 regulation. However it is not possible to relate regulation through phosphorylation to levels of mRNA (microarray results). How ERK and PDK1 contribute to activation of RPS6KA3, and therefore invasion in MCF7H3erbB2, is therefore uncertain.

However, results from the present study have demonstrated that siRNA silencing of RPS6KA3 alone had a considerable effect on invasion in SKBR3 and DLKP4E. Although RPS6KA3 has not been directly associated with invasion, it is evident from the literature that it plays a significant role in several signalling pathways that are often disrupted in cancer, such as MAPK/ERK (Smith *et al.*, 1999). Comparison studies of the docking site of RPS6KA3 and the carboxyl-terminal tails of other MAPK-activated kinases revealed similar docking sites within each of these MAPK-targeted kinases. Also, the number and placement of lysine and arginine residues within the conserved region correlated with specificity for activation by ERK and p38 MAPKs *in vivo* (Smith *et al.*, 1999). MAPK plays a major role in inducing proteolytic enzymes that degrade the basemant membrane, enhancing cell migration, initiating several pro-survival genes and maintaining growth. The MAPK pathways can be divided into ERK (extracellular

regulated kinase), JNK (c-Jun N-terminal kinase) and p38 isoforms. Activated MAPK pathways have been detected in many tumours including breast, lung, colon and kidney, implicating it in in tumour progression and metastasis (Reddy *et al.*, 2003). RPS6KA3 is activated via the ERK pathway following mitogen stimulation by phosphorylation on four sites: Ser227 in the activation loop of the N-terminal kinase domain (NTK), Ser369 in the linker, Ser386 in the hydrophobic motif and Thr577 in the C-terminal kinase (CTK) domain (Doehn *et al.*, 2004). ERK dissociates when the NTK domain phosphorylates Ser736 next to the ERK docking site.

It is clear from the above that RPS6KA3 has a broad range of substrates and actions, and is likely to participate in many cellular processes. RPS6KA3 acts as a vital regulator of key transcription factors involved in early gene response, such as c-Fos, Elk-1 and CREB which are known for their role in tumour progression (Sassone *et al.*, 1999; Aksan Kurnaz, 2004; Xing *et al.*, 1996). Immediate early genes (IEGs) are activated transiently and rapidly in response to a wide variety of cellular stimuli. They represent a standing response mechanism that is activated at the transcription level in the first round of response to stimuli, before any new proteins are synthesized. Thus IEGs are distinct from "late response" genes, which can only be activated later following the synthesis of early response gene products. Thus IEGs have been called the "gateway to the genomic response". It is well established that several specific early response genes are activated in response to exogenous agents that induce intracellular stress including several therapeutic modalities such as chemotherapeutic agents, heat, and ionizing radiation (IR). In this regard, these gene products may function in coupled short-term changes in cellular phenotype by modulating the expression of specific target genes involved in cellular defences to the damaging effects of IR (Wang *et al.*, 2005a; Gius *et al.*, 1999). RPS6KA3 therefore holds a powerful position in determining cellular response.

RPS6KA3 may also contribute to increased invasion through promotion of ani-apopotic proteins. Defective apoptosis can facilitate metastasis by allowing cells to ignore restraining signals from neighboring cells, survive detachment from the extracellular matrix, and persist in hostile environments. The development and maintenance of healthy tissues is dependent on a balance between cell survival and cell death (apoptosis). Disruption of this balance and prevention of apoptotsis contributes to uncontrolled growth and clonal expansion of cancer cells. The Bcl-2 family member Bad is a pro-apoptotic protein, and phosphorylation of Bad by cytokines and growth factors promotes cell survival in many cell types. The Bcl-2 family of related proteins

contains protein-protein interaction domains that facilitate homo- and heterodimerization. Bcl-X_L, an anti-apoptotic member, forms a hetrodimer with Bad, which is pro-apoptotic (Reed, 1998). Phosphorylation of Bad results in its release from Bcl-xl, increasing levels of Bcl-xl in the cell and causing a decrease in apoptosis. She *et al.*, illustrated that UVB-induced phosphorylation of Bad at serine 112 was mediated through MAP kinase signaling pathways in which RPS6KA3 served as direct mediator (She *et al.*, 2002). More recent reports have confirmed this and show that RPS6KA3 mediated phosphorylation of Bad is activated by the Ras signaling pathway (Gu *et al.*, 2004).

Though RSK family mechanism of action has been the subject of many studies, few have examined their biological function. Results here demonstrate a functional effect of RPS6KA3 in invasion of both DLKP4E and SKBR3. Although its exact role in the invasion process is unclear, RPS6KA3 documented overexpression in breast and prostate cancer tissue, along with its obvious association with so many other invasion markers strongly implicates RPS6KA3 in the invasion process. This knowledge combined with the functional effects observed after RPS6KA3 siRNA silencing in DLKP4E and SKBR3, makes RPS6KA3 a probable marker of invasion, and a promising target for future anti-invasion interventions.

4.4.2.4 Effect of TNFAIP8 siRNA on DLKP4E and SKBR3

Comparison of parent MCF7H3 to MCF7H3erbB2 found a +2.47 fold increase in levels of TNFAIP8 expression in MCF7H3erbB2 compared to the parent cell line. No change in expression was seen in DLKP4E or DLKP4Emut. Unlike the other siRNA targets, TNFAIP8 was examined only using proliferation and invasion assays. Due to the novelty of the target, no antibody was commercially available, and qPCR primers failed to detect the target. In previous work rabbit polyclonal antiserum was custom generated against a TNFAIP8-specific peptide for western blot analysis (Kumar *et al.*, 2004; Zhang *et al.*, 2006). This was not possible in the present study due to time constraints.

4.4.2.4.1 Effect of TNFAIP8 siRNA on proliferation

Proliferation assays results were similar to previous targets. Again, little change in growth rate was observed in DLKP4E after TNFAIP8 siRNA transfection, but SKBR3 showed a 40% increase in growth. As already explained, this was most likely due to scrambled siRNA having a negative effect on growth, which based on this and previous results appears to be specific to SKBR3 (Section 3.8.1). Overexpression of TNFAIP8 in cancer cells has been associated with enhanced survival (You *et al.*, 2001). Kumar *et al.*, (2000) found that TNFAIP8 overexpression was a negative mediator of apoptosis though its death effector domian. Apoptosis signaling is regulated and executed by specialized proteins that often carry protein/protein interaction domains. One of these domains is the death effector domain (DED), found in components of the death-inducing signaling complex (DISC), which also contains death receptors, adaptor proteins, caspase-8 and caspase-10. The DED protein family comprises both proapoptotic- and antiapoptotic-DED-containing proteins, and not surprisingly, these proteins play a pivotal role in the regulation of apoptosis (Barnhart *et al.*, 2003). Accumulating evidence now suggests that DED-containing proteins have additional roles in controlling pathways of cellular activation and proliferation. In this regard the DED family may be important to cellular homeostasis by co-regulating proliferation and apoptosis in parallel (Tibbetts *et al.*, 2003). By decreasing the level of apoptosis TNFAIP8 enhances survival, and may also enhance the rate of proliferation. Apoptosis and proliferation of arthritis synovial fibroblasts (RASFs) was significantly decreased after treatment with siRNA for TNFAIP8 as compared with controls treated with siRNA for luciferase or untreated control RASFs (Zhang *et al.*, 2004). MDA-MB 435 human cancer cells transfected with the TNFAIP8 cDNA also exhibited increased growth rate

compared to control vector transfectants (Kumar *et al.*, 2004). Based on published data, TNFAIP8 siRNA transfection of DLKP4E and SKBR3 would be expected to decrease proliferation. An increase in proliferation of SKBR3 may have been due to an effect of the scrambled control (as already discussed), and no decrease in proliferation was observed in DLKP4E. It is possible that TNFAIP8 extends the life of DLKP4E cells without increasing the rate of proliferation, which would explain why TNFAIP8 siRNA transfection had little effect on the outcome of proliferation assays.

4.4.2.4.2 Effect of TNFAIP8 siRNA on invasion

A considerable decline in the number of invading cells was observed in DLKP4E after siRNA silencing of TNFAIP8. Cells transfected with TNFAIP8 siRNA were 50-60% less invasive than DLKP4E transfected with a scrambled control. Results for SKBR3 are less impressive, with siRNA A and B having no significant effect. The siRNA C however, caused the greatest effect with a 65% drop in invasion (Section 3.8.2). However, there was no evidence of TNFAIP8 reduction at an mRNA or protein level in either cell line. Considering the fact that there was no measured silencing of TNFAIP8 it may be suggested that the functional effects observed were due to non-specific transfection-selected effects. This is unlikely however as the same stringent controls and policies outlined for TFPI were adhered to in this case. These include the use of three different siRNA oligos against the same target, all of which caused a decrease in invasion when transfected into DLKP4E. The same cells had also been transfected with kinesin and GAPDH as controls, and both controls proved a successful transfection (kinesin visually through changes in the morphology of the cells, and GAPDH showed mRNA knock-down under the same transfection conditions). This strongly suggests that the siRNAs are functioning in silencing TNFAIP8. An earlier study looking at differentially displayed transcripts in human primary and matched metastatic head and neck squamous cell carcinoma cell lines, identified TNFAIP8 as having association with a invasive phenotype (Patel *et al.*, 1997). Results of the present study concur, finding TNFAIP8 differentially expressed in an invasive MCF7H3erbB2 compared to the non-invasive parent MCF7H3.The most recent study published demonstrated that expression of TNFAIP8 cDNA in MDA-MB 435 human breast cancer cells was associated with enhanced invasion *in vitro* and increased frequency of pulmonary colonization of tumour cells in athymic mice. They also showed that treatment of athymic mice with TNFAIP8 antisense oligo led to decreased incidence of pulmonary

metastasis and inhibition of TNFAIP8 in vivo. Inhibition of endogenous TNFAIP8 correlated with decreased expression of VEGF receptor-2 in tumour cells and human lung microvascular endothelial cells and loss of endothelial cell viability. Inhibition was also was associated with decreased expression MMP-1 and MMP-9, both well documented as invasion-associated genes (Zhang *et al.*, 2006). These results show TNFAIP8 as a novel invasion marker, and confirm the accuracy of the microarray analysis used in the present work to identify invasion-associated genes in MCF7H3erbB2.

The TNFAIP8 open reading frame contains a sequence in the amino terminus that shows a significant homology to death effector domain II of cell death regulatory protein, Fas-associated death domain-like interleukin-1b-converting enzyme-inhibitory protein (FLIP). Unlike FLIP, the TNFAIP8 open reading frame contains only one death effector domain and lacks the carboxyl-terminal caspase-like homology domain, raising the possibility that TNFAIP8 may be a novel member of the FLIP family (Kumar *et al.*, 2000). FLIP family proteins are involved in the intrinsic apoptotic pathway. Both intrinsic and extrinsic apoptotic pathways exists, the extrinsic modulates mitochondrial function, and the intrinsic regulates the activation of caspases responsible for activation and execution of the apoptotic cascade (Harada and Grant, 2003). FLIP resembles Caspase-8 in structure but lacks protease activity. It interacts with both fas-associated death domain (FADD) and Caspase-8 to inhibits the apoptotic signal of death receptors and, at the same time, can activate other signalling pathways such as that leading to NF-kappa B activation (Schneider and Tschopp, 2000). TNFAIP8 mRNA expression is induced by NFkB and TNFα in human cancer cells, vascular endothelial cells and primary rheumatoid arthritis synovial fibroblasts (Zhang *et al.*, 2005). NFkB comprises a family of transcription factors involved in the regulation of a wide variety of biological responses. NF-kB plays a well-known function in the regulation of immune responses and inflammation, and is believed to play a major role in oncogenesis. NF-kB regulates the expression of genes involved in proliferation, migration and apoptosis which are important in the progression of cancer. Overexpression of NF-kB has been detected in many human malignancies (Dolcet *et al.*, 2005), and although most well know for its role in regulating anti-apoptotic molecules, inhibition of NF-kB has recently been found to contribute to a reduction of the in vitro invasion of colo 205 cells (human colon cancer) (Su *et al.*, 2006). Transcriptional regulation of TNFAIP8 by NF-

kB may therefore be an important factor in the mechanism by which invasion is increased in DLKP4E and SKBR3.

TNFα, which induces TNFAIP8, is a cytokine involved in mediating the inflammatory process in tumours. Tumour promotion can come about as a result of persistant and unresolved inflammation, and therefore TNFα is a vital component in the initial promotion of tumour growth (Szlosarek *et al.*, 2006). Evidence for a role of TNF-α in human cancer has been provided by several clinical studies. To date, TNF-α expression has been confirmed in the tumour micro-environment in the following malignancies: breast, ovarian, colorectal, prostate, bladder, oesophageal, renal cell cancer, melanoma, and lymphomas and leukaemias (Szlosarek and Balkwill, 2003). Exogenous expression of TNFAIP8 causes suppression of TNF-mediated apoptosis, and is thought to work by specifically inhibiting TNF-induced caspases-8 (You *et al.*, 2001). Through inhibition of apoptosis, TNFAIP8 contributes to the invasion process by allowing cells to survive detachment and persist in hostile environments.

More specific studies looking at the role of TNFAIP8 in invasion showed MDA-MB-231 cells stably transfected with TNFAIP8 cDNA displayed an increase in cell migration in collagen I as compared to control transfectants, and the same study provided evidence TNFAIP8 overexpression significantly enhanced tumor growth as compared to control transfectants in athymic mice (Kumar *et al.*, 2004). In May 2006, Zhang *et al.* published data confirming the role played by TNFAIP8 in experimental metastasis (Zhang *et al.*, 2006). Through stable transfection of TNFAIP8 in MDA-MB-435 cells, they showed TNFAIP8 overexpressing cells demonstrated a significant increase in invasion compared to control transfectants. In the present study, TNFAIP8 was not found differentially expressed in DLKP4E compared to parent, yet siRNA silencing caused a marked decrease in invasion, which implied TNFAIP8 was involved in invasion of lung cancer cells. This concurs with results found by Zhang *et al.* (2006), who found mice inoculated with TNFAIP8 showed visible lung metastasis. The same study also used siRNA strategies to inhibit endogenous TNFAIP8 in MDA-MB 435 cells. This inhibition of TNFAIP8 expression was associated with inhibition of MMP-1 and MMP-9 and no change in MMP-2 and VEGF expression. TNFAIP8 siRNA-treated tumour cells also showed inhibition of TNFAIP8, lower molecular weight MMP-1 and MMP-9, 47%; MMP-1. This study supports the present work and helps to validate microarray analysis. Therefore, it is safe to say that TNFAIP8 has a role in cellular

invasion, and taken together, the present studies demonstrate TNFAIP8 as a novel oncogenic factor in cancer cells.

4.4.2.5 Effect of THBS1 siRNA on DLKP4E and SKBR3

Unlike the other targets chosen from this analysis, THBS1 was down-regulated in an invasive cell line (MCF7H3erbB2) by -2.3 fold. Therefore a reduction of THBS1 in a non-invasive cell line was expected to induce an invasive phenotype. For this reason MCF7 (non-invasive) and DLKP (mildly invasive) were selected for transfection with THBS1 siRNAs. DLKP4E and SKBR3, which had been used with all other siRNA targets from this analysis, were also included.

4.4.2.5.1 Effect of THBS1 on proliferation

Results of proliferation assays from MCF7, DLKP and DLKP4E showed very minor changes in growth when transfected with the THBS1 siRNAs, indicating that THBS1 did not play an important role in proliferation in any of these cell lines (Section 3.9.1). THBS1 has been found to both increase (Straume and Akslen, 2003) and decrease (Ren *et al.*, 2006) the rate of proliferation of cells. Microarray results indicate that in this model, THBS1 is associated with a decrease in invasion, and therefore reducing THBS1 should lead to an increase in invasion. As the experimental design was based on finding genes relevant to invasion, there was no guarantee that a proliferation effect would also be observed. THBS1 siRNA may not have had an effect on proliferation of DLKP4E due to the fact that it is a highly invasive cell line, therefore expressing low levels of endogenous THBS1. As with the majority of siRNAs used, SKBR3 showed a more marked increase in proliferation. This may have been due to siRNA silencing, but this would contradict results found in DLKP4E, as SKBR3 is also an invasive cell line. It is most likely due to the effect of the scrambled siRNA on SKBR3 than due to THBS1 effects on proliferation, as the same results were observed for the majority of siRNAs transfected into SKBR3. The varied phenotypic responses which are experienced as a result of THBS1 expression in different cell lines can be contributed to the specific receptor repertoire of the cells. It is therefore possible that THBS1 both enhances and inhibits proliferation depending on the cell type and its pattern of gene expression.

4.4.2.5.2 Effect of THBS1 on mRNA and protein

Real time PCR was carried out on all four cells lines transfected with all three THBS1 siRNAs to determine if THBS1 mRNA had been successfully silenced. Taken as a whole the results showed transfection of 2 out of 3 THBS1 siRNAs caused knock-down of THBS1 at an mRNA level in four different cell lines (Section 3.9.2). Western blots

were use to examine THBS1 protein levels 72hrs post-siRNA transfection in all cell lines. MCF7 was the only cell line that had sufficient levels of THBS1 protein for detection by western blot, which fits with the THBS1 anti-invasion model, as MCF7 is the only non-invasive of the cell lines studied. The results showed that THBS1 protein was reduced after transfection with all three of the THBS1 siRNAs (Section 3.9.3). Also noteworthy that the pattern of silencing which was similar to that observed at mRNA level. Result confirmed that the TBS1 siRNAs used were capable of knock-down of THBS1 at mRNA and protein level.

4.4.2.5.3 Effect of THBS1 on invasion

As predicted from array analysis, reduction of THBS1 caused an increase in invasion (Section 3.9.4). The most dramatic results were seen in DLKP and MCF7. DLKP, a mildly invasive cell line, showed a 3.5 to 4-fold increase in the number of invading cells when transfected with all three siRNA oligos. MCF7, a completely non-invasive cell line, became invasive after transfection with THBS1 siRNA. Cell counts revealed that a 1.3 to 1.7 fold increase was seen in SKBR3 THBS1 siRNA transfected cells. DLKP4E, already a highly invasive cell line, showed a negligible change. These results show that transfection of THBS1 siRNA produces dramatic increases in invasion across SKBR3 and DLKP, with the increase in invasive capacity being inversely proportional to the original level of invasion, and subsequently THBS1 of the cell lines. A recent study showed THBS1 played an important role in the regulation of MMP activity, and by doing so acted as an inhibitor of migration, invasion and angiogenesis. What is most interesting about this study is that is showed mammary tumours progress more rapidly in mice that lack THBS1 and express erbB2. Furthermore, they demonstrated that overexpression of THBS1 suppressed tumour growth (Rodríguez-Manzaneque *et al.*, 2001). This result agrees with those of the present study, and strengthens the argument in favour of THBS1 as an inhibitor of invasion.

Figure 4.5: THBS1 function

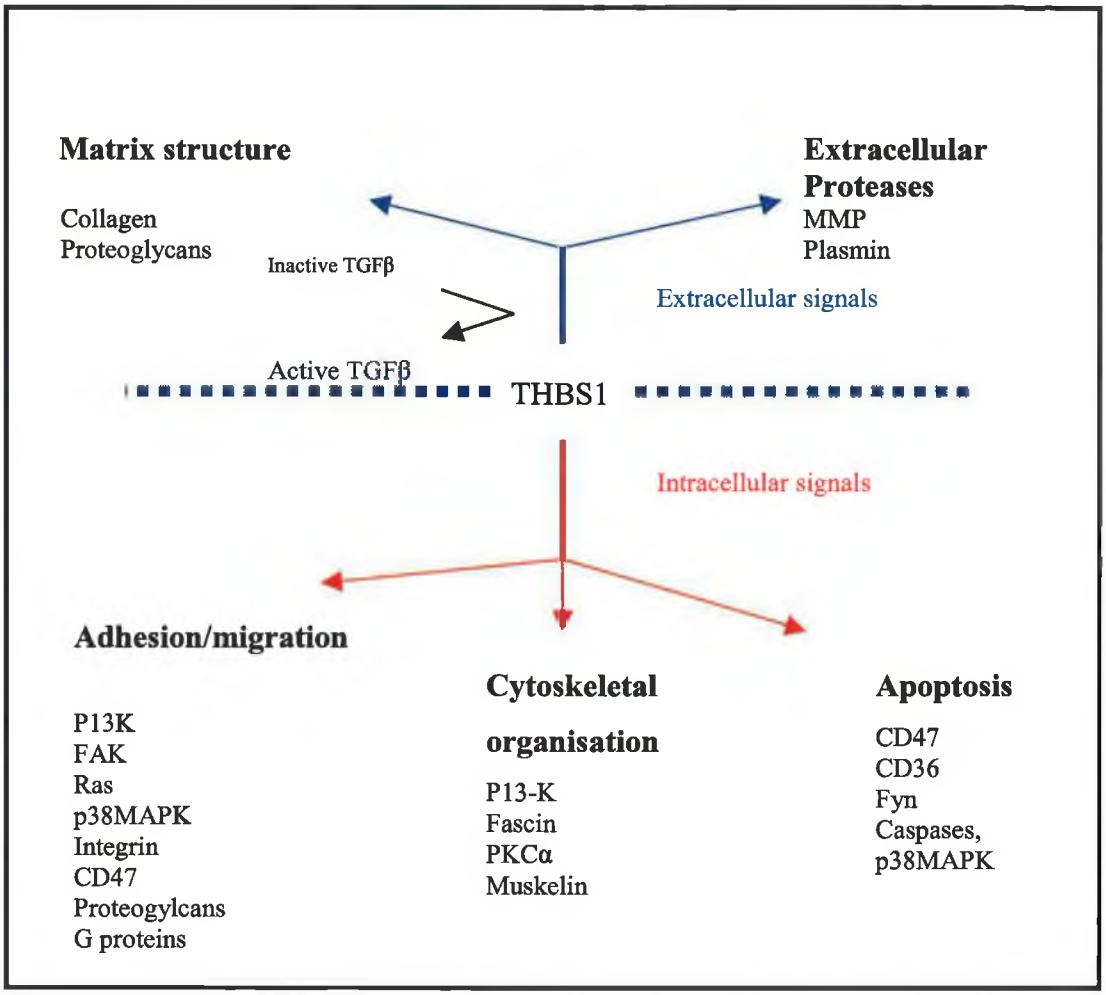

Figure 4.5: Cell-surface-associated thrombospondins provide information that directs changes to the extracellular matrix and interior of the cell. This schematic illustrates how the flow of information provides the direction for extracellular and intracellular responses during tissue genesis and remodelling. Proteins that are involved in some aspects of the responses are listed. The specific subset of molecules that are involved will depend on the cell type and the experimental conditions (Lawler, 2000).

4.4.2.5.4 Pro-invasive role of THBS1

Many studies have supported the idea of THBS1 contributing to increases in tumour cell motility and invasion. Yabkowitz *et al.*, (1993) showed that THBS1 increased migration of a highly invasive squamous cancer cell line, and antibodies against THBS1 reduced invasion (Yabkowitz *et al.*, 1993). Increased invasion in vitro was also seen in breast and squamous cancer cells after exposure to THBS1 (Wang *et al.*, 1996). The same work also demonstrated growth inhibition of malignant breast cancer in mice when injected with a THBS1 antibody.

As already mentioned THBS1 acts as an adhesion factor (Taraboletti *et al.*, 1990) and is also involved in migration in many cancer tissues (Li *et al.*, 2001b). In the presence of THBS1 tumour cells and platelets are more likely to attach to epithelial cells and cross capillary and lymphatic endothelia. This is aided by the conversion of plasminogen to plasmin facilitated by THBS1. It has also been suggested that THBS1 activation of growth factors such as TGFβ may play a role in plasmin production through an amplification loop. TGFβ is a latent growth factor stored in the tumour-associated stroma and activated by plasmin. This activation causes an up-regulation of uPA and uPRA, and therefore plasmin generation (Keski-Oja *et al.*, 1991). Plasmin is very efficient at generating active MMP-3 from exogenously added pro-MMP-3. The activated MMP-3 becomes a potent activator of the 92-kDa pro-MMP-9, yielding an 82-kDa species that is enzymatically active in solution and represents up to 50-75% conversion of the zymogen. It has been demonstrated that the activated MMP-9 enhanced the invasive phenotype of cultured cells as their ability to both degrade extracellular matrix and transverse basement membrane was significantly increased following zymogen activation (Ramos-DeSimone *et al.*, 1999). THBS-1 has been found localized in tumor stroma surrounding pancreatic tumour cells expressing MMP-9, and stromally-derived THBS-1 up-regulates the production of MMP-9 by pancreatic adenocarcinoma. These data are also consistent with the conclusion that THBS-1-rich stroma is involved in regulating matrix remodeling in tumour invasion (Qian, 2001).

The thrombin-induced increase in THBS1 mRNA was proved to be due to direct thrombin receptor, plasminogen activator receptor (PAR1) stimulation (Olson *et al.*, 1999). A more recent study provided further evidence for the role of THBS1 in invasion through protease-activated receptor-1 (PAR1) (Boire *et al.*, 2005). Boire *et al.* (2005) found that expression of PAR1 was both required and sufficient to promote growth and invasion of breast carcinoma cells in a xenograft mouse model. MMP1 acted as a protease agonist of PAR1, cleaving the receptor at the proper site to generate PAR1-dependent Ca (2+) signals and migration. MMP1 activity was derived from fibroblasts and was absent from the breast cancer cells. These results demonstrated that MMP1 in the stromal-tumor microenvironment could alter the behavior of cancer cells through PAR1 to promote cell migration and invasion. A similar study showed THBS1 caused an increase in tumour cell invasion through the Urokinase PAR (uPAR) (Albo and Tuszynski, 2004). Taken together, these studies support a central role for THBS1 in the regulation of the plasminogen/plasmin system and tumour cell invasion.

4.4.2.5.5 Anti-invasion role of THBS1

In contrast with the above studies, much work has supported THBS1 as an inhibitor of invasion. There are several studies which found THBS1 overexpression decreased tumor growth for certain cell lines when they were implanted into nude mice. It was reported that highly invasive breast, melanoma, and bronchial cancer cells secreted lower THBS1 than their less invasive counterparts (Zabrenetzky *et al.*, 1994).A decrease in the metastatic potential of these highly malignant tumors after THBS1 overexpression strongly pointed towards an invasion inhibitory role for THBS1. Similarly, metastatic hemangioma and cutaneous squamous cancer cells made to overexpress THBS1 also lost their metastatic potential (Sheibani and Frazier, 1995; Streit *et al.*, 1999). In addition THBS1 secretion by a fibrosarcoma cell line prevented the progression of metastatic melanoma in mice (Volpert *et al.,* 1998). Similarly, after resection of a THBS1 secreting malignant sarcoma there was widespread metastasis, which may have been due to the loss of THBS1 inhibition on metastatic tumor growth (Crawford *et al.* 1998).

Another study demonstrating the anti-invasive effects of THBS1 showed tumor burden and vasculature were significantly increased in THBS1-deficient animals, in contrast to THBS1 overexpressors which displayed delayed tumour growth or lacked tumour development. The absence of THBS1 resulted in increased association of vascular endothelial growth factor (VEGF) with its receptor VEGFR2 and higher levels of active matrix metalloproteinase-9 (MMP9), a molecule known to facilitate both angiogenesis and tumor invasion (Rodríguez-Manzaneque *et al.*, 2001). This study also found that exogenous THBS1 added to microvascular endothelial cultures lead to accumulation and stabilization of proMMP9. This had been demonstrated previously, and what made this study interesting was they found this increase occurs with a parallel reduction in MMP9 activation/processing. THBS1 has been seen to bind MMP2 and MMP9 *in vitro* (Bien and Simons, 2000). The authors also demonstrated that presence of THBS1 blocks gelatinolytic activity of these enzymes and speculated that the effect of THBS1 might be mediated via block of proMMP2 and proMMP9 processing. Together these findings are consistent with a role of THBS1 in MMP regulation, and are in agreement with the reported effects of TSP1 as an inhibitor of invasion in the present study.

Also of note are expression levels of PTEN in the present microarray study. PTEN decreases phosphorylation of AKT by dephosphorylating 3-phosphorylated inositol phospholipids, and by repressing AKT signalling prevents transcription of downstream

tumour-associated genes. Upregulation of PTEN expression in glioma cell lines was seen to decrease levels of phosphorylated Akt, transactivation of p53 and increase levels of THBS1 gene expression (Su *et al.*, 2003). This is in agreement with microarray results from the present study. Results showed when PTEN expression was downregulated, so too was THBS1 expression in the invasive MCF7H3erbB2 (relative to the non-invasive parent cell line). Both studies suggest a role for THBS1 in tumour suppression.

The work presented here suggests THBS1 to have anti-invasive properties in DLKP and MCF7. Gene silencing of THBS1 alone was enough to change the phenotype of MCF7 cells from non-invasive to invasive, and cause a marked increase in invasion of DLKP. Research studies to date provide experimental evidence indicating that THBS1 can be both adhesive and anti-adhesive, can foster and retard metastasis, stimulate and inhibit angiogenesis and increase and reduce proteolytic activity and fibrinolysis. THBS1 exerts its function by binding to various matrix proteins and cell-surface receptors, and by interaction with these receptors functions in directing formation of multi-protein complexes that modulate cellular phenotype. As a result, diverse intracellular pathways are activated relevant to embryonic development, tissue differentiation, inflammations, wound healing, and coagulation (Figure 4.5). Previous studies have shown THBS1 displays distinct biological activities in different cell types, which is attributed to its multiple functional domains that engage corresponding receptors on the surface of targeted cells. It is clear that THBS1 is capable of initiating a variety of intracellular signals, not only through binding of receptors but also its ability to activate latent transforming growth factor beta (TGFβ) and inhibit several proteases. The varied phenotypic responses which are experienced as a result of THBS1 expression can be contributed to the combined effect of TGFβ activation and the specific receptor repertoire of the cells. It is therefore possible that THBS1 has both invasive and non-invasive functions depending on the cell type and its pattern of gene expression.

As with all of the siRNAs used in this study, stringent controls were adhered to. This included the use of three non-homologous siRNAs (Figure 4.6), each of which was transfected into four different cell lines. Consequently, the present study provides strong evidence for THBS1 as anti-invasive in a variety of breast and lung cell lines.

Figure 4.6 Exon targets of THBS1 siRNA A, B & C.

Targeted Exon(s): NM_003246: Exon 22

THBS1A

Targeted Exon(s): NM_003246: Exon 3

THBS1B

Targeted Exon(s): NM_003246: Exon 22 - THBS1C (diagram not available)

4.4.3 Genes related to invasion and specific to DLKP4E/DLKP4Emut

Five genes were chosen as siRNA targets based on analysis of DLKP4E and DLKP4Emut microarray data (Section 3.3.4.3). All five genes displayed increased expression in invasive DLKP4E and DLKP4Emut, and evidence in the literature suggested, in most cases that they may play a role in invasion. siRNA analysis was chosen to silence these genes in order to observe the effect on invasion. As all genes were over-expressed in invasive cell lines, silencing of these genes was expected to reduce invasion. As with all targets, siRNA was transfected into DLKP4E and SKBR3. Results for proliferation assays were similar to those for MCF7H3erbB2 targets, with little change in DLKP4E and an increase in growth of SKBR3 (thought to be due to scrambled siRNA having an effect on proliferation of SKBR3).

Invasion assays revealed that none of the siRNA transfections resulted in any change in invasion of DLKP4E (Figure 3.10.2). Cell counts were not performed on DLKP4E because the extent of the invading cells on most inserts made accurate counting impossible. Initially, the photograph of the SKBR3 invasion inserts indicated some decrease in invasion (Figure 3.10.3). However, cell counts revealed no change in the number of invading cells (Figure 3.10.4), and when repeated results for this cell line were inconsistent. These results showed that transfection of SKBR3 and DLK4E with this set of siRNAs did not result in reduced invasion.

A kinesin-silencing reduction in proliferation, and also real-time PCR showing GAPDH knock-down in these cells (Figure 3.4.3), demonstrated that optimal transfection conditions were used. Therefore invasion assay results suggest that these targets alone didn't play a significant role in invasion in SKBR3 or DLKP4E. Because of this further analysis was not performed.

4.4.4 Why MCF7H3erbB2 targets were successful and DLKP4E were not

It is unclear why target genes from the MCF7H3erbB2 list proved to be involved in invasion as indicated by microarray analysis, but those from the DLKP4E/4Emut list did not. One explanation could be that siRNA silencing of the DLKP4E/4Emut targets did not take place. As only proliferation and invasion functional effects were examined, there is no evidence of siRNA silencing at either mRNA or protein level. However, considering that

stringent measures were employed to ensure accurate transfection (as with TFPI), it is possible that targets were silenced but had no functional effect.

Bioinformatics analysis performed to obtain both final gene lists was very similar. The main difference between lists was that targets chosen for MCF7H3erbB2 were all inter-related, and as such may have been part of an important network involved in the invasion process. Therefore it is possible that silencing one gene from this pathway may have had a knock-on effect on the other genes, amplifying the anti-invasive effect. Targets chosen for DLKP4E were not all inter-related. A pathway was identified by Pathway Assist®, but only one gene from this pathway (NRG) was chosen. It was hoped that this gene would have a knock-on effect on the other genes in the pathway, and if they were involved in invasion this would lead to a greater effect of NRG siRNA silencing. However, NRG had no effect on the level of invasion post-siRNA transfection. It is possible that NRG was not a key component of this pathway, and that some or all of the other members should be examined using siRNA. Three members of the HOXB gene family were examined. Because five HOXB members appeared in the final list, all of which were highly up-regulated (fold changes for HOXB2, 4, 5, 6 &7, ranged from 5.83 to 98.39), it was thought likely that they were involved in invasion. However, individual HOXB siRNA transfection was not suffice to reduce the level of invasion.

The success of targets chosen based on MCF7H3erbB2 analysis may have been due to more stringent elimination of non-invasion related genes. Targets chosen from DLKP4E and DLKP4Emut were based on differentially expressed genes in both cell lines compared to parent and vector-transfected cells. In the case of MCF7H3erbB2, genes differentially expressed in MCF7H3erbB2 compared to parent were further reduced by removing any gene changes which were common to non-invasive MCF7 cell lines (MCF74E, MCF74Emut, MCF7pcDNA, and also clonal variation between MCF7 and MCF7H3). In the MCF7H3erbB2 system, the major difference being examined is invasion. MCF7H3 is completely non-invasive, and overexpression of erbB2 changes this phenotype to invasive. This is not the case in DLKP, where the parental cell line is mildly invasive. Therefore the MCF7H3erbB2 model is more suitable for the selection of invasion-specific targets. It is important to remember that the final list of DLKP4E /DLKP4Emut genes were chosen based on specificity to an invasive phenotype *and* eIF4E overexpression. eIF4E is the

limiting translation initiation factor in most cells. Thus, eIF4E activity plays a principal role in determining global translation rates. Consistent with this role, eIF4E is required for cell cycle progression, cell proliferation and differentiation. Overexpression of eIF4E leads to anti-apoptotic activity and transformation of cells. It is therefore possible that the HOXB genes, NRG and MYO are upregulated as a consequence of eIF4E over-expression, but do not play a role in invasion. It is possible that they do play a part in the invasion process, but are only effective in concert with other genes. In some cases, such as the HOXB genes, silencing of one family member may result in another member with similar function taking its place. For this reason, further analysis using joint transfection of multiple siRNAs, for instance some of those genes found to be related through pathway assist analysis, may help to answer this question.

It is also significant that three of the five targets from the MCF7H3erbB2 list (EGR1, RPS6KA3 and TFPI) were also differentially expressed in DLKP4E or DLKP4Emut. Two were filtered out of the DLKP4E/4Emut list because they were either differentially expressed in DLKPpcDNA (e.g. EGR1, which was down-regulated in pcDNA) or not common to all lists (TFPI1, not differentially expressed in DLKP4E, but DLKP4Emut and MCF7H3erbB2). RPS6KA3 was the only target chosen which proved common to both lists.

4.4.5 Effect of eIF4E on the invasive status of MCF7 and DLKP cells

To form metastases, individual tumour cells must break from the primary tumour mass, degrade extracellular matrix, invade the surrounding normal tissue, enter the blood or lymphatic circulation, exit the circulation at a distal tissue and establish satellite colonies within this new tissue environment. This aberrant behaviour of cancer cells requires the cooperative function of numerous proteins – those that facilitate angiogenesis (e.g. VEGF), cell survival (e.g. Bcl-2), invasion (e.g. MMPs), and autocrine growth stimulation (e.g. c-myc, cyclin D1). Although expression of these proteins is regulated at many levels, translation of these key malignancy-related proteins is regulated primarily by the activity of eIF-4E. This is because the above mRNA contain long, G-C-rich 5'UTRs which are capable of forming stable secondary structures and upstream AUGs, and therefore are dependent on the presence of eIF4E for efficient translation. Many of the gene products that drive metastasis are not altered by mutation, but by altered patterns of gene expression. Therefore it is the quantity not the nature of key genes that drives the metastatic program (Graff and Zimmer, 2003). Not surprisingly, eIF4E is elevated in most solid tumours, contributing to metastatic progression by selectively upregulating the translation of key malignancy-related proteins that together conspire to drive the metastatic process. The present study did not look in detail at differential expression of mRNA as a result of eIF4E overexpression, but rather related these changes specifically to invasion. It does however provide valuable data relating eIF4E phosphorylation-dependent and independent translation to mRNA profiles for future work.

It has long since been established that eIF4E plays a critical role in breast cancer (Kerekatte *et al.*, 1995; Byrnes *et al.*, 2006). A marked increased in eIF4E in vascularized malignant ductiles of invasive breast carcinomas has been reported (Nathan *et al.*, 1997), and recent studies have shown direct correlation between invasion and eIF4E in breast cancer cells (Yoon *et al.*, 2006). However, stable expression of the eIF4E and eIF4Emut plasmids alone was not sufficient to cause an increase in invasion in MCF7 (Section 3.1.8). DLKP on the other hand, changed considerably after eIF4E transfection (Section 2.3.6). At a 200X magnification the average number of invading cells was 20 in DLKP parent, whereas for DLKP4E and DLKP4Emut clones the average count ranged from 40 to 160. This result

concurs with previous studies, which have associated eIF4E with increased invasiveness and metastasis of the lung (Graff *et al.*, 1995; Seki *et al.*, 2002).

Why then did eIF4E produce a different effect in MCF7 and DLKP? Microarray analysis of eIF4E and eIF4Emut clones compared to the parent MCF7 and DLKP showed lists of genes differentially expressed when clones were compared to parents. Looking at the eIF4E clones alone, of those changes specific to DLKP4E, almost 900 genes appeared that were not differentially expressed in MCF74E. Likewise, over 200 genes differentially expressed in MCF74E did not change significantly in DLKP4E. Without any further analysis it is clear from this observation that eIF4E overexpression has a very different effect on DLKP and MCF7. To further investigate this phenomenon, Pathway Assist® was used to examine if there was a pattern in the type of genes changes due to eIF4E/eIF4Emut in both cell lines. This was investigated using the following approaches:

4. Genes present in both DLKP and MCF7 with different patterns of expression
5. Gene changes due to eIF4E overexpression in DLKP4E and not in MCF74E
6. Genes common to DLKP4E and MCF7H3erbB2 but not MCF74E (with the same pattern of expression).

The first factor taken into consideration was the invasion status of parental DLKP and MCF7 cell lines. As DLKP displayed mildly-invasive characteristics prior to eIF4E transfection, it may have been pre-disposed to an invasive phenotype, already having some of the genes necessary for invasion 'switched on'. Stable transfection of eIF4E cDNA may then have resulted in the expression or up-regulation of some key genes which pushed the phenotype to highly-invasive. Gene expression in MCF7 was compared to that in DLKP to identify genes with significantly different patterns of expression. Only genes with an expression level < 50 in MCF7 and a fold change of > 10 when compared to DLKP were used for further analysis. Genes from this list were found to be important in cell survival, proliferation and inflammation, all of which have previously been associated with cancer progression. So, DLKP was initially a more aggressive *in vitro* cell line, which may explain why it had a marked increase in invasion upon eIF4E overexpression as opposed to MCF7

cells. This analysis highlights the impact of different initial mRNA profiles on the phenotypical outcome of overexpression of a single gene.

The next logical step in analysis was to look at changes post-eIF4E overexpression in both cell lines. Genes changes in DLKP4E compared to MCF74E were predominantly involved in motility and proliferation, which would agree with the phenotypical changes seen in DLKP4E compared to MCF74E. No significant change in these genes in the MCF74E cell line may be contributing to the cells lack of invasion.

MCF7H3erbB2 is an invasive clone of MCF7, and many of the gene changes which occur in this cell line compared to parent MCF7H3 are related to its invasive phenotype. One important gene recognised by Pathway Assist® as being common to DLKP4E and MCF7H3erbB2 was erbB2. However, in MCF74E there was no change in the level of expression of erbB2. This further strengthens the case for erbB2 as a vital promoter of invasion, and suggests that in DLKP overexpression of eIF4E leads to erbB2 expression at mRNA level, but does not in MCF7.

To further investigate gene changes that occur due to eIF4E in DLKP4E and are related to invasion, genes that were common to both MCF7H3erbB2 and DLKP4E but not MCF74E were examined using Pathway Assist ®. This created a list of genes with a phenotypical change from non-invasive to invasive in an MCF7 cell line, and also relevant to invasion as a result of eIF4E overexpression. Several pathways were generated which showed common targets for this list of genes. Of the 351 genes on the list 34 were involved in cell survival, 12 in invasion, 30 in motility and 54 in apoptosis. Of most significance to this study were those involved in invasion and motility. The fact that these genes are significantly changed in two invasive cell lines, and not in non-invasive MCF74E, strongly suggest they play an important role in invasion in both DLKP and MCF7. This pre-existing relationship with an invasive phenotype validates the list of MCF7H3erbB2 and DLKP4E common genes as being related to invasion. Many other genes on this list, especially those poorly annotated or with yet unknown association to invasion, will prove valuable for further analysis of invasion in MCF7 and DLKP.

4.4.6 The relationship between MCF7H3erbB2 target genes and erbB2

All five target genes which performed successfully (that is increased or decreased invasion as predicted by microarray analysis) were all chosen from the list of genes differentially expressed in MCF7H3erbB2. It is therefore likely that these genes, as well as being related to an invasive phenotype, also have some connection with erbB2. Previous studies have shown overexpression of erbB2 in vivo (Meteoglu *et al.*, 2005) and in vitro (Dittmar *et al.*, 2002) results in cellular transformation, and more specifically invasion (Zhan *et al.*, 2006). Work carried out in the NICB also showed that stable expression of erbB2 cDNA in a breast cell line resulted in invasion. The resulting clone, MCF7H3erbB2 was used in the present study.

erbB2 is a member of the epidermal growth factor receptor (EGRF) family of receptor tyrosine kinases, the normal function of which is to mediate cell-cell interactions in organogenesis and adulthood through binding to their ligands (Burden and Yarden, 1997). In epithelium, the basolateral location of erbBs allows them to mediate cell-cell interactions through signaling between the mesenchymal and epithelium (Borg *et al.*, 2000). Ligands binding the erbBs are divided into two categories; EGF-like ligands and neuregulins. These ligands influence which receptor subtype or subtypes dimerization and oligomerisation occurs with and promotes self-phosphorylation on tyrosine residues (Navolanic *et al.*, 2002). The result of ligand-receptor binding is the initiation of several signaling cascades, producing a specific physiological outcome. Cellular transformation mediated by erbB2 is as a result of the inappropriate expression of signaling pathways that promote cell proliferation and survival. Both homodimers and heterodimers containing erbB2 are effective in activating Ras/Raf/ERK and phosphoinositide 3'-kinase (PI3K) pathways (Zhan *et al.*, 2006). MAPK pathways induce proteolytic enzymes that degrade the extracellular matrix (ECM), enhance migration, initiate pro-survival genes and maintain growth (Kaladhar *et al.*, 2003). PI3K is a lipid kinase that catalyzes the synthesis of the membrane phospholipid PtdIns-3,4,5-P_3 from PtdIns-4,5-P_2, effectively recruiting Akt to the plasma membrane by direct interaction of PtdIns-3,4,5-P_3 with the Akt pleckstrin homology domain. In normal and cancer cells, Akt regulates both growth and survival mechanisms and does so by phosphorylating a large number of substrates (Toker and Yoeli-Lerner, 2006).

Figure 4.7 demonstrates the diversity of signalling pathways initiating from erbB2.

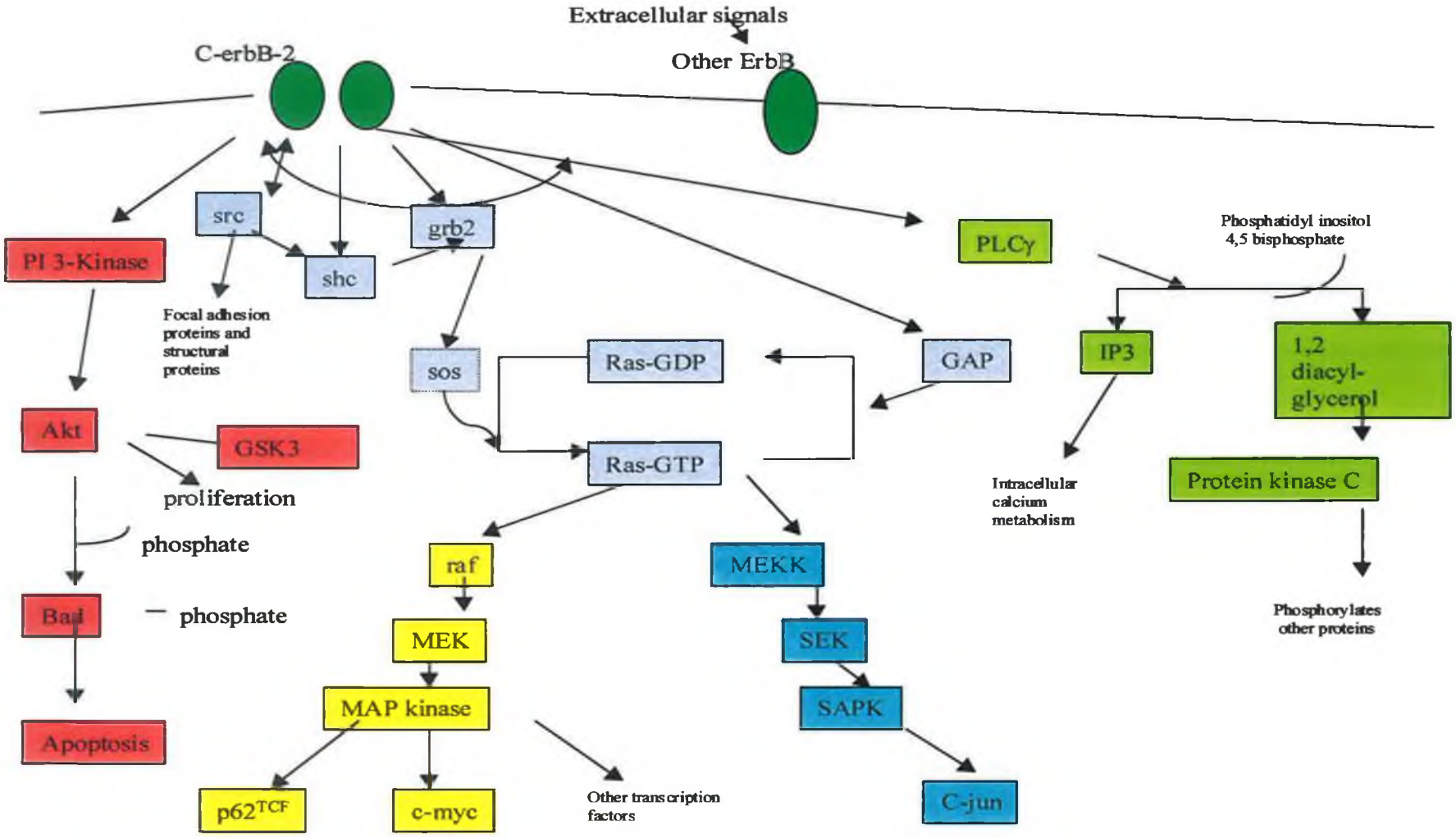

4.4.6.1 Relationship of target genes to eIF4E

The AKT/mammalian target of rampamycin (mTOR)/4EBP1 pathway is a central regulator of protein synthesis. Phosphorylation of 4EBP1 leads to the release of eIF4E, which can then bind with eIF4E and initiate translation. erbB2 has been shown to trigger the AKT/mTOR/4EBP1 signaling cascade, and therefore influence the level of eIF4E available for translation initiation (Zhou *et al.*, 2004). In addition to initiating the AKT signalling pathway, erbB2 can also cause initiation of the Ras/Raf/MEK/ERK signalling cascade, which is associated with the invasive phenotype through up-regulation of several transcription factors. Although much attention has been given to the role of Akt activation in the regulation of protein synthesis, recent evidence suggest signalling through the MAP kinases also converge on eIF4E, making this another means of mediating translational control (Kelleher *et al.*, 2004). Ras-ERK signalling leads to the phosphorylation of eIF4E at serine 209 (Wang *et al.*, 1998a), which has been directly associated with translation of mRNAs with complex 5'UTRs (Andersson and Sundler, 2006; Grund *et al.*, 2005; Pyronnet *et al.*, 2000). eIF4E translation of complex mRNAs in particular has previously been associated with cancer progression, and is also involved in the translation of erbB2 (Yoon *et al.*, 2006). In this way erbB2 and eIF4E are involved in a positive feedback loop, and therefore cells over-expressing erbB2 or eIF4E may contain similar mechanisms and/or novel markers for invasion, which would explain why targets chosen from an erbB2 overexpressing cell line were also relevant in an eIF4E overexpressing cell line.

Both erbB2 and eIF4E have been associated with metastasis in vivo (Marx *et al.*, 1990; Byrnes *et al.*, 2006). However, the fact that erbB2 overexpression caused invasion in a MCF7 cell line, where overexpression of eIF4E was unable to, coupled with the fact that erbB2 targets for invasion were more successful than those for eIF4E, suggest that erbB2 plays a more significant role in invasion than eIF4E *in vitro*. This is probably due to the activation of different signalling pathways, which lead not only to activation of eIF4E and increased translation of eIF4E sensitive mRNAs, but also to other factors important to the invasion process.

4.4.6.2 RPS6KA3 and erbB2

RPS6KA3 is a mitogen-activated protein kinase-activated protein kinase (MAPKAPKs), and a downstream effector of the mitogen-activated protein kinases (MAPK) family of kinases (Zhao *et al.*, 1996). Activation of the Ras/Raf/MEK/ERK signalling cascade by erbB2 results in the direct stimulation of RPS6KA3 (Murphy *et al.*, 2002). RPS6KA3 acts as a vital regulator of key transcription factors involved in early gene response, such as c-Fos, Elk-1 and CREB which know for their role in tumour progression (Sassone *et al.*, 1999; Aksan Kurnaz, 2004; Xing *et al.*, 1996).

4.4.6.3 RPS6KA3 and EGR1

Immediate early response gene activation upon mitogenic activation occurs through the serum response element (SRE). The enhanced transcription of genes through transcriptional regulatory elements such as the SRE makes the characterization of the upstream pathways a powerful means to engineer cellular responses. Mitogen signaling activates the MAPKs through increased binding of the ternary complex factor (TCF), such as Elk-1 to the SRE in the DNA promoter region, activating transcription. In response to serum stimulation, Elk-1 is phosphorylated at multiple sites, and can be phosphorylated by all three of the MAPK families (Sharrocks, 2000). This activation through phosphorylation is a crucial step in SRE-driven transcription, and phor-Elk-1 is thought to recruit a variety of proteins to the promoter through protein-protein interactions. The MEK/ERK/RPS6KA3 cascade, through phosphorylation of the ternary complex factor Elk-1, leads to the expression of EGR1 (Anderson *et al.*, 2004).

4.4.6.4 EGR1 and erbB2

We know that erbB2 stimulates the MEK/ERK/RPS6KA3 cascade, which leads to expression of EGR1 (Anderson *et al.*, 2004). Recent reports have demonstrated that ERG1 is also capable of regulating transcription of erbB2. Promoter deletion assays and site-directed mutageneses identified a binding site for the transcription of EGR1 in erbB2 promoter as a putative curcumin response element in regulating the promoter activity of the gene in colon cancer cells (Chen *et al.*, 2006). Therefore, EGR1 and erbB2 are involved in a positive feed-back loop, and one of the knock-on effects of down regulation of EGR1

may also be inhibition of erbB2.This may also contribute to the anti invasive effect observed in DLKP4E and SKBR3 after siRNA silencing of EGR1.

4.4.6.5 EGR1 and THBS1

Extracellular stimuli regulate an array of cellular events such as growth, differentiation and death by altering the gene expression profile. These include induction of dormant genes and repression of active genes. In response, immediate early genes (IEGs) are induced and trigger transcriptional cascades, which ultimately lead to the different biological phenotypes. THBS1 is transcriptionally regulated by EGR1, and rapidly induced by serum, PDGF, and basic fibroblast growth factor. Both EGR1 and THBS1 are immediate early response genes, and have both been found dependent on the Ras/Raf/MEK/ERK pathway (Inuzuka *et al.*, 1999), which is activated by erbB2. As a transcriptional regulator of THBS1, up-regulation of EGR1 may be expected to result in up-regulation of THBS1. This was not observed in MCF&H3erbB2. Other studies have shown a similar relationship between the two based on a global microarray analysis, with THBS1 reversing the changes in immediate-early gene expression induced by TCR-mediated T cell activation. One set of genes, including EGR1, which were induced after TCR stimulation, were down-regulated by THBS1 treatment (Li *et al.*, 2001). This concurs with results showing an increase in EGR1 and decrease in THBS1 contributed to invasion in MCF7H3erbB2 cells. It also suggests that up-regulation of erbB2 results in up-regulation of ERG1, possibly by inducing the MEK/ERK signalling pathway. It also implies negative regulation of THBS1 involving EGR1 and most likely several other factors, the precise mechanism of which remains to be fully explained.

4.4.6.6 THBS1 and TFPI

TFPI binds specifically to thrombospondin-1 (THBS1), and TFPI bound to immobilized THBS1 remains an active proteinase inhibitor. THBS1 secreted by platelets plays an important role in recruiting and localizing TFPI to surfaces within the extravascular matrix. In solution phase assays measuring TFPI inhibition of factor TF-VIIa catalytic activity, the rate of factor Xa generation was decreased 55% in the presence of THBS-1 compared with TFPI alone. Once localized, TFPI-THBS1 can efficiently down-regulate the procoagulant activity of tissue factor (TF), therefore showing thrombospondin enhances the coagulation-

inhibition ability of TFPI when bound (Mast *et al.*, 2000). The down-regulation of THBS1 and sequential up-regulation of TFPI observed in MCF7H3erbB2 suggests that TFPI is inhibiting TF with maximum efficiency, and therefore may serve another purpose within the cells. Based on the reduction in invasion detected post-TFPI silencing, it is possible this novel function of TFPI is important in the invasion process.

4.4.6.7 TNFAIP8 and erbB2

TNFAIP8 may be a novel member of the FLIP family (Kumar *et al.*, 2000). FLIP family proteins are involved in the intrinsic apoptotic pathway, regulating the activation of caspases responsible for activation and execution of the apoptotic cascade (Harada and Grant, 2003). TNFAIP8 causes suppression of TNF-mediated apoptosis by specifically inhibiting TNF-induced caspases-8 (You *et al.*, 2001).

A recent study found that erbB2 is a substrate for caspase-8 and that TNF-α stimulation leads to an early caspase-8-dependent erbB2 cleavage in MCF7 A/Z breast adenocarcinoma cells defective for NFkB activation. They showed that the antiapoptotic transcription factor NFkB counteracts this cleavage through induction of the caspase-8 inhibitor c-FLIP (Benoit *et al.*, 2004). It is possible that TNFAIP8 performs a similar role in MCF7H3erbB2, as its anti-apoptotic action is also through caspase-8 inhibition.

Also, ERK phosphorylation (which can be attributed to erbB2 expression) is linked to VEGFR2 expression in breast cancer (Svensson *et al.*, 2005). VEGFR2 expression has in turn been related to TNFAIP8 expression (Zhang *et al.*, 2006). Therefore up-regulation of VEGFR2 in response to overexpression of erbB2 could somehow be involved in TNFAIP8 expression, the exact mechanism of which has not been elucidated.

Table 4.3: Summary of results in relation to literature

Gene	Function	Role in the cell	Previous association with invasion
RPS6KA3	**MAPK-activated protein kinase**	Regulator of key transcription factors involved in early gene response, such as c-Fos, Elk-1 and CREB which know for their role in tumour progression	**No functional effect previously observed from reduction of RPS6KA3 alone.**
EGR1	**Transcription factor**	p53, through EGR1, could facilitate the up-regulation of VEGF expression. Bcl2, fibronectin and NFkB, all of which are associated with differentiation and cell survival, and VEGF and TF, both of which are involved in angiogenesis, are regulated by EGR1.	**Shown to have both pro- and ani-invsive effect depending on cell line. Pro-invasive in prostate, as in breast in present study.**
TFPI	**Protease inhibitor**	Endogenous anticoagulant protein of the serine protease family, TFPI inhibition of TF shifts coagulation from the extrinsic to the intrinsic pathway.	**Has been detected in advanced tumours, but no functional effect previously observed from reduction of TFPI alone.**
THBS1	**Immediate early response gene, extracellular matrix glycoprotein**	Mediates cell-to-cell and cell-to-matrix interactions through binding of fibronectin, fibrinogen, laminin, type V collagen, integrins α_V/β_1, TGFβ, and PDGF. Enhances the coagulation-inhibition ability of TFPI when bound.	**Both pro- and anti-invasive effect observed previously. Present study shows anti-invasive effect across breast and lung cell lines**
TNFAIP8	**novel member of the FLIP family**	TNFAIP8 causes suppression of TNF-mediated apoptosis by specifically inhibiting TNF-induced caspases-8.	**Prevoiusly shown to be pro-invasive, as in present study.**

4.4.6.8 Summary

It is clear from the present study that erbB2 plays a very important role in promoting an invasive phenotype in both MCF7 and DLKP cell lines. This is most likely as a result of the diversity of signalling pathways initiating from erbB2. Key target genes involved in invasion and activated through erbB2 signalling were examined in this study. The possible role of each of these genes is depicted in Figure 4.8, which demonstrates the diversity of genes effected by erbB2 signalling.

Figure 4.8: The signalling relationship between MCF7H3erbB2 target genes, eIF4E and erbB2

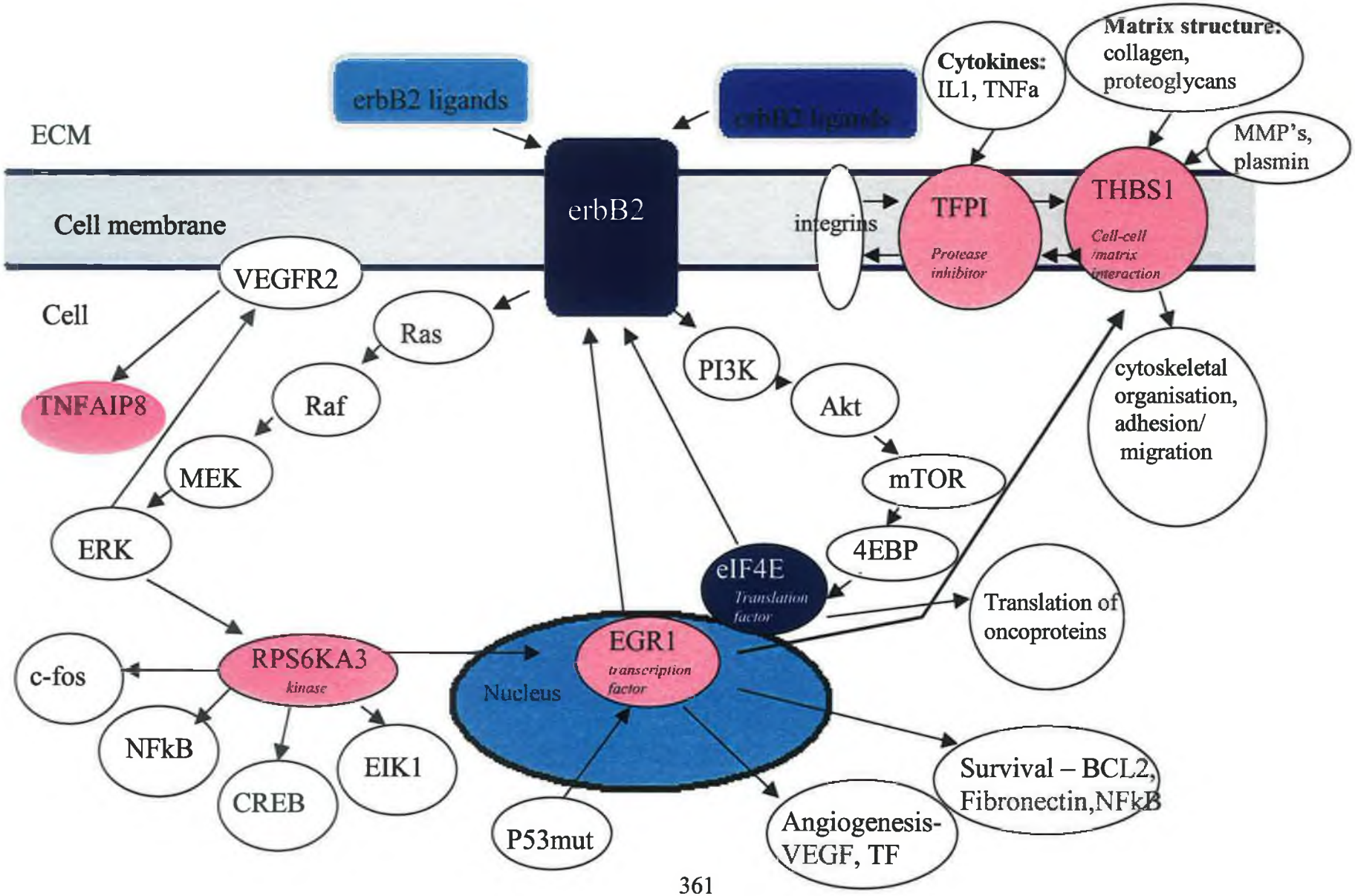

4.5 Effect of up-regulation of eIF4E on mRNA profiles

Previous studies have shown that an excess of eIF4E does not affect global translation rates, but instead leads to an increase in translation of mRNAs with complex 5'UTRs (eIF4E 'sensitive' mRNAs). Many of these mRNAs code for oncoproteins, regulators of cell cycle, growth factors and their receptors (De Benedetti *et al.*,1994). Therefore prolonged overexpression of eIF4E can lead to oncogenic transformation. In the present study, overexpression of eIF4E resulted in phenotypic changes *in vitro*, including increased invasion in DLKP4E/4Emut and increased colony forming efficiency in MCF74E/4Emut. These *in vitro* events are frequently associated with malignant transformation, and are in agreement with current models for eIF4E overexpression. However, as a translation factor, eIF4E may not have been expected to have such a profound effect on mRNA profiles as observed in the present study. Microarray data showed a considerable number of differentially expressed genes in stable eIF4E/eIF4Emut transfected DLKP and MCF7 clones, compared to the parent cell lines.

4.5.1 eIF4E translation of transcription factors

This result may be partially explained by an increase in the translation of eIF4E 'sensitive' mRNAs, many of which include transcription factors. In this way eIF4E can have a considerable effect on transcriptional regulation, which may lead to significant changes in mRNA profiles. An example of this is Ets1. The Ets1 proto-oncoprotein is a member of the Ets family of transcription factors that share a unique DNA binding domain, the Ets domain (Dittmer, 2003). Ets transcription factors regulate the expression of genes that are involved in various biological processes including proliferation, differentiation, development, transformation and apoptosis (Seth and Watson, 2005). An increase in Ets1 protein expression has been directly correlated with the phosphorylation of MNK1 and eIF4E in natural killer (NK) cells (Grund *et al.*, 2005). This not only suggests Ets1 is an eIF4E sensitive mRNA, but also that its translation is eIF4E phosphorylation dependent. An examination of genes directly regulated by Ets1 in DLKP4E and DLKP4Emut was carried out using Pathway Assist ®. Results showed different groups of Ets1-regulated genes depending on the cell lines and whether cells had been transfected with wild type eIF4E or phosphorylation deficient eIF4Emut. Ets1 was not differentially expressed in any of the cell lines, but genes regulated by Ets1 were.

Figure 4.9: ETS1 regulation in DLKP4E

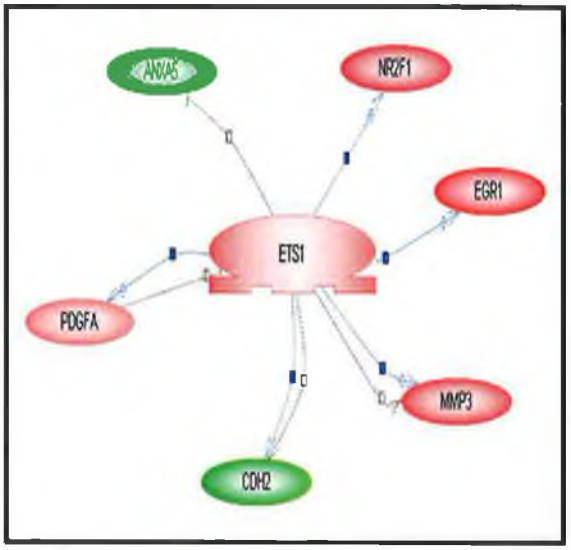

Gene	Description	Fold Change
NR2F1	nuclear receptor subfamily 2, group F, member 1	+2.72
ANXA5	annexin A5	+2.47
MMP3	MMP3 matrix metallopeptidase 3 (stromelysin 1, progelatinase)	+2.15
CDH2	cadherin 2, type 1, N-cadherin (neuronal)	+2.52
PDGFA	platelet-derived growth factor alpha polypeptide	+4.83
EGR1	Early growth response 1	+2.4

Figure 4.10: ETS1 regulation in MCF74E

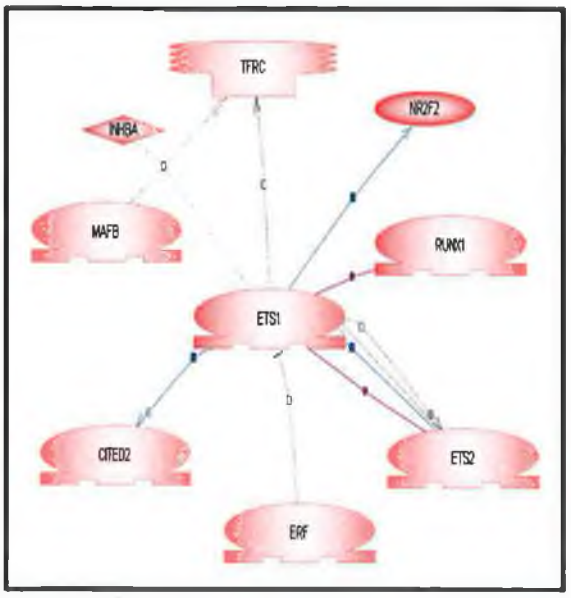

Gene	Description	Fold Change
TFRC	transferrin receptor (p90, CD71)	+2.24
NR2F2	nuclear receptor subfamily 2, group F, member 2	-2.04
RUNX1	runt-related transcription factor 1 (acute myeloid leukemia 1; aml1 oncogene)	+1.5
ETS2	v-ets erythroblastosis virus E26 oncogene homolog 2 (avian)	+1.62
ERF	Ets2 repressor factor	-1.34
CITED2	Cbp/p300-interacting transactivator, with Glu/Asp-rich carboxy-terminal domain, 2	-1.74

It appeared that genes regulated by Ets1 were predominantly amplified in cells transfected with eIF4E (Figure 4.9; 4.10), compared to those with eIF4Emut (Figure 4.11; 4.12). This suggests up-regulation of Ets1 at a protein level, which would not be detected by microarray analysis. Up-regulation of Ets1 protein in the presence of phosphorylated eIF4E concurs with previous models (Grund *et al.*, 2005). However, Ets1 regulated genes were also differentially expressed in eIF4E phosphorylation deficient eIF4Emut clones. This implies that either eIF4E translation of Ets1 is not phosphorylation-dependent, or that the Ets1 regulated genes expressed in MCF74Emut

and DLKP4Emut are actually being regulated by an alternative transcription factor, which is not eIF4E phosphorylation dependent. It is also interesting that a different set of Ets1 regulated genes were differentially expressed in eIF4E and eIF4Emut clones in both cells lines.

Figure 4.11: ETS1 regulation in DLKP4Emut

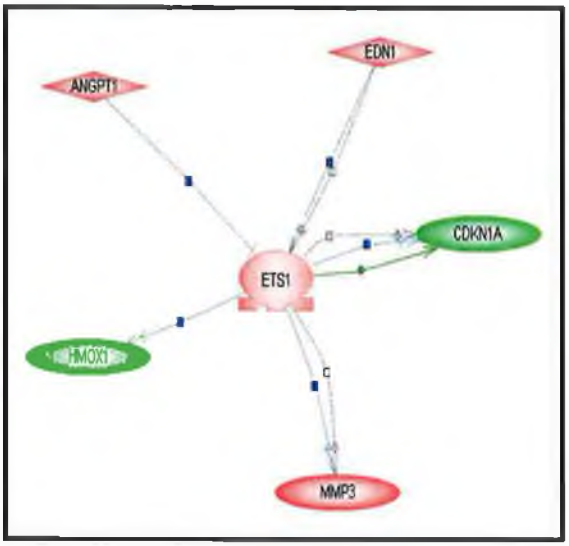

Gene	Description	Fold Change
MMP3	matrix metallopeptidase 3 (stromelysin 1, progelatinase)	+10.15
CDKN1A	endothelin 1	+ 2.33
ANGPT1	cyclin-dependent kinase inhibitor 1A (p21, Cip1)	-2.02
HMOX1	angiopoietin 1	-2.25
EDN1	heme oxygenase (decycling)	-4.89

Figure 4.12: ETS1 regulation in MCF74Emut

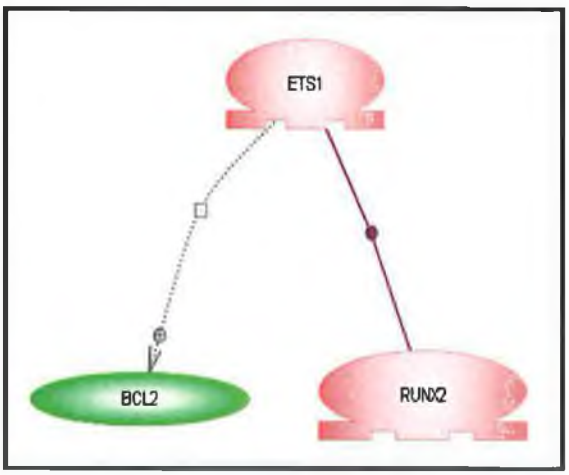

Gene	Description	Fold Change
BCL2AF1	BCL2-associated transcription factor 1	-1.21
RUNX2	runt-related transcription factor 2	+3.08

Tumour necrosis factor (TNF)-α mRNA also requires phosphorylation of eIF4E at serine 209 for initiation of translation (Andersson and Sundler, 2006). TNF-α can in turn induce activation of nuclear factor kappa B (NFkB). The introduction of IkappaB, the repressor of NFkB, has also been found to lead to suppression of eIF4E (Topisirovic *et al.*, 2003). NFkB comprises a group of dimeric transcription factors consisting of various members of the NFkB/ Rel family (Verma *et al.*, 1995). NF-kB proteins are

involved in the transcriptional activation of a huge number of inflammatory-related genes in response to a number of cytokines, including TNF-α (Pahl, 1998; Baud and Karin, 2001). An examination of genes directly regulated by NFkB1 in DLKP4E and DLKP4Emut was carried out using Pathway Assist ®. Again NFkB1, as with Ets1 was not differentially expressed at mRNA level in any of the cell lines but differential expression of NFkB-regulated genes would suggest it was being expressed at protein level, possibly due to overexpression of eIF4E. My results showed NFkB1-regulated genes were differentially expressed after eIF4E and eIF4Emut overexpression in DLKP. Again as with Ets1, different groups of genes were expressed at mRNA level depending on whether cells had been transfected with wild type eIF4E (Figure 4.13; 4.14) or phosphorylation deficient eIF4Emut (Figure 4.15). This contradicts work carried out by Andersson and Sundler (2006), and suggests Phosphorylation of eIF4E is not necessary for TNF-α translation, and subsequent activation of NFkB. It is also possible however, that the NFkB regulated genes detected in DLKP4Emut can also be regulated through other transcription factors. No genes known to be regulated by NFkB were detected in MCF74Emut. The fact that NFkB genes were differentially expressed at mRNA level in a different cell line means this is likely due to genotypic differences between MCF7 and DLKP rather than eIF4E phosphorylation dependency.

Figure 4.13: NFkB1 regulation in DLKP4E

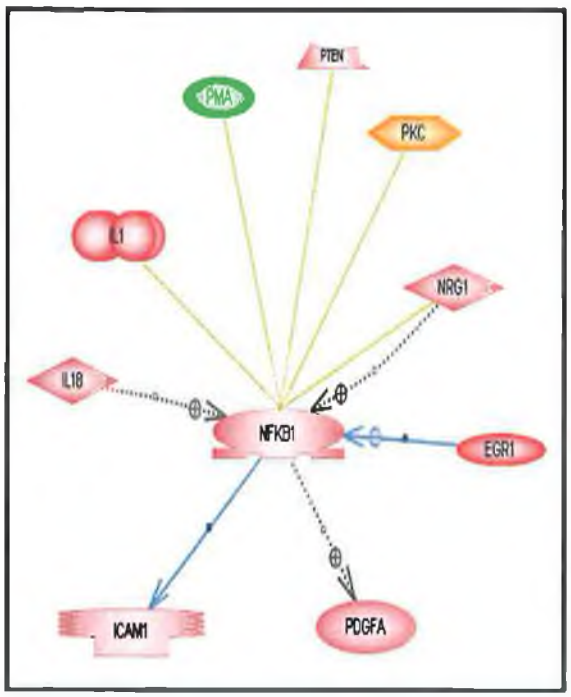

Gene	Description	Fold Change
PTEN	phosphatase and tensin homolog (mutated in multiple advanced cancers 1)	-1.42
NRG1	Neuregulin	+8.36
EGR1	Early growth response 1	+2.4
PDGFA	platelet-derived growth factor alpha polypeptide	+4.83
ICAM1	intercellular adhesion molecule 1 (CD54), human rhinovirus receptor	-7.39
IL18	interleukin 18 (interferon-gamma-inducing factor)	+5.42

Figure 4.14: NFkB1 regulation in MCF74E

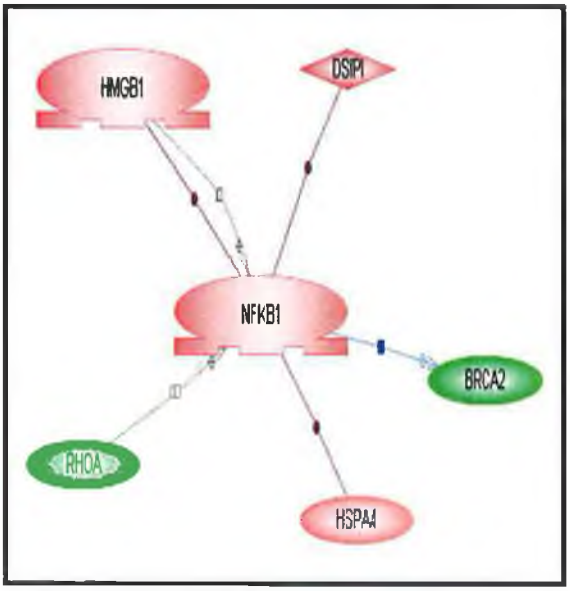

Gene	Description	Fold Change
HMGB1	high-mobility group box 1	-1.31
BRCA2	breast cancer 2, early onset	-1.65
HSPA4	heat shock 70kDa protein 4	+1.32
RHOA	ras homolog gene family, member A	+1.35

Figure 4.15: NFkB1 regulation in DLKP4Emut

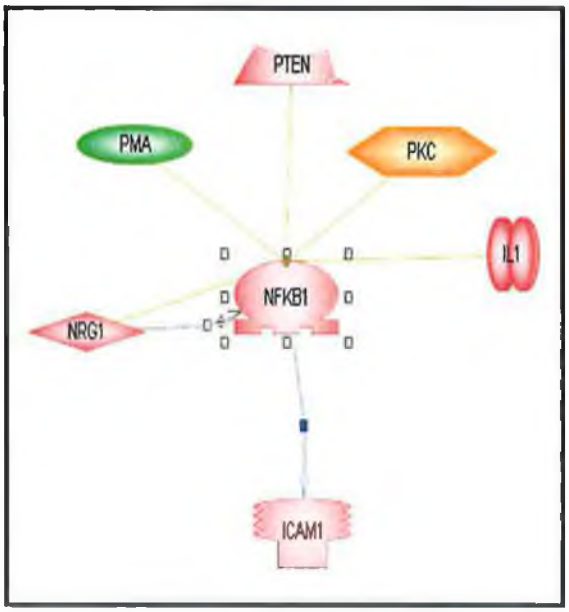

Gene	Description	Fold Change
PTEN	phosphatase and tensin homolog (mutated in multiple advanced cancers 1)	-2.0
NRG1	Neuregulin	+5.32
ICAM1	intercellular adhesion molecule 1 (CD54), human rhinovirus receptor	-5.37
IL1	interleukin 1	-1.22

Much work is needed to fully assess the role of eIF4E-translation dependent transcription factors. However, the examination of only two such transcription factors in DLKP4E/4Emut and MCF74E/4Emut showed the potential effect of eIF4E overexpression on mRNA levels.

Another way in which eIF4E can bring about changes at mRNA level is by increasing translation of factors such as cytokines, and growth factors, which activate different signaling cascades. As already mentioned, TNF is an eIF4E 'sensitive' mRNA. TNF is

also involved in the activation of the p38-MAPK and JNK signaling pathways, both of which lead to the activation of a variety of transcription factors, which may also be reflected in the genes differentially expressed as a result of eIF4E overexpression (Figure 4.16) (Wajant *et al.*, 2003).

Figure 4.16: TNF activation of p38-MAPK and JNK

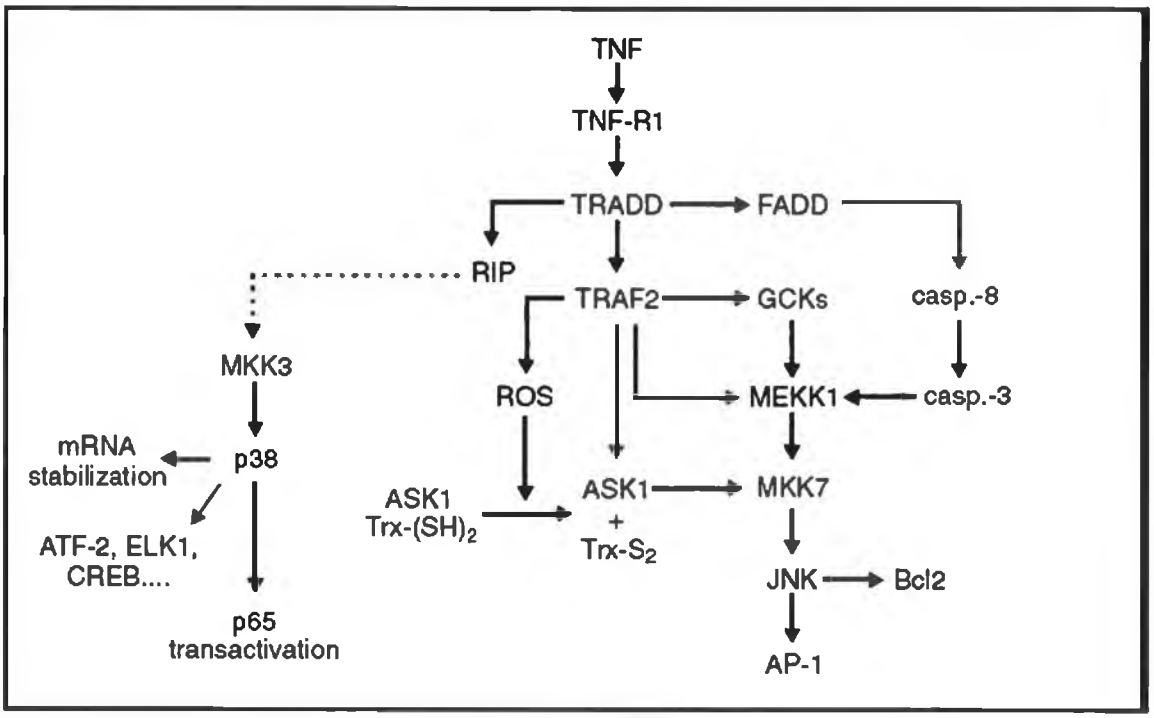

4.5.2 mRNA Stability

Steady state mRNA levels are determined by the balance between the rate of transcription and the rate of mRNA decay (Raghavan and Bohjanen, 2004). Most microarray experiments only look at steady state levels and do not examine the relative effects of transcription and mRNA decay. The assumption that changes in gene expression, as measured by microarray experiments, are directly correlated with changes in the rate of new gene synthesis form the basis of attempts to connect coordinated changes in gene expression with shared transcription regulatory elements. However, it is important to consider mRNA stability regulation. It has been proposed that regulation of mRNA stability in response to external stimuli contributes significantly to observed changes in gene expression as measured by high throughput systems (Cheadle *et al.*, 2005).

Nonsense mediated mRNA decay (NMD) is a conserved process which leads to the detection of premature termination codons within an mRNA molecule. This nonsense mRNA is subsequently targeted for decay thus preventing this nonsense mRNA from being continually translated and consequently producing potentially deleterious truncated polypeptides. The decay of this nonsense mRNA occurs at a more rapid rate than if the mRNA were to decay through the default decay pathway. This increased decay rate allows the cell to rapidly remove these mRNAs from the pool of translatable mRNAs.In mammalian cells NMD does not detectably target eIF4E-bound mRNA (Ishigaki *et al.*, 2001). This suggests that increases in the activity of eIF4E may lead to mRNA stabilization under certain conditions.

The role of eIF4E outside the process of translation also effects mRNA levels. Regulation of nucleocytoplasmic transport, cytoplasmic localisation of mRNA and splicing can all play a role in mRNA stability. eIF4E is known to play a role in nucleocytoplasmic mRNA transport (Lejbkowicz *et al.*, 1992) and splicing (Dostie *et al.*, 2000), and Cohen *et al.*, (2001) found that an eIF4E mutant, with negligible cap-binding activity, could still act as an oncogene by increasing the export of growth regulatory mRNAs. Therefore, it is possible that eIF4E could influence the levels of mRNA detected by microarray analysis through its roles in nucleoplasmic transport and mRNA stability.

Summary & Conclusions

Effect of overexpression of eIF4E in MCF7 and DLKP

Stable transfection of DLKP with eIF4E and eIF4Emut cDNA resulted in a set of highly invasive clones, demonstrating that in DLKP, eIF4E plays a significant role in the invasion process, and also that phosphorylation of eIF4E does not affect the role of eIF4E in invasion in this cell line. Transfection of MCF7 with the same set of eIF4E, eIF4Emut and pcDNA had no effect on the level of invasion, thus showing that overexpression of eIF4E alone is not sufficient to induce an invasive phenotype in this cell line. However, up-regulation of eIF4E did cause a marked increase in growth rate, loss of adhesion and an increase in the ability to form colonies in soft agar in the MCF74E clones, all important *in vitro* correlates of cancer. It is worth noting that both anchorage-independent growth and colony forming ability were affected more by the wild-type eIF4E, suggesting a role for phosphorylation of eIF4E in these processes.

eIF4E control of mRNA levels

Microarray analysis of MCF74E/4Emut and DLKP4E/4Emut showed a considerable change in mRNA profiles between parental and eIF4E/eIF4Emut clonal populations. While overexpression of a translation factor might not at first glance have been expected to have such a profound effect on mRNA profiles. This could possibly be explained by the increased eIF4E-dependent translation of transcription factors, or the role of eIF4E in mRNA stability. Microarray results provide valuable data for further analysis of the role of eIF4E in regulation of mRNA levels, specifically and globally.

Why eIF4E caused an increase in invasion of DLKP4E but not MCF74E

Further analysis of MCF74E compared to DLKP4E using microarray data, suggest that a significant number of genes involved in motility (e.g. Raf1, PDGFA, HGF) and proliferation (e.g. BIRC3, RFP, GTF2IRD1) were differentially expressed in DLKP4E compared to DLKP, but not MCF74E compared to MCF7. It is possible that this set of genes plays a key role in the invasion processes, and their absence in MCF74E may have been sufficient to prevent invasion. In addition, there were genes differentially expressed (compared to parent cell lines) and common to DLKP4E and

MCF7erbB2 which did not appear to change in MCF74E compared to parent MCF7. These genes were involved in the regulation of many key processes including cell survival, invasion, motility and apoptosis. In particular, 12 genes (A2M, RRM1, TFPI2, TIMP2, LMNA, CD99, ERBB2, CAPG, CD24, EFNA1, FBLN1 and SLC7A5) which from the literature are known to be involved in invasion, could at least partially answer the question as to why MCF7 did not become invasive.

The fact that erbB2 overexpression caused invasion in an MCF7 cell line, where overexpression of eIF4E was unable to, confirms that erbB2 plays a significant role in invasion. This may be due to the fact that in addition to initiating the AKT signalling pathway, erbB2 can also cause initiation of the Ras/Raf/MEK/ERK signalling cascade, which is associated with the invasive phenotype, through up-regulation of several key transcription factors.

Another important factor is the invasion status of the parental DLKP and MCF7 cell lines. As DLKP displayed mildly-invasive characteristics prior to eIF4E transfection, it may have been pre-disposed to an invasive phenotype, already having some of the genes necessary for invasion 'switched on'. It may have required only the up regulation of some key genes to push the phenotype to highly-invasive. The 12 genes common to MCF7H3erbB2 and DLP4E/4Emut may be part of a group of genes essential for invasion. More interesting will be the study of novel and unannotated genes which are common to both lists. A list of ~300 gene that were differentially expressed, related to an invasive phenotype, and with the same pattern of expression in both MCF7H3erbB2 and DLKP4E was generated. This list contained both well and poorly annotated genes. Several of the previously annotated genes can be related to invasion, cell survival, motility and apoptosis. The possibility that some of the unnanotated genes are also relevant to cancer invasion awaits further investigation.

Markers for invasion in breast and lung

A combination of the development of stable invasive and non-invasive clones, microarray analysis of same, and siRNA silencing has led to the identification of five genes which have significant roles in the invasion process of both lung (DLKP) and breast (SKBR3) cells. These genes are early growth response 1(EGR1), tissue factor pathway inhibitor (TFPI1), thrombospondin (THBS1), tumour necrosis factor alpha-induced protein A (TNFAIP8) and ribosomal protein S6 kinase-90kDa-polypeptide 3

(RPS6KA3). EGR1, TFPI1, TNFAIP8 and RPS6KA3, were all upregulated in invasive MCF7H3erbB2.

They cause significant reduction in invasion when silenced in DLKP4E and SKBR3. Silencing of THBS1, the only one of the targets to have been down regulated in MCF7H3erbB2, caused invasion of non-invasive MCF7 and an increase in invasion of mildly invasive DLKP. These genes represent a combination of those previously reported to have an involvement in invasion (EGR1, TNFAIP8, THBS1), and those whose functional role is yet to be fully elucidated (RPS6KA3 and TFPI1).

EGR1 (early growth response 1)

The transcription factor EGR1 is overexpressed in many tumours and regulates the expression of several genes implicated in tumor progression. Although EGR1 deficiency has been shown to impair the transition of tumour cells to invasion in mouse models, it can have a repressive or activating role depending on the tumour type. This study shows EGR1 to be directly related to invasion of both a breast and a lung cell line. Further study of genes regulated by EGR1 in these cell systems will establish a clearer picture of EGR1 influence on invasion.

TFPI1 (tissue factor pathway inhibitor 1)

The nature of TFPI1 increase in patients with cancer is not fully understood; increased synthesis by tumour cells or by host cells could be involved. Tumour-associated macrophages and various cancer cells have been shown to express TFPI1, whereas small lung cell carcinoma, renal cell carcinoma and malignant melanoma did not. Up-regulation of TFPI1 has not previously been directly linked to an increase in invasion, but results represented in this thesis clearly show an increase in TFPI1 in an invasive cell line, and reduction of this TFPI1 leading to a decline in invasion.

THBS1 (thrombospondin)

THBS1 is an adhesive, extracellular matrix glycoprotein that mediates cell-to-cell and cell-to-matrix interactions, and the majority of work to date shows that overexpression of THBS1 is involved in migration in many cancer tissues. Tumour cells and platelets expressing THBS1 are more likely to attach to epithelial cells and cross capillary and lymphatic endothelia. In contrast to previous studies, this thesis suggests THBS1 to have anti-invasive properties in DLKP and MCF7. Gene silencing of THBS1 alone

was enough to change the phenotype of MCF7 cells from non-invasive to invasive, and cause a marked increase in invasion of DLKP. THBS1 exerts its function by binding to various matrix proteins and cell-surface receptors, and by interaction with these receptors functions in directing formation of multi-protein complexes that modulate cellular phenotype. As a result, diverse intracellular pathways are activated relevant to embryonic development, tissue differentiation, inflammations, wound healing, and coagulation. Evidence to date suggests that THBS1 displays distinct biological activities in different cell types, which is attributed to its multiple functional domains that engage corresponding receptors on the surface of targeted cells. It is therefore possible that THBS1 has both pro- and anti-invasive functions.

RPS6KA3 (ribosomal protein S6 kinase, 90kDa, polypeptide 3)

The RSK genes are a subfamily of mitogen-activated protein kinase-activated protein kinases (MAPKAPKs). Little evidence exists to show whether or not RPS6KA3 plays an important role in cancer, although it is capable of activation of the Ras-dependent mitogen-activated protein kinase (MAPK) cascade, and is also a target of ERK, both of which are well-characterised instigators of invasion. RPS6KA3 was found to be up-regulated in both invasive cell lines DLKP4E and MCF7H3erbB2, and subsequent siRNA gene-silencing resulted in considerable loss of invasion. This evidence presents RPS6KA3 as a pro-invasive gene in DLKP4E and SKBR3. Analysis of data from microarray experiments on clinical samples also found RPS6KA3 to be statistically relevant.

TNFAIP8 (tumour necrosis factor, alpha-induced protein 8)

TNFAIP8 is a recently discovered antiapoptotic molecule induced by the activation of the transcription factor NF-kappaB. It has been implicated in metastasis and a recent study has linked it with enhanced invasion of breast cancer cells *in vitro*, along with increased frequency of pulmonary colonization of tumor cells in athymic mice. The results of this thesis agrees with this work, demonstrating up-regulation of TNFAIP8 in an invasive cell line. Transfection of an invasive lung cell line with three separate THBS1 siRNA's resulted in reduced invasion, which also point to TNFAIP8 having an important functional role in invasion.

Future Work

Role of eIF4E in chemotherapeutic drug sensitivity/resistance

Toxicity assays were caried out to look at the effect of eIF4E and eIF4Emut overexpression on drug resistance in DLKP and MCF7. Although other studies have found eIF4E increases drug resistance, results of the present study were inconclusive and must be repeated. To obtain the maximum data it would be best to look at the MCF74E/4Emut and DLKP4E/4Emut clones used in array analysis. If a pattern of resistance to a particular drug was found, this could then be related back to microarray results for further elucidation of the mechanism involved.

Role of successful target genes in invasion

TFPI, RPS6KA3, EGR1 and TNFAIP8 were all found up-regulated in MCF7H3erbB2, and subsequent silencing of these genes using siRNA was sufficient to reduce the level of invasion in breast and lung cell lines. These genes can be further analysed by transfection of their cDNA into non-invasive cell lines. It would be interesting to see if these genes, most of which are end- or by-products of erbB2 induced signalling, were capable of inducing invasion. It would also be interesting to see if any one of these targets were capable of inducing invasion in MCF7, the invasion status of which was greatly influenced by erbB2 signalling.

Further analysis of DLKP4E/DLKP4Emut common genes related to invasion

Apart from RPS6KA3, which was also common to the MCF7H3erbB2 list, silencing of none of the chosen DLKP targets had an effect on invasion in DLKP4E or SKBR3. It is possible that individual silencing of any one of these genes was not enough to reduce invasion, and therefore the next step would be combined silencing of two or more simultaneously. It is possible, for example, that silencing one of the HOXB genes only results in another HOXB family member taking over its role.

MCF7H3erbB2 unannotated genes

As all five of the targets chosen from the list of genes differentially expressed in MCF7H3 erbB2 were shown to be relevant to the invasion process, it is likely that other genes obtained from the same analysis would also. There were many genes on

the list which were unannotated or poorly annotated prior connection to invasion. These genes may prove important novel markers for invasion. It would be possible to design siRNA against such genes using sequences from Affymetrix probe sets. If silencing resulted in a decrease in invasion then it would also be possible to clone mammalian cells transfected with the novel gene cDNA. Overexperessing novel genes would allow further determination of functional effects such as drug resistance.

Why DLKP4E was invasive and MCF74E was not

Further analysis of microarray data, in an attempt to determine why eIF4E overexpression had resulted in increased invasion in DLKP but not MCF7, found several genes that were common to invasive MCF7H3erbB2 and DLKP4E. Several of the gene on this list were found in the current literature to be associated with an invasive phenotype. This validates the analysis, the purpose of which was to find genes important to invasion in MCF7 and DLKP. It is likely therefore that other genes on the list are important to invasion, but have not yet been identified as such. It would be interesting to look at other genes on this list, both well and poorly-annotated, to determine their role in the invasion process.

The effect of eIF4E phosphorylation on mRNA profiles

Both wild type eIF4E and an eIF4E phosphorylation deficient mutant were overexpressed in DLKP and MCF7, and the resultant clones examined using microarray analysis. The result was a valuable data set relating mRNA profiles to eIF4E phosphorylation. There is currently much debate about the function of eIF4E phosphorylation at both mRNA and protein level. This data will permit examination of the regulation of expression of transcription factors, and patterns of gene expression as a result of this regulation in response to eIF4E phosphorylation.

Bibliography

Abdulkadir, S.A., Qu, Z., Garabedian, E., Song, S.K., Peters, T.J., Svaren, J., Carbone, J.M., Naughton, C.K., Catalona, W.J., Ackerman, J.J., Gordon, J.I., Humphrey, P.A. & Milbrandt, J. 2001, "Impaired prostate tumorigenesis in Egr1-deficient mice", *Nature medicine* 7: 101-107.

Adams, J.C. 1997, "Thrombospondin-1", *The international journal of biochemistry & cell biology* 29: 861-865.

Adamson, E., de Belle, I., Mittal, S., Wang, Y., Hayakawa, J., Korkmaz, K., O'Hagan, D., McClelland, M. & Mercola, D. 2003, "Egr1 signaling in prostate cancer", *Cancer.Biol.Ther.* 2: 617-622.

Aggarwal, B.B., Shishodia, S., Takada, Y., Jackson-Bernitsas, D., Ahn, K.S., Sethi, G. & Ichikawa, H. 2006, "TNF blockade: an inflammatory issue", *Ernst Schering Research Foundation workshop* 56: 161-186.

Aggarwal, S., Kim, S.W., Cheon, K., Tabassam, F.H., Yoon, J.H. & Koo, J.S. 2006, "Nonclassical action of retinoic acid on the activation of the cAMP response element-binding protein in normal human bronchial epithelial cells", *Molecular biology of the cell.* 17: 566-575.

Agrawal, N., Dasaradhi, P.V., Mohmmed, A., Malhotra, P., Bhatnagar, R.K. & Mukherjee, S.K. 2003, "RNA interference: biology, mechanism, and applications", *Microbiology and molecular biology reviews : MMBR* 67: 657-685.

Ahmad, A. & Hart, I.R. 1997, "Mechanisms of metastasis", *Critical reviews in oncology/haematology* 26: 163-173.

Aksan Kurnaz, I. 2004, "Kinetic analysis of RSK2 and Elk-1 interaction on the serum response element and implications for cellular engineering", *Biotechnology and bioengineering,* 88: 890-900.

Albo, D. & Tuszynski, G.P. 2004, "Thrombospondin-1 up-regulates tumor cell invasion through the urokinase plasminogen activator receptor in head and neck cancer cells", *The Journal of surgical research* 120: 21-26.

Altmann, M., Muller, P.P., Pelletier, J., Sonenberg, N. & Trachsel, H. 1989, "A mammalian translation initiation factor can substitute for its yeast homologue in vivo", *Journal of Biological Chemistry* 264: 12145-12147.

Ambs, S., Merriam, W.G., Ogunfusika, M.O., Bennett, W.P., Ishibe, N., Hussain, S.P., Tzeng, E.E., Geller, D.A., Billiar, T.R. & Harris, C.C. 1998, "p53 and vascular endothelial growth factor regulate tumor growth of NOS2-expressing human carcinoma cells", *Nature medicine* 4:. 1371-1376.

Amundson, S.A., Myers, T.G., Scudiero, D., Kitada, S., Reed, J.C. & Fornace, A.J.,Jr 2000, "An informatics approach identifying markers of chemosensitivity in human cancer cell lines", *Cancer research.* 60: 6101-6110.

Andersson, K. & Sundler, R. 2006, "Posttranscriptional regulation of TNFalpha expression via eukaryotic initiation factor 4E (eIF4E) phosphorylation in mouse macrophages", *Cytokine* 33: 52-57.

Andjelkovic, M., Alessi, D.R., Meier, R., Fernandez, A., Lamb, N.J., Frech, M., Cron, P., Cohen, P., Lucocq, J.M. & Hemmings, B.A. 1997, "Role of translocation in the activation and function of protein kinase B", *Journal of Biological Chemistry* 272: 31515-31524.

Andrade, A.A., Silva, P.N., Pereira, A.C., De Sousa, L.P., Ferreira, P.C., Gazzinelli, R.T., Kroon, E.G., Ropert, C. & Bonjardim, C.A. 2004, "The vaccinia virus-stimulated mitogen-activated protein kinase (MAPK) pathway is required for virus multiplication", *The Biochemical journal.* 381: 437-446.

Archiniegas, E., Neves, C.Y., Candelle, D. & Cardier, J.E. 2004, "Thrombin and its protease-activated receptor-1 (PAR1) participate in the endothelial-mesenchymal transdifferentiation process", *DNA and cell biology* 23: 815-825.

Arii, S., Ishigami, S., Mori, A., Onodera, H. & Imamura, M. 1998, "Implication of VEGF and MMPs in hepatic metastasis of human colon cancer", *Nippon Geka Gakkai zasshi* 99: 436-440.

Avdulov, S., Li, S., Michalek, V., Burrichter, D., Peterson, M., Perlman, D.M., Manivel, J.C., Sonenberg, N., Yee, D., Bitterman, P.B. & Polunovsky, V.A. 2004, "Activation of translation complex eIF4F is essential for the genesis and maintenance of the malignant phenotype in human mammary epithelial cells", *Cancer.Cell* 5: 553-563.

Bai, F., Feng, J., Cheng, Y., Shi, J., Yang, R. & Cui, H. 2006, "Analysis of gene expression patterns of ovarian cancer cell lines with different metastatic potentials", *Internationa journal of gynecological cancer : official journal of the International Gynecological Cancer Society* 16: 202-209.

Bajaj, M.S., Birktoft, J.J., Steer, S.A. & Bajaj, S.P. 2001, "Structure and biology of tissue factor pathway inhibitor", *Thrombosis and haemostasis.* 86: 959-972.

Bang, M.L., Mudry, R.E., McElhinny, A.S., Trombitas, K., Geach, A.J., Yamasaki, R., Sorimachi, H., Granzier, H., Gregorio, C.C. & Labeit, S. 2001, "Myopalladin, a novel 145-kilodalton sarcomeric protein with multiple roles in Z-disc and I-band protein assemblies", *The Journal of cell biology* 153: 413-427.

Barkett, M. & Gilmore, T.D. 1999, "Control of apoptosis by Rel/NF-kappaB transcription factors", *Oncogene.* 18: 6910-6924.

Barnhart, B.C., Lee, J.C., Alappat, E.C. & Peter, M.E. 2003, "The death effector domain protein family", *Oncogene* 22: 8634-8644.

Baron, V., Adamson, E.D., Calogero, A., Ragona, G. & Mercola, D. 2006, "The transcription factor Egr1 is a direct regulator of multiple tumor suppressors including TGFbeta1, PTEN, p53, and fibronectin", *Cancer gene therapy* 13: 115-124.

Bastian, M., Steiner, M. & Schuff-Werner, P. 2005, "Expression of thrombospondin-1 in prostate-derived cell lines", *International journal of molecular medicine* 15: 49-56.

Baud, V. & Karin, M. 2001, "Signal transduction by tumor necrosis factor and its relatives", *Trends in cell biology* 11: 372-377.

Behlke, M.A. 2006, "Progress towards in vivo use of siRNAs", *Molecular therapy : the journal of the American Society of Gene Therapy* 13: 644-670.

Bein, K. & Simons, M. 2000, "Thrombospondin type 1 repeats interact with matrix metalloproteinase 2. Regulation of metalloproteinase activity", *Journal of Biological Chemistry* 275: 32167-32173.

Bein, K. & Simons, M. 2000, "Thrombospondin type 1 repeats interact with matrix metalloproteinase 2. Regulation of metalloproteinase activity", *Journal of Biological Chemistry* 275: 32167-32173.

Bertucci, F., Nasser, V., Granjeaud, S., Eisinger, F., Adelaide, J., Tagett, R., Loriod, B., Giaconia, A., Benziane, A., Devilard, E., Jacquemier, J., Viens, P., Nguyen, C., Birnbaum, D. & Houlgatte, R. 2002, "Gene expression profiles of poor-prognosis primary breast cancer correlate with survival", *Human molecular genetics* 11: 863-872.

Bhattacharyya, M. & Lemoine, N.R. 2006, "Gene therapy developments for pancreatic cancer", *Best Pract.Res.Clin.Gastroenterol.* 20: 285-298.

Bieche, I., Lerebours, F., Tozlu, S., Espie, M., Marty, M. & Lidereau, R. 2004, "Molecular profiling of inflammatory breast cancer: identification of a poor-prognosis gene expression signature", *Clinical cancer research : an official journal of the American Association for Cancer Research* 10: 6789-6795.

Birchmeier, C. & Gherardi, E. 1998, "Developmental roles of HGF/SF and its receptor, the c-Met tyrosine kinase", *Trends in cell biology* 8: 404-410.

Birchmeier, C., Birchmeier, W., Gherardi, E. & Vande Woude, G.F. 2003, "Met, metastasis, motility and more", *Nature reviews. Molecular cell biology* 4: 915-925.

Bitko, V., Musiyenko, A., Shulyayeva, O. & Barik, S. 2005, "Inhibition of respiratory viruses by nasally administered siRNA", *Nature medicine* 11: 50-55.

Blaszczyk, J., Tropea, J.E., Bubunenko, M., Routzahn, K.M., Waugh, D.S., Court, D.L. & Ji, X. 2001, "Crystallographic and modeling studies of RNase III suggest a mechanism for double-stranded RNA cleavage", *Structure (London, England)* 9: 1225-1236.

Boado, R.J. 2005, "RNA interference and nonviral targeted gene therapy of experimental brain cancer", *Neurology Reactionsx* 2: 139-150.

Bodey, B., Bodey, B.,Jr, Groger, A.M., Siegel, S.E. & Kaiser, H.E. 2000a, "Immunocytochemical detection of homeobox B3, B4, and C6 gene product expression in lung carcinomas", *Anticancer Research* 20: 2711-2716.

Bodey, B., Bodey, B.,Jr, Siegel, S.E. & Kaiser, H.E. 2000b, "Immunocytochemical detection of the homeobox B3, B4, and C6 gene products in breast carcinomas", *Anticancer Research* 20: 3281-3286.

Bodey, B., Bodey, B.,Jr, Siegel, S.E., Luck, J.V. & Kaiser, H.E. 2000c, "Homeobox B3, B4, and C6 gene product expression in osteosarcomas as detected by immunocytochemistry", *Anticancer Research* 20: 2717-2721.

Boire, A., Covic, L., Agarwal, A., Jacques, S., Sherifi, S. & Kuliopulos, A. 2005, "PAR1 is a matrix metalloprotease-1 receptor that promotes invasion and tumorigenesis of breast cancer cells", *Cell* 120: 303-313.

Bonneau, A.M. & Sonenberg, N. 1987, "Involvement of the 24-kDa cap-binding protein in regulation of protein synthesis in mitosis", *Journal of Biological Chemistry* 262: 11134-11139.

Bonnefoy, A., Hantgan, R., Legrand, C. & Frojmovic, M.M. 2001, "A model of platelet aggregation involving multiple interactions of thrombospondin-1, fibrinogen, and GPIIbIIIa receptor", *Journal of Biological Chemistry* 276: 5605-5612.

Borg, J.P., Marchetto, S., Le Bivic, A., Ollendorff, V., Jaulin-Bastard, F., Saito, H., Fournier, E., Adelaide, J., Margolis, B. & Birnbaum, D. 2000, "ERBIN: a basolateral PDZ protein that interacts with the mammalian ERBB2/HER2 receptor", *Nature cell biology* 2: 407-414.

Bornstein, P. 1995, "Diversity of function is inherent in matricellular proteins: an appraisal of thrombospondin 1", *The Journal of cell biology* 130: 503-506.

Brazma, A., Hingamp, P., Quackenbush, J., Sherlock, G., Spellman, P., Stoeckert, C., Aach, J., Ansorge, W., Ball, C.A., Causton, H.C., Gaasterland, T., Glenisson, P., Holstege, F.C., Kim, I.F., Markowitz, V., Matese, J.C., Parkinson, H., Robinson, A., Sarkans, U., Schulze-Kremer, S., Stewart, J., Taylor, R., Vilo, J. & Vingron, M. 2001, "Minimum information about a microarray experiment (MIAME)-toward standards for microarray data", *Nature genetics* 29: 365-371.

Brennan, D.J., O'Brien, S.L., Fagan, A., Culhane, A.C., Higgins, D.G., Duffy, M.J. & Gallagher, W.M. 2005, "Application of DNA microarray technology in determining breast cancer prognosis and therapeutic response", *Expert Opinion in.Bioogica .Theapy* 5: 1069-1083.

Bridge, A.J., Pebernard, S., Ducraux, A., Nicoulaz, A.L. & Iggo, R. 2003, "Induction of an interferon response by RNAi vectors in mammalian cells", *Nature genetics* 34: 263-264.

Brown, L.F., Guidi, A.J., Schnitt, S.J., Van De Water, L., Iruela-Arispe, M.L., Yeo, T.K., Tognazzi, K. & Dvorak, H.F. 1999, "Vascular stroma formation in carcinoma in

situ, invasive carcinoma, and metastatic carcinoma of the breast", *Clinical cancer research : an official journal of the American Association for Cancer Research* 5: 1041-1056.

Broze, G.J.,Jr & Miletich, J.P. 1987, "Isolation of the tissue factor inhibitor produced by HepG2 hepatoma cells", *Proceedings of the National Academy of Sciences of the United States of America* 84: 1886-1890.

Broze, G.J.,Jr 1995, "Tissue factor pathway inhibitor and the current concept of blood coagulation", *Blood coagulation & fibrinolysis : an international journal in haemostasis and thrombosis* 6: S7-13.

Burden, S. & Yarden, Y. 1997, "Neuregulins and their receptors: a versatile signaling module in organogenesis and oncogenesis", *Neuron* 18: 847-855.

Bushell, M., Wood, W., Clemens, M.J. & Morley, S.J. 2000, "Changes in integrity and association of eukaryotic protein synthesis initiation factors during apoptosis", *European journal of biochemistry / FEBS* 267: 1083-1091.

Byrnes, K., White, S., Chu, Q., Meschonat, C., Yu, H., Johnson, L.W., Debenedetti, A., Abreo, F., Turnage, R.H., McDonald, J.C. & Li, B.D. 2006, "High eIF4E, VEGF, and microvessel density in stage I to III breast cancer", *Annals of Surgery* 243: 684-90.

Calin, G.A., Sevignani, C., Dumitru, C.D., Hyslop, T., Noch, E., Yendamuri, S., Shimizu, M., Rattan, S., Bullrich, F., Negrini, M. & Croce, C.M. 2004, "Human microRNA genes are frequently located at fragile sites and genomic regions involved in cancers", *Proceedings of the National Academy of Sciences of the United States of America* 101: 2999-3004.

Canto, C., Suarez, E., Lizcano, J.M., Grino, E., Shepherd, P.R., Fryer, L.G., Carling, D., Bertran, J., Palacin, M., Zorzano, A. & Guma, A. 2004, "Neuregulin signaling on glucose transport in muscle cells", *Journal of Biological Chemistry* 279: 12260-12268.

Cardillo, M.R., Monti, S., Di Silverio, F., Gentile, V., Sciarra, F. & Toscano, V. 2003, "Insulin-like growth factor (IGF)-I, IGF-II and IGF type I receptor (IGFR-I) expression in prostatic cancer", *Anticancer Research* 23: 3825-3835.

Carey, L.A., Perou, C.M., Livasy, C.A., Dressler, L.G., Cowan, D., Conway, K., Karaca, G., Troester, M.A., Tse, C.K., Edmiston, S., Deming, S.L., Geradts, J., Cheang, M.C., Nielsen, T.O., Moorman, P.G., Earp, H.S. & Millikan, R.C. 2006, "Race, breast cancer subtypes, and survival in the Carolina Breast Cancer Study", *JAMA : the journal of the American Medical Association* 295: 2492-2502.

Carraway, K.L.,3rd, Soltoff, S.P., Diamonti, A.J. & Cantley, L.C. 1995, "Heregulin stimulates mitogenesis and phosphatidylinositol 3-kinase in mouse fibroblasts transfected with erbB2/neu and erbB3", *Journal of Biological Chemistry* 270: 7111-7116.

Chambers, A.F., Groom, A.C. & MacDonald, I.C. 2002, "Dissemination and growth of cancer cells in metastatic sites", *Nature`Review Cancer* 2: 563-572.

Chang, J.Y., Monroe, D.M., Oliver, J.A. & Roberts, H.R. 1999, "TFPIbeta, a second product from the mouse tissue factor pathway inhibitor (TFPI) gene", *Thrombosis and haemostasis* 81: 45-49.

Chang, L. & Karin, M. 2001, "Mammalian MAP kinase signalling cascades", *Nature* 410: 37-40.

Chavany, C., Connell, Y. & Neckers, L. 1995, "Contribution of sequence and phosphorothioate content to inhibition of cell growth and adhesion caused by c-myc antisense oligomers", *Molecular pharmacology* 48:. 738-746.

Cheadle, C., Fan, J., Cho-Chung, Y.S., Werner, T., Ray, J., Do, L., Gorospe, M. & Becker, K.G. 2005, "Stability regulation of mRNA and the control of gene expression", *Annals of the New York Academy of Sciences* 1058:. 196-204.

Chen, A., Xu, J. & Johnson, A.C. 2006, "Curcumin inhibits human colon cancer cell growth by suppressing gene expression of epidermal growth factor receptor through reducing the activity of the transcription factor Egr-1", *Oncogene* 25: 278-287.

Chen, C.N., Hsieh, F.J., Cheng, Y.M., Lee, P.H. & Chang, K.J. 2004, "Expression of eukaryotic initiation factor 4E in gastric adenocarcinoma and its association with clinical outcome", *Journal of surgical oncology* 86: 22-27.

Chen, J.J., Peck, K., Hong, T.M., Yang, S.C., Sher, Y.P., Shih, J.Y., Wu, R., Cheng, J.L., Roffler, S.R., Wu, C.W. & Yang, P.C. 2001, "Global analysis of gene expression in invasion by a lung cancer model", *Cancer research* 61: 5223-5230.

Cho, H.S. & Leahy, D.J. 2002, "Structure of the extracellular region of HER3 reveals an interdomain tether", *Science*. 297: 1330-1333.

Cillo, C., Barba, P., Freschi, G., Bucciarelli, G., Magli, M.C. & Boncinelli, E. 1992, "HOX gene expression in normal and neoplastic human kidney", *International journal of cancer. Journal international du cancer* 51: 892-897.

Cillo, C., Faiella, A., Cantile, M. & Boncinelli, E. 1999, "Homeobox genes and cancer", *Experimental cell research* 248:. 1-9.

Cirisano, F.D. & Karlan, B.Y. 1996, "The role of the HER-2/neu oncogene in gynecologic cancers", *Journal of the Society for Gynecologic Investigation*. 3: 99-105.

Clark, D.E., Errington, T.M., Smith, J.A., Frierson, H.F.,Jr, Weber, M.J. & Lannigan, D.A. 2005, "The serine/threonine protein kinase, p90 ribosomal S6 kinase, is an important regulator of prostate cancer cell proliferation", *Cancer research* 65: 3108-3116.

Clark, D.E., Poteet-Smith, C.E., Smith, J.A. & Lannigan, D.A. 2001, "Rsk2 allosterically activates estrogen receptor alpha by docking to the hormone-binding domain", *The EMBO journal* 20: 3484-3494.

Cogswell, P.C., Mayo, M.W. & Baldwin, A.S.,Jr 1997, "Involvement of Egr-1/RelA synergy in distinguishing T cell activation from tumor necrosis factor-alpha-induced NF-kappa B1 transcription", *The Journal of experimental medicine* 185: 491-497.

Cohen, N., Sharma, M., Kentsis, A., Perez, J.M., Strudwick, S. & Borden, K.L. 2001, "PML RING suppresses oncogenic transformation by reducing the affinity of eIF4E for mRNA", *The EMBO journal* 20: 4547-4559.

Cohen, P. 2002, "The origins of protein phosphorylation", *Nature cell biology* 4: E127-30.

Cohen, S.J., Cohen, R.B. & Meropol, N.J. 2005, "Targeting signal transduction pathways in colorectal cancer--more than skin deep", *Journal of clinical oncology : official journal of the American Society of Clinical Oncology* 23: 5374-5385.

Colomer, R., Shamon, L.A., Tsai, M.S. & Lupu, R. 2001, "Herceptin: from the bench to the clinic", *Cancer investigation* 19: 49-56.

Crawford, S.E., Flores-Stadler, E.M., Huang, L., Tan, X.D., Ranalli, M., Mu, Y. & Gonzalez-Crussi, F. 1998, "Rapid growth of cutaneous metastases after surgical resection of thrombospondin-secreting small blue round cell tumor of childhood", *Human pathology* 29 1039-1044.

Dahlberg, P.S., Ferrin, L.F., Grindle, S.M., Nelson, C.M., Hoang, C.D. & Jacobson, B. 2004, "Gene expression profiles in esophageal adenocarcinoma", *The Annals of Thoracic Surgery* 77: 1008-1015.

De Benedetti, A. & Graff, J.R. 2004, "eIF-4E expression and its role in malignancies and metastases", *Oncogene* 23:. 3189-3199.

De Benedetti, A. & Harris, A.L. 1999, "eIF4E expression in tumors: its possible role in progression of malignancies", *The international journal of biochemistry & cell biology* 31: 59-72.

De Cesare, D., Jacquot, S., Hanauer, A. & Sassone-Corsi, P. 1998, "Rsk-2 activity is necessary for epidermal growth factor-induced phosphorylation of CREB protein and transcription of c-fos gene", *Proceedings of the National Academy of Sciences of the United States of America* 95: 12202-12207.

de Groot, R.P., Ballou, L.M. & Sassone-Corsi, P. 1994, "Positive regulation of the cAMP-responsive activator CREM by the p70 S6 kinase: an alternative route to mitogen-induced gene expression", *Cell* 79: 81-91.

De la Haba-Rodriguez, J.R., Ruiz Borrego, M., Gomez Espana, A., Villar Pastor, C., Japon, M.A., Travado, P., Moreno Nogueira, J.A., Lopez Rubio, F. & Aranda Aguilar, E. 2004, "Comparative study of the immunohistochemical phenotype in breast cancer and its lymph node metastatic location", *Cancer investigation* 22: 219-224.

De Martin, R., Hoeth, M., Hofer-Warbinek, R. & Schmid, J.A. 2000, "The transcription factor NF-kappa B and the regulation of vascular cell function", *Arteriosclerosis,*

Deiss, L.P. & Kimchi, A. 1991, "A genetic tool used to identify thioredoxin as a mediator of a growth inhibitory signal", *Science* 252: 117-120.

Demicheli, R. 2001, "Tumour dormancy: findings and hypotheses from clinical research on breast cancer", *Seminars in cancer biology* 11: 297-306.

Deng, X., Ewton, D.Z., Li, S., Naqvi, A., Mercer, S.E., Landas, S. & Friedman, E. 2006, "The kinase Mirk/Dyrk1B mediates cell survival in pancreatic ductal adenocarcinoma", *Cancer research* 66: 4149-4158.

Dimova, I., Zaharieva, B., Raitcheva, S., Dimitrov, R., Doganov, N. & Toncheva, D. 2006, "Tissue microarray analysis of EGFR and erbB2 copy number changes in ovarian tumors", *International journal of gynecological cancer : official journal of the International Gynecological Cancer Society* 16: 145-151.

Dittadi, R., Calderazzo, F., Cabrelle, A., Di Fresco, S., Gion, M. & Chieco-Bianchi, L. 1996, "c-erbB-2/neu protein expression, DNA ploidy and S phase in breast cancer", *Cell proliferation* 29: 403-412.

Dittmar, T., Husemann, A., Schewe, Y., Nofer, J.R., Niggemann, B., Zanker, K.S. & Brandt, B.H. 2002, "Induction of cancer cell migration by epidermal growth factor is initiated by specific phosphorylation of tyrosine 1248 of c-erbB-2 receptor via EGFR", *The FASEB journal : official publication of the Federation of American Societies for Experimental Biology* 16: 1823-1825.

Dittmer, J. 2003, "The biology of the Ets1 proto-oncogene", *Moecular Cancer* 2: 29-39.

Doehn, U., Gammeltoft, S., Shen, S.H. & Jensen, C.J. 2004, "p90 ribosomal S6 kinase 2 is associated with and dephosphorylated by protein phosphatase 2Cdelta", *The Biochemical journal.* 382: 425-431.

Doench, J.G., Petersen, C.P. & Sharp, P.A. 2003, "siRNAs can function as miRNAs", *Genes & development* 17: 438-442.

Dolcet, X., Llobet, D., Pallares, J. & Matias-Guiu, X. 2005, "NF-kB in development and progression of human cancer", *Virchows Archiv : an international journal of pathology* 446: 475-482.

Dostie, J., Lejbkowicz, F. & Sonenberg, N. 2000, "Nuclear eukaryotic initiation factor 4E (eIF4E) colocalizes with splicing factors in speckles", *The Journal of cell biology* 148: 239-247.

Eid, M.A., Kumar, M.V., Iczkowski, K.A., Bostwick, D.G. & Tindall, D.J. 1998, "Expression of early growth response genes in human prostate cancer", *Cancer research* 58: 2461-2468.

Eisen, M.B., Spellman, P.T., Brown, P.O. & Botstein, D. 1998, "Cluster analysis and display of genome-wide expression patterns", *Proceedings of the National Academy of Sciences of the United States of America* 95: 14863-14868.

Elenbaas, B. & Weinberg, R.A. 2001, "Heterotypic signaling between epithelial tumor cells and fibroblasts in carcinoma formation", *Experimental cell research* 264: 169-184.

Erman, M., Abali, H., Oran, B., Haznedaroglu, I.C., Canpinar, H., Kirazli, S. & Celik, I. 2004, "Tamoxifen-induced tissue factor pathway inhibitor reduction: a clue for an acquired thrombophilic state?", *Annals of Oncology : Official Journal of the European Society for Medical Oncology / ESMO* 15: 1622-1626.

Esemuede, N., Lee, T., Pierre-Paul, D., Sumpio, B.E. & Gahtan, V. 2004, "The role of thrombospondin-1 in human disease", *The Journal of surgical research* 122: 135-142.

Evans, C.W. 1991, "A genetic basis for metastasis", *Cell biology international reports* 15: 1175-1181.

Even-Ram, S.C., Maoz, M., Pokroy, E., Reich, R., Katz, B.Z., Gutwein, P., Altevogt, P. & Bar-Shavit, R. 2001, "Tumor cell invasion is promoted by activation of protease activated receptor-1 in cooperation with the alpha vbeta 5 integrin", *Journal of Biological Chemistry* 276: 10952-10962.

Ezzat, S. & Asa, S.L. 2005, "FGF receptor signaling at the crossroads of endocrine homeostasis and tumorigenesis", *Hormone and metabolic research. Hormon- und Stoffwechselforschung. Hormones et metabolisme* 37: 355-360.

Faivre, S., Regnauld, K., Bruyneel, E., Nguyen, Q.D., Mareel, M., Emami, S. & Gespach, C. 2001, "Suppression of cellular invasion by activated G-protein subunits Galphao, Galphai1, Galphai2, and Galphai3 and sequestration of Gbetagamma", *Molecular pharmacology* 60: 363-372.

Falls, D.L. 2003, "Neuregulins: functions, forms, and signaling strategies", *Experimental cell research* 284: 14-30.

Fang, J.Y. & Richardson, B.C. 2005, "The MAPK signalling pathways and colorectal cancer", *Lancet Oncology* 6: 322-327.

Ferraro, B., Bepler, G., Sharma, S., Cantor, A. & Haura, E.B. 2005, "EGR1 predicts PTEN and survival in patients with non-small-cell lung cancer", *Journal of clinical oncology : official journal of the American Society of Clinical Oncology* 23: 1921-1926.

Fidler, I.J., Wilmanns, C., Staroselsky, A., Radinsky, R., Dong, Z. & Fan, D. 1994, "Modulation of tumor cell response to chemotherapy by the organ environment", *Cancer metastasis reviews* 13:. 209-222.

Finlay, T.H., Tamir, S., Kadner, S.S., Cruz, M.R., Yavelow, J. & Levitz, M. 1993, "alpha 1-Antitrypsin- and anchorage-independent growth of MCF-7 breast cancer cells", *Endocrinology* 133: 996-1002.

Fire, A., Xu, S., Montgomery, M.K., Kostas, S.A., Driver, S.E. & Mello, C.C. 1998, "Potent and specific genetic interference by double-stranded RNA in Caenorhabditis elegans", *Nature* 391: 806-811.

Fischer, E.G., Riewald, M., Huang, H.Y., Miyagi, Y., Kubota, Y., Mueller, B.M. & Ruf, W. 1999, "Tumor cell adhesion and migration supported by interaction of a receptor-protease complex with its inhibitor", *The Journal of clinical investigation* 104: 1213-1221.

Fiucci, G., Ravid, D., Reich, R. & Liscovitch, M. 2002, "Caveolin-1 inhibits anchorage-independent growth, anoikis and invasiveness in MCF-7 human breast cancer cells", *Oncogene* 21: 2365-2375.

Flynn, A. & Proud, C.G. 1996a, "The role of eIF4 in cell proliferation", *Cancer surveys* 27: 293-310.

Flynn, A. & Proud, G. 1996b, "Insulin-stimulated phosphorylation of initiation factor 4E is mediated by the MAP kinase pathway", *FEBS letters* 389: 162-166.

Frodin, M., Jensen, C.J., Merienne, K. & Gammeltoft, S. 2000, "A phosphoserine-regulated docking site in the protein kinase RSK2 that recruits and activates PDK1", *The EMBO journal* 19: 2924-2934.

Fudge, K., Wang, C.Y. & Stearns, M.E. 1994, "Immunohistochemistry analysis of platelet-derived growth factor A and B chains and platelet-derived growth factor alpha and beta receptor expression in benign prostatic hyperplasias and Gleason-graded human prostate adenocarcinomas", *Modern pathology : an official journal of the United States and Canadian Academy of Pathology, Inc* 7: 549-554.

Gartel, A.L. & Kandel, E.S. 2006, "RNA interference in cancer", *Biomolecular engineering* 23: 17-34.

Gehring, W.J., Qian, Y.Q., Billeter, M., Furukubo-Tokunaga, K., Schier, A.F., Resendez-Perez, D., Affolter, M., Otting, G. & Wuthrich, K. 1994, "Homeodomain-DNA recognition", *Cell* 78: 211-223.

Ghosh, S., Spagnoli, G.C., Martin, I., Ploegert, S., Demougin, P., Heberer, M. & Reschner, A. 2005, "Three-dimensional culture of melanoma cells profoundly affects gene expression profile: a high density oligonucleotide array study", *Journal of cellular physiology* 204: 522-531.

Gingras, A.C., Raught, B. & Sonenberg, N. 1999, "eIF4 initiation factors: effectors of mRNA recruitment to ribosomes and regulators of translation", *Annual Review of Biochemistry* 68: 913-963.

Gius, D., Botero, A., Shah, S. & Curry, H.A. 1999, "Intracellular oxidation/reduction status in the regulation of transcription factors NF-kappaB and AP-1", *Toxicology letters* 106: 93-106.

Goetze, S., Xi, X.P., Kawano, Y., Kawano, H., Fleck, E., Hsueh, W.A. & Law, R.E. 1999, "TNF-alpha-induced migration of vascular smooth muscle cells is MAPK dependent", *Hypertension* 33: 183-189.

Golpon, H.A., Geraci, M.W., Moore, M.D., Miller, H.L., Miller, G.J., Tuder, R.M. & Voelkel, N.F. 2001, "HOX genes in human lung: altered expression in primary pulmonary hypertension and emphysema", *American Journal of Pathology*. 158: 955-966.

Gotzmann, J., Mikula, M., Eger, A., Schulte-Hermann, R., Foisner, R., Beug, H. & Mikulits, W. 2004, "Molecular aspects of epithelial cell plasticity: implications for local tumor invasion and metastasis", *Mutation research* 566: 9-20.

Graff, J.R. & Zimmer, S.G. 2003, "Translational control and metastatic progression: enhanced activity of the mRNA cap-binding protein eIF-4E selectively enhances translation of metastasis-related mRNAs", *Clinical & experimental metastasis* 20: 265-273.

Graff, J.R., Boghaert, E.R., De Benedetti, A., Tudor, D.L., Zimmer, C.C., Chan, S.K. & Zimmer, S.G. 1995, "Reduction of translation initiation factor 4E decreases the malignancy of ras-transformed cloned rat embryo fibroblasts", *International journal of cancer. Journal international du cancer* 60: 255-263.

Graus-Porta, D., Beerli, R.R., Daly, J.M. & Hynes, N.E. 1997, "ErbB-2, the preferred heterodimerization partner of all ErbB receptors, is a mediator of lateral signaling", *The EMBO journal* 16: 1647-1655.

Greenberg, V.L. & Zimmer, S.G. 2005, "Paclitaxel induces the phosphorylation of the eukaryotic translation initiation factor 4E-binding protein 1 through a Cdk1-dependent mechanism", *Oncogene* 24: 4851-4860.

Grille, S.J., Bellacosa, A., Upson, J., Klein-Szanto, A.J., van Roy, F., Lee-Kwon, W., Donowitz, M., Tsichlis, P.N. & Larue, L. 2003, "The protein kinase Akt induces epithelial mesenchymal transition and promotes enhanced motility and invasiveness of squamous cell carcinoma lines", *Cancer research* 63: 2172-2178.

Grishok, A., Pasquinelli, A.E., Conte, D., Li, N., Parrish, S., Ha, I., Baillie, D.L., Fire, A., Ruvkun, G. & Mello, C.C. 2001, "Genes and mechanisms related to RNA interference regulate expression of the small temporal RNAs that control C. elegans developmental timing", *Cell* 106: 23-34.

Grund, E.M., Spyropoulos, D.D., Watson, D.K. & Muise-Helmericks, R.C. 2005, "Interleukins 2 and 15 regulate Ets1 expression via ERK1/2 and MNK1 in human natural killer cells", *Journal of Biological Chemistry* 280: 4772-4778.

Gu, Q., Wang, D., Wang, X., Peng, R., Liu, J., Deng, H., Wang, Z. & Jiang, T. 2004, "Basic fibroblast growth factor inhibits radiation-induced apoptosis of HUVECs. II. The RAS/MAPK pathway and phosphorylation of BAD at serine 112", *Radiation research* 161: 703-711.

Guo, H.S., Xie, Q., Fei, J.F. & Chua, N.H. 2005, "MicroRNA directs mRNA cleavage of the transcription factor NAC1 to downregulate auxin signals for arabidopsis lateral root development", *The Plant Cell* 17: 1376-1386.

Guy, P.M., Carraway, K.L.,III & Cerione, R.A. 1992, "Biochemical comparisons of the normal and oncogenic forms of insect cell-expressed neu tyrosine kinases", *Journal of Biological Chemistry* 267: 13851-13856.

Guy, P.M., Platko, J.V., Cantley, L.C., Cerione, R.A. & Carraway, K.L.,3rd 1994, "Insect cell-expressed p180erbB3 possesses an impaired tyrosine kinase activity", *Proceedings of the National Academy of Sciences of the United States of America* 91: 8132-8136.

Hamik, A., Setiadi, H., Bu, G., McEver, R.P. & Morrissey, J.H. 1999, "Down-regulation of monocyte tissue factor mediated by tissue factor pathway inhibitor and the low density lipoprotein receptor-related protein", *Journal of Biological Chemistry* 274: 4962-4969.

Hamilton, A., Voinnet, O., Chappell, L. & Baulcombe, D. 2002, "Two classes of short interfering RNA in RNA silencing", *The EMBO journal* 21: 4671-4679.

Hamilton, A.J. & Baulcombe, D.C. 1999, "A species of small antisense RNA in posttranscriptional gene silencing in plants", *Science* 286: 950-952.

Hammond, S.M. 2006, "MicroRNA therapeutics: a new niche for antisense nucleic acids", *Trends in molecular medicine* 12: 99-101.

Hammond, S.M., Bernstein, E., Beach, D. & Hannon, G.J. 2000, "An RNA-directed nuclease mediates post-transcriptional gene silencing in Drosophila cells", *Nature* 404: 293-296.

Hamuro, T., Kamikubo, Y., Nakahara, Y., Miyamoto, S. & Funatsu, A. 1998, "Human recombinant tissue factor pathway inhibitor induces apoptosis in cultured human endothelial cells", *FEBS letters* 421: 197-202.

Hanks, S.K. & Hunter, T. 1995, "Protein kinases 6. The eukaryotic protein kinase superfamily: kinase (catalytic) domain structure and classification", *The FASEB journal : official publication of the Federation of American Societies for Experimental Biology* 9: 576-596.

Hannemann, J., Oosterkamp, H.M., Bosch, C.A., Velds, A., Wessels, L.F., Loo, C., Rutgers, E.J., Rodenhuis, S. & van de Vijver, M.J. 2005, "Changes in gene expression associated with response to neoadjuvant chemotherapy in breast cancer", *Journal of clinical oncology : official journal of the American Society of Clinical Oncology.* 23: 3331-3342.

Harada, H. & Grant, S. 2003, "Apoptosis regulators", *Reviews Clinical Experiments Hematology* 7: 117-138.

Harrington, L.S., Findlay, G.M. & Lamb, R.F. 2005, "Restraining PI3K: mTOR signalling goes back to the membrane", *Trends in biochemical sciences* 30: 35-42.

Hartmann, T.N., Burger, J.A., Glodek, A., Fujii, N. & Burger, M. 2005, "CXCR4 chemokine receptor and integrin signaling co-operate in mediating adhesion and chemoresistance in small cell lung cancer (SCLC) cells", *Oncogene* 24: 4462-4471.

Hay, E.D. 1995, "An overview of epithelio-mesenchymal transformation", *Acta Anatomica* 154: 8-20.

He, L., Thomson, J.M., Hemann, M.T., Hernando-Monge, E., Mu, D., Goodson, S., Powers, S., Cordon-Cardo, C., Lowe, S.W., Hannon, G.J. & Hammond, S.M. 2005, "A microRNA polycistron as a potential human oncogene", *Nature* 435: 828-833.

Hembrough, T.A., Ruiz, J.F., Papathanassiu, A.E., Green, S.J. & Strickland, D.K. 2001, "Tissue factor pathway inhibitor inhibits endothelial cell proliferation via association with the very low density lipoprotein receptor", *Journal of Biological Chemistry* 276: 12241-12248.

Hennessy, B.T., Smith, D.L., Ram, P.T., Lu, Y. & Mills, G.B. 2005, "Exploiting the PI3K/AKT pathway for cancer drug discovery", *Nature Review Drug Discovery* 4: 988-1004.

Henrikson, K.P., Salazar, S.L., Fenton, J.W.,2nd & Pentecost, B.T. 1999, "Role of thrombin receptor in breast cancer invasiveness", *British journal of cancer* 79: 401-406.

Heyder, C., Gloria-Maercker, E., Hatzmann, W., Zaenker, K.S. & Dittmar, T. 2006, "Visualization of tumor cell extravasation", *Contributions to microbiology* 13: 200-208.

Hiscox, S. & Jiang, W.G. 1997, "Quantification of tumour cell-endothelial cell attachment by 1,1'-dioctadecyl-3,3,3',3'-tetramethylindocarbocyanine (DiI)", *Cancer letters* 112: 209-217.

Hoffmann, S., He, S., Jin, M., Ehren, M., Wiedemann, P., Ryan, S.J. & Hinton, D.R. 2005, "A selective cyclic integrin antagonist blocks the integrin receptors alphavbeta3 and alphavbeta5 and inhibits retinal pigment epithelium cell attachment, migration and invasion", *BMC ophthalmology* 5: 16.

Holbro, T., Civenni, G. & Hynes, N.E. 2003, "The ErbB receptors and their role in cancer progression", *Experimental cell research* 284: 99-110.

Huang, R.P., Fan, Y., de Belle, I., Niemeyer, C., Gottardis, M.M., Mercola, D. & Adamson, E.D. 1997, "Decreased Egr-1 expression in human, mouse and rat mammary cells and tissues correlates with tumor formation", *International journal of cancer. Journal international du cancer* 72: 102-109.

Hung, M.C. & Lau, Y.K. 1999, "Basic science of HER-2/neu: a review", *Seminars in oncology* 26: 51-59.

Idriss, H.T. & Naismith, J.H. 2000, "TNF alpha and the TNF receptor superfamily: structure-function relationship(s)", *Microscopy research and technique* 50: 184-195.

Inoki, K., Li, Y., Zhu, T., Wu, J. & Guan, K.L. 2002, "TSC2 is phosphorylated and inhibited by Akt and suppresses mTOR signalling", *Nature cell biology* 4: 648-657.

Inuzuka, H., Nanbu-Wakao, R., Masuho, Y., Muramatsu, M., Tojo, H. & Wakao, H. 1999, "Differential regulation of immediate early gene expression in preadipocyte cells through multiple signaling pathways", *Biochemical and biophysical research communications* 265: 664-668.

Ishigaki, Y., Li, X., Serin, G. & Maquat, L.E. 2001, "Evidence for a pioneer round of mRNA translation: mRNAs subject to nonsense-mediated decay in mammalian cells are bound by CBP80 and CBP20", *Cell* 106: 607-617.

Ishikawa, T., Kobayashi, M., Mai, M., Suzuki, T. & Ooi, A. 1997, "Amplification of the c-erbB-2 (HER-2/neu) gene in gastric cancer cells. Detection by fluorescence in situ hybridization", *American Journal of Pathology* 151: 761-768.

Iversen, N., Lindahl, A.K. & Abildgaard, U. 1998, "Elevated TFPI in malignant disease: relation to cancer type and hypercoagulation", *British journal of haematology* 102: 889-895.

Jackson, A.L., Bartz, S.R., Schelter, J., Kobayashi, S.V., Burchard, J., Mao, M., Li, B., Cavet, G. & Linsley, P.S. 2003, "Expression profiling reveals off-target gene regulation by RNAi", *Nature biotechnology* 21: 635-637.

Jackson, J.G., White, M.F. & Yee, D. 1998, "Insulin receptor substrate-1 is the predominant signaling molecule activated by insulin-like growth factor-I, insulin, and interleukin-4 in estrogen receptor-positive human breast cancer cells", *Journal of Biological Chemistry* 273: 9994-10003.

Jackson, R.J. 2005, "Alternative mechanisms of initiating translation of mammalian mRNAs", *Biochemical Society transactions* 33: 1231-1241.

Jaeschke, A., Dennis, P.B. & Thomas, G. 2004, "mTOR: a mediator of intracellular homeostasis", *Current topics in microbiology and immunology* 279: 283-298.

Jariel-Encontre, I., Salvat, C., Steff, A.M., Pariat, M., Acquaviva, C., Furstoss, O. & Piechaczyk, M. 1997, "Complex mechanisms for c-fos and c-jun degradation", *Molecular biology reports* 24: 51-56.

Jechlinger, M., Grunert, S. & Beug, H. 2002, "Mechanisms in epithelial plasticity and metastasis: insights from 3D cultures and expression profiling", *Journal of mammary gland biology and neoplasia* 7: 415-432.

Jensen, C.J., Buch, M.B., Krag, T.O., Hemmings, B.A., Gammeltoft, S. & Frodin, M. 1999, "90-kDa ribosomal S6 kinase is phosphorylated and activated by 3-phosphoinositide-dependent protein kinase-1", *Journal of Biological Chemistry* 274: 27168-27176.

Jiang, W.G., Martin, T.A., Parr, C., Davies, G., Matsumoto, K. & Nakamura, T. 2005, "Hepatocyte growth factor, its receptor, and their potential value in cancer therapies", *Critical reviews in oncology/hematology* 53: 35-69.

Jin, H., Hwang, S.K., Yu, K., Anderson, H.K., Lee, Y.S., Lee, K.H., Prats, A.C., Morello, D., Beck, G.R.,Jr & Cho, M.H. 2006, "A high inorganic phosphate diet perturbs brain growth, alters Akt-ERK signaling, and results in changes in cap-dependent translation", *Toxicological sciences : an official journal of the Society of Toxicology* 90: 221-229.

Jones, R.M., Branda, J., Johnston, K.A., Polymenis, M., Gadd, M., Rustgi, A., Callanan, L. & Schmidt, E.V. 1996, "An essential E box in the promoter of the gene encoding the mRNA cap-binding protein (eukaryotic initiation factor 4E) is a target for activation by c-myc", *Molecular and cellular biology* 16: 4754-4764.

Joshi, B., Cai, A.L., Keiper, B.D., Minich, W.B., Mendez, R., Beach, C.M., Stepinski, J., Stolarski, R., Darzynkiewicz, E. & Rhoads, R.E. 1995, "Phosphorylation of eukaryotic protein synthesis initiation factor 4E at Ser-209", *Journal of Biological Chemistry* 270: 14597-14603.

Kamikubo, Y., Nakahara, Y., Takemoto, S., Hamuro, T., Miyamoto, S. & Funatsu, A. 1997, "Human recombinant tissue-factor pathway inhibitor prevents the proliferation of cultured human neonatal aortic smooth muscle cells", *FEBS letters* 407: 116-120.

Kane, L.P., Shapiro, V.S., Stokoe, D. & Weiss, A. 1999, "Induction of NF-kappaB by the Akt/PKB kinase", *Current biology* 9: 601-604.

Kang, M.J., Ahn, H.S., Lee, J.Y., Matsuhashi, S. & Park, W.Y. 2002, "Up-regulation of PDCD4 in senescent human diploid fibroblasts", *Biochemical and biophysical research communications* 293: 617-621.

Kang, Y. & Massague, J. 2004, "Epithelial-mesenchymal transitions: twist in development and metastasis", *Cell* 118: 277-279.

Kapitein, L.C., Peterman, E.J., Kwok, B.H., Kim, J.H., Kapoor, T.M. & Schmidt, C.F. 2005, "The bipolar mitotic kinesin Eg5 moves on both microtubules that it crosslinks", *Nature* 435: 114-118.

Karrison, T.G., Ferguson, D.J. & Meier, P. 1999, "Dormancy of mammary carcinoma after mastectomy", *Journal of the National Cancer Institute* 91: 80-85.

Kaufmann, K. & Thiel, G. 2001, "Epidermal growth factor and platelet-derived growth factor induce expression of Egr-1, a zinc finger transcription factor, in human malignant glioma cells", *Journal of the neurological sciences* 189: 83-91.

Kelleher, R.J.,3rd, Govindarajan, A. & Tonegawa, S. 2004, "Translational regulatory mechanisms in persistent forms of synaptic plasticity", *Neuron* 44: 59-73.

Kerekatte, V., Smiley, K., Hu, B., Smith, A., Gelder, F. & De Benedetti, A. 1995, "The proto-oncogene/translation factor eIF4E: a survey of its expression in breast

carcinomas", *International journal of cancer. Journal international du cancer* 64: 27-31.

Keski-Oja, J., Koli, K., Lohi, J. & Laiho, M. 1991, "Growth factors in the regulation of plasminogen-plasmin system in tumor cells", *Seminars in thrombosis and hemostasis* 17:. 231-239.

Kevil, C., Carter, P., Hu, B. & DeBenedetti, A. 1995, "Translational enhancement of FGF-2 by eIF-4 factors, and alternate utilization of CUG and AUG codons for translation initiation", *Oncogene* 11: 2339-2348.

Kim, H.H., Vijapurkar, U., Hellyer, N.J., Bravo, D. & Koland, J.G. 1998, "Signal transduction by epidermal growth factor and heregulin via the kinase-deficient ErbB3 protein", *The Biochemical journal* 334: 189-195.

Kim, J., Lee, Y.H., Kwon, T.K., Chang, J.S., Chung, K.C. & Min do, S. 2006, "Phospholipase D prevents etoposide-induced apoptosis by inhibiting the expression of early growth response-1 and phosphatase and tensin homologue deleted on chromosome 10", *Cancer research* 66: 784-793.

Kim, J., Mori, T., Chen, S.L., Amersi, F.F., Martinez, S.R., Kuo, C., Turner, R.R., Ye, X., Bilchik, A.J., Morton, D.L. & Hoon, D.S. 2006, "Chemokine receptor CXCR4 expression in patients with melanoma and colorectal cancer liver metastases and the association with disease outcome", *Annals of Surgery* 244: 113-120.

Kim, V.N. 2004, "MicroRNA precursors in motion: exportin-5 mediates their nuclear export", *Trends in cell biology* 14: 156-159.

Kirsch, M., Schackert, G. & Black, P.M. 2004, "Metastasis and angiogenesis", *Cancer treatment and research* 117: 285-304.

Klapper, L.N., Glathe, S., Vaisman, N., Hynes, N.E., Andrews, G.C., Sela, M. & Yarden, Y. 1999, "The ErbB-2/HER2 oncoprotein of human carcinomas may function solely as a shared coreceptor for multiple stroma-derived growth factors", *Proceedings of the National Academy of Sciences of the United States of America* 96: 4995-5000.

Krichevsky, A.M., King, K.S., Donahue, C.P., Khrapko, K. & Kosik, K.S. 2003, "A microRNA array reveals extensive regulation of microRNAs during brain development", *RNA* 9: 1274-1281.

Kristiansen, G., Yu, Y., Petersen, S., Kaufmann, O., Schluns, K., Dietel, M. & Petersen, I. 2001, "Overexpression of c-erbB2 protein correlates with disease-stage and chromosomal gain at the c-erbB2 locus in non-small cell lung cancer", *European journal of cancer* 37: 1089-1095.

Krones-Herzig, A., Mittal, S., Yule, K., Liang, H., English, C., Urcis, R., Soni, T., Adamson, E.D. & Mercola, D. 2005, "Early growth response 1 acts as a tumor suppressor in vivo and in vitro via regulation of p53", *Cancer research* 65: 5133-5143.

Kuesters, S., Maurer, M., Burger, A.M., Metz, T. & Fiebig, H.H. 2006, "Correlation of ErbB2 gene status, mRNA and protein expression in a panel of >100 human tumor xenografts of different origin", *Onkologie* 29: 249-256.

Kumar, D., Gokhale, P., Broustas, C., Chakravarty, D., Ahmad, I. & Kasid, U. 2004, "Expression of SCC-S2, an antiapoptotic molecule, correlates with enhanced proliferation and tumorigenicity of MDA-MB 435 cells", *Oncogene*. 23: 612-616.

Kumar, D., Whiteside, T.L. & Kasid, U. 2000, "Identification of a novel tumor necrosis factor-alpha-inducible gene, SCC-S2, containing the consensus sequence of a death effector domain of fas-associated death domain-like interleukin- 1beta-converting enzyme-inhibitory protein", *Journal of Biological Chemistry* 275: 2973-2978.

Kureishi, Y., Kobayashi, S., Amano, M., Kimura, K., Kanaide, H., Nakano, T., Kaibuchi, K. & Ito, M. 1997, "Rho-associated kinase directly induces smooth muscle contraction through myosin light chain phosphorylation", *Journal of Biological Chemistry* 272: 12257-12260.

Lachance, P.E., Miron, M., Raught, B., Sonenberg, N. & Lasko, P. 2002, "Phosphorylation of eukaryotic translation initiation factor 4E is critical for growth", *Molecular and cellular biology* 22: 1656-1663.

Lachance, P.E., Miron, M., Raught, B., Sonenberg, N. & Lasko, P. 2002, "Phosphorylation of eukaryotic translation initiation factor 4E is critical for growth", *Molecular and cellular biology* 22: 1656-1663.

Lai, E.C. 2005, "miRNAs: whys and wherefores of miRNA-mediated regulation", *Current biology* 15: R458-60.

Larue, L. & Bellacosa, A. 2005, "Epithelial-mesenchymal transition in development and cancer: role of phosphatidylinositol 3' kinase/AKT pathways", *Oncogene* 24: 7443-7454.

Lassus, H., Sihto, H., Leminen, A., Joensuu, H., Isola, J., Nupponen, N.N. & Butzow, R. 2006, "Gene amplification, mutation, and protein expression of EGFR and mutations of ERBB2 in serous ovarian carcinoma", *Journal of Molecular Medicine* 84:671-81

Law, E., Gilvarry, U., Lynch, V., Gregory, B., Grant, G. & Clynes, M. 1992, "Cytogenetic comparison of two poorly differentiated human lung squamous cell carcinoma lines", *Cancer genetics and cytogenetics* 59: 111-118.

Lawler, J. 2000, "The functions of thrombospondin-1 and-2", *Current opinion in cell biology* 12: 634-640.

Lawler, J.W., Chao, F.C. & Fang, P.H. 1977, "Observation of a high molecular weight platelet protein released by thrombin", *Thrombosis and haemostasis* 37: 355-357.

Lawrence, J.C.,Jr & Abraham, R.T. 1997, "PHAS/4E-BPs as regulators of mRNA translation and cell proliferation", *Trends in biochemical sciences* 22: 345-349.

Lazaris-Karatzas, A. & Sonenberg, N. 1992, "The mRNA 5' cap-binding protein, eIF-4E, cooperates with v-myc or E1A in the transformation of primary rodent fibroblasts", *Molecular and cellular biology* 12: 1234-1238.

Lee, H. & Bai, W. 2002, "Regulation of estrogen receptor nuclear export by ligand-induced and p38-mediated receptor phosphorylation", *Molecular and cellular biology* 22: 5835-5845.

Lejbkowicz, F., Goyer, C., Darveau, A., Neron, S., Lemieux, R. & Sonenberg, N. 1992, "A fraction of the mRNA 5' cap-binding protein, eukaryotic initiation factor 4E, localizes to the nucleus", *Proceedings of the National Academy of Sciences of the United States of America* 89: 9612-9616.

Leng, Q. & Mixson, A.J. 2005, "Small interfering RNA targeting Raf-1 inhibits tumor growth in vitro and in vivo", *Cancer gene therapy* 12: 682-690.

Levine, A.J. 1997, "p53, the cellular gatekeeper for growth and division", *Cell* 88: 323-331.

Li, B.D., Liu, L., Dawson, M. & De Benedetti, A. 1997, "Overexpression of eukaryotic initiation factor 4E (eIF4E) in breast carcinoma", *Cancer* 79: 2385-2390.

Li, B.D., McDonald, J.C., Nassar, R. & De Benedetti, A. 1998, "Clinical outcome in stage I to III breast carcinoma and eIF4E overexpression", *Annals of Surgery* 227: 756-761

Li, S., Crothers, J., Haqq, C.M. & Blackburn, E.H. 2005, "Cellular and gene expression responses involved in the rapid growth inhibition of human cancer cells by RNA interference-mediated depletion of telomerase RNA", *Journal of Biological Chemistry* 280: 23709-23717.

Li, S., Perlman, D.M., Peterson, M.S., Burrichter, D., Avdulov, S., Polunovsky, V.A. & Bitterman, P.B. 2004, "Translation initiation factor 4E blocks endoplasmic reticulum-mediated apoptosis", *Journal of Biological Chemistry* 279: 21312-21317.

Li, S., Takasu, T., Perlman, D.M., Peterson, M.S., Burrichter, D., Avdulov, S., Bitterman, P.B. & Polunovsky, V.A. 2003, "Translation factor eIF4E rescues cells from Myc-dependent apoptosis by inhibiting cytochrome c release", *Journal of Biological Chemistry* 278: 3015-3022.

Li, Z., He, L., Wilson, K. & Roberts, D. 2001, "Thrombospondin-1 inhibits TCR-mediated T lymphocyte early activation", *Journal of immunology* 166: 2427-2436.

Liang, Y., McDonnell, S. & Clynes, M. 2002, "Examining the relationship between cancer invasion/metastasis and drug resistance", *Curr.Cancer.Drug Targets* 2: 257-277.

Lim, S.J., Lopez-Berestein, G., Hung, M.C., Lupu, R. & Tari, A.M. 2000, "Grb2 downregulation leads to Akt inactivation in heregulin-stimulated and ErbB2-overexpressing breast cancer cells", *Oncogene* 19: 6271-6276.

Lin, M., Wei, L.J., Sellers, W.R., Lieberfarb, M., Wong, W.H. & Li, C. 2004, "dChipSNP: significance curve and clustering of SNP-array-based loss-of-heterozygosity data", *Bioinformatics* 20: 1233-1240.

Lin, X., Buff, E.M., Perrimon, N. & Michelson, A.M. 1999, "Heparan sulfate proteoglycans are essential for FGF receptor signaling during Drosophila embryonic development", *Development* 126: 3715-3723.

Lindahl, A.K., Boffa, M.C. & Abildgaard, U. 1993, "Increased plasma thrombomodulin in cancer patients", *Thrombosis and haemostasis* 69: 112-114.

Lindahl, A.K., Jacobsen, P.B., Sandset, P.M. & Abildgaard, U. 1991, "Tissue factor pathway inhibitor with high anticoagulant activity is increased in post-heparin plasma and in plasma from cancer patients", *Blood coagulation & fibrinolysis : an international journal in haemostasis and thrombosis* 2: 713-721.

Lindahl, A.K., Odegaard, O.R., Sandset, P.M. & Harbitz, T.B. 1992, "Coagulation inhibition and activation in pancreatic cancer. Changes during progress of disease", *Cancer* 70:. 2067-2072.

Lindahl, A.K., Sandset, P.M. & Abildgaard, U. 1992, "The present status of tissue factor pathway inhibitor", *Blood coagulation & fibrinolysis : an international journal in haemostasis and thrombosis* 3: 439-449.

Lindahl, A.K., Sandset, P.M., Abildgaard, U., Andersson, T.R. & Harbitz, T.B. 1989, "High plasma levels of extrinsic pathway inhibitor and low levels of other coagulation inhibitors in advanced cancer", *Acta Chirurgica Scandinavica* 155: 389-393.

Linn, F., Heidmann, I., Saedler, H. & Meyer, P. 1990, "Epigenetic changes in the expression of the maize A1 gene in Petunia hybrida: role of numbers of integrated gene copies and state of methylation", *Molecular & general genetics* 222: 329-336.

Liotta, L.A. 1986, "Tumor invasion and metastases--role of the extracellular matrix: Rhoads Memorial Award lecture", *Cancer research* 46: 1-7.

Lippman, Z. & Martienssen, R. 2004, "The role of RNA interference in heterochromatic silencing", *Nature* 431: 364-370.

Liu, C., Yao, J., Mercola, D. & Adamson, E. 2000, "The transcription factor EGR-1 directly transactivates the fibronectin gene and enhances attachment of human glioblastoma cell line U251", *Journal of Biological Chemistry* 275: 20315-20323.

Liu, E., Thor, A., He, M., Barcos, M., Ljung, B.M. & Benz, C. 1992, "The HER2 (c-erbB-2) oncogene is frequently amplified in in situ carcinomas of the breast", *Oncogene* 7: 1027-1032.

Lopez, R., Garrido, E., Pina, P., Hidalgo, A., Lazos, M., Ochoa, R. & Salcedo, M. 2006, "HOXB homeobox gene expression in cervical carcinoma", *International journal of gynecological cancer: official journal of the International Gynecological Cancer Society* 16: 329-335.

Louvain-Quintard, V.B., Bianchini, E.P., Calmel-Tareau, C., Tagzirt, M. & Le Bonniec, B.F. 2005, "Thrombin-activable factor X re-establishes an intrinsic amplification in tenase-deficient plasmas", *Journal of Biological Chemistry* 280: 41352-41359.

Lwaleed, B.A. & Bass, P.S. 2006, "Tissue factor pathway inhibitor: structure, biology and involvement in disease", *The Journal of pathology* 208: 327-339.

Lynch, M., Chen, L., Ravitz, M.J., Mehtani, S., Korenblat, K., Pazin, M.J. & Schmidt, E.V. 2005, "hnRNP K binds a core polypyrimidine element in the eukaryotic translation initiation factor 4E (eIF4E) promoter, and its regulation of eIF4E contributes to neoplastic transformation", *Molecular and cellular biology* 25: 6436-6453.

Mader, S., Lee, H., Pause, A. & Sonenberg, N. 1995, "The translation initiation factor eIF-4E binds to a common motif shared by the translation factor eIF-4 gamma and the translational repressors 4E-binding proteins", *Molecular and cellular biology* 15: 4990-4997.

Magrath, I. 1990, "The pathogenesis of Burkitt's lymphoma", *Advances in Cancer Research* 55: 133-270.

Makiyama, K., Hamada, J., Takada, M., Murakawa, K., Takahashi, Y., Tada, M., Tamoto, E., Shindo, G., Matsunaga, A., Teramoto, K., Komuro, K., Kondo, S., Katoh, H., Koike, T. & Moriuchi, T. 2005, "Aberrant expression of HOX genes in human invasive breast carcinoma", *Oncology reports* 13: 673-679.

Mallory, A.C., Reinhart, B.J., Jones-Rhoades, M.W., Tang, G., Zamore, P.D., Barton, M.K. & Bartel, D.P. 2004, "MicroRNA control of PHABULOSA in leaf development: importance of pairing to the microRNA 5' region", *The EMBO journal* 23: 3356-3364.

Manning, B.D. & Cantley, L.C. 2003, "Rheb fills a GAP between TSC and TOR", *Trends in biochemical sciences* 28: 573-576.

Marcotrigiano, J., Gingras, A.C., Sonenberg, N. & Burley, S.K. 1997, "Cocrystal structure of the messenger RNA 5' cap-binding protein (eIF4E) bound to 7-methyl-GDP", *Cell* 89: 951-961.

Marques, J.T. & Williams, B.R. 2005, "Activation of the mammalian immune system by siRNAs", *Nature biotechnology* 23: 1399-1405.

Martinez, J., Patkaniowska, A., Urlaub, H., Luhrmann, R. & Tuschl, T. 2002, "Single-stranded antisense siRNAs guide target RNA cleavage in RNAi", *Cell* 110: 563-574.

Marx, D., Schauer, A., Reiche, C., May, A., Ummenhofer, L., Reles, A., Rauschecker, H., Sauer, R. & Schumacher, M. 1990, "c-erbB2 expression in correlation to other biological parameters of breast cancer", *Journal of cancer research and clinical oncology* 116: 15-20.

Mast, A.E., Stadanlick, J.E., Lockett, J.M., Dietzen, D.J., Hasty, K.A. & Hall, C.L. 2000, "Tissue factor pathway inhibitor binds to platelet thrombospondin-1", *Journal of Biological Chemistry* 275: 31715-31721.

Matsumoto, G., Kushibiki, T., Kinoshita, Y., Lee, U., Omi, Y., Kubota, E. & Tabata, Y. 2006, "Cationized gelatin delivery of a plasmid DNA expressing small interference RNA for VEGF inhibits murine squamous cell carcinoma", *Cancer Science* 97: 313-321.

Matsuo, H., Li, H., McGuire, A.M., Fletcher, C.M., Gingras, A.C., Sonenberg, N. & Wagner, G. 1997, "Structure of translation factor eIF4E bound to m7GDP and interaction with 4E-binding protein", *Nature structural biology* 4: 717-724.

Matuoka, K., Shibasaki, F., Shibata, M. & Takenawa, T. 1993, "Ash/Grb-2, a SH2/SH3-containing protein, couples to signaling for mitogenesis and cytoskeletal reorganization by EGF and PDGF", *The EMBO journal* 12: 3467-3473.

Matzke, M.A., Primig, M., Trnovsky, J. & Matzke, A.J. 1989, "Reversible methylation and inactivation of marker genes in sequentially transformed tobacco plants", *The EMBO journal* 8: 643-649.

Maulbecker, C.C. & Gruss, P. 1993, "The oncogenic potential of deregulated homeobox genes", *Cell growth & differentiation : the molecular biology journal of the American Association for Cancer Research* 4: 431-441.

McClusky, D.R., Chu, Q., Yu, H., Debenedetti, A., Johnson, L.W., Meschonat, C., Turnage, R., McDonald, J.C., Abreo, F. & Li, B.D. 2005, "A prospective trial on initiation factor 4E (eIF4E) overexpression and cancer recurrence in node-positive breast cancer", *Annals of Surgery* 242: 584-90.

McGary, E.C., Lev, D.C. & Bar-Eli, M. 2002, "Cellular adhesion pathways and metastatic potential of human melanoma", *Cancer Biology Therapy* 1: 459-465.

McKendrick, L., Morley, S.J., Pain, V.M., Jagus, R. & Joshi, B. 2001, "Phosphorylation of eukaryotic initiation factor 4E (eIF4E) at Ser209 is not required for protein synthesis in vitro and in vivo", *European journal of biochemistry / FEBS* 268: 5375-5385.

McKendrick, L., Pain, V.M. & Morley, S.J. 1999, "Translation initiation factor 4E", *The international journal of biochemistry & cell biology* vol. 31: 31-35.

Melnick, A. & Licht, J.D. 1999, "Deconstructing a disease: RARalpha, its fusion partners, and their roles in the pathogenesis of acute promyelocytic leukemia", *Blood* 93: 3167-3215.

Meteoglu, I., Dikicioglu, E., Erkus, M., Culhaci, N., Kacar, F., Ozkara, E. & Uyar, M. 2005, "Breast carcinogenesis. Transition from hyperplasia to invasive lesions", *Saudi medical journal* 26: 1889-1896.

Metzler, M., Wilda, M., Busch, K., Viehmann, S. & Borkhardt, A. 2004, "High expression of precursor microRNA-155/BIC RNA in children with Burkitt lymphoma", *Genes, chromosomes & cancer* 39: 167-169.

Michael, M.Z., O'Connor, S.M., van Holst Pellekaan, N.G., Young, G.P. & James, R.J. 2003, "Reduced accumulation of specific microRNAs in colorectal neoplasia", *Molecular Cancer Research* 1: 882-891.

Michelotti, E.F., Michelotti, G.A., Aronsohn, A.I. & Levens, D. 1996, "Heterogeneous nuclear ribonucleoprotein K is a transcription factor", *Molecular and cellular biology* 16: 2350-2360.

Mikhailenko, I., Kounnas, M.Z. & Strickland, D.K. 1995, "Low density lipoprotein receptor-related protein/alpha 2-macroglobulin receptor mediates the cellular internalization and degradation of thrombospondin. A process facilitated by cell-surface proteoglycans", *Journal of Biological Chemistry* 270:. 9543-9549.

Minakuchi, Y., Takeshita, F., Kosaka, N., Sasaki, H., Yamamoto, Y., Kouno, M., Honma, K., Nagahara, S., Hanai, K., Sano, A., Kato, T., Terada, M. & Ochiya, T. 2004, "Atelocollagen-mediated synthetic small interfering RNA delivery for effective gene silencing in vitro and in vivo", *Nucleic acids research* 32: e109-116.

Mine, S., Yamazaki, T., Miyata, T., Hara, S. & Kato, H. 2002, "Structural mechanism for heparin-binding of the third Kunitz domain of human tissue factor pathway inhibitor", *Biochemistry (John Wiley & Sons)* 41: 78-85.

Minich, W.B., Balasta, M.L., Goss, D.J. & Rhoads, R.E. 1994, "Chromatographic resolution of in vivo phosphorylated and nonphosphorylated eukaryotic translation initiation factor eIF-4E: increased cap affinity of the phosphorylated form", *Proceedings of the National Academy of Sciences of the United States of America* 91: 7668-7672.

Mitsuuchi, Y., Johnson, S.W., Selvakumaran, M., Williams, S.J., Hamilton, T.C. & Testa, J.R. 2000, "The phosphatidylinositol 3-kinase/AKT signal transduction pathway plays a critical role in the expression of p21WAF1/CIP1/SDI1 induced by cisplatin and paclitaxel", *Cancer research* 60: 5390-5394.

Moon, Y., Bottone, F.G.,Jr, McEntee, M.F. & Eling, T.E. 2005, "Suppression of tumor cell invasion by cyclooxygenase inhibitors is mediated by thrombospondin-1 via the early growth response gene Egr-1", *Molecular CancerTherapeutics* 4 1551-1558.

Morley, S.J. & McKendrick, L. 1997, "Involvement of stress-activated protein kinase and p38/RK mitogen-activated protein kinase signaling pathways in the enhanced phosphorylation of initiation factor 4E in NIH 3T3 cells", *Journal of Biological Chemistry* 272: 17887-17893.

Morrison, C., Zanagnolo, V., Ramirez, N., Cohn, D.E., Kelbick, N., Copeland, L., Maxwell, L.G. & Fowler, J.M. 2006, "HER-2 is an independent prognostic factor in endometrial cancer: association with outcome in a large cohort of surgically staged patients", *Journal of clinical oncology : official journal of the American Society of Clinical Oncology* 24: 2376-2385.

Mukaida, N. 2003, "Pathophysiological roles of interleukin-8/CXCL8 in pulmonary diseases", *American Journal of Physiology. Lung Cellular and Molecular Physiology* 284: L566-77.

Mulkeen, A.L., Silva, T., Yoo, P.S., Schmitz, J.C., Uchio, E., Chu, E. & Cha, C. 2006, "Short interfering RNA-mediated gene silencing of vascular endothelial growth factor: effects on cellular proliferation in colon cancer cells", *Archives of Surgery* 141: 367-374.

Murphy, L.O., Smith, S., Chen, R.H., Fingar, D.C. & Blenis, J. 2002, "Molecular interpretation of ERK signal duration by immediate early gene products", *Nature cell biology* 4: 556-564.

Mutter, G.L., Lin, M.C., Fitzgerald, J.T., Kum, J.B., Baak, J.P., Lees, J.A., Weng, L.P. & Eng, C. 2000, "Altered PTEN expression as a diagnostic marker for the earliest endometrial precancers", *Journal of the National Cancer Institute* 92: 924-930.

Nakajima, M., Morikawa, K., Fabra, A., Bucana, C.D. & Fidler, I.J. 1990, "Influence of organ environment on extracellular matrix degradative activity and metastasis of human colon carcinoma cells", *Journal of the National Cancer Institute* 82: 1890-1898.

Napoli, C., Lemieux, C. & Jorgensen, R. 1990, "Introduction of a Chimeric Chalcone Synthase Gene into Petunia Results in Reversible Co-Suppression of Homologous Genes in trans", *The Plant Cell* 2: 279-289.

Nathan, C.A., Carter, P., Liu, L., Li, B.D., Abreo, F., Tudor, A., Zimmer, S.G. & De Benedetti, A. 1997, "Elevated expression of eIF4E and FGF-2 isoforms during vascularization of breast carcinomas", *Oncogene* 15:. 1087-1094.

Navolanic, P.M., Steelman, L.S. & McCubrey, J.A. 2003, "EGFR family signaling and its association with breast cancer development and resistance to chemotherapy (Review)", *International journal of oncology* 22: 237-252.

Nemoto, T., Vana, J., Bedwani, R.N., Baker, H.W., McGregor, F.H. & Murphy, G.P. 1980, "Management and survival of female breast cancer: results of a national survey by the American College of Surgeons", *Cancer* 45: 2917-2924.

Nevins, J.R., Huang, E.S., Dressman, H., Pittman, J., Huang, A.T. & West, M. 2003, "Towards integrated clinico-genomic models for personalized medicine: combining gene expression signatures and clinical factors in breast cancer outcomes prediction", *Human molecular genetics* 12: R153-157.

Nguyen, Q.D., De Wever, O., Bruyneel, E., Hendrix, A., Xie, W.Z., Lombet, A., Leibl, M., Mareel, M., Gieseler, F., Bracke, M. & Gespach, C. 2005, "Commutators of PAR-1 signaling in cancer cell invasion reveal an essential role of the Rho-Rho kinase axis and tumor microenvironment", *Oncogene* 24: 8240-8251.

Nicholson, A.W. 1999, "Function, mechanism and regulation of bacterial ribonucleases", *FEMS microbiology reviews* 23: 371-390.

Nicholson, K.M. & Anderson, N.G. 2002, "The protein kinase B/Akt signalling pathway in human malignancy", *Cellular signalling* 14: 381-395.

Niedzwiecka, A., Darzynkiewicz, E. & Stolarski, R. 2004, "Thermodynamics of mRNA 5' cap binding by eukaryotic translation initiation factor eIF4E", *Biochemistry (John Wiley & Sons)* 43:13305-13317.

Nogawa, M., Yuasa, T., Kimura, S., Tanaka, M., Kuroda, J., Sato, K., Yokota, A., Segawa, H., Toda, Y., Kageyama, S., Yoshiki, T., Okada, Y. & Maekawa, T. 2005, "Intravesical administration of small interfering RNA targeting PLK-1 successfully prevents the growth of bladder cancer", *The Journal of clinical investigation* 115: 978-985.

Noske, A., Kaszubiak, A., Weichert, W., Sers, C., Niesporek, S., Koch, I., Schaefer, B., Sehouli, J., Dietel, M., Lage, H. & Denkert, C. 2006, "Specific inhibition of AKT2 by RNA interference results in reduction of ovarian cancer cell proliferation: Increased expression of AKT in advanced ovarian cancer", *Cancer letters 235: 1-11* .

Novina, C.D. & Sharp, P.A. 2004, "The RNAi revolution", *Nature* 430: 161-164.

Novotny, W.F., Girard, T.J., Miletich, J.P. & Broze, G.J.,Jr 1989, "Purification and characterization of the lipoprotein-associated coagulation inhibitor from human plasma", *Journal of Biological Chemistry* 264: 18832-18837.

O-charoenrat, P., Rhys-Evans, P.H., Modjtahedi, H. & Eccles, S.A. 2002, "The role of c-erbB receptors and ligands in head and neck squamous cell carcinoma", *Oral oncology* 38: 627-640.

O'Donovan, K.J., Tourtellotte, W.G., Millbrandt, J. & Baraban, J.M. 1999, "The EGR family of transcription-regulatory factors: progress at the interface of molecular and systems neuroscience", *Trends in neurosciences* 22: 167-173.

Oft, M., Akhurst, R.J. & Balmain, A. 2002, "Metastasis is driven by sequential elevation of H-ras and Smad2 levels", *Nature cell biology* 4: 487-494.

Ogiso, H., Ishitani, R., Nureki, O., Fukai, S., Yamanaka, M., Kim, J.H., Saito, K., Sakamoto, A., Inoue, M., Shirouzu, M. & Yokoyama, S. 2002, "Crystal structure of the complex of human epidermal growth factor and receptor extracellular domains", *Cell* 110: 775-787.

Ohnishi, K., Tobita, T., Sinjo, K., Takeshita, A. & Ohno, R. 1998, "Modulation of homeobox B6 and B9 genes expression in human leukemia cell lines during myelomonocytic differentiation", *Leukemia & lymphoma* 31: 599-608.

Olayioye, M.A., Graus-Porta, D., Beerli, R.R., Rohrer, J., Gay, B. & Hynes, N.E. 1998, "ErbB-1 and ErbB-2 acquire distinct signaling properties dependent upon their dimerization partner", *Molecular and cellular biology* 18: 5042-5051.

Olson, B.A., Day, J.R. & Laping, N.J. 1999, "Age-related expression of renal thrombospondin 1 mRNA in F344 rats: resemblance to diabetes-induced expression in obese Zucker rats", *Pharmacology* 58: 200-208.

Ostareck-Lederer, A. & Ostareck, D.H. 2004, "Control of mRNA translation and stability in haematopoietic cells: the function of hnRNPs K and E1/E2", *Biologie cellulaire* 96: 407-411.

Otey, C.A., Rachlin, A., Moza, M., Arneman, D. & Carpen, O. 2005, "The palladin/myotilin/myopalladin family of actin-associated scaffolds", *International review of cytology* 246: 31-58.

Overhoff, M., Alken, M., Far, R.K., Lemaitre, M., Lebleu, B., Sczakiel, G. & Robbins, I. 2005, "Local RNA target structure influences siRNA efficacy: a systematic global analysis", *Journal of Molecular Biology* 348: 871-881.

Paddison, P.J., Caudy, A.A. & Hannon, G.J. 2002, "Stable suppression of gene expression by RNAi in mammalian cells", *Proceedings of the National Academy of Sciences of the United States of America* 99: 1443-1448.

Pai, S.I., Lin, Y.Y., Macaes, B., Meneshian, A., Hung, C.F. & Wu, T.C. 2006, "Prospects of RNA interference therapy for cancer", *Gene therapy* 13: 464-477.

Pain, V.M. 1996, "Initiation of protein synthesis in eukaryotic cells", *European journal of biochemistry / FEBS* 236: 747-771.

Pal-Bhadra, M., Bhadra, U. & Birchler, J.A. 2002, "RNAi related mechanisms affect both transcriptional and posttranscriptional transgene silencing in Drosophila", *Molecular cell* 9: 315-327.

Panner, A., James, C.D., Berger, M.S. & Pieper, R.O. 2005, "mTOR controls FLIPS translation and TRAIL sensitivity in glioblastoma multiforme cells", *Molecular and cellular biology* 25: 8809-8823.

Pantel, K. & Brakenhoff, R.H. 2004, "Dissecting the metastatic cascade", *Nat.Rev.Cancer* 4: 448-456.

Patel, S., Wang, F.H., Whiteside, T.L. & Kasid, U. 1997, "Identification of seven differentially displayed transcripts in human primary and matched metastatic head and neck squamous cell carcinoma cell lines: implications in metastasis and/or radiation response", *Oral oncology* 33: 197-203.

Pedersen, N., Mortensen, S., Sorensen, S.B., Pedersen, M.W., Rieneck, K., Bovin, L.F. & Poulsen, H.S. 2003, "Transcriptional gene expression profiling of small cell lung cancer cells", *Cancer research* 63: 1943-1953.

Perona, R. 2006, "Cell signalling: growth factors and tyrosine kinase receptors", *Clinical & translational oncolog.* 8: 77-82.

Persengiev, S.P., Zhu, X. & Green, M.R. 2004, "Nonspecific, concentration-dependent stimulation and repression of mammalian gene expression by small interfering RNAs (siRNAs)", *RNA* 10: 12-18.

Pfeffer, S., Zavolan, M., Grasser, F.A., Chien, M., Russo, J.J., Ju, J., John, B., Enright, A.J., Marks, D., Sander, C. & Tuschl, T. 2004, "Identification of virus-encoded microRNAs", *Science* 304: 734-736.

Pfeiffer, P., Clausen, P.P., Andersen, K. & Rose, C. 1996, "Lack of prognostic significance of epidermal growth factor receptor and the oncoprotein p185HER-2 in patients with systemically untreated non-small-cell lung cancer: an immunohistochemical study on cryosections", *British journal of cancer* 74: 86-91.

Pille, J.Y., Denoyelle, C., Varet, J., Bertrand, J.R., Soria, J., Opolon, P., Lu, H., Pritchard, L.L., Vannier, J.P., Malvy, C., Soria, C. & Li, H. 2005, "Anti-RhoA and anti-RhoC siRNAs inhibit the proliferation and invasiveness of MDA-MB-231 breast cancer cells in vitro and in vivo", *Molecular therapy : the journal of the American Society of Gene Therapy* 11: 267-274.

Piro, O. & Broze, G.J.,Jr 2005, "Comparison of cell-surface TFPIalpha and beta", *Journal of thrombosis and haemostasis* 3: 2677-2683.

Pisegna, S., Pirozzi, G., Piccoli, M., Frati, L., Santoni, A. & Palmieri, G. 2004, "p38 MAPK activation controls the TLR3-mediated up-regulation of cytotoxicity and cytokine production in human NK cells", *Blood* 104:. 4157-4164.

Polunovsky, V.A., Rosenwald, I.B., Tan, A.T., White, J., Chiang, L., Sonenberg, N. & Bitterman, P.B. 1996, "Translational control of programmed cell death: eukaryotic translation initiation factor 4E blocks apoptosis in growth-factor-restricted fibroblasts with physiologically expressed or deregulated Myc", *Molecular and cellular biology* 16: 6573-6581.

Pratt, M.A., Satkunaratnam, A. & Novosad, D.M. 1998, "Estrogen activates raf-1 kinase and induces expression of Egr-1 in MCF-7 breast cancer cells", *Molecular and cellular biochemistry* 189: 119-125.

Pratt, M.M. 1984, "ATPases in mitotic spindles", *International review of cytology* 87: 83-105.

Prenzel, N., Fischer, O.M., Streit, S., Hart, S. & Ullrich, A. 2001, "The epidermal growth factor receptor family as a central element for cellular signal transduction and diversification", *Endocrine-related cancer* 8: 11-31.

Price, G.C., Thompson, S.A. & Kam, P.C. 2004, "Tissue factor and tissue factor pathway inhibitor", *Anaesthesia* 59: 483-492.

Proud, C.G. 1992, "Protein phosphorylation in translational control", *Current topics in cellular regulation* 32: 243-369.

Pyronnet, S. 2000, "Phosphorylation of the cap-binding protein eIF4E by the MAPK-activated protein kinase Mnk1", *Biochemical pharmacology* 60: 1237-1243.

Qian, X., Rothman, V.L., Nicosia, R.F. & Tuszynski, G.P. 2001, "Expression of thrombospondin-1 in human pancreatic adenocarcinomas: role in matrix metalloproteinase-9 production", *Pathology oncology research* 7: 251-259.

Quenel, N., Wafflart, J., Bonichon, F., de Mascarel, I., Trojani, M., Durand, M., Avril, A. & Coindre, J.M. 1995, "The prognostic value of c-erbB2 in primary breast carcinomas: a study on 942 cases", *Breast cancer research and treatment* 35: 283-291.

Raghavan, A. & Bohjanen, P.R. 2004, "Microarray-based analyses of mRNA decay in the regulation of mammalian gene expression", *Briefings in functional genomics & proteomics* 3: 112-124.

Rak, J., Milsom, C., May, L., Klement, P. & Yu, J. 2006, "Tissue factor in cancer and angiogenesis: the molecular link between genetic tumor progression, tumor neovascularization, and cancer coagulopathy", *Seminars in thrombosis and hemostasis* 32: 54-70.

Ramaswamy, S. & Perou, C.M. 2003, "DNA microarrays in breast cancer: the promise of personalised medicine", *Lancet* 361: 1576-1577.

Ramos-DeSimone, N., Hahn-Dantona, E., Sipley, J., Nagase, H., French, D.L. & Quigley, J.P. 1999, "Activation of matrix metalloproteinase-9 (MMP-9) via a converging plasmin/stromelysin-1 cascade enhances tumor cell invasion", *Journal of Biological Chemistry* 274: 13066-13076.

Rao, G.N. 2000, "Oxidant stress stimulates phosphorylation of eIF4E without an effect on global protein synthesis in smooth muscle cells. Lack of evidence for a role of H202 in angiotensin II-induced hypertrophy", *Journal of Biological Chemistry* 275: 16993-16999.

Rapaport, S.I. & Rao, L.V. 1995, "The tissue factor pathway: how it has become a "prima ballerina"", *Thrombosis and haemostasis* 74: 7-17.

Rau, M., Ohlmann, T., Morley, S.J. & Pain, V.M. 1996, "A reevaluation of the cap-binding protein, eIF4E, as a rate-limiting factor for initiation of translation in reticulocyte lysate", *Journal of Biological Chemistry* 271: 8983-8990.

Raught, B. & Gingras, A.C. 1999, "eIF4E activity is regulated at multiple levels", *The international journal of biochemistry & cell biology* 31: 43-57.

Raught, B., Gingras, A.C., Gygi, S.P., Imataka, H., Morino, S., Gradi, A., Aebersold, R. & Sonenberg, N. 2000, "Serum-stimulated, rapamycin-sensitive phosphorylation sites in the eukaryotic translation initiation factor 4GI", *The EMBO journal* 19: 434-444.

Reddy, K.B., Nabha, S.M. & Atanaskova, N. 2003, "Role of MAP kinase in tumor progression and invasion", *Cancer metastasis reviews* 22: 395-403.

Reed, J.C. 1998, "Bcl-2 family proteins", *Oncogene* 17: 3225-3236.

Reese, D.M. & Slamon, D.J. 1997, "HER-2/neu signal transduction in human breast and ovarian cancer", *Stem cells* 15: 1-8.

Reis-Filho, J.S., Westbury, C. & Pierga, J.Y. 2006, "The impact of expression profiling on prognostic and predictive testing in breast cancer", *Journal of clinical pathology* 59: 225-231.

Ren, B., Yee, K.O., Lawler, J. & Khosravi-Far, R. 2006, "Regulation of tumor angiogenesis by thrombospondin-1", *Biochimica et biophysica acta* 1765: 178-188.

Revillion, F., Hebbar, M., Bonneterre, J. & Peyrat, J.P. 1996, "Plasma c-erbB2 concentrations in relation to chemotherapy in breast cancer patients", *European journal of cancer* 32A: 231-234.

Richter, J.D. & Sonenberg, N. 2005, "Regulation of cap-dependent translation by eIF4E inhibitory proteins", *Nature* 433: 477-480.

Riese, D.J.,2nd & Stern, D.F. 1998, "Specificity within the EGF family/ErbB receptor family signaling network", *BioEssays : news and reviews in molecular, cellular and developmental biology* 20:. 41-48.

Robinson, M.J. & Cobb, M.H. 1997, "Mitogen-activated protein kinase pathways", *Current opinion in cell biology* 9: 180-186.

Rodrigues, S.P., Fathers, K.E., Chan, G., Zuo, D., Halwani, F., Meterissian, S. & Park, M. 2005, "CrkI and CrkII function as key signaling integrators for migration and invasion of cancer cells", *Molecular cancer research* 3: 183-194.

Rodriguez-Manzaneque, J.C., Lane, T.F., Ortega, M.A., Hynes, R.O., Lawler, J. & Iruela-Arispe, M.L. 2001, "Thrombospondin-1 suppresses spontaneous tumor growth and inhibits activation of matrix metalloproteinase-9 and mobilization of vascular endothelial growth factor", *Proceedings of the National Academy of Sciences of the United States of America* 98: 12485-12490.

Rogers, S.J., Harrington, K.J., Rhys-Evans, P., O-Charoenrat, P. & Eccles, S.A. 2005, "Biological significance of c-erbB family oncogenes in head and neck cancer", *Cancer metastasis reviews* 24: 47-69.

Rollin, J., Iochmann, S., Blechet, C., Hube, F., Regina, S., Guyetant, S., Lemarie, E., Reverdiau, P. & Gruel, Y. 2005, "Expression and methylation status of tissue factor pathway inhibitor-2 gene in non-small-cell lung cancer", *British journal of cancer* 92: 775-783.

Ronski, K., Sanders, M., Burleson, J.A., Moyo, V., Benn, P. & Fang, M. 2005, "Early growth response gene 1 (EGR1) is deleted in estrogen receptor-negative human breast carcinoma", *Cancer* 104: 925-930.

Rosenwald, I.B., Lazaris-Karatzas, A., Sonenberg, N. & Schmidt, E.V. 1993a, "Elevated levels of cyclin D1 protein in response to increased expression of eukaryotic initiation factor 4E", *Molecular and cellular biology* 13: 7358-7363.

Rosenwald, I.B., Rhoads, D.B., Callanan, L.D., Isselbacher, K.J. & Schmidt, E.V. 1993b, "Increased expression of eukaryotic translation initiation factors eIF-4E and eIF-2 alpha in response to growth induction by c-myc", *Proceedings of the National Academy of Sciences of the United States of America* 90:. 6175-6178.

Rowinsky, E.K. 2003, "Signal events: Cell signal transduction and its inhibition in cancer", *The oncologist* 8: 5-17.

Ryther, R.C., Flynt, A.S., Phillips, J.A.,3rd & Patton, J.G. 2005, "siRNA therapeutics: big potential from small RNAs", *Gene therapy* 12: 5-11.

Sager, R. 1997, "Expression genetics in cancer: shifting the focus from DNA to RNA", *Proceedings of the National Academy of Sciences of the United States of America* 94: 952-955.

Sahai, E. 2005, "Mechanisms of cancer cell invasion", *Current opinion in genetics & development* 15: 87-96.

Sandset, P.M. 1996, "Tissue factor pathway inhibitor (TFPI)--an update", *Haemostasis* 26: 154-165.

Sansal, I. & Sellers, W.R. 2004, "The biology and clinical relevance of the PTEN tumor suppressor pathway", *Journal of clinical oncology : official journal of the American Society of Clinical Oncology* 22: 2954-2963.

Santel, A., Aleku, M., Keil, O., Endruschat, J., Esche, V., Durieux, B., Loffler, K., Fechtner, M., Rohl, T., Fisch, G., Dames, S., Arnold, W., Giese, K., Klippel, A. & Kaufmann, J. 2006, "RNA interference in the mouse vascular endothelium by systemic administration of siRNA-lipoplexes for cancer therapy", *Gene therapy* 13:1360-1370

Sassone-Corsi, P., Mizzen, C.A., Cheung, P., Crosio, C., Monaco, L., Jacquot, S., Hanauer, A. & Allis, C.D. 1999, "Requirement of Rsk-2 for epidermal growth factor-activated phosphorylation of histone H3", *Science* 285: 886-891.

Sato, Y., Asada, Y., Marutsuka, K., Hatakeyama, K., Kamikubo, Y. & Sumiyoshi, A. 1997, "Tissue factor pathway inhibitor inhibits aortic smooth muscle cell migration induced by tissue factor/factor VIIa complex", *Thrombosis and haemostasis* 78: 1138-1141.

Saxena, A., Yashar, C., Taylor, D.D. & Gercel-Taylor, C. 2005, "Cellular response to chemotherapy and radiation in cervical cancer", *American Journal of Obstetrics and Gynecology* 192: 1399-1403.

Saxena, S., Jonsson, Z.O. & Dutta, A. 2003, "Small RNAs with imperfect match to endogenous mRNA repress translation. Implications for off-target activity of small inhibitory RNA in mammalian cells", *Journal of Biological Chemistry* 278: 44312-44319.

Scacheri, P.C., Rozenblatt-Rosen, O., Caplen, N.J., Wolfsberg, T.G., Umayam, L., Lee, J.C., Hughes, C.M., Shanmugam, K.S., Bhattacharjee, A., Meyerson, M. & Collins, F.S.

2004, "Short interfering RNAs can induce unexpected and divergent changes in the levels of untargeted proteins in mammalian cells", *Proceedings of the National Academy of Sciences of the United States of America* 101: 1892-1897.

Scheper, G.C. & Proud, C.G. 2002, "Does phosphorylation of the cap-binding protein eIF4E play a role in translation initiation?", *European journal of biochemistry / FEBS* 269: 5350-5359.

Schiffelers, R.M., Mixson, A.J., Ansari, A.M., Fens, M.H., Tang, Q., Zhou, Q., Xu, J., Molema, G., Lu, P.Y., Scaria, P.V., Storm, G. & Woodle, M.C. 2005, "Transporting silence: design of carriers for siRNA to angiogenic endothelium", *Journal of controlled release : official journal of the Controlled Release Society* 109: 5-14.

Schneider, P. & Tschopp, J. 2000, "Modulation of death receptor signalling", *Symposia of the Society for Experimental Biology* 52: 31-42.

Seftor, E.A., Meltzer, P.S., Kirschmann, D.A., Pe'er, J., Maniotis, A.J., Trent, J.M., Folberg, R. & Hendrix, M.J. 2002, "Molecular determinants of human uveal melanoma invasion and metastasis", *Clinical & experimental metastasis* 19: 233-246.

Seki, N., Takasu, T., Mandai, K., Nakata, M., Saeki, H., Heike, Y., Takata, I., Segawa, Y., Hanafusa, T. & Eguchi, K. 2002, "Expression of eukaryotic initiation factor 4E in atypical adenomatous hyperplasia and adenocarcinoma of the human peripheral lung", *Clinical cancer research : an official journal of the American Association for Cancer Research* 8: 3046-3053.

Shantz, L.M. & Pegg, A.E. 1994, "Overproduction of ornithine decarboxylase caused by relief of translational repression is associated with neoplastic transformation", *Cancer research* 54: 2313-2316.

Sharrocks, A.D., Yang, S.H. & Galanis, A. 2000, "Docking domains and substrate-specificity determination for MAP kinases", *Trends in biochemical sciences* 25: 448-453.

Shaw, R.J. & Cantley, L.C. 2006, "Ras, PI(3)K and mTOR signalling controls tumour cell growth", *Nature* 441: 424-430.

She, Q.B., Ma, W.Y., Zhong, S. & Dong, Z. 2002, "Activation of JNK1, RSK2, and MSK1 is involved in serine 112 phosphorylation of Bad by ultraviolet B radiation", *Journal of Biological Chemistry* 277: 24039-24048.

Sheibani, N. & Frazier, W.A. 1995, "Thrombospondin 1 expression in transformed endothelial cells restores a normal phenotype and suppresses their tumorigenesis", *Proceedings of the National Academy of Sciences of the United States of America* 92: 6788-6792.

Shelton, J.G., Steelman, L.S., Lee, J.T., Knapp, S.L., Blalock, W.L., Moye, P.W., Franklin, R.A., Pohnert, S.C., Mirza, A.M., McMahon, M. & McCubrey, J.A. 2003, "Effects of the RAF/MEK/ERK and PI3K/AKT signal transduction pathways on the

abrogation of cytokine-dependence and prevention of apoptosis in hematopoietic cells", *Oncogene* 22: 2478-2492.

Shi, Y., Zou, M., Collison, K., Baitei, E.Y., Al-Makhalafi, Z., Farid, N.R. & Al-Mohanna, F.A. 2006, "Ribonucleic acid interference targeting S100A4 (Mts1) suppresses tumor growth and metastasis of anaplastic thyroid carcinoma in a mouse model", *The Journal of clinical endocrinology and metabolism* 91: 2373-2379.

Shingu, T. & Bornstein, P. 1994, "Overlapping Egr-1 and Sp1 sites function in the regulation of transcription of the mouse thrombospondin 1 gene", *Journal of Biological Chemistry* 269: 32551-32557.

Silverman, E.S. & Collins, T. 1999, "Pathways of Egr-1-mediated gene transcription in vascular biology", *American Journal of Pathology* 154: 665-670.

Singh, R., Pan, S., Mueske, C.S., Witt, T.A., Kleppe, L.S., Peterson, T.E., Caplice, N.M. & Simari, R.D. 2003, "Tissue factor pathway inhibitor deficiency enhances neointimal proliferation and formation in a murine model of vascular remodelling", *Thrombosis and haemostasis* 89: 747-751.

Skobe, M., Hawighorst, T., Jackson, D.G., Prevo, R., Janes, L., Velasco, P., Riccardi, L., Alitalo, K., Claffey, K. & Detmar, M. 2001, "Induction of tumor lymphangiogenesis by VEGF-C promotes breast cancer metastasis", *Nature medicine* 7: 192-198.

Slamon, D.J., Clark, G.M., Wong, S.G., Levin, W.J., Ullrich, A. & McGuire, W.L. 1987, "Human breast cancer: correlation of relapse and survival with amplification of the HER-2/neu oncogene", *Science* 235: 177-182.

Slamon, D.J., Godolphin, W., Jones, L.A., Holt, J.A., Wong, S.G., Keith, D.E., Levin, W.J., Stuart, S.G., Udove, J. & Ullrich, A. 1989, "Studies of the HER-2/neu proto-oncogene in human breast and ovarian cancer", *Science* 244: 707-712.

Sledz, C.A., Holko, M., de Veer, M.J., Silverman, R.H. & Williams, B.R. 2003, "Activation of the interferon system by short-interfering RNAs", *Nature cell biology* 5: 834-839.

Slepenkov, S.V., Darzynkiewicz, E. & Rhoads, R.E. 2006, "Stopped-flow kinetic analysis of eIF4E and phosphorylated eIF4E binding to cap analogs and capped oligoribonucleotides: evidence for a one-step binding mechanism", *Journal of Biological Chemistry* 281: 14927-14938.

Smith, C.J., Watson, C.F., Bird, C.R., Ray, J., Schuch, W. & Grierson, D. 1990, "Expression of a truncated tomato polygalacturonase gene inhibits expression of the endogenous gene in transgenic plants", *Molecular & general genetics* 224: 477-481.

Smith, J.A., Poteet-Smith, C.E., Malarkey, K. & Sturgill, T.W. 1999, "Identification of an extracellular signal-regulated kinase (ERK) docking site in ribosomal S6 kinase, a sequence critical for activation by ERK in vivo", *Journal of Biological Chemistry* 274: 2893-2898.

Smith, J.A., Poteet-Smith, C.E., Xu, Y., Errington, T.M., Hecht, S.M. & Lannigan, D.A. 2005, "Identification of the first specific inhibitor of p90 ribosomal S6 kinase (RSK) reveals an unexpected role for RSK in cancer cell proliferation", *Cancer research* 65: 1027-1034.

Soltoff, S.P. & Cantley, L.C. 1996, "p120cbl is a cytosolic adapter protein that associates with phosphoinositide 3-kinase in response to epidermal growth factor in PC12 and other cells", *Journal of Biological Chemistry* 271: 563-567.

Sonenberg, N. 1994, "Regulation of translation and cell growth by eIF-4E", *Biochimie* 76: 839-846.

Song, G., Ouyang, G. & Bao, S. 2005, "The activation of Akt/PKB signaling pathway and cell survival", *Journal of Cellular and Molecular Medicine* 9: 59-71.

Song, J.H., Choi, C.H., Yeom, H.J., Hwang, S.Y. & Kim, T.S. 2006, "Monitoring the gene expression profiles of doxorubicin-resistant acute myelocytic leukemia cells by DNA microarray analysis", *Life Sciences* 79: 193-202.

Sorrells, D.L., Meschonat, C., Black, D. & Li, B.D. 1999, "Pattern of amplification and overexpression of the eukaryotic initiation factor 4E gene in solid tumor", *The Journal of surgical research* 85: 37-42.

Spencer, K.S., Graus-Porta, D., Leng, J., Hynes, N.E. & Klemke, R.L. 2000, "ErbB2 is necessary for induction of carcinoma cell invasion by ErbB family receptor tyrosine kinases", *The Journal of cell biology* 148: 385-397.

Stark, G.R., Kerr, I.M., Williams, B.R., Silverman, R.H. & Schreiber, R.D. 1998, "How cells respond to interferons", *Annual Review of Biochemistry* 67: 227-264.

Stebbins-Boaz, B., Cao, Q., de Moor, C.H., Mendez, R. & Richter, J.D. 1999, "Maskin is a CPEB-associated factor that transiently interacts with eIF-4E", *Molecular cell* 4: 1017-1027.

Stephen, R.L., Shaw, L.E., Larsen, C., Corcoran, D. & Darbre, P.D. 2001, "Insulin-like growth factor receptor levels are regulated by cell density and by long term estrogen deprivation in MCF7 human breast cancer cells", *Journal of Biological Chemistry* 276: 40080-40086.

Stove, C. & Bracke, M. 2004, "Roles for neuregulins in human cancer", *Clinical & experimental metastasis* 21: 665-684.

Straume, O. & Akslen, L.A. 2003, "Increased expression of VEGF-receptors (FLT-1, KDR, NRP-1) and thrombospondin-1 is associated with glomeruloid microvascular proliferation, an aggressive angiogenic phenotype, in malignant melanoma", *Angiogenesis* 6: 295-301.

Streit, M., Velasco, P., Brown, L.F., Skobe, M., Richard, L., Riccardi, L., Lawler, J. & Detmar, M. 1999, "Overexpression of thrombospondin-1 decreases angiogenesis and

inhibits the growth of human cutaneous squamous cell carcinomas", *American Journal of Pathology* 155: 441-452.

Su, C.C., Chen, G.W., Lin, J.G., Wu, L.T. & Chung, J.G. 2006, "Curcumin inhibits cell migration of human colon cancer colo 205 cells through the inhibition of nuclear factor kappa B /p65 and down-regulates cyclooxygenase-2 and matrix metalloproteinase-2 expressions", *Anticancer Research* 26: 1281-1288.

Su, J.D., Mayo, L.D., Donner, D.B. & Durden, D.L. 2003, "PTEN and phosphatidylinositol 3'-kinase inhibitors up-regulate p53 and block tumor-induced angiogenesis: evidence for an effect on the tumor and endothelial compartment", *Cancer research* 63: 3585-3592.

Subramanian, R., Gondi, C.S., Lakka, S.S., Jutla, A. & Rao, J.S. 2006, "siRNA-mediated simultaneous downregulation of uPA and its receptor inhibits angiogenesis and invasiveness triggering apoptosis in breast cancer cells", *International journal of oncology* 28: 831-839.

Sugita, M., Geraci, M., Gao, B., Powell, R.L., Hirsch, F.R., Johnson, G., Lapadat, R., Gabrielson, E., Bremnes, R., Bunn, P.A. & Franklin, W.A. 2002, "Combined use of oligonucleotide and tissue microarrays identifies cancer/testis antigens as biomarkers in lung carcinoma", *Cancer research* 62: 3971-3979.

Sugiyama, Y., Tomoda, K., Tanaka, T., Arata, Y., Yoneda-Kato, N. & Kato, J. 2001, "Direct binding of the signal-transducing adaptor Grb2 facilitates down-regulation of the cyclin-dependent kinase inhibitor p27Kip1", *Journal of Biological Chemistry* 276: 12084-12090.

Sun, X., Skorstengaard, K. & Mosher, D.F. 1992, "Disulfides modulate RGD-inhibitable cell adhesive activity of thrombospondin", *The Journal of cell biology* 118: 693-701.

Suo, Z., Emilsen, E., Tveit, K.M. & Nesland, J.M. 1998, "Type 1 protein tyrosine kinases in benign and malignant breast lesions", *Histopathology* 33: 514-521.

Svensson, S., Jirstrom, K., Ryden, L., Roos, G., Emdin, S., Ostrowski, M.C. & Landberg, G. 2005, "ERK phosphorylation is linked to VEGFR2 expression and Ets-2 phosphorylation in breast cancer and is associated with tamoxifen treatment resistance and small tumours with good prognosis", *Oncogene* 24: 4370-4379.

Svitkin, Y.V., Ovchinnikov, L.P., Dreyfuss, G. & Sonenberg, N. 1996, "General RNA binding proteins render translation cap dependent", *The EMBO journal* 15: 7147-7155.

Szlosarek, P., Charles, K.A. & Balkwill, F.R. 2006, "Tumour necrosis factor-alpha as a tumour promoter", *European journal of cancer* 42: 745-750.

Szlosarek, P.W. & Balkwill, F.R. 2003, "Tumour necrosis factor alpha: a potential target for the therapy of solid tumours", *Lancet Oncology* 4: 565-573.

Takahashi, Y., Ishii, Y., Nishida, Y., Ikarashi, M., Nagata, T., Nakamura, T., Yamamori, S. & Asai, S. 2006, "Detection of aberrations of ubiquitin-conjugating enzyme E2C gene (UBE2C) in advanced colon cancer with liver metastases by DNA microarray and two-color FISH", *Cancer genetics and cytogenetics* 168: 30-35.

Taki, K., Kogai, T., Kanamoto, Y., Hershman, J.M. & Brent, G.A. 2002, "A thyroid-specific far-upstream enhancer in the human sodium/iodide symporter gene requires Pax-8 binding and cyclic adenosine 3',5'-monophosphate response element-like sequence binding proteins for full activity and is differentially regulated in normal and thyroid cancer cells", *Molecular endocrinology* 16: 2266-2282.

Tao, L., Zhou, L., Zheng, L. & Gao, Y. 2002, "Study on the expression of proto-oncogene eIF4E in laryngeal squamous carcinoma", *Lin Chuang Er Bi Yan Hou Ke Za Zhi = Journal of clinical otorhinolaryngology* 16: 62-64.

Taraboletti, G., Roberts, D., Liotta, L.A. & Giavazzi, R. 1990, "Platelet thrombospondin modulates endothelial cell adhesion, motility, and growth: a potential angiogenesis regulatory factor", *The Journal of cell biology* 111: 765-772.

Thiery, J.P. & Morgan, M. 2004, "Breast cancer progression with a Twist", *Nature medicine* 10: 777-778.

Tibbetts, M.D., Zheng, L. & Lenardo, M.J. 2003, "The death effector domain protein family: regulators of cellular homeostasis", *Nature immunology* 4: 404-409.

Toker, A. & Yoeli-Lerner, M. 2006, "Akt signaling and cancer: surviving but not moving on", *Cancer research* 66: 3963-3966.

Topisirovic, I., Culjkovic, B., Cohen, N., Perez, J.M., Skrabanek, L. & Borden, K.L. 2003, "The proline-rich homeodomain protein, PRH, is a tissue-specific inhibitor of eIF4E-dependent cyclin D1 mRNA transport and growth", *The EMBO journal* 22: 689-703.

Toretsky, J.A. & Helman, L.J. 1996, "Involvement of IGF-II in human cancer", *The Journal of endocrinology* 149: 367-372.

Tsai, C.M., Chang, K.T., Wu, L.H., Chen, J.Y., Gazdar, A.F., Mitsudomi, T., Chen, M.H. & Perng, R.P. 1996, "Correlations between intrinsic chemoresistance and HER-2/neu gene expression, p53 gene mutations, and cell proliferation characteristics in non-small cell lung cancer cell lines", *Cancer research* 56: 206-209.

Tsiambas, E., Karameris, A., Dervenis, C., Lazaris, A.C., Giannakou, N., Gerontopoulos, K. & Patsouris, E. 2006, "HER2/neu expression and gene alterations in pancreatic ductal adenocarcinoma: a comparative immunohistochemistry and chromogenic in situ hybridization study based on tissue microarrays and computerized image analysis", *JOP* 7: 283-294.

Tsutsui, S., Ohno, S., Murakami, S., Kataoka, A., Kinoshita, J. & Hachitanda, Y. 2002, "EGFR, c-erbB2 and p53 protein in the primary lesions and paired metastatic regional lymph nodes in breast cancer", *European journal of surgical oncology: the journal of*

the European Society of Surgical Oncology and the British Association of Surgical Oncology 28: 383-387.

Tuazon, P.T., Morley, S.J., Dever, T.E., Merrick, W.C., Rhoads, R.E. & Traugh, J.A. 1990, "Association of initiation factor eIF-4E in a cap binding protein complex (eIF-4F) is critical for and enhances phosphorylation by protein kinase C", *Journal of Biological Chemistry* 265: 10617-10621.

Tuschl, T., Zamore, P.D., Lehmann, R., Bartel, D.P. & Sharp, P.A. 1999, "Targeted mRNA degradation by double-stranded RNA in vitro", *Genes & development* 13: 3191-3197.

Ullrich, A., Gray, A., Tam, A.W., Yang-Feng, T., Tsubokawa, M., Collins, C., Henzel, W., Le Bon, T., Kathuria, S. & Chen, E. 1986, "Insulin-like growth factor I receptor primary structure: comparison with insulin receptor suggests structural determinants that define functional specificity", *The EMBO journal* 5: 2503-2512.

Vaidyanathan, H. & Ramos, J.W. 2003, "RSK2 activity is regulated by its interaction with PEA-15", *Journal of Biological Chemistry* 278: 32367-32372.

Valentin, S., Ostergaard, P., Kristensen, H. & Nordfang, O. 1991, "Simultaneous presence of tissue factor pathway inhibitor (TFPI) and low molecular weight heparin has a synergistic effect in different coagulation assays", *Blood coagulation & fibrinolysis : an international journal in haemostasis and thrombosis* 2: 629-635.

van der Krol, A.R., Mur, L.A., Beld, M., Mol, J.N. & Stuitje, A.R. 1990, "Flavonoid genes in petunia: addition of a limited number of gene copies may lead to a suppression of gene expression", *The Plant Cell* 2: 291-299.

van der Velden, A.W. & Thomas, A.A. 1999, "The role of the 5' untranslated region of an mRNA in translation regulation during development", *The international journal of biochemistry & cell biology* 31: 87-106.

Van Roy, F. & Mareel, M. 1992, "Tumour invasion: effects of cell adhesion and motility", *Trends in cell biology,* vol. 2, no. 6, pp. 163-169.

van 't Veer, L.J., Dai, H., van de Vijver, M.J., He, Y.D., Hart, A.A., Mao, M., Peterse, H.L., van der Kooy, K., Marton, M.J., Witteveen, A.T., Schreiber, G.J., Kerkhoven, R.M., Roberts, C., Linsley, P.S., Bernards, R. & Friend, S.H. 2002, "Gene expression profiling predicts clinical outcome of breast cancer", *Nature* 415: 530-536.

Van Trappen, P.O., Ryan, A., Carroll, M., Lecoeur, C., Goff, L., Gyselman, V.G., Young, B.D., Lowe, D.G., Pepper, M.S., Shepherd, J.H. & Jacobs, I.J. 2002, "A model for co-expression pattern analysis of genes implicated in angiogenesis and tumour cell invasion in cervical cancer", *British journal of cancer* 87: 537-544.

Vande Woude, G.F., Jeffers, M., Cortner, J., Alvord, G., Tsarfaty, I. & Resau, J. 1997, "Met-HGF/SF: tumorigenesis, invasion and metastasis", *Ciba Foundation symposium,* 212: 119-30.

Verma, I.M., Stevenson, J.K., Schwarz, E.M., Van Antwerp, D. & Miyamoto, S. 1995, "Rel/NF-kappa B/I kappa B family: intimate tales of association and dissociation", *Genes & development* 9: 2723-2735.

Vider, B.Z., Zimber, A., Hirsch, D., Estlein, D., Chastre, E., Prevot, S., Gespach, C., Yaniv, A. & Gazit, A. 1997, "Human colorectal carcinogenesis is associated with deregulation of homeobox gene expression", *Biochemical and biophysical research communications* 232: 742-748.

Virolle, T., Adamson, E.D., Baron, V., Birle, D., Mercola, D., Mustelin, T. & de Belle, I. 2001, "The Egr-1 transcription factor directly activates PTEN during irradiation-induced signalling", *Nature cell biology* 3: 1124-1128.

Virolle, T., Krones-Herzig, A., Baron, V., De Gregorio, G., Adamson, E.D. & Mercola, D. 2003, "Egr1 promotes growth and survival of prostate cancer cells. Identification of novel Egr1 target genes", *Journal of Biological Chemistry* 278: 11802-11810.

Virtanen, C., Ishikawa, Y., Honjoh, D., Kimura, M., Shimane, M., Miyoshi, T., Nomura, H. & Jones, M.H. 2002, "Integrated classification of lung tumors and cell lines by expression profiling", *Proceedings of the National Academy of Sciences of the United States of America* 99:12357-12362.

Volm, M., Efferth, T. & Mattern, J. 1992, "Oncoprotein (c-myc, c-erbB1, c-erbB2, c-fos) and suppressor gene product (p53) expression in squamous cell carcinomas of the lung. Clinical and biological correlations", *Anticancer Research* 12: 11-20.

Volpert, O.V., Lawler, J. & Bouck, N.P. 1998, "A human fibrosarcoma inhibits systemic angiogenesis and the growth of experimental metastases via thrombospondin-1", *Proceedings of the National Academy of Sciences of the United States of America* 95: 6343-6348.

von der Haar, T. & McCarthy, J.E. 2002, "Intracellular translation initiation factor levels in Saccharomyces cerevisiae and their role in cap-complex function", *Molecular microbiology* 46: 531-544.

Wajant, H., Pfizenmaier, K. & Scheurich, P. 2003, "Tumor necrosis factor signaling", *Cell death and differentiation* 10: 45-65.

Wall, N.R. & Shi, Y. 2003, "Small RNA: can RNA interference be exploited for therapy?", *Lancet* 362: 1401-1403.

Walsh, D., Meleady, P., Power, B., Morley, S.J. & Clynes, M. 2003, "Increased levels of the translation initiation factor eIF4E in differentiating epithelial lung tumor cell lines", *Differentiation; research in biological diversity* 71: 126-134.

Wang, M.J., Kuo, J.S., Lee, W.W., Huang, H.Y., Chen, W.F. & Lin, S.Z. 2006, "Translational event mediates differential production of tumor necrosis factor-alpha in hyaluronan-stimulated microglia and macrophages", *Journal of neurochemistry* 97:857-871.

Wang, T., Hu, Y.C., Dong, S., Fan, M., Tamae, D., Ozeki, M., Gao, Q., Gius, D. & Li, J.J. 2005, "Co-activation of ERK, NF-kappaB, and GADD45beta in response to ionizing radiation", *Journal of Biological Chemistry* 280: 12593-12601.

Wang, T.N., Qian, X., Granick, M.S., Solomon, M.P., Rothman, V.L., Berger, D.H. & Tuszynski, G.P. 1996, "Thrombospondin-1 (TSP-1) promotes the invasive properties of human breast cancer", *The Journal of surgical research* 63: 39-43.

Wang, W., Wyckoff, J.B., Frohlich, V.C., Oleynikov, Y., Huttelmaier, S., Zavadil, J., Cermak, L., Bottinger, E.P., Singer, R.H., White, J.G., Segall, J.E. & Condeelis, J.S. 2002, "Single cell behavior in metastatic primary mammary tumors correlated with gene expression patterns revealed by molecular profiling", *Cancer research* 62: 6278-6288.

Wang, X., Flynn, A., Waskiewicz, A.J., Webb, B.L., Vries, R.G., Baines, I.A., Cooper, J.A. & Proud, C.G. 1998, "The phosphorylation of eukaryotic initiation factor eIF4E in response to phorbol esters, cell stresses, and cytokines is mediated by distinct MAP kinase pathways", *Journal of Biological Chemistry* 273: 9373-9377.

Weiss, L. 1990, "Metastatic inefficiency", *Advances in Cancer Research* 54: 159-211.

Weisz, L., Zalcenstein, A., Stambolsky, P., Cohen, Y., Goldfinger, N., Oren, M. & Rotter, V. 2004, "Transactivation of the EGR1 gene contributes to mutant p53 gain of function", *Cancer research* 64: 8318-8327.

Wen, S., Stolarov, J., Myers, M.P., Su, J.D., Wigler, M.H., Tonks, N.K. & Durden, D.L. 2001, "PTEN controls tumor-induced angiogenesis", *Proceedings of the National Academy of Sciences of the United States of America* 98:4622-4627.

Wendel, H.G. & Lowe, S.W. 2004b, "Reversing drug resistance in vivo", *Cell.Cycle* 3: 847-849.

Wendel, H.G., De Stanchina, E., Fridman, J.S., Malina, A., Ray, S., Kogan, S., Cordon-Cardo, C., Pelletier, J. & Lowe, S.W. 2004a, "Survival signalling by Akt and eIF4E in oncogenesis and cancer therapy", *Nature* 428: 332-337.

Werling, R.W., Zacharski, L.R., Kisiel, W., Bajaj, S.P., Memoli, V.A. & Rousseau, S.M. 1993, "Distribution of tissue factor pathway inhibitor in normal and malignant human tissues", *Thrombosis and haemostasis* 69: 366-369.

Whiteside, M.A., Chen, D.T., Desmond, R.A., Abdulkadir, S.A. & Johanning, G.L. 2004, "A novel time-course cDNA microarray analysis method identifies genes associated with the development of cisplatin resistance", *Oncogene* 23: 744-752.

Williams, F.M. & Flintoff, W.F. 1995, "Isolation of a human cDNA that complements a mutant hamster cell defective in methotrexate uptake", *Journal of Biological Chemistry* 270: 2987-2992.

Woo, M.S., Ohta, Y., Rabinovitz, I., Stossel, T.P. & Blenis, J. 2004, "Ribosomal S6 kinase (RSK) regulates phosphorylation of filamin A on an important regulatory site", *Molecular and cellular biology* 24: 3025-3035.

Worden, B., Yang, X.P., Lee, T.L., Bagain, L., Yeh, N.T., Cohen, J.G., Van Waes, C. & Chen, Z. 2005, "Hepatocyte growth factor/scatter factor differentially regulates expression of proangiogenic factors through Egr-1 in head and neck squamous cell carcinoma", *Cancer research* 65: 7071-7080.

Wyckoff, J.B., Jones, J.G., Condeelis, J.S. & Segall, J.E. 2000, "A critical step in metastasis: in vivo analysis of intravasation at the primary tumor", *Cancer research* 60: 2504-2511.

Wyckoff, J.B., Jones, J.G., Condeelis, J.S. & Segall, J.E. 2000, "A critical step in metastasis: in vivo analysis of intravasation at the primary tumor", *Cancer research* 60: 2504-2511.

Wymann, M.P., Zvelebil, M. & Laffargue, M. 2003, "Phosphoinositide 3-kinase signalling--which way to target?", *Trends in pharmacological sciences* 24: 366-376.

Xie, Z., Yuan, H., Yin, Y., Zeng, X., Bai, R. & Glazer, R.I. 2006, "3-phosphoinositide-dependent protein kinase-1 (PDK1) promotes invasion and activation of matrix metalloproteinases", *BMC cancer* 6: 77.

Xing, J., Ginty, D.D. & Greenberg, M.E. 1996, "Coupling of the RAS-MAPK pathway to gene activation by RSK2, a growth factor-regulated CREB kinase", *Science* 273: 959-963.

Yabkowitz, R., Mansfield, P.J., Ryan, U.S. & Suchard, S.J. 1993, "Thrombospondin mediates migration and potentiates platelet-derived growth factor-dependent migration of calf pulmonary artery smooth muscle cells", *Journal of cellular physiology* 157: 24-32.

Yamashita, T., Tazawa, S., Yawei, Z., Katayama, H., Kato, Y., Nishiwaki, K., Yokohama, Y. & Ishikawa, M. 2006, "Suppression of invasive characteristics by antisense introduction of overexpressed HOX genes in ovarian cancer cells", *International journal of oncology* 28: 931-938.

Yang, D., Buchholz, F., Huang, Z., Goga, A., Chen, C.Y., Brodsky, F.M. & Bishop, J.M. 2002, "Short RNA duplexes produced by hydrolysis with Escherichia coli RNase III mediate effective RNA interference in mammalian cells", *Proceedings of the National Academy of Sciences of the United States of America* 99: 9942-9947.

Yarden, Y. & Sliwkowski, M.X. 2001, "Untangling the ErbB signalling network", *Nature reviews. Molecular cell biology* 2: 127-137.

Yiu, G.K. & Toker, A. 2006, "NFAT induces breast cancer cell invasion by promoting the induction of cyclooxygenase-2", *Journal of Biological Chemistry* 281: 12210-12217.

Yoon, S.O., Shin, S. & Lipscomb, E.A. 2006, "A novel mechanism for integrin-mediated ras activation in breast carcinoma cells: the alpha6beta4 integrin regulates ErbB2 translation and transactivates epidermal growth factor receptor/ErbB2 signaling", *Cancer research* 66: 2732-2739.

You, Z., Ouyang, H., Lopatin, D., Polver, P.J. & Wang, C.Y. 2001, "Nuclear factor-kappa B-inducible death effector domain-containing protein suppresses tumor necrosis factor-mediated apoptosis by inhibiting caspase-8 activity", *Journal of Biological Chemistry* 276: 26398-26404.

Yu, D. & Hung, M.C. 2000, "Overexpression of ErbB2 in cancer and ErbB2-targeting strategies", *Oncogene* 19: 6115-6121.

Zabrenetzky, V., Harris, C.C., Steeg, P.S. & Roberts, D.D. 1994, "Expression of the extracellular matrix molecule thrombospondin inversely correlates with malignant progression in melanoma, lung and breast carcinoma cell lines", *International journal of cancer. Journal international du cancer* 59: 191-195.

Zeniou, M., Ding, T., Trivier, E. & Hanauer, A. 2002, "Expression analysis of RSK gene family members: the RSK2 gene, mutated in Coffin-Lowry syndrome, is prominently expressed in brain structures essential for cognitive function and learning", *Human molecular genetics* 11: 2929-2940.

Zhan, L., Xiang, B. & Muthuswamy, S.K. 2006, "Controlled activation of ErbB1/ErbB2 heterodimers promote invasion of three-dimensional organized epithelia in an ErbB1-dependent manner: implications for progression of ErbB2-overexpressing tumors", *Cancer research 66*: 5201-5208.

Zhang, C., Chakravarty, D., Sakabe, I., Mewani, R.R., Boudreau, H.E., Kumar, D., Ahmad, I. & Kasid, U.N. 2006, "Role of SCC-S2 in experimental metastasis and modulation of VEGFR-2, MMP-1, and MMP-9 expression", *Molecular therapy : the journal of the American Society of Gene Therapy* 13: 947-955.

Zhang, H.G., Hyde, K., Page, G.P., Brand, J.P., Zhou, J., Yu, S., Allison, D.B., Hsu, H.C. & Mountz, J.D. 2004, "Novel tumor necrosis factor alpha-regulated genes in rheumatoid arthritis", *Arthritis and Rheumatism* 50: 420-431.

Zhang, Y., Gao, X., Saucedo, L.J., Ru, B., Edgar, B.A. & Pan, D. 2003, "Rheb is a direct target of the tuberous sclerosis tumour suppressor proteins", *Nature cell biology* 5: 578-581.

Zhao, Y., Bjorbaek, C. & Moller, D.E. 1996, "Regulation and interaction of pp90(rsk) isoforms with mitogen-activated protein kinases", *Journal of Biological Chemistry* 271: 29773-29779.

Zhou, X., Tan, M., Stone Hawthorne, V., Klos, K.S., Lan, K.H., Yang, Y., Yang, W., Smith, T.L., Shi, D. & Yu, D. 2004, "Activation of the Akt/mammalian target of rapamycin/4E-BP1 pathway by ErbB2 overexpression predicts tumor progression in breast cancers", *Clinical cancer research : an official journal of the American Association for Cancer Research* 10: 6779-6788.

Zhu, N., Gu, L., Findley, H.W. & Zhou, M. 2005, "Transcriptional repression of the eukaryotic initiation factor 4E gene by wild type p53", *Biochemical and biophysical research communications* 335: 1272-1279.

Zilberman, D., Cao, X. & Jacobsen, S.E. 2003, "ARGONAUTE4 control of locus-specific siRNA accumulation and DNA and histone methylation", *Science* 299: 716-719.

Zimmermann, T.S., Lee, A.C., Akinc, A., Bramlage, B., Bumcrot, D., Fedoruk, M.N., Harborth, J., Heyes, J.A., Jeffs, L.B., John, M., Judge, A.D., Lam, K., McClintock, K., Nechev, L.V., Palmer, L.R., Racie, T., Rohl, I., Seiffert, S., Shanmugam, S., Sood, V., Soutschek, J., Toudjarska, I., Wheat, A.J., Yaworski, E., Zedalis, W., Koteliansky, V., Manoharan, M., Vornlocher, H.P. & MacLachlan, I. 2006, "RNAi-mediated gene silencing in non-human primates", *Nature* 441: 111-114.

Zuberek, J., Wyslouch-Cieszynska, A., Niedzwiecka, A., Dadlez, M., Stepinski, J., Augustyniak, W., Gingras, A.C., Zhang, Z., Burley, S.K., Sonenberg, N., Stolarski, R. & Darzynkiewicz, E. 2003, "Phosphorylation of eIF4E attenuates its interaction with mRNA 5' cap analogs by electrostatic repulsion: intein-mediated protein ligation strategy to obtain phosphorylated protein", *RNA* 9: 52-61.